





---

INVESTIGATION OF THE  
BIOCHEMICAL BASIS OF BROWNING  
DURING THE STORAGE OF  
SULTANAS

---

---

INVESTIGATION OF THE  
BIOCHEMICAL BASIS OF BROWNING  
DURING THE STORAGE OF  
SULTANAS

---

A THESIS SUBMITTED FOR THE DEGREE OF  
DOCTOR OF PHILOSOPHY



DAMIAN FRANK  
B. Sc. (Biochemistry)

Centre for Bioprocessing and Food Technology  
(Food Safety Authenticity and Quality Unit)  
Victoria University of Technology  
Werribee  
Victoria Australia

September 2002

WER THESIS

664.8048 FRA

30001007614409

Frank, Damian

Investigation of the  
biochemical basis of  
browning during the storage

## DECLARATION

---

I hereby declare that all of the work contained within this thesis was carried out at the Centre for Bioprocessing and Food Technology (Food Safety Authenticity and Quality Unit) at the Werribee campus of Victoria University of Technology during my candidature as a PhD student. To my best knowledge no part of this thesis has been submitted in part or full for any other degree or diploma at any other University. Moreover, I declare that no material contained within this thesis has been written or published by any other person, excepting where due reference has been made to individuals in the text.

Damian Frank

December 2001

## ABSTRACT

---

High quality Australian sultanas are marketed largely on the basis of their light-golden colour and soft skins. Significant browning occurs in sultanas during storage and shipping, which seriously degrades sultana colour as well as overall quality. Whilst the cause of sultana browning during drying has been attributed to polyphenol oxidase (PPO) mediated oxidation of sultana phenolic substrates, the browning which occurs during sultana storage is less well-defined. The occurrence of non-enzymatic Maillard reactions has been suggested by a number of researchers, yet there has been no specific research conducted to elucidate these reactions in sultanas. In this thesis, PPO mediated browning, non-enzymatic Maillard reactions and, to a limited extent, lipid oxidation reactions were examined in two long-term storage trials.

Sultana grapes from two seasons (1995 and 1996) were used in multi-factor storage trials to investigate the effects of sultana sunfinishing ( $a_w$ ), storage temperature (10°C and 30°C), oxygen and storage time (10 and 14 months) on colour ( $L^*a^*b^*$  tristimulus values). ANOVA data for both years indicated that storage temperature and sunfinishing ( $a_w$ ) were the most important main effects on storage browning, with the presence of oxygen being less important. The  $b^*$  values were strongly effected by sunfinishing, oxygen exposure and to a lesser extent temperature. In both years intense browning was observed only at 30°C storage, aerobically and anaerobically, consistent with Maillard type reactions. The reactions were also strongly time-dependent, also in accordance with slower Maillard processes. The 1996 trial indicated that sultana maturity also might effect sultana storage colour.

Evidence of Maillard reactions was indicated through the disappearance of free-arginine in sultanas at 30°C after 4 months storage and the appearance of 5-hydroxymethyl furfural (5-HMF) a key intermediate of Maillard reactions. The concentration of 5-HMF was generally significantly lower in oxygen-exposed sultanas indicating different rates of Maillard browning in the presence of oxygen. In a further experiment Sultana grapes were also grown with four levels of soil nitrogen application (severely deficient, marginal, adequate and high) and dried. Total nitrogen, free-arginine and -proline content of the sultanas increased with soil nitrogen application. Browning was proportional to the skin free-arginine, regardless of whether the sultanas were stored in the presence or absence of oxygen. The concentration of the main PPO substrate, *trans*-caftaric acid, did not decrease significantly despite intense browning, indicating that phenolic oxidation reactions did not contribute to the storage browning reactions in those sultanas. Evidence of oxidation of sultana surface wax components at 30°C was also shown.

Specific arginine-glucose Maillard reaction products were also indicated in both sultanas and model systems through a number of compounds identified by high performance liquid chromatography diode array detection (HPLC-DAD) as well as gas chromatography-mass spectrometry (GC-MS). In the last chapter, reflectance Near Infrared Spectroscopy (NIR) was examined as a possible browning prediction technology. Preliminary data indicated that NIR may be useful in measuring  $L^*a^*b^*$ ,  $a_w$ , Kjeldahl Nitrogen and skin free-arginine in sultanas; these parameters were shown in simple regression models to be indicators of sultana storage browning potential.

## ACKNOWLEDGEMENTS

---

Many people have had input into the long process which has culminated in the form of this final document, and their efforts are gratefully acknowledged. Firstly, a general heartfelt thank you is extended to all those friends, family and colleagues who motivated me through those seemingly endless periods of technical problems and difficulties. Thanks for sticking by me.

Specific thanks must be extended to a number of people who played key roles in this project:

- Dr Mary Millikan, for her consistent optimism in her role as supervisor; and her technical advice and suggestions. On numerous occasions her patience and kindness prevented me from giving up.
- Ian Gould, for his rational and realistic approach to things and general assistance.
- Robert Hayes, for his advice and practical support at the Sunraysia Horticultural Centre.
- Peter Flinn, for his patience and advice with NIR.
- Dr Nagarajah, for the provision of the soil nitrogen sultana samples for Chapter 5.0 and his general assistance in obtaining grape and sultana samples.
- Mr John Reynolds at Food Science Australia for his advice on experimental design and statistical analysis.

Moreover, thanks must be extended to staff at the Centre for Bioprocessing and Food Technology and the School of Biological and Life Sciences at Victoria University of Technology, specifically to Vilnis Ezerniecks for his technical support.

General thanks are also expressed to the staff at the Sunraysia Horticultural Centre and CSIRO Merbein, especially Peter Clingeffer, Carolyn Tarr and Paul Burrow. Financial support from the Dried Fruits Research and Development Council of Australia and from the Centre for Bioprocessing and Food Technology are gratefully acknowledged. A number of friends must be acknowledged, who have been supportive at various crucial times during the project:

- George Phillips, for both his friendship and his unflinching patience in unravelling the mysteries of document formatting.
- Anne Wilson, for her friendship, support and inspiration.
- Alex Green, for his friendship and support.
- Katie, my sister who was there through frustrating moments.
- bryan Andy for being there for the last leg.

Finally, I thank Anne, my mother, John, my father and Lynn my stepfather, for their general support and belief in me.

# TABLE OF CONTENTS

---

<b>DECLARATION</b>	<b>i</b>
<b>ABSTRACT</b>	<b>ii</b>
<b>ACKNOWLEDGEMENTS</b>	<b>iii</b>
<b>TABLE OF CONTENTS</b>	<b>iv</b>
<b>LIST OF FIGURES</b>	<b>viii</b>
<b>LIST OF TABLES</b>	<b>xi</b>
<b>LIST OF ABBREVIATIONS</b>	<b>xiii</b>
<b>1.0 INTRODUCTION</b>	<b>1</b>
1.01 Sultana production	1
1.02 The Sultana grape in Australia	2
1.03 Production of sultanas	5
1.04 Browning processes in sultanas	9
1.05 General thesis aims	10
<b>2.0 BROWNING REACTIONS: LITERATURE REVIEW</b>	<b>11</b>
2.01 Enzymatic Browning Processes	11
2.02 Secondary reactions of <i>o</i> -quinones	12
2.03 Browning in sultanas	15
2.04 Phenolic compounds	16
2.05 Grape phenolics	16
2.06 Synthesis of phenolic substrates	18
2.07 Grape surface lipids and action of dipping oils	19
2.08 Maillard non-enzymatic browning reactions	20
2.09 Maillard reaction mechanisms	20
2.10 Evidence of Maillard reactions in sultanas and grape products	23
2.11 Maillard coloured compounds and melanoidin	24
2.12 Nitrogenous compounds in grapes and sultanas	27
2.13 Biosynthesis of proline	28
2.14 Biosynthesis of arginine	29
2.15 Arginine as a Maillard amino acid	29
2.16 Plant senescence processes	32
2.17 Water activity	32
2.18 Crystallisation phenomena	34
2.19 Fatty acid oxidation	35
2.20 Conventional browning prevention strategies	36
2.21 Colour definition and measurement	38
2.22 Natural colour chemistry	39
2.23 Near infrared spectroscopy	41
2.24 Near infrared: theoretical	42
2.25 Spectral pre-processing and derivative spectroscopy	44
2.26 Multivariate calibration techniques: multiple linear regression (MLR) calibration	45
2.27 Partial least squares (PLS) calibrations	46

<b>3.0</b>	<b>SULTANA STORAGE EXPERIMENT I 1995</b>	<b>49</b>
3.01	Introduction	49
3.02	Experimental aims	49
3.03	Materials and methods: source of grape material	50
3.04	Determination of TSS and TA	50
3.05	Substrate PPO activity	50
3.06	Oxygen-free packaging	51
3.07	Colour measurement—tristimulus values ( $L^*a^*b^*$ )	53
3.08	Water activity	54
3.09	Total phenolics	54
3.10	Analysis of grape and sultana free amino acids	54
3.11	Ortho-phthalaldehyde (OPA) amino acid derivatisation	55
3.12	9-fluorenylmethylchloroformate (F-moc) amino acid derivatisation	56
3.13	Measurement of 5-Hydroxymethylfurfural (GC and GC-MS)	57
3.14	Statistical analysis	58
3.15	Analytical results	58
3.16	Preparation of sultanas for the storage trial	59
3.17	Analysis of pre-storage sultanas	61
3.18	Pre-storage $a_w$	61
3.19	Pre-storage total phenolics	62
3.20	Pre-storage sultana PPO activity in skin and flesh	62
3.21	Pre-storage sultana colour	62
3.22	Storage trial preparation	63
3.23	Storage colour change and statistical analysis	63
3.24	Storage changes in $L^*$ tristimulus coordinate	63
3.25	Storage change in $a^*$ tristimulus coordinate	65
3.26	Storage changes in $b^*$ tristimulus coordinate	70
3.27	Storage changes in sultana free-amino acid profiles	73
3.28	Free-arginine in pre-storage sultanas (skin and flesh)	78
3.29	5-Hydroxymethylfurfural (5-HMF) in sultanas	79
3.30	$A_w$ change during sultana storage	81
3.31	Internal sugaring in sultanas	82
3.32	Change in total phenolics during storage	83
3.33	Regression analysis of storage trial data	84
3.34	Regression model for $L^*$ tristimulus value	85
3.35	Regression model for $b^*$ tristimulus value	88
3.36	Data interpretation and conclusions	91
<b>4.0</b>	<b>SULTANA STORAGE EXPERIMENT II 1996</b>	<b>94</b>
4.01	Introduction	94
4.02	Experimental aims	94
4.03	Source of grape material	94
4.04	Experimental: analysis of grape TSS, TA, total phenolics and $L^*a^*b^*$ tristimulus values	95
4.05	Grape pH	97
4.06	Grape glucose	97
4.07	Grape free-amino acid analysis	97
4.08	Hydroxycinnamic esters (HPLC)	97
4.09	Fresh grape maturity data	98
4.10	Grape skin-flesh PPO activity	98
4.11	Free-amino acids in grapes	100
4.12	Grape total phenolics	100
4.13	HPLC analysis of grape phenolic profiles	100
4.14	Drying of grapes	104
4.15	Iron and copper analysis	105
4.16	Kjeldahl protein	105

4.17	Analytical data for pre-storage sultanas	106
4.18	Pre-storage substrate PPO activity	106
4.19	Pre-storage total phenolics	107
4.20	Pre-storage sultana $a_w$	107
4.21	Pre-storage free-amino acids in sultanas	107
4.22	Pre-storage sultana Kjeldahl protein, copper and iron	108
4.23	Pre-storage sultana colour	110
4.24	Pre-storage sultana HPLC profiles	111
4.25	Preparation of samples for the storage trial	113
4.26	Storage colour changes	116
4.27	Storage changes in $L^*$ tristimulus coordinate	116
4.28	Storage changes in $a^*$ tristimulus coordinate	122
4.29	Storage changes in $b^*$ tristimulus coordinate	126
4.30	Storage changes of $a_w$	130
4.31	Internal sugaring	130
4.32	Changes in 5-HMF in sultanas	132
4.33	Regression model of colour prediction	133
4.34	Regression model of storage browning using combined 1995 and 1996 data	143
4.35	Discussion of data	146
<b>5.0</b>	<b>SOIL NITROGEN AND SULTANA BROWNING</b>	<b>150</b>
5.01	Soil nitrogen and sultana colour—introduction	150
5.02	Experimental aims	150
5.03	Source of sultana material	150
5.04	Experimental-storage trial	152
5.05	HPLC diode-array analysis of Maillard model system and sultana extracts	152
5.06	Pre-storage sultana chemical data	152
5.07	Pre-storage free-amino acid profiles	153
5.08	Storage trial	154
5.09	Storage colour changes	154
5.10	Changes in the $L^*$ tristimulus coordinate	155
5.11	Changes in $a^*$ tristimulus coordinate	155
5.12	Changes in $b^*$ tristimulus coordinate	158
5.13	Changes in HPLC Profiles of sultana MeOH extracts	163
5.14	Changes in 5-HMF during storage	167
5.15	Conformation experiment	168
5.16	Maillard reaction products	175
5.17	Discussion	183
<b>6.0</b>	<b>SULTANA SURFACE LIPID OXIDATION DURING STORAGE</b>	<b>188</b>
6.01	Introduction	188
6.02	Experimental aims	188
6.03	Gas chromatography-mass spectrometry (GC-MS)	188
6.04	Sample preparation	188
6.05	Experimental results	190
6.06	Mass spectra of lipid peaks and statistical analysis	192
6.07	Saturated fatty acid esters	192
6.08	Mono-unsaturated fatty acid esters	196
6.09	Polyunsaturated lipid material	198
6.10	Saturated hydrocarbon material	198
6.11	Interpretation of data	203

<b>7.0</b>	<b>MAILLARD REACTION INTERMEDIATES IN SULTANAS AND ARGININE-GLUCOSE MODEL SYSTEMS</b>	<b>205</b>
7.01	Introduction	205
7.02	Experimental aims	205
7.03	Sample preparation—sultana and model systems	205
7.04	Ethyl acetate (EtAc) and methanol (MeOH) extracts	206
7.05	Maillard reaction products GC-MS	206
7.06	Analysis of EtAc extracts	207
7.07	Interpretation of mass spectral data	213
7.08	Semi-quantification of Maillard intermediates in sultanas	216
7.09	Methanol extracts	217
7.10	Solid-phase micro-extraction (SPME)—GC-MS	223
7.11	SPME sampling	223
7.12	Interpretation of mass spectral data	230
7.13	Conclusions	231
<b>8.0</b>	<b>BROWNING MODEL SYSTEMS</b>	<b>234</b>
8.01	Maillard model systems—introduction	234
8.02	Experimental aims	234
8.03	Influence of arginine concentration, temperature and $a_w$ on Maillard browning systems	234
8.04	Results	235
	Influence of pH on arginine- glucose interaction	241
8.06	Maillard model systems—discussion	243
<b>9.0</b>	<b>NEAR INFRARED SPECTROSCOPY OF SULTANAS</b>	<b>244</b>
9.01	Introduction	244
9.02	Experimental aims	244
9.03	Materials and methods	244
9.04	Water activity	246
9.05	Colour $L^*a^*b^*$	253
9.06	Free-arginine in sultanas	258
9.07	Kjeldahl protein in sultanas	260
9.08	Conclusions	263
<b>10.0</b>	<b>CONCLUSIONS AND FURTHER WORK</b>	<b>264</b>
10.01	Summary of data	264
10.02	Further research	268
	<b>BIBLIOGRAPHY</b>	<b>270</b>
	<b>APPENDIX I—MASS SPECTRA FROM CHAPTER 7.0</b>	<b>296</b>

# LIST OF FIGURES

---

## Chapter 1.0

- Figure 1.1 Recent trends in the export of dried grapes (almost entirely sultanas) and import of dried grapes. 4

## Chapter 2.0

- Figure 2.1 True polyphenoloxidases have both cresolase (left) and catecholase activity (right). 11
- Figure 2.2 Secondary reactions of ortho-quinones with phenolic compounds. 13
- Figure 2.3 Secondary reactions of ortho-quinones with non-phenolic compounds. 14
- Figure 2.4 Structures of the main phenolic compounds in Sultana grapes 18
- Figure 2.5 Structures of the initial Maillard colourless intermediates 21
- Figure 2.6 General scheme showing the generation of dicarbonyl intermediates 22
- Figure 2.7 General scheme of Strecker decarboxylation of amino acids by  $\alpha$ -dicarbonyl compound. 23
- Figure 2.8 Common furanoid Maillard reaction intermediates. 25
- Figure 2.9 Typical pyrrole-derived Maillard heterocycles isolated from model and food systems. 26
- Figure 2.10 Some common two-nitrogen heterocycles formed in Maillard reactions. 26
- Figure 2.11 Structures of proline (left) and arginine (right). 29
- Figure 2.12 Products formed from the interaction of the guanidine group with dicarbonyl intermediates. 30
- Figure 2.13 Furyl-pyrrolines and cyclopentazepinone products from arginine glucose models. 31
- Figure 2.14 Structure of the intense red-brown cross-linked product formed by N- $\alpha$ -arginine, glyoxal and furfural. 31
- Figure 2.15 Water adsorption isotherms for sultanas at 20°C, 25°C, 30°C and 35°C. 33

## Chapter 3.0

- Figure 3.1 Data for optimisation of assay conditions for PPO with 4-methyl catechol as a substrate 51
- Figure 3.2 Diagram showing grape and sultana field treatments and packaging. 60
- Figure 3.3 Effects of sunfinishing and oxygen exposure on L\* values for exposed and protected sultana combined. 66
- Figure 3.4 Average a\* tristimulus values at 4, 8 and 14 months at 10°C (top) and 30°C (bottom). 68
- Figure 3.5 Effect of vine exposure on a\* tristimulus values. 70
- Figure 3.6 Average b\* tristimulus values at 4, 8 and 14 months at 10°C (top) and 30°C (bottom). 71
- Figure 3.7 Concentration of F-moc derivatised free-amino acids. 75
- Figure 3.8 HPLC profiles of F-moc derivatised free-amino acids after 14 months storage. 76
- Figure 3.9 HPLC profiles of F-moc derivatised free-amino acids after 14 months storage. 77
- Figure 3.10 Changes in free L-arginine over 14 months storage at 30°C. 78
- Figure 3.11 EI-mass spectrum of peak identified as 5-hydroxymethyl furfural from sultana DCM extract. 80
- Figure 3.12 Decrease in free-arginine and generation of 5-hydroxymethyl furfural in sultanas. 81
- Figure 3.13 The effect of sunfinishing and oxygen exposure on changes in aw 82
- Figure 3.14 Total phenolics in sultanas pre-storage and after 14 months at each storage condition 84
- Figure 3.15 Regression model for L\* using pre-storage L\*, skin free-arginine, aw, time and temperature. 86
- Figure 3.16 Regression model for L\* using aw, time and temperature. 87
- Figure 3.17 Regression model for b\* using pre-storage b\*, skin free-arginine, aw, time and temperature. 89
- Figure 3.18 Regression model for b\* using aw, time and temperature 90

## Chapter 4.0

Figure 4.1	Flow diagram showing field shading, sample codes and storage experiment.	96
Figure 4.2	Typical HPLC profiles of MeOH extracts of 1996 grape skin phenolics at 320 nm.	102
Figure 4.3	HPLC phenolic profiles of skins and flesh of the fresh grapes.	103
Figure 4.4	Skin and flesh concentration of free-arginine and free-proline in pre-storage sultanas.	109
Figure 4.5	Skin and flesh concentration of the unidentified compound in pre-storage sultanas.	110
Figure 4.6	Pre-storage L* a* b* tristimulus values for 1996 sultanas.	112
Figure 4.7	Typical HPLC profiles of MeOH extracts of pre-storage sultanas at 320 nm	114
Figure 4.8	Concentration of HPLC peaks in pre-storage sultana skin and flesh for early and late harvest fruit.	115
Figure 4.9	Change in L* values at 10 °C (top) and 30 °C (bottom) averaged for level of exposure.	118
Figure 4.10	Effect of vine solar exposure on L* values averaged for early (21 February) harvested sultanas.	119
Figure 4.11	Change in a* values at 10 °C (top) and 30 °C (bottom): averaged for early and late fruit.	123
Figure 4.12	Effect of vine solar exposure on a* values averaged for early harvested sultanas.	124
Figure 4.13	Change in b* values at 10 °C (top) and 30 °C (bottom)— averaged for early and late fruit.	127
Figure 4.14	Effect of vine solar exposure on average b* values for early and late harvested sultanas	128
Figure 4.15	Changes in a <sub>w</sub> in early (top) and late (bottom) sultanas over 10 months storage at 10 °C and 30 °C.	131
Figure 4.16	Concentration of 5-hydroxymethyl furfural after 10 months storage in 1996 sultanas.	132
Figure 4.17	Graphical representation of regression prediction equation of sultana L*.	134
Figure 4.18	Graphical representation of regression prediction equation of sultana L*.	135
Figure 4.19	Graphical representation of regression prediction equation of sultana b*.	136
Figure 4.20	Graphical representation of regression prediction equation of sultana b*.	137
Figure 4.21	Graphical representation of fitted (predicted) L* (above) and b* (below) tristimulus values.	139
Figure 4.22	Graphical representation of fitted (predicted) L* (above) and b* (below) tristimulus values.	141
Figure 4.23	Graphical representation of the multiple term linear regression equation.	144
Figure 4.24	Graphical representation of the multiple term linear regression equation.	145

## Chapter 5.0

Figure 5.1	Pre-storage free-proline and arginine in sultanas from vines given four amounts of nitrogen fertiliser.	154
Figure 5.2	Change in L* values for soil nitrogen sultanas stored for 10 months.	156
Figure 5.3	Change in a* (Lightness) values for soil nitrogen sultanas stored for 10 months.	159
Figure 5.4	Change in b* (Lightness) values for soil nitrogen sultanas stored for 10 months.	160
Figure 5.5	Colours of soil nitrogen sultanas after 5 months at each of the storage conditions	161
Figure 5.6	Colours of soil nitrogen sultanas after 10 months at each of the storage conditions.	162
Figure 5.7	Changes in HPLC profiles of sultana MeOH extracts.	164
Figure 5.8	Change in the relative concentrations of HPLC peaks in sultana MeOH extracts.	165
Figure 5.9	5-HMF measured in DCM extracts of the soil nitrogen sultanas pre-storage and after 10 months storage.	167
Figure 5.10	HPLC profiles at 320 nm of MeOH sultana extract before storage (top) and after storage for 12 days at 55 °C	169
Figure 5.11	HPLC profile at 280 nm of a typical MeOH sultana extract.	170
Figure 5.12	Areas of the major compounds evolving in MeOH extracts of sultanas stored at 55°C over 12 days.	170

Figure 5.13	Diode array UV-spectra of peaks eluting at 8.2 min. (top) and 8.3 min. (bottom) in MeOH extracts.	173
Figure 5.14	Diode array UV-spectra of peaks eluting at 10.2 min. (top) and 13.07 min. (bottom) in MeOH extracts.	174
Figure 5.15	Typical HPLC profile of arginine-glucose model system.	176
Figure 5.16	UV spectrum of Maillard peak eluting at 5.3 min.	177
Figure 5.17	UV-spectra for the peak eluting at 6.5 min. (5-Hydroxymethyl furfural).	178
Figure 5.18	Characteristic UV spectra for the peak eluting at 4.1 min. (see Table 5-4).	181
Figure 5.19	Typical UV spectra for characteristic peaks discussed in Table 5-4.	182
<b>Chapter 6.0</b>		
Figure 6.1	GC profiles of DCM extracts of sultanas after 10 months storage at 30 °C.	191
Figure 6.2	Mass spectra for peaks described in Table 6.3.	193
Figure 6.3	Quantitative changes in individual lipids after 10 months storage at 10 °C and 30 °C.	200
Figure 6.4	Quantitative changes in individual lipids after 10 months storage at 10 °C and 30 °C.	202
<b>Chapter 7.0</b>		
Figure 7.1	Total ion chromatogram of EtAc extract of sultanas (30°C) and model systems (37°C).	208
Figure 7.2	Total ion chromatograms of EtAc extracts of sultanas (50°C) and model system (50°C).	209
Figure 7.3	Total ion chromatograms of EtAc extracts of sultanas (60 °C ) and model system (60°).	210
Figure 7.4	Total ion chromatogram of HPLC separated MeOH extract.	211
Figure 7.5	Structures of some of the Maillard intermediates tentatively identified in EtAc extracts.	215
Figure 7.6	Relative concentration of Maillard intermediates in EtAc extracts from sultanas.	218
Figure 7.7	Structures of some of the Maillard intermediates tentatively identified in EtAc extracts.	219
Figure 7.8	Total ion chromatograms of MeOH extracts of sultanas stored at 30 °C (top) and arginine-glucose model stored at 37 °C (bottom).	220
Figure 7.9	Total ion chromatograms of MeOH extracts of sultanas (top) and arginine-glucose model (bottom) stored at 50 °C	221
Figure 7.10	Total ion chromatograms of MeOH extracts of sultanas (top) and arginine-glucose model (bottom) stored at 60 °C	222
Figure 7.11	Total ion chromatogram for SPME analysis of sultana and arginine-glucose model headspace.	225
Figure 7.12	Expanded view of total ion chromatogram for Carboxen fibre sampling (0.5-12 minutes)	226
Figure 7.13	Expanded view of total ion chromatogram for Carboxen fibre sampling (12-25 minutes)	227
Figure 7.14	Expanded view of total ion chromatogram for Carboxen fibre sampling (25-41 minutes).	228
Figure 7.15	Structures of some of the Maillard compounds present in SPME extracts.	230
Figure 7.16	Typical arginine-specific Maillard products.	232
<b>Chapter 8.0</b>		
Figure 8.1	Time course for L* values in arginine-glucose model systems with different initial $a_w$ values.	237
Figure 8.2	Time course for a* values in arginine-glucose model systems with different initial $a_w$ values.	239
Figure 8.3	Time course for b* values in arginine-glucose model systems with different initial $a_w$ values.	240
Figure 8.4	The effect of pH on rates of arginine-D-glucose Maillard browning at 37 °C and 50 °C.	242

## Chapter 9.0

Figure 9.1	Typical reflectance NIR spectra of sultanas.	247
Figure 9.2	Detail of spectral variation of NPS 2nd D spectra.	248
Figure 9.3	Detail of spectral variation of NPS 2nd D spectra	249
Figure 9.4	Plot of MRL predicted and PLS predicted water activity.	251
Figure 9.5	Calibration data for $\lambda_1$ 1276 nm, $\lambda_2$ 1026 nm and $\lambda_3$ 1962 nm.	252
Figure 9.6	Plot of PLS predicted for L*	254
Figure 9.7	Plot of PLS predicted for a*	255
Figure 9.8	Plot of predicted PLS for b*	256
Figure 9.9	Plot of predicted skin free-arginine	259
Figure 9.10	Plot of PLS predicted for Kjeldahl Protein (KP)	262

# LIST OF TABLES

---

## Chapter 1.0

Table 1.1	Major world producers of dried Sultana grapes	3
Table 1.2	Tonnes of dried vine fruit produced annually in Australia 1996-1999.	3
Table 1.3	Crown grade classification system adapted from ADFA Dried Vine Fruit Manual July 1998	8

## Chapter 3.0

Table 3.1	Properties of OPP and PVDC polymers, based on a film thickness of 25 $\mu\text{m}$ (1 mil).	52
Table 3.2	Analytical data for fresh berries collected from exposed and protected vines of experiment I 1995.	58
Table 3.3	Codes for the sultana samples used in storage experimentII, 1995..	59
Table 3.4	Pre-storage data for sultanas used in the 1995 experiment.	61
Table 3.5	ANOVA table for L* showing all main effects and two-way interactions.	67
Table 3.6	ANOVA table for a* showing all main effects and two-way interactions.	69
Table 3.7	ANOVA table for b* showing all main effects and two-way interactions.	73
Table 3.8	Distribution of free-arginine in pre-storage sultana skin and flesh.	78
Table 3.9	Internal sugaring measured as number of surface crystal nuclei per berry	83
Table 3.10	Table of regression coefficients (top) and cumulative ANOVA table (bottom)	85
Table 3.11	Table of regression model coefficients (top) and cumulative ANOVA table (bottom)	88

## Chapter 4.0

Table 4.1	Data for total soluble solids TSS ( $^{\circ}$ Brix), pH, titratable acidity (TA), glucose concentration and tristimulus values.	98
Table 4.2	Skin-flesh substrate PPO activity and total phenolics for grapes.	99
Table 4.3	Whole F-moc grape free-amino acids (arginine and proline) and unidentified compound in 80% MeOH extracts of grapes.	99
Table 4.4	Codes used for the 16 unique sultana samples used in the 1996 storage trial.	104
Table 4.5	Pre-storage sultana data: substrate PPO activity, total phenolics and $a_w$ .	106
Table 4.6	Pre-storage concentration of Kjeldahl protein, iron and copper in early and late harvested sultanas.	108
Table 4.7	ANOVA table for L*: treatment harvest time included.	120
Table 4.8	ANOVA table for L* for early (top) and late harvest (bottom) sultanas.	121
Table 4.9	ANOVA table for a*: treatment harvest time included.	124
Table 4.10	ANOVA table for a* for early (top) and late harvest (bottom) sultanas.	125
Table 4.11	ANOVA table for b*: early and late harvest fruit together.	128
Table 4.12	ANOVA table for b* early (top) and late harvest (bottom) sultanas	129
Table 4.13	Internal sugaring expressed as average number of nuclei per sultana and $a_w$	130
Table 4.14	Statistical data for L* and b* tristimulus regression models.	130
Table 4.15	Top: calculated constant and regression coefficients with their respective standard errors	142
Table 4.16	ANOVA data showing the effect of season in the combined equation for L* tristimulus values	146

## Chapter 5.0

Table 5.1	Analytical data for grape petiole nitrate, percent nitrogen, total soluble solids (TSS), titratable acidity (TA) and sultana yield.	151
Table 5.2	Pre-storage analytical data for soil nitrogen sultanas.	153
Table 5.3	ANOVA table for the effects of nitrogen, oxygen, temperature, time on L*a*b* tristimulus values.	157
Table 5.4	$\lambda$ max for the Maillard HPLC peaks.	179

## Chapter 6.0

Table 6.1	Temperature program for the gas chromatograph—DB-1 column.	189
Table 6.2	The Varian Saturn II instrument settings used in the analysis of sultana DCM extracts.	190
Table 6.3	Retention times and most intense ion fragments in mass spectra (decreasing intensity).	197
Table 6.4	Table of significance of effects on lipid peaks in DCM extracts.	199

## Chapter 7.0

Table 7.1	Varian Saturn II ITMS settings used in the analysis of EtAc and MeOH extracts.	206
Table 7.2	Mass spectral fragments for the peaks in EtAc sultana and model system extracts.	212
Table 7.3	Varian Saturn 2000-ITMS instrument settings for SPME analyses	224
Table 7.4	Most abundant mass spectral fragments for the peaks from 'Carboxen'- SPME fibre.	229
Table 7.5	Expected m/z values for M <sup>+</sup> fragment of imidazolone and pyrimidine structures.	232

## Chapter 8.0

Table 8.1	ANOVA table for L* a* b* data for model systems.	238
-----------	--	-----

## Chapter 9.0

Table 9.1	Calibration data for water activity.	251
Table 9.2	Calibration statistics for L* and a* tristimulus coordinates.	254
Table 9.3	Calibration statistics for b* tristimulus coordinate	257
Table 9.4	Multiple Linear Regression wavelengths for L a* b* calibrations	258
Table 9.5	Calibration validation data for L*, a* and b* tristimulus values	258
Table 9.6	Calibration statistics for skin free-arginine	258
Table 9.7	Calibration statistics for whole sultana Kjeldahl Protein for 1996 samples.	261
Table 9.8	Calibration data for 1998 and 1996 & 1998 PLS calibrations for KP.	262

## Chapter 10.0

Table 10.1	Summary of the single effects and two-way interactions from the ANOVA analyses of the sultana storage trials (trials I, II and the soil-nitrogen experiment).	267
------------	---	-----

## LIST OF ABBREVIATIONS

---

$\nu$	Frequency
$\lambda$	Wavelength (nanometres)
$\lambda_{\text{max}}$	Wavelength of maximum absorption
1 <sup>st</sup> D	First derivative
5-HMF	5-hydroxymethyl furfural
a*	Tristimulus red-green coordinate
ADFA	Australian Dried Fruits Association
AFISC	Australian Food Industry Science Centre
amu	Atomic Mass Unit
ANOVA	Analysis of Variance
a <sub>w</sub>	Water Activity
b*	Tristimulus yellow-blue coordinate
c	Speed of light <i>in vacuo</i>
CBFT	Centre for Bioprocessing and Food Technology
CSIRO	Commonwealth Scientific and Industrial Research Organisation
DCM	Dichloromethane
DFRDC	Dried Fruits Research and Development Council
DHA	Dehydroascorbic acid
DVF	Dried Vine Fruit
DW	Dry weight
EtAc	Ethyl Acetate
F	Factor
FID	Flame Ionisation Detector
F-moc	9-Flourenylmethylchloroformate
FSA	Food Science Australia
FW	Fresh weight
GC	Gas Chromatography
GC/MS	Gas Chromatography/ Mass Spectrometry
GRP	Grape reaction product
HPLC	High Pressure Liquid Chromatography
IR	Infrared
KP	Kjeldahl Protein
L*	Tristimulus lightness coordinate
LV	Latent Variable
m/z	Mass/ Charge ratio
M+	Parent ion

MeOH	Methanol
Milli-Q	Trade name for distilled/ deionised water Millipore Company
MLR	Multiple Linear Regression
MW	Molecular Weight
NIR	Near Infrared Spectroscopy
NPS	N point smooth
NSAS®	Near Infrared Spectral Analysis Software
OPA	Ortho Phthaldialdehyde
OPP	Oriented polypropylene
PC	Principal Component
PLS	Partial Least Squares
PPO	Polyphenoloxidase
PVDC	Polyvinylidene chloride
SS	Sum of Residual Squared Errors
SD	Standard Deviation
SDS-PAGE	Sodium dodecyl sulphate-polyacrylamide gel electrophoresis
SEC	Standard Error of Calibration
SECV	Standard Error of Cross Validation
SEM	Scanning Electron Microscopy
SEP	Standard Error of Prediction
SHC	Sunraysia Horticultural Centre, Irymple, Victoria.
TA	Titrateable Acidity
$t_R$	Retention Time
VUT	Victoria University of Technology



## 1.0 INTRODUCTION

---

### 1.01 Sultana production

The grape (*Vitis vinifera*) is the most widely cultivated fruit crop in the world, with global annual production estimated at approximately 60 million tonnes (Olmo 1993 and Australian Bureau of Statistics—ABS 1999). In terms of area of vine coverage, Australia is ranked in position 22 (90,000 ha) on a comparative world basis, in position 14 in terms of grape tonnage (942,100 tonnes) and 9 vis-à-vis wine production (743,000 tonnes). In Australia, approximately 79% of all grapes are used for wine production, with the remainder sold as table grapes (61,600 tonnes or 6.5%) or dried grapes (137,000 tonnes or 14%). In 1997 Australia contributed 3% to total world dry grape production (ABS 1999).

Drying of fruits and vegetables is one of the most ancient methods of food preservation. The low water activity of these foods prevents the spoilage by microorganisms and allows for extended storage without refrigeration or the application of sophisticated storage technology. The drying of grapes originated in the Middle East, mainly Afghanistan and Iran. The main grape cultivars in use worldwide for the production of dried vine fruit were derived from these countries; they are characterised by their thin skins, firm flesh and high sugar content (Patil *et al.* 1995). The main *Vitis vinifera* drying grape variety is Sultana, known in different parts of the world as *Sultana*, *Sultanina*, *Kish-mish* and *Thompson Seedless*. In Australia this grape variety is commonly referred to as either Sultana or sometimes Thompson Seedless—the dried fruit thereof is always referred to as sultanas. Other drying grape varieties such as currants (produced from the small grape cultivar *Zante Currant*—synonym: *Black Corinth*) and raisins (produced from the slightly larger grape cultivar *Muscat Gordo Blanco*—synonyms: *Muscat of Alexandria* and *Waltham Cross*) are also popular, but constitute a small percentage of all dried vine fruit. It is a matter of confusion that North Americans generically refer to dried fruit from Sultana and Muscat Gordo Blanco cultivars as raisins, although the predominant drying grape in the United States is, by far, Sultana. This thesis focuses entirely on the Sultana grape, as this cultivar is the most economically important drying grape in Australia. There is quite a degree of variation in how Sultana grapes are dried in various countries (Table 1.1 and Patil *et al.* 1995).

The United States is the largest producer of sultanas. The bulk of sultanas there are produced by laying fresh grapes on paper trays between rows of vines, and left to dry in the sun. Americans refer to these dark-coloured characteristically malty-flavoured sultanas as 'sun-dried naturals'. Simple sun-drying also in use in other countries (Afghanistan, South Africa, Mexico and others)—generally wherever the climate will allow. In some countries, rather than directly drying undipped grapes in the sun, grapes are placed in dehydrators and dried at around 60-70°C—

sultanas produced in this manner are tough-skinned, dark in colour and malty in flavour. In the USA, in addition to 'naturals', a small percentage of grapes are dipped in alkali solution and subjected to fumes of burning sulphur in a 'sulphur house' and subsequently dried in a dehydrator at 60-70°C. Light coloured raisins are produced by this technique. This method of sultana production is also followed in some other countries, such as Chile and South Africa.

In many parts of the world (Table 1.1), mainly Turkey, Iran, Greece and Australia, grapes of the Sultana cultivar are dried after being dipped in an emulsion of potassium carbonate and vegetable oil. The dipped grapes are dried either in direct or indirect sunlight. In Australia dipped grapes are dried on multi-tiered wire mesh in open-sided drying racks covered with a corrugated iron roof to protect the fruit from rain damage and direct sunlight. Sultanas produced in this manner possess soft skins, a fleshy appearance and are generally of a light golden to amber colour.

A small proportion of dried Sultana grapes, called 'Sogoyashi', is produced in Iran and Afghanistan. Typically, grape clusters are threaded onto strings and hung in specially designed well-ventilated drying houses. Grapes dehydrate slowly and have a characteristic light-green colour and soft texture.

## **1.02 The Sultana grape in Australia**

Sultana is one of Australia's most important white grape varieties, with approximately 13,000 ha of fruit bearing vines in 1999, coming second only to Chardonnay (ca. 15,200 ha—ABS 1999). In terms of tonnes per year, the Sultana grape is produced in the highest quantity of all grape varieties (red and white) with 250,000 tonnes produced in 1999. Of this total, approximately 42% of grapes were dried, 47% were used for winemaking and the remainder sold as table grapes. It should be noted that the production of dried grapes has declined over recent years (Table 1.2).

The yearly fluctuation in dried fruit yield is due to a number of factors, such as weather conditions, international dried fruit markets and the increasing demand on Sultana grapes from the wine industry. In some seasons it is more profitable for Sultana farmers to sell their grapes to wineries than to dry them. Although Sultana grapes are almost always used as a 'blending' grape in winemaking, they still constitute one of the most important white wine grapes in terms of tonnage used. In 1999 Sultana grapes were second only to Chardonnay grapes in terms of grapes used for wine-making. Although there are a number of other grape varieties used in Australia for drying purposes, such as currants and raisins, over 90% of all dried grapes are Sultana. Sultana grapes are almost exclusively cultivated in the Murray Valley, extending from Waikerie in the Riverland region in South Australia, to Sunraysia in northwest Victoria and southwest New South Wales, to Robinvale and up to Swan Hill.

NORTHERN HEMISPHERE	TONNAGE	DRYING METHOD	CHARACTERISTICS
<b>United States Of America</b>			
Naturals	280,000	Ground trays in sun	Dark and malty
Emulsion treated sultanas	1,000	Emulsion sprayed on vine	Light, golden, soft
Sulphur bleached raisins	28,000	Sulphur bleached and dehydrated	Soft golden.
<b>Mexico</b>			
Naturals	15,000	Ground trays in sun	Dark and malty.
<b>Turkey</b>			
Sultanas	180,000	Emulsion on rack or ground	Soft, golden
<b>Iran</b>			
Sultanas	90,000	Emulsion on ground or roof	Soft, golden
<b>Greece</b>			
Sultanas	35,000	Emulsion on ground	Soft, golden
<b>Afghanistan</b>			
Raisins	40,000	Ground or roof dried in sun	Dark and malty
Sogayashi	5,000	Shade house dried	Soft, green fruit
<b>India</b>			
Sultanas	9,000	Emulsion, ground or racks	Soft green or golden
Sulphur bleached raisins	2,000	Bleached and dehydrated	Soft golden
Raisins	4,000	Ground dried	Dark and malty
<b>SOUTHERN HEMISPHERE</b>			
<b>Australia</b>			
Sultanas	40,000	Emulsion on rack or trellis	Soft, golden.
Naturals	1,000	Dehydrator	Dark and malty
<b>South Africa</b>			
Raisins	20,000	Slab dried in sun	Dark and malty
Sultanas	8,000	Emulsion on rack	Soft, golden
Sulphur bleached	4,000	Bleached and dehydrated	Soft golden
<b>Chile</b>			
Raisins	30,000	Dehydrator dried	Dark and malty
Sulphur bleached	5,000	Bleached and dehydrated	Golden
<b>Argentina</b>			
Raisins	7,000	Dehydrator	Dark and malty
<b>WORLD TOTAL</b>	<b>804,000</b>		

Table 1.1 Major world producers of dried Sultana grapes  
Average tonnage, production methods and final characteristics. Table adapted from the  
Dried Vine Fruit Manual 1998.

Year	Currants '000 tonnes	Raisins '000 tonnes	Sultanas '000 tonnes	Total '000 tonnes
1996	4.4	2.1	48.1	54.6
1997	2.9	1.7	25.3	29.9
1998	2.4	2.5	33.8	38.6
1999	2.0	1.1	23.0	26.1

Table 1.2 Tonnes of dried vine fruit produced annually in Australia 1996-1999.  
Source: ABS 1999.

At present, Australia ranks around sixth place in world terms of overall production of dried grapes (29,500 tonnes in 1997), a substantial decrease in Australia's world standing compared to production levels in previous years. Exports of dried grapes have generally decreased over the last decade with a concomitant rise in imports of dried grapes (Figure 1.1). Fresh grape exports have, however, risen substantially in the same time period. The decreases in dried grape production and exports are due to a complex set of factors; increasing competition from sultana producing countries where labour costs are much lower than Australia, increasingly attractive prices for Sultana grapes sold as table grapes and for wine-making. There are also climatic factors which effect grape yield from season to season.

A large proportion of dried grapes are exported each year, the major destinations being Canada, Germany, the United Kingdom, New Zealand and Japan (ABS 1999). Most of these countries impose strict limits regarding residual pesticides, fumigants and sulphur dioxide on dried fruit. Typically these countries also prefer light-coloured, fleshy sultanas, in contrast to tough-skinned dark sultanas produced elsewhere. These countries are prepared to pay more for high-quality, soft, light-coloured fruit. If Australia is to continue satisfying these buyers it is essential that Australian sultanas be of consistently high quality.

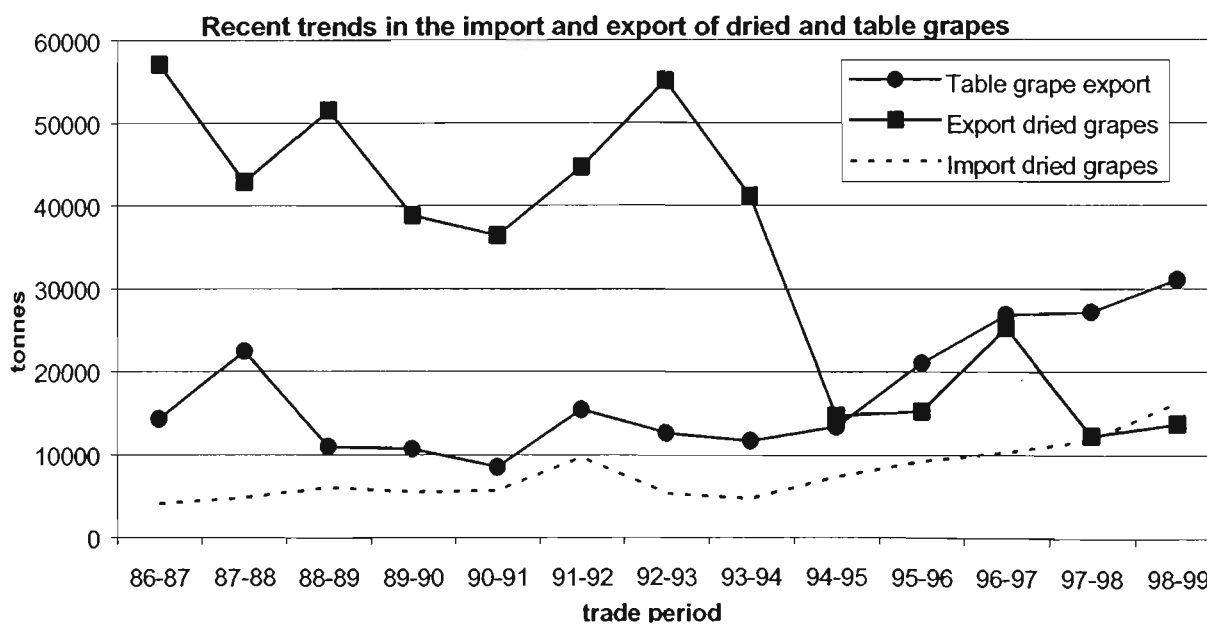


Figure 1.1 Recent trends in the export of dried grapes (almost entirely sultanas) and import of dried grapes. The concomitant increase in export of table grapes (mainly Sultana) is also shown (imports of table grapes during this period was patchy and very low). Adapted from ABS (1999).

### 1.03 Production of sultanas

Climatic conditions limit the successful drying of grapes to between 25° and 40° latitude in both northern and southern hemispheres, with a mean temperature requirement of greater than 23°C for the hottest month (Whiting 1992).

Comparison of meteorological data of major world sultana producing regions shows that the drying conditions in the Murray Valley are less favorable than elsewhere (Whiting 1992). The mean monthly maximum and minimum temperatures in Mildura are lower than in Afghanistan, California and South Africa, our major sultana growing competitors. More significant are the differences in average rainfall during ripening and drying periods. Low average rainfall is encountered both in California and Afghanistan, whereas comparatively high rainfall is common in the Murray Valley. Heavy rainfall, winds and declining temperatures during the drying season can damage fruit on the vines, leading to poor quality dried fruit. Moreover, low temperatures can severely retard the drying of grapes to their optimal storage moisture level (18% moisture or less) leaving fruit susceptible to microbial infestation and undesirable quality changes, such as sticky fruit and darkening or browning of fruit. As a response to the unpredictable drying conditions encountered in the sultana producing regions of Australia, a number of techniques have been employed to accelerate grape drying.

The alkaline cold dip method, first introduced by Greek settlers in the 1920s, has since become the standard practice among Australian sultana producers. Historical records indicate that the dipping of grapes was first practiced in Mesopotamia and in Ancient Greece, where grapes were immersed in a dipping mixture containing olive oil and potash (Whiting 1992). Today in Australia, dipping emulsions are commonly made up from around 2.5% (w/v) of potassium carbonate and around 2% (v/v) of a commercial oil blend in water. Commercial drying oils vary slightly in composition but mainly contain a combination of ethyl and methyl esters of C14, C16 and C18 fatty acids, free fatty acids and emulsifiers. Approximately 80 % of the drying oil is lost during drying with free fatty acids being the principal breakdown product (Australian Dried Fruit Manual-ADFM 1998). The potassium carbonate in the dipping preparation maintains an alkaline pH between 9.5-11.5, which not only accelerates moisture loss in its own right, but also inhibits the growth of moulds and yeasts and keeps the oil homogeneously distributed in solution.

In Australia the commencement of sultana grape harvest for drying is recommended when grapes have reached a sugar level of about 20° Brix. In a typical year this sugar level is reached in the last week of February (ADFM 1998). Harvest of grapes at higher Brix levels, later in the season generally results in darker, lower quality fruit (Uhlig and Clingeffer 1998). Grapes are usually hand-harvested, placed in buckets and transported to drying racks, where they are alkaline dipped

and then spread out on wire mesh racks. Grapes are placed onto the wire mesh about one bunch deep, and spread out to ensure an even distribution of air around grapes, and hence optimum drying rates. The wire racks are covered from rain, thus relying on cross winds and ambient air temperature to promote moisture loss. Some growers spray the grapes after placement in drying racks using a fully mechanised spray application system. Under favourable weather conditions, emulsion-treated grapes require around two weeks to dry down to approximately 16% moisture. If the drying process has been successful, sultanas of a uniformly light golden to light amber colour are produced. In contrast, undipped grapes, which have either been dried on the vine, or dried in direct sunlight without dipping, require about three to five weeks to attain a 16% moisture level. Undipped grapes dry to a dark purple brown colour with a 'malty' flavour, which is quite different to the acid-fruity flavour of light-coloured, dipped sultanas. If low temperature weather conditions and/or excessive rainfall prevail during the harvest and drying period, sultanas require longer drying time, despite having been dipped, and the light golden colour shifts towards a darker brown colour. Protracted drying times also leave fruit more susceptible to general contamination with moulds and insects such as vinegar fly (ADFM 1998).

Once a moisture level of around 16% has been reached, fruit is shaken down from the drying racks, placed on black plastic ground sheets and raked out to an evenly distributed single layer of fruit. Ground sheet temperatures are significantly higher than ambient temperature and can attain average temperatures of 65°C, 55°C and 45°C for the months of March, April and May respectively (ADFM 1998). The fruit is sunfinished until moisture levels are reduced to 13% or less, which may require two or three hot days. Not only is the moisture level of sultanas reduced during the sunfinishing process, but the skins of sultanas become more durable and less susceptible to processing damage (ADFM 1998). Sultanas with a moisture level above 13% incur penalties from fruit packing sheds to cover the cost of dehydrating sultanas using gas fired dehydrators. The penalty is commensurate with the amount of excess moisture. Artificial dryers are generally operated at around 50°C to 60°C and may require up to 24 hours to reduce moisture levels. This technique can be applied on a large scale as a last alternative to salvage sultanas during years with particularly bad drying conditions.

In the late 1960s, a salvage technique was developed by the CSIRO called trellis drying or summer pruning. Many sultana farmers have since adopted this technique of sultana production as a normal production method. Trellis drying methods involve spraying mature grapes on vines with drying emulsions using a specialised tractor with appropriate spraying equipment. The drying emulsion is either applied before or after canes have been cut on the trellis and grapes are left *in situ* on the trellis to dry in the sun. After about 20 days, the grapes dry down to about 16% moisture, and can be collected by an automated harvester. When the grapes have reached this moisture level, bunches can be easily knocked-off the trellis into an appropriate collection

system. After harvesting, sultanas are either spread on the ground and sunfinished or dried down to 13% moisture using a dehydrator. Delays in drying can result in significant browning. Extended periods in gas dehydrators, or temperatures above 60°C can also lead to dark fruit (ADFM 1998). Trellis drying techniques consistently produce high quality fruit, with light-golden colour and good processing characteristics. The development of the 'Shaw swing arm trellis' has further improved the quality of trellis-dried sultanas (Hayes *et al.* 1991). This technique involves use of a trellis system design, which not only facilitates easier harvesting, but also spreads the vine canopy out. Fruiting canes are exposed to maximum sunlight during growth periods, and better canopy air circulation and sun exposure results in faster and more homogeneous vine drying. The resulting quality and colour of fruit produced from this trellising method is consistently high and offers growers other benefits such as reduced labour costs.

When sultanas have been dried down to around 13% moisture, regardless of production method, they are transferred to storage bins for transportation to packing sheds. It is important that sultanas have cooled sufficiently, before boxing. 'Hot boxing' i.e. putting hot sultanas directly from drying sheets into storage bins, can result in high temperatures, especially in the centre of containers, which can persist for up to months. Temperatures in excess of 60°C can damage fruit and cause otherwise light coloured sultanas to rapidly become dark (ADFM 1998). After boxing, sultanas are taken to packing sheds, where the fruit is inspected by trained staff and awarded a crown grade based on a number of quality criteria. Each year prices are set for crown grades with some consideration of seasonal factors, such as years with exceptionally low average yields or very high yield seasons. As listed by the Australian Dried Fruits Association (ADFA), the major criteria considered in determination of crown grade are:

- ?? Colour: base colour and homogeneity of colour
- ?? Maturity: boldness, fleshiness, texture and flavour
- ?? Size: base size of berries and uniformity of size
- ?? Defects: compliance with scheduled defect limits for waste, mould and moisture content.

Defects include excessive moisture, mould and waste, excessive vine stalks and leaves, hot fruit and excessively large sultanas. The crown grade system ranges from seven crown, for highest quality fruit, down to one crown. A brief summary of crown grades is shown in Table 1.3.

After inspection, fruit is labelled according to when and from which farmer it was delivered and valued, based on the crown classification. Fruit is stored in large sheltered warehouses until it is processed and sold to specific buyers depending on their quality demands. Fruit may remain in storage sheds for up to twelve months before it is processed and during this time significant deterioration of colour and overall quality may occur.

CROWN GRADE	COLOUR	TEXTURE	DARK FRUIT CONTENT
Seven Crown	Bold, bright golden colour	Typical texture and flavour	No amber or dark berries
Six Crown	Bold, bright amber colour	Typical texture and flavour	No more than 5% dark sultanas
Five Crown	Be either light amber colour or light brown and homogeneous	Typical texture and flavour	No more than 10% dark sultanas
Four Crown	Be either light amber colour or light brown and homogeneous	Typical texture and flavour	No more than 15% dark sultanas
Three Crown	Be either light amber colour or light brown and homogeneous	Typical texture and flavour	No more than 20% dark sultanas
Two Crown	Be either light brown colour or uniformly dark brown	Typical texture and flavour	No more than 50% dark sultanas
One Crown	Be of reasonable, typical colour, may be slightly green, or dark and heterogeneous	Typical texture and flavour	May be quite heterogeneous in colour

*Table 1.3 Crown grade classification system adapted from ADFA Dried Vine Fruit Manual July 1998*

During late summer and early autumn, high temperatures and humidity often prevail in packing sheds, which promotes both browning reactions and internal and external sugaring in sultanas. Moreover, after processing, fruit colour may deteriorate substantially during transport and shipment, where sultanas may be exposed to high temperatures and humidity. There is a highly differential degree of colour and quality deterioration, which occurs in what ostensibly appear to be similar quality fruit upon receipt and classification. The differential browning propensity of sultanas can be a serious problem for packers, growers and buyers. If fruit is sold on the basis of being light and golden, but in fact arrives at its ultimate destination in a dark brown and degraded condition, consumer confidence is compromised.

One of the major quality factors upon which Australian sultanas are marketed is their softness and lightness of colour. As can be seen in Table 1.1, many countries produce light golden fruit through sulphur drying. Sulphite is an aggressive inhibitor of chemical browning processes in sultanas, however due to negative flavour changes and some health concerns regarding sulphite use in foodstuffs, the Australian sultana industry is committed to alternative means of producing light-coloured sultanas.

#### 1.04 Browning processes in sultanas

Browning processes in sultanas are thought to occur via two distinct processes; enzymatic and non-enzymatic. Enzymatic browning occurs when the grape enzyme polyphenol oxidase (PPO) comes into contact with endogenous grape phenolic compounds located in vacuoles, mainly within grape skins and seeds (Moskowitz and Hrazdina 1981). In the presence of oxygen, the PPO enzyme oxidises grape phenolics to reactive quinones, which can go on to form intense dark pigments via a number of complex secondary reactions. In healthy living-tissue, both the enzyme and colourless non-oxidised phenolic substrates are separately compartmentalised within grape tissue. During drying processes, loss of compartmentalisation of enzyme and substrate are thought to occur, where oxidation, and subsequent browning, can commence (Radler 1964, Grncarevic and Hawker 1971). PPO, like all enzymes, can only function within specific parameters, such as pH, water activity ( $a_w$ ) and temperature. Dipping accelerates drying, inducing a rapid increase in sugar concentration. It is thought that when compartmentalisation is lost at c. 50% moisture content, the sugar concentration has become too high for PPO to be active (Radler 1964, Grncarevic and Hawker 1971). The darker fruit produced in bad years, where rainfall and low temperatures retard drying rates, is assumed to occur because a certain degree of cellular breakdown has already taken place, allowing both enzyme and substrate to come into contact at a sufficiently high  $a_w$  to promote oxidative browning.

Non-enzymatic browning processes are also known as Maillard reactions. These occur when amino acids catalyse the degradation of reducing sugars to form a complex array of colour-forming chromophores and dark-coloured end-products generically referred to as melanoidin. Maillard reactions contrast with PPO browning reactions primarily in their ability to occur in the absence of oxygen. Maillard reactions can occur at low temperatures, but accelerate rapidly with increased temperature: browning rates generally double with an increase of 10°C. Although Maillard reactions are not oxygen dependent, the kinetics of colour formation are generally faster in the presence of oxygen. Like all chemical reactions, Maillard processes are affected by pH, amino acid type and concentration, sugar type and concentration,  $a_w$  and temperature. Maillard reactions not only produce coloured compounds but also bring about flavour changes in food products, producing, in many cases, sweet caramel, malty flavours and aromas. The presence of Maillard reactions has always been suspected in longer-term sultana browning processes especially during storage (Grncarevic and Hawker 1971). Whilst an abundance of literature has focused on PPO and phenolic based browning, reactions in grapes and to a lesser extent sultanas, Maillard processes in sultanas have not been specifically researched or elucidated.

In addition to PPO and Maillard browning processes, a number of other browning mechanisms are known to promote browning in natural products. Oxidation of lipid compounds produces highly reactive intermediates, which may interact with other browning systems to accelerate and intensify browning products. Interaction of Maillard products with phenolic browning intermediates can also enhance browning processes.

### **1.05 General thesis aims**

Australia must be able to produce consistently high-quality sultanas if it is to maintain its export markets. Competition is increasingly strong, due to the high cost of labour in Australia. Having less than optimal weather conditions in the Sunraysia region, local industry must constantly find new innovations to optimise yield and quality. To guarantee the quality of the fruit from the farmer to the buyer is essential if the Australian sultana industry is to remain viable in the long-term.

To predict the long-term colour stability of sultanas is an important part of the overall quality control process. The aims of this research were:

- to generate basic information regarding the nature of browning reactions during long-term storage of sultanas
- to establish whether sultana storage browning is essentially caused by PPO and oxidation of grape phenolic compounds or other processes such as Maillard reactions and lipid oxidation
- to partially address why some sultanas darken faster than others during storage and, if possible, define some measurable parameters for use in prediction of long-term storage colour stability, and
- to develop an objective method for prediction of sultana colour stability.

## 2.0 BROWNING REACTIONS: LITERATURE REVIEW

### 2.01 Enzymatic Browning Processes

Enzymatic browning reactions in fruit and vegetable crops that are estimated to cost up to 20% per annum in lost revenue, due to the activity of endogenous plant enzymes (Vamos-Vigyazo 1981). Enzymatic browning is commonly associated with the oxidation of plant phenols by the oxido-reductase enzymes, peroxidase (POD) and polyphenoloxidase (PPO). The common initial event in enzymatic browning processes involves the rapid oxidation of endogenous plant phenolic compounds to form coloured, reactive quinone intermediates. The further interactions of quinones with each other and other substrates, largely non-enzymatic in nature, lead to the formation of considerably darker pigments over time (Mason and Peterson 1965, Pierpont 1969, Singleton 1987 and Valero *et al.* 1988).

Polyphenoloxidases are categorised into two broad classes: the catechol oxidases (E.C. 1.10.3.1) and the laccases (E.C. 1.10.3.2). Catechol oxidases can catalyse two distinct reactions: the ortho hydroxylation of a monophenol to form an *o*-diphenol, and the oxidation of an *o*-diphenol to form an *o*-quinone. The former reaction is commonly referred to as cresolase activity and the latter as catecholase activity. Cresolase activity is not always present and, if it is, it is generally 10 to 40 times less active than the catecholase activity (Vamos-Vigyazo 1981). Catalysis occurs at a copper prosthetic group, which is essential for activity, and both reactions require molecular oxygen. Cresolase and catecholase reactions are shown in Figure 2.1.

Laccases can be distinguished from catechol oxidases through their ability to oxidise *p*-diphenolic compounds in addition to *o*-diphenolic substrates. A third polyphenoloxidase exists in the form of tyrosinase or monophenol mono-oxygenase, which is basically the same as catechol oxidase except that it only acts on monophenolic substrates.

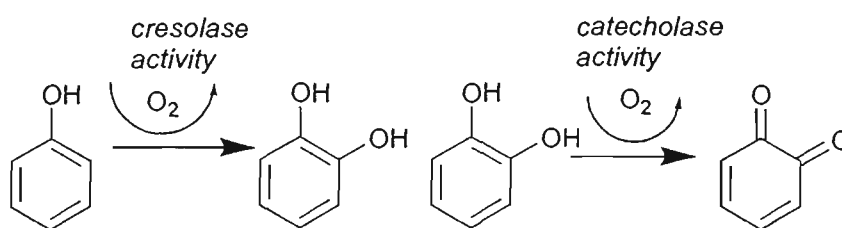


Figure 2.1 True polyphenoloxidases have both cresolase (left) and catecholase activity (right). Both reactions involve the presence of molecular oxygen. Source Vamos-Vigyazo 1981.

PPO is ubiquitous in the plant kingdom and is present in most angiosperm families (Mayer and Harel 1979). PPO is known to be present in different forms in fruits and vegetables and thus displays a considerable degree of polymorphism. The distribution of PPO varies widely depending on maturity (Sapis *et al.* 1983), tissue type and storage conditions (Vamos-Vyazgo 1981). The number and type of PPO forms present is largely dependent on extraction methods. In grapes, multiple forms of PPO have been widely reported (Wolfe 1976, Wisseman and Montgomery 1981 and Sánchez-Ferrer *et al.* 1989). Nakamura *et al.* (1983) purified one homogenous band with PPO activity from Koshu grapes, with a molecular weight of 39 kDa and 41 kDa. Dry and Robinson (1994) purified a single PPO protein band with a molecular weight of 40 kDa. The same authors showed that active PPO enzyme is initially transcribed as a part of a larger precursor protein of 67 kDa. The precursor protein consists of a 10.6 kDa chloroplast transit peptide, a 40.5 kDa active catalytic protein with 2 copper binding regions and a final 16.2 kDa terminal protein sequence. Post-translational processing of the 67 kDa protein is believed to occur in the chloroplast. Okuda *et al.* (1999) isolated and characterised PPO from the Muscat Bailey grape variety with a MW of 40 kDa: the purified PPO had an optimum activity at a pH of 6.3 and temperature of 25°C to 30°C. The PPO contained only *o*-dihydroxyphenol activity and showed no activity toward mono-hydroxy phenols.

## 2.02 Secondary reactions of *o*-quinones

Secondary reactions of *o*-quinones formed through primary oxidation of diphenolic compounds play an important role in the intensity of final browning pigments. Initial quinones formed vary widely in colour, ranging from golden yellow for catechin ( $\lambda_{\text{max}}$  380 nm) and pink for *o*-dihydroxyphenylalanine or DOPA ( $\lambda_{\text{max}}$  480 nm), depending on the structure of the original phenolic and pH (Nicolas *et al.* 1994 and Taylor and Clydesdale 1987). Quinones are very reactive and it is largely through secondary non-enzymatic interactions that intensely brown pigments are formed.

*O*-quinones react with each other or with non-oxidised phenolic substrates (through coupled oxidation reactions) to form dimers. Polymerisation of dimers to form oligomers results in changes in the colour of the products formed. Figure 2.2 shows diagrammatically the nature of coupled oxidation reactions.

The high reactivity of the adjacent carbonyl groups with the *o*-quinone allows facile reaction with other non-phenolic groups, such as ascorbic acid, sulphites and amino acids.

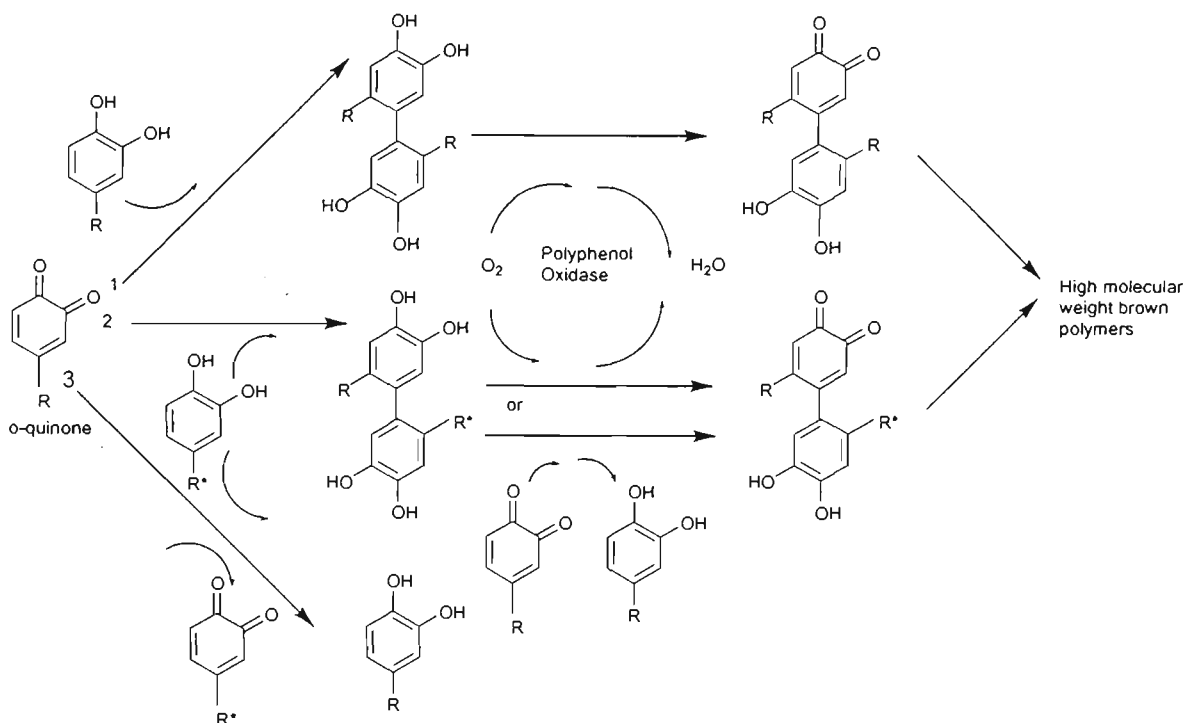


**Figure 2.2** Secondary reactions of ortho-quinones with phenolic compounds. Highly unstable o-quinones react (1) with parent non-oxidised o-diphenolics to produce dimers, or (2) react with other o-diphenols to produce hybrid dimers. Coupled oxidation (3) of a non-enzymatic reduction of o-quinone or further PPO oxidation of dimers leads to dimeric quinones which in turn can react to form larger polymeric pigments. Adapted from Nicolas *et al.* 1994.

Ascorbic acid is commonly used as an anti-browning agent due to its strong reducing potential. Ascorbic acid reacts with o-quinones to generate dehydroascorbic acid (DHA) and regenerates the original diphenol (Täufel and Voigt 1964 and Golan-Goldhirsh and Whitaker 1984), however DHA is a highly reactive intermediate, which can eventually lead to the formation of coloured pigments.

The reaction of o-quinones with sulphites leads to colourless addition-compounds and some regenerated phenol (Haisman 1974). O-quinones also react readily with thiol groups (R-SH), through nucleophilic addition reactions. Cysteine has been widely studied for its ability to form colourless compounds (Molnar-Perl and Friedman 1990 a, b & c, Richard-Forget *et al.* 1991 and 1992), either in free form or bound in peptides or proteins. Cysteine o-diphenolic adducts are not a substrate of PPO and effectively inhibit further enzyme mediated oxidation. The formation of a colourless adduct of *trans*-caftaric acid with the cysteine residue in glutathione in grapes, known as Grape Reaction Product (GRP) or 2-S-glutathionyl caftaric acid has been well described in the literature (Singleton *et al.* 1984, Cheynier *et al.* 1986, Cheynier and Van Hulst 1988 and Cheynier *et al.* 1990). Singleton (1987) hypothesised in his review that sultanas may darken because of an initial failure to form GRP. Nucleophilic addition of various other amino acids to o-quinones can form intensely coloured pigments (Mason and Peterson 1965, Pierpont 1969, Cabanes *et al.* 1987 and Valero *et al.* 1988).

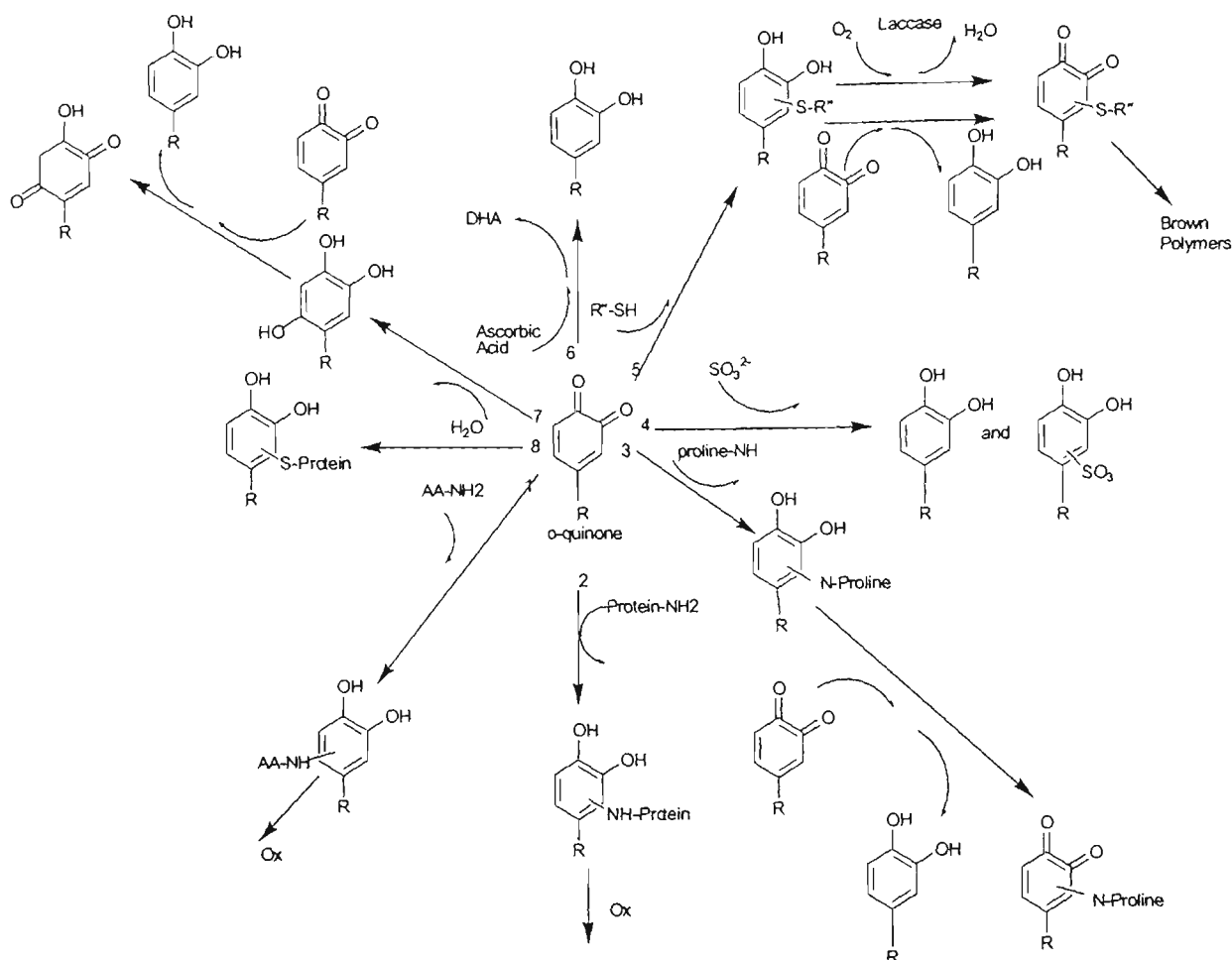


Figure 2.3 Secondary reactions of ortho-quinones with non-phenolic compounds. (1) General reaction with free  $\alpha$ -amino group (2) reaction with amino group on a protein (3) specific reaction with free proline (4) reaction with sulphite (5) reaction with sulphhydryl group and subsequent reaction with laccase (6) reaction with ascorbic acid (7) reaction with water and (8) reaction with sulphur amino acid on protein (adapted from Nicolas *et al.* 1994)

*O*-diphenols also react readily with amino residues in proteins often forming extensive cross-linking. At low pH, a reaction is favoured in which *o*-diquinones become hydrated by a water molecule to form a triphenolic compound, which can be subsequently oxidised to para-quinones by PPO. It has generally been found that wines with relatively high pH (~ 4.0 and above) are much less stable towards phenolic oxidation and hence colour changes than more acidic wines (Singleton 1987 and Fernández-Zurbano *et al.* 1995 and 1998).

The relative stability of various *o*-quinones is highly dependent on the substituents attached to the phenolic compound and other factors such as pH. A summary of the secondary colour reactions of *o*-diphenolics is shown in Figure 2.3. The Peroxidase enzymes (POD E.C. 1.11.1.17) may also play a role in enzymatic browning reactions, however it is generally believed that POD plays only a minor role in browning processes in grapes, with the contribution of PPO being far more significant. Zapata *et al.* (1995) failed to find a correlation between POD levels and browning in white and red grape varieties.

### 2.03 Browning in sultanas

Based on a large body of research, the browning occurring during drying is considered to be mainly due to enzymatic reactions. Radler (1964) showed that the major effect of dipping oils was to increase the rate of drying such that sugar concentrations become high enough to inhibit the PPO enzyme. Radler also demonstrated that the PPO activity of crude sultana extracts was inhibited rapidly with increasing addition of glucose: an experiment was conducted in which grape berries were cut, rinsed with water and dried at 50°C, together with whole grapes. It was observed that the cut grapes dried in about one third of the time as the whole grapes, and that their final colour was yellow-green rather than dark brown. In the same study, a mutant variegated Sultana variety—Bruce's Sport—was examined, which produces grape berries with characteristic white stripes, lacking chlorophyll. This grapevine mutant was observed to produce consistently lighter sultanas than the non-variegated Sultana variety by Antcliff and Webster (1962) and Radler (1964). Later Rathjen and Robinson (1992a) found that the mutant grapes contained only a fraction of the PPO activity of normal Sultana grapes although there were negligible differences in their total phenolic content. Both groups of researchers concluded that the lack of enzyme activity in the mutant was responsible for its low browning potential, rather than lack of phenolic substrate.

The biochemical basis of the low browning grape Bruce's Sport was further elucidated by Rathjen and Robinson (1992a). They confirmed that Bruce's Sport dried to produce lighter sultanas and also found that the mutant had 25% less PPO activity than the other varieties. They examined PPO activity in both white (low-chlorophyll) and green sections of the grape skin tissue and found that although there was not a significant difference in the PPO activity in green sections (compared to other Sultana clones), the white tissue had only about 19% of the PPO activity. The total phenolic content of both the mutant and normal grapes was comparable, supporting the conclusions of Radler (1964), i.e. that intensity of browning during drying was more a function of PPO activity rather than the phenolic substrate content. Rathjen and Robinson (1992a) also showed that by staining hand-sections of sultana grapes with exogenous phenolic substrate (4-methylcatechol), most of the browning observed was restricted to green areas of grape skin. In a further study, Rathjen and Robinson (1992b) demonstrated that the low-chlorophyll, white-coloured areas of the variegated mutant contained low PPO activity. The low activity was due to aberrant post-translational processing of the 60-kD PPO precursor-protein. Protease treatment of the 60-kD protein was demonstrated to cleave the protein to produce a 40-kD protein, which had an identical amino-terminal sequence to that of functional PPO. The 40-kD protein obtained after trypsin treatment of the 60-kD precursor failed, however, to display PPO activity when treated with exogenous phenolic substrate. Two reasons were given for the lack of PPO activity in the 40-kD protein. It was suggested that the protein might not have contained

copper atom in the prosthetic site, or that the position of trypsin cleavage of the protein precursor may not have occurred at a position leading to active PPO. The findings of these researchers has opened the possibility of using genetic manipulation (anti-sense m-RNA techniques) to effectively silence the expression of PPO protein and hence create a Sultana grape with an inherently low PPO browning potential.

#### 2.04 Phenolic compounds

Several thousand phenolic compounds have been identified in plants, fruits and vegetables; their significance in the physiology of plants and human nutrition is extremely broad. Plant phenolics are ubiquitous secondary metabolites with wide-ranging effects. Amongst the many physiological functions ascribed to phenolics is their role as plant cell signal transducers and growth molecules, allelopathic compounds, defence and their protection functions both against invading pathogenic microorganisms and UV-frequency solar radiation. Grape and wine phenolics are also important in their role as powerful natural antioxidants (Kanner *et al.* 1994), their *in vivo* protective effect against lipid peroxidation and platelet aggregation (Bagchi *et al.* 1998, Xia *et al.* 1998 and Satue-Gracia *et al.* 1999) and as flavour compounds and browning substrates. Rates of synthesis of phenolic compounds are affected by a number of environmental stresses such as mineral nutrient deficiency, soil carbon-nitrogen nutritional balance, plant hormonal changes, invasion of plant tissues by pathogen, physical damage, seasonality and plant age. Low soil fertility, drought stress, salinity and application of exogenous hormones can also affect phenolic biosynthesis (Di Cosmo and Towers 1984, Gershenzon 1984 and Balsberg and Phalsson 1989). In grapes, certain phenolic metabolites such as resveratrol,  $\epsilon$ -viniferin,  $\alpha$ -viniferin, stilbene and pterostilbene have been shown to assist in grapevine defence against pathogens such as the grape fungus *Botrytis cinerea* and UV radiation (Langcake 1981 and Liswidowati *et al.* 1991). In addition, many grape phenolics exert positive effects on human health (Soleas *et al.* 1997). Multi-gene families (Sparvoli *et al.* 1994) code most of the genes responsible for phenolic synthesis.

#### 2.05 Grape phenolics

In ripe *Vitis vinifera* berries, five major classes of phenolic compounds have been identified: phenolic acids, anthocyanins, flavanols, flavan-3-ols and tannins, and flavanonols (Macheix *et al.* 1990). Grapes are unique in that they do not contain quinic esters of cinnamic acids (chlorogenic acid), which are abundant in most other fruits. Instead, hydroxycinnamic acid is present as tartaric acid ester derivatives rather than glucose esters (Singleton *et al.* 1978 and Romeyer *et al.* 1983). Anthocyanins are only present in red grape varieties. Flavan-3-ols, especially (-) epicatechin-3-*o*-gallate have been identified in both white and red cultivars (Singleton and Trousdale 1983). The last major class of phenolics is the condensed tannins (proanthocyanidins) which are present in both white and red cultivars—predominantly as the dimers B-1 and B-2. The distribution of grape

phenolics varies widely according to cultivar, and the various phenolics are distributed unevenly within the grape itself. The bulk of grape phenolics is present in grape skins and seed traces. Tartaric acid esters of hydroxycinnamic acids are higher in grape skins than pulp. Catechins are mainly present in grape seeds and skins, with only a small amount present in the pulp and the remainder in the stalks. Most investigators have found (+) catechin to be more abundant than (-) epicatechin, however in some varieties the reverse has been observed (Lee and Jaworski 1989).

In white grape varieties the hydroxycinnamates are by far the most concentrated phenolic compounds, present as: *monocaffeoyl tartaric acid* (caftaric acid), *mono-p-coumaroyl tartaric acid* (coutaric acid) and *monoferuloyl tartaric acid* (fertaric acid). Ong and Nagel (1978a) surveyed the concentration of hydroxycinnamates in a number of red and white grape cultivars and found that caftaric acid was present at highest concentration (average white grapes  $107 \text{ mg.L}^{-1}$  -average red grapes  $170 \text{ mg.L}^{-1}$ ), followed by coutaric ( $16.3 \text{ mg.L}^{-1}$  and  $25 \text{ mg.L}^{-1}$ ) and fertaric ( $6.1 \text{ mg.L}^{-1}$  and  $6.3 \text{ mg.L}^{-1}$ ). In Sultana grapes caftaric acid is the main phenolic substrate in terms of concentration and PPO oxidation (Singleton 1987). Approximately 10% of the phenolic content is made up of flavonoids such as catechins and soluble tannins. The chemical structures of important phenolics in Sultana grapes are shown in Figure 2.4.

Both caftaric and coutaric acids exist in *trans* and *cis* conformation, however it has been shown that at least for caftaric acid, the *trans* isomer is by far the more dominant in both white and red grape cultivars (Macheix *et al.* 1991). The specific role of *trans*-caftaric acid in enzymatic browning is however ambiguous. *Trans*-caftaric acid has the highest oxidation potential of all grape phenolics and thus is always the first phenolic to undergo oxidation in wine musts (Cheynier *et al.* 1988 and Cheynier and Moutounet 1992). Despite its facile oxidation, researchers have failed to find a strong correlation between absolute levels of *trans*-caftaric acid and degree of browning in grape juice and wines (Romeyer *et al.* 1985); this was confirmed more recently by Fernández-Zurbano *et al.* (1998). Both authors found a much stronger correlation of browning with less concentrated phenolic substrates such as the flavanol phenolics, catechin and epicatechin, all of which have a much lower affinity for grape PPO compared to caftaric acid (Singleton 1987) and are thus slowly oxidised by PPO. Cheynier *et al.* (1988) and Cheynier and Van Hulst (1988) demonstrated that these low concentration compounds are easily oxidised in binary model systems through coupled reactions with quinones formed through the initial oxidation of caftaric acid.

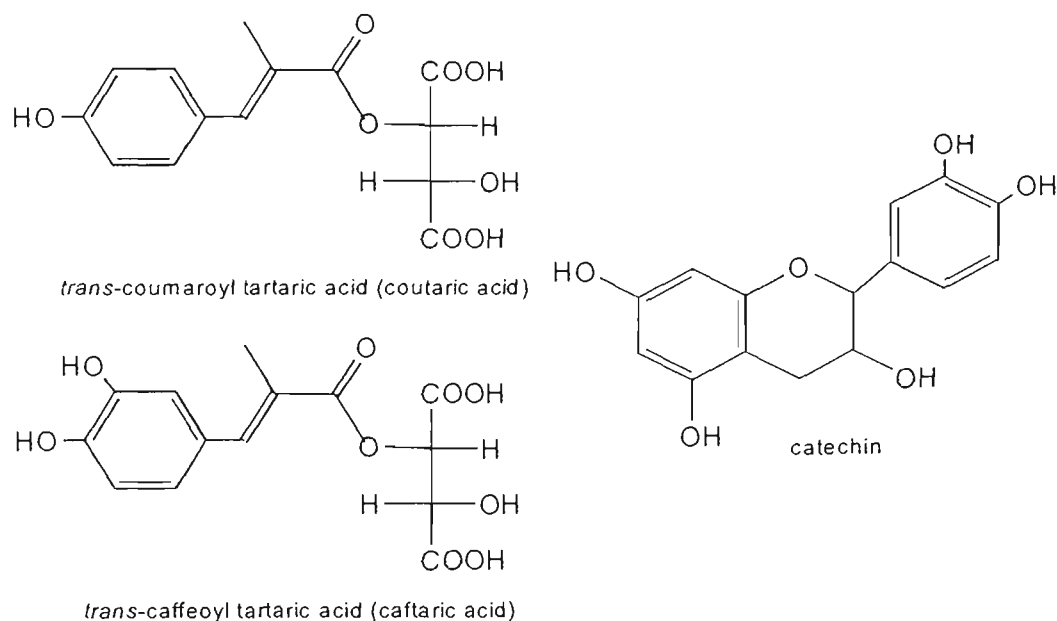


Figure 2.4 Structures of the main phenolic compounds in Sultana grapes  
Source: Machiex *et al.* 1991.

Thus it is generally assumed that oxidation of caftaric acid must always take place before coupled oxidation of other phenolic substrates can occur. Caftaric acid has been shown to react easily with glutathione to form Grape Reaction Product (GRP) 2-*S*-glutathionyl *trans*-caffeoyl-tartaric acid. GRP is colourless and not a direct substrate of PPO, and has been implicated as an important mechanism in minimising browning in grape musts (Singleton *et al.* 1984, 1985). Whilst GRP may be important in wine, it has not been detected in sultanas (Singleton *et al.* 1985).

## 2.06 Synthesis of phenolic substrates

Phenolic compounds in grapes are synthesised via the phenylpropanoid metabolic pathway where L-phenylalanine is converted to 4-coumaroyl-coenzyme A or via the conversion of acetyl Co-A to malonyl-CoA (Hahlbrock and Scheel 1989). Phenylalanine ammonia lyase (PAL; EC 4.3.1.5) is the enzyme which diverts phenylalanine from protein-synthetic processes by removing ammonia from phenylalanine to produce *trans*-cinnamic acid and ammonium, the former being the initial substrate for the phenylpropanoid pathway, and the synthesis of further phenolic compounds. PAL is mainly located in grape epidermal tissue: it peaks during the early stages of berry development and rapidly drops off after veraison in white grape varieties (Kataoka *et al.* 1983, Hrazdina *et al.* 1984 and Roubelakis-Angelakis and Kliever 1985 and 1986). Sparvoli *et al.* (1994) found that PAL and stilbene synthase genes were expressed at the same rate in darkness and light, however expression of other phenolic-synthesis genes were dramatically increased by UV light exposure. Other researchers, however, found that levels of irradiation rapidly stimulated transcription of PAL genes, accumulation of PAL mRNA and enzyme activity in bean cells (Edwards *et al.* 1985). Ishizuka *et al.* (1991) demonstrated that PAL specific m-RNA was rapidly induced in wounded potato tubers. Other researchers have demonstrated that induction of PAL

transcripts and that the activity of the enzyme itself are strongly regulated by *trans*-cinnamic acid, the initial product of PAL activity (Mavandad *et al.* 1990).

A number of researchers have examined the effects of field conditions on synthesis of grape phenolics. Kliewer (1977) found that the synthesis of anthocyanins in pigmented Emperor grapes was not inhibited by UV light but rather higher temperatures (day temperatures of 37°C and night temperatures of 32°C). High temperature grapes failed to colour significantly, whereas grapes at field temperatures and low temperature hot house grapes coloured normally. Kliewer and Torres (1972) observed that day temperatures above 35°C completely inhibited development of anthocyanins in Tokay grapes and greatly reduced synthesis of anthocyanins in Cardinal and Pinot Noir grapes, regardless of night temperatures. UV light can have a variable effect on anthocyanin formation. Crippen and Morrison (1986) found that there was no significant difference in soluble phenols, or anthocyanins at harvest between shaded and exposed *Cabernet Sauvignon* grapes. Small differences in percent-polymerised soluble phenols were observed, however, in grapes with different sun exposure.

## 2.07 Grape surface lipids and action of dipping oils

Grape skins naturally possess a complex lipid matrix, which provides an effective barrier to water loss from grape berries. The non-living, non-cellular cuticle is made up of a number of non-discrete layers, which have distinct lipophilic and hydrophilic regions. The cuticular membrane is bound to the cellulosic wall by pectic substances (Chambers and Possingham 1963). The epicuticular wax consists of a 3 µm layer of partially overlapping wax platelets, which, due to both their spatial arrangement and chemical properties, impart high hydrophobicity of the surface waxes (Grncarevic and Radler 1971). Despite the relatively facile transfer of water from the inside of the grape into the cuticular membrane, the high hydrophobicity of the normal surface waxes prevents droplets of water forming in the capillary spaces, thus efficiently retarding water vapour escaping from grape surfaces (Chambers and Possingham 1963). The application of free fatty acids and fatty acid esters in dipping oils brings about a conformational change in platelet primary structure and an increase in the hydrophilic groups of the waxes. This lowers the surface tension and creates a hydrophilic capillary effect within the wax-layers, which pulls water from inside the grape to the skin surface where it evaporates (Chambers and Possingham 1963). The application of potassium alone to grape berry surfaces has been shown to increase rates of evaporation (Grncarevic 1963), through saponification of free fatty acids on grape surfaces; it is the synergistic effect of both oil fatty acid esters and potassium cations which promotes accelerated grape water loss.

## 2.08 Maillard non-enzymatic browning reactions

Non-enzymatic browning is often referred to with the blanket term 'Maillard reactions'. Since the discovery by Maillard in 1912 that sugar degradation and sugar browning were accelerated in the presence of amino acids, the terminology has become entrenched. Since Maillard, many subtleties of sugar degradation processes have been elucidated and much still remains poorly understood. Maillard reactions are responsible for many of the positive flavour and aroma characteristics of foods and both negatively and positively perceived colour changes. Maillard reactions can also decrease the nutritional value of foods by reducing available amino acids, especially essential amino acids such as lysine (Ledl and Schleicher 1990). Maillard reactions can cause many of the health complications due to high blood glucose gradients in diabetics (Lederer and Buhler 1999). Maillard reactions are also fundamental to the ageing process and formation of advanced glycosylation end products (Monnier and Cerami 1981, Monnier *et al.* 1984, Kohn *et al.* 1984 and Chen and Cerami 1993). Formation of reactive radical intermediates in Maillard processes have been characterised by a number of authors (Hofmann *et al.* 1999a and 1999b). Particular Maillard reactions between creatinine and glucose in meat have been shown to produce powerful heterocyclic amines, mutagens and carcinogens (Jägerstad *et al.* 1991 and Felton *et al.* 1992). Maillard reaction products (MRPs) have been shown to exert strong anti-oxidative effects in food systems especially as natural inhibitors of lipid oxidation. (Elizalde *et al.* 1991, Aliaz and Barragan 1995, Aliaz *et al.* 1995, Nienaber and Eichner 1995, Aliaz *et al.* 1996, Bressa *et al.* 1996 and Jayathilakan *et al.* 1997). Recent work has indicated the widespread inhibitory effects of MRPs on many enzymes. Glycine-glucose crude MRP extracts have been shown to inhibit trypsin and chymotrypsin (Pittoti *et al.* 1993 and Hirano *et al.* 1996), and apple PPO was inhibited and activated by various MRPs (Tan and Harris 1995) as well as POD (Nicoli *et al.* 1991). MRPs are known to react with a wide variety of endogenous substrates, such as lipids, phenolic compounds and proteins. Interest in Maillard reactions in the context of food quality comes from mainly three areas: their antioxidant behaviour, their role in colour formation, and their contribution to flavour and aroma in heat-processed foods.

## 2.09 Maillard reaction mechanisms

Maillard reactions generally share similar initial reaction pathways, which have been widely examined in the literature (Hodge 1953 and Ledl and Schleicher 1990). Beyond initial reactions, Maillard chemistry becomes increasingly complex; many of these reactions are only superficially understood. Maillard reaction kinetics and reactions are sensitive to many chemical and physical factors (Namiki 1988). Factors include: source of  $\alpha$ -amino acid (Birch *et al.* 1984), carbonyl moiety (sugar, aldehyde, fatty acid), concentration, pH, temperature, time, water activity ( $a_w$ ), UV light, the presence of metal ions (Cheng and Kawakishi 1994, Hayase *et al.* 1996 and O'Brien and Morrissey 1997), the presence and absence of molecular oxygen and external pressure (Tamoaka *et al.* 1991). In the literature, most studies of Maillard reactions consider high temperature

(>100°C) processes. It is, however, becoming increasingly clear that Maillard reactions also occur at lower temperatures: at 30°C in orange juice concentrates (Del Castillo *et al.* 1999), 37°C in sweet fortified wines (Cutzach *et al.* 1999), in sun-dried raisins (Karadeniz *et al.* 2000). Maillard reactions have been shown to occur during refrigeration (Whitfield 1992) and at sub-zero temperatures (-15°C) in Thompson Seedless grapes (Karadeniz *et al.* 2000).

Many of the principal interactions in Maillard processes were outlined by Hodge (1953) in his landmark review. Amines can react in Maillard reactions as either acids or bases in the initial stages of the reaction. The initial step involves an amine functionality—amino acid, ammonia, protein—behaving as a nucleophile which interacts with a carbonyl moiety typically on a reducing sugar, such as glucose (an aldose sugar) to form an imine (Schiff base) and eliminating a water molecule. The imine base cyclises and forms an *N*-substituted aldosylamine, which isomerises to form a stable 1-amino-1-deoxy-2-ketose intermediate, better known as an ‘Amadori product’ (AP). APs are colourless intermediates. Similar interactions of an amine group with a ketose sugar (fructose) leads to the formation of a ketosylamine, which undergoes Heyn’s rearrangement to form the ketose Amadori analogue, 2-amino-2-deoxyaldose: ‘Heyn’s product’. The general structures of the Amadori and Heyn’s product are shown in Figure 2.5.

Amino acids can also behave as acids and bases, catalysing the transformation of aldoses and ketoses into reactive  $\alpha$ -dicarbonyl compounds without the formation of aminoketoses or aminoaldose, via the ‘Lobry de Bruyn-Alberda van Eckenstein rearrangement’ (Hayashi and Namiki 1986). These reactive  $\alpha$ -dicarbonyl compounds are formed at pH conditions (4-7) encountered in biological systems, and can react with other Maillard intermediates to form flavour and coloured compounds. The amino acid catalysis of sugars to form  $\alpha$ -dicarbonyl compounds is significant, because their formation in sugar systems in the absence of amino catalysts would require extremes of pH (pH >9 or < 3) or extreme temperatures i.e. above 130°C such as those required for caramelisation reactions.

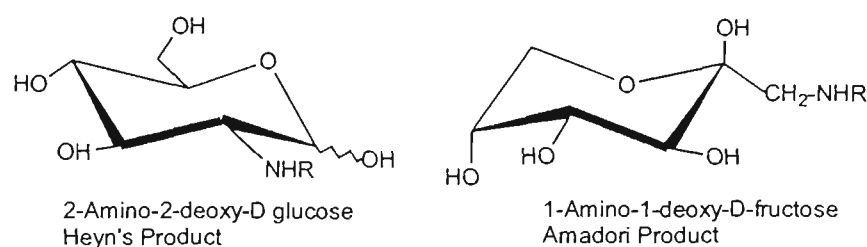


Figure 2.5 Structures of the initial Maillard colourless intermediates  
Left, Heyn's Product and right Amadori Product.  
Source: Yaylayan and Huyghues-Despointes 1994.

APs are strongly affected by pH. Under alkaline conditions APs and the Schiff base intermediate can rapidly undergo chain fragmentation (2,3 enolisation) to form 2 and 3 carbon fragments, which react to form high-molecular-weight melanoidins. Under acidic pH conditions APs undergo 1,2 enolisation, eliminating the original amine to generate a 3-deoxy-2-hexulose (3-deoxysone). APs can also behave as nucleophiles and react with a second sugar molecule to form a diglycated compound, or react with a second amino acid (Figure 2.6). Reactive dicarbonyl compounds formed in Maillard reactions can form heterocyclic compounds with other amino bearing fragments or other carbonyl fragments (Weenen 1998). 3 deoxy-2-hexuloses (3-deoxyglucosones) produced through 1,2 enolisation of APs react slowly to form 5-hydroxymethylfurfural (5-HMF), furfural and 5-methylfurfural. 5-HMF is the furfural analogue formed from glucose. Labelling experiments indicate that 5-HMF is formed through direct dehydration of 3-deoxy-2-hexuloses and formation of the furylium ion (Ledl and Schleicher 1990).

In the presence of air and trace amounts of transition metals, APs can undergo autoxidation to produce  $\alpha$ -dicarbonyl compounds, which can undergo different reactions to form  $\beta$ -elimination products (Yaylayan and Huyghues-Despointes 1994). Strecker degradations involve the nucleophilic addition of  $\alpha$ -dicarbonyl intermediates with unreacted amino acids, catalysing decarboxylation to produce reactive aldehydes and ammonia. Condensation of these compounds result in diverse nitrogen containing heterocycles such as pyridine, pyrazine, imidazole and their derivatives. A general reaction scheme for Strecker degradation is shown in Figure 2.7.

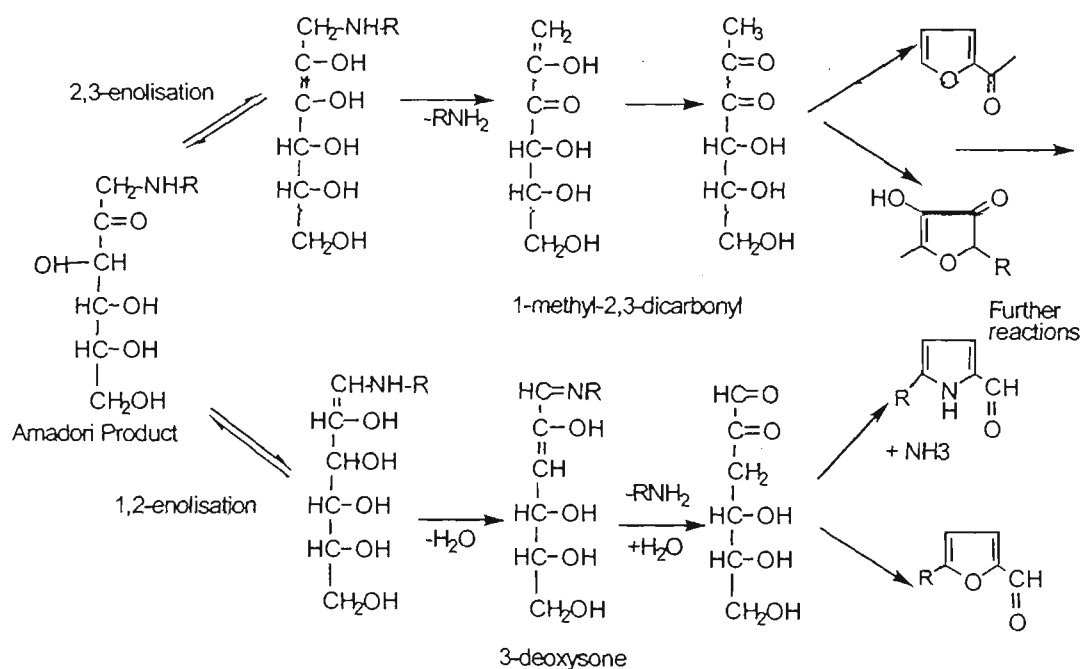


Figure 2.6 General scheme showing the generation of dicarbonyl intermediates through the degradation of APs (adapted from Ledl and Schleicher 1990)

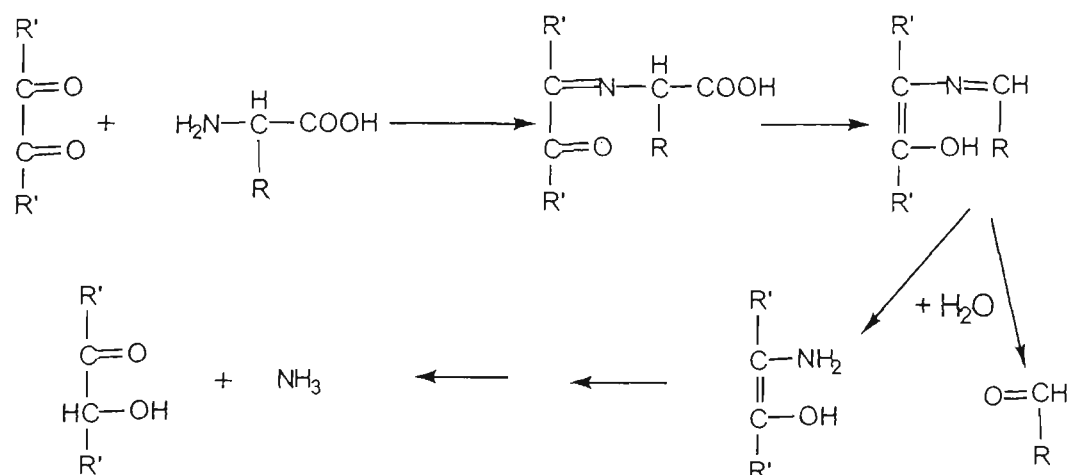


Figure 2.7 General scheme of Strecker decarboxylation of amino acids by  $\alpha$ -dicarbonyl compound. Adapted from Ledl and Schleicher 1990.

## 2.10 Evidence of Maillard reactions in sultanas and grape products

The temperature dependence of *storage* browning in sultanas has been confirmed in long-term trials by Bolin (1980), Mc Bride *et al.* (1984) and Cañellas *et al.* (1993), who observed that significant storage colour change occurred, but only above 20°C. Simal *et al.* (1996) observed no statistically significant differences between holding dried Seedless Flame grapes at 14°C and 21°C, however large differences in colour and texture in dried grapes stored at 28°C and 35°C were observed. Aguilera *et al.* (1987) found that both enzymatic and non-enzymatic browning kinetics were maximal at  $a_w$  0.8, however the mechanism of non-enzymatic browning was not elucidated.

The existence of Maillard reactions in grapes, grape products and sultanas is also evinced from a number of sources; furfural, 5-HMF and other typical Maillard intermediates have been found in sweet aged fortified wines (Cutzach *et al.* 1999 and Ho *et al.* 1999). Investigations by Spanos and Wrolstad (1990) found high levels of 5-HMF (up to 33 mg.L<sup>-1</sup>) in concentrated juice from Sultana grapes after nine months storage at 25°C supporting the presence of Maillard reactions at low temperature in grape systems. Bozkurt *et al.* (1999) modelled non-enzymatic browning in grapes and found extensive browning and 5-HMF after 10 days at 55°C and at pH 4. In a recent paper, Karadeniz *et al.* (2000) measured large concentrations of 5-HMF and also losses of amino acids—tyrosine and tryptophan—in sultanas via HPLC detection at 280 nm. Whilst there is clear evidence of Maillard reactions occurring in sultanas, there has been no concrete evidence that Maillard reactions actually lead to *coloured* compounds i.e. 5-HMF and other intermediates are colourless.

## 2.11 Maillard coloured compounds and melanoidin

As Ledl and Schleicher (1990) outlined in their review article, very few Maillard chromophores have been well characterised, and moreover, no coloured compounds have been isolated from natural products or food systems. The high reactivity of MRPs, their facile interaction with each other and protein residues to form high-molecular-weight coloured products, present difficulties for isolation and characterisation of specific chromophores. The condensation product of 5-HMF and pyranone has been shown to produce yellow compounds (Ledl and Severin 1978). Condensation products of furfural in the presence of primary amino acids yielded red-coloured heterocyclic 4-ring systems and an intense red-brown coloured compound was formed through reaction of furan-2-carboxaldehyde and L-alanine (Ledl and Schleicher 1990). Pyrroles and condensation products containing these molecules have also been shown to produce coloured compounds (Hofmann 1998a and 1998c and Zamora *et al.* 2000). Furthermore, intense coloured chromophores have been shown to form through the interaction of some low molecular weight Maillard intermediates such as methyl-hydroxyfuranones and pyrrolinones with metal ions, (Ledl and Schleicher 1990).

Characterisation of the chemical nature of melanoidins has been limited to basic information, such as MW, and  $^{13}\text{C}$ ,  $^{15}\text{N}$  NMR profiles. Exclusion chromatography studies have isolated compounds with MWs of around 7 KD and greater (Ledl and Schleicher 1990). NMR studies have strongly supported the existence of pyrrole- and indole-type nitrogens within Melanoidin structure (Benzig-Purdie and Ratcliffe 1986 and Zamora *et al.* 2000). Tressl *et al.* (1998) verified the high polymerisation potential of N-substituted pyrroles, 2-furaldehyde and N-substituted formyl-pyrroles—typical hexose Maillard intermediates—to form repetitive polymeric structures with more than 30 monomer units and intense brown to black colour.

Furan derivatives are commonly formed from monosaccharides such as the hexose sugars D-glucose or D-fructose or pentose sugars such as D-xylose. The basic furanoid structure derives its origin from the sugar backbone and the type of ring substitution is more dependent on the amine-bearing fragment and interactions with other reactive substrates within the food chemical matrix. At high pH furan derivatives generally produce sweet, spicy, burnt and caramel aromas, consistent with the type of sensory compounds expected in dried fruit. Some common furan derivatives isolated from model systems include furfural, 5-methyl furfural, furfuryl alcohol, and 5- and 2-hydroxymethyl furfural. A number of di- and tetra-hydrofuran and furanone compounds are also important in Maillard systems, which are thought to arise from Amadori degradation reactions. A number of typical furan-derived molecules, which have been identified in Maillard model systems and food systems, are shown in Figure 2.8.

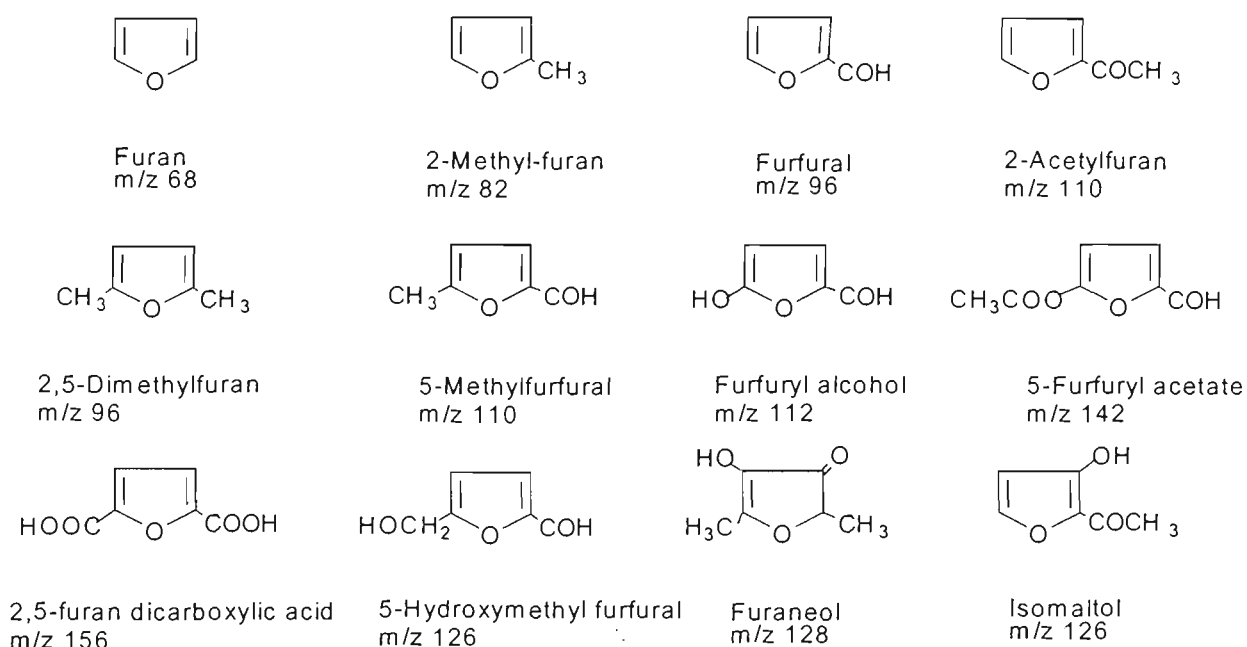


Figure 2.8 Common furanoid Maillard reaction intermediates. Isolated from model and natural systems with corresponding m/z values for M<sup>+</sup> ion. Source: Vernin and Vernin, 1982, and Vernin and Párkányi 1982.

Pyrazines are mainly formed via the Strecker degradation pathway, where an  $\alpha$ -dicarbonyl compound generated through sugar degradation reacts with an amino acid and forms a Strecker aldehyde and an  $\alpha$ -amino carbonyl intermediate. Condensation of  $\alpha$ -amino carbonyls and subsequent oxidation produce characteristic pyrazine derivatives (Shu and Lawrence 1994). Pyrazines are typically present in Maillard browning products and are important flavour components. Numerous pyrazines are produced in the reaction of D-glucose and ammonia, and pyrazine formation occurs readily in the absence of oxygen although the exact mechanism of formation has not been elucidated (Shibamoto and Bernhard 1976 and Shibamoto *et al.* 1979). Various methyl pyrazines are commonly found in Maillard model systems (Shibamoto and Bernhard 1976 and Vernin and Párkányi 1982).

Pyrroles are found widely in processed foods such as roasted coffee and, although not generally considered to be important flavour precursors, they play an important role in colour development reactions (Vernin and Párkányi 1982). Commonly encountered pyrroles isolated from amino acid-D-glucose systems include 2-acetylpyrrole, 5-methylpyrrole-2-carboxaldehyde and 5-hydroxymethylpyrrole-2-carboxaldehyde (Figure 2.9). Furfural and its derivatives can react with amino acids, through the Strecker degradation pathways, to form pyrroles, further increasing the array of structural variation.

Imidazoles and their derivatives are highly soluble in aqueous phase, and are rarely identified in non-aqueous organic solvent extractions from Maillard model system (Ledl and Schleicher 1990 and Vernin and Párkányi 1982). However, imidazole, various methyl-imidazoles and hydroxymethyl-imidazoles have been isolated from browning systems. Other browning heterocycles such as oxazoles and pyridine have been isolated from browning systems, but these components are generally present only at trace concentration. The chemical structures of common nitrogen containing Maillard heterocycles—pyrroles, imidazoles, pyrazoles and pyrazines—are shown in Figure 2.10, together with their molecular weight or the mass/charge ratio ( $m/z$ ) of the parent ion in mass spectrometry.

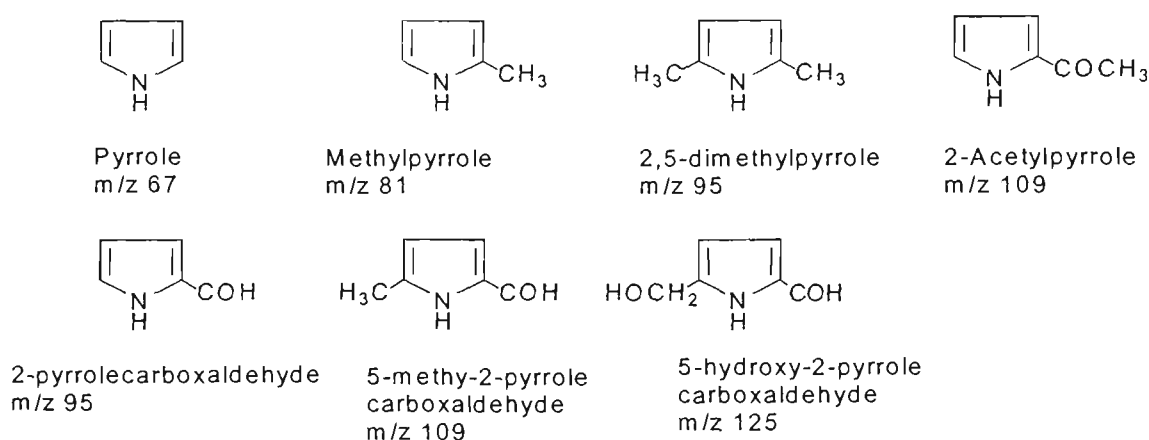


Figure 2.9 Typical pyrrole-derived Maillard heterocycles isolated from model and food systems. Source: Vernin and Vernin (1982) and Vernin and Párkányi (1982).

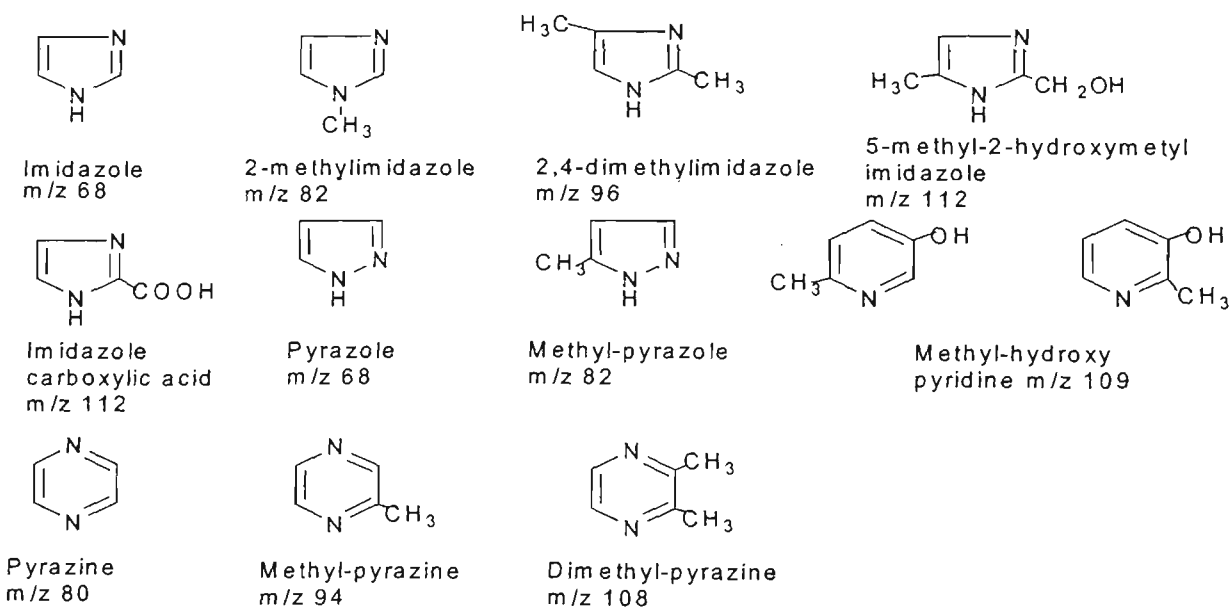
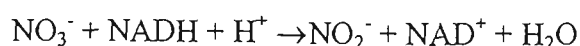


Figure 2.10 Some common two-nitrogen heterocycles formed in Maillard reactions.  $m/z$  values for  $M^+$  mass spectral fragments. Source: Vernin and Vernin (1982) and Vernin and Párkányi (1982).

## 2.12 Nitrogenous compounds in grapes and sultanas

The presence of amino nitrogen or ammonia is essential for Maillard processes. Free-amino acids may also play a role in sultana browning through interaction with quinone intermediates to form dark-coloured compounds. The grapevine assimilates nitrogen from nitrate and ammonium in the soil. Nitrate absorbed by vine roots is reduced to nitrite and ammonium ions and is either converted to amino acids or transported to aerial parts of the grapevine. Berry nitrate concentration is maximal at veraison with maximum nitrate levels of around 1.6 mM, with highest levels found in grape skins (Schaller *et al.* 1985). Depending on the cultivar, the free-amino acid fraction of total nitrogen in grapes can account for 50 to 90 % of total nitrogen. Across red and white grape cultivars, eight major amino acids—arginine, proline, alanine,  $\gamma$ -amino butyric acid, glutamic acid, aspartic acid, serine, and threonine—make up 50 to 95 % of total amino nitrogen. In sultanas it was found that arginine, proline and glutamic acid made up the bulk of amino nitrogen with concentrations of 7.4 mg.g<sup>-1</sup>, 4.0 mg.g<sup>-1</sup> and 2.5 mg.g<sup>-1</sup> respectively (Bolin and Petrucci 1985). Total nitrogen in ripening grapes was found to correlate with soil nitrogen (Kanellis and Roubelakis-Angelakis 1993). As amino acid synthesis increases during berry ripening, concentrations of ammonia decrease. Kliewer (1968) found that total free-amino acids in grape juice increased two- to five-fold during the last six to eight weeks of berry ripening, ranging from two to eight g.L<sup>-1</sup>. Concentrations of proline and arginine can differ from two- to six-fold between early- and late-harvested grapes of the same cultivar (Kanellis and Roubelakis-Angelakis 1993). Hernandez-Orte *et al.* (1999) determined the concentration of free-amino acids for *Tempranillo*, *Riesling*, *Cabernet Sauvignon* and *Moristel* grapes at harvest over a period of three consecutive years, and found that arginine, proline, histidine and glutamine were the most prominent amino acids in that order for all four varieties. The four major amino acids accounted for 62% to 88% of the total free-amino acids. Stines *et al.* (2000) surveyed white and red grape varieties in Australia, and found that arginine and proline were always the most abundant free-amino acids. Synthesis of proline appears to be temperature sensitive, with proline levels being generally higher in warmer years (Flanzy and Poux 1965).

Virtually all plants, fungi and bacteria have the ability to reduce soil nitrate to ammonia. The first step of nitrogen accumulation involves the reduction of nitrate (NO<sub>3</sub><sup>-</sup>) to nitrite (NO<sub>2</sub><sup>-</sup>) by the complex enzyme *nitrate reductase*, requiring bound FAD (flavin adenine dinucleotide), molybdenum and cytochrome 557 as cofactors and NADH as an electron donor. Nitrate reductase carries out the following reaction:



Nitrite is subsequently reduced to ammonia in three steps by the enzyme *nitrite reductase*, with ferredoxin used as an electron donor in each step. Incorporation of ammonium ions into amino acids is due to the activities of glutamine synthetase (GS), glutamate synthase (GOGAT) and glutamate hydrogenase (GDH) (Hall *et al.* 1984). The enzymes responsible for mediating arginine synthesis—ornithine transcarbamoylase (OTC), arginosuccinate synthetase and arginosuccinate lyase and arginase—have been extensively examined by Roubelakis and Kliewer (1978 a, b & c). OTC and arginase activities were found to be higher at veraison (Roubelakis and Kliewer 1981).

The ligation of ammonia into a molecule of L-glutamate is catalysed by the enzyme glutamate synthetase, shown in the reaction:



GS is present in large amounts in all plant tissue and has a very high affinity for ammonia generally preventing any appreciable accumulation of ammonia which is toxic (Lea *et al.* 1985).

The molecule of ammonia which is added to the amide group of L-glutamate is then transferred to the 2-amino position of  $\alpha$ -ketoglutarate via the action of *glutamate synthase* (Gsyn), to produce two molecules of L-glutamate:



One molecule continuously recycles, whilst the other can be transaminated to other amino acids or used directly for proline and arginine synthesis. The activities of glutamate synthase and glutamate synthetase form the glutamate synthase cycle. Ornithine, arginine and proline are the major amino acids synthesised from glutamate (Lea *et al.* 1985).

### 2.13 Biosynthesis of proline

Glutamate is first acetylated by acetyl coenzyme A and reduced to *N*-acetyl glutamate. The  $\gamma$ -carboxyl group on this molecule is then reduced to glutamic  $\gamma$ -semialdehyde, which is the precursor to proline. The aldehyde and amino group undergo a spontaneous non-enzymatic cyclisation to form  $\Delta^1$ -pyrroline carboxylic acid, and then an NADPH (nicotinamide adenine dinucleotide phosphate) dependent reduction to form proline (Lea *et al.* 1985). Proline is considered a non-essential amino acid, as it is readily synthesised from metabolic intermediates and does not need to be provided in the diet. Chemically, proline is categorised as a cyclic amino acid with primarily aliphatic character (Lea *et al.* 1985).

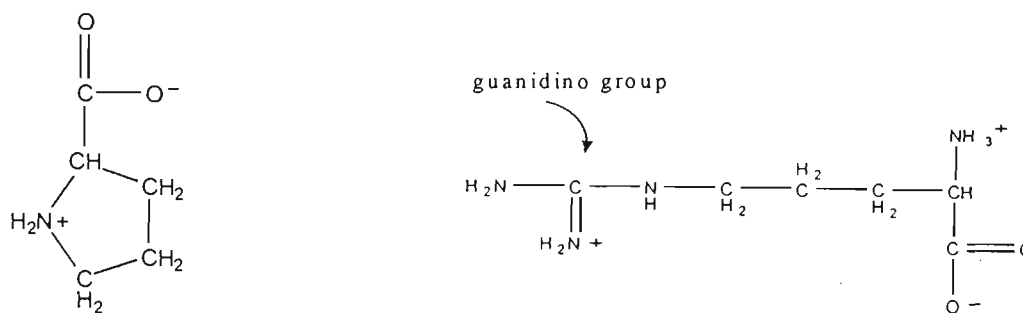


Figure 2.11 Structures of proline (left) and arginine (right). Proline has a cyclic side group and aliphatic character. Arginine has a basic guanidino side group with a  $pK_a$  of around 12.5. Under physiological conditions the guanidino group is ionised.

## 2.14 Biosynthesis of arginine

$\gamma$ -Glutamic semialdehyde is also a precursor to arginine synthesis via ornithine. Ornithine is formed by the transamination of ammonia, the activated semialdehyde. Arginine is synthesised via the Krebs-Henselate cycle from ornithine. A third nitrogen is incorporated into the molecule by the addition of the energetically activated carbomoyl phosphate by the enzyme *ornithine transcarbamoylase* to form citrulline. Citrulline is combined with aspartate in an ATP requiring reaction catalysed by *argininosuccinate synthetase*. Finally *arginosuccinase* cleaves arginosuccinate in a non-oxidative, non-hydrolytic reaction to produce arginine (Lea *et al.* 1985). Arginine is considered an essential amino acid in humans and rats because it is necessary during growth of juveniles. Dietary arginine, however, is not essential for fully developed humans. Arginine is classified as a basic amino acid, because of the guanidino group with a  $pK_a$  of around 12.5 (Mathews and van Holde 1990).

## 2.15 Arginine as a Maillard amino acid

References to arginine as a principal Maillard reactant in food or model systems in the scientific literature are scant compared to other amino acids such as: alanine and lysine (Blank and Fay 1996, Hofmann 1998c, 1999a and Pischetsrieder *et al.* 1998) or proline (Tressl *et al.* 1985, Helak *et al.* 1989, Huyghues-Despointes and Yaylayan 1996). The lack of focus on arginine as a Maillard amino acid specifically may arise from the non-essentiality of arginine in the adult human diet. Recently a number of studies have emerged in the literature demonstrating the *in vivo* reactivity of arginine in the formation of cross-linked products (Lederer and Buhler 1999, Oya *et al.* 1999, Franke *et al.* 2000). Fennema (1985) states that both lysine and arginine undergo more facile interaction with carbonyl compounds due to the basicity of their side chain nitrogens. However, in the case of arginine it has been demonstrated that the guanidino functionality of the side chain does not in fact initiate the Maillard reaction with sugars. The reaction of N- $\alpha$ -acetyl arginine, where the  $\alpha$ -amino moiety was effectively blocked, failed to initiate browning in the presence of D-glucose (Heyns and Noack 1962 and Ledl and Schleicher 1990). Thus the

guanidino group is not an initiator of the Maillard reaction. After reaction of the  $\alpha$ -amino group of arginine, formation of the arginine Amadori compound and subsequent generation of  $\alpha$ - and  $\beta$ -dicarbonyl compounds, the reactions of arginine become more complicated. Dicarbonyl groups react easily with the guanidino group via 'Strecker degradation' to produce imidazolones and pyrimidines with structures as shown in Figure 2.12 (Ledl and Schleicher 1990).

Baltes (1990) reports in his study that L-arginine underwent much faster degradation in the presence of diacetyl and pyruvic aldehyde compared with other amino acids such as lysine, to produce nitrogen containing heterocycles. Hwang *et al.* (1995) on the other hand, rated arginine as the least reactive amino acid in terms of its ability to produce pyridines, pyrroles and oxazoles in the presence of glycine and glucose.

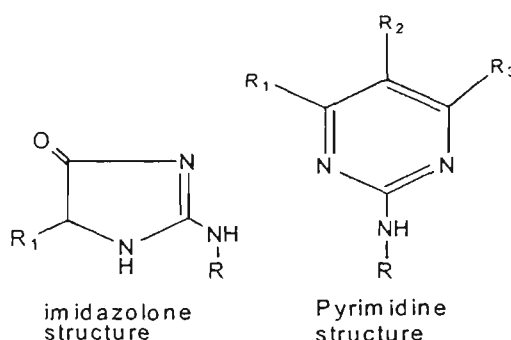


Figure 2.12 Products formed from the interaction of the guanidine group with dicarbonyl intermediates.  
Source: Ledl and Schleicher 1990

Arginine has also been shown to form a cross-linked product 'imidazopyridinium' and other cross-linked products with lysine and sugar which has been isolated from human tendon. Others (Lederer and Buhler 1999 and Oya *et al.* 1999) have described cross-linked arginine products. A similar arginine cross-linked compound was partially characterised by Hayase *et al.* (1997). The high reactivity of the guanidino group however has been demonstrated through studies of the *in vivo* inhibitory effect of aminoguanidine (guanidine hydrazine) on advanced Maillard reactions in the context of diabetes (Brownlee *et al.* 1986, Hirsch *et al.* 1992 and Jerums *et al.* 1994). The molecule reacts rapidly with dicarbonyl intermediates in Maillard reactions to form triazines, which are relatively stable and prevent further Maillard reactions. Although the guanidino group of arginine clearly does not prevent Maillard browning in model systems, it is certain that this moiety is highly reactive and capable of interacting with carbonyl intermediates of the Maillard reaction to form more complex molecules. Tressl *et al.* (1990) reported some furyl-pyrrolines and cyclopentazepinone products isolated from arginine-D glucose model systems held at 150°C for 1.5 hours. These products were postulated to occur via a 1-pyrroline intermediate formed through the Strecker degradation of arginine and the elimination of a urea moiety. The structures of these compounds are shown in Figure 2.13.

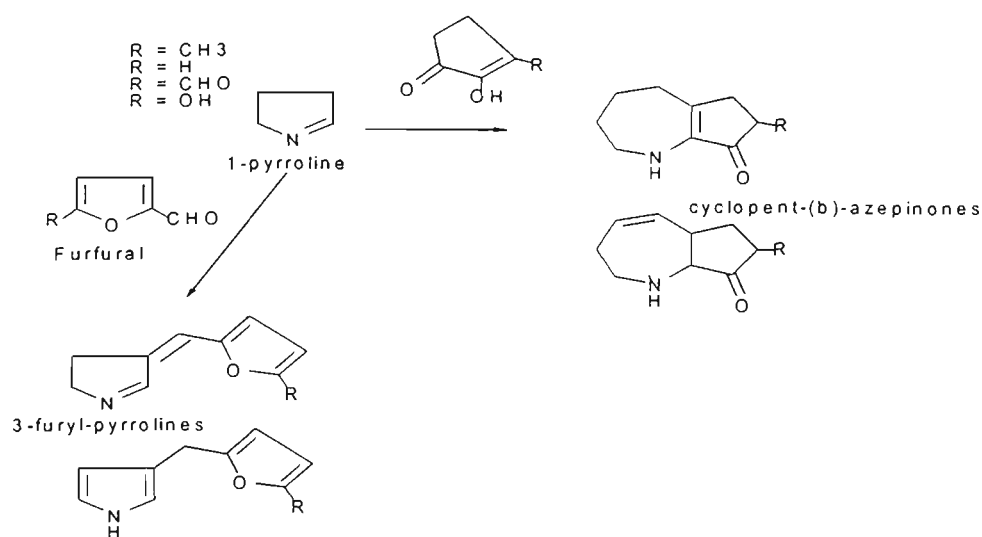


Figure 2.13 Furyl-pyrrolines and cyclopentazepinone products from arginine glucose models.  
Source: Tressl 1990

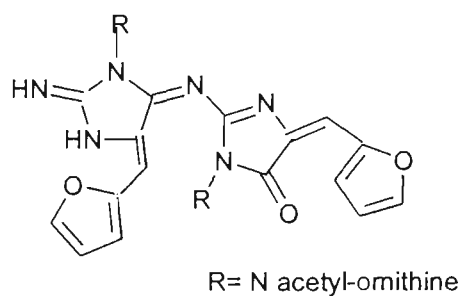


Figure 2.14 Structure of the intense red-brown cross-linked product formed by N- $\alpha$ -arginine, glyoxal and furfural.  
Source: Hofmann (1998b)

Hofmann (1998 b) recently characterised a potent red-brown chromophore from a model system of N- $\alpha$ -acetyl arginine, together with furfural (furan 2-carboxaldehyde) and the dicarbonyl compound glyoxal. The author proposed that the formation of arginine cross-linked products was a significant substructure in melanoidin. The proposed structure of the arginine-cross-linked product is shown in Figure 2.14.

Recent investigations of the antioxidant effect of aged garlic extract have identified the glucose-arginine Amadori compound, fructosyl-arginine, as a potent inhibitor of oxidation of low-density lipids (Ide *et al.* 1997 and 1999). Finally, the ability of L-arginine to increase the pH of its chemical environment by virtue of the basicity of the guanidino group may well promote more facile interaction of the  $\alpha$ -amino group; alkaline pH favours Maillard browning.

## 2.16 Plant senescence processes

Plant senescence describes the gradual breakdown of plant cellular components which can occur in all parts of annual plants—flowers, fruit, leaves and roots—or in perennial plants, where only the flowers and fruit senesce, with leaves and roots surviving another season. In fruits, the first stages of senescence occur during ‘ripening’, with further breakdown occurring during post-harvest storage. Many positive changes associated with fruit ripening, such as increase in sugars, generation of volatile flavour compounds, partial breakdown of plant walls and protein bodies, are in fact the earliest stages of senescence (Thimann 1987). The ultra-structural changes, which occur during senescence, follow a general sequence as outlined by Thomson *et al.* (1987). Firstly, the content of protein bodies undergoes degradation and interruption of vacuoles to form larger vacuoles. Vesiculation of endoplasmic reticulum then occurs with little degradation of mitochondria or nuclei. Final stages of senescence involve the fragmentation of the tonoplast membrane of the vacuole and subsequent loss of compartmentalisation of the cell. Breakdown of chloroplasts is a key event in the senescence process, and breakdown of foliar-chloroplasts results in mobilisation of nitrogen, potassium and phosphorus and transport into fruiting bodies. As senescence processes advance, protease activity increases significantly. Martin and Thimann (1972) stored oat leaves (*Avena sativa*) in darkness at 25°C and measured rapid loss of chlorophyll after 24 hours and protein after 6 hours. After 72 hours, total free-amino acids increased by almost seven-fold. Tseng and Mau (1999) observed an increase in free-amino acids in mushrooms stored at 12°C and Brierly *et al.* (1997) observed a steady increase in free-amino acids with a rise in protease activity in potato tubers stored at 5°C and 10°C. In addition vacuolar enzymes such as acid endoproteinases can rapidly degrade plant proteins and enzymes such as ribulose-1,5-biphosphate carboxylase (Thayer *et al.* 1987).

## 2.17 Water activity

All foods contain water; it is largely the case that foods with a higher water content undergo more rapid biological and chemical change. As solutes such as sugars are added to water, the entropy of the water decreases as water molecules become oriented with respect to the dissolved solutes, and solute-solvent electrostatic interactions make it more difficult for water molecules to escape from the liquid to the vapour phase. These interactions are translated to a decrease in the vapour pressure of water above the solution, relative to the vapour pressure above pure water at the same temperature.

Water activity ( $a_w$ ) is defined as the ratio of the partial pressure of water vapour above a food substance and the partial pressure of water vapour above pure water at the same temperature (Troller and Christian 1978). The concept of  $a_w$  is one of the most important factors governing the propensity of low and intermediate moisture food systems towards spoilage and browning. In any

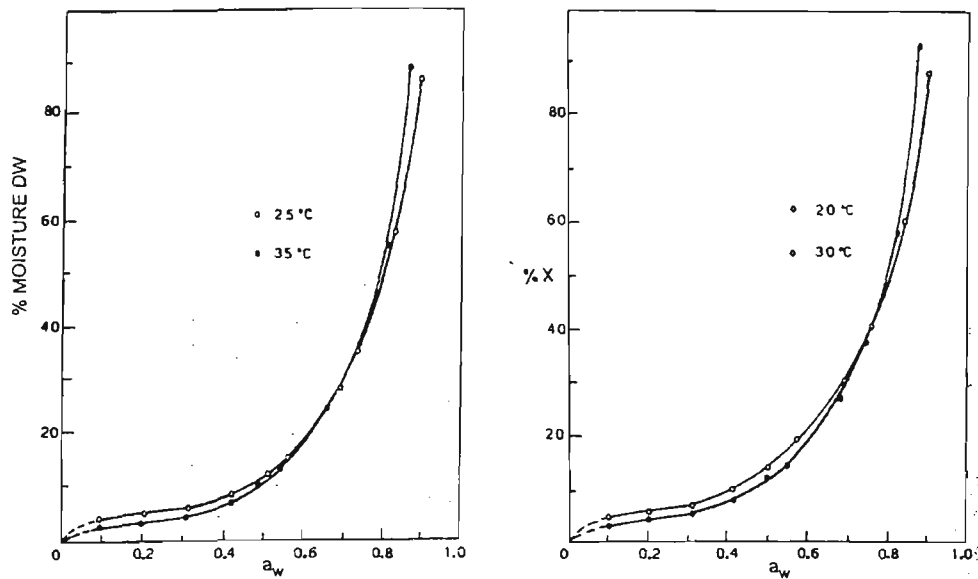


Figure 2.15 Water adsorption isotherms for sultanas at 20°C, 25°C, 30°C and 35°C.  
Source: Saravacos *et al.* (1986)

complex biochemical matrix a percentage of all water is bound in tissues and is not available for chemical interaction, i.e. to act as a solvent. Measurement of  $a_w$  does not measure bound water, whereas percent moisture determinations do not discriminate between bound and unbound water, which can often result in an erroneous assessment of a food's stability. The percent moisture can be related to  $a_w$  through a water sorption isotherm, which must be experimentally determined for a specific matrix. Typically water is added to a dry food matrix and the  $a_w$  is plotted against the percent moisture content to form a sorption isotherm. Conversely water can be removed in increments from the matrix to form a desorption isotherm. Frequently there is a difference in the plots of both, forming a hysteresis loop due to capillary condensation. In sultanas however, hysteresis effects are minimal (Bolin 1980). As  $a_w$  is temperature dependent, sorption isotherms differ slightly with changes in temperature. Figure 2.15 shows adsorption water isotherms for sultanas determined by Saravacos *et al.* (1986). It can be seen that the adsorption isotherms changed slightly at different temperatures. Bolin (1980) found that the sorption isotherms were slightly different for sultanas from grapes of different °Brix, which is often the case for high sugar foods. The same author also derived equations for the prediction of percent moisture as a function of  $a_w$  in the range 0.51-0.60, shown below:

$$\% \text{ moisture} = 36.60 - (122.5 \times a_w) + (144.3 \times a_w^2) \quad 17^\circ \text{Brix}$$

$$\% \text{ moisture} = 39.310 - (126.9 \times a_w) + (1.46.5 \times a_w^2) \quad 22^\circ \text{Brix}$$

Chirife and Buera (1996) compared sorption isotherm data for raisins from four independent research groups (Bolin 1980, Saravacos *et al.* 1986, Ayranci *et al.* 1990 and Tsami *et al.* 1990) and found good agreement between all data, despite the fact that sultanas are a 'non-equilibrium' system.

Because of the slow rates of water exchange in dried fruits, sultanas can be viewed as an essentially pseudo-equilibrium system (Chirife and Buera 1996). Dried fruits have a sugar content of between 50 and 85% (Tsami *et al.* 1990) The sugar content of sultanas (glucose and fructose) is 83 - 85% of berry dry weight.

A large number of  $a_w$  measurement techniques exists: manometric, whereby the vapour pressure above a food matrix is measured, electric-hygrometric, whereby differences in the electrical conduction of an hygroscopic salt (such as lithium chloride) in equilibrium with the ambient atmosphere surrounding the food item is measured, or dew point methods. The latter method has been incorporated in highly accurate benchtop devices, which provide an accurate and easy method of  $a_w$  determination. The dew point phenomenon relies on the fact that water vapour condenses at a specific temperature depending on its relative humidity. A food sample is placed in a closed chamber with a mirror, which is electronically cooled with a peltier device—condensation is determined by a reflected light beam with an electronically controlled feedback circuit. Generally after a few cycles equilibrium is reached and the relative humidity above the sample, and hence  $a_w$ , is calculated and a digital readout is given. Commercially available instruments are usually calibrated against standard saturated salt solutions, i.e. analytical grade NaCl and KCl, and are capable of determining  $a_w$  to  $\pm 0.005$ .

## 2.18 Crystallisation phenomena

In high sugar foods undesirable sugar crystallisation processes can occur over time. Sugar crystallisation is an important process for achieving desirable textural qualities in many food products. Formation of solid-phase sugar can have a negative organoleptic effect, however, in many foods, such as sugar crystals in maple syrup, large lactose crystals in ice cream products or graining of hard candy during storage. In the case of sultanas and other dried fruits the phenomenon of internal sugaring occurs during long-term storage and can have a negative impact on consumer desirability. Glucose and fructose make up more than 99% of total carbohydrate in grapes and account for around 25-30% of total weight of mature grapes. In immature berries, glucose accounts for approximately 85% of the sugar, and as the fruit ripens, fructose levels increase until a 1:1 ratio is reached between the two sugars at veraison. Over-ripe grapes typically have slightly higher levels of fructose (Peynaud and Ribereau-Gayon 1971, Possner and Kliever 1985 and Coombe 1987).

The interaction of water molecules with sugars is fundamental in crystallisation processes. The chemico-physical processes behind the clustering of sugar molecules to form nucleation centres are not understood in detail (Hartel and Shastry 1991). For any crystallisation process to occur the sugar solution must be supersaturated. The solubility point is the concentration of a sugar solution when the solid (crystalline) and liquid (sugar solution) phases are in equilibrium and the chemical

potential difference is zero. Sugar solutions with solubilities below the equilibrium concentration will allow the crystal to dissolve into it. If the solution has a higher solubility concentration (supersaturated), sugar molecules will transfer from the liquid phase in to the solid phase and the crystal will grow. The crystal size becomes static when the supersaturated solution has reached the equilibrium sugar concentration. In any supersaturated sugar solution, a driving force exists towards crystallisation. Critical energy barriers must be exceeded before a solid phase will form.

In phase diagrams for sugar-water solubility, this region is called the metastable region of super saturation. The presence of other compounds, such as amino acids, proteins, mineral salts, trace metals and physical and chemico-physical factors such as pH and temperature all affect the metastable region. The solubilities of common sugars at a given temperature differ markedly. At 15°C, glucose is approximately 42% (w/w) soluble, sucrose is 65% (w/w) and fructose is 80% (w/w) soluble (Chirife and Buera 1996): the difference in solubility for these sugars is thought to lie largely in differences in mutarotation behaviour of sugars in solution. Bolin (1980) observed internal sugaring in sultanas stored at 1°C for twelve months and sub-surface crystallisation in sultanas stored at 21°C for the same length of time; neither internal nor surface sugaring was observed for sultanas stored at 32°C.

## 2.19 Fatty acid oxidation

Lipid-containing foods are susceptible to oxidation processes, due to oxygen-initiated free radical deterioration. Oxidative deterioration reactions can have negative effects on flavour, texture, appearance and colour. Even the low concentration of lipids found in most fruits and vegetables can affect storage quality. In grapes and sultanas most of the lipid material is present in the form of surface waxes. Lipid oxidation occurs via peroxidation of unsaturated fatty acids by activated free radical oxygen-containing species. These include singlet oxygen—initiated by chemical and photochemical reactions—superoxide and perhydroxyl radicals, hydrogen peroxide and hydroxyl radicals. Hydroxyl radicals are produced by metal activated breakdown of lipids, especially Fe (II). A wide variety of natural enzymatic processes and autoxidation of ascorbic acid (Kanner 1992) produce hydrogen peroxide.

A major pathway to lipid peroxidation in plant tissues is mediated by the enzyme lipoxygenase (LOX EC. 1.13.11.12). LOXs are widespread in the plant kingdom (Hildebrand *et al.* 1988). LOX is a soluble cytoplasmic enzyme localised in chloroplast and photosynthetic tissues and lipid bodies in oilseeds (Zhuang *et al.* 1998). LOXs contain a catalytic non-haem iron centre which cycles between Fe (II) and Fe (III) oxidation states during catalysis. When a 18:2 fatty acid (linolenic acid) is used as a substrate, the LOX catalysed peroxidation initially involves the abstraction of a hydrogen from the C-11 methylene group. This is facilitated by the presence of a basic amino acid, for example arginine (Gardner 1991 and Whitfield 1992). Removal of the

hydrogen results in an unpaired electron forming a linoleoyl radical. Molecular oxygen reacts with the radical to form a peroxy radical, which then accepts an electron from LOX-Fe(II) and then acquires a proton forming a hydroperoxide end-product, linoleoyl hydroperoxide in the case of linoleic acid. Under conditions of depleted oxygen, LOX-Fe(II) can abstract the hydrogen, to form a linoleoyl radical, which after dissociation from the enzyme can react with a large variety of substrates to form fatty acid dimers, ketones and epoxides (Gardner 1991).

Radicals formed by LOX activity are highly reactive and can catalyse the breakdown of terpenoid compounds such as the grape triterpenoid wax component, oleonolic acid and carotenoids (Klein *et al.* 1985) and also reaction with amino acid and protein residues (Gardner 1979). The reaction of LOX products, both fatty acid hydroperoxides and radicals have led many researchers to assume that LOX activity plays an important role in general cellular breakdown and loss of membrane integrity, especially in senescence processes (Pauls and Thompson 1984, Fobel *et al.* 1987 and Zhuang *et al.* 1995). Zamora and co-workers (1985) found an increase in LOX activity in the grape cultivar Maelaleo during maturity. Fatty acid esters are known to readily react with ammonia at high temperature but similar reactions have been shown to take place at ambient temperature even with basic amino acids (Whitfield 1992). Rates of lipid oxidation are strongly influenced by  $a_w$ . Lipids present in food are bound almost exclusively as esters, which can be hydrolysed by chemical and enzymatic means. In cereal grains the enzyme lipase (E.C. 3.1.1.3), which is mainly present in the bran component, can hydrolyse triacylglycerols, diglycerols and ester linkages during storage, releasing free fatty acids.

The interaction between MRPs and lipids is an area of food chemistry receiving increased attention. Lipid oxidation can cause deterioration in proteins and amino acids and interact with MRPs to form coloured compounds (Elizalde *et al.* 1991 and Alaiz *et al.* 1995).

## 2.20 Conventional browning prevention strategies

The food industry has developed a number of general strategies to control undesirable browning reactions such as salting, blanching, lowering  $a_w$ , the use of exogenous antioxidants and reducing agents, acidulants and sulphiting agents. Reduction of  $a_w$  is one of the oldest and most effective methods of controlling browning processes in foods. The availability of water in a food system exerts an influence by providing a solvent for dissolution of reactants (Troller and Christian 1978) and also as a reactant in itself (Nicolas *et al.* 1994). Many enzyme proteins in their fully active, native state are surrounded by a hydration shell of water molecules; water acts as a plasticiser, increasing the conformational flexibility of enzyme active-sites and general structure (Bone 1987 and Affleck *et al.* 1992). In complex biological systems such as foods, minimum inhibitory values of  $a_w$  differ widely for different classes of enzymes (Ashie *et al.* 1996). There is limited information in the literature regarding the effect of  $a_w$  on PPO activity. Tome *et al.* (1978) found

that water activities at which the limit of detectable PPO activity was found, varied widely depending on the co-solvent used to lower  $a_w$  in binary model systems: sorbitol (0.75), glycerol (0.43), ethanol (0.71), methanol (0.61) and propylene glycol (0.68).

Blanching and high temperature techniques are used extensively to denature enzymes, such as pectinases and PPO. At elevated temperatures denaturation can be achieved by interrupting the tertiary protein structure, such as irreversible changes in hydrogen and disulphide bonds which cause prosthetic groups to become inactive. Sensitivity of PPO to heat inactivation varies widely in various fruits and vegetables and can vary significantly for different cultivars. In green coconut water, temperatures of 90°C maintained for about nine minutes were required to completely inactivate coconut PPO (Campos *et al.* 1996).

Inactivation of PPO through treatment with microwave heating has been applied in various fruits and vegetables. Abd-El-Al *et al.* (1994) reported that shorter heating times were required using microwave techniques compared to conventional methods, to inactivate PPO in guava, papaya and mango. Kostaropoulos and Saravacos (1995) found that microwaving sultana grapes after dipping improved final sultana colour. Microwaving reduced grape moisture content by 10-20% and increased drying times twice that of non-microwaved controls. Aguilera *et al.* (1987) studied the effects of blanching sultana grapes in water at various temperatures and times. PPO inactivation was a function of both heating time and temperature and up to 87.9% of activity was reduced with heating at 98°C for 2 minutes, 93°C for 2.5 minutes and 80°C for 3 minutes. The same authors found a high correlation between PPO inactivation and  $L^*$  values in dried sultanas.

Sulphiting agents have been used for many years as a general blanket method of inhibiting browning reactions in foods. Sulphiting involves the bombing of foodstuffs with  $SO_2$ , generally liberated from a non-organic sulphites (sodium bisulphate and sodium metabisulphite) or through burning sulphur crystals. Sulphiting inhibits both enzymatic and non-enzymatic browning, because of the high reactivity of  $SO_2$  for many common browning substrates such as carbonyl compounds, reducing sugars, proteins, metal ions and phenolics (Berke *et al.* 1998 and Karadeniz *et al.* 2000). Sulphur dioxide reacts directly with quinones (Haisman 1974) to prevent further browning and also inhibits PPO through interaction with the copper prosthetic group. Sulphiting as a method of inhibition of browning is generally extremely effective; a small proportion of consumers, however, may have an allergic response to the small amount of sulphur dioxide which may remain (Taylor *et al.* 1986, Steinman *et al.* 1993 and Lester 1995). Perhaps more importantly, the use of sulphur dioxide may impart a residual sulphur taste to (dried fruits) which is undesirable. There may also be an exaggerated negative consumer perception: for these reasons, many of Australia's export buyers have very low tolerances for  $SO_2$ . As a response, the

Australian sultana industry has completely phased out the use of SO<sub>2</sub>, choosing to utilise other approaches to minimise browning.

Ascorbic acid and sulphhydryl compounds can also inhibit browning processes. Sulphydryl groups are strong reductants and can retard browning processes, primarily by reacting with quinones formed via PPO oxidation (Cheynier and Van Hulst 1988 and Richard-Forget *et al.* 1992) to form colourless stable adducts. Allowable food sulphhydryls include the sulphur containing amino acids cysteine and the polypeptide glutathione. Examples of the positive effects of ascorbic acid on browning prevention are too numerous to cite, however ascorbic acid itself, once oxidised to DHA, becomes very reactive and can actually form brown pigments through Maillard-like reactions.

## 2.21 Colour definition and measurement

Food colour has a strong effect on consumer perception of wholesomeness, nutritional value, freshness and general organoleptic desirability. In some cases decisions regarding the suitability of a food item for a particular application are based solely on colour aesthetic considerations. In most cases with natural foods there is a strong intercorrelation between food colour and other organoleptic parameters such as firmness, acidity, bitterness, sweetness, crunchiness and overall mouth-feel.

Enzymatic browning phenomena are generally regarded in a negative context, being associated with negative qualities such as damage, bruising, oxidation, decreased nutritional value and general lack of freshness. Non-enzymatic browning such as Maillard browning can be perceived as either desirable or non-desirable depending on the context and the nutritional knowledge of the consumer. Due to the fact that Maillard reactions are inextricably linked with the generation of flavour and aroma compounds as well as coloured chromophores, it is simplistic to rate Maillard browning generally as a positive or negative phenomenon in a given food system. The anti-nutritional effects of Maillard reactions, such as loss of essential and non-essential amino acids, production of free radicals and production of potential mutagenic compounds, is contrasted with more recent knowledge regarding the anti-oxidative properties of Maillard reaction intermediates.

In the food industry, accurate measurement and definition of colour is important for consistency and quality control. Human colour perception can vary widely due to factors such as source of object illumination, angle of object illumination, subject viewing angle, surrounding colour landscape and age and sex of viewer. Genetic factors also play a role in colour perception with various forms of colour blindness affecting colour vision. Objective colour measurement technologies to reliably define and reproduce colour characteristics are therefore essential.

In human observers colour or scotopic vision predominates under high illumination conditions. Scotopic vision is mediated by a homogeneous array of each of the three cone types denoted  $\rho$ ,  $\gamma$  and  $\beta$  which are present in numerically different proportions (40:20:1) on the retina surface (Jacobs 1981). The three cone types exhibit different sensitivity and absorption maxima in the visible region, corresponding to red, green and blue portions of the visible electromagnetic spectrum respectively. A large degree of overlap of sensitivity curves allows a basis for discrimination of colour hue and intensity.

Scotopic vision can accurately be reproduced using trichromatic matching functions, which correspond to the absorption maxima of the cones of the retina (Jacobs 1981). The  $\rho$ ,  $\gamma$  and  $\beta$  receptors are reproduced at wavelengths 700 nm (red), 546.1 nm (green) and 435.8 nm (blue) respectively. All colours can be represented as combinations of these three monochromatic stimuli at specific power intensities. Because colour perception is dependent on viewing angle, most colour systems operate on a  $2^\circ$  viewing angle system, which reproduces human colour perception. In 1931 the Commission Internationale de l'Eclairage (CIE) developed a set of new tristimulus-derived values, X, Y and Z, based on the trichromatic colour matching functions, which has become the basis for derived colour space systems. In 1976, the  $L^*a^*b^*$  colour space was developed by the CIE, and since has become the most widespread colour measurement system.  $L^*$  is a measure of lightness and  $a^*$  and  $b^*$  are the hue or chromaticity coordinates ( $a^*$  green-red and  $b^*$  blue-yellow).  $L^*$  values can range from 0 for a black or completely absorbing surface and 100 for a white or completely reflecting surface. The  $a^*$  colour dimension ranges from -60 for vivid green to +60 for vivid red. Similarly the  $b^*$  dimension ranges from -60 for vivid blue to +60 for vivid yellow hue (Precise Color Communication, Minolta Co. Ltd, Osaka, Japan).

## 2.22 Natural colour chemistry

Two processes can explain organic colour phenomenology: chemical bond conjugation and charge transfer processes (Nassau 1983). Most organic dyes fall under the former category. To discuss the chemical behaviour of coloured organic compounds a number of definitions of common nomenclature are important. A *chromogen* is a colour-producing compound, which by definition must contain a *chromophore*. A chromophore by itself may not necessarily produce colour but through interaction with an *auxochrom* (colour enhancer), colour may be produced. Chromophores contain one or more conjugated double bonds, such as  $-C=C-$  (carbon double bond),  $-N=N-$  (azo group),  $-N=O$  (nitroso group) and  $C=S$  (thio group). Auxochromes may be electron donors or acceptors, common examples being  $-NH_2$  (amino),  $-NR_2$  (amine),  $-NO_2$  (nitro),  $-CH_3$  (methyl),  $-OH$  (hydroxyl) and the halogens  $-Br$  and  $-Cl$ . Quantum mechanical methods describe light absorption in the UV-visible region as resulting from electronic excitation (Jürgen and Horst 1980). The presence of different auxochromes with chromophores can cause a shift in the absorbed frequency. If the absorption is shifted from a shorter to longer wavelength, the

auxochrome is *bathochromic*, or red shifting. A long to short wavelength shift is *hypsochromic* or blue shifting (Jürgen and Horst 1980).

Molecular orbital theory is required to understand quantum mechanical models of colour. The ubiquitous C=O double bond can be used as an illustration. Both the carbon and oxygen atom are  $sp^2$  hybridized, with three trigonal planar orbitals, which form  $\sigma$  bonds. A single electron also occupies a  $p_x$  atomic orbital which lies in an orthogonal plane above and below the plane of the  $\sigma$  bonds. Non-bonding ( $n$ ) electron pairs occupy the two remaining  $sp^2$  orbitals on the oxygen atom. Overlap of these  $p_x$  orbital electrons form a second  $\pi$  orbital. Both  $\sigma$  and  $\pi$  molecular bonds have a bonding orbital where a net attraction results from the two electrons in the orbital, and an antibonding orbital, where an overall electronic repulsion exists between the two atoms.

Antibonding orbitals are denoted  $\sigma^*$  and  $\pi^*$  respectively. In terms of energy and stability the order of orbitals is  $\sigma < \pi < n < \pi^* < \sigma^*$ . Absorption of UV or visible light is sufficiently energetic to excite an electron from the highest energy occupied molecular orbitals (HOMO) to the lowest energy unoccupied orbitals (LUMO) which are generally antibonding orbitals (Jürgen and Horst 1980).

For the C=O bond the top two highest energy orbitals and the lowest unoccupied orbitals can be shown as  $\pi^2 n^4 \pi^{*0} \sigma^{*0}$ . Transitions from HOMO to LUMO levels can occur with an electron moving from a lower energy to higher energy orbital. Common transitions are  $n \rightarrow \pi^*$ ,  $\pi \rightarrow \pi^*$ ,  $n \rightarrow \sigma^*$  and  $\pi \rightarrow \sigma^*$ . Other higher energy transitions are possible but will not absorb energy in the visual region. In a simple molecule containing the C=O moiety, such as formaldehyde ( $H_2C=O$ ), the  $\pi \rightarrow \pi^*$  transition occurs at 185 nm (UV region). Addition of a C=C double bond to formaldehyde to form a conjugated system causes a bathochromic shift in the  $\pi \rightarrow \pi^*$  transition such that the wavelength of absorption is at 330 nm—within the visible region. Further addition of conjugated bonds shifts the absorbing wavelength further into the visible region. Most colour in organic molecules originates from similar p orbital  $\pi \rightarrow \pi^*$  transitions in conjugated molecules. Conjugated double bonds are collectively known as *polyenes*. Polyenes can be broadly classified as non-cyclic polyenes, non-benzenoid ring systems and benzenoid systems (Nassau 1983).

Of particular relevance to PPO mediated browning is the quinoid colour systems which can give rise to a full spectrum of colours from yellow through to intense black. Quinoid chromophore pairs generate  $n \rightarrow \pi^*$  transitions, which occur at longer wavelengths depending on the specific chemical environment. Caffeic acid is oxidised by PPO to form what is essentially an ortho-benzoquinone analogue. Ortho benzoquinones are characterised by intense absorption in the near UV region due to a  $\pi \rightarrow \pi^*$  transition ( $\lambda_{max}$  390 nm) and a weaker  $n \rightarrow \pi^*$  electron transition which occurs in the visible region. Most studies on the effect of substituents on absorption have focused on para-quinone structures, as the para conformation is commonly encountered in

industrial dyes, however the effect of substituents is very similar for ortho-benzoquinones (Jürgen and Horst 1980). Common substituents such as amine groups can easily react with quinone intermediates to form azomethine derivatives, which shift the strong  $\pi \rightarrow \pi^*$  transition well into the visible region. The presence of a non-oxidised hydroxyl group on the benzenoid structure produce pronounced dark colour in an alkaline medium. In model Maillard reaction systems a large number of highly conjugated moieties are generated which absorb in the visible region. In model systems, a large number of low-molecular-weight coloured compounds have been identified (Nursten and O'Reilly 1986, Bailey *et al.* 1996, Ames *et al.* 1993 and 1999), however the chromo-chemical nature of melanoidin remains largely uncharacterised (Benzig-Purdie and Ratcliffe 1986 and Yaylayan and Kaminsky 1998). The ability of Maillard intermediates possessing adjacent carbonyl and enol functionality to form coloured complexes with metal ions, especially with ferric cations, leads to intense dark coloured melanoidin pigments (Ledl and Schleicher 1990).

### 2.23 Near infrared spectroscopy

Near Infrared Spectroscopy (NIR) is rapidly becoming a widely applied technology in food and agricultural quality assessment. The NIR region of the electromagnetic spectrum was discovered by Herschel in 1800 (Sharma *et al.* 2000). Abney and Festing demonstrated the absorption of organic compounds within the NIR region of the electromagnetic spectrum as early as 1881. The NIR region extends from 700-2500 nm, with signals arising from harmonic overtones and overlapping combination bands of fundamental molecular vibrations of C-H, N-H and O-H bonds. The lower absorptivity of hydrogen bonds in the near infrared, compared to the infrared region (2,500-50,000 nm), allows the use of longer path lengths and determination of higher concentrations of analyte than comparable spectroscopic techniques. The practical consequence of this is that NIR techniques are especially well suited to analysis of chemical components in unprocessed materials in their native state, without any prior sample preparation or extraction process. The region 700-1100 nm is called the short wave or very near infrared which is mainly due to second and third overtone signals. Absorption from 1100-2500 nm is the classic near infrared analytical region with signals arising from resonance of first overtones and combination bands.

Despite early experiments in NIR, it was not until after World War II that developmental research of NIR as an analytical tool gained momentum. Commercially available instruments appeared in the early 1970s. Early spectrometers were filter instruments with a limited range of bandwidths available for analysis of a number of specific chemico-physical properties. Much of the developmental research of applied NIR was in the grain industry, where a non-invasive, rapid analytical technique was required for wheat protein and moisture content. Extensive use of digital technology and high speed computer processors has allowed the application of complex

chemometric data analysis to be applied to the processing of information-rich spectral data, in order to create calibrations for many traditional quality parameters measured in food products. Recent applications of NIR calibrations include measurement of various sugars and moisture in honey (Qiu *et al.* 1999), moisture, fat and protein in sheep milk (Albanell *et al.* 1999), soluble solids in apple juice (Ventura *et al.* 1998) and gluten protein in a number of cereal products (Kays *et al.* 2000). Some more esoteric parameters measured by NIR include chemico-physical qualities such as viscosity and enthalpy values of cocoa butter used in chocolate manufacture (Bollinger 1999), mineral contents of soil samples such as Na, K, Fe, N, Ca and Mg (Malley *et al.* 1999), sensory qualities of ripened cheeses (Sorenson 1998), rapid measurement of the amount of illicit drugs in whole tablets (Sondermann and Kovar 1999) and non-destructive measurement of pharmaceutical tablet hardness (Kirsch and Drennen 1999). Advances in optical technology and fibre optic components have facilitated highly accurate dispersing monochromators, which are superseding earlier filter instruments. Attachment of fibre optic probes to NIR devices allows transmission of signals at a distance from the radiation source, which makes a wide range of warehouse or factory floor in-line applications viable. Because of the high accuracy of many NIR calibrations, a number of NIR calibrations have or are in the process of being adopted as official analytical standard methods by the Association of Official Analytical Chemists (AOAC) such as protein content in whole wheat (Delwiche *et al.* 1998).

## 2.24 Near infrared: theoretical

The process of absorption and the origin of signals in NIR can be described by a number of theoretical models. NIR radiation can be described as a typical sinusoidal harmonic wave-form, with a perpendicular magnetic component. The wave form can be described in terms of frequency ( $\nu$ ) and as shown in the following equation:

$$y = A \sin 2\pi \nu t$$

Where  $A$ , is equal to amplitude,  $\nu$  is frequency and  $t$  is time in seconds.

The absorption wavelength of a vibrating molecule occurs at a specific resonant frequency, which is related to the frequency of vibration of a particular molecular bond. A typical diatomic bond can be described as a harmonic oscillator, which can be characterised by a purely mechanical model or as a quantum mechanical model. Using the former, a bond can be described analogous to a mass (isolated atom) attached via a spring to a fixed rigid body. When the spring is displaced from equilibrium, Hooke's Law can describe the force ( $F$ ) required to restore the spring to equilibrium:

$$F = -kd$$

Where,  $d$  is the distance displaced from the equilibrium position and  $k$  is the force constant, which is dependent on the strength of the spring and by analogy chemical bond strength. The frequency of vibration, can be also described by the equation:

$$\nu = \frac{1}{2\pi} \sqrt{\frac{k}{\mu}}$$

where,  $k$  is the force constant and  $\mu$  is the reduced mass, which is defined as:

$$\mu = \frac{m_1 m_2}{m_1 + m_2}$$

and  $m_1$  and  $m_2$  are the atomic masses of two atoms bonded together. The harmonic oscillator model however fails to account for the fact that absorption of energy by matter is not continuous, but rather it occurs in discrete quantised energy units. Emission or absorption phenomena can only occur at specific discrete energy states. It is the discrete nature of vibrational energy absorption by different bonds, which is exploited to produce spectra. Near infrared absorption is due to overtone bands, which like fundamental frequencies, are quantised. The origin of overtone bands derives from the coulombic repulsion, which occurs when two nuclei approach each other. An anharmonic oscillator model better describes molecular vibration, where spacing between discrete energy bands decrease as frequency increases (Chang 1990), consistent with observed behaviour in molecules. The energy of an oscillation for an anharmonic oscillator can be represented in the following simplified equation:

$$E_{vib} = (\nu + \frac{1}{2})h\nu - (\nu + \frac{1}{2})^2 h(\nu x)$$

where  $\nu$  = quantised vibrational state, which can have values of 0 (ground state) through 1, 2, 3..... $\infty$ ,  $\nu$  = vibrational frequency,  $h$  = Planck's constant and  $\nu x$  is the anharmonicity constant.

Only first, second and to a lesser extent, third overtones are of significance in NIR spectroscopy. Fundamental IR bands are well characterised and extensive overtone bands have also been defined experimentally. Tables of overtone bands—first, second and third—for hydrogenic bonds have been reasonably well characterised and interpretive tables are available for chemical assignment.

## 2.25 Spectral pre-processing and derivative spectroscopy

Spectral pre-processing techniques are commonly applied to raw spectral data to maximise spectral differences due to variations in analyte concentration and to minimise and or eliminate

spectral effects due to stochastic causes such as particle size differences in samples and small differences in detector output and response behaviour.

A number of common algorithms exist to minimise purely random noise factors from raw spectra, the simplest being the N-point smooth (NPS) operation. In this process a small segment N of a spectrum, usually between 2 and 10 nm, is used to calculate and average absorption, and this segment is then shifted one wavelength along and the averaging process repeats until the whole spectrum has been 'smoothed'. Because of the broadness of NIR signals, stochastic noise is reduced and the analyte signal is generally enhanced (Osborne *et al.* 1993).

The use of derivative spectroscopy has been applied in various spectroscopic fields, but is particularly effective in NIR applications. Raw spectral curves are mathematically treated to convert them into first, second and less commonly, third derivative spectra. Derivatisation techniques magnify spectral 'fine structure' and can often lead to better NIR calibrations. In NIR spectroscopy, 1<sup>st</sup> and 2<sup>nd</sup> derivative treatments are most commonly applied.

The first derivative finds the gradient function for two adjacent segments of contiguous spectral width (10-20 nm) by subtraction. In a first derivative transformation, maxima in raw spectra, with a gradient function of zero, are set at the zero crossing point, with the originally positive gradients set above the abscissa and negative gradients set below. In reflectance NIR, as the wavelength is increased, the baseline slopes upwards, due to increasing penetration of the radiation in highly granular materials. Slight differences in sample packing of samples also affect the penetration of incident radiation. The offset is essentially a constant, so the first derivatisation obviates major particle size effects.

Application of the second derivative algorithm restores original maxima in an inverted fashion, and points of inflection or shoulders on original raw spectra are shown as positive maxima. Second derivatisation enhances valuable information and virtually eliminates particle size and surface irregularity contributions. Second derivative manipulation of spectral data is most widely used in reflectance NIR.

## 2.26 Multivariate calibration techniques: multiple linear regression (MLR) calibration

Linear regression calibration techniques infer a correlation between absorbance at one or more wavelengths in the spectrum, with different analyte concentrations in the sample matrix. In NIR spectroscopy, there is rarely a single wavelength, which satisfactorily calibrates for a particular analyte, especially in raw products, due to chemical interactions and particularly due to particle size effects, which can have a dominant effect on spectra. In order to eliminate these particle differences a second wavelength is typically incorporated in the calibration equation with a wavelength algorithm which corrects for differences in scattering due to different particle size. A

line of best fit is fitted to the data, using the method of least squares. For  $n$  spectra, at the wavelength of interest there are 1 to  $n$ , sets of  $(x_i, y_i)$  data pairs, and a line with the equation  $(y = a + bx)$  is fitted to them so as to minimise the sum of residual squared errors ( $SS$ ), where  $\hat{y}$  is the predicted value of  $y$ :

$$SS = \sum_{(i=1 \rightarrow n)} (y_i - a - bx_i)^2 \quad \text{or} \quad SS = \sum_{(i=1 \rightarrow n)} (y_i - \hat{y}_i)^2$$

$$b = \frac{\sum_{(i=1 \rightarrow n)} (x_i - \bar{x})(y_i - \bar{y})}{\sum_{(i=1 \rightarrow n)} (x_i - \bar{x})^2}$$

where  $b$  is the gradient for the line of best fit and  $a$  is the intercept determined for the line of best fit and  $\bar{x}$  and  $\bar{y}$  are the mean values of all  $x$  and  $y$  values in the data set. Two further measures of goodness of fit for a linear equation, are the standard error of calibration ( $SEC$ ) and the coefficient of multiple determination ( $R^2$ ), also known as the R-squared statistic. The  $SEC$  or standard error of estimation ( $SEE$ ) is described algebraically by the following equation:

$$SEC = \sqrt{\sum_{(i=1 \rightarrow n)} \frac{(y_i - a - bxi)^2}{(n - 2)}}$$

where  $n$  is the number of data pairs, and two degrees of freedom are removed to account for the data used to calculate the constants  $a$  and  $b$  (Martens and Naes, 1991). The  $SEC$  is an indication of the total residual remaining unexplained error between actual laboratory measured values and NIR predicted data.  $R^2$  measure is an indication of how much of the variation in the data is modelled by the equation expressed as a fraction of 1. As  $R^2$  values approach 1, the amount of variation in the laboratory or reference data is modelled by the calibration equation approaches 100%. As  $R^2$  values decrease, the model explains less and less variation in the laboratory data. Low values of  $SEC$  indicate that measured values lie very close to a straight line. The R squared statistic complements  $SEC$ , and gives a measure of the degree of variability in  $y$  values which can be successfully described by the fitted linear equation.  $R^2$  is explained mathematically by the equation:

$$R^2 = 1 - \left( \frac{\sum_{(i=1 \rightarrow n)} (y_i - \hat{y}) / (n - k - 1)}{\sum_{(i=1 \rightarrow n)} (y_i - \bar{y})^2 / (n - 1)} \right)$$

where  $n$  = number of spectra in data set and  $k$  = number of wavelengths used in the calibration. Often  $R$  or the *simple correlation coefficient* is used which is simply equal to the square root of  $R^2$ . Both  $R$  and  $R^2$  are dependent not only on the goodness of fit of the linear equation, but also the spread of  $y$  values in the data set. Extreme values of  $y$  in the data set may generate a high value of

$R$  or  $R^2$ , but may have a low level of predictive accuracy. When assessing the validity of an NIR linear regression model, both  $R$  and  $SEC$  must be considered. Often use of two or more optical terms (wavelengths) are used to generate a superior predictive model. In this case a multiple linear model (MLR) is calculated from multiple wavelength data. Additional constants ( $b_2, b_3, b_4 \dots b_p$ ) are added to give the following equation:

$$y = a + b_1x_1 + b_2x_2 + b_3x_3 + \dots + b_px_p$$

Constants are derived such that  $SS$  is minimised as shown below:

$$SS = \sum_{(i=1 \text{ to } n)} (y_i - a - b_1x_{1i} - b_2x_{2i} - b_3x_{3i} - \dots - b_px_{pi})^2$$

Although there is no mathematical limit to the number of terms used to generate an MLR calibration, it is generally accepted that a model with fewer wavelengths is superior to a complex multiple term equation (Osborne *et al.* 1993).

MLR techniques can be applied to spectral data, which has been mathematically, transformed, such as application of first, second or third derivative processes. MLR techniques can be very successfully applied to relatively clean systems, where sample matrix variation is low and does not interfere with analytes of interest. In most natural products, however, a large degree of spectral variation within a group of spectra is often not due to variation in analytes of interest, but rather due to other stochastic sources. MLR is inadequate in modelling this natural matrix variation and hence may not sufficiently predict analyte concentration or identify unusual or atypical samples.

## 2.27 Partial least squares (PLS) calibrations

Linear regression techniques are known as 'local' methods of calibration because they utilise a small number of discrete wavelengths from an entire spectrum, which typically may include 2000 or more wavelengths. Increasingly a number of alternative 'global' or 'full-spectrum techniques' are being used in chemometric analysis (Mark 1992). With these techniques a larger portion of spectral data is incorporated in the calibration equation through compression of original data into principal components (PC), also known as factors (F) or latent variables (LV). Principal component regression (PCR) and partial least squares (PLS) regression use full spectrum techniques to generate calibrations. PCR data reduction techniques are commonly used in qualitative NIR applications where discrimination between different natural products is desired. PLS is a commonly applied approach to generation of quantitative NIR calibration models using multivariate statistical processing. Both PCR and PLS methods calibrate for desired components and also implicitly model for other sources of variation in the data set. Both methods use signal

averaging techniques, where a large number of redundant measurements may be used to generate a mean factor which is a better representation of analyte concentration. Data compression or rank reduction are the fundamental motivation for use of PCR and PLS. Martens and Naes (1991) list three typical shortcomings of MLR calibration methods:

- No single X-variable is sufficient to predict Y. Commonly this may be caused by interference of matrix constituents other than the analyte. A number of X variables ( $x_1, x_2, x_3, \dots, x_k$ ) may be required.
- High co-linearity between X-data. Inter-correlation or redundancy of X-data is common in spectral data, where a number of wavelengths may have a linear relationship with analyte concentration. Inclusion of multiple redundant wavelengths in a model provides increased robustness and better ability to detect true outliers in the data set.
- In a complex natural product matrix, a high degree of chemical interaction may occur between the analyte and other chemical components. The nature of this interaction or covariance structure is often not obvious and may not be accounted for by other calibration methods.

PLS differs from PCR in the process of determination of latent factors. For PCR, factors are determined entirely through modelling variation in the X data, independently of Y data. In PLS, factors are determined by modelling the variation in both X and Y data simultaneously. Through active use of Y data in the modelling, the potential of including irrelevant variation in the calibration model is minimised. Commonly PLS methods are described as PLS1 and PLS2. The former method generates a calibration model for one analyte only, whereas the latter creates a model for two or more analytes simultaneously. PLS1 is more straightforward and is the most commonly used method in NIR spectroscopy. PLS calibration can be described in terms of complex matrix algebra operations (Martens and Naes 1991) or in a more graphical manner (Osborne *et al.* 1993). A much-simplified account for the basic ideas of PLS follows.

In PLS reliable predictors of X data are generated from projecting many x variables (absorption at many specific wavelengths  $\lambda$ ) to form new factors ( $\hat{T}$ ) which are used as regressors for y data.

$$\hat{Y} = f(X)$$

$$\hat{T} = X\hat{V}$$

where  $X$  is the vector sum of  $x_k$  data and  $\hat{V}$  is the loading matrix of  $X$ . In PLS1 operations the X data is first scaled so that all data has comparable noise levels. X and y variables are subsequently centered, by subtracting the mean values of x and y from all variables. Loading weight vectors

(eigenvectors) are calculated to maximise the covariance between X and Y data for each factor. Factor scores are calculated which correspond to the maximum correlation of each loading vector with chemical values. Residual unexplained variation in the data matrix is modelled by the generation of a new factor. Stepwise iteration occurs until a sufficient number of factors are created to explain the variation in the chemical data. An important statistical property for calculated factors is their orthogonality to one another, which eliminates the multicollinearity normally problematic in MLR calibration approaches (Bjørsvik and Martens 1991). The efficacy of a PLS calibration is assessed in much the same way as MLR calibrations. A standard technique for measuring the predictive ability of PLS equations is through cross validation, where a nominal subset of spectra is removed from the original spectral population, withheld from the calibration process, and later used as a validation set. During the cross validation process, through iterative algorithms, each sample is used both as an independent validation sample and as a member of the calibrating set. This form of validation generates the mean standard error of cross validation (MSECV). The number of factors used in models is usually recommended by the chemometric software, which corresponds with the ratio of the most recently generated MSECV to the lowest MSCEV, which is closest to the statistically significant value of 1.25 (NSAS Reference Manual 1996).

## 3.0 SULTANA STORAGE EXPERIMENT I 1995

---

### 3.01 Introduction

The largely enzymatic nature of browning during grape drying is reasonably well understood; in contrast the browning processes which occur during storage remain relatively undefined. The objectives of this experimental section were to obtain a broad outline of the chemical nature of *storage* browning processes in sultanas. Some farmers to minimise the risk of weather damage to grape berries have adopted vine-shading techniques. Anecdotal evidence from sultana farmers and packers indicated a positive relationship between sultana colour lightness and a high level of grapevine solar exposure. Vine trellising techniques such as the Shaw trellis, where the vine canes and fruiting canes are managed to maximise solar exposure of grape berries, have also been demonstrated to produce better quality and lighter coloured sultanas, compared to more conventional trellising methods (Hayes *et al.* 1991).

Solar exposure levels in other grape cultivars and other fruits are known to affect synthesis of phenolic substrates, a key parameter in browning processes. Heat has generally been shown to suppress expression of phenolic-synthesis enzymes, whereas UV light can have a stimulating effect on certain phenolics as a natural plant defence mechanism (see section 2.04). The 'sunfinishing' step is important to produce high quality, light-coloured and colour-stable fruit (ADFM 1998). It is unknown whether sunfinishing improves sultana colour quality simply by lowering  $a_w$  or by irreversibly inhibiting PPO activity. PPO mediated browning reactions are generally assumed to occur within the time frame of days (24-120 hrs at 40°C, Radler 1964). Slower oxidative phenomena, such as the slow autoxidation of phenolic substrates and subsequent reaction of quinone intermediates with other components within the sultana chemical matrix may occur over a longer time frame. Maillard reactions occur at a slower rate at ambient temperatures, generally requiring months before substantial browning occurs.

### 3.02 Experimental aims

The specific aims of this experiment were:

- to determine whether vine shading and sunfinishing have an effect on the storage browning potential of sultanas,
- to characterise the oxygen dependence of sultana storage browning processes,
- and assess the relative contribution of Maillard and/or PPO-browning processes.

### 3.03 Materials and methods: source of grape material

Fruit from Sultana vines—clone H5 on Ramsey rootstock—growing in two adjacent rows of a vineyard of the Sunraysia Horticultural Centre (SHC, Irymple, Victoria) were used in this experiment. The vines of one row were covered between fruit-set and harvest with medium-weave polythene shade cloth (~25% shading), typically used by sultana farmers in the Sunraysia region (purchased from the Irymple Co-op). Grapes and dried sultanas from these vines will be referred to as 'protected' hereafter. The vines of the adjacent row were left uncovered, and their grapes and dried sultanas will be referred to as 'exposed' hereafter. Both rows were given the same fertiliser and irrigation treatments. Whole bunches of fruit were removed from the outside and top of the foliage canopy on the morning of March 6 from each of the two treatment rows. A total of 39 kg of protected and 45 kg of exposed grapes were collected and held at 4°C overnight in the cold storage facility at SHC. Samples of whole bunches from both treatments were placed in insulated containers (Esky) with dry ice and were transported to Victoria University of Technology (VUT-Werribee campus, Victoria) for chemical analysis. Total soluble solids (TSS) and titratable acidity (TA) were measured on the juice of 100 berries. The remaining Sultana grapes, approximately 35 kg from each treatment, were dipped in a typical cold dipping solution—whole grape bunches were placed into dipping buckets and submerged for 120 seconds. Grape berries were dipped in an emulsion of 2.4% m/m of potassium carbonate and 1.4 % v/v of the commercial dipping oil 'Ee-muls-oyle'<sup>TM</sup> (Voullaire's, Australia) in 10 L of water.

### 3.04 Determination of TSS and TA

Frozen grapes (n=100) were removed from -80°C storage and were placed in a stainless steel Waring blender and allowed to thaw slightly before blending at the lowest speed setting in order to roughly break up grape skins. The juice was filtered through clean cheese cloth. At least five determinations were performed for each test. TA was determined via titration with 0.1 M NaOH and phenolphthalein indicator to determine the end point. TA was expressed as g.L<sup>-1</sup> tartaric acid. TSS were determined at 22°C by placing a drop of the grape juice on the glass reading surface of a hand-held refractometer (Atago Instruments, Japan) with the °Brix read directly from the scale. TSS values were temperature corrected and final values were the means of 5 determinations.

### 3.05 Substrate PPO activity

The PPO assay was based on the protocol described by Rathjen and Robinson (1992a). 4-methylcatechol (4-methyl-1,2-*o*-dihydroxybenzene, Sigma-Aldrich, Australia) was used as the substrate for all PPO activity assays. An optimal saturated working substrate concentration was experimentally determined. Grape skins (n=20) were homogenised in 20 mL ice-cold grinding buffer (0.1 M NaH<sub>2</sub>PO<sub>4</sub>, 0.4 M sucrose and 1 mM MgCl<sub>2</sub>) and a 300 µL aliquot of the homogenate was added to 20 mL of 0.05 M NaH<sub>2</sub>PO<sub>4</sub> buffer (pH 5, temperature 22°C). An

aliquot of 4-methylcatechol was added over the concentration range 1-6 mM and rates of disappearance of dissolved oxygen were monitored with a digital dissolved oxygen electrode (HI 9141 electrode, Hanna Instruments). Beyond a concentration of 3 mM no increase in PPO activity was observed as can be seen in Figure 3.1. In subsequent assays, the substrate was added to give a final concentration of 4 mM. For skin and flesh PPO substrate measurements grapes were removed from  $-80^{\circ}\text{C}$  storage and allowed to thaw slightly on a bed of ice in the laboratory. Skin and flesh were separated from semi-frozen grapes with a scalpel ( $n=20$  grapes) and weighed and homogenised in 20 mL ice cold grinding buffer (0.1 M  $\text{NaH}_2\text{PO}_4$ , 0.4 M sucrose and 1 mM  $\text{MgCl}_2$ ). Two sub-samples of either twenty grapes or sultanas were prepared and at least two assays were performed. A 300  $\mu\text{L}$  aliquot of either skin or flesh extract was immediately added to phosphate buffer (pH 5,  $22^{\circ}\text{C}$ ) and 4-methylcatechol was added for a final concentration of 4 mM. A magnetic stirrer was added and the decrease in dissolved oxygen was measured. The instrument was conditioned and calibrated according to the manufacturer's instructions every two hours during measurements. Determinations of PPO activity in sultanas were performed in a similar manner.

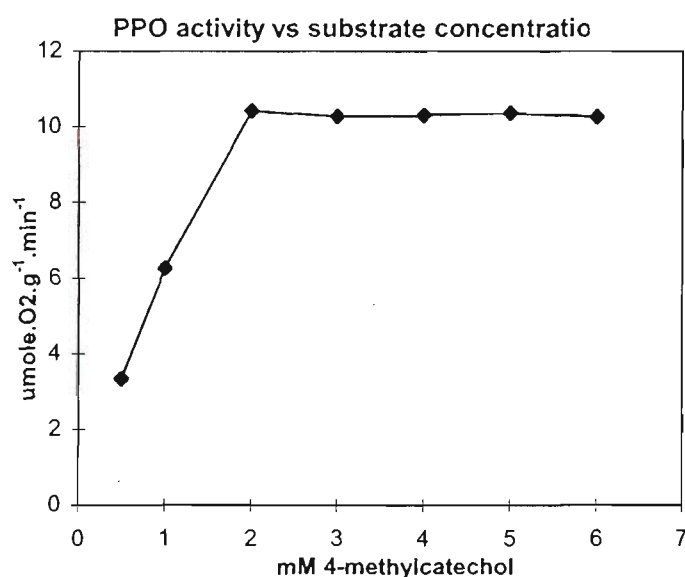


Figure 3.1 Data for optimisation of assay conditions for PPO with 4-methyl catechol as a substrate. Beyond a concentration of 3 mM the enzyme was saturated with substrate.

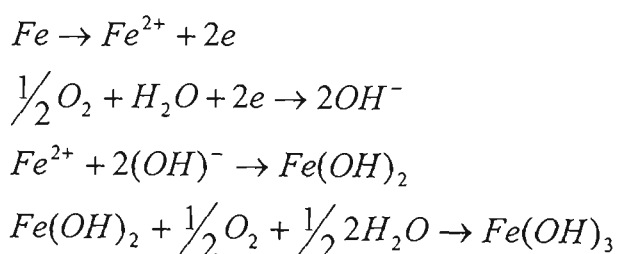
### 3.06 Oxygen-free packaging

Advice and packaging materials were obtained from the Cryovac Division of W & R Grace Co. Packaging (Fawkner, Australia). Samples were packaged in polyvinylidene chloride (PVDC) coated biaxially orientated polypropylene (OPP) pouches about  $11 \times 15 \text{ cm}^2$  in size (25  $\mu\text{m}$  film thickness-PVDC). PVDC has a high impermeability to gases ( $\text{O}_2$ ,  $\text{CO}_2$  and  $\text{H}_2\text{O}$ ) and operates effectively over a wide moisture range.

	Biaxially-orientated OPP	PVDC
Density (g.cc <sup>-1</sup> )	0.90	1.6 - 1.7
Tensile Strength (kp.cm <sup>2</sup> )	8 - 12	8 - 16
Tensile Modulus 1% secant (kp.cm <sup>2</sup> )	138	19.5-59
Elongation at break (%)	50 - 275	50-100
Tear strength (Elmendorf) (g.mil <sup>-1</sup> )	1000 - 1500	2
Water Vapour Transfer Rate (g.100 cm <sup>2</sup> -24 hr) at 37.7°C and 90% RH	0.16	0.02 - 0.0.12
O <sub>2</sub> permeability (cc/100 cm <sup>2</sup> -24 hr-atm) at 37.7°C and 0% RH	39 - 63	0.04 - 0.18
Functional Temperature °C	5 - 120	-18 -135

Table 3.1 Properties of OPP and PVDC polymers, based on a film thickness of 25  $\mu\text{m}$  (1 mil).  
Adapted from Zagory 1995.

Co-extrusion of the two polymer materials creates a highly effective oxygen and water vapour barrier, which exploits the very low oxygen transfer rate of PVDC and the high strength of OPP. The physical properties of these materials are summarised in Table 3.1. The vapour permeability specification for the bags used in the experiment was  $< 4 \text{ g.m}^{-2} \cdot 24 \text{ hrs.}$  and the oxygen permeability was  $1\text{-}5 \text{ mL.m}^{-2} \cdot 24 \text{ hrs.}$  Remaining oxygen was removed from packages with two sachets of Ageless®-Z-100 powdered iron oxygen scavenger (Mitsubishi Chemical Company Inc., Japan). The Ageless product has been widely used in Japan and the USA for many years and is by far the most widely used oxygen scavenger technology (Smith *et al.* 1995). Ageless sachets can rapidly reduce the package headspace oxygen concentration to below 0.01% in combination with the correct barrier packaging. The sachets consist of finely divided powdered iron which, in the presence of water vapour, react with residual O<sub>2</sub> to form non-toxic iron hydroxide. The oxidation mechanism can be expressed by the following series of chemical equations (Smith *et al.* 1995):



Within a few days all residual oxygen is removed from the packaging headspace and the food is protected from oxygen dependent reactions such as browning of phenolic substrates and lipid oxidation reactions.

Ageless Z-100 type oxygen scavengers are suitable for samples with water activities of 0.85 or less. Each sachet can absorb 100 mL of O<sub>2</sub> or approximately 500 mL of air. Deoxygenation occurs within 1-4 days at 25°C. Ageless Eye® oxygen indicators were used to monitor oxygen-free status: pink when oxygen concentration is 0.1% or less, blue when oxygen is present at 0.5% or more. After filling with sultanas, the pouches were flushed with N<sub>2</sub> gas and vacuum-sealed with a Multivac® A-300-16 bag sealer (Sepp-Hagenmüller KG-Wolfertschwenden, Germany). The oxygen-free condition of the pouches was also verified using gas chromatography-mass spectrometry (GC-MS). After storage (10 months) a teflon-lined silicone GC septum was attached to the side of the unopened package with silicone glue (Silastic). After allowing to dry overnight, the septum had securely adhered to the packaging material allowing a gastight sampling syringe (1 mL) to be inserted into the plastic film without tearing the polymer material. A Saturn II® ion trap mass spectrometer (ITMS) (Varian Australia, Mulgrave, Victoria) connected to a Varian 3400-CX gas chromatograph was tuned and set up to determine the oxygen status of the package gas headspace. The GC column temperature was set at 50°C (DB-1 Column) the injector temperature at 250°C and the ion trap was turned on with the mass window set to 15 - 50 amu. A 0.5 mL volume of the packaging headspace was immediately injected onto the column (a large volume injector liner was used). The presence of oxygen was monitored visually at 32 m/z. Replicate injections from a number of packages resulted in no detectable increase in the ion current at 32 m/z indicating that the packages had remained oxygen-free to the limits of MS detection during the storage experiment.

### 3.07 Colour measurement—tristimulus values (L\*a\*b\*)

Objective colour measurement was achieved using a Minolta CR-300 Chromameter (Minolta Camera Co. Ltd. Osaka, Japan) with a glass light projection tube (CR-A33F) with an 8 mm-diameter specimen area. The illumination source was a pulsed-xenon arc lamp used with a 0° viewing angle. Reflected and incident light was measured via a double array of silicon photocells filtered to match the CIE (Commission Internationale de l'Eclairage) 2° Standard Colorimetric Observer Curves  $x\lambda$ ,  $y\lambda$ ,  $z\lambda$ . All data were acquired using the CIE standard illuminant C. The instrument was calibrated using the calibrating ceramic tile according to the manufacturer's instructions.

A representative sample of approximately 100 g of sultanas was tightly packed into a deep petri dish and the colour reading head was placed flush with the sultana surface layer. Grape stem or waste material was removed prior to colour measurements. After data acquisition the reading head aperture was moved to another position on the sample surface and the process was repeated until five measurements had been collected. The sultanas were then taken out of the petri dish and repacked and a further five readings were performed. This was repeated a total of 10 times until

50 readings were obtained. The Chromameter software automatically calculated the mean data. This procedure was repeated and the mean colour data for 2×50 readings were used in the statistical analyses.

For determination of grape colour, 2×25 grapes were removed from -80°C storage and allowed to thaw. The grapes were placed on a clean piece of white paper on the laboratory bench and the reading aperture (8 mm) of the Chromameter was placed directly on a grape surface and a reading was taken. The reading head was moved to another grape and colour was determined for a total of 25 grapes. The Chromameter determined the statistical average.

### **3.08 Water activity**

Water activity ( $a_w$ ) was measured using a Decagon CX-2 Water Activity Meter (Decagon Devices Inc., Pullman, WA, USA). The device utilises a cooled-mirror dewpoint technique to measure the relative humidity above sultana samples, and hence  $a_w$ . The instrument was calibrated prior to use using saturated salt solutions of pure sodium chloride ( $a_w=0.755$ ) and potassium chloride ( $a_w=0.851$ ), according to the manufacturers specifications. In order to measure the  $a_w$  of sultanas a representative sample of sultanas ( $n=50$ ) was ground in a mortar and pestle and small duplicate samples were placed in covered sample cups and immediately measured. Readings were taken until two concordant  $a_w$  values were obtained.

### **3.09 Total phenolics**

Total phenolic compounds in grapes and sultanas were analysed colorimetrically using the Folin-Ciocalteu Phenolic reagent (Sigma Chemicals, Sigma-Aldrich, Australia). Two sub-samples ( $n=20$  sultanas) for each grape/sultana treatment were ground in ice-cold 80:20 MeOH-Milli-Q with a Polytron aggregate and centrifuged as for free-amino acids (see next section). A 25  $\mu\text{L}$  volume of sultana or grape MeOH-Milli-Q extract was diluted in 525  $\mu\text{L}$  of Milli-Q water and a 50  $\mu\text{L}$  aliquot of the Folin-Ciocalteu Reagent was added. After 2 minutes a 400  $\mu\text{L}$  volume 1 M sodium carbonate ( $\text{Na}_2\text{CO}_3$ ) was added and colour was allowed to develop for 30 minutes before transfer to a cuvette. Absorption was monitored at 765 nm with a Pharmacia Ultraspec-III spectrophotometer. Quantification was achieved using caffeic acid in an external calibration standard curve. Two instrumental determinations were performed on the two sub-samples and the mean values were used in statistical tests.

### **3.10 Analysis of grape and sultana free amino acids**

Free amino acids in grape and sultana samples were analysed via HPLC using two pre-column derivatisation agents—ortho-phthalaldehyde (OPA) and 9-fluorenylmethylchloroformate (F-moc)—with subsequent fluorescence detection. The F-moc derivatisation was used for measurement of both free-arginine and proline, whereas OPA derivatisation was used to measure arginine only.

### 3.11 Ortho-phthalaldehyde (OPA) amino acid derivatisation

OPA (*o*-phthalaldehyde) is a fluorescent substrate, which reacts with the  $\alpha$ -amino group of primary amino acids in about 60 seconds in the presence of 2-mercaptoethanol to form a stable amino acid/ OPA/ mercaptoethanol complex. The following method was adapted from Umagat *et al.* (1982).

Accurately weighed samples of grapes, sultanas or parts thereof were transferred into screw-top polycarbonate centrifuge tubes (40 mL) and a sufficient volume (20-25 cm<sup>3</sup>) of ice-cold methanol (HyperSolv® HPLC Reagent, BDH Chemicals, Poole, England) and Milli-Q water (80:20) was added. In the case of sultanas the samples were allowed to rehydrate in the freezer overnight. Samples were subsequently homogenised in centrifuge tubes with a Polytron aggregate (Kinematica, Luzern, Switzerland) at speed setting 3 for 120 seconds. Samples were centrifuged at 4°C, at 17,400 × *g* for 15 minutes in a Beckman J2-HS centrifuge (Beckman Instruments, Palo Alto, CA, USA). Supernatants were transferred to plastic Falcon™ tubes and the pellets were re-suspended in a further volume of ice cold MeOH/Milli-Q buffer and further homogenised for 120 seconds. Samples were re-centrifuged for ten minutes and supernatants were pooled. Samples were made up to a constant volume and an aliquot was passed through a 0.2 micron nylon filter with a 10 mL syringe ready for HPLC analyses.

A 50  $\mu$ L aliquot of sample was diluted together with internal standard (glycine) in borax (0.1 M) buffer to make a final volume of 1 mL in 2 mL amber HPLC vials with screw top lids and teflon coated septa (Alltech, Australia). Samples were made up such that the final composition was: 50  $\mu$ L sample, 50  $\mu$ L internal standard and 900  $\mu$ L borax buffer. The OPA derivatisation mix was made up as follows: 50 mg of OPA reagent (Sigma-Aldrich, Australia) were weighed out and dissolved in 500  $\mu$ L of HPLC grade MeOH. A 50  $\mu$ L volume of 2-mercaptoethanol (Sigma Aldrich, Australia) was added together with 10 mL of the 0.1 M borax buffer. The OPA solution was prepared fresh weekly and covered with silver foil and stored at 4°C until used.

Sample derivatisation and injection were fully automated using a Varian 9100 autosampler connected to a Varian 9010 solvent pump and a Varian 9070 fluorescence detector (Varian Australia). The Varian proprietary 'Star' software (Version 5.34) was used to program the derivatisation sequence described in the following. A 20  $\mu$ L aliquot of the sultana or grape amino acid MeOH extract was automatically delivered to a 100  $\mu$ L glass vial insert (Alltech, Australia) which was placed inside an empty amber HPLC vial. The autosampler was programmed to deliver 80  $\mu$ L of the OPA derivatising mixture with the sample. The sample was derivatised for 120 seconds with mixing (3 mixing cycles). A 30 $\mu$ L volume of the sample was injected automatically through a Rheodyne 10  $\mu$ L HPLC sample loop onto the analytical column.

A secondary solvent system was used for elution of the derivatised amino acids. Separation was performed with gradient elution using the following buffers: solvent 'A' was made up of 0.05 M sodium dihydrogen phosphate ( $\text{NaH}_2\text{PO}_4$ ) and solvent 'B' was made up with an 80:20 mix of HPLC grade methanol (HyperSolv) and solvent 'A'. Solvents were filtered through a nylon 66, 47 mm diameter 0.45 micron membrane (Alltech, Australia) and degassed under vacuum with stirring for two hours prior to use. Separation was achieved on a 25 cm reverse phase Phenomenex Ultracarb-5 ODS(30) column with a 5 micron particle size (Phenomenex, Torrance, CA., USA). The HPLC solvent elution gradient was as follows:

Time (minutes)	Solvent A	Solvent B
0.00	90%	10%
2.00	90%	10%
29.00	15%	85%
30.00	100%	0%
35.00	100%	0%

The column was equilibrated for ten minutes at initial solvent conditions. The column flow rate was  $1.0 \text{ mL min}^{-1}$ . OPA derivatives were detected with a Varian 9070-fluorescence detector with an excitation wavelength of 360 nm and an emission wavelength of 455 nm.

Amino acids were identified on the basis of retention times and spiking experiments. Quantification was achieved for arginine and proline using an external standard method. Both arginine and proline were greater than 99% purity (Sigma Aldrich, Australia). The unknown compound was semi-quantitatively measured using the proline calibration curve. Integrated areas for the internal standard were all within 5% for chromatograms and two instrumental measurements were performed on each sample. The OPA method was used initially because of the considerably shorter derivatisation time, 2 min., and shorter run times, 35 min. per run, and greater precision compared to F-moc derivatisation (see the following section).

### 3.12 9-fluorenylmethylchloroformate (F-moc) amino acid derivatisation

The following protocol was adapted from Cunico *et al.* 1995. F-moc reacts with proline and primary amino acids, but the method is considerably longer than the OPA method and requires an extraction step to remove F-moc-OH, which is the stable reaction product formed with water in the samples. As the F-moc water product becomes a dominant artefact, it must be removed before HPLC analysis. F-moc-OH was extracted into a solvent phase made up of a 80:20 pentane: ethyl acetate (HPLC grade) mixture. Grape and sultana samples were prepared as described in the previous section.

Filtered grape/sultana methanolic extracts were diluted 1:50 in 0.1 M NaHCO<sub>3</sub> buffer (pH 9). Internal standard (L-glycine) was added to sultana-buffer samples at an appropriate concentration. All samples were derivatised using a Varian 9100 autosampler module. The F-moc derivatising mixture was made with 20 mg of the F-moc reagent (Sigma Aldrich Chemicals, Australia) dissolved in 10 mL of acetone (HyperSolv). A 20 µL aliquot of the diluted sultana extract was derivatised with 20 µL of the F-moc derivatising mixture for 10 minutes and mixed. In order to remove F-moc-OH, 60 µL of the extraction buffer was added to the mixture and mixed automatically 6 times by the autosampler. A 30 µL volume of the aqueous phase was injected through a 10 µL Rheodyne sample loop. Solvent A was made up of 0.02 M tri-sodium citrate (AnalaR, BDH Chemicals) with 2.5 mM tetramethylammonium chloride TMAC (5.0 M solution Sigma Aldrich, Australia) and the pH was adjusted to 2.85 with undiluted orthophosphoric acid and an Orion 420A pH meter. Solvent B was made up of 0.02 M tri-sodium citrate with the pH adjusted to 4.5—HPLC grade MeOH was added to the sodium citrate buffer in a 20:80 v/v ratio. Solvent C consisted of 100% HPLC grade acetonitrile. All solvents (except acetonitrile) were filtered through a 0.45 µm, 47 mm diameter nylon 66 membrane (Alltech Australia) and degassed under vacuum for two hours before use. Separation was achieved on a 25 cm reverse-phase Phenomenex Ultracarb-5 ODS(30) column, with a 5 µm particle size (Phenomenex, Torrance CA, USA). The F-moc tertiary solvent gradient was as follows:

Time (minutes)	Solvent A	Solvent B	Solvent C
0.00	75%	0%	25%
11.50	60%	0%	40%
13.00	60%	0%	40%
18.01	0%	60%	40%
20.00	0%	62%	38%
30.00	0%	70%	30%
35.00	0%	75%	25%
40.00	75%	0%	25%

Column flow was set at 1.40 mL minute<sup>-1</sup>. Derivatives were detected on a Varian 9070 fluorescence detector with excitation and emission wavelengths of 268 nm and 340 nm.

### 3.13 Measurement of 5-Hydroxymethylfurfural (GC and GC-MS)

5-Hydroxymethylfurfural (5-hydroxymethyl-2-furancarboxaldehyde) or 5-HMF is a key intermediate of glucose degradation via Maillard reactions. This compound was measured simultaneously with sultana lipid material (see chapter 6.0) in dichloromethane (DCM-HyperSolv) extracts of sultanas (see 6.03 for details of sample preparation) and identified on the basis of retention times and mass spectral data as compared to an authentic 5-HMF standard (Sigma Aldrich, Australia, 99% purity by HPLC). Under the GC conditions described in 6.03,

both the putative 5-HMF and the authentic 5-HMF eluted at the same time (7.09 min.), and had identical mass spectra under the same EI conditions. The peak at  $m/z$  126 corresponded to the  $M^+$  parent ion, the peak at  $m/z$  109 corresponded to a loss of  $OH^+$ ,  $m/z$  97 was loss of  $CHO^+$ , and  $m/z$  81 was the methylene furan ring. Two important diagnostic ions for the presence of a furan ring were present:  $m/z$  29 and  $m/z$  39 which correspond to the fragments  $HC\equiv O^+$  and  $C_3H_3^+$  respectively, produced when cleavage occurs at the oxygen heteroatom. The mass spectra of the peaks in sultana extracts and of the authentic standard are shown in Figure 3.11. The mass spectra matched closely to that in the NIST-98 mass spectral library.

### 3.14 Statistical analysis

All statistical evaluations of data were performed using Genstat-5 ® for Microsoft Windows™ (Release 4.1, Fourth Edition, Statistics Department, IACR-Rothamsted, Harpenden, Hertsfordshire, England). The storage experiment was treated as a randomised, non-replicated, factorial design. Analysis of variance (ANOVA) was performed on storage trial data to evaluate the effect on the factors on the  $L^* a^* b^*$  data. Least significant difference data (LSD) was calculated for the appropriate level of factor interaction. More detailed information on the spreadsheet format for data is given in the each section.

### 3.15 Analytical results

The values for TSS and TA (Table 3.2) indicated that the maturity of the exposed fruit was more advanced than that of the protected fruit, although both were in the maturity range at which grapes may be harvested commercially to produce dried fruit. The tristimulus data show that the exposed berries were somewhat lighter, less green and more yellow than the protected fruit. Substrate PPO activity in both grape skin and flesh was similar in both exposed and shaded fruit. The PPO substrate activity data did not indicate large initial differences in either skin or flesh activity of the enzyme between exposed and protected fresh grapes.

Treatment	TSS	Titratable Acidity g.L <sup>-1</sup> n=5	Tristimulus Colour			Substrate PPO activity	
	(°Brix) n=5		L*	a*	b*	µmoles O <sub>2</sub> gram <sup>-1</sup> min <sup>-1</sup> Skin n=4	Flesh
exposed	26.3 ± 0.10	4.5 ± 0.1	47.49 0.98	-3.15 ± 0.75	27.96 ± 0.90	10.56 ± 1.80	3.66 ± 0.24
protected	20.4 ± 0.05	5.1 ± 0.1	41.14 ± 0.82	-9.14 ± 0.25	26.34 ± 0.61	11.20 ± 1.52	3.64 ± 0.40

Table 3.2 Analytical data for fresh berries collected from exposed and protected vines of experiment I 1995. Standard errors for total soluble solids (TSS) and titratable acidity are for the replicate measures on the juice of 100 berries.  $L^*a^*b^*$  tristimulus values are the means of 2 determinations performed on 25 individual berries. The standard error for PPO activity was determined for two analytical determinations on the skin and flesh of 2 × 20 fresh berries.

### 3.16 Preparation of sultanas for the storage trial

Sultanas were subjected to a number of treatments and stored according to the multi-factorial design shown in Figure 3.2. Thirty-kg lots each of exposed and protected grapes bunches were dipped in a standard dipping solution and allowed to dry on drying racks until they had reached approximately 15% moisture by 21 March 1995. Half of the dipped sultanas (approximately 5 kg), exposed and protected, were hosed down with water on racks late in the afternoon to simulate rain wetting and left overnight. Sultanas, which were sprayed down with water, will be referred to as 'rehydrated' hereafter. Those sultanas, which were not rehydrated, are referred to as 'non-rehydrated'. Rehydrated and non-rehydrated samples were further divided and one group was then subsequently 'sunfinished' and the other left 'non-sunfinished'. In order to sunfinish sultanas, fruit was spread out on black plastic ground sheets from 9.30am to 5.30pm on 22, 23 and 24 March. A thermometer was placed on the surface of the sultanas and temperatures recorded at 1.00pm on each of the days were 37.5°C, 49.5°C and 30.5°C respectively. A second temperature reading taken at 4.30pm on the same days was 39.0 °C, 46.5°C and 32.0 °C respectively. The various treatments produced 8 unique dipped sultana samples, which were produced as shown in Figure 3.2. Individual sultana treatments will be referred to by their corresponding codes in

Table 3.3 henceforth. A sub-sample of sultanas from each of the treatments was transported on dry ice to VUT and stored at -80°C until further chemical analysis. The bulk of the samples were transported in plastic bags on dry ice in insulated containers to VUT for use in the following storage experiment.

Sample Code	Sunfinishing	Vine Solar Exposure	Rehydration
SED	Sunfinished	Exposed	
NED	Non-sunfinished	Exposed	
SRED	Sun-finished	Exposed	Rehydrated
NRED	Non-sunfinished	Exposed	Rehydrated
SPD	Sunfinished	Protected	
NPD	Non-sunfinished	Protected	
SRPD	Sunfinished	Protected	Rehydrated
NRPD	Non-sunfinished	Protected	Rehydrated

Table 3.3 Codes for the sultana samples used in storage experiment I, 1995..

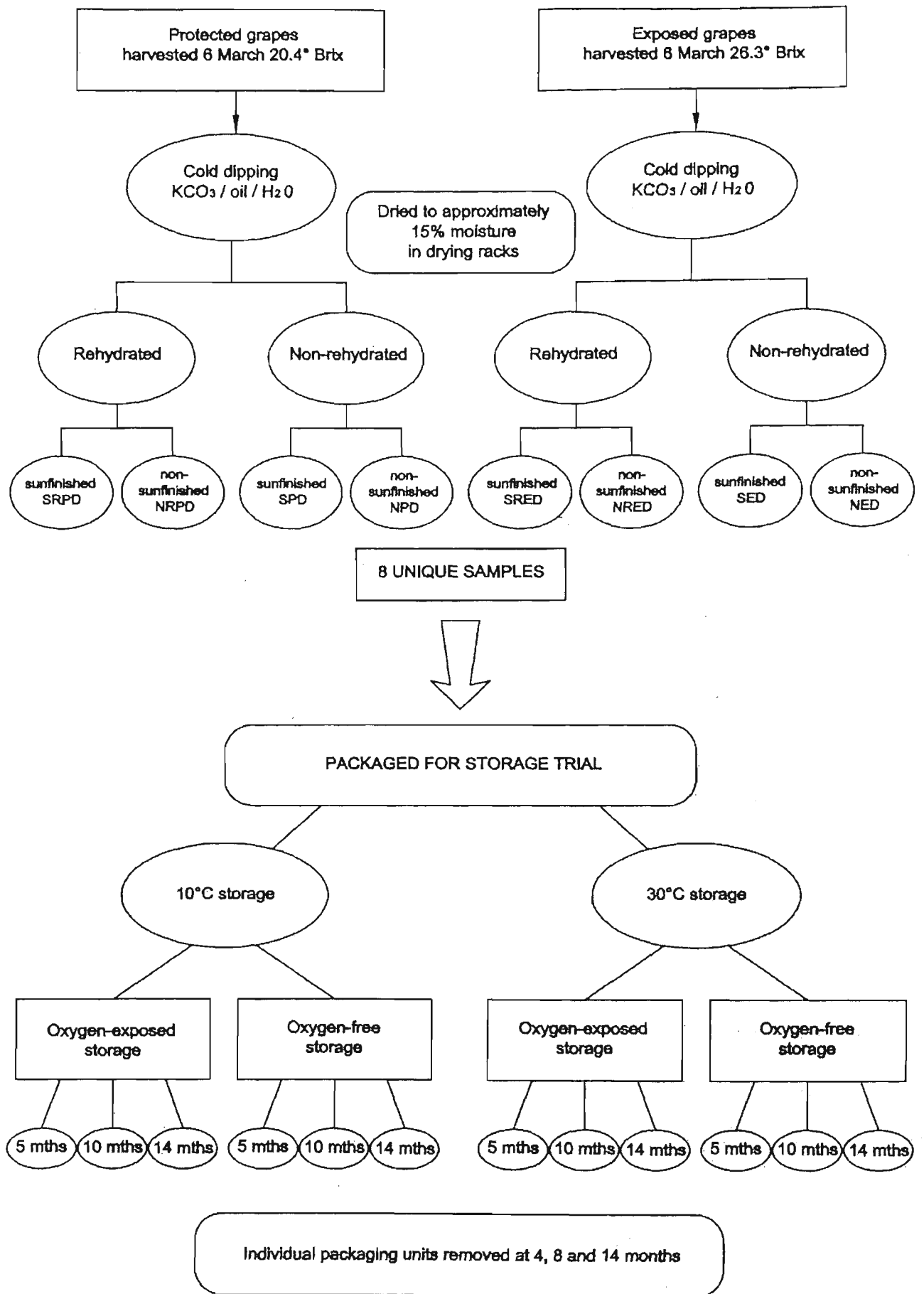


Figure 3.2 Diagram showing grape and sultana field treatments and packaging. There were 8 grape and 96 sultana samples.

### 3.17 Analysis of pre-storage sultanas

Analytical data for the sultanas at the beginning of the storage period (pre-storage) are shown in Table 3.4. Determinations were made on sultanas immediately after drying before packaging for storage. Individual replicate measurements for  $a_w$ , total phenolics, substrate skin and flesh PPO activity and mean  $L^*a^*b^*$  tristimulus data were arranged in spreadsheet format and subjected to ANOVA. The significance of any of these treatments on the variate data— $a_w$ , total phenolics, substrate PPO activity and  $L^*a^*b^*$  data—was assessed.

The combinations of the field and storage treatments were applied to provide variation in initial chemical and physical properties, hopefully being representative of typically sultanas arriving at packing sheds in a typical year. Whilst the design may have been able to test the significance of all the post-harvest and storage treatments, the interpretation of the significance of the effect of shading must be considered with the caveat that this treatment was not replicated.

### 3.18 Pre-storage $a_w$

Initial variation in  $a_w$  in 1995 sultanas can be seen in Table 3.4. The effects of exposure, rehydration and sunfinishing on initial  $a_w$  were assessed by ANOVA. Sunfinished sultanas had significantly lower  $a_w$  values (0.419- 0.458), than non-sunfinished sultanas (0.527-0.558) for every comparable treatment pair. The effect of Sultana vine exposure on  $a_w$  was not statistically significant. Rehydrated exposed fruit had slightly higher  $a_w$  values, however the difference was not statistically significant.

	Water activity	Total phenolics	Substrate PPO activity		Colour determination		
	$a_w$	caffeic acid equiv. $\text{mg.g}^{-1}$	$\mu\text{moles g}^{-1} \text{min}^{-1}$		Tristimulus values		
			Skin	Flesh	$L^*$	$a^*$	$b^*$
LSD ( $p=0.05$ )	0.053	0.50	0.576	1.366	4.42	2.18	2.96
SED	0.419	1.37	13.97	13.88	36.26	6.95	22.08
SRED	0.458	1.23	9.05	11.10	34.55	6.25	19.28
NED	0.527	1.22	12.71	10.81	33.26	3.12	18.20
NRED	0.558	1.30	12.22	11.58	34.45	4.81	19.21
SPD	0.448	1.76	12.60	16.81	34.67	3.55	21.00
SRPD	0.433	2.01	13.52	16.11	35.14	2.35	21.21
NPD	0.557	1.98	11.53	16.18	33.65	0.76	19.81
NRPD	0.543	1.57	13.62	15.94	33.67	0.85	20.27

Table 3.4 Pre-storage data for sultanas used in the 1995 experiment. LSD values were determined for the interaction of exposure, rehydration and sunfinishing using the mean values of the multiple determinations for each parameter.

### 3.19 Pre-storage total phenolics

Total phenolics are shown for whole sultanas in Table 3.4. Sunfinishing was found not to produce a significant decrease in initial total phenolics for comparable treatment pairs. The effect of rehydration was also not significant. The effect of exposure was found to be significant. All protected sultanas had higher total phenolics than comparable exposed sultanas: the small differences were not significant for all comparable exposed and protected pairs, however.

### 3.20 Pre-storage sultana PPO activity in skin and flesh

Skin-flesh PPO activity was assayed using 4-methylcatechol as a substrate. The effect of sultana exposure and sunfinishing on PPO skin-flesh activity was assessed using ANOVA analysis. Although there were small significant differences in PPO skin activity for all treatments—exposure, rehydration and sunfinishing—there were no clear trends in the data. Generally the treatments rehydration and sunfinishing were found not to have a significant effect. Pre-storage PPO activity was consistently higher in protected flesh compared to exposed sultanas.

In nearly all cases, the measured PPO activity in sultana skins was higher than in the corresponding grape skin samples (see Table 3.2), indicating that the PPO enzyme was not significantly denatured by the dipping or drying process. The overall increase in PPO activity measured in sultana flesh was most likely due to concentration of the enzyme during the dehydration process; during drying grape mass decreases by a factor of around four (DVFM 1998).

### 3.21 Pre-storage sultana colour

Pre-storage tristimulus  $L^*a^*b^*$  values are shown in Table 3.4. High values for  $L^*$  (lightness) and  $b^*$  (yellowness) are desirable and indicate light golden sultanas. The  $a^*$  (redness) coordinate is not as critical, but is useful to indicate the chlorophyll content of sultanas. Typical  $L^*a^*b^*$  values for five crown sultanas are around 35, 4.5 and 16 respectively (DVFM). The influence of the treatments exposure, rehydration and sunfinishing on initial  $L^*a^*b^*$  values was assessed. ANOVA data indicated grape exposure, rehydration and sunfinishing did not have a statistically significant effect on initial  $L^*$  or  $b^*$  values. Pre-storage sultana  $L^*$  values ranged from 33.26 to 36.26, and initial  $b^*$  values ranged from 18.20 to 22.08. Large variations in initial  $a^*$  values are clearly shown in Table 3.4. Protected sultanas were greener (indicating a higher chlorophyll content—not measured) and thus had relatively low  $a^*$  values. In contrast  $a^*$  values were significantly higher in exposed sultanas. Sunfinishing significantly lowered sultana greenness. Sunfinished fruit had significantly higher  $a^*$  values than non-sunfinished counterparts. For all samples, initial  $L^*$  and  $b^*$  values were within the five crown classification, however  $a^*$  values of the protected sultanas were lower than would be normally be desirable.

### 3.22 Storage trial preparation

Oxygen-free storage was created using oxygen barrier packaging and commercial oxygen scavenger sachets as described previously. In order that the oxygen-free status was not disturbed during storage, fruit from each unique sultana treatment was divided into thirds (each of around 150g) and packaged in separate individual oxygen-free packages. Sultanas stored in this manner will be referred to as 'oxygen-free' for the remainder of this chapter. The remaining fruit was divided into three portions (150g each) and packaged in open snap-lock polyethylene bags (Glad, Australia) which were stored fully exposed to oxygen and will be referred to hereafter as 'oxygen-exposed' sultanas. Oxygen-free and oxygen-exposed samples were stored at 10°C and 30°C in temperature-controlled, computer-monitored environments at the Australian Food Industry Science Centre (AFISC). The data logger for the temperature-controlled rooms indicated that the temperatures were maintained within  $\pm 1.0^\circ\text{C}$  for the entirety of the storage experiment. Samples were removed at 4, 8 and 14 months for physical and chemical analysis. Thus after 4, 8 and 14 months storage an entire packaging unit was removed, obviating the need to open bulk packages and disturb the oxygen-free status brought about by the packaging technology. As previously described, commercial Ageless-Eye oxygen indicators were used in all oxygen-free packages to monitor the oxygen-free status. After 14 months storage at both 10°C and 30°C, oxygen indicators were still bright pink indicating oxygen levels of 0.1% or less. Further evidence of the oxygen-free status was obtained by GC-MS.

### 3.23 Storage colour change and statistical analysis

The effect of the various treatments on the storage colour of sultanas was investigated via ANOVA. The data was first arranged in a spreadsheet format and then imported into Genstat. An unblocked-randomised statistical analysis was applied to the data. It was assumed that there were no inherent differences between the plastic storage pouch units which were removed at specific time intervals i.e. 4, 8 and 14 months. ANOVA tables are shown for each of the main effects and significant interactions for the  $L^*a^*b^*$  tristimulus coordinates. There were significant interactions up to the four-way level; no five-way interactions were found to be statistically significant. Tables of mean data were used for the graphical presentation of the data and LSD data were generated for the appropriate level of interaction. Sample packaging units were removed from storage after 4, 8 and 14 months, opened and colour was measured using the Minolta Chromameter; an average of  $2 \times 50$  readings was used for each sample. Changes in the individual  $L^*a^*b^*$  tristimulus values are presented in the following sections.

### 3.24 Storage changes in $L^*$ tristimulus coordinate

The  $L^*$  or lightness tristimulus value is the most indicative single measure of the overall brightness of sultanas, generally when  $L^*$  is high so is the  $b^*$  value. High  $L^*$  values can be accompanied by either high or low  $a^*$  values, as has already been seen with the large differences in pre-storage  $a^*$  values, with relatively constant  $L^*$  and  $b^*$  values (Table 3.4). The ANOVA data for sultana lightness (Table 3.5) indicated that the main effect on  $L^*$  was due to the storage temperature. The main significant factors ( $p < 0.05$ ) attributed to changes in  $L^*$  were the storage

temperature, sunfinishing, the temperature×time interaction, the level of oxygen exposure and time. Exposure level and the rehydration treatments were both statistically significant, but were relatively small effects. As the rehydration treatment was not found to have a significant effect on either  $a^*$  or  $b^*$  values, its effect was not further examined. The four-way interaction of sunfinishing×oxygen×temperature×time, are presented graphically in Figure 3.3. The average values of  $L^*$  for both protected and exposed +fruit together, and the overall effects of sunfinishing and oxygen level are shown at 10°C (top) and 30°C (bottom). The bars represent the LSD (1.76  $p=0.05$ ). The two columns on the left-hand side of each graph represents the mean pre-storage  $L^*$  value for all sunfinished sultanas (left) and all non-sunfinished sultanas (right). As was previously stated, initially there was not a significant difference between sunfinished or non-sunfinished fruit (Table 3.4).

The upper graph in Figure 3.3 shows the effect on  $L^*$  of time, sunfinishing and oxygen exposure for sultanas stored at 10°C. Under these conditions, sunfinished sultanas stored in oxygen (s-ox) did not undergo significant decrease in  $L^*$  over the first four-month period, however a small significant decrease in  $L^*$  values was measured after 8 and 14 months. In contrast, sunfinished sultanas stored in an oxygen-free environment did not undergo significant decrease in  $L^*$  over time. Non-sunfinished sultanas stored in oxygen-exposed (n-ox) and oxygen-free (n-nox) storage environments underwent significantly more browning than sunfinished controls. The  $L^*$  values were significantly lower for non-sunfinished, oxygen-exposed sultanas compared with oxygen-free sultanas, however the difference was only small. The increase in  $L^*$  values at 14 months for non-sunfinished sultanas was most likely due to the extensive internal sugaring which occurred from 8 to 14 months, which presumably greatly increased the luminosity of sultana surfaces and hence  $L^*$  values. Internal sugaring is discussed in section 3.31.

At 30°C storage (Figure 3.3 -bottom graph), significant decreases in  $L^*$  were observed for all treatments (sunfinishing, oxygen and time).  $L^*$  values for sunfinished sultanas were significantly higher than non-sunfinished controls at 4 and 8 months and significant for all treatments except for the oxygen-free stored sample at 14 months. The largest decreases in  $L^*$  occurred in higher moisture, non-sunfinished, oxygen-exposed (n-ox) sultanas. The second greatest decreases in  $L^*$  were measured in similar sultanas stored under oxygen-free conditions (n-nox). This data indicates that the browning processes affecting  $L^*$  occurred more rapidly at the higher temperature (30°C) and were strongly affected by  $a_w$  regardless of the oxygen exposure level. Since both PPO and Maillard processes are strongly  $a_w$  sensitive, higher rates of browning at a higher  $a_w$  alone would not indicate PPO or Maillard processes. The fact that large decreases in  $L^*$  values occurred also in the absence of oxygen indicated that non-oxygen dependent reactions, such as Maillard type reactions, must have occurred in sultanas even at fairly low storage temperatures, such as at 10°C and 30°C.

Although the effect of vine shading was rated significant ( $p=0.003$ ) it accounted for only a small portion of variance in storage  $L^*$  values. Comparisons for means of treatments indicated that

average  $L^*$  values were slightly significantly lower for non-sunfinished-protected fruit (pro-n) compared to non-sunfinished-exposed sultanas (ex-n) after 8 and 14 months storage (graph not shown). No significant difference was found between protected and exposed sultanas for the other storage conditions.

### 3.25 Storage change in $a^*$ tristimulus coordinate

Redness ( $a^*$ ) values changed mainly for high temperature stored fruit. For oxygen-exposed and oxygen-free samples at 30°C,  $a^*$  increased during storage as the sultanas became redder. Generally for non-oxygen-exposed fruit,  $a^*$  values increased steadily during the 14 months. In contrast for oxygen exposed fruit  $a^*$  values increased to reach a lower maximum and then decreased, especially for non-sunfinished fruit (high  $a_w$ ). Redness values remained fairly static throughout the storage period in low temperature stored sultanas, both oxygen-exposed and oxygen-free.

ANOVA analysis of  $a^*$  data indicated that temperature was the most important single factor, followed by exposure, time and oxygen (Table 3.6). In Figure 3.4 the effects of sunfinishing, storage, oxygen, exposure, sunfinishing and time on  $a^*$  values is shown at 10°C (top) and 30°C (bottom). At 10°C in the presence of oxygen  $a^*$  values remained close to initial values; significant changes were not observed. Average  $a^*$  values for sunfinished fruit stored at 10°C in an oxygen-free environment were significantly higher at 8 months and then decreased up to 14 months. The  $a^*$  tristimulus values for non-sunfinished higher moisture sultanas increased over time at 10°C, both in the presence and absence of oxygen:  $a^*$  values were significantly higher for oxygen-free samples compared to oxygen-exposed controls.

At 30°C storage all sultanas increased significantly in redness. At 4 months average  $a^*$  values were similar, with no significant effect observed for the treatments oxygen or sunfinishing. After 8 months storage, lower  $a_w$  sunfinished fruit had increased in redness, with sultanas stored in the absence of oxygen being significantly redder at 8 months. Higher  $a_w$  non-sunfinished fruit did not undergo significant increases in  $a^*$  values after 4 months. Overall the lowest  $a^*$  values were observed in non-sunfinished fruit stored in the presence of oxygen. It is important to note that the  $a^*$  tristimulus value is not as strong an indicator of overall sultana colour as the  $L^*$  and  $b^*$  tristimulus values. For example a low  $a^*$  value may be found for light sultanas which have a green tinge, whilst a comparable  $a^*$  value may be found on a dark brown sultana which also has relatively low  $L^*$  and  $b^*$  values.

The effect of vine exposure on sultana  $a^*$  values is shown in Figure 3.4. The lower  $a^*$  values measured pre-storage in protected sultanas were maintained for all sunfinishing and storage temperature conditions. At 10°C  $a^*$  values increased from 4 to 8 months for both protected and exposed fruit (sunfinished and non-sunfinished) and then decreased to 14 months. At 10°C exposed sultanas were significantly redder than protected at all times. At 30°C storage  $a^*$  values increased substantially for exposed and protected fruit;  $a^*$  values were higher in exposed sultanas than protected at all times.

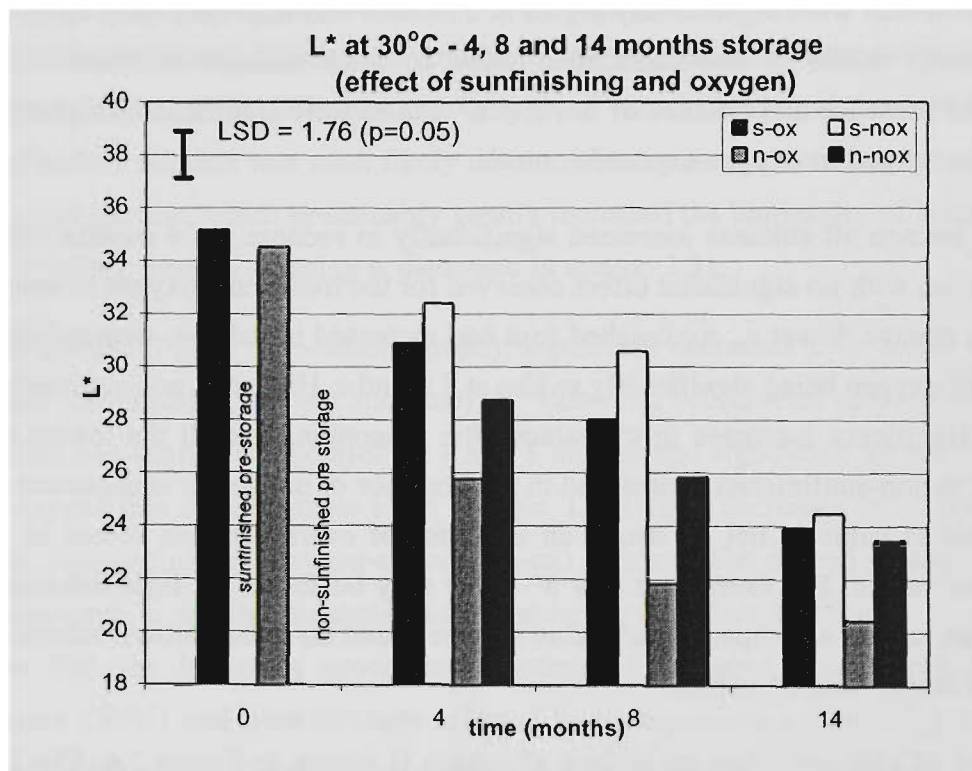
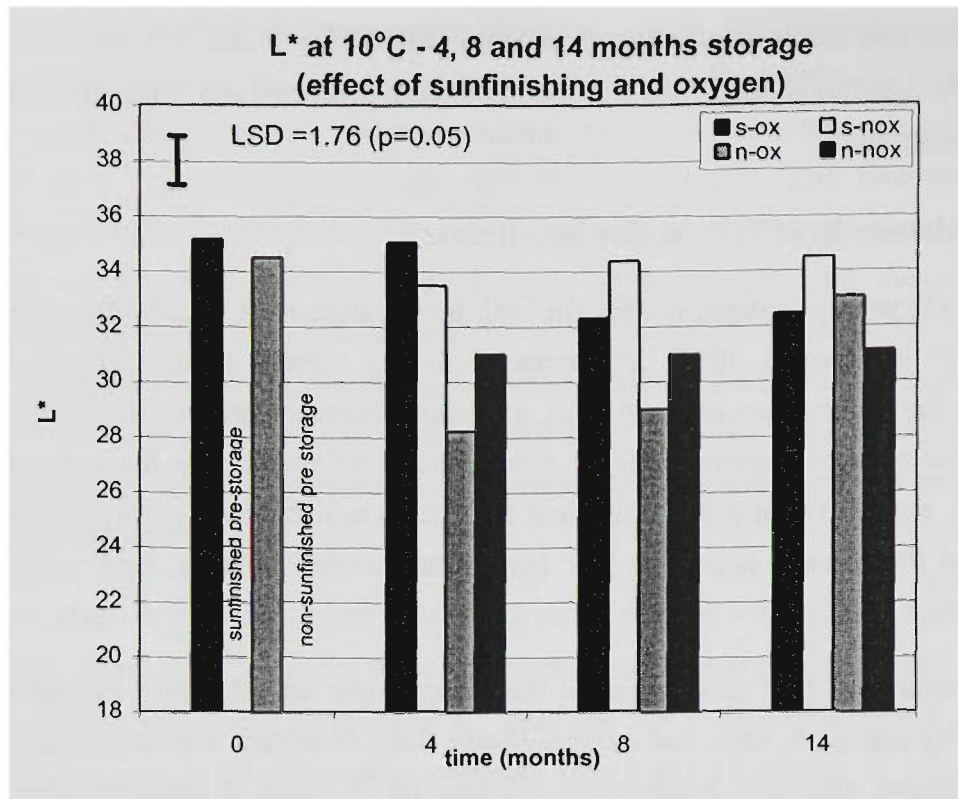


**Figure 3.3** Effects of sunfinishing and oxygen exposure on  $L^*$  values for exposed and protected sultana combined.

$L^*$  tristimulus values at 4, 8 and 14 months at 10°C (top) and 30°C (bottom). The two single columns on the far left are the average pre-storage  $L^*$  values for sunfinished (left column) and non-sunfinished (right column) protected and exposed sultanas. Codes are s-ox (sunfinished + oxygen), n-ox (non-sunfinished + oxygen), s-nox (sunfinished no oxygen) and n-nox (non-sunfinished no oxygen). LSD was calculated for the treatments sunfinishing, oxygen, temperature and time.

Source of variation for L*	d.f.	s.s	m.s.	v.r.	F pr.
exposure	1	16.484 (0.90%)	16.484	13.20	0.003
rehydration	1	6.966 (0.38%)	6.966	5.58	0.034
sunfinishing	1	307.307 (16.85%)	307.307	246.03	<0.001
oxygen	1	66.560 (3.64%)	66.567	53.29	<0.001
temperature	1	798.107 (43.76%)	798.107	638.96	<0.001
time	2	123.166 (6.75%)	61.583	49.30	<0.001
exposure.rehydration	1	0.725	0.725	0.58	0.460
exposure.sunfinishing	1	5.626	5.626	4.50	0.054
Rehydration.sunfinishing	1	3.92	3.920	3.14	0.100
exposure.oxygen	1	0.004	0.004	0.00	0.959
rehydration.oxygen	1	8.604	8.604	6.89	0.021
sunfinishing.oxygen	1	5.134	5.134	4.11	0.064
exposure.temperature	1	1.949	1.949	1.56	0.234
rehydration.temperature	1	4.472	4.472	3.58	0.081
sunfinis.temperature	1	4.905	4.905	3.93	0.069
oxygen.temperature	1	14.477 (0.79%)	14.477	11.59	0.005
exposure.time	2	4.347	2.174	1.74	0.214
rehydration.time	2	0.752	0.376	0.3	0.745
sunfinishing.time	2	37.373	18.687	14.96	<0.001
oxygen.time	2	12.616	6.308	5.05	0.024
temperature.time	2	213.007 (11.67%)	106.504	85.27	<0.001
exposure.rehydrat.sunfinish	1	15.296	15.296	12.25	0.004
exposure.sunfinish.temperature	1	9.767	9.767	7.82	0.015
rehydrat.oxygen.temperature	1	9.102	9.102	7.29	0.018
sunfinish.oxygen.time	2	13.721	6.861	5.49	0.019
exposure.rehydrat.temp.time	2	15.599	7.800	6.24	0.013
exposure.sunfinis.temp.time	2	12.516	6.258	5.01	0.024
sunfinis.oxygen.temp.time	2	21.286	10.643	8.52	0.004
<b>Pooled non-significant three and four-way interactions</b>		<b>74.708</b>			
<b>Residual</b>	<b>13</b>	<b>16.238</b>	<b>1.249</b>		
<b>Total</b>	<b>95</b>	<b>1824.734</b>			

Table 3.5 ANOVA table for L\* showing all main effects and two-way interactions. Interactions which were significant ( $p=0.05$ ) are highlighted in grey. Only the significant three- and four-way interactions are shown. Non-significant three and four-way interaction SS was pooled.

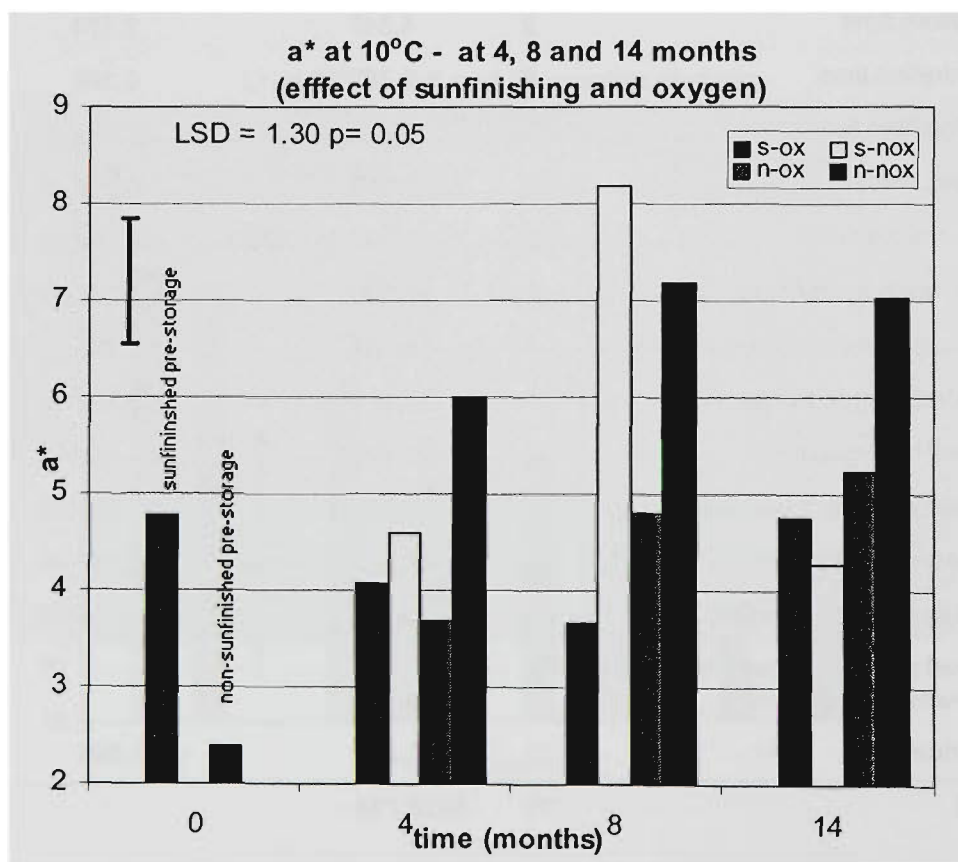
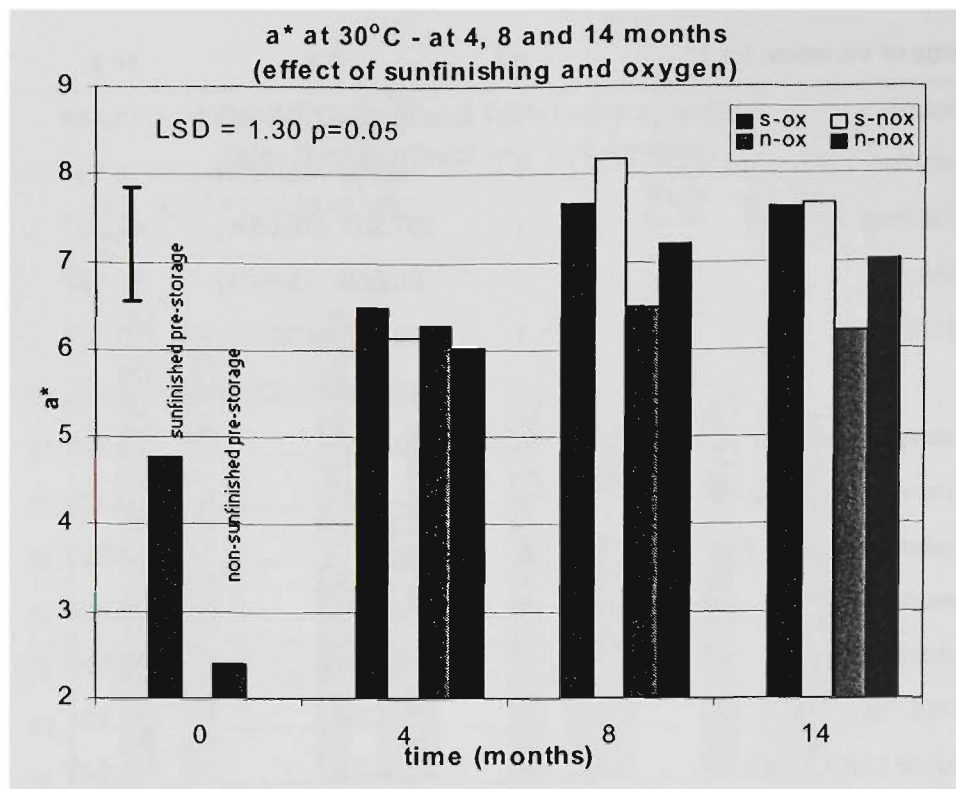


**Figure 3.4** Average  $a^*$  tristimulus values at 4, 8 and 14 months at 10°C (top) and 30°C (bottom). Effects of sunfinishing and oxygen exposure on average  $a^*$  values for exposed and protected sultanas. The two single columns on the far left are average pre-storage  $a^*$  values for sunfinished (left column) and non-sunfinished (right column). Codes are s-ox (sunfinished + oxygen), n-ox (non-sunfinished+ oxygen), s-nox (sunfinished no oxygen) and n-nox (non-sunfinished no oxygen). LSD was calculated for the treatments sunfinishing, oxygen, temperature and time.

Source of variation for a*	d.f.	s.s	m.s.	v.r.	F pr.
exposure	1	74.836 (21.92%)	74.836	115.06	<0.001
rehydration	1	1.7173	1.7173	2.64	0.128
sunfinishing	1	2.5611	2.5611	3.94	0.069
oxygen	1	12.9213 (3.7%)	12.9213	19.87	<0.001
temperature	1	89.7453 (26.30%)	89.7453	137.99	<0.001
time	2	37.7278 (11.05%)	18.8639	29	<0.001
exposure.rehydration	1	4.6552 (1.36%)	4.6552	7.16	0.019
exposure.sunfinishing	1	2.5938	2.5938	3.99	0.067
rehydrat.sunfinishing	1	0.3015	0.3015	0.46	0.508
exposure.oxygen	1	0.3553	0.3553	0.55	0.473
rehydration.oxygen	1	2.7473	2.7473	4.22	0.061
sunfinishing.oxygen	1	0.0793	0.0793	0.12	0.732
exposure.temperature	1	4.335	4.335	6.67	0.023
rehydration.temperature	1	0.0122	0.0122	0.02	0.893
sunfinishing.temperature	1	4.4893	4.4893	6.9	0.021
oxygen.temperature	1	5.733	5.733	8.81	0.011
exposure.time	2	2.7515	1.3758	2.12	0.16
rehydration.time	2	1.2848	0.6424	0.99	0.399
sunfinishing.time	2	0.6236	0.3118	0.48	0.63
oxygen.time	2	20.4296	10.2148	15.71	<0.001
exposure.oxygen.temp	1	5.0968	5.0968	7.84	0.015
sunfinish.temp.time	2	5.288	2.644	4.07	0.043
oxygen.temp.time	2	11.9389	5.9694	9.18	0.003
<b>Pooled non-significant three and four-way interactions</b>		<b>40.610</b>			
<b>Residual</b>	<b>13</b>	<b>8.455</b>	<b>0.6504</b>		
<b>Total</b>	<b>95</b>	<b>341.2855</b>			

Table 3.6 ANOVA table for a\* showing all main effects and two-way interactions. Interactions which were significant ( $p=0.05$ ) are highlighted in grey. Only the significant three- and four-way interactions are shown. Non-significant three and four-way interaction SS was pooled

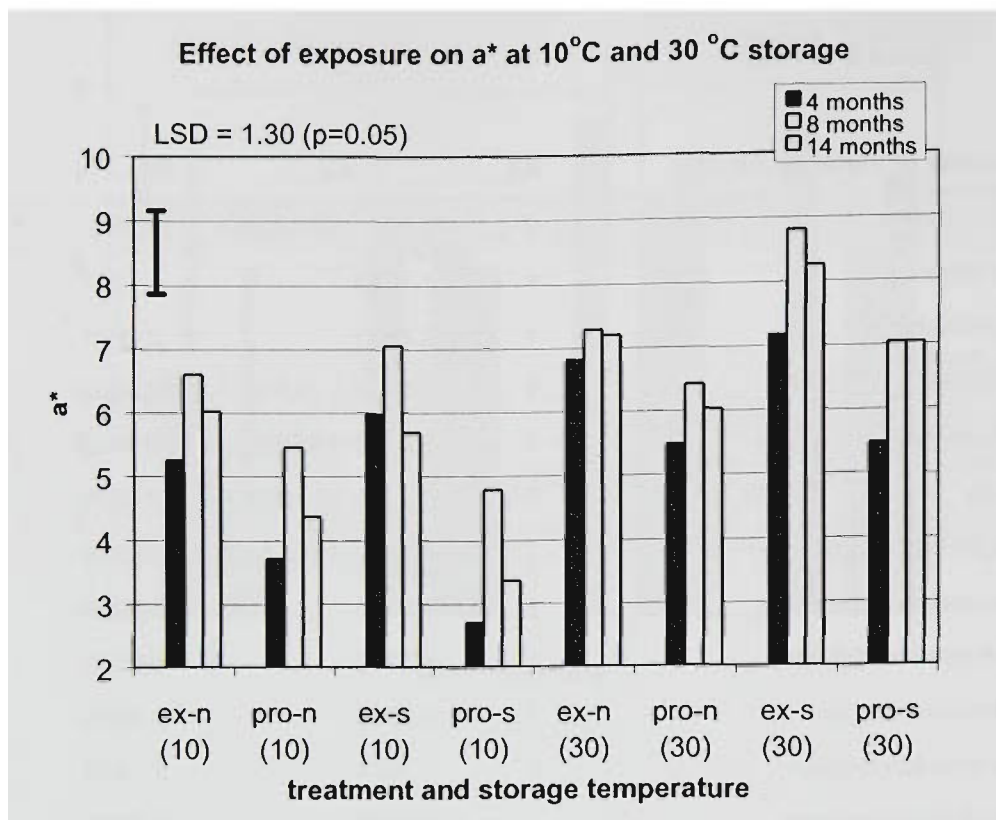
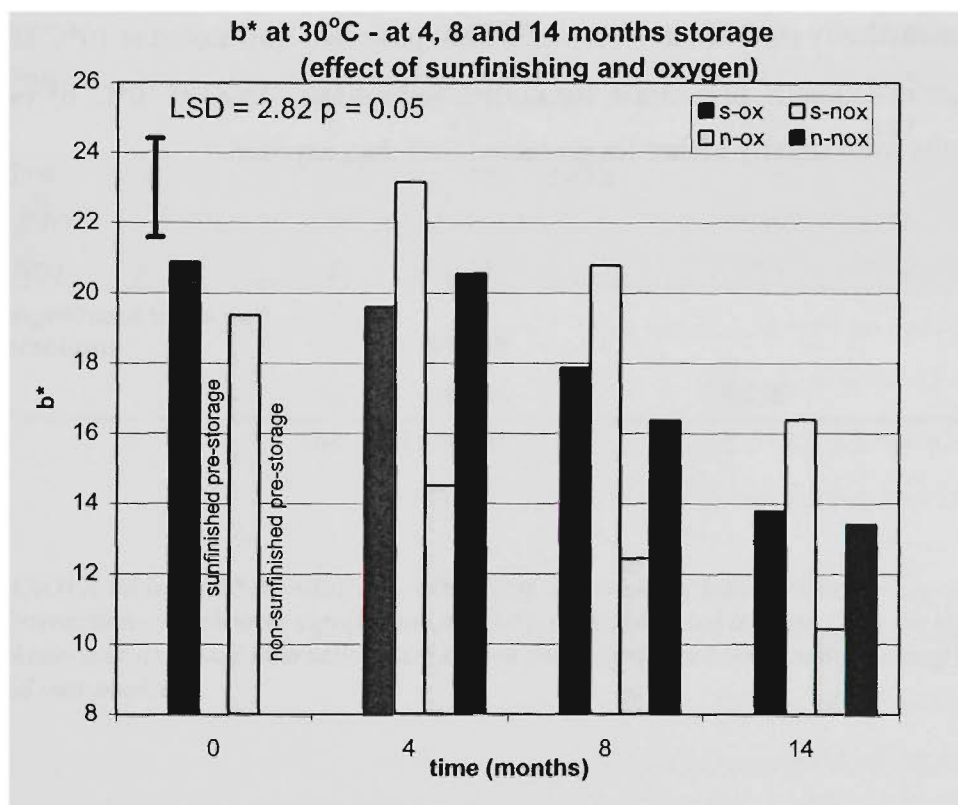
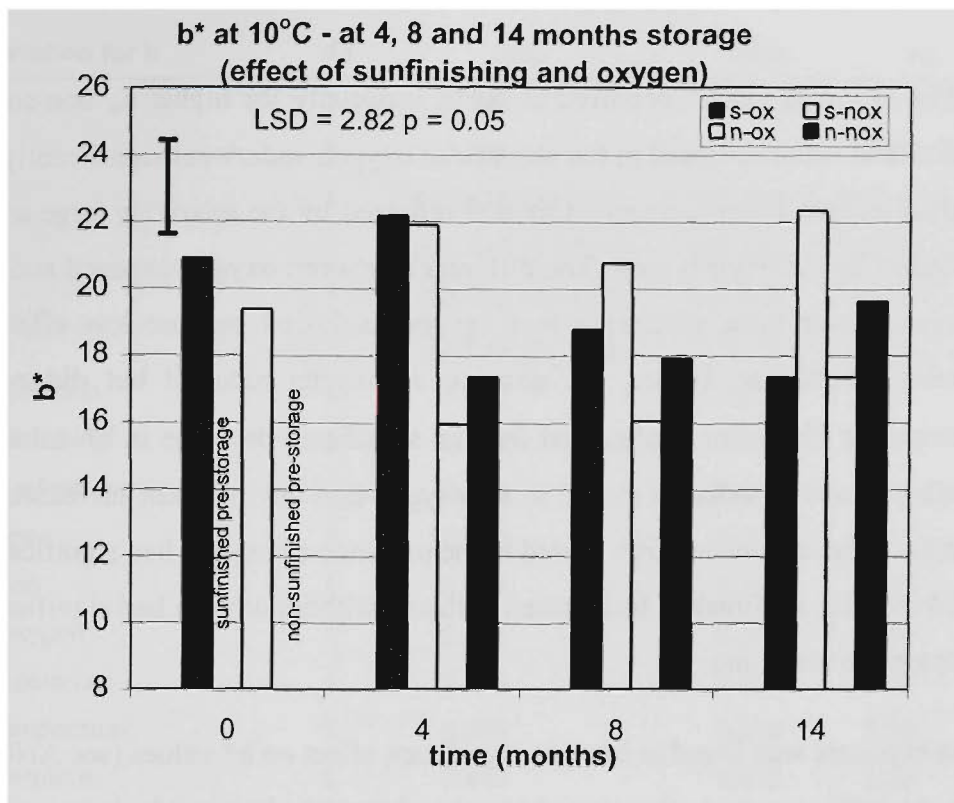


Figure 3.5 Effect of vine exposure on a\* tristimulus values. Sunfinished (s) and non-sunfinished (n) exposed (ex) and protected (pro) sultanas at 10°C (10) and 30°C (30) storage. LSD was determined for the interaction of exposure, sunfinishing, temperature and time.

### 3.26 Storage changes in b\* tristimulus coordinate

The b\* tristimulus coordinate (yellowness) is also a strong measure of overall sultana lightness. High b\* values indicate a high yellow index which is desirable for sultanas. Generally as browning processes advance, b\* values decrease, along with decreases in L\* values. ANOVA data showed that the strongest single factors influencing b\* values were sunfinishing, oxygen, temperature and time in that order.

Changes in average b\* values over time at 10°C are shown in Figure 3.6. Low a<sub>w</sub>, sunfinished sultanas stored at 10°C in the absence of oxygen did not undergo significant decreases in b\* at any time. In the presence of oxygen, sunfinished fruit decreased in b\* values slowly over time, however the decrease was statistically significant only at 14 months. The increase in values at 14 months was once again most likely due to internal sugaring effects and should be interpreted with some caution. The effect of non-sunfinishing on b\* values at 10°C is illustrated by the fact that non-sunfinished fruit was significantly lower than sunfinished controls stored either in the presence or absence of oxygen at 4 months. At 8 months, although average b\* values were lower for oxygen-exposed sultanas, the difference was not significant for oxygen-free fruit.



*Figure 3.6 Average b\* tristimulus values at 4, 8 and 14 months at 10°C (top) and 30°C (bottom). Effects of sunfinishing and oxygen exposure on average b\* values for exposed and protected sultanas. The two single columns on the far left are average pre-storage b\* values for sunfinished (left column) and non-sunfinished (right column). Codes are s-ox (sunfinished + oxygen), n-ox (non-sunfinished + oxygen), s-nox (sunfinished no oxygen) and n-nox (non-sunfinished no oxygen). LSD was calculated for the treatments sunfinishing, oxygen, temperature and time.*

Largest decreases in  $b^*$  occurred at 30°C, especially for higher  $a_w$  non-sunfinished fruit. Non-sunfinished sultanas stored in the absence of oxygen underwent significantly smaller decreases in  $b^*$  than oxygen stored sultanas; this was reflected by the relatively large amount of SS variance explained by the oxygen term. The difference between oxygen-exposed and oxygen-free samples decreased over time, indicating that oxygen exclusion became less effective with increasing duration of storage. Hence, the absence of oxygen retarded but did not prevent browning processes at 30°C. For sunfinished fruit no significant decrease in  $b^*$  values was measured at 4 months, however, sultanas stored in an oxygen-free environment increased in yellowness. At 8 months, only sunfinished fruit stored in the presence of oxygen had significantly lower  $b^*$  values. At 14 months, sunfinished fruit stored with and without oxygen had significantly lower  $b^*$  values compared to zero time.

Vine exposure was found to have no significant effect on  $b^*$  values (see ANOVA data in Table 3.7). At 30°C storage, both exposed (ex-n) and protected (pro-n) had almost identical  $b^*$  values at each time: sunfinished -protected fruit had slightly lower  $b^*$  values, however the differences were not statistically significant. Non-sunfinished protected fruit stored at 10°C had slightly lower  $b^*$  values at 8 months. In contrast, for sunfinished sultanas stored at 10°C,  $b^*$  values at 8 and 14 months were slightly higher for protected fruit than exposed.

Source of variation for b	d.f	s.s.	m.s.	v.r.	F pr.
exposure	1	2.100	2.100	1.04	0.326
rehydration	1	0.756	0.756	0.37	0.551
sunfinishing	1	321.494 (27.32%)	321.494	159.35	<0.001
oxygen	1	207.329 (17.62%)	207.329	102.76	<0.001
temperature	1	123.216 (10.47%)	123.216	61.07	<0.001
time	2	138.668 (11.7%)	69.334	34.36	<0.001
exposure.rehydration	1	0.018	0.018	0.01	0.927
exposure.sunfinishing	1	0.803	0.803	0.40	0.539
rehydration.sunfinishing	1	2.350	2.350	1.16	0.300
exposure.oxygen	1	0.226	0.226	0.11	0.743
rehydrat.oxygen	1	5.714	5.714	2.83	0.116
sunfinishing.oxygen	1	2.301	2.300	1.14	0.305
exposure.temperature	1	2.933	2.933	1.45	0.249
rehydration.temperature	1	6.816	6.816	3.38	0.089
sunfinis.temperature	1	2.413	2.413	1.20	0.294
oxygen.temperature	1	12.951	12.951	6.42	0.025
exposure.time	2	0.371	0.185	0.09	0.913
rehydration.time	2	5.825	2.912	1.44	0.272
sunfinishing.time	2	27.682	13.841	6.86	0.009
oxygen.time	2	1.085	0.542	0.27	0.768
temperature.time	2	152.111 (12.93%)	76.055	37.7	<0.001
sunfinis.temp.time	2	21.298	10.649	5.28	0.021
oxygen.temp.time	2	20.64	10.320	5.12	0.023
<b>Pooled non-significant three and four-way interactions</b>		<b>91.203</b>			
<b>Residual</b>	<b>13</b>	<b>26.228</b>	<b>2.018</b>		
<b>Total</b>	<b>95</b>	<b>1176.531</b>			

Table 3.7 ANOVA table for b\* showing all main effects and two-way interactions. Interactions which were significant ( $p=0.05$ ) are highlighted in grey. Only the significant three- and four-way interactions are shown. Non-significant three and four-way interaction SS was pooled

### 3.27 Storage changes in sultana free-amino acid profiles

The storage trial data indicated that a reasonable degree of the browning which occurred in sultanas was not inherently oxygen dependent and hence pointed towards the possibility of non-oxygen dependent Maillard-type reactions. Identification of a decrease in amino acids during storage would provide *prima facie* evidence that Maillard reactions may have occurred.

Samples from the storage trial—removed at 4, 8 and 14 months—were stored at  $-80^{\circ}\text{C}$  for later chemical analysis. In an initial investigation, SED, NED, SPD and NPD sultanas were analysed for free-amino acid profiles at 0 time and after 14 months at each of the four storage conditions. Triple 80% methanol extracts from two sub-samples of sultanas ( $n=20$ ) were analysed for free-amino acids using F-moc pre-column derivatisation and HPLC fluorescence detection. Figure 3.8 shows typical F-moc HPLC profiles for sultana extracts after 14 months storage in an oxygen-free environment at  $10^{\circ}\text{C}$  (top) and  $30^{\circ}\text{C}$  (bottom). Figure 3.9 shows HPLC profiles of sultana extracts stored at  $10^{\circ}\text{C}$  and  $30^{\circ}\text{C}$  in an oxygen-exposed environment. The dominant peaks on the chromatograms were an unidentified compound eluting at 10.2 min., arginine at 12.3 min., glycine internal standard (IS) at 15.5 min., F-moc-OH at 17.3 min. (an artefact of derivatisation) and proline at 19.7 min. As can be seen from the chromatograms, the only amino acid to decrease over time was arginine, only at  $30^{\circ}\text{C}$  storage, indicating that this amino acid may be involved in Maillard type browning processes. The small peaks at 5.4 min., 6.5 min. etc. were not identified, however, as the concentration of these compounds did not change for any of the storage conditions, it was assumed that they did not play a role in Maillard processes. The unidentified compound increased significantly in concentration only at  $30^{\circ}\text{C}$  storage, both in the presence and absence of oxygen, implying that it may be a Maillard reaction intermediate e.g. the arginine Amadori product. Figure 3.7 shows concentrations of each of the two main free-amino acids prior to storage and after storage for 14 months at each of the four conditions. After storage at  $30^{\circ}\text{C}$  for 14 months almost all free-arginine had disappeared from the sultana extracts irrespective of the presence or absence of oxygen. The concentration of arginine also underwent smaller significant decreases in a number of samples stored at  $10^{\circ}\text{C}$ , especially in the presence of oxygen. The concentration of the unidentified compound (peak at 10.2 min.) increased in samples stored at  $30^{\circ}\text{C}$  and did not change in those stored at  $10^{\circ}\text{C}$ .

Changes in the concentration of free-arginine in 80% MeOH extracts of whole sultanas were quantified by OPA-pre-column derivatisation and HPLC analysis, in pre-storage samples and in samples stored at  $30^{\circ}\text{C}$  (with and without oxygen) at 4, 8 and 14 months. Figure 3.10 shows the changes in concentration of free-arginine, which occurred over the 14-month storage period. Similar behaviour was observed for samples stored in the presence of oxygen (results not shown). Pre-storage protected fruit had significantly higher concentrations of arginine ( $4.6\text{--}3.2\text{ mg.g}^{-1}$ ) than exposed sultanas ( $1.4\text{--}1.7\text{ mg.g}^{-1}$ ). After 4 months storage, the arginine concentration in protected sultanas had already decreased to an average concentration of  $0.81\text{ mg.g}^{-1}$  and in exposed sultanas to an average value of  $0.65\text{ mg.g}^{-1}$ . Only trace amounts of arginine were measured at 8 and 14 months. The relative distribution of arginine in sultana skin and flesh was analysed (Table 3.8). The concentration of free-arginine was greater in the skins of sultanas, especially in protected sultanas.

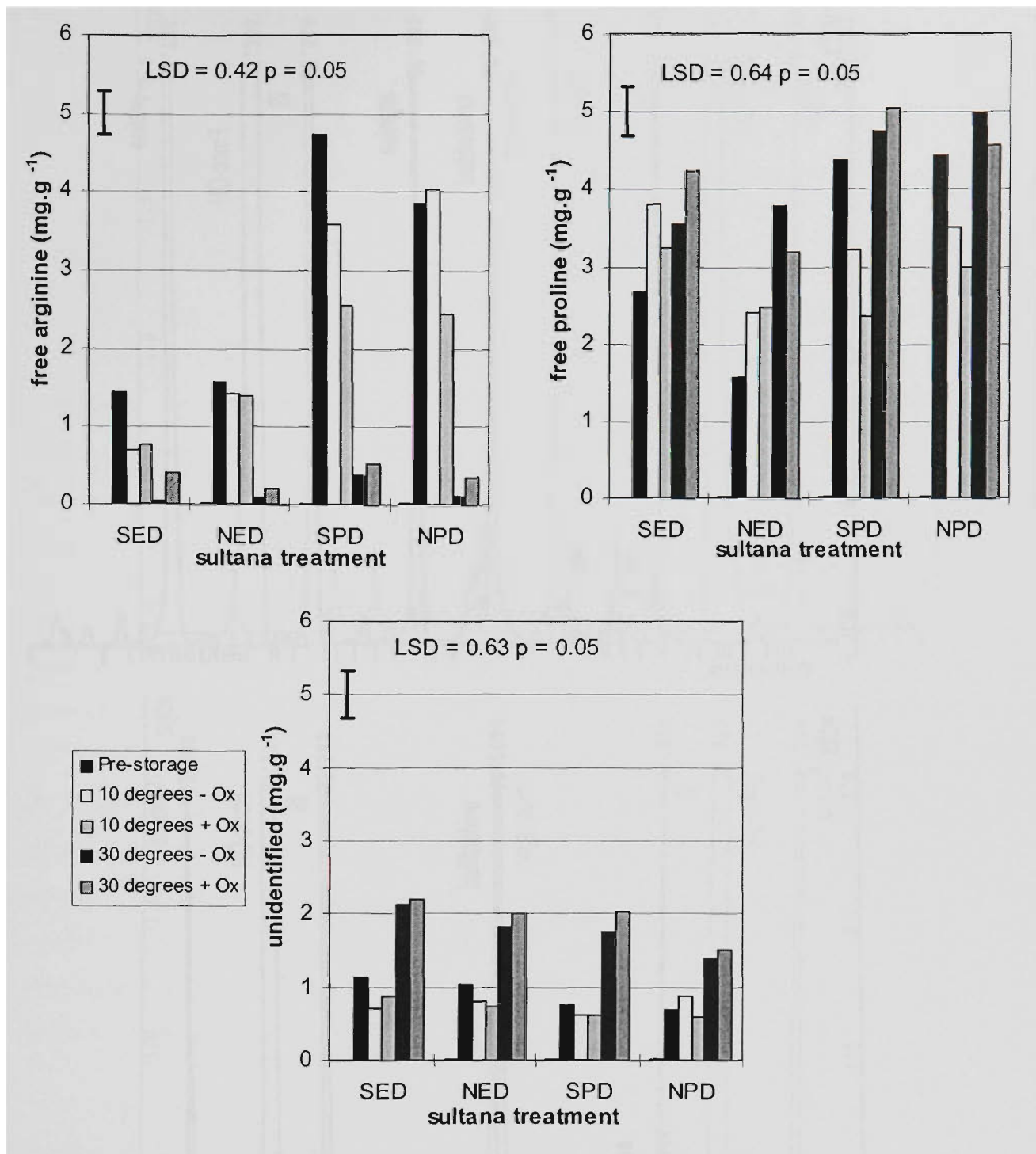


**Figure 3.7** Concentration of *F*-moc derivatised free-amino acids. Arginine, proline and an unidentified compound in triple extracts of whole sultanas made prior to storage and after storage for 14 months at 10°C or 30°C, with (+) or without (-) oxygen (Ox). Two samples of 20 sultanas were extracted for each treatment and duplicate measurements were made. The LSD was determined on the mean values for the sub-samples by ANOVA for the four-way interaction of exposure, sunfinishing, oxygen and temperature.

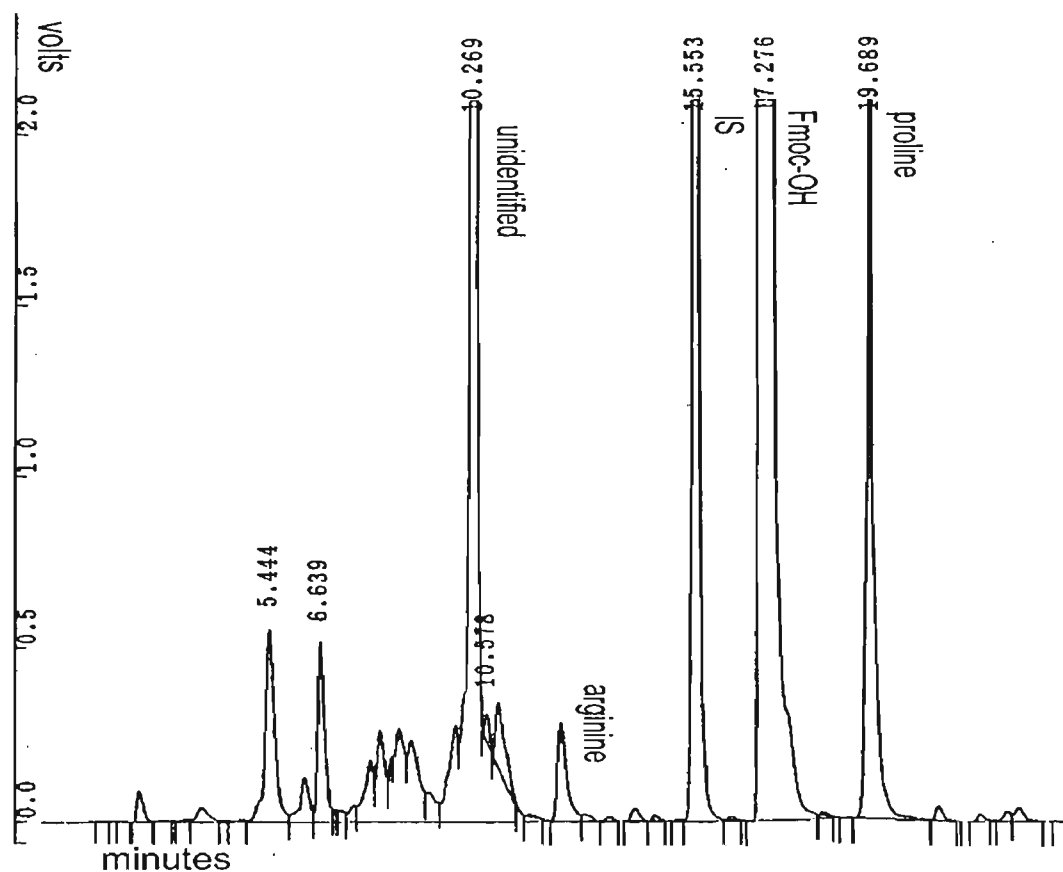
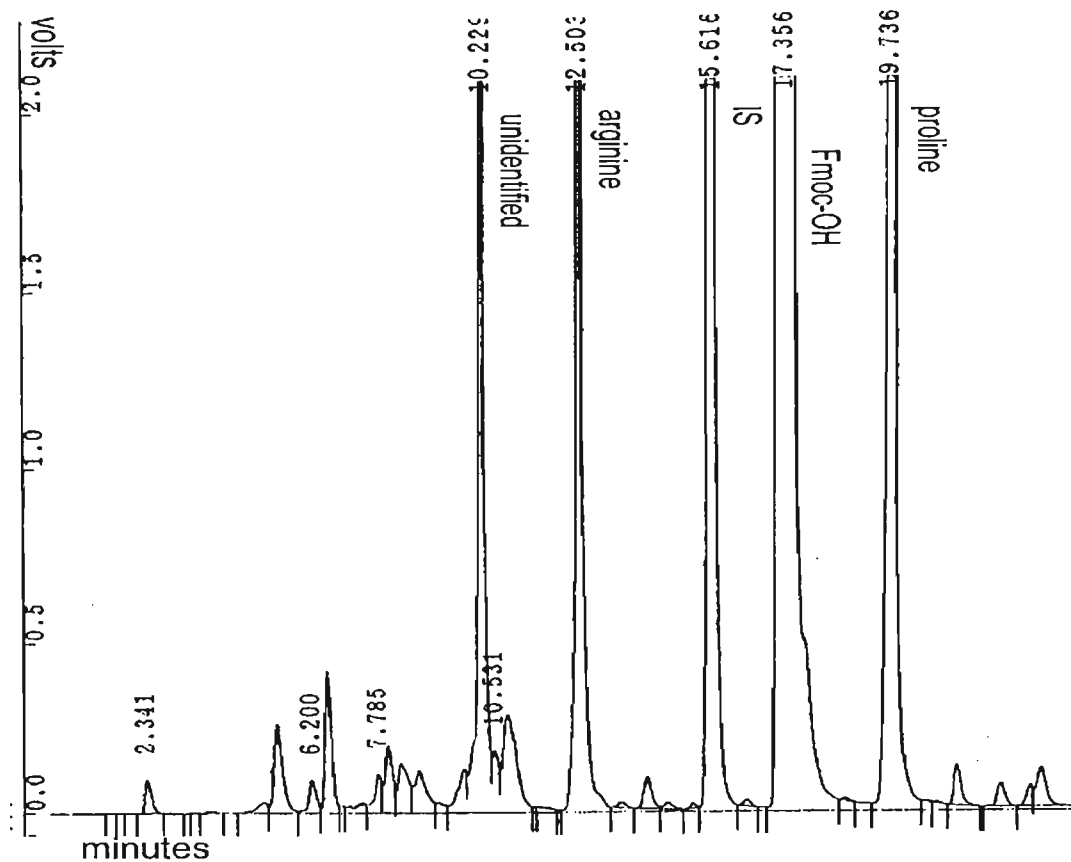


Figure 3.8 HPLC profiles of F-moc derivatised free-amino acids after 14 months storage. In an oxygen-free atmosphere at 10°C (top) and 30°C (bottom). Peak at 10.2 min. (unidentified), 12.5 min. (arginine), 15.5 min. (internal standard, IS), 17.30 min. (F-moc-OH) and 19.7 min. (proline)

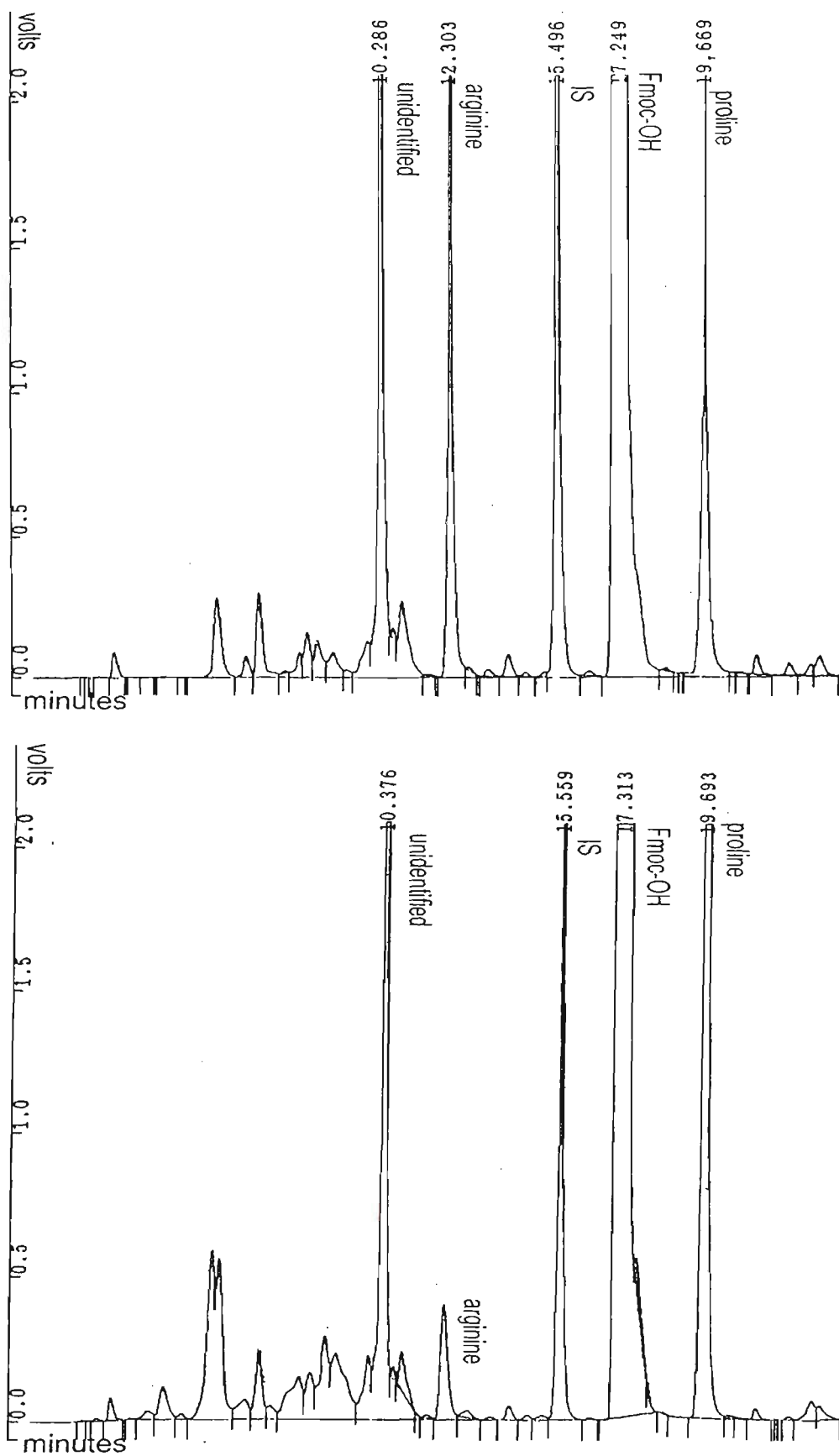


Figure 3.9 HPLC profiles of *F*-moc derivatised free-amino acids after 14 months storage. In an oxygen-free atmosphere at 10°C (top) and 30°C (bottom). Peak at 10.2 min. (unidentified), 12.5 min. (arginine), 15.5 min. (internal standard, IS), 17.30 min. (*F*-moc-OH) and 19.7 min. (proline).

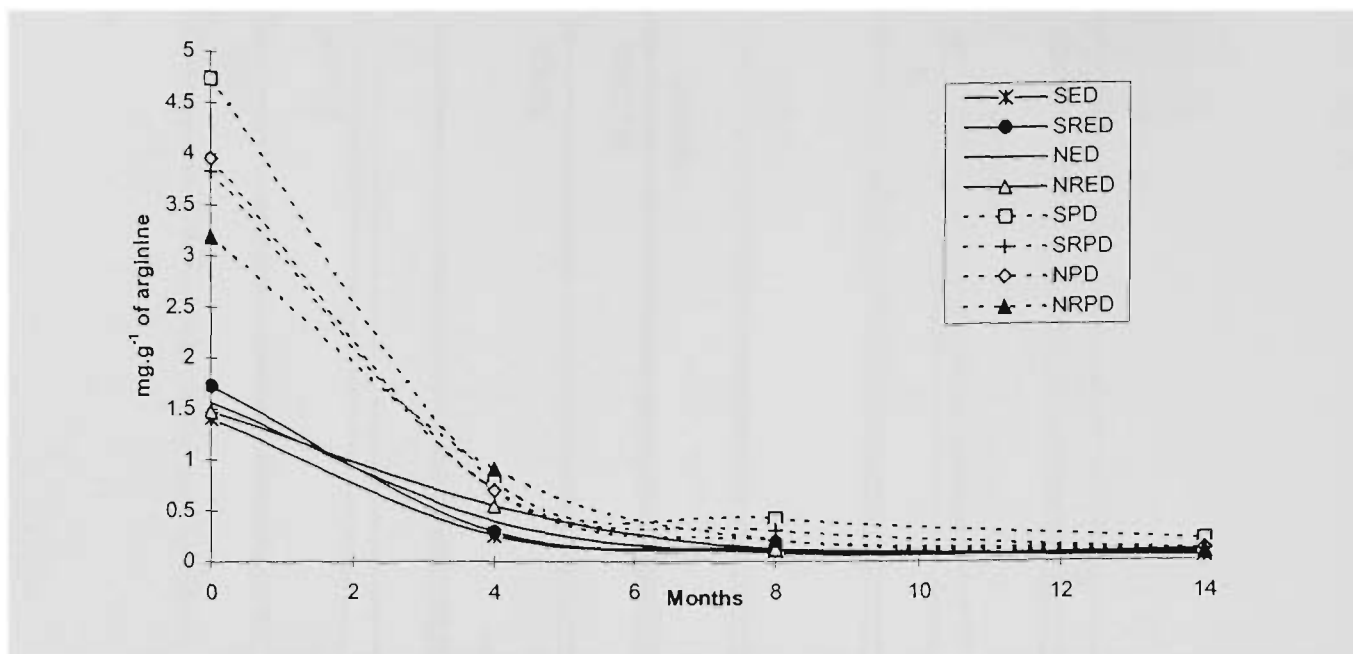


Figure 3.10 Changes in free L-arginine over 14 months storage at 30°C. In the absence of oxygen for 1995 harvested sultanas. The decrease of free-arginine under oxygen-exposed storage conditions was almost identical.

### 3.28 Free-arginine in pre-storage sultanas (skin and flesh)

The skin and flesh was separated with a scalpel from sultanas (n=20) which had been stored at -80°C until analysis. Separated skin and flesh were triple extracted in 80% MeOH/Milli-Q as previously described and subjected to OPA HPLC analysis. Two instrumental determinations were performed on each sub-sample. Generally the concentration of free-arginine was significantly lower in sultana flesh compared to skins for both exposed and protected fruit. The concentration of free-arginine in the flesh, and especially the skin of sultanas, was significantly higher in protected fruit.

	Exposed	Protected	Exposed	Protected
	Free-arginine-flesh mg.g <sup>-1</sup>		Free-arginine-skin mg.g <sup>-1</sup>	
<b>LSD=0.05</b>		<b>0.478</b>		<b>0.376</b>
S	1.41	2.41	1.98	3.81
SR	1.50	2.50	2.31	3.95
N	1.52	1.75	2.19	3.82
NR	1.42	2.20	2.32	3.91

Table 3.9 Distribution of free-arginine in pre-storage sultana skin and flesh. Concentrations were determined by OPA pre-derivatisation and HPLC. Analyses were performed on two 80% MeOH extracts of 20 sultanas. LSD calculated for the interaction of exposure and sunfinishing for the mean of duplicate determinations of two sub-samples.

### 3.29 5-Hydroxymethylfurfural (5-HMF) in sultanas

5-HMF was semi-quantitatively analysed using GC and GC-MS and identified from mass spectral data. Figure 3.11 shows the mass spectrum of the peak believed to be 5-HMF from dichloromethane (DCM) sultana extracts (top), the mass spectrum of an authentic sample of 5-HMF (middle) and the NIST-98 library spectrum of 5-HMF. Both the commercial standard 5-HMF (Sigma Aldrich, Australia) and the sultana peak had the same retention time on the same capillary column under the same GC conditions (see section 6.03) and had almost identical mass spectra. It can be seen that the major fragments for 5-HMF in the NIST-98 reference spectrum were present in the sultana spectrum, however the relative intensities of fragments were not exactly identical with the NIST-98 library reference. Some variation in relative ion intensity is common for spectra acquired with different mass spectrometers; this is especially true when comparing spectra acquired with an ion-trap spectrometer to a transmission-quadrupole device (Todd 1995).

Relative concentrations of 5-HMF in sultanas were semi-quantitatively measured using n-tetradecane as an internal standard. 5-HMF was analysed in DCM extracts from SED and SPD fruit at 0, 4, 8 and 14 months for each of the 4 storage conditions. Relative concentrations of 5-HMF ( $\mu\text{g.g}^{-1}$  DW) are shown plotted together with the free-arginine concentration ( $\text{mg.g}^{-1}$  DW) in Figure 3.12. In pre-storage SED fruit very low traces of 5-HMF were measured, indicating that some Maillard reactions may have already occurred. There was no detectable 5-HMF in DCM extracts of pre-storage SPD fruit. During storage at 30°C, the concentration of 5-HMF increased with time in both types of fruit.

Only small increases in the concentration of 5-HMF were measured in SED sultanas stored at 10°C (data not shown). Large concentrations of 5-HMF were measured at 8 months, indicating the occurrence of earlier Maillard reaction steps, such as the formation of Amadori intermediates. The rate of increase in the concentration of 5-HMF was significantly different for both oxygen-exposed and oxygen-free samples. For both SPD and SED sultanas, the concentration of 5-HMF accumulated steadily up until 14 months, whereas for oxygen-exposed samples, after reaching a maximum at 8 months, levels of 5-HMF decreased, especially for SPD fruit. ANOVA of the data indicated that all main effects had a significant influence on the 5-HMF concentration as well as a number of higher interactions. The major influences accounting for SS variance were, in decreasing rank: temperature, time, temperature×time, shading×time×oxygen, and exposure.

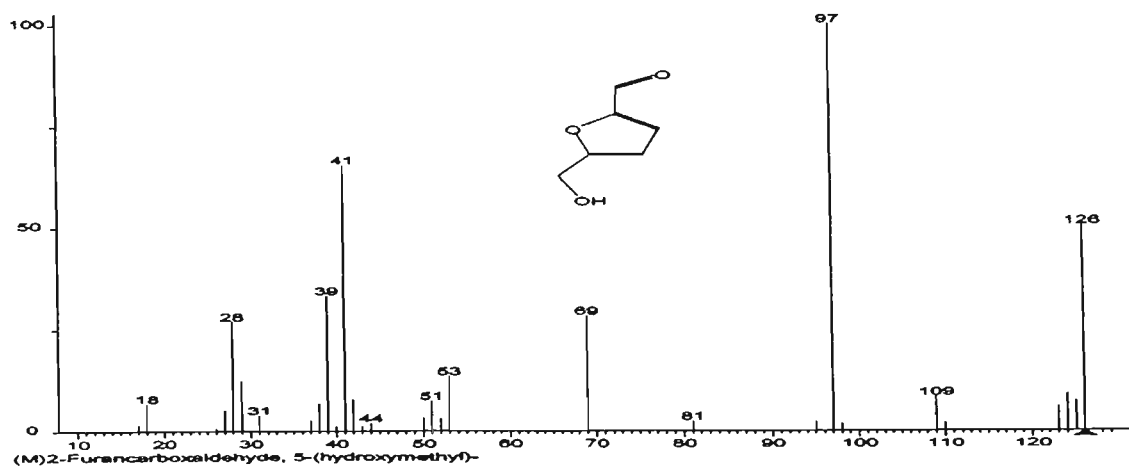
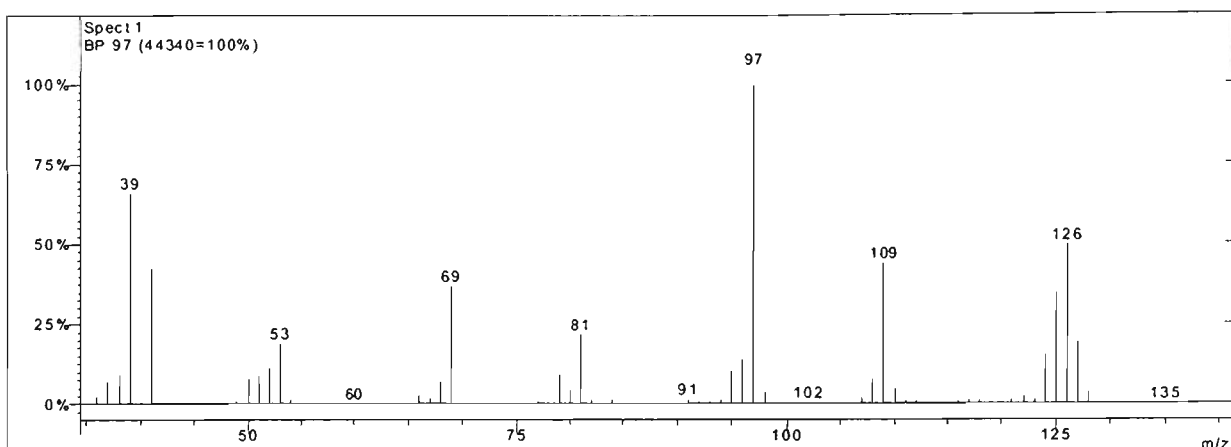
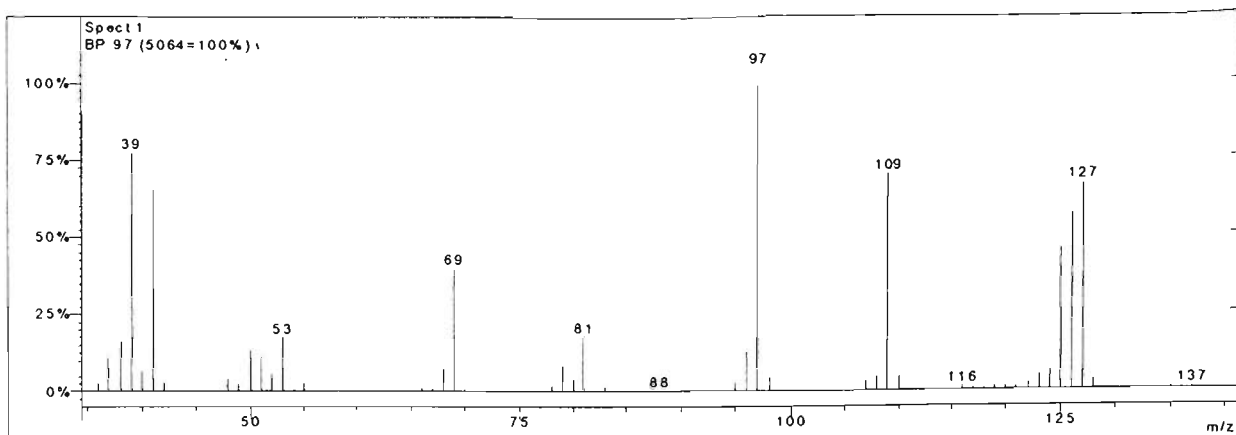


Figure 3.11 EI-mass spectrum of peak identified as 5-hydroxymethyl furfural from sultana DCM extract. (top) and authentic 5-HMF (middle) (Sigma Chemical Co.) The peak agrees well in terms of ions present and relative intensity with the spectrum present in the NIST 98 library (bottom) (CAS-67-47-0). Mass spectra were acquired with a Varian Saturn ion trap mass spectrometer as described in section 6.03.

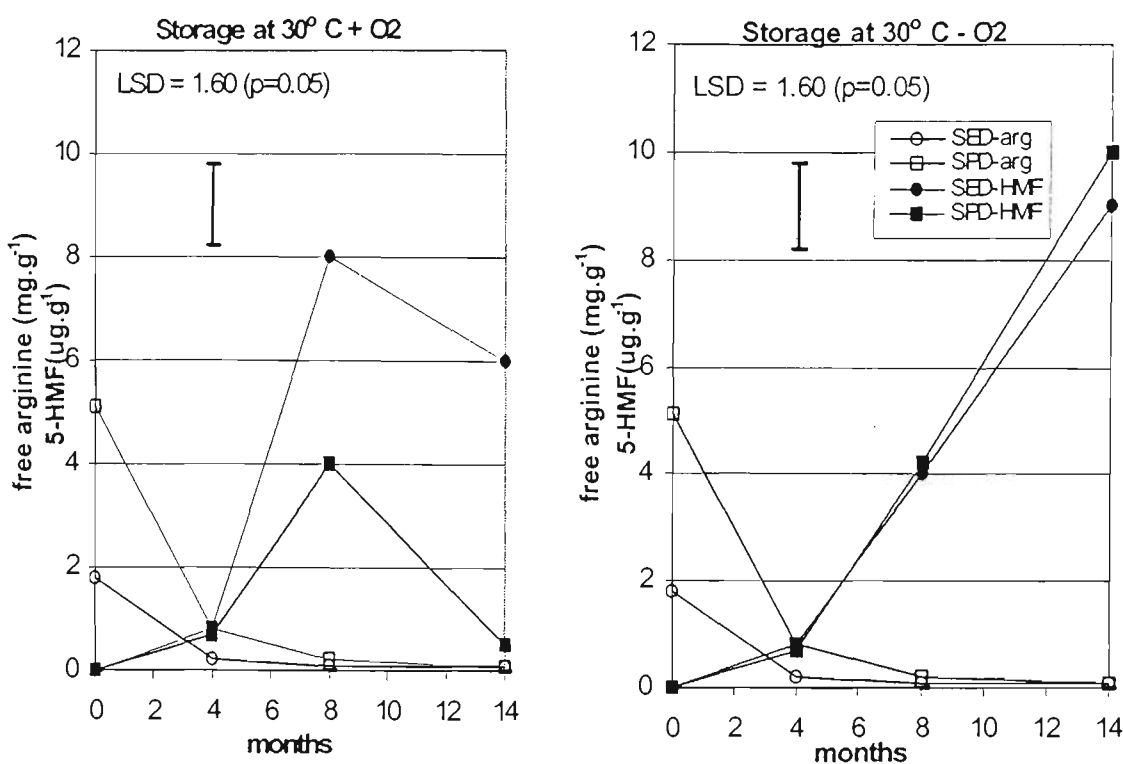


Figure 3.12 Decrease in free-arginine and generation of 5-hydroxymethyl furfural in sultanas. Exposed (SED) and protected (SPD) sultanas pre-storage, and after 4, 8 and 14 months storage at 30°C. Free-arginine was analysed by OPA- HPLC and 5-HMF was analysed by GC-MS (see section 6.03) The LSD for comparison of 5-HMF was determined using the duplicate determinations for each sub-sample for the treatments temperature, time and oxygen.

### 3.30 $A_w$ change during sultana storage

Sultana  $a_w$  was monitored at 0, 4, 8 and 14 months of storage. In Figure 3.13 changes in  $a_w$  for this level of interaction are graphically shown for sultanas stored at 10°C (left) and 30°C (right). Changes in  $a_w$  over time at each of these storage temperatures are shown for the combinations of sunfinished sultanas stored in the presence of oxygen (s-ox), non-sunfinished sultanas stored in the presence of oxygen (n-ox), sunfinished sultanas stored in an oxygen-free environment (s-nox) and non-sunfinished sultanas stored in an oxygen-free environment (n-nox).

At 10°C  $a_w$  values in sultanas increased for all treatments. Sultanas stored in the oxygen-free packaging had significantly lower  $a_w$  values than comparable sultanas stored in an oxygen-exposed environment at 8 and 14 months. As well as creating an oxygen-free environment, the packaging material also provided a partial barrier to water mass-transfer. For sultanas stored at 10°C in the presence of oxygen, sunfinished fruit had lower  $a_w$  values than non-sunfinished sultanas under the same conditions. Sunfinished fruit underwent a large increase in  $a_w$  up to 8

months, to reach an  $a_w$  close to non-sunfinished sultanas. Hence it appeared that sunfinishing sultanas did not prevent uptake of atmospheric water vapour over time at 10°C storage. At 30°C storage,  $a_w$  decreased over time. There was not a statistically significant difference in average  $a_w$  values at any time between sultanas stored in the oxygen-free packaging and in an oxygen-exposed environment. Despite higher pre-storage  $a_w$  in non-sunfinished sultanas compared to sunfinished, by 8 and 14 months the differences were not significant.

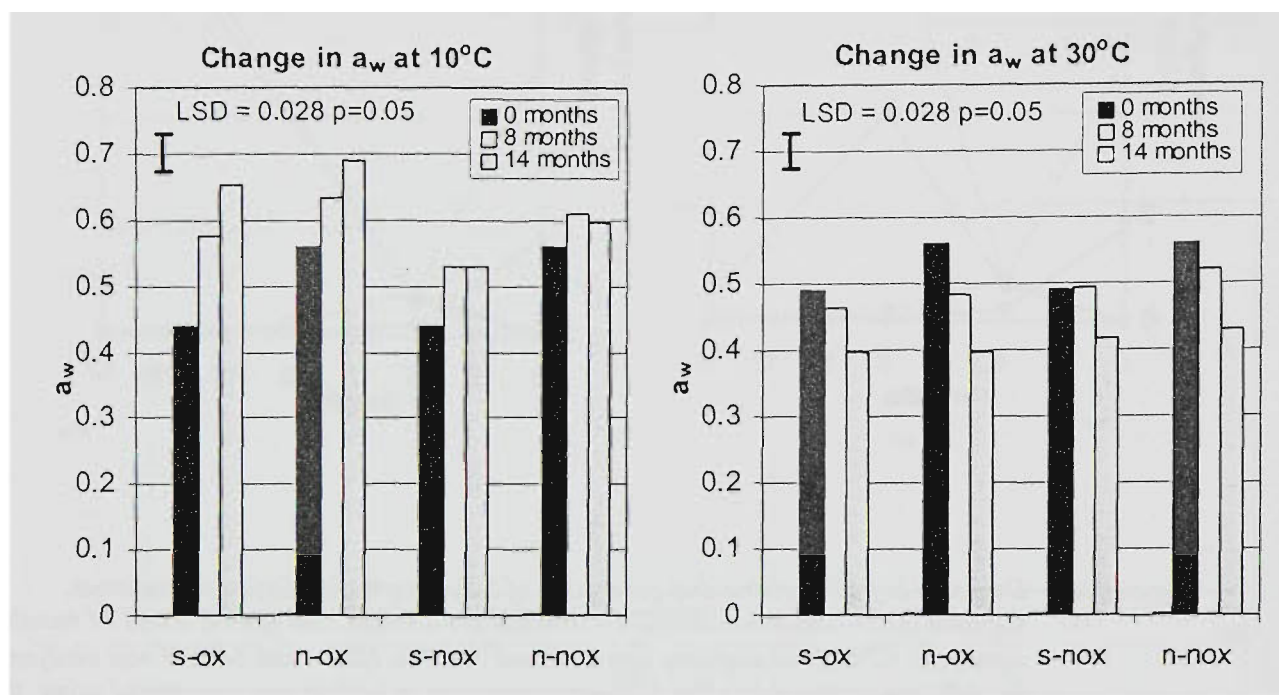


Figure 3.13 The effect of sunfinishing and oxygen exposure on changes in  $a_w$  at 10°C storage (left) and 30°C storage (right). The LSD was determined for the duplicate determinations of  $a_w$  on sub-samples for the interaction of temperature, time, sunfinishing and oxygen. S-ox (sunfinished-oxygen), n-ox (non-sunfinished-oxygen), s-nox (sunfinished-no oxygen) and n-nox (non-sunfinished-no oxygen).

### 3.31 Internal sugaring in sultanas

Internal sugaring beneath sultana skins, which is undesirable, is characterised by individual white sugar crystals with a diameter ranging between 1 to 3 mm. To estimate the degree of crystallisation, the total number of nuclei was visually counted on 20 randomly selected sultanas and averaged. Internal sugaring was only observed in fruit stored at 10°C. Table 3.10 shows  $a_w$  and the average number of crystals for sultanas stored with oxygen and without oxygen at 4, 8 and 14 months. As was observed in the previous section,  $a_w$  increased more slowly in sultanas stored in the oxygen-free packaging. After 4 months some internal sugaring appeared in NED and NRED sultanas, for both oxygen-exposed and oxygen-free storage conditions. Note these sultanas had reached an  $a_w$  of, or very close to, 0.6 at this time. As time elapsed and  $a_w$  increased to 0.6 in sultanas of other treatments, internal sugaring became apparent in them also. For all oxygen-

exposed fruit,  $a_w$  reached or surpassed the 0.6  $a_w$  mark and internal sugaring had occurred in all of them by 14 months storage. The oxygen barrier packaging retarded increases in  $a_w$  and thus kept more sultana samples below the critical  $a_w$  of 0.6, however all sultanas which were at or above  $a_w$  0.6 were affected by internal sugaring.

	10°C, + O <sub>2</sub>						10°C, - O <sub>2</sub>					
	4 months		8 months		14 months		4 months		8 months		14 months	
	$a_w$	Nuclei (No.)	$a_w$	Nuclei (No.)	$a_w$	Nuclei (No.)	$a_w$	Nuclei (No.)	$a_w$	Nuclei (No.)	$a_w$	Nuclei (No.)
SED	0.490	—	0.561	—	<b>0.606</b>	12	0.460	—	0.516	—	0.510	—
NED	0.586	15	<b>0.639</b>	20	<b>0.692</b>	20	0.570	15	0.595	20	<b>0.623</b>	20
SRED	0.526	—	0.594	—	<b>0.696</b>	20	0.494	—	0.53	—	0.530	—
NRED	<b>0.601</b>	20	<b>0.644</b>	20	<b>0.679</b>	30	0.588	15	<b>0.618</b>	20	<b>0.635</b>	30
SPD	0.513	—	0.578	—	<b>0.655</b>	12	0.485	—	0.522	—	0.534	—
NPD	0.593	—	<b>0.628</b>	—	<b>0.694</b>	30	0.580	—	<b>0.603</b>	—	0.528	—
SRPD	0.503	—	0.573	—	<b>0.662</b>	10	0.488	—	0.544	—	0.539	—
NRPD	0.582	—	<b>0.621</b>	10	<b>0.690</b>	25	0.579	—	<b>0.615</b>	5	<b>0.601</b>	12

Table 3.10 Internal sugaring measured as number of surface crystal nuclei per berry as a function of  $a_w$  at 4, 8 and 14 months storage. Note: in nearly all cases sultanas reached an  $a_w$  of approximately 0.60 before crystals were observed.  $a_w$  values at or over 0.60 are shown in bold in the table. A dash indicates absence of crystals.

### 3.32 Change in total phenolics during storage

Total phenolics were measured in whole sultana extracts of pre-storage sultanas and after 14 months at each of the four storage conditions. Total phenolic values for exposed and protected sultanas are displayed graphically in Figure 3.14. ANOVA analysis was conducted for the effects of vine exposure, oxygen exposure, sunfinishing and temperature. Both vine exposure and temperature were found to have a statistically significant effect ( $p < 0.001$ ), however sunfinishing ( $p > 0.461$ ) and oxygen exposure ( $p > 0.561$ ) did not.

Significantly lower concentrations of total phenolics were observed after 14 months storage in most 10°C-stored fruit compared to 30°C-stored samples irrespective of the presence or absence of oxygen. In a number of cases (NRED, SRPD and NRPD) there were significantly lower concentrations observed in the presence of oxygen, implying some oxidation of phenolics may have occurred. Phenolic content either increased significantly or did not change in sultanas stored at 30°C with or without oxygen, indicating that little oxidation occurred in those samples.

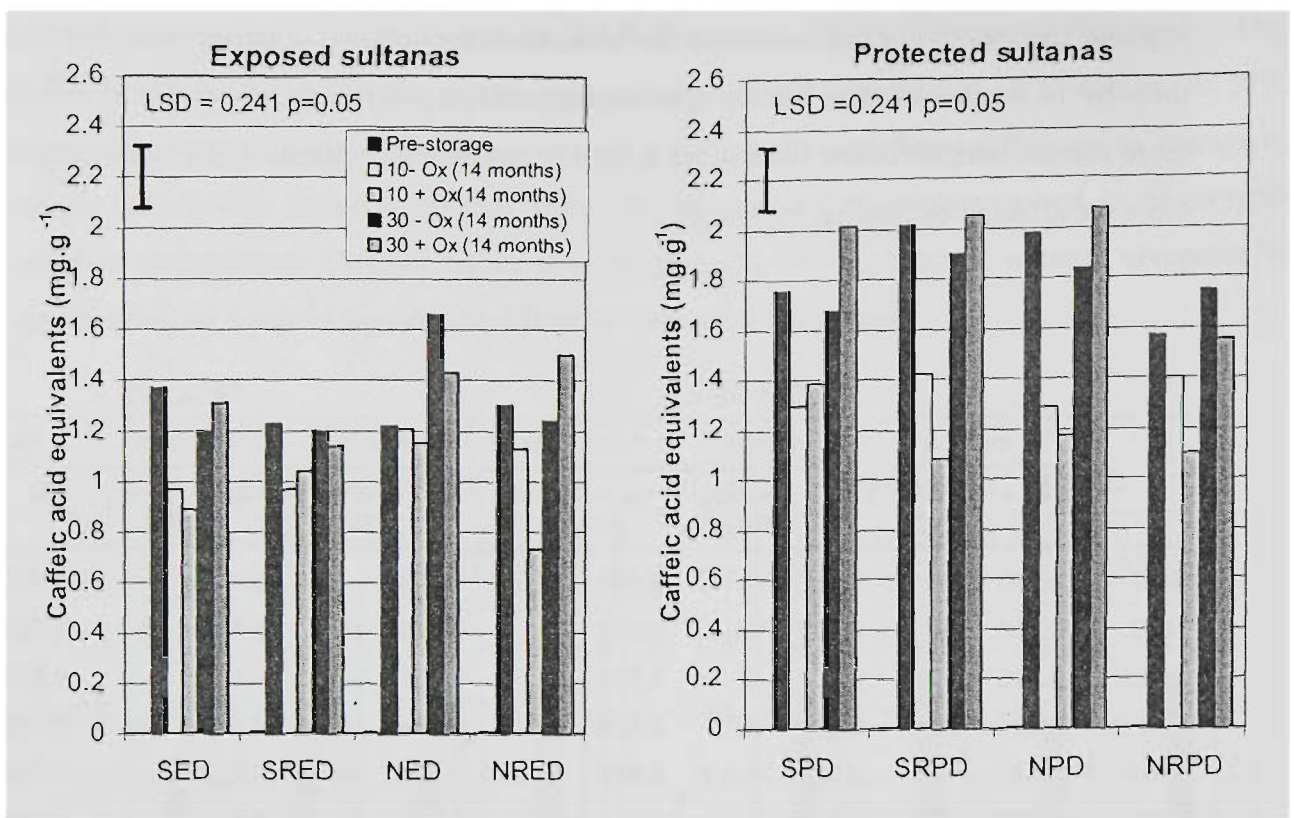


Figure 3.14 Total phenolics in sultanas pre-storage and after 14 months at each storage condition 10 - Ox (10°C no oxygen), 10 + Ox (10°C + oxygen), 30 - Ox (30°C no oxygen) and 30 + Ox (30°C + oxygen). Data are the mean of two determinations each performed on 80% MeOH extracts of 2 × 20 sultanas. LSD data were calculated for the interaction of exposure, sunfinishing, oxygen, temperature and time.

### 3.33 Regression analysis of storage trial data

Prediction of the future colour of sultanas stored in the presence of oxygen as a function of pre-storage parameters was modelled using multiple linear regression (MLR). Pre-storage sultana data—initial  $a_w$ , initial skin arginine, initial total phenolics, initial skin PPO substrate activity and initial  $L^*a^*b^*$  data were used to generate predictive models of  $L^*a^*b^*$  tristimulus values for sultanas stored in oxygen at 10°C and 30°C, at 4, 8 and 14 months. The multiple linear regression option in Genstat 5 was used to generate predictive models. As an initial ‘screening’ method all variate parameters were used to predict either  $L^*a^*$  or  $b^*$ , and the statistical power of these predictors was assessed from ANOVA data and regression coefficient estimates. Those parameters with the least significance were eliminated to generate plausible models. In the data set there was a total of 48 individual samples. After removal of outliers by Genstat, the fitted (predicted) values of  $L^*a^*$  or  $b^*$  were listed together with the measured values. These data were then transferred into Microsoft Excel® and  $R^2$  (Pearson’s correlation coefficient squared) values were determined.

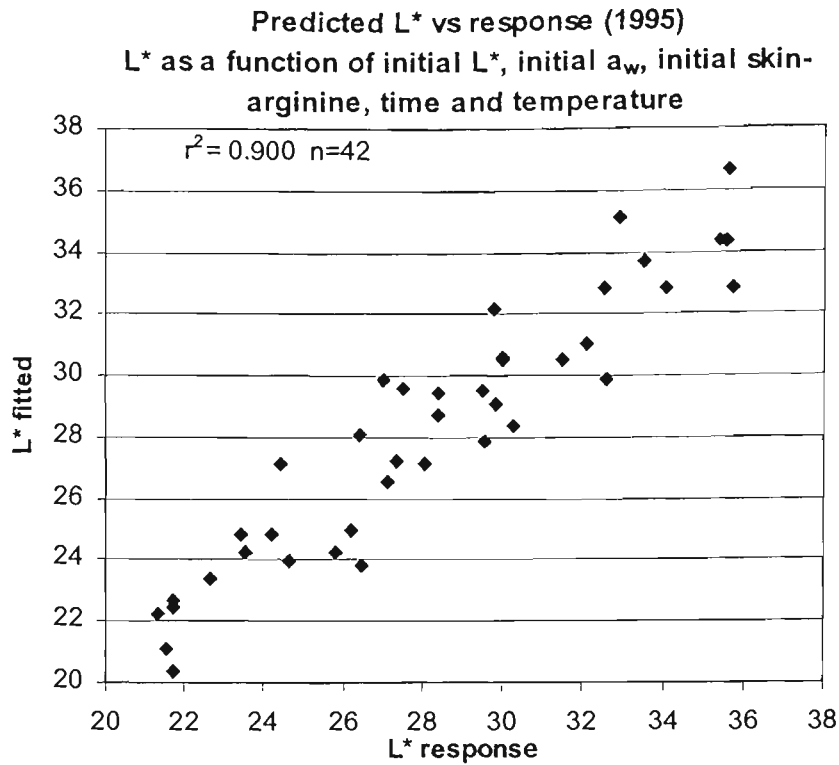
### 3.34 Regression model for L\* tristimulus value

Data generated for a model using all variates are shown in Table 3.12. The data indicated that only  $a_w$ , temperature and time were statistically significant parameters; pre-storage skin substrate PPO, total phenolics, skin arginine and initial L\* values were not found to be statistically significant. Optimised models, with outliers removed, were generated with the pre-storage free-arginine and initial L\* values included (Figure 3.15) and removed (Table 3.13). A small improvement in  $r^2$  values was obtained with the inclusion of the arginine and initial L\* terms, compared to the model without these terms. The use of these non-significant terms was justified on the basis that in the following years storage trial, both of these terms were found to contribute significantly to the prediction model.

	coefficient	s.e.	t(40)	t pr.
Constant	44.7	16.4	2.73	0.009
L* initial	0.232	0.37	0.63	0.534
$a_w$	-30.4	9.66	-3.15	0.003
temp	-0.3272	0.0355	-9.22	<0.001
time	-0.236	0.0863	-2.73	0.009
arginine	-1.17	1.06	-1.1	0.278
phenolic	2.7	2.98	0.91	0.370
ppo	-0.118	0.207	-0.57	0.573

Source of variation	d.f.	s.s.	m.s.	v.r.	F pr.
L* initial	1	150.52 (14.7%)	150.523	24.92	<0.001
$a_w$	1	61.052 (5.9%)	61.052	10.11	0.003
temperature	1	513.78 (50.3%)	513.783	85.06	<0.001
time	1	45.14 (4.4%)	45.14	7.47	0.009
arginine	1	4.872	4.872	0.81	0.375
phenolic	1	4.002	4.002	0.66	0.42
ppo	1	1.95	1.95	0.32	0.573
Residual	40	241.606	6.04		
<b>Total</b>	<b>47</b>	<b>1022.926</b>	<b>21.764</b>		

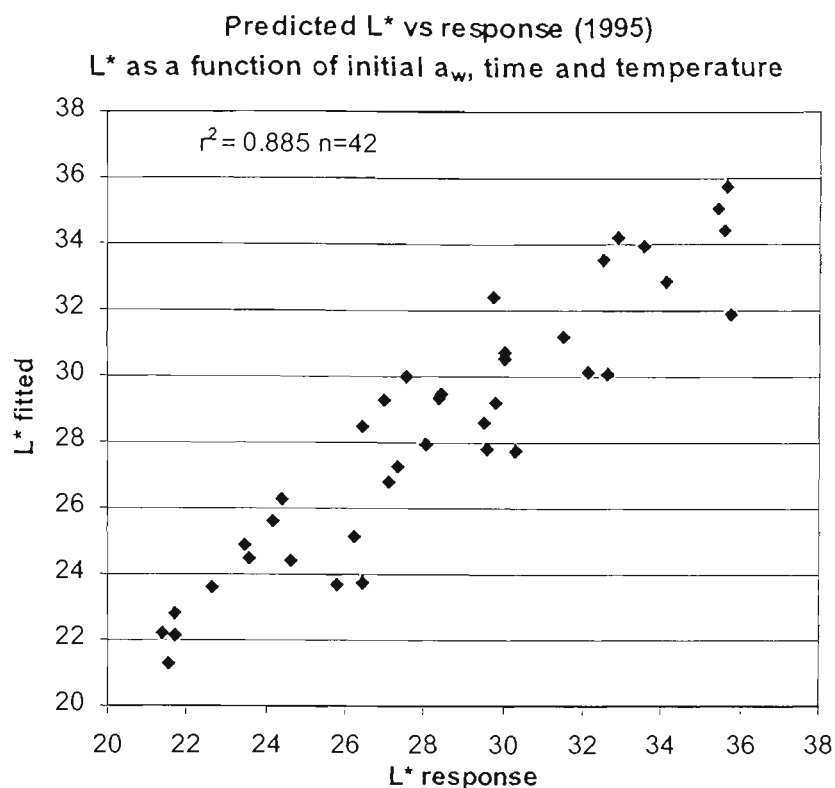
Table 3.12 Table of regression coefficients (top) and cumulative ANOVA table (bottom) generated for variates used to predict L\*.



Source of variation	coefficient	s.e.	t(36)	t pr.
Constant	43.3	10.8	4.00	<0.001
L* initial	0.372	0.232	1.61	0.117
arginine	-0.338	0.298	-1.13	0.265
a <sub>w</sub>	-37.82	6.61	-5.72	<0.001
temperature	-0.2815	0.0255	-11.02	<0.001
time	-0.3853	0.0652	-5.91	<0.001

Source of variation	d.f.	s.s.	m.s.	v.r.	F pr.
L* initial	1	211.55 (23.5%)	211.553	82.60	<0.001
arginine	1	4.28	4.282	1.67	0.204
a <sub>w</sub>	1	97.04 (10.8%)	97.046	37.89	<0.001
temperature	1	406.51 (45.12%)	406.514	158.72	<0.001
time	1	89.34 (9.9%)	89.342	34.88	<0.001
Residual	36	92.202	2.561		
<b>Total</b>	<b>41</b>	<b>900.94</b>	<b>21.974</b>		

*Figure 3.15 Regression model for L\* using pre-storage L\*, skin free-arginine, a<sub>w</sub>, time and temperature. Top table: Graphical representation of predicted L\* vs measured L\*. Middle table: statistical data for regression coefficients. Bottom table: cumulative ANOVA table for model parameters.*



Source of variation	coefficient	s.e.	t(38)	t pr.
Constant	59.54	2.44	24.42	<0.001
a <sub>w</sub>	-46.39	4.70	-9.87	<0.001
temperature	-0.2803	0.0263	-10.66	<0.001
time	-0.3887	0.0672	-5.79	<0.001

Source of variation	d.f.	s.s.	m.s.	v.r.	F pr.
a <sub>w</sub>	1	302.48 (33.6%)	302.483	111.31	<0.001
temperature	1	404.21 (44.9%)	404.211	148.74	<0.001
time	1	90.98 (10.1%)	90.98	33.48	<0.001
Residual	38	103.26	2.718		
<b>Total</b>	<b>41</b>	<b>900.9</b>	<b>21.974</b>		

Figure 3.16 Regression model for L\* using a<sub>w</sub>, time and temperature.  
 Top: graphical representation of predicted L\* vs measured L\*(response)  
 Middle table: statistical data for regression coefficients.  
 Bottom: cumulative ANOVA table for model parameters.

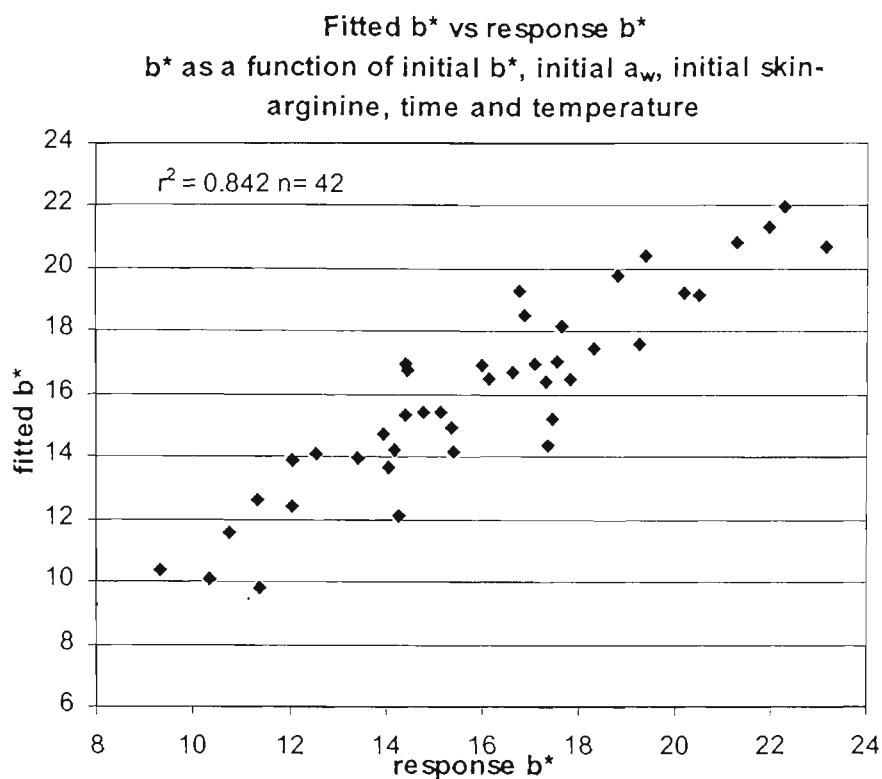
### 3.35 Regression model for b\* tristimulus value

An initial regression model was estimated using all parameters as was performed for L\* in the previous section. Once again pre-storage PPO, total phenolics, skin-arginine and initial b\* data did not have a statistically significant effect in terms of prediction of b\* (Table 3.13). Following the rationale given in the preceding section, initial arginine and initial b\* were used. In Figure 3.17, the optimised regression model for prediction of b\* using pre-storage arginine and initial b\* tristimulus values is shown. Figure 3.18 shows the prediction model without the terms pre-storage arginine and initial b\*.

Source of variation	coefficient	s.e.	t(40)	t pr.
Constant	32.7	10.6	3.08	0.004
a <sub>w</sub>	-29.51	8.17	-3.61	<0.001
time	-0.3033	0.0644	-4.71	<0.001
temperature	-0.15	0.0264	-5.67	<0.001
ppo	-0.359	0.236	-1.52	0.137
phenolics	1.03	2.12	0.49	0.629
b*initial	0.389	0.472	0.82	0.415
arginine	-0.401	0.735	-0.55	0.588

Source of variation	d.f.	s.s.	m.s.	v.r.	F pr.
a <sub>w</sub>	1	182.92 (35.9%)	182.922	54.48	<0.001
time	1	74.55 (14.6%)	74.553	22.20	<0.001
temperature	1	108.03 (21.1%)	108.03	32.17	<0.001
ppo	1	5.16	5.160	1.54	0.222
phenolic	1	1.208	1.208	0.36	0.552
b* initial	1	2.528	2.528	0.75	0.391
arginine	1	1.001	1.001	0.30	0.588
Residual	40	134.304	3.358		
<b>Total</b>	<b>47</b>	<b>509.706</b>	<b>10.845</b>		

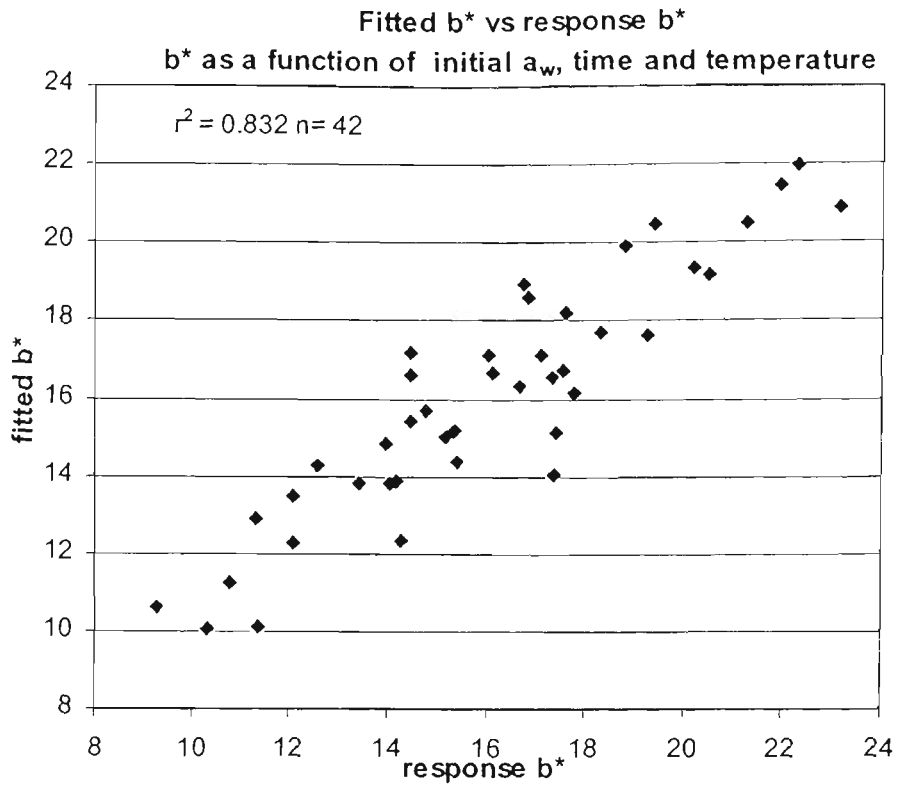
Table 3.13 Table of regression model coefficients (top) and cumulative ANOVA table (bottom) generated for variates used to predict b\*.



Source of variation	coefficient	s.e.	t(36)	t pr.
Constant	46.41	8.36	5.55	<0.001
temperature	-0.14	0.0225	-6.22	<0.001
time	-0.3818	0.0573	-6.66	<0.001
a <sub>w</sub>	-41.1	6.45	-6.37	<0.001
b* initial	-0.184	0.298	-0.62	0.54
arginine	-0.126	0.299	-0.42	0.676

Source of variation	d.f.	s.s.	m.s.	v.r.	F pr.
temperature	1	146.56 (31.6%)	146.565	72.04	<0.001
time	1	56.82 (12.2%)	56.821	27.93	<0.001
a <sub>w</sub>	1	185.77 (39.9%)	185.77	91.31	<0.001
b* initial	1	1.729	1.729	0.85	0.363
arginine	1	0.361	0.361	0.18	0.676
Residual	36	73.239	2.034		
<b>Total</b>	<b>41</b>	<b>464.485</b>	<b>11.329</b>		

Figure 3.17 Regression model for b\* using pre-storage b\*, skin free-arginine, a<sub>w</sub>, time and temperature. Top: graphical representation of predicted b\* vs measured b\*(response) Middle table: statistical data for regression coefficients. Bottom table: cumulative ANOVA table for model parameters.



	estimate	s.e.	t(38)	t pr.
Constant	41.0	2.06	19.93	<0.001
temperature	-0.1409	0.0222	-6.36	<0.001
time	-0.3743	0.0558	-6.7	<0.001
a <sub>w</sub>	-38.51	3.98	-9.68	<0.001

Change	d.f.	s.s.	m.s.	v.r.	F pr.
temperature	1	146.56 (31.5%)	146.565	73.94	<0.001
time	1	56.82 (12.2%)	56.821	28.66	<0.001
a <sub>w</sub>	1	185.77 (39.9%)	185.77	93.71	<0.001
Residual	38	75.329	1.982		
<b>Total</b>	<b>41</b>	<b>464.485</b>	<b>11.329</b>		

Figure 3.18 Regression model for b\* using a<sub>w</sub>, time and temperature  
 Top: graphical representation of predicted b\* vs measured b\*(response)  
 Middle table: statistical data for regression coefficients  
 Bottom: cumulative ANOVA table for model parameters.

### 3.36 Data interpretation and conclusions

Both Maillard and PPO processes are sensitive to chemical and physical factors: pH,  $a_w$  and temperature, often exhibiting similar optimal conditions. A major difference between the two browning systems is the role of molecular oxygen; PPO mediated browning, phenolic auto-oxidation and lipid oxidation reactions all require molecular oxygen to occur. Maillard reactions in contrast can proceed in the absence of molecular oxygen. ANOVA analysis of storage colour changes indicated that the browning processes which took place were temperature sensitive—highest browning occurred mainly at 30°C—and sensitive to pre-storage  $a_w$  values—greater browning occurred in higher  $a_w$  sultanas. Although the browning processes were oxygen sensitive, significant browning also occurred in samples from which oxygen had been excluded. The colour of non-sunfinished sultanas stored at 10°C, which underwent significant decreases in  $L^*$  and  $b^*$ , were a dull mousy grey colour, in contrast to the dark brown colour of 30°C stored fruit. This lower temperature process appeared to be different to those occurring at 30°C. Significant colour change occurred at 10°C storage regardless of the oxygen exposure, indicating that whatever processes occurred were not inherently oxygen dependent. It was seen that there was an overall small decrease in total phenolics in 10°C stored samples—both oxygen-free and oxygen-exposed—and also some small decreases in free-arginine and proline in some samples.

Another possible explanation was a slow non-oxygen dependent polymerisation of MRPs. Some 5-HMF was already present at a low concentration in pre-storage sultanas. It is conceivable that 5-HMF and other compounds, e.g. free proline and arginine, may have interacted with metal cations over time; proline has been shown to produce dark pigments with phenolics in the presence of iron (Mason and Peterson 1965 and Nicolas 1994). The  $a_w$  of sultanas stored at 10°C increased slowly over time, increasing the chemical mobility. The higher  $a_w$  of these samples may have allowed some latent PPO to become active (at least in sultanas stored in the presence of oxygen). The lack of significant difference in  $L^*$  or  $b^*$  values in 10°C stored samples with or without oxygen would indicate, however, that PPO processes contributed little to the colour changes in these samples.

The data demonstrated that the most intense browning occurred at 30°C. Both PPO and Maillard browning increase with storage temperature, however the fact that browning was observed without oxygen indicated the occurrence of Maillard reactions. Storage trials identified that arginine was the main free-amino acid to decrease during storage (at 30°C), with rates of decrease being equal either in an oxygen-free or exposed storage environment. The heat sensitive decrease in free-arginine implicated this amino acid as the main amino acid involved in Maillard reactions. As free-proline did not decrease at 30°C, it was not considered to be important in Maillard type browning which occurred in these samples. The finding that free-arginine and free-proline were

the most abundant amino acids in sultana extracts was in accordance with Treeby *et al.* (1998) and Stines *et al.* (2000), who found that both amino acids were dominant in Australian grapes across a number of red and white grape cultivars. Many other researchers have reported these amino acids in high concentration in grapes (in Sultana grapes, Bolin and Petrucci 1985, Kanellis and Roubelakis-Angelakis 1993 and Hernandez-Orte *et al.* 1999).

Evidence of Maillard-type browning reactions was indicated by increases in concentration of 5-HMF during storage at 30°C; increases were not observed at 10°C. The time-course study indicated that the rate of synthesis and degradation of 5-HMF was different in the presence of oxygen. Since 5-HMF is essentially a colourless Maillard reaction intermediate, the data might be interpreted as evidence that the presence of oxygen accelerated the rate of polymerisation of the substrate and hence Maillard browning. The greater browning observed in the presence of oxygen at 30°C may also have been due to other reactions, such as the oxidation of sultana surface lipids and possible subsequent interaction with other browning systems: phenolics and Maillard intermediates. It has been demonstrated that browning in oxidative Maillard reactions occurs at a faster rate in the presence of oxygen and trace metals (Saltmarsh and Labuza 1982 and Yayalayan and Huyghues-Despointes 1994). Cutzach *et al.* (1999) examined phenolic and Maillard compounds in aged fortified wines during a storage period of 12 months. They found significant differences in the concentration of 5-HMF in wines stored with and without oxygen, with higher concentrations found in the wines stored without oxygen. This was in agreement with the trend observed in the storage experiment. Melanoidins are also known to produce significantly darker pigments in the presence of metal cations such as copper and iron, which may occur more readily in the presence of oxygen.

ANOVA analysis of colour change of L\*a\*b\* tristimulus data indicated that the effect of vine solar exposure accounted for only a small amount of the variation in L\* and a\* and was insignificant for b\*. The data from this particular storage trial generally did not strongly support the 'anecdotal' evidence, which suggested that vine shading results in darker fruit. The slightly faster browning rates observed in protected sultanas may have been due to both higher pre-storage levels of free-arginine and total phenolic compounds, however the lack of significance of these terms in the regression data would indicate that these effects were relatively unimportant.

The hypothesis that sunfinishing exerts a positive effect on sultana lightness and storage colour stability by lowering initial PPO activity was not supported by the experimental data. Active PPO enzyme was neither substantially inactivated through dipping or drying in either protected or exposed grapes, nor was the sunfinishing process shown to result in significantly lower PPO activity in sultanas. These results attest to the general robustness of Sultana PPO which has been shown to require temperatures in excess of 93° C for up to 120 seconds in order to substantially decrease activity (Radler 1964). The fact that latent PPO enzyme was measured in sultanas does

not, however, imply that this could necessarily result in the oxidation of grape phenolics. The essential pre-condition of phenolic substrates and enzyme coming into contact (loss of compartmentalisation) at a suitable  $a_w$  must be met before this type of browning can occur. The positive effect of sunfinishing on sultana storage browning was likely to be due to the simple fact of reducing  $a_w$ . The storage data clearly showed the  $a_w$  sensitivity of browning, regardless of the oxygen exposure, temperature or mechanism of browning; oxidative or non-oxidative.

The ion trap mass-spectrometer is an extremely sensitive device, and space charge effects can induce some secondary ionisation within the trap, leading to some distortion of mass spectra; high concentrations and some specific molecular species are particularly prone to these effects. 5-HMF is a highly labile compound, which has a tendency to acquire an extra proton under ion trap conditions. This was seen in the spectra in Figure 3.11, where there was a strong peak at  $m/z$  127. The fact that the authentic standard had the same retention time and mass spectrum as the putative peak indicated that it was in fact 5-HMF. It should be noted that other authors have reported its presence in wine and sultanas at relatively high concentration (Cutzach *et al.* 1999 and Karadeniz *et al.* 2000).

Oxygen barrier packaging was not only an effective method of eliminating oxygen and slowing rates of browning in sultanas during storage, but was also an effective method to retard water uptake which can lead to undesirable internal sugaring phenomena. It would seem that internal sugaring only occurs at low storage temperatures ( $<10^\circ\text{C}$ ). Bolin (1980) reported some sub-cuticular sugaring in sultanas, which had been stored at  $1^\circ\text{C}$  for 12 months. Some surface sugaring was also observed in samples stored at  $21^\circ\text{C}$  and  $32^\circ\text{C}$ , however no surface sugaring was observed in the  $30^\circ\text{C}$  stored samples in this trial. Cañelas *et al.* (1993) stored sultanas with an initial  $a_w$  of 0.61 at  $21^\circ\text{C}$  for 11 months and found an increase in  $a_w$  from 0.61 to 0.65, but did not report any signs of internal sugaring. The same workers measured a decrease in glucose concentration in sultanas during storage and assumed that it was evidence of the presence of Maillard reactions.

Overall, the data indicated that non-oxygen dependent reactions made a significant contribution to sultana browning and future sultana storage colour could be predicted to a certain extent by a simple regression model.

## 4.0 SULTANA STORAGE EXPERIMENT II 1996

---

### 4.01 Introduction

In the previous section (storage experiment I 1995) significant browning occurred in sultanas stored at 30°C in the absence of oxygen, indicating that non-oxygen dependent reactions play an important role in storage browning. Maillard-type reactions were indicated by (1) the loss of free-arginine, (2) the occurrence of significant browning at 30°C in the absence of oxygen and (3) the formation of 5-HMF over time. Vine shading was again employed with the intention of providing a range of grape chemico-physical characteristics, which may affect sultana storage browning. In addition, the influence of grape maturity on sultana colour was examined. There is evidence that grape maturity can affect final sultana colour and storage colour stability (Uhlig and Clingeffer 1998). In this experiment, grapes were harvested and dried at two periods within the 1996-season: at the optimal time, the third week in February and late in the season, the second week in March. Although the primary purpose of the investigation was to gain further insight into storage browning, the effect of grape maturity on sultana colour and storage browning was also investigated.

### 4.02 Experimental aims

The specific aims of this experiment were:

- To examine the temperature,  $a_w$  and oxygen dependence of storage browning on a second season's fruit in a similar storage trial,
- To further explore the effect of vine shading on sultana colour and storage colour stability and also free-arginine and free-proline concentrations,
- To examine changes in HPLC phenolic profiles, specifically *trans*-caftaric acid, by comparing profiles of fresh grapes and dried sultanas, and
- To examine the effect of grape maturity on the browning potential of sultanas and, where possible, relate chemico-physical properties to browning.

### 4.03 Source of grape material

Sultana grapes were produced in an experimental plot at the SHC from vines given three different levels of solar radiation. Shading was achieved using woven polythene shade-cloth widely used by Sultana farmers (purchased from the Irymple Co-op). One row of vines was covered with medium-density (approximately 25% shading) shade cloth and a second with high-density shade-cloth (approximately 50% shading). Shade-cloth material was placed at fruit set. A third row was left uncovered and fully exposed to direct sun. The grapes were harvested on the mornings of 21

February and 13 March and were placed in cool storage (4°C) overnight to be dipped the next day. The following mass of fruit was collected on each of the dates: 21 February, 'exposed' 60 kg, 'medium-shaded' 55 kg, and 'high-shaded' 50 kg; 13 March, 'exposed' 55 kg, 'medium-shaded' 48 kg, and 'high-shaded' 48 kg. Bunches were taken only from the top of the vine canopies for each of the shading levels in order to make valid comparisons for exposure to solar radiation. Grapes were coded as 'High Shaded' 21 February (HS21), 'High Shaded' 13 March (HS13), 'Medium Shaded' 21 February (MS21), 'Medium Shaded' 13 March (MS13), 'Exposed' 21 February (EX21) and 'Exposed' 13 March (EX13). In addition to grapes taken from the top of vine canopy, grapes were harvested from bunches hanging underneath fully exposed vines which had not received direct sun exposure and were slightly green in colour. These grapes were coded 'Green' 21 February (GR21) and 'Green' 13 March (GR13). 52 kg and 55 kg of these grapes were collected on the respective dates.

Grape and sultana samples will be referred to by these codes henceforth. Figure 4.1 shows diagrammatically an outline of the shading and subsequent drying and packaging treatments. Representative bulk whole-bunch grape samples for each vine exposure treatment (approximately 1.5 kg) and harvest date were retained and stored at 4°C in the cold storage facility at SHC (approximately 48 hrs) until transportation to VUT on dry ice in a number of insulated storage containers. Grape samples arrived cold and in good condition. Upon arrival, bulk samples of grape material (approximately 1 kg) were packaged and stored at -20°C for pH, titratable acidity, and total phenolic determinations. Remaining grapes (approximately 500 g) were packaged into sealed plastic boxes, labelled and stored at -80°C until the determination of PPO activity, glucose, hydroxycinnamic acid and free-amino acids.

#### **4.04 Experimental: analysis of grape TSS, TA, total phenolics and L\*a\*b\* tristimulus values**

Frozen grapes for each treatment (n=100) were removed from -20°C storage for maturity analyses. The frozen grapes were removed from stems and other plant material; before weighing. Grapes were added to an ice-cold Waring blender and were homogenised at the low speed setting for 60 seconds to roughly break them up. Semi-frozen grape homogenates were transferred to 250 mL screw-top polycarbonate centrifuge tubes and centrifuged at 4°C at 13,900×g for ten minutes. The solid precipitate of grape material was discarded and the liquid homogenates were used for analyses. Triplicate analyses were performed for each sample. Total soluble solids and titratable acidity were determined as described previously. Total phenolics were determined on two separate sub-samples of 25 whole grapes or sultanas in the manner previously described. L\*a\*b\* values were determined on whole thawed grapes (2×25) as described in section 3.07.

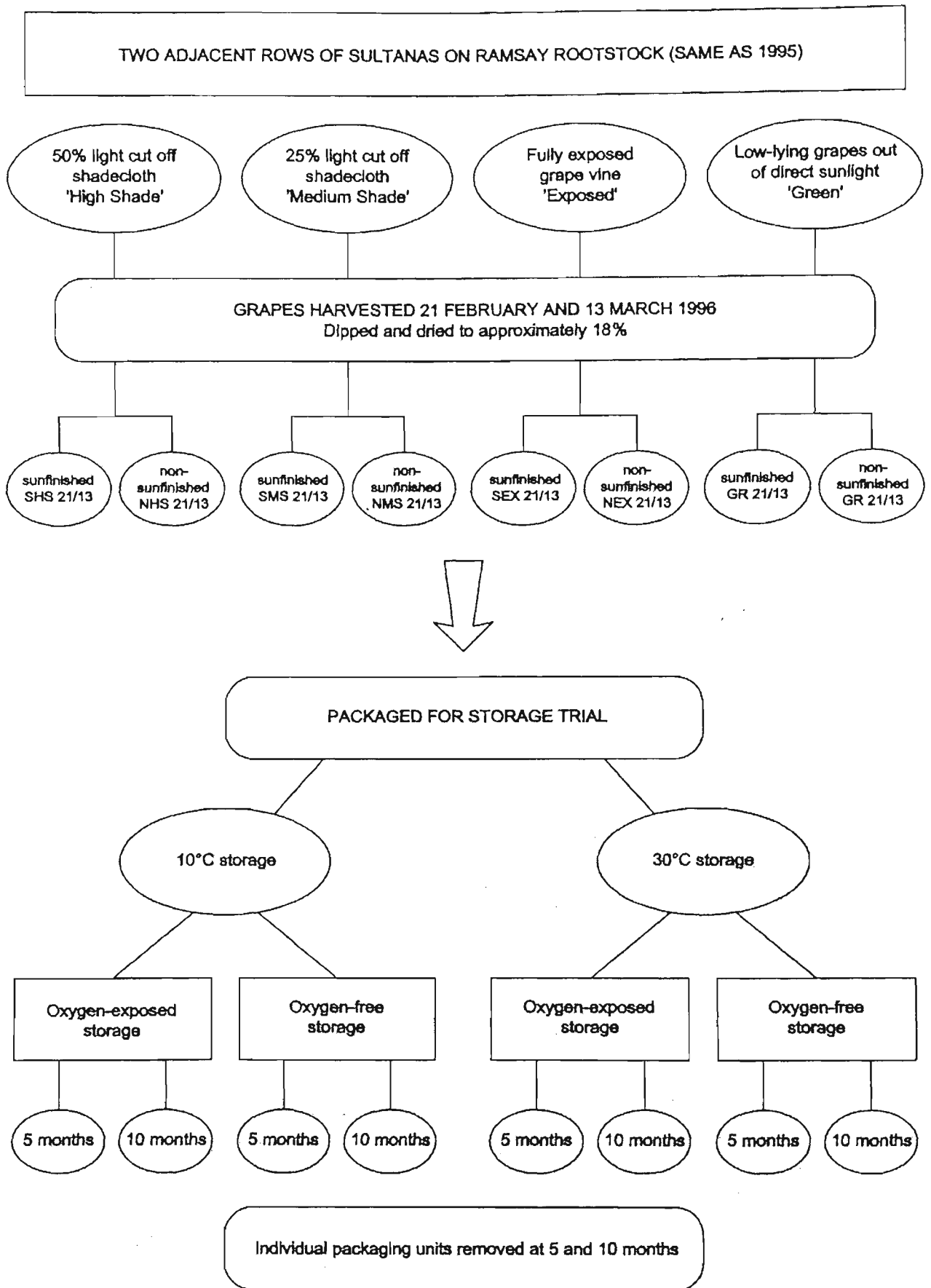


Figure 4.1 Flow diagram showing field shading, sample codes and storage experiment. Sultanas were harvested on 21 February and 13 March 1996. There were 16 unique samples of grapes and 128 samples of sultanas.

#### 4.05 Grape pH

An Orion 420A hydrogen ion electrode was used for pH determinations. The glass electrode was calibrated according to the manufacturer's instructions. Cold 20 mL samples were transferred to McCartney bottles and allowed to warm to ambient temperature (approximately 22°C). Determinations were performed on duplicate sub-samples.

#### 4.06 Grape glucose

The glucose concentration of fresh grapes was determined enzymatically using the Trinder® glucose-oxidase method (Sigma Aldrich Chemicals). Triplicate glucose determinations were performed on the juice from 100 grapes from each treatment level. A 5 µL aliquot of a 1:10 dilution of the juice extract was added to the reagent, made up as per instructions, and incubated at 37°C for ten minutes. An appropriate external calibration curve was made with glucose standards and also incubated at 37°C. Samples were measured in an Ultraspec-III (Pharmacia-Biotech) UV-visible spectrophotometer at 505 nm.

#### 4.07 Grape free-amino acid analysis

Grape 80:20 MeOH-Milli-Q extracts were made as described previously and subjected to F-moc amino acid analysis.

#### 4.08 Hydroxycinnamic esters (HPLC)

Frozen (-80°C) grapes were removed from the freezer and transferred to an ice-cold tray. Skins from 20 grapes were quickly removed from the frozen flesh using a scalpel and skin and flesh were weighed and put into an approximately 15 mL aliquot of ice cold extraction buffer (9:1 methanol/ Milli-Q water v/v and 2% ascorbic acid w/v). Samples were prepared in duplicate (2×20 grapes) and HPLC analyses were performed in duplicate. Sultanas were similarly prepared except they were allowed to warm to room temperature before the skin and flesh were separated. Skin and flesh samples were homogenised with the Polytron and transferred into 20 mL polycarbonate centrifuge tubes and centrifuged at 4°C for 15 minutes at 17,400×g. Supernatants were decanted into clean plastic Falcon tubes and the pellets were re-suspended in approximately 10 mL ice-cold extraction buffer and re-homogenised and centrifuged as previously. The two supernatant volumes were pooled and made to a constant volume of 30 mL. An aliquot (5 mL) was passed through a Whatman 0.45 µm teflon filter with a plastic 10 mL syringe and then immediately manually injected into a 20 µL Rheodyne sample loop and delivered onto the column for analysis. All samples were prepared individually immediately prior to HPLC analysis. A Varian HPLC system was used with a Varian 9010 solvent pump and a Varian 9050 UV-visible detector set at 320 nm. Separation was achieved on a reverse phase Ultracarb-5 ODS(30) (Phenomenex, Torrance, CA, USA), with a length of 25 cm and a particle size of 5 µm. Phenolics were eluted with a binary solvent gradient. Solvent 'A' consisted of 0.05 M NaH<sub>2</sub>PO<sub>4</sub> buffer

adjusted to pH 2.5 with orthophosphoric acid and solvent 'B' was HPLC grade acetonitrile (HyperSolv). The acetonitrile was increased from 10% linearly up to 40% over 15 min. and was held until the end of the 40 min. run. A constant flow rate of 1.0 mL min<sup>-1</sup> was used. The HPLC protocol was based on methods cited by Singleton *et al.* (1984) and Ong and Nagel (1978).

#### 4.09 Fresh grape maturity data

It can be seen from Table 4.1 that the TSS (° Brix) was higher for each grape shading treatment on 13 March, compared to the earlier harvested grapes (21 February). The pH levels were slightly higher and TA slightly lower in later harvested grapes, indicating greater maturity. Glucose concentrations were higher in later harvested fruit and it appeared that the glucose concentration also increased with the level of vine solar exposure. L\*a\*b\* tristimulus data indicated that all grapes were light; L\* ranged between 50.74 and 62.65. The a\* values show that all grapes were slightly green with negative a\* values. Lower a\* values were observed in all shaded grapes in late harvest fruit compared with early fruit. All b\* values ranged from 23.57 to 27.15, except the early harvest GR grapes which had average b\* values of 17.11.

#### 4.10 Grape skin-flesh PPO activity

Semi-frozen grapes were separated into skin and flesh and prepared for the PPO substrate assay as described in section 3.05. The skin and flesh were separated from two sub-samples of 20 berries and at least two assays were performed on each. The data were analysed by ANOVA using the two factors: exposure and harvest. LSD data were generated for the interaction of exposure and harvest.

Treatment	TSS (°Brix)	pH	TA g.L <sup>-1</sup>	Glucose mg.g <sup>-1</sup>	L*	a*	b*
EX21	19.16	3.5	3.7	89.79	57.18	-4.49	26.36
GR21	18.20	3.4	5.7	85.83	50.74	-5.31	17.11
MS21	15.16	3.7	5.6	70.06	57.62	-6.09	24.45
HS21	14.40	3.3	6.0	55.92	57.46	-10.83	26.01
EX13	23.50	3.9	2.3	119.4	62.65	-4.37	23.57
GR13	19.10	4.1	3.6	92.01	58.23	-10.54	26.96
MS13	20.56	4.0	4.2	84.83	54.97	-8.59	23.14
HS13	17.96	4.0	5.2	71.83	58.76	-10.07	27.15

Table 4.1 Data for total soluble solids TSS (° Brix), pH, titratable acidity (TA), glucose concentration and tristimulus values. For fresh sultana grape berries sampled at harvest on 21 February and 13 March. TSS, pH, TA and glucose values are the mean of triplicate determinations on samples from the juice of 100 berries. L\*a\*b\* values are the mean of 2 × 25 separate determinations on single berries.

Grape treatment	PPO activity—skin ( $\mu\text{mole O}_2\cdot\text{min}^{-1}\cdot\text{g}^{-1}\text{ FW}$ )		PPO activity—flesh ( $\mu\text{mole O}_2\cdot\text{min}^{-1}\cdot\text{g}^{-1}\text{ FW}$ )		Total Phenolics caffeic acid equivalents ( $\text{mg}\cdot\text{g}^{-1}$ )	
	21 Feb early	13 Mar late	21 Feb early	13 Mar late	21 Feb early	13 Mar late
LSD ( $p=0.05$ )	0.232		0.104		0.148	
EX	4.51	4.43	0.72	1.03	1.01	1.19
GR	4.52	4.68	0.84	0.93	1.17	0.97
MS	3.25	3.63	0.93	1.06	1.22	1.03
HS	5.06	5.13	0.56	0.78	1.29	1.05

Table 4.2 *Skin-flesh substrate PPO activity and total phenolics for grapes. Harvested on 21 February and 13 March 1996. PPO values are the mean of three determinations on  $2 \times 20$  sub-samples for each grape treatment. Total phenolics values are the mean of two determinations on 80% MeOH extracts of  $2 \times 25$  sub-samples of whole grapes. LSD values were calculated by ANOVA on the replicate determinations for the interaction of exposure and harvest.*

Grape treatment	Free-arginine Whole grape $\text{mg}\cdot\text{g}^{-1}\text{ FW}$		Free-proline Whole grape $\text{mg}\cdot\text{g}^{-1}\text{ FW}$		Unidentified amino Whole grape $\text{mg}\cdot\text{g}^{-1}\text{ FW}$	
	21 Feb early	13 Mar late	21 Feb early	13 Mar late	21 Feb early	13 Mar late
LSD ( $p=0.05$ )	0.17		0.11		0.075	
EX	0.17	0.63	0.22	0.40	0.40	0.47
GR	0.26	0.77	0.15	0.47	0.37	0.51
MS	0.72	1.45	0.08	0.32	0.32	0.44
HS	0.30	0.70	0.09	0.13	0.20	0.34

Table 4.3 *Whole F-moc grape free-amino acids (arginine and proline) and unidentified compound in 80% MeOH extracts of grapes. Harvested 21 February and 13 March 1996. Stated values are the mean of two analytical determinations performed on two sub-samples of 25 grapes. LSD values were generated using replicate determinations for the interaction of exposure and harvest.*

The data (Table 4.2) indicated that the skin substrate PPO activity did not differ significantly between harvest dates. There were significant differences in skin PPO activity for the level of exposure but the differences were small and did not show an obvious tendency to increase or decrease with vine solar exposure. Grape flesh PPO activity was significantly higher in earlier harvested fruit, except for in exposed fruit, where it was lower.

#### 4.11 Free-amino acids in grapes

As observed in the sultanas from the previous year, the predominant free-amino acids in grape extracts were proline and arginine and the unidentified peak; only traces of other free-amino acids were present. Arginine was the most concentrated amino acid in whole grape extracts. A significantly higher ( $p < 0.05$ ) concentration of each amino acid was present in nearly all cases in late harvested grapes, compared to comparable early harvested grapes (Table 4.3). This was especially apparent in the case of free-arginine. The unidentified amino compound and proline generally increased with the level of sun exposure, however free-arginine concentrations decreased with the level of sun exposure. The treatments exposure and harvest date both had a significant effect on the concentration of each amino acid ( $p < 0.001$ ).

#### 4.12 Grape total phenolics

Total phenolics were measured using the Folin-Ciocalteu phenolic reagent. The concentration of total phenolics in grapes was similar for all shading treatments, between 1 and 1.3 mg.g<sup>-1</sup> FW caffeic acid equivalents. There were, however, significantly higher total phenolic levels recorded in the earlier harvest fruit for all shading treatments except for EX fruit (Table 4.2). ANOVA analysis of the data confirmed that the harvest date was the most important effect ( $p = 0.024$ ). Grapevine solar exposure was not significant at the  $p = 0.05$  level.

#### 4.13 HPLC analysis of grape phenolic profiles

Figure 4.2 shows typical HPLC profiles of grape MeOH extracts, detected at 320 nm. The HPLC conditions used were similar to the conditions cited by other authors (Singleton *et al.* 1984 and Somers *et al.* 1987). The peaks were identified from their elution order and tentatively confirmed in later experiments (section 5.06). HPLC integrated peak areas were used to semi-quantitatively measure the relative concentration of individual grape phenolics expressed as integrated area counts (IAC/1000) per gram of grape skin or flesh ( $IAC \times 10^{-3}$  g<sup>-1</sup> FW). The large peak eluting at 8.3 min dominated HPLC profiles. The UV spectrum of this peak, with an absorption maximum at 328 nm, was identified as *trans*-caftaric acid. The peak eluting at 6.5 min was identified as 5-HMF from UV spectral data agreement with spectral and retention time ( $t_R$ ) data of an authentic sample of 5-HMF (Sigma Aldrich, Australia). The 'cluster' of peaks eluting at around 2.7 min.

was tentatively identified as being early formed arginine Maillard reaction products (MRPs) as described in more detail in the following chapter.

Figure 4.3 shows relative amounts for each of these peaks in grapes subjected to different shading treatments for each of the harvest dates. Data for each of these peaks were subjected to ANOVA analysis to determine LSD data. The concentration of the 'cluster' ( $t_R$  2.7 min.) was present at significantly higher concentration in MeOH extracts of late harvest grape skins, compared to early harvest grapes; lower concentrations of these compounds were present in grape flesh. There were no significant differences in the concentration of this peak for the different levels of grape exposure in the early harvested fruit. In the later harvest fruit there were large differences in the skin concentrations of this compound, however no clear relationship with shading level was apparent. The treatment harvest date was significant ( $p < 0.001$ ) for this peak.

The peak eluting at 6.5 min. (5-HMF) was present at relatively low concentration (approximately  $2-30 \text{ IAC} \times 10^{-3} \cdot \text{g}^{-1}$ ) compared to the peak at 8.3 min. This peak was identified as 5-HMF and was present at significantly higher concentration in early harvest GR and EX grapes, compared to late harvest fruit; this was not observed for the other shade treatments. Much lower concentrations of this compound were measured in the grape flesh, except for MS21 grapes, indicating that Maillard reactions may occur predominantly in grape skins. Both harvest date and vine solar exposure had a significant effect on the concentration of this compound ( $p < 0.001$ ). The higher skin concentration of 5-HMF was probably due to higher mean temperatures throughout the season on grape surfaces.

The peak eluting at 8.3 min., later identified as *trans*-caftaric acid, was present in similar concentration in grapes of each shading level; there was not a significant difference in the concentration of this compound between harvest dates. Once again much lower levels of this compound were measured in grape flesh. Neither the solar exposure nor harvest date were found to have a statistically significant effect ( $p = 0.10$ ) on the concentration of this phenolic compound in grape skins.

The small peak eluting after the main peak was tentatively identified as *trans*-coumaroyl tartaric acid ester from UV spectra (see section 5.09). The last small peak on HPLC profiles was not readily identifiable from UV spectral data (also see section 5.09).

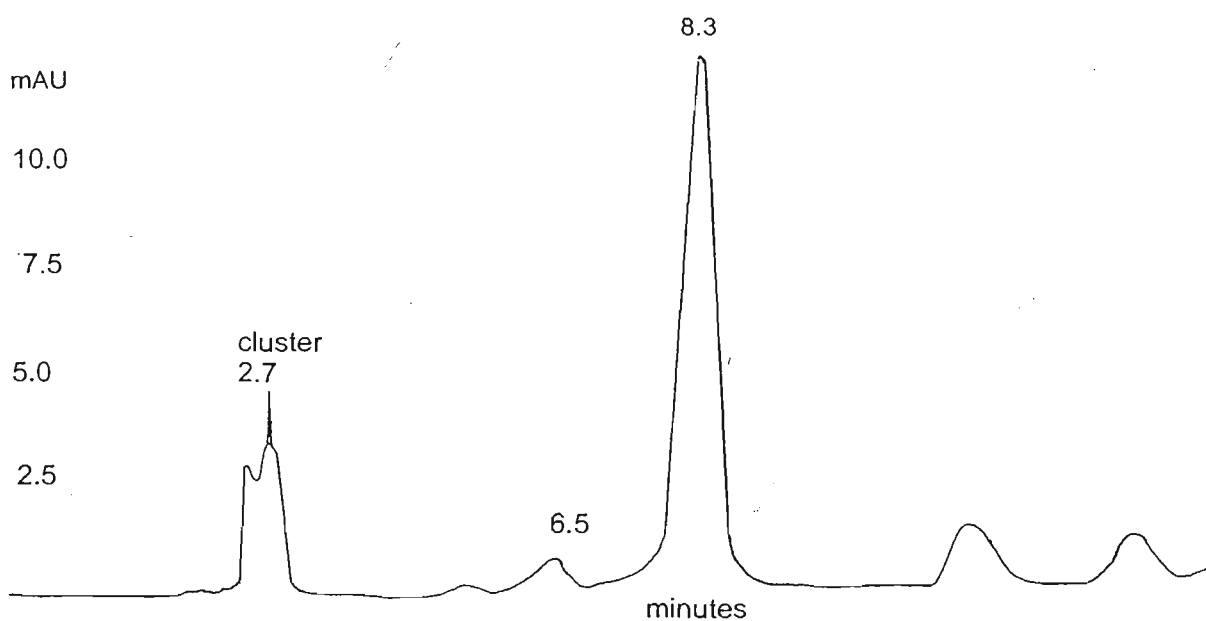
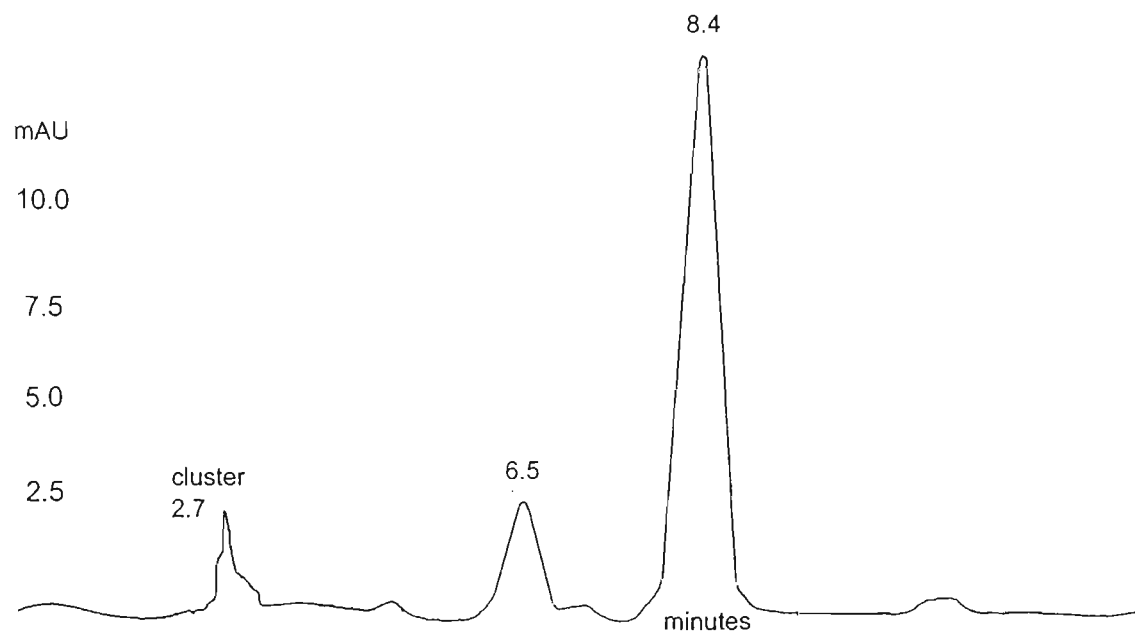


Figure 4.2 Typical HPLC profiles of MeOH extracts of 1996 grape skin phenolics at 320 nm. EX21-skin (top) and EX13-skin (bottom). The peak eluting at 8.3 min. was identified as *trans*-castaric acid and the peak at 6.5 min as 5-HMF. The cluster of peaks at approximately 2.7 min. was identified as MRPs.

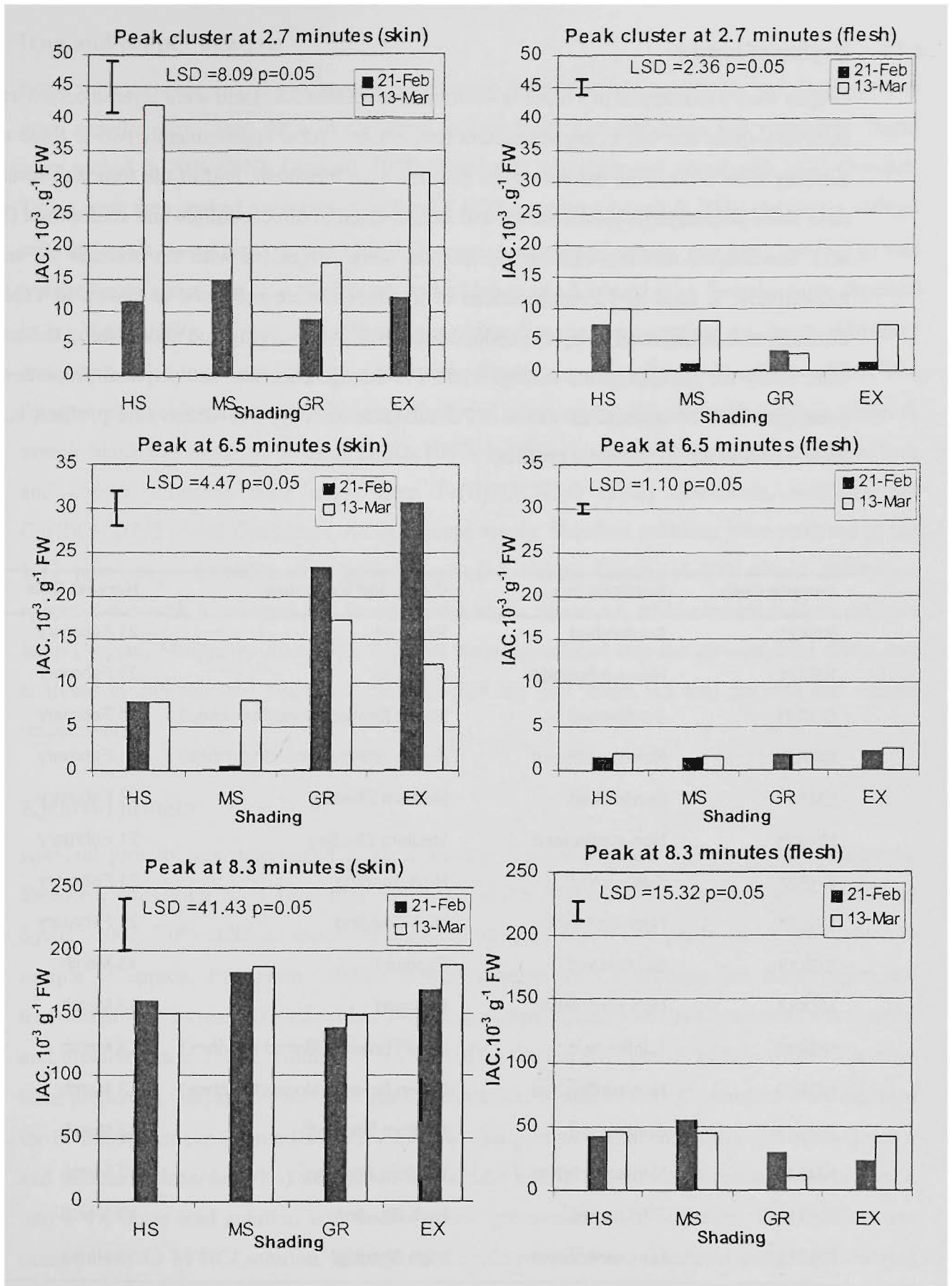


Figure 4.3 HPLC phenolic profiles of skins and flesh of the fresh grapes. Harvested on 21 February and 13 March 1996. LSD was calculated on using the means of two analytical determinations on two grape sub-samples ( $n=20$  berries).

#### 4.14 Drying of grapes

Grapes were hand dipped in a dipping solution (see section 3.03) and were layered onto wire trays in drying-sheds and left to dry at ambient temperature. After approximately two to three weeks, sultanas were taken from the wire trays and, for each treatment, half of the fruit was spread out onto black polyethylene plastic sheets and further dried in direct sunlight and sunfinished (Figure 4.1). Sunfinished and non-sunfinished samples were designated with the prefixes 'S' and 'N' respectively. A total of 16 combinations of treatments were produced as shown in Table 4.4. Sultanas will be referred to by the codes henceforth. After drying and sunfinishing the sultanas were ready for packaging and storage trials. Pre-storage chemical and physical properties were measured:  $L^*a^*b^*$  tristimulus values, PPO substrate activity, free-amino acid profiles,  $a_w$ , total phenolics and HPLC phenolic profiles.

Sample Code	Sunfinishing	Vine Solar Exposure	Harvest Date
SEX21	Sunfinished	Exposed	21 February
NEX21	Non-sunfinished	Exposed	21 February
SGR21	Sunfinished	Green (low-positioned bunches)	21 February
NGR21	Non-sunfinished	Green (low-positioned bunches)	21 February
SMS21	Sunfinished	Medium Shading	21 February
NMS21	Non-sunfinished	Medium Shading	21 February
SHS21	Sunfinished	High Shading	21 February
NHS21	Non-sunfinished	High Shading	21 February
SEX13	Sunfinished	Exposed	13 March
NEX13	Non-sunfinished	Exposed	13 March
SGR13	Sunfinished	Green (low-positioned bunches)	13 March
NGR13	Non-sunfinished	Green (low-positioned bunches)	13 March
SMS13	Sunfinished	Medium Shading	13 March
NMS13	Non-sunfinished	Medium Shading	13 March
SHS13	Sunfinished	High Shading	13 March
NHS13	Non-sunfinished	High Shading	13 March

Table 4.4 Codes used for the 16 unique sultana samples used in the 1996 storage trial.

#### 4.15 Iron and copper analysis

Forty sultanas were mixed to a homogeneous paste using a mortar and pestle and duplicate one gram samples were used for acid digestion and analysis. Kjeldahl tubes and volumetric flasks were soaked in 20% HNO<sub>3</sub> (AnalaR, BDH chemicals) overnight and rinsed with Milli-Q water. Tubes were then soaked overnight in a 50 g.L<sup>-1</sup> EDTA solution (AnalaR, BDH chemicals-sodium salt) and again rinsed three times in Milli-Q water. A sample of approx. one gram ( $\pm 0.005$  g) was weighed onto a nitrogen free filter paper and added to the Kjeldahl tube. Samples were digested in 1:1 H<sub>2</sub>SO<sub>4</sub>:HNO<sub>3</sub> at 120°C for 90 minutes. After digestion and cooling, a volume of Milli-Q water was added to the acid digests, which were filtered through a Whatman cellulose filter. The filtrate was transferred into a volumetric flask and made up to 100 mL with Milli-Q water. A sample blank was prepared by using H<sub>2</sub>SO<sub>4</sub>:HNO<sub>3</sub> in Milli-Q water without sample. Standard iron and copper solutions were made from Fe(II)SO<sub>4</sub>.7H<sub>2</sub>O (BDH Chemicals, AnalaR) and Cu(II)Cl<sub>2</sub>.2H<sub>2</sub>O (BDH Chemicals, AnalaR) respectively. Standard solutions were analysed in the 1-10 ppm range. Samples were analysed using a Varian Spectra A-400 atomic absorption spectrometer with a conventional flame burner and a SpectrAA multi-element hollow cathode lamp (Varian, Mulgrave, Australia). Samples were introduced into the air-acetylene flame and analysed at 248 nm (slit width 0.2 nm) and 324 nm (slit width 0.5 nm) for iron and copper respectively.

#### 4.16 Kjeldahl protein

Kjeldahl protein was determined using a Tecator Kjelttech-System I (Foss-Tecator, Höganäs, Sweden), consisting of a Digestion System 20-1015 heating block and a Kjelttec Distilling System-1002. Fifty sultanas were homogenised using a mortar and pestle and a representative sample of approx. two grams  $\pm 0.005$  g was weighed onto a nitrogen-free filter paper and transferred into a clean Kjeldahl tube. Two copper type Kjeltabs (BDH Chemicals) were added and dissolved in a 15 mL volume of H<sub>2</sub>SO<sub>4</sub> (BDH Chemicals, AnalaR nitrogen free). Samples were prepared in duplicate and the digestion block was heated to 400°C. Samples were digested for 60 minutes as per instructions in the manual. Samples were diluted with 70 mL Milli-Q water and sodium hydroxide (40%) was added to the tube before distillation. Ammonia was collected into a 4% boric acid solution with bromo-cresol green-methyl red indicator. The solution was titrated with 0.1 M HCl solution. Nitrogen and crude protein were calculated using the following formulae:

$$\%N = 14.01 \times (\text{mL HCl titrant}) \times 0.1 \text{ M} / \text{g of sample} \times 10$$

$$\%P = N \times \text{factor } 6.25$$

	Substrate PPO activity whole sultanas $\mu\text{mole O}_2\cdot\text{min}^{-1}\cdot\text{g}^{-1}\text{ DW}$		Total phenolics whole sultanas $\text{mg}\cdot\text{g}^{-1}\text{ DW}$		Pre-storage $a_w$	
	21 Feb early	13 March late	21 Feb early	13 March late	21 Feb early	13 March late
LSD	0.66		0.10		0.019	
P=0.05						
SEX	4.40	4.10	0.89	0.93	0.485	0.564
NEX	6.81	5.00	1.00	0.81	0.553	0.690
SGR	4.75	4.42	0.88	0.94	0.480	0.577
NGR	6.50	5.01	0.86	0.87	0.546	0.691
SMS	5.31	6.63	1.02	0.83	0.481	0.523
NMS	6.02	7.42	1.01	0.76	0.529	0.638
SHS	6.31	7.35	1.13	0.81	0.481	0.507
NHS	9.05	8.81	0.99	0.70	0.528	0.644

Table 4.5 *Pre-storage sultana data: substrate PPO activity, total phenolics and  $a_w$ . LSD values were calculated for all samples for the interaction of exposure, harvest and sunfinishing.*

#### 4.17 Analytical data for pre-storage sultanas

$A_w$  determinations were performed immediately prior to packaging of the bulk sultana samples. Substrate PPO activity, total phenolics, HPLC phenolic profiles and free-amino acid determinations were performed on sultana samples which had been stored at  $-80^\circ\text{C}$ . The analyses were performed in the manner described in the appropriate sections of chapter 3.0.

#### 4.18 Pre-storage substrate PPO activity

Mean substrate PPO values are shown in Table 4.5. For all early (21 February) harvest and most late (13 March) harvested sultanas the substrate PPO activity was significantly higher in non-sunfinished sultanas compared to sunfinished sultanas. This was in contrast to the previous year's data, where no such sunfinishing effect was observed. Although the sunfinishing effect was significant, it can be seen that considerable active PPO enzyme was still present in sunfinished sultanas. There were some differences in PPO activity for different levels of vine solar exposure treatments on both harvest dates; skin and flesh PPO concentrations were higher in MS and HS sultanas on both harvest dates. This was especially true for non-sunfinished HS fruit. Overall, however, there was not a strong trend in the effect of harvest date on PPO activity. Comparison of PPO substrate data for 1995 season sultanas ( $9.06\text{--}16.18 \mu\text{mole}\cdot\text{O}_2\cdot\text{g}^{-1}\text{ min}^{-1}$ ) with 1996 values indicated that PPO activity for 1996 season was considerably lower than the previous year's values.

#### 4.19 Pre-storage total phenolics

Total phenolics measurements fell within the range 0.70-1.13 mg.g<sup>-1</sup> caffeic acid equivalents (Table 4.5). ANOVA analysis of the data indicated that neither vine solar exposure nor the effect of sunfinishing had a significant effect on pre-storage total phenolics ( $p < 0.05$ ). Harvest date was found to be significant ( $p < 0.001$ ). Many late harvest sultanas had significantly lower total phenolic concentrations indicating that some oxidation of phenolics may have occurred during drying (*cf.* fresh grape total phenolics Table 4.2).

#### 4.20 Pre-storage sultana $a_w$

Water activity data for 1996 sultanas can be seen in Table 4.5. All early harvest fruit had significantly lower values of  $a_w$  than later harvested fruit (both sunfinished and non-sunfinished). Early harvest fruit had  $a_w$  values in the range 0.480-0.553, whereas the pre-storage  $a_w$  values for late harvest fruit ranged from 0.507-0.690. Non-sunfinished late harvest sultanas had pre-storage  $a_w$  values well above the critical  $a_w$  of 0.6, which was identified in the 1995 storage trial as the  $a_w$  at which internal sugaring was observed in sultanas (see 3.11). The effect of vine solar exposure was not significant ( $p < 0.05$ ).

#### 4.21 Pre-storage free-amino acids in sultanas

Mean concentrations of skin and flesh free-arginine, free-proline and the unidentified compound are shown in Figure 4.4. Analyses were performed on HS, MS and EX samples only. Initial concentrations of the unidentified compound in MeOH extracts of 1996 sultanas did not indicate a particularly strong relationship with harvest date or solar exposure, with levels of this amino acid being similar in sultana skin and flesh. The distribution of free-arginine however, did follow the trend previously observed in 1995 season's sultanas. Shaded sultanas had higher skin-flesh free-arginine concentrations than exposed sultanas, on both harvest dates. The concentration of skin free-arginine in late harvest sultanas was significantly higher than in comparable early harvest fruit in nearly all cases. This was especially apparent for HS and MS sultanas. Significantly higher concentrations of skin free-arginine compared with that in the flesh were observed in most cases. Exposure, harvest and sunfinishing were all significant (in decreasing order) at the  $p < 0.001$  level.

The pre-storage concentration of free L-proline did not show a strong relationship with the level of vine exposure for early harvested fruit. In late harvested fruit, however, there was a significantly higher concentration of free-proline measured in the skins of HS fruit. ANOVA analysis showed that harvest date was the most important effect followed by vine exposure ( $p < 0.001$ ). Sunfinishing was found not to be statistically significant at the  $p < 0.05$  level, although significantly lower concentrations of free-proline were measured in late harvest HS and EX sultanas.

## 4.22 Pre-storage sultana Kjeldahl protein, copper and iron

Kjeldahl protein (KP) analyses were performed in triplicate on whole sultana samples (Table 4.6). The data shows that significantly higher KP was found in MS and HS fruit compared to both GR and EX fruit. No significant differences were observed for each of the harvest dates; only the exposure term was significant ( $p < 0.001$ ). In light of the free-amino acid data, the fact that the total KP on a w/w basis did not change significantly between the harvest dates would indicate that free-amino acids were released from some source, rather than being the product of *de novo* synthesis.

Copper and iron content of sultanas was analysed using atomic absorption spectroscopy. Data for each of these elements are shown in Table 4.6. The concentration of iron in sultanas ranged from 24.01 to 26.00  $\mu\text{g.g}^{-1}$  DW. There was not a significant difference in the iron concentration in any of the samples. The concentration of copper in sultanas ranged between 5.64 - 9.41  $\mu\text{g.g}^{-1}$  and was present at significantly higher levels in shaded fruit ( $p < 0.05$ ). The effect of harvest date did not have a significant effect on the concentration of copper. It can be seen in Table 4.6 that there were only small differences in the copper concentration in early- and late-harvest sultanas.

	Kjeldahl Protein $\text{mg.g}^{-1}$ DW	Copper $\mu\text{g.g}^{-1}$ DW	Iron $\mu\text{g.g}^{-1}$ DW
LSD ( $p=0.05$ )	0.99	1.24	4.30
EX21	17.03	6.49	24.87
EX13	16.40	5.64	24.72
GR21	17.27	n.d.	n.d.
GR13	17.24	n.d.	n.d.
MS21	26.05	7.28	26.00
MS13	25.33	7.01	24.01
HS21	27.00	9.41	25.05
HS13	27.18	9.35	25.75

Table 4.6 Pre-storage concentration of Kjeldahl protein, iron and copper in early and late harvested sultanas. LSD values were determined for the duplicate analytical determinations on two sub-samples for the interaction of exposure and harvest. N.d =not done.

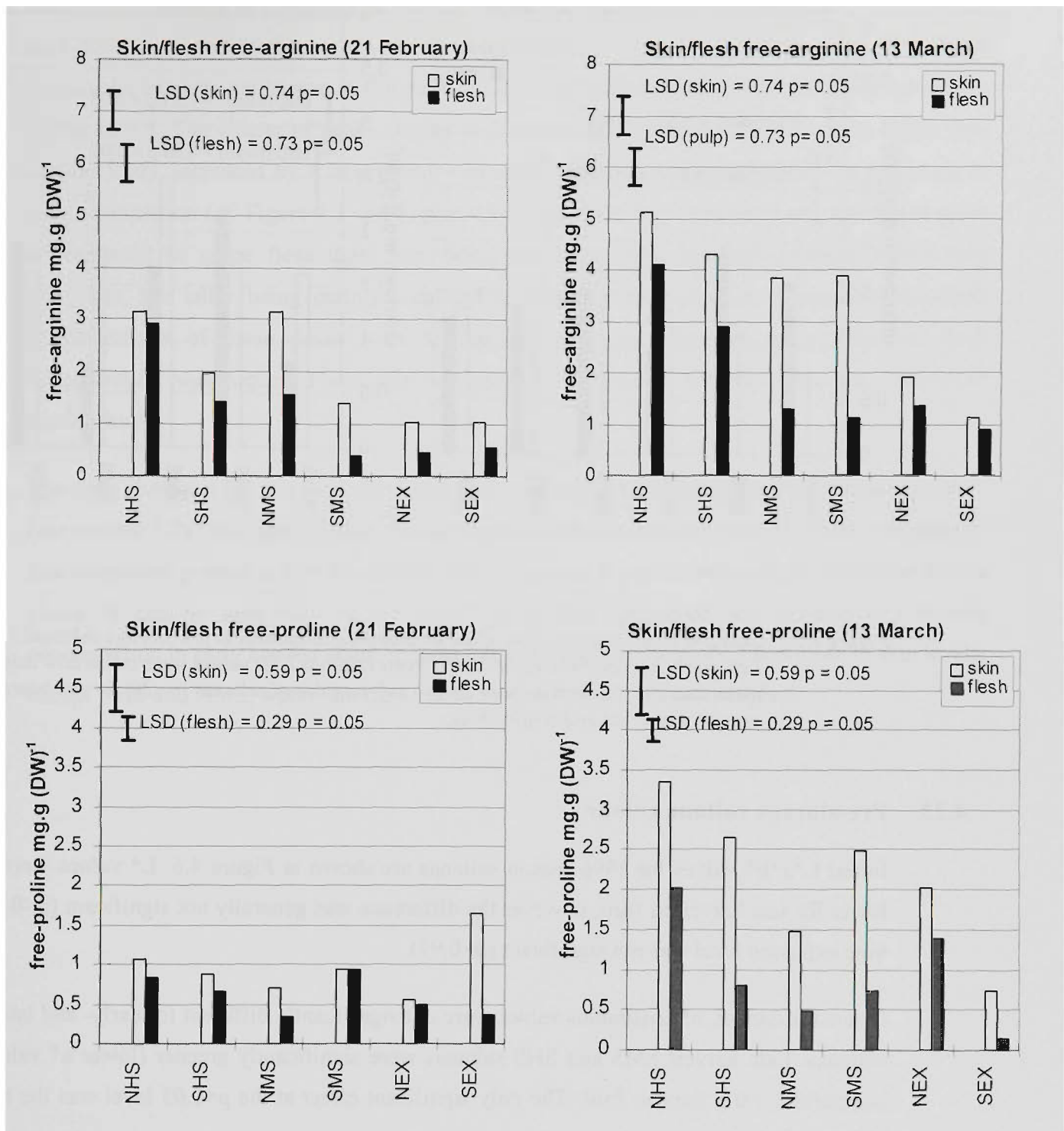


Figure 4.1 Skin and flesh concentration of free-arginine and free-proline in pre-storage sultanas. Left: early harvest fruit, right: late harvest sultanas. LSD values were calculated using the mean analytical determinations on two sub-samples of sultanas ( $n=20$ ) for the interaction of exposure, harvest and sunfinishing.

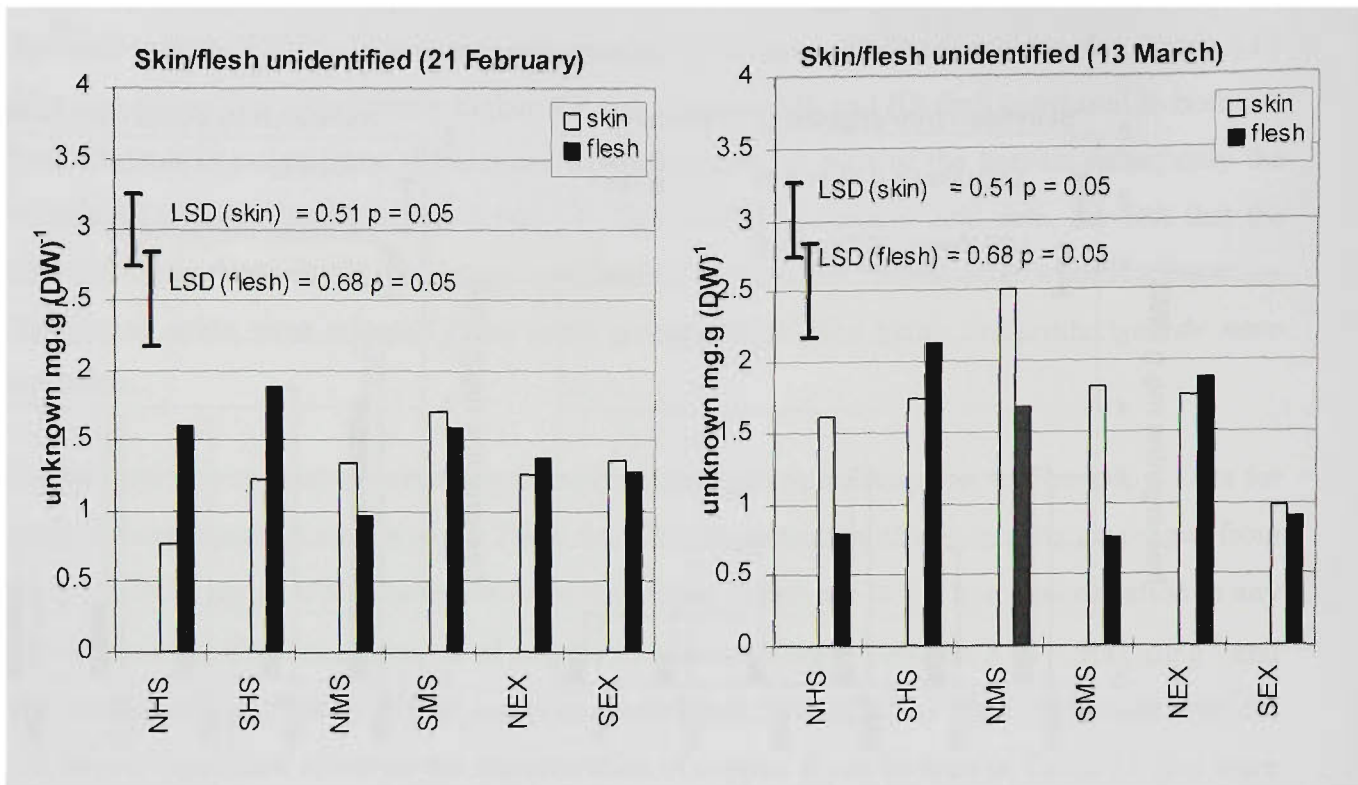


Figure 4.2 Skin and flesh concentration of the unidentified compound in pre-storage sultanas. Left: early harvest fruit, right: late harvest sultanas LSD values were calculated using the mean analytical determinations on two sub-samples of sultanas ( $n=20$ ) for the interaction of exposure, harvest and sunfinishing.

### 4.23 Pre-storage sultana colour

Initial  $L^*a^*b^*$  values for 1996 season sultanas are shown in Figure 4.6.  $L^*$  values were slightly lower for late harvested fruit, however the difference was generally not significant ( $p<0.05$ ). The vine exposure level was not significant ( $p=0.97$ ).

In most instances,  $a^*$  tristimulus values were not significantly different for early- and late-harvest sultanas. Late harvest SMS and SHS sultanas were significantly greener (lower  $a^*$  values) than comparable early harvest fruit. The only significant effect at the  $p<0.05$  level was the treatment exposure.

Pre-storage  $b^*$  values were not significantly different for the treatment harvest date, except in the case of the late harvest non-sunfinished sultanas NEX and NGR, which both had significantly lower  $b^*$  values, than comparable early harvest fruit. The treatment exposure was not significant ( $p=0.05$ ).

#### 4.24 Pre-storage sultana HPLC profiles

Methanolic extracts of phenolics in sultana skin and flesh were examined for any changes that may have occurred in the grape to sultana transition. Typical HPLC profiles for sultana methanolic extracts are shown in Figure 4.7. The relative concentrations of the peaks are shown in Figure 4.8. The cluster of peaks eluting at 2.7 min, which was identified as early MRPs (see section 5.09), increased by a large factor—in some cases more than a 30-fold—in the grape to sultana transition (*cf.* Figure 4.3 and Figure 4.8). In addition this compound was equally or more concentrated in grape flesh than skin, being consistent with Maillard products rather than phenolics, the latter being mainly localised in grape or sultana skins. Generally, skin-flesh concentrations of these peaks were similar, although in a number of samples the flesh concentration was higher. There was no apparent relationship between exposure, harvest or sunfinishing.

The peak eluting at 5.3 min. was also identified as being a later-forming Maillard reaction product (see section 5.09) also identified in glucose-arginine Maillard model systems. There was none of this compound present in MeOH extracts of fresh grapes: it was formed entirely during the drying phase. It can be seen that the concentration of this compound was present at a similar concentration in early harvest skins; in most cases the flesh concentration was close to skin levels, except NHS and NMS, where the flesh concentration was significantly higher.

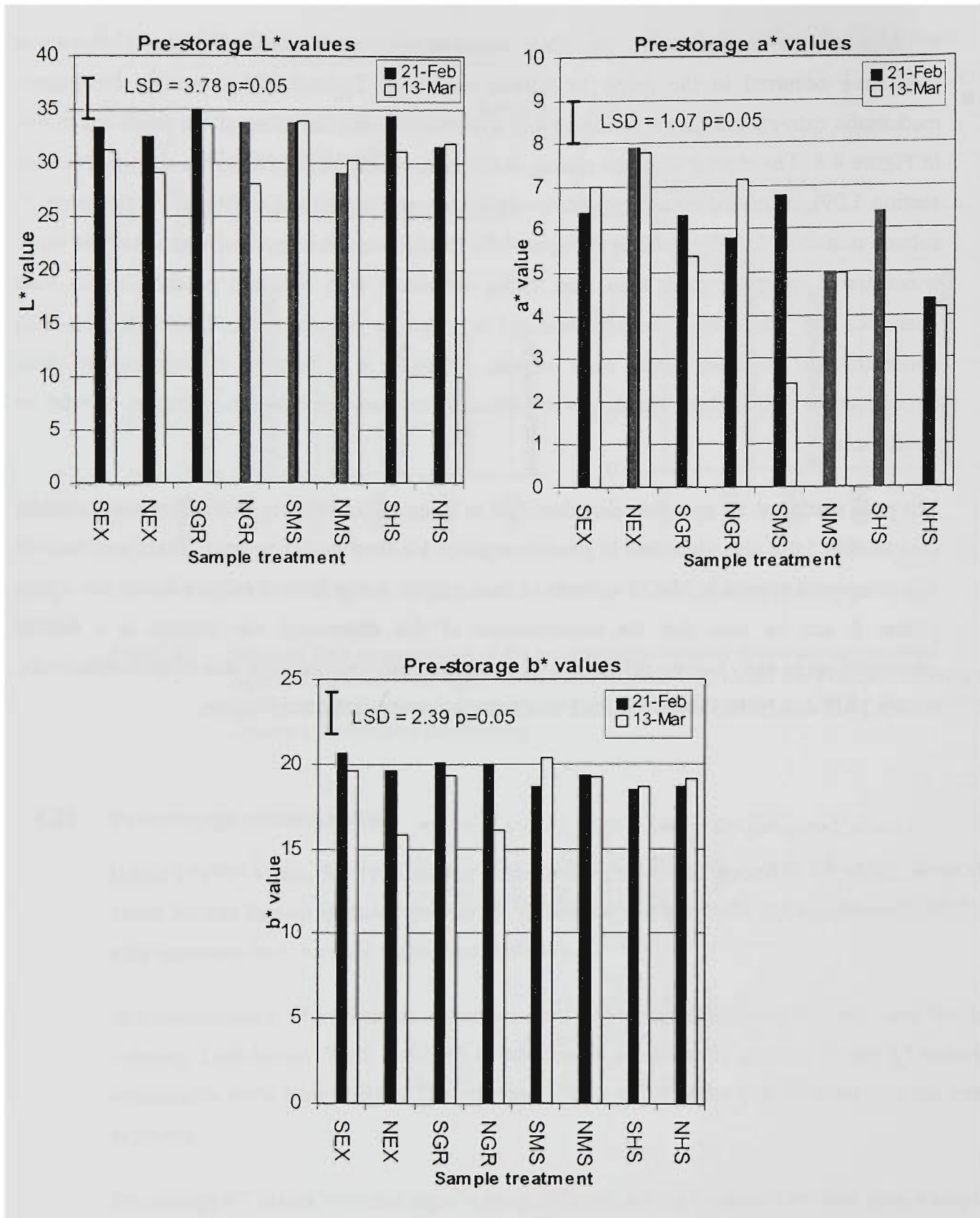


Figure 4.6 Pre-storage L\* a\* b\* tristimulus values for 1996 sultanas. Harvested 21 February and 13 March. LSD calculated using the mean of the duplicate determinations on two sub-samples of sultanas for the interaction of exposure, harvest and sunfinishing.

Significantly lower levels of this compound were present in both skin and flesh in every higher  $a_w$  non-sunfinished treatment compared to the lower  $a_w$  unfinished treatment, indicating that this Maillard reaction product was  $a_w$  sensitive. Both exposure and sunfinishing were significant effects ( $p < 0.001$ ).

The relative concentration of the peak eluting at 6.5 min.—identified as 5-HMF from spectral data (see next chapter)—increased by a large factor (ca.  $\times 10$  for HS sultanas) in the grape to sultana transition in most samples, indicating that Maillard reactions occurred during the drying process. There was some evidence that 5-HMF was also  $a_w$  sensitive; a significantly lower concentration of this compound was measured in non-sunfinished late harvest fruit compared to unfinished fruit. The effects of harvest and sunfinishing were statistically significant ( $p < 0.001$ ).

The relative concentration of the peak with a  $t_R$  time of 8.3 min.—identified in the next chapter as *trans*-caftaric acid on the basis of UV spectral data—increased in concentration in the grape to sultana transition. In grapes the skin concentration of *trans*-caftaric acid ranged ca.  $140\text{--}180 \text{ IAC} \times 10^{-3} \cdot \text{g}^{-1}$  (Figure 4.3). In sultanas this compound was present in higher concentration in the skins of all early harvest sultanas (ca.  $245\text{--}340 \text{ IAC} \times 10^{-3} \cdot \text{g}^{-1}$ ). The skin concentration of this compound in late-harvest unfinished sultanas was higher than in grapes, however lower than the concentration in comparable early-harvest sultanas. This indicated that there was some oxidation of *trans*-caftaric acid in the grape to sultana transition. The concentration of this phenolic in the skin of non-sunfinished late-harvest sultanas was significantly lower compared to the grape concentration, indicating that significant oxidation had taken place in the drying process; this was, however, not necessarily reflected in the pre-storage colour of these sultanas (Figure 4.6). In Figure 4.7 (bottom) the considerable loss of *trans*-caftaric acid can be seen from the profile of typical non-sunfinished, late-harvest sultanas. All effects; harvest, exposure and sunfinishing had a statistically significant effect on the skin concentration of *trans*-caftaric acid ( $p < 0.001$ ).

#### 4.25 Preparation of samples for the storage trial

Sultanas for each of the treatments were packaged as described in section 3.03, in oxygen-free and oxygen-exposed plastic pouches. Samples were stored in a thermostatically controlled insulated rooms as described previously, again at  $10^\circ\text{C}$  and  $30^\circ\text{C}$ . Individual package units were removed from their respective storage rooms at 5 and 10 months for physical and chemical analysis.

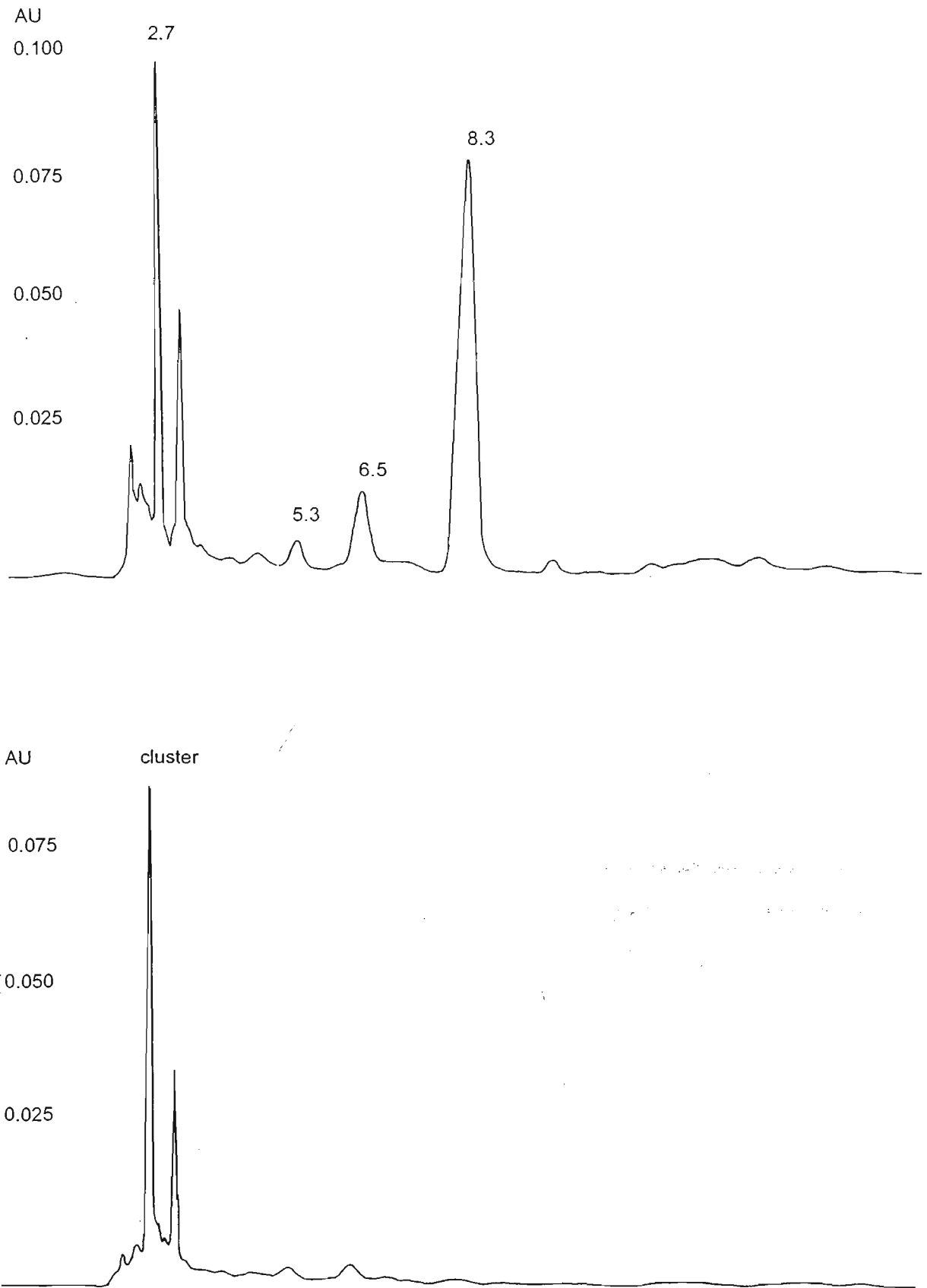


Figure 4.7 Typical HPLC profiles of MeOH extracts of pre-storage sultanas at 320 nm  
 Top: sultana skin extract (20 berries), showing *trans*-caftaric acid (8.3 min), 5-HMF (6.5 min) and other Maillard reaction peaks at ~2.7 min. and 5.3 min. Bottom: typical profile of non-sunfinished, late harvest sultanas (extract of 20 berries) showing extensive disappearance of *trans*-caftaric acid and other MRPs.

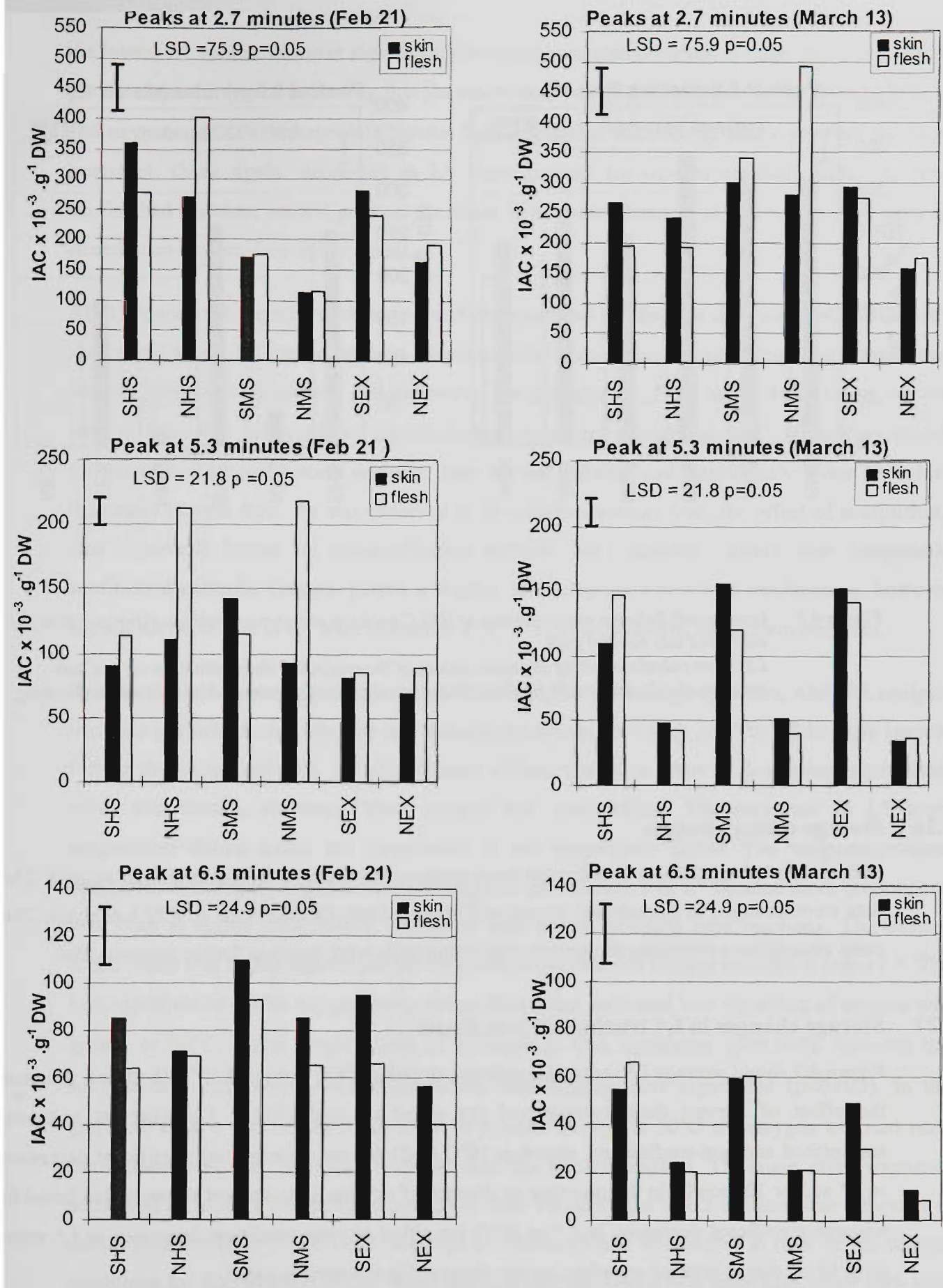


Figure 4.8 Concentration of HPLC peaks in pre-storage sultana skin and flesh for early and late harvest fruit.

LSD was calculated using the mean values of the analytical determinations on two subsamples of sultanas (n=20 berries) for the interaction of exposure, harvest and sunfinishing.

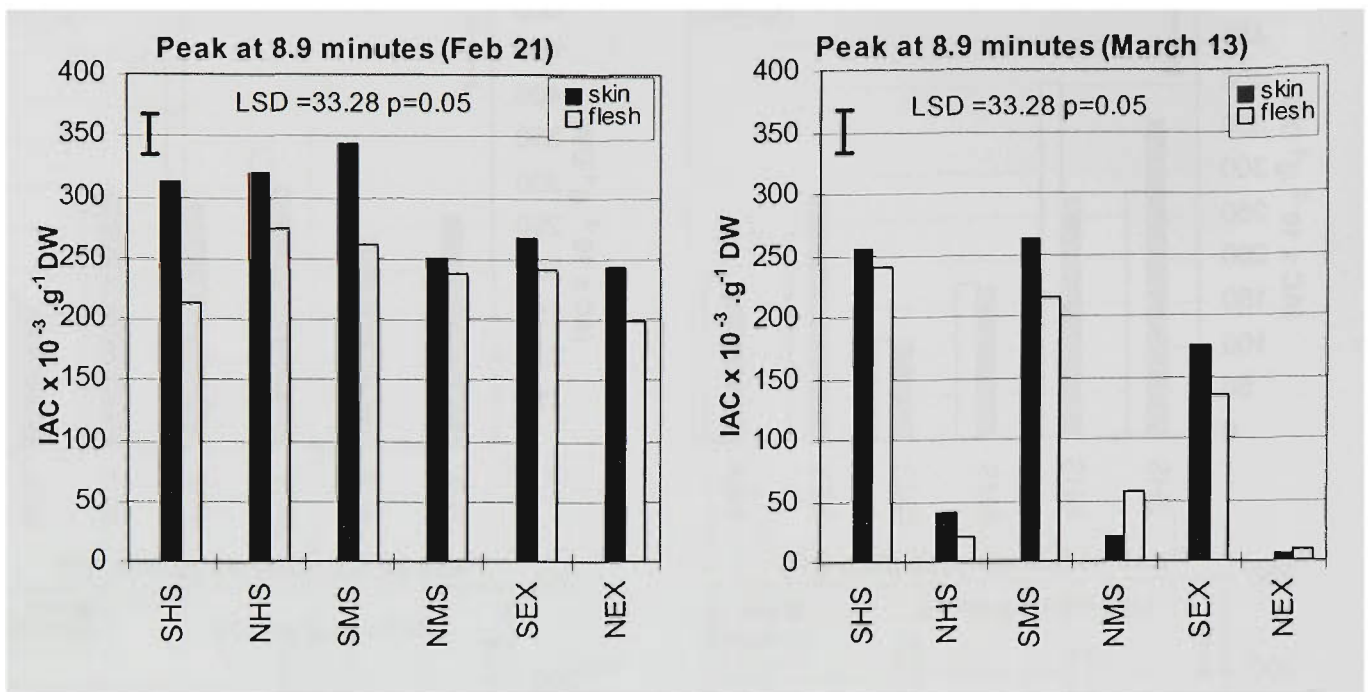


Figure 4.8 (continued) Relative concentration of HPLC peaks in pre-storage sultana skins and flesh for early and late harvest fruit. LSD was calculated using the mean values of the analytical determinations on two subsamples of sultanas ( $n=20$  berries) for the interaction of exposure, harvest and sunfinishing.

#### 4.26 Storage colour changes

Sultana  $L^*a^*b^*$  tristimulus coordinates were measured at times 0, 5 months and 10 months. The data were arranged in spreadsheet format and imported into Genstat 5 for ANOVA analysis. The same assumptions regarding the storage-packaging units were made as for the previous trial.

#### 4.27 Storage changes in $L^*$ tristimulus coordinate

Figure 4.9 shows average  $L^*$  values for sultanas stored at  $10^\circ\text{C}$  (top) and  $30^\circ\text{C}$  (bottom), showing the effect of harvest date, oxygen and the effect of sunfinishing. Early-harvest sultanas, sunfinished and non-sunfinished, stored at  $10^\circ\text{C}$  (left) did not undergo any significant decreases in  $L^*$  at 5 or 10 months in the presence or absence of oxygen. Late-harvest sultanas also failed to undergo significant decreases in  $L^*$  at  $10^\circ\text{C}$  for either oxygen condition. Increases in  $L^*$  were most likely due to internal sugaring, as was observed in the previous trial.

Significant decreases in  $L^*$  were observed only at  $30^\circ\text{C}$ . For early harvest sultanas significant decreases in  $L^*$  were observed at 5 months only for oxygen-exposed sultanas, both sunfinished and non-sunfinished, however all treatments had significantly lower  $L^*$  values after 10 months storage. After 10 months storage, all sunfinished sultanas had comparable  $L^*$  values, regardless of their oxygen exposure. After 10 months non-sunfinished oxygen-exposed sultanas clearly had

the lowest  $L^*$  values, however significant decreases were also observed in these samples stored in the absence of oxygen, indicating that the reaction(s) which took place were sensitive to both  $a_w$  and oxygen. At 30°C storage, late harvest fruit was darker than comparable early fruit for every treatment. Once again, decreases in  $L^*$  were greatest for oxygen-exposed, higher  $a_w$  non-sunfinished sultanas; second greatest decreases in  $L^*$  were observed in non-sunfinished sultanas stored in an oxygen-free environment.

ANOVA analyses were performed on combined early and late harvest sultanas. ANOVA data are shown in Table 4.7. Significant main effects in order of decreasing importance were temperature, harvest, oxygen, sunfinishing and exposure. The importance of the temperature effect, as was seen in Table 4.7, indicated that significant browning only occurred at 30°C. Harvest accounted for the second largest portion variance; later harvest sultanas had significantly lower  $L^*$  values than early harvest fruit. As was observed in the previous storage trial, the effect of sunfinishing was important; higher  $a_w$  non-sunfinished sultanas were generally darker than comparable sunfinished controls. Oxygen played a slightly more important role than sunfinishing, however significant decreases in  $L^*$  were measured at 30°C in an oxygen-free storage environment.

Because the late-harvest sultanas had significantly higher pre-storage  $a_w$  values, ANOVA analysis was also performed on early and late sultanas separately. ANOVA data for  $L^*$  in early harvest fruit is shown in Table 4.8. Significant main effects, ranked in order of decreasing importance, were; temperature, exposure, time, oxygen and sunfinishing. The decreases in  $L^*$  were temperature driven hence the importance of the temperature factor. The temperature×time interaction was highly significant, indicating that the decreases in  $L^*$  became more pronounced with time at higher temperature, consistent with slower Maillard type reactions. The oxygen single effect was highly significant showing that the presence of oxygen resulted in lower  $L^*$ . The high significance of the oxygen×temperature interaction indicated that the effect of oxygen was greater at 30°C. The single effect of sunfinishing was significant ( $p<0.047$ ), however the sunfinishing×oxygen×temperature interaction was slightly more significant ( $p<0.025$ ). In the graphical data it can be seen that after 10 months storage at 30°C the oxygen exposed non-sunfinished fruit was significantly darker than the non-sunfinished. The main effect exposure accounted for a highly significant portion of total variance; the effect of vine solar exposure is shown graphically in Figure 4.10. Average  $L^*$  values (5 and 10 months) at each of the storage conditions for EX, MS and HS sultanas indicated that sultanas which were from vines with high solar exposure were generally lighter than shaded controls.

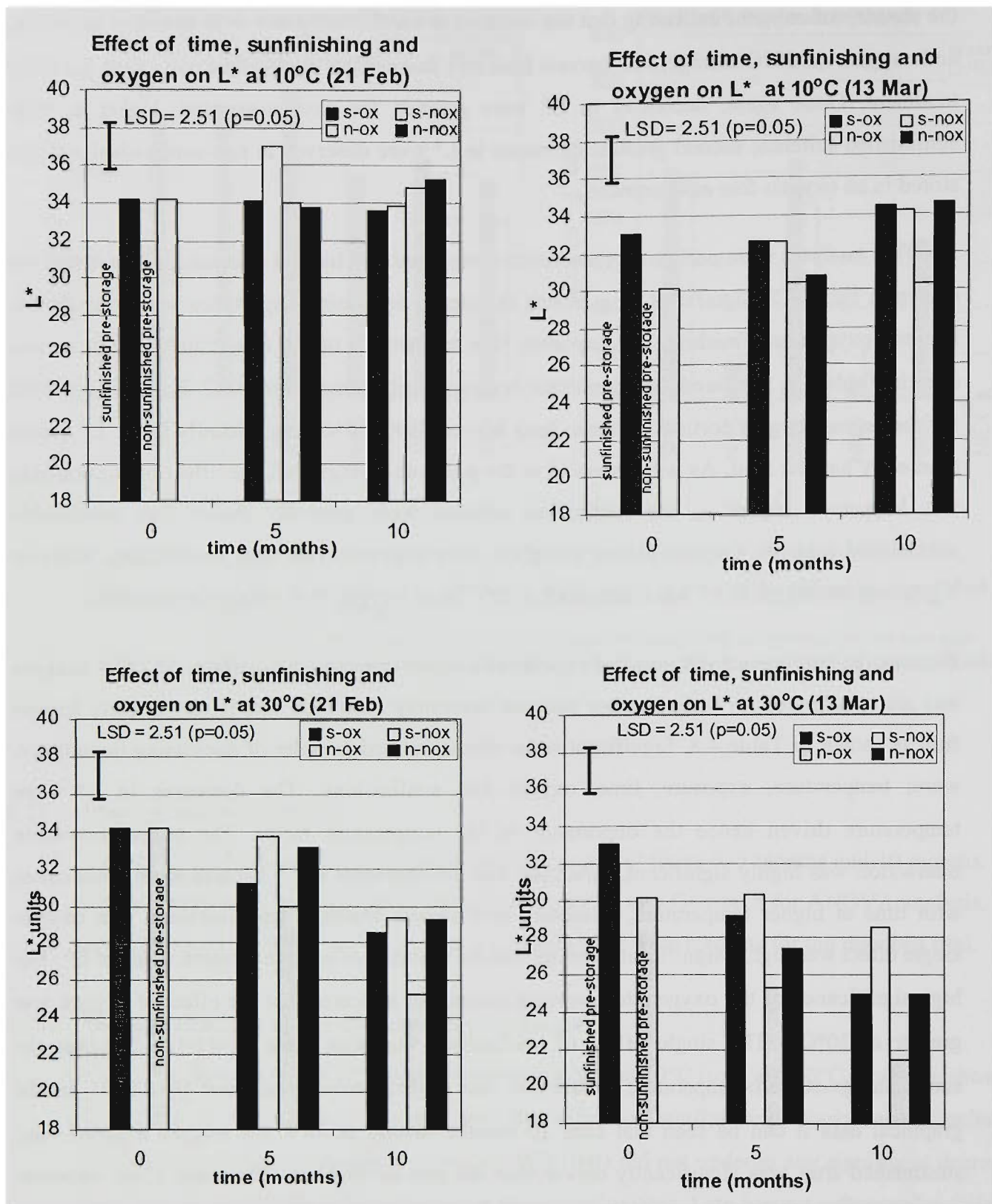


Figure 4.9 Change in L\* values at 10°C (top) and 30°C (bottom) averaged for level of exposure. Sunfinished (s) and non-sunfinished (n) sultanas stored in the presence of oxygen (-ox) and without oxygen (-nox). LSD values were calculated for the interaction of harvest × sunfinishing × oxygen × temperature × time for all samples.

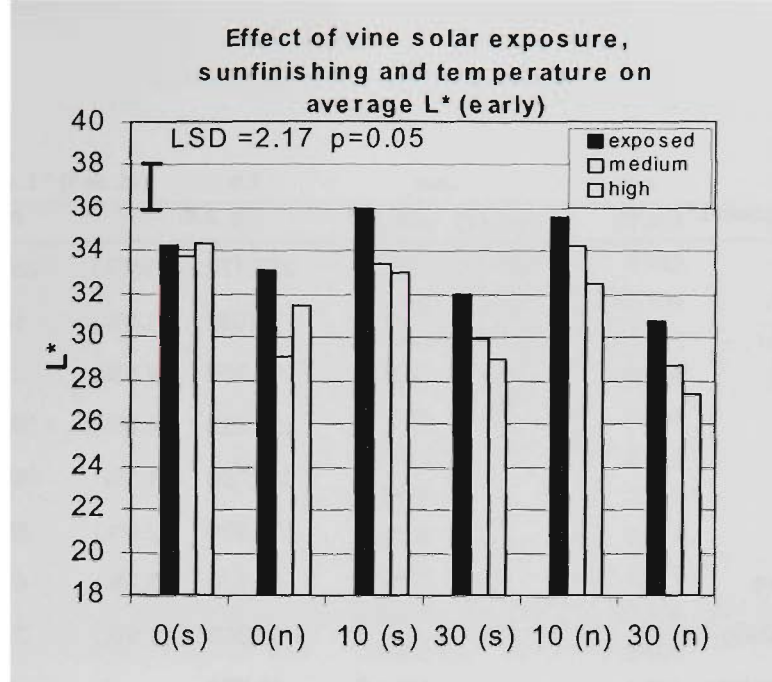


Figure 4.10 Effect of vine solar exposure on  $L^*$  values averaged for early (21 February) harvested Sultanas.  
LSD was calculated for the interaction of harvest  $\times$  exposure  $\times$  sunfinishing  $\times$  temperature.

Separate ANOVA analysis for late harvest Sultanas indicated that vine solar exposure was not significant (Table 4.8); no apparent trend was observed as for the early exposed sample (graph not shown). The main effects, temperature, sunfinishing and oxygen were all highly significant, as was the interaction of temperature $\times$ time. The large effect of temperature is shown clearly in Figure 4.9. At 10°C storage there were no significant decreases in  $L^*$  for the late harvest Sultanas stored under any conditions. In contrast all Sultanas stored at 30°C underwent significant decreases in  $L^*$  regardless of their oxygen exposure or sunfinishing status. The clear time dependence of the decreases in  $L^*$  were seen at 30°C storage. In addition to the significant oxygen term, the interaction of time $\times$ oxygen was close to reaching significance ( $p=0.05$ ), which implied that the effect of oxygen was enhanced with time. This can be supported by the observation that 5 months difference in  $L^*$  between oxygen-exposed and anaerobically stored treatment pairs was not significant but by 10 months clearly was significant. The important effect of sunfinishing was observed in Figure 4.9: at both 5 and 10 months, regardless of the oxygen status, the non-sunfinished fruit were darker than sunfinished controls. The low of significance of the oxygen $\times$ sunfinishing term ( $p=0.13$ ) indicated that the sunfinishing effect was important in itself to promote decreases in  $L^*$  and did not require oxygen to be present to take effect.

Source of variation L*	d.f	s.s.	m.s.	v.r.	F pr.
Harvest	1	252.170 (11.9%)	252.17	95.36	<0.001
exposure	2	36.980 (1.8%)	18.491	6.99	0.002
sunfinishing	1	95.358 (4.5%)	95.358	36.06	<0.001
oxygen	1	100.320 (4.8%)	100.324	37.94	<0.001
temperature	1	869.760 (41.3%)	869.758	328.91	<0.001
time	1	59.590 (2.8%)	59.596	22.54	<0.001
harvest.exposure	2	83.730 (3.9%)	41.868	15.83	<0.001
harvest.sunfinishing	1	30.380 (1.5%)	30.381	11.49	0.001
exposure.sunfinishing	2	12.570	6.284	2.38	0.104
harvest.oxygen	1	0.171	0.171	0.06	0.8
exposure.oxygen	2	6.588	3.294	1.25	0.297
sunfinis.oxygen	1	5.503	5.503	2.08	0.156
harvest.temperature	1	16.603	16.603	6.28	0.016
exposure.temperature	2	7.075	3.537	1.34	0.273
sunfinishing.temperature	1	15.015	15.015	5.68	0.021
oxygen.temperature	1	20.995	20.995	7.94	0.007
harvest.time	1	17.390	17.39	6.58	0.014
exposure.time	2	2.785	1.393	0.53	0.594
sunfinis.time	1	2.453	2.453	0.93	0.341
oxygen.time	1	2.703	2.703	1.02	0.317
temperature.time	1	139.740 (6.6%)	139.737	52.84	<0.001
harvest.oxygen.time	1	13.939	13.939	5.27	0.026
exposure.oxygen.time	2	20.423	10.212	3.86	0.028
harvest.sunfinishing.oxygen.temperature	1	14.567	14.567	5.51	0.023
exposure.sunfinishing.oxygen.temperature	2	34.636	17.318	6.55	0.003
<b>Pooled SS for non-significant three- and four-way interactions</b>		<b>128.36</b>			
<b>Residual</b>	<b>45</b>	<b>118.995</b>	<b>2.644</b>		
<b>Total</b>	<b>127</b>	<b>2108.8</b>			

Table 4.7 ANOVA table for L\*: treatment harvest time included. All main and two-way interactions shown. Significant ( $p > 0.05$ ) effects are highlighted in grey. Only significant three-way and four-way interactions are shown. SS variance for the non-significant three- and four-way interactions was pooled.

Source of variation. L* (Feb 21)	d.f.	s.s.		m.s.	v.r.	F pr.
exposure	2	114.700	(14.1%)	57.353	28.7	<0.001
sunfinishing	1	9.045	(1.1%)	9.045	4.53	0.047
oxygen	1	46.100	(5.7%)	46.104	23.07	<0.001
temperature	1	323.010	(39.8%)	323.011	161.65	<0.001
time	1	70.680	(8.7%)	70.686	35.38	<0.001
exposure.sunfinishing	2	1.791		0.896	0.45	0.646
exposure.oxygen	2	5.222		2.611	1.31	0.295
sunfinis.oxygen	1	0.107		0.107	0.05	0.819
exposure.temperature	2	0.028		0.014	0.01	0.993
sunfinis.temperature	1	5.267		5.267	2.64	0.122
oxygen.temperature	1	12.408		12.408	6.21	0.023
exposure.time	2	4.852		2.426	1.21	0.320
sunfinishing.time	1	4.796		4.796	2.40	0.139
oxygen.time	1	2.183		2.183	1.09	0.310
temp.time	1	49.070	(6.0%)	49.07	24.56	<0.001
sunfinis.oxygen.temp	1	11.937		11.937	5.97	0.025
exposure.sunfinis.time	2	6.951		3.476	1.74	0.204
exposure.oxygen.time	2	32.776		16.388	8.20	0.003
sunfinis.oxygen.time	1	9.030		9.030	4.52	0.048
sunfinis.temp.time	1	14.612		14.612	7.31	0.015
exposure.sunfinis.oxygen.temp	2	34.06		17.033	8.52	0.002
<b>Pooled SS for non-significant three- and four- way interactions</b>						
<b>Residual</b>	<b>18</b>	<b>35.967</b>		<b>1.998</b>		
<b>Total</b>	<b>63</b>	<b>812.673</b>				

Source of variation L* (13 Mar)	d.f.	s.s.		m.s.	v.r.	F pr.
Exposure	2	6.01		3.005	0.85	0.445
sunfinish	1	116.69	(11.1%)	116.694	32.91	<0.001
oxygen	1	54.391	(5.2%)	54.391	15.34	0.001
temp	1	563.35	(54.0%)	563.35	158.87	<0.001
time	1	6.32		6.3	1.78	0.199
exposure.sunfinis	2	22.57		11.29	3.18	0.065
exposure.oxygen	2	1.808		0.904	0.25	0.778
sunfinis.oxygen	1	8.94		8.94	2.52	0.13
exposure.temp	2	13.003		6.501	1.83	0.188
sunfinis.temp	1	10.144		10.144	2.86	0.108
oxygen.temp	1	8.747		8.747	2.47	0.134
exposure.time	2	5.91		2.955	0.83	0.451
sunfinis.time	1	0.001		0.001	0.00	0.99
oxygen.time	1	14.459		14.459	4.08	0.059
temp.time	1	94.33	(9.0%)	94.333	26.60	<0.001
<b>Pooled SS for non-significant three-and four-way interactions</b>						
<b>Residual</b>	<b>18</b>	<b>63.829</b>		<b>3.546</b>		
<b>Total</b>	<b>63</b>	<b>1043.957</b>				

Table 4.8 ANOVA table for L\* for early (top) and late harvest (bottom) sultanas.

#### 4.28 Storage changes in a\* tristimulus coordinate

Table 4.9 shows the ANOVA data for a\* (redness) for both early and late harvest sultanas together. The single effects of exposure, temperature, sunfinishing and harvest were highly significant. Neither oxygen ( $p=0.21$ ) nor time ( $p=0.60$ ) were significant. A number of two-way interactions were also significant.

Mean a\* values, average of all solar exposure levels, are shown graphically in Figure 4.11. for early and late sultanas stored at 10°C (top) and 30°C (bottom). At all temperatures, average a\* increased compared to pre-storage values. The effect pronounced effect of temperature on a\* was especially apparent for early harvest fruit stored at 30°C, for which a large significant increase was observed, regardless of the oxygen status. Separate ANOVA analysis of early harvest fruit (Table 4.9) indicated that temperature was the most important effect followed by sunfinishing and exposure. The effects of neither time nor oxygen were significant. It can be seen that 30°C stored early-harvest sultanas were significantly redder than 10°C stored fruit. Non-sunfinished sultanas generally had lower a\* values than sunfinished controls, hence the high significance of sunfinishing term. The lack of significance of the effect of time was illustrated by the small differences observed between 5 and 10 months. The largest changes in a\* occurred in the 0-5 month interval with only small changes occurring thereafter. In Figure 4.12 the effect of vine exposure on a\* is shown graphically: for early-harvest fruit, average EX fruit was slightly redder than MS and HS sultanas, however the differences were generally not statistically significant.

For late harvest fruit, the largest single factor accounting for variation in a\* was exposure, followed by temperature, sunfinishing and a number of significant two-and three-way interactions. The effect of oxygen was not statistically significant ( $p=0.1$ ). In Figure 4.11 it can be seen that non-sunfinished fruit had slightly lower a\* values than sunfinished fruit at 30°C storage irrespective of oxygen exposure. The strong effect of vine solar exposure is clearly seen in Figure 4.12: nearly all EX fruit was redder than MS or HS fruit. This trend was already apparent in pre-storage fruit and persisted throughout the storage trial. It can also be seen that overall, a\* increased significantly in all fruit under all storage conditions.

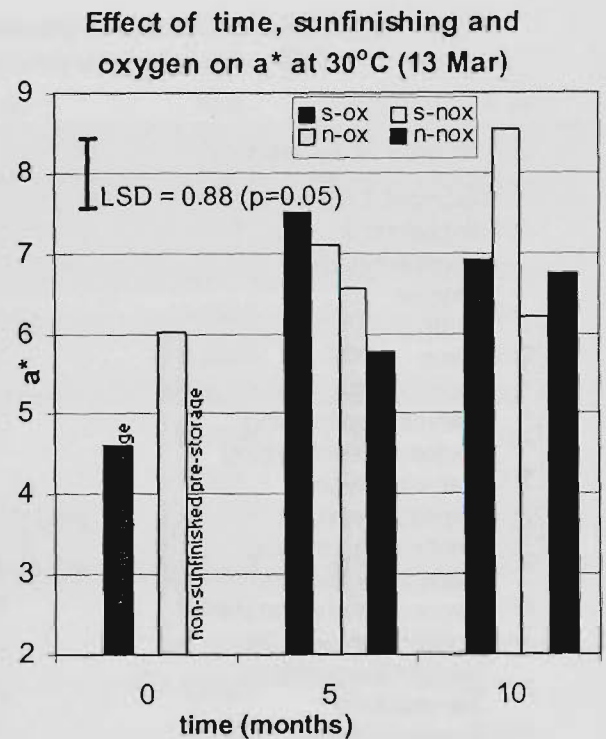
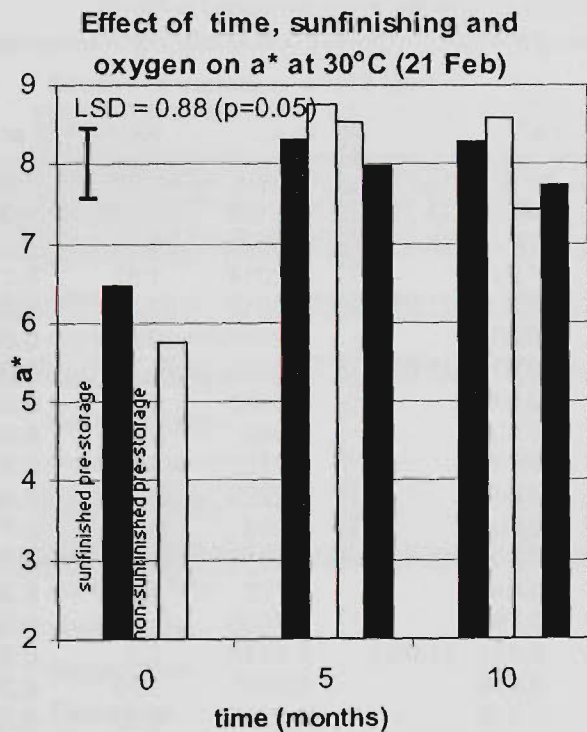
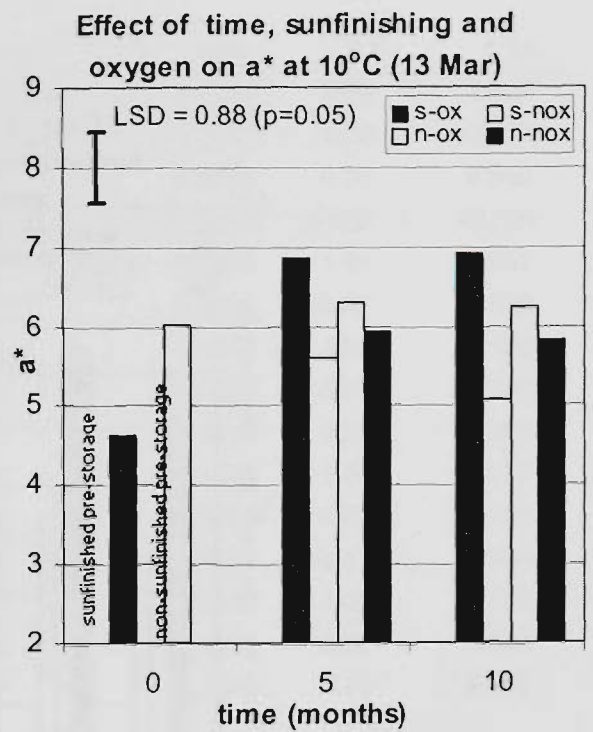
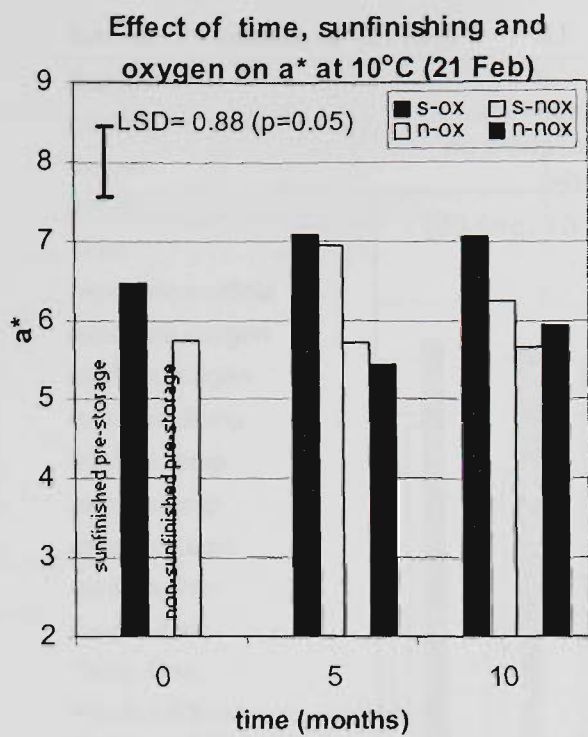


**Figure 4.11** Change in  $a^*$  values at 10°C (top) and 30°C (bottom): averaged for early and late fruit. Sunfinished (s) and non-sunfinished (n) sultanas stored in the presence of oxygen (-ox) and without oxygen (-nox). LSD values were calculated for the interaction of harvest  $\times$  sunfinishing  $\times$  oxygen  $\times$  temperature  $\times$  time for all samples.

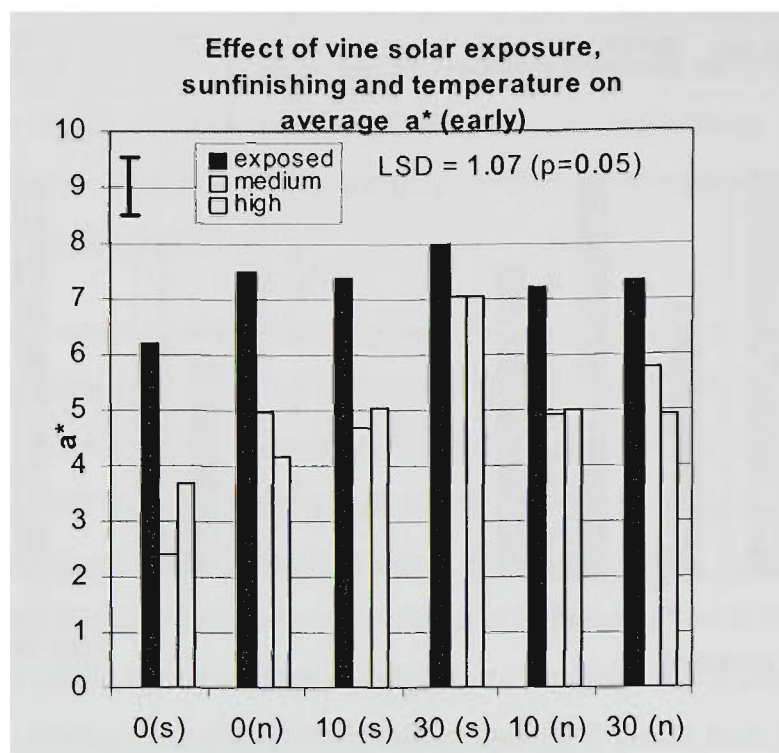


Figure 4.12 Effect of vine solar exposure on  $a^*$  values averaged for early harvested sultanas.  
LSD value calculated for the interaction of harvest  $\times$  exposure  $\times$  sunfinishing  $\times$  temperature.

Source of variation $a^*$	d.f	s.s.	m.s.	v.r.	F pr.
Harvest	1	15.820 (5.7%)	15.821	21.33	<.001
exposure	2	60.250 (21.7%)	30.1133	40.61	<.001
sunfinishing	1	17.860 (6.4%)	17.8645	24.09	<.001
oxygen	1	1.200	1.2014	1.62	0.21
temp	1	60.880 (21.9%)	60.8842	82.1	<.001
Time	1	0.200	0.2047	0.28	0.602
harvest.exposure	2	10.020 (3.6%)	5.0124	6.76	0.003
harvest.sunfinishing	1	0.548	0.5488	0.74	0.394
exposure.sunfinishing	2	0.106	0.053	0.07	0.931
harvest.oxygen	1	0.775	0.7752	1.05	0.312
exposure.oxygen	2	4.440	2.2229	3	0.06
sunfinishing.oxygen	1	0.098	0.098	0.13	0.718
harvest.temperature	1	9.500 (3.4%)	9.5053	12.82	<0.001
exposure.temperature	2	1.546	0.773	1.04	0.361
sunfinis.temperature	1	0.796	0.7968	1.07	0.306
oxygen.temperature	1	5.411 (1.9%)	5.4116	7.3	0.01
harvest.time	1	0.959	0.9593	1.29	0.262
exposure.time	2	0.478	0.2395	0.32	0.726
sunfinishing.time	1	0.000	0.0001	0.00	0.992
oxygen.time	1	1.5315	1.5315	2.07	0.158
temperature.time	1	0.0392	0.0392	0.05	0.819
harvest.sunfinis.temperature	1	5.7711	5.7711	7.78	0.008
sunfinishing.oxygen.temperature	1	3.9407	3.9407	5.31	0.026
oxygen.temperature.time	1	3.0879	3.0879	4.16	0.047
<b>Pooled SS for all non-significant three- and four- way interactions</b>					
<b>Residual</b>	<b>44</b>	<b>32.63</b>	<b>0.7416</b>		
<b>Total</b>	<b>127</b>	<b>277.13</b>			

Table 4.9 ANOVA table for  $a^*$ : treatment harvest time included.

Source of variation a* (21 Feb)	d.f.	s.s.	m.s.	v.r.	F pr.
Exposure	2	11.540 (10.3%)	5.7737	7.92	0.003
sunfinis	1	12.330 (10.4%)	12.3377	16.93	<0.001
oxygen	1	0.0233	0.0233	0.03	0.860
temp	1	59.250 (49.7%)	59.2515	81.31	<0.001
Time	1	1.0252	1.0252	1.41	0.251
exposure.sunfinis	2	0.6922	0.3461	0.47	0.630
exposure.oxygen	2	2.8525	1.4263	1.96	0.170
sunfinis.oxygen	1	0.0039	0.0039	0.01	0.942
exposure.temp	2	0.3291	0.1646	0.23	0.800
sunfinis.temp	1	1.1396	1.1396	1.56	0.227
oxygen.temp	1	0.6931	0.6931	0.95	0.342
exposure.time	2	0.1442	0.0721	0.1	0.906
sunfinis.time	1	0.0046	0.0046	0.01	0.938
oxygen.time	1	0.1620	0.162	0.22	0.643
Temp.time	1	0.5293	0.5293	0.73	0.405
<b>Pooled SS for non-significant three- and four-way interactions</b>					
<b>Residual</b>	<b>18</b>	<b>13.1167</b>	<b>0.7287</b>		
<b>Total</b>	<b>63</b>	<b>119.5475</b>			

Source of variation a* (13 Mar)	d.f.	s.s.	m.s.	v.r.	F pr.
Exposure	2	58.210 (41.3%)	29.1097	42.83	<0.001
sunfinis	1	5.920 (4.2%)	5.9204	8.71	0.009
oxygen	1	2.043	2.043	3.01	0.101
temp	1	10.920 (7.7%)	10.9275	16.08	<0.001
Time	1	0.1635	0.1635	0.24	0.63
exposure.sunfinis	2	1.1738	0.5869	0.86	0.439
exposure.oxygen	2	4.5314	2.2657	3.33	0.06
sunfinis.oxygen	1	0.1696	0.1696	0.25	0.624
exposure.temp	2	4.332	2.166	3.19	0.067
sunfinis.temp	1	5.280 (3.6%)	5.2816	7.77	0.013
oxygen.temp	1	5.8839 (4.2%)	5.8839	8.66	0.009
exposure.time	2	1.7688	0.8844	1.3	0.298
sunfinis.time	1	0.0023	0.0023	0	0.954
oxygen.time	1	1.9025	1.9025	2.8	0.113
Temp.time	1	1.0802	1.0802	1.59	0.224
sunfinis.oxygen.temp	1	3.5652	3.5652	5.25	0.035
oxygen.temp.time	1	4.0776	4.0776	6	0.025
exposure.sunfinis.oxygen.time	2	4.5342	2.2671	3.34	0.06
<b>Residual</b>	<b>17</b>	<b>11.5544</b>	<b>0.6797</b>		
<b>Total</b>	<b>62</b>	<b>11.0934</b>			

Table 4.10 ANOVA table for a\* for early (top) and late harvest (bottom) sultanas.

#### 4.29 Storage changes in $b^*$ tristimulus coordinate

ANOVA data for  $b^*$  (yellowness) for early and late harvest fruit indicated a large number of significant single effects and interactions (Table 4.11). The single effects of temperature, harvest, oxygen and sunfinishing were all highly significant, as were a number two-way interactions. The four-way interaction of exposure $\times$ sunfinishing $\times$ oxygen $\times$ temperature was also highly significant, indicating that the  $b^*$  tristimulus values were affected by a complex interplay of factors. The mean  $b^*$  values across all exposure-levels are shown in Figure 4.13.

The ANOVA table for  $b^*$  for early-harvest sultanas (Table 4.12) indicated that temperature was the most important effect followed by time, the oxygen $\times$ temperature interaction and oxygen and other significant interactions. At 10°C storage some small decreases in  $b^*$  values were observed, however the decreases were not significant ( $p=0.05$ ). After 5 months storage at 30°C significant decreases were observed only in oxygen exposed samples. After 10 months storage at the same temperature, all samples had significantly lower  $b^*$  values compared to pre-storage values. It was clear, however, that high  $a_w$  sultanas stored in the presence of oxygen had the lowest  $b^*$  values. The effect of vine solar exposure on average  $b^*$  values is shown in Figure 4.14. Most sultanas from MS and HS treatments had lower  $b^*$  values compared to EX sultanas.

ANOVA data for late harvest fruit (Table 4.12) indicated that the most important effects were temperature, sunfinishing, oxygen and the temperature $\times$ time interaction. At 10°C storage decreases in  $b^*$  were observed for all conditions after 5 months, with similar values for sultanas stored in the presence and absence of oxygen. After 10 months storage at this temperature, increases in  $b^*$  were measured in all samples except oxygen-exposed non-sunfinished fruit. Increases in  $b^*$  were explained by the extensive internal sugaring in these samples (see later sections). At 30°C storage, significant decreases in  $b^*$  were measured for all storage conditions. Sunfinished fruit stored in an oxygen-free environment underwent the smallest decrease in  $b^*$ , emphasising the positive effect of exclusion of oxygen in these samples. The effect of oxygen exclusion was, however not nearly as effective for higher- $a_w$ , non-sunfinished sultanas, which after 10 months storage were almost as dark as non-sunfinished samples stored in the presence of oxygen. The lack of significance of the sunfinishing $\times$ oxygen term ( $p=0.853$ ) was seen in the graphical data:  $b^*$  values of non-sunfinished were lower regardless of the oxygen status. As for the  $L^*$  values, this interaction would be expected to be highly significant if the chemical reactions affecting decreases in  $b^*$  were mainly PPO driven, i.e at higher  $a_w$  the oxygen effect would become more important. In contrast to the sunfinishing $\times$ oxygen term, the sunfinishing $\times$ temperature and the oxygen $\times$ temperature interactions were both highly significant ( $p<0.001$ ). This may be interpreted in the following manner: at 30°C the more important determinant of decreases in  $b^*$  was sunfinishing (ie initial  $a_w$ ) rather than oxygen being present (Figure 4.14). This can be seen in the very low  $b^*$  values found after 10 months for the non-sunfinished sultanas, regardless of the oxygen status.

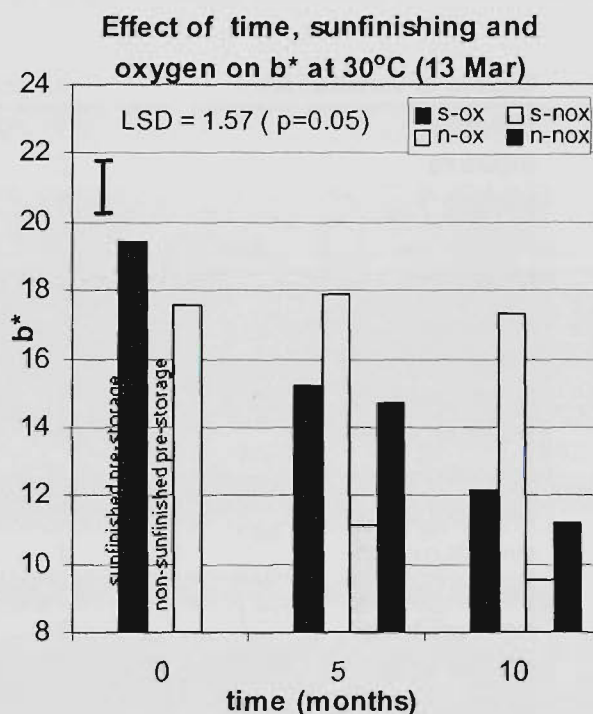
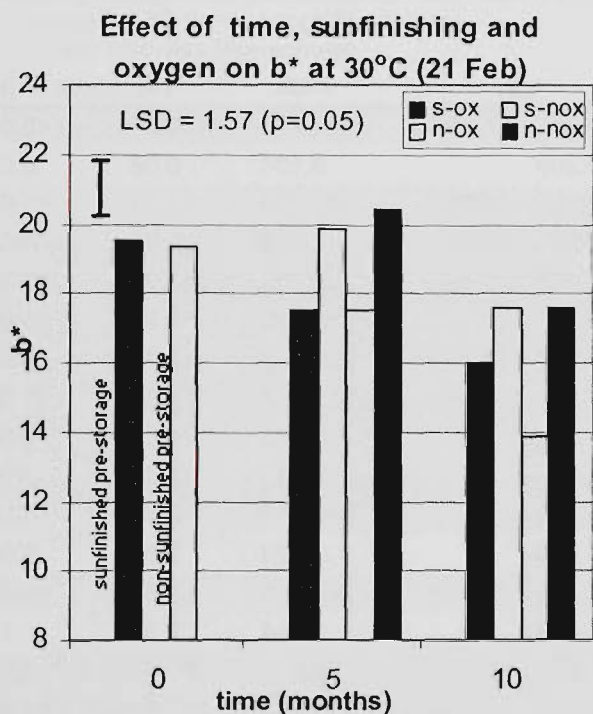
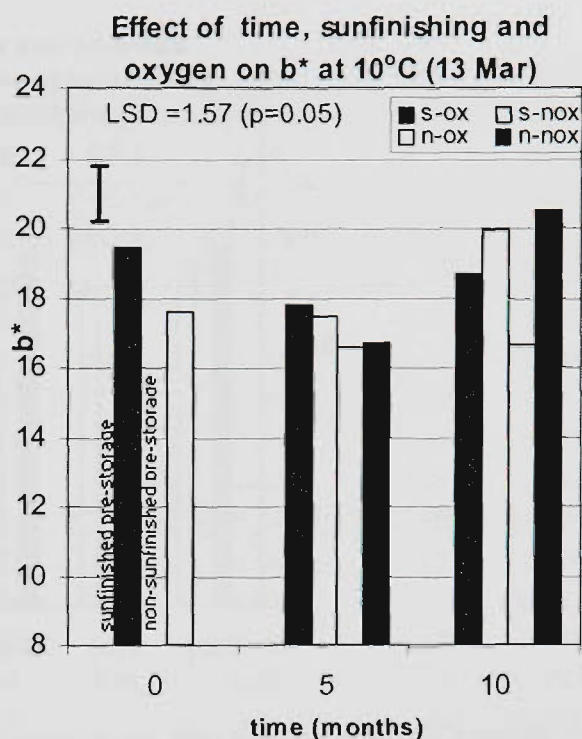
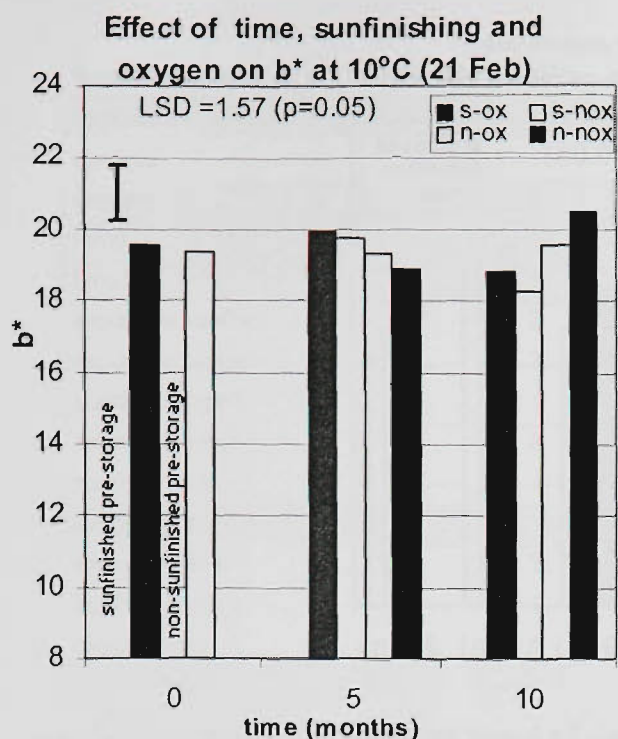


**Figure 4.13** Change in  $b^*$  values at 10°C (top) and 30°C (bottom)— averaged for early and late fruit. Sunfinished (s) and non-sunfinished (n) sultanas stored in the presence of oxygen (-ox) and without oxygen (-nox). LSD values calculated for the interaction of harvest  $\times$  sunfinishing  $\times$  oxygen  $\times$  temperature  $\times$  time for all samples.

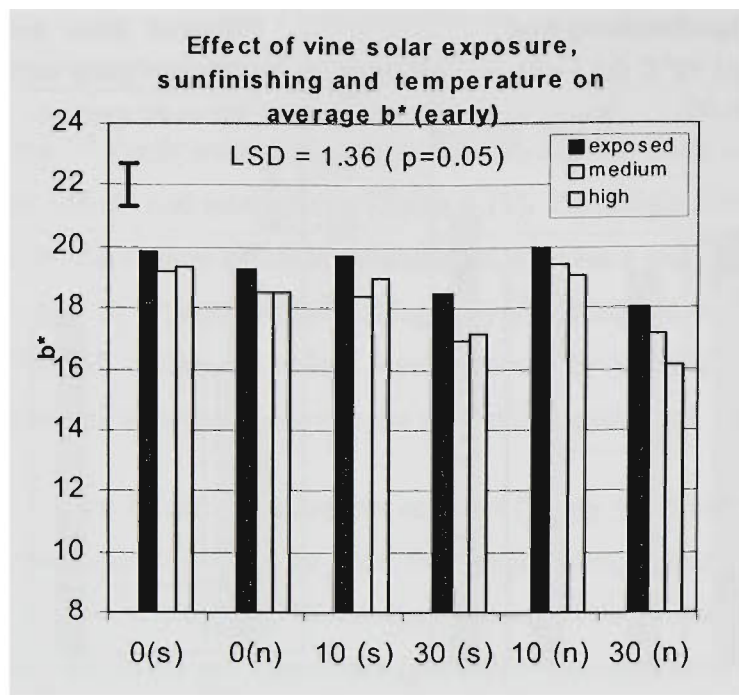


Figure 4.14 Effect of vine solar exposure on average b\* values for early and late harvested sultanas  
LSD values calculated for the interaction of harvest × exposure × sunfinishing × temperature.

Source of variation b*	d.f	s.s.	m.s.	v.r.	F pr.
Harvest	1	209.27 (17.7%)	209.274	170.3	<0.001
exposure	2	0.209	0.104	0.08	0.919
sunfinis	1	42.42 (3.6%)	42.426	34.52	<0.001
oxygen	1	105.57 (8.9%)	105.574	85.91	<0.001
temp	1	297.70 (25.3%)	297.703	242.25	<0.001
time	1	16.32 (1.4%)	16.325	13.28	<0.001
harvest.exposure	2	41.247 (3.5%)	20.623	16.78	<0.001
harvest.sunfinis	1	41.80 (3.5%)	41.807	34.02	<0.001
exposure.sunfinis	2	13.53	6.766	5.51	0.007
harvest.oxygen	1	9.11	9.11	7.41	0.009
exposure.oxygen	2	8.423	4.212	3.43	0.041
sunfinis.oxygen	1	3.529	3.529	2.87	0.097
harvest.temp	1	47.51 (4.0%)	47.516	38.67	<0.001
exposure.temp	2	5.088	2.544	2.07	0.138
sunfinis.temp	1	26.69 (2.28%)	26.693	21.72	<0.001
oxygen.temp	1	48.91 (4.2%)	48.916	39.8	<0.001
harvest.time	1	13.538	13.538	11.02	0.002
exposure.time	2	1.364	0.682	0.56	0.578
sunfinis.time	1	0.371	0.371	0.3	0.585
oxygen.time	1	7.877	7.877	6.41	0.015
temp.time	1	74.164 (6.29%)	74.164	60.35	<0.001
harvest.exposure.sunfinis	2	8.845	4.423	3.6	0.035
harvest.sunfinis.temp	1	8.795	8.795	7.16	0.01
sunfinis.temp.time	1	8.337	8.337	6.78	0.012
exposure.sunfinis.oxygen.temp	2	18.846	9.423	7.67	0.001
<b>Pooled SS for non-significant three- and four-way interactions</b>					
Residual	4	55.3	1.229		
<b>Total</b>	<b>12</b>	<b>7</b>	<b>1178.466</b>		

Table 4.11 ANOVA table for b\*: early and late harvest fruit together.

Source of variation b* (21 Feb 1996)	d.f.	s.s.	m.s.	v.r.	F pr.	
Exposure	2	21.03	(8.2%)	10.516	10.27	0.001
sunfinis	1	0.001		0.001	0	0.974
oxygen	1	26.33	(10.24%)	26.33	25.7	<0.001
temp	1	53.67	(20.8%)	53.674	52.4	<0.001
time	1	29.79	(11.6%)	29.798	29.09	<0.001
exposure.sunfinis	2	2.545		1.273	1.24	0.312
exposure.oxygen	2	5.013		2.506	2.45	0.115
sunfinis.oxygen	1	3.807		3.807	3.72	0.07
exposure.temp	2	1.804		0.902	0.88	0.432
sunfinis.temp	1	2.422		2.422	2.36	0.142
oxygen.temp	1	28.55	(11.1%)	28.556	27.88	<0.001
exposure.time	2	3.335		1.668	1.63	0.224
sunfinis.time	1	0.666		0.666	0.65	0.43
oxygen.time	1	0.222		0.222	0.22	0.647
temp.time	1	22.38	(8.6%)	22.385	21.85	<0.001
exposure.oxygen.time	2	9.173		4.587	4.48	0.026
sunfinis.temp.time	1	12.825		12.825	12.52	0.002
<b>Pooled SS for non-significant three- and four-way interactions</b>						
Residual	18	18.438		1.024		
<b>Total</b>	<b>63</b>	<b>257.541</b>				

Source of variation b* (13 Mar 1996)	d.f.	s.s.	m.s.	v.r.	F pr.	
Exposure	2	21.204		10.602	10.15	0.001
sunfinis	1	93.926		93.926	89.89	<0.001
oxygen	1	78.96		78.96	75.57	<0.001
temp	1	309.354		309.354	296.07	<0.001
time	1	0.591		0.591	0.57	0.462
exposure.sunfinis	2	18.298		9.149	8.76	0.002
exposure.oxygen	2	3.88		1.94	1.86	0.185
sunfinis.oxygen	1	0.037		0.037	0.04	0.853
exposure.temp	2	2.634		1.317	1.26	0.307
sunfinis.temp	1	39.238		39.238	37.55	<0.001
oxygen.temp	1	16.269		16.269	15.57	<0.001
exposure.time	2	0.124		0.062	0.06	0.943
sunfinis.time	1	0.219		0.219	0.21	0.652
oxygen.time	1	8.904		8.904	8.52	0.009
temp.time	1	63.386		63.386	60.67	<.001
exposure.sunfinis.temp	2	9.453		4.726	4.52	0.026
sunfinis.oxygen.temp	1	7.873		7.873	7.54	0.013
oxygen.temp.time	1	5.825		5.825	5.57	0.03
exposure.sunfinis.oxygen.temp	2	12.32		6.16	5.9	0.011
sunfinis.oxygen.temp.time	1	10.524		10.524	10.07	0.005
<b>Pooled SS for non-significant three- and four-way interactions</b>						
Residual	18	18.807		1.045		
<b>Total</b>	<b>63</b>	<b>736.574</b>				

Table 4.12 ANOVA table for b\* early (top) and late harvest (bottom) sultanias

### 4.30 Storage changes of $a_w$

Changes in  $a_w$  can be seen in Figure 4.15. ANOVA data confirmed that vine solar exposure did not have a significant effect on  $a_w$ ; maturity, sunfinishing, temperature and time were all significant ( $p < 0.001$ ). Some small increases in average  $a_w$  values were observed in 10°C stored fruit, however the increases were mostly not statistically significant. In some cases an average decrease in  $a_w$  values was observed. In the previous storage trial the oxygen barrier packaging significantly inhibited the increase in  $a_w$  at 10°C storage compared to oxygen exposed controls; this effect was not apparent in the present storage trial. Figure 4.15 shows that late harvest non-sunfinished fruit was well over the critical  $a_w$  of 0.6—the  $a_w$  at which internal sugaring was observed in the previous storage trial—throughout the 10 month storage period. The data also shows that the average  $a_w$  of non-sunfinished sultanas was significantly higher than sunfinished sultanas.

At 30°C storage, all  $a_w$  values decreased regardless of pre-storage levels. In nearly all samples, the average  $a_w$  decreased to close to 0.4 after 10 months. Decrease in  $a_w$  appeared to be slightly retarded by the packaging material at 30°C for non-sunfinished fruit.

### 4.31 Internal sugaring

As for the 1995 trial, sugar internal crystallisation processes occurred in some 10°C stored fruit. Internal sugaring (IS) occurred only in late-harvest sultanas stored at 10°C. Table 4.13 shows number of sugar nuclei and the  $a_w$  of sultanas. It can be seen that IS was observed only in those sultanas which reached an  $a_w$  value of just below or above 0.6 or more, as in the earlier storage trial.

	10°C + O <sub>2</sub>				10°C no O <sub>2</sub>			
	5 months		10 months		5 months		10 months	
	$a_w$	Nuclei (No.)	$a_w$	Nuclei (No.)	$a_w$	Nuclei (No.)	$a_w$	Nuclei (No.)
SEX	<b>0.641</b>	20	0.594	20	0.569	—	0.587	5
NEX	<b>0.715</b>	13	<b>0.715</b>	15	<b>0.726</b>	19	<b>0.732</b>	22
SGR	<b>0.658</b>	40	<b>0.607</b>	20	0.575	—	<b>0.644</b>	20
NGR	<b>0.722</b>	16	<b>0.732</b>	22	<b>0.712</b>	22	<b>0.723</b>	25
SMS	0.534	—	0.529	—	0.546	—	0.550	—
NMS	<b>0.654</b>	9	<b>0.638</b>	20	<b>0.654</b>	7	<b>0.653</b>	12
SHS	0.557	—	0.578	—	0.529	—	0.529	—
NHS	<b>0.689</b>	6	<b>0.670</b>	13	<b>0.656</b>	9	<b>0.691</b>	15

Table 4.13 Internal sugaring expressed as average number of nuclei per sultana and  $a_w$  10°C stored sultanas (late harvest sultanas).  $A_w$ s over 0.60 are shown in bold.

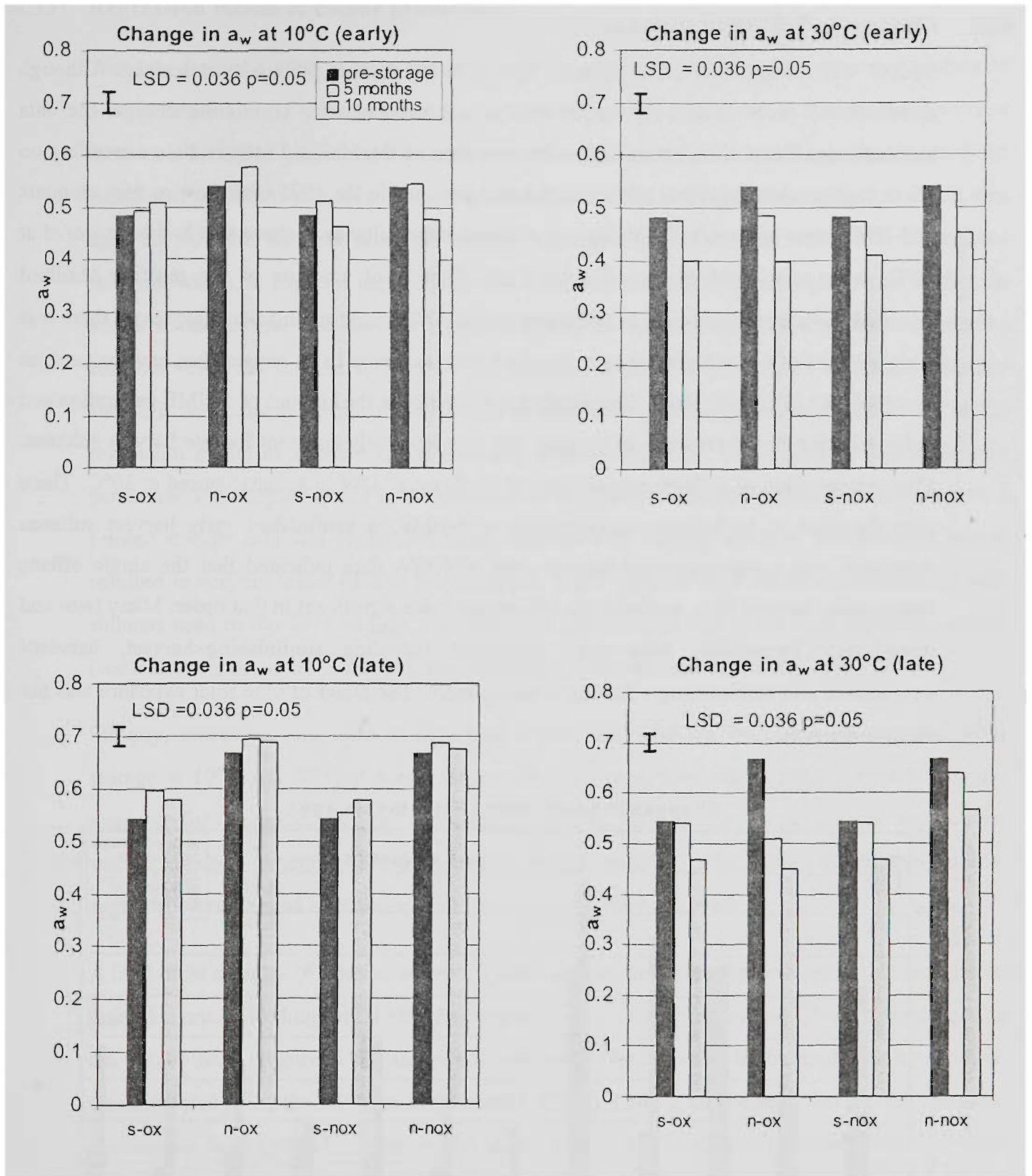


Figure 4.15 Changes in  $a_w$  in early (top) and late (bottom) sultanas over 10 months storage at 10°C and 30°C. S-ox (sunfinished + oxygen), n-ox (non-sunfinished + oxygen), s-nox (sunfinished no-oxygen) and n-nox (non-sunfinished no-oxygen). LSD data calculated using the mean of the determinations of two sub-samples for the interaction of sunfinishing  $\times$  oxygen  $\times$  temperature  $\times$  time.

#### 4.32 Changes in 5-HMF in sultanas

5-HMF was measured in DCM extracts by GC in the manner previously described. Although measurements were made only on pre-storage sultanas and after 10 months storage, the data indicated significant differences in the concentration of the Maillard intermediate depending on the storage oxygen exposure, similar to the data obtained in the 1995 trial. Low or zero amounts of 5-HMF were present in DCM extracts of pre-storage sultanas or those that had been stored at 10°C, with or without oxygen (Figure 4.16). Significant amounts of the reactive Maillard intermediate were present only in DCM extracts of 30°C stored sultanas. In many cases there was a higher level of 5-HMF present in extracts of sultanas stored in an oxygen-free environment, as was observed in the 1995 trial. This implied a difference in the kinetics of 5-HMF generation and polymerisation in the presence of oxygen; this was especially apparent for late harvest sultanas. The concentration of 5-HMF ranged from ~5 to 40  $\mu\text{g.g}^{-1}$  DW in sultanas stored at 30°C. There also appeared to be higher concentrations of 5-HMF in sunfinished early harvest sultanas compared with comparable late harvest fruit. ANOVA data indicated that the single effects temperature, harvest date, sunfinishing and oxygen were significant in that order. Many two- and three- way interactions were also significant including sunfinishing $\times$ harvest, harvest $\times$ temperature and sunfinishing  $\times$  harvest  $\times$  temperature. The effect of vine solar exposure was not significant.

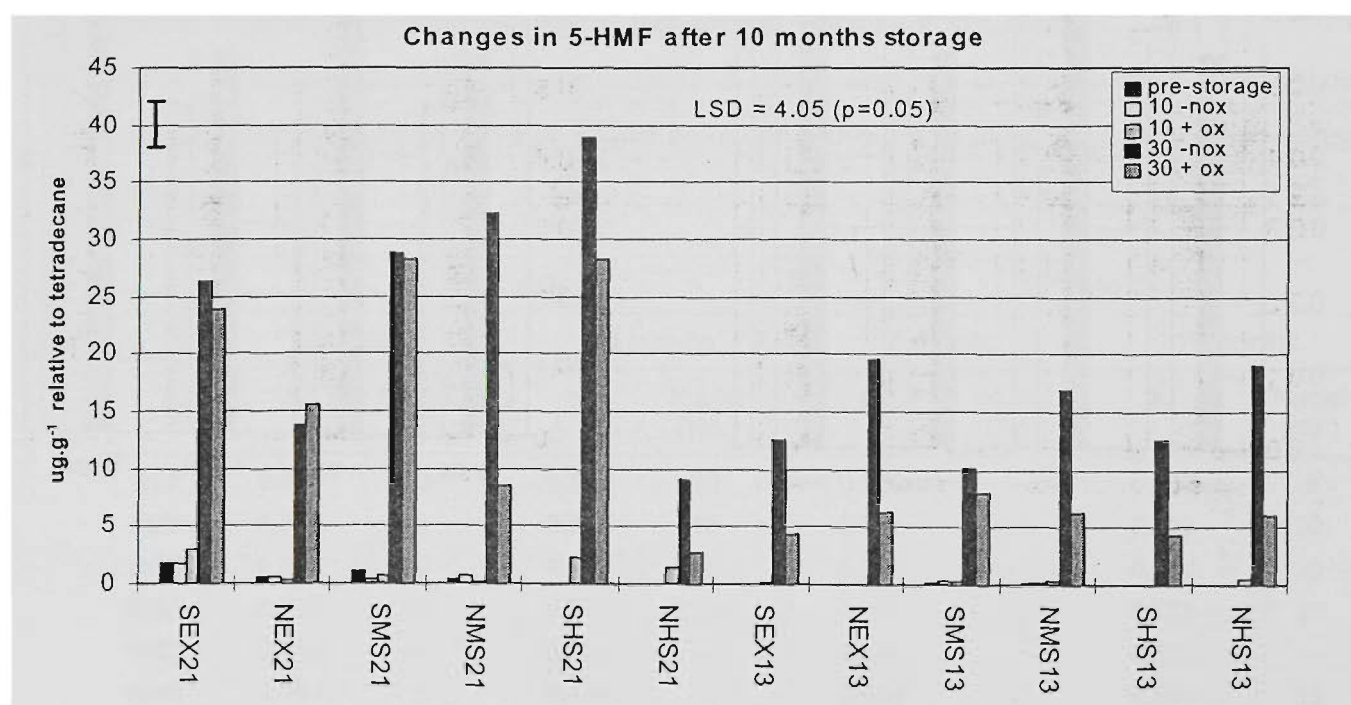


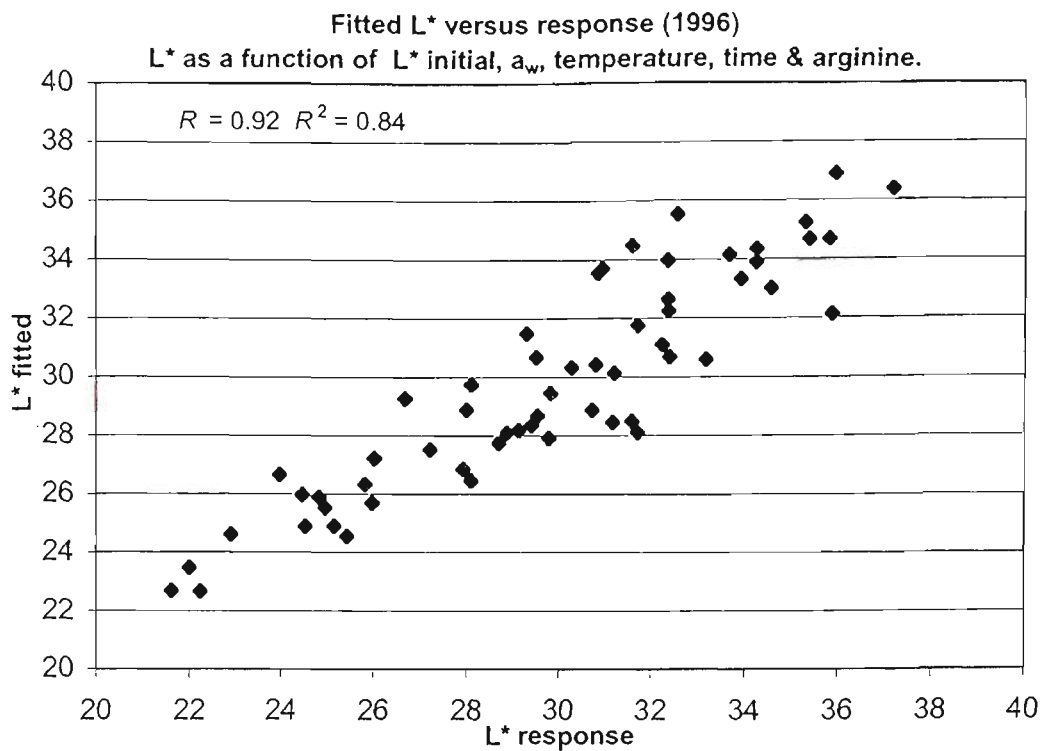
Figure 4.16 Concentration of 5-hydroxymethyl furfural after 10 months storage in 1996 sultanas. 5-HMF was low or not detectable in samples stored at 10°C, and was present in significant concentrations only in samples stored at 30°C. Each value is the mean of replicate measurements of 2 $\times$ 25 g of sultana DCM extracts.

### 4.33 Regression model of colour prediction

The data from the 1996 storage trial was used to generate multiple term regression models to predict future  $L^*$  and  $b^*$  from pre-storage chemico-physical parameters in the manner described in section 3.13. The vine solar exposure term was significant for  $L^*$   $a^*$   $b^*$  in early-harvest fruit: significantly lower tristimulus values were measured in MS and HS fruit compared to EX. It was apparent that the KP and skin free-arginine concentration in sultanas was lower in exposed sultanas, which, at least for the early harvest fruit, remained significantly lighter than shaded. In addition, late-harvest sultanas had significantly higher levels of skin free-arginine compared to early-harvest fruit. Late-harvest fruit were generally darker than early fruit. Using the rationale stated, it was considered potentially useful to use either pre-storage skin-arginine or KP in the regression model in addition to the time and temperature terms. Regression models were only performed for samples stored in the presence of oxygen. As outlined in the following chapter, a limited storage trial was performed using sultanas with varying levels of soil-nitrogen, which resulted in varying levels of skin free-arginine. These samples were stored simultaneously with sultanas used in the 1996 storage trial and were also incorporated in the final regression model (see following sections) to increase the robustness of the regression model.

Initially, however, only 1996 storage trial II data was used for the regression models. After storage at 10°C and 30°C at 5 and 10 months in oxygen, there was a total of (n=64) samples available for the model. Genstat was used to calculate MLR prediction models and any outliers were removed: generally low-temperature stored samples, which had undergone internal sugaring, were flagged as outliers by the software and were removed.

A total of 58 samples (6 samples removed) were used in the  $L^*$  prediction equation. It can be seen that all terms, including initial skin free-arginine and initial (pre-storage)  $L^*$  were significant at the  $p < 0.05$  level (Figure 4.17), and hence valid terms for inclusion in the model. Sultana colour was predicted using the KP term in the model (Figure 4.18). It can be seen that the KP term was statistically valid ( $p < 0.05$ ), however,  $L^*$  initial did not add much useful information. In Figure 4.19, a model predicting sultana  $b^*$  values, is shown using the arginine term. It can be seen that the arginine and the  $b^*$  initial terms were statistically valid ( $p < 0.05$ ). In Figure 4.20 the model using KP is shown; both the KP and  $b^*$  initial terms were significant.

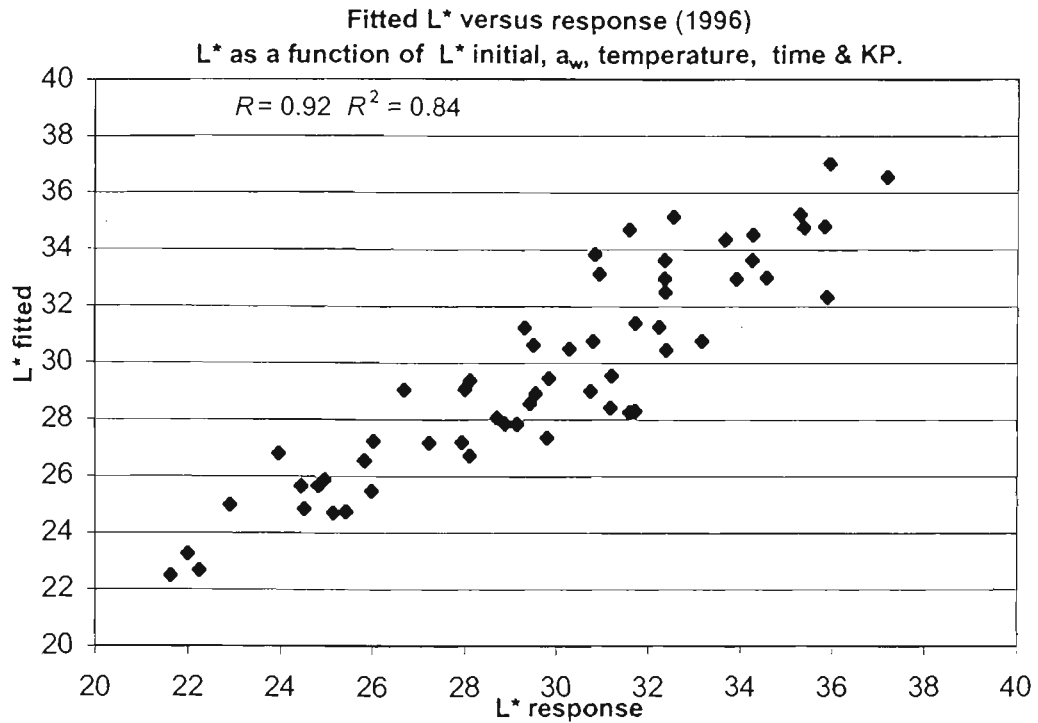


Source of variation	coefficient	s.e.	t(53)	t pr.
Constant	43.5	5.530	7.86	<0.001
L* initial	0.207	0.098	2.11	0.040
a <sub>w</sub>	-19.040	4.590	-4.15	<0.001
temperature	-0.289	0.022	-12.93	<0.001
time	-0.443	0.089	-4.96	<0.001
arginine	-0.416	0.164	-2.53	0.014

estimate	reference	correlation					
Constant	1	1					
L* initial	2	-0.936	1				
a <sub>w</sub>	3	-0.896	0.73	1			
temperature	4	-0.104	0.019	0.041	1		
time	5	-0.115	-0.003	-0.007	-0.053	1	
arginine	6	-0.066	0.038	-0.056	-0.034		1
		1	2	3	4	5	6

variance	d.f.	s.s.		m.s.	v.r.	F pr.
L* initial	1	174.358	(17.8%)	174.358	59.39	<0.001
a <sub>w</sub>	1	42.451	(4.3%)	42.451	14.46	<0.001
temperature	1	518.452	(52.9%)	518.452	176.60	<0.001
time	1	68.721	(7.0%)	68.721	23.41	<0.001
arginine	1	18.775	(1.9%)	18.775	6.40	0.014
residual	53	155.592		2.936		
<b>Total</b>	<b>58</b>	<b>978.349</b>		<b>16.868</b>		

Figure 4.17 Graphical representation of regression prediction equation of sultana L\*. L\* as a function of initial L\*, a<sub>w</sub>, temperature, time and initial skin arginine. Statistical data for regression: calculated constant and regression coefficients with their respective standard errors (s.e.), t test values (t=53) level of statistical significance and cumulative variance.

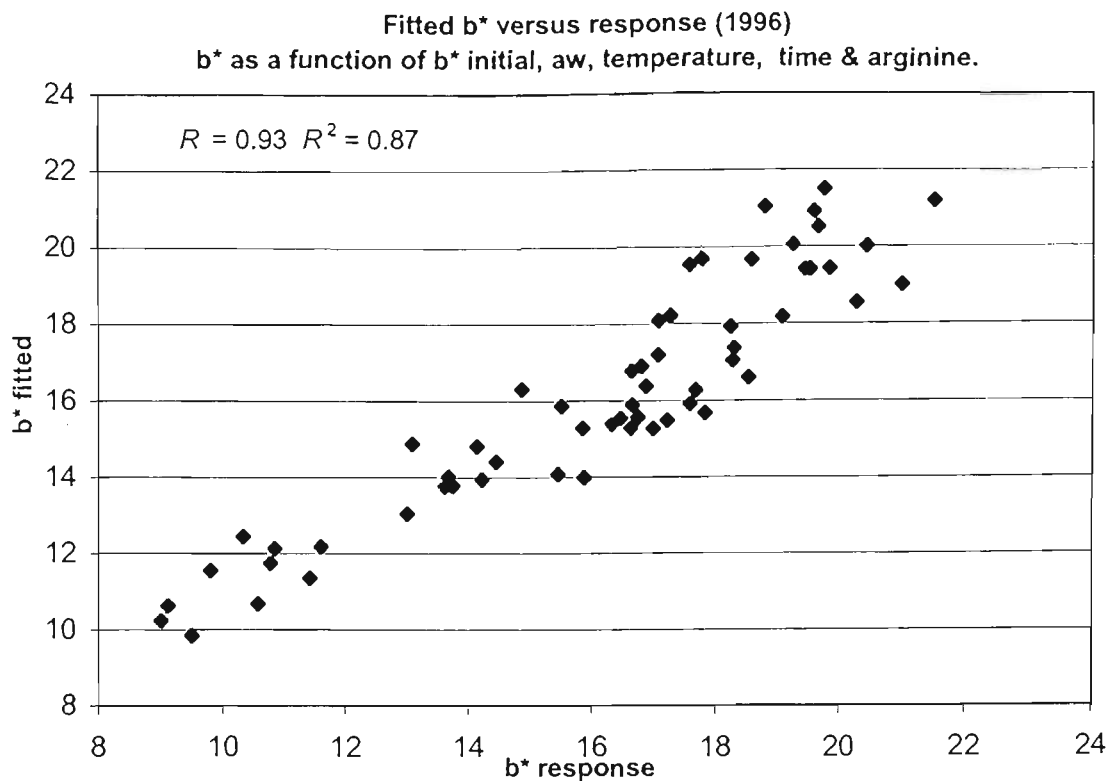


Source of variation	coefficient	s.e.	t(53)	t pr.
Constant	48.91	5.92	8.25	<0.001
L* initial	0.1724	0.0987	1.75	0.086
a <sub>w</sub>	-23.31	4.72	-4.94	<0.001
temperature	-0.2886	0.0222	-13.01	<0.001
time	-0.44	0.0885	-4.97	<0.001
KP	-0.13	0.0471	-2.76	0.008

estimate	ref	correlations					
Constant	1	1					
L* initial	2	-0.915	1				
a <sub>w</sub>	3	-0.908	0.741	1			
temperature	4	-0.08	0.012	0.024	1		
time	5	-0.115	0	0.005	-0.053	1	
KP	6	-0.387	0.164	0.278	-0.047	0.031	1
		1	2	3	4	5	6

Variance	d.f.	s.s.		m.s.	v.r.	F pr.
L* initial	1	174.358	(17.8%)	174.358	60.62	<0.001
a <sub>w</sub>	1	42.451	(4.34%)	42.451	14.76	<0.001
temperature	1	518.452	(53.0%)	518.452	180.26	<0.001
time	1	68.721	(7.0%)	68.721	23.89	<0.001
KP	1	21.936	(2.2%)	21.936	7.63	0.008
residual	53	152.431	(15.6%)	2.876		
total	58	978.349		16.868		

Figure 4.18 Graphical representation of regression prediction equation of sultana L\*. L\* as a function of initial L\*, a<sub>w</sub>, temperature, time and initial KP. Statistical data for regression: calculated constant and regression coefficients with their respective standard errors (s.e.), t test values (t=53) level of statistical significance and cumulative variance.



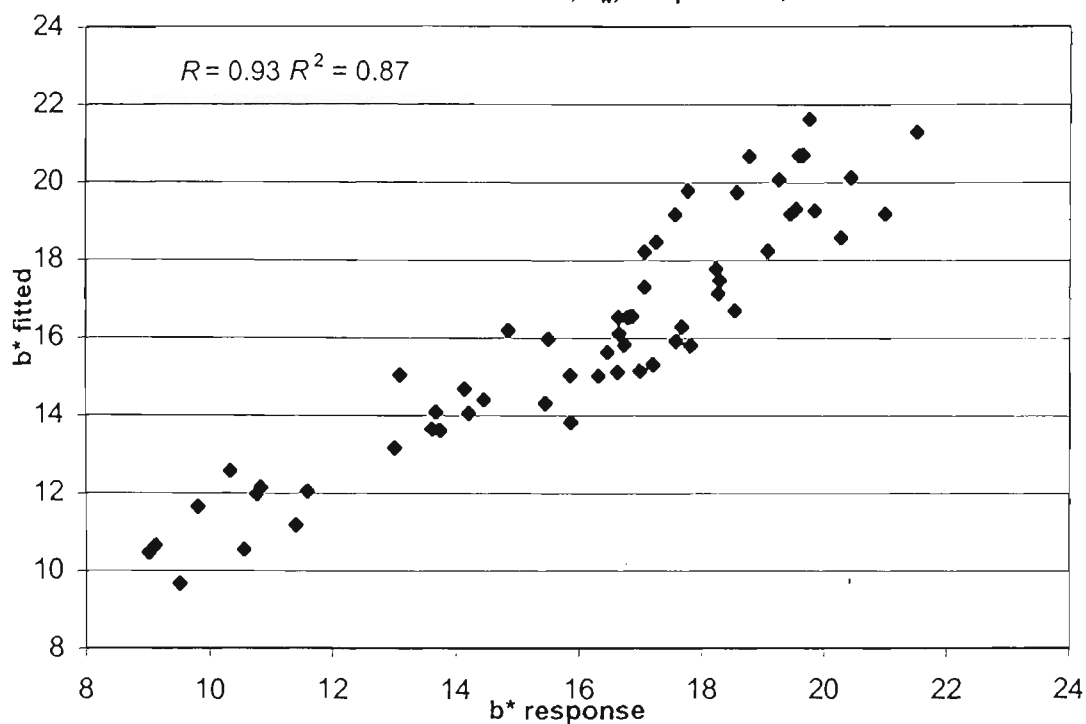
Source of variation	coefficient	s.e.	t(53)	t pr.
Constant	26.72	3.68	7.26	<0.001
b* initial	0.376	0.114	3.29	0.002
a <sub>w</sub>	-18.62	3.45	-5.4	<0.001
temperature	-0.207	0.0165	-12.53	<0.001
time	-0.2999	0.0658	-4.56	<0.001
arginine	-0.278	0.131	-2.13	0.038

estimate	ref	correlations					
Constant	1	1					
b*initial	2	-0.92	1				
a <sub>w</sub>	3	-0.916	0.742	1			
temperature	4	-0.096	0.031	0.007	1		
time	5	-0.112	-0.038	-0.001	-0.061	1	
arginine	6	0.211	-0.285	-0.244	-0.115	0.077	1
		1	2	3	4	5	6

variance	d.f.	s.s.	m.s.	v.r.	F pr.
b* initial	1	174.19 (27.6%)	174.193	110.25	<.001
a <sub>w</sub>	1	62.74 (9.9%)	62.749	39.72	<.001
temperature	1	271.59 (43.0%)	271.598	171.9	<.001
time	1	30.63 (4.9%)	30.638	19.39	<.001
arginine	1	7.183 (1.1%)	7.183	4.55	0.038
Residual	53	83.736	1.580		
<b>Total</b>	<b>58</b>	<b>630.099</b>	<b>10.864</b>		

Figure 4.19 Graphical representation of regression prediction equation of sultana b\*. b\* as a function of initial b\*, a<sub>w</sub>, temperature, time and initial skin free-arginine. Statistical data for regression: calculated constant and regression coefficients with their respective standard errors (s.e.), t test values (t=53) level of statistical significance and cumulative variance.

Fitted  $b^*$  versus response (1996)  
 $b^*$  as a function of  $b^*$  initial,  $a_w$ , temperature, time & KP.



Source of variation	coefficient	s.e.	t(53)	t pr.
Constant	29.18	3.63	8.03	<0.001
$b^*$ initial	0.363	0.113	3.2	0.002
$a_w$	-20.78	3.36	-6.19	<0.001
temperature	-0.2076	0.0166	-12.54	<0.001
time	-0.3009	0.0661	-4.55	<0.001
KP	-0.074	0.0362	-2.04	0.046

estimate	ref	correlations					
Constant	1	1					
$b^*$ initial	2	-0.859	1				
$a_w$	3	-0.911	0.688	1			
temperature	4	-0.062	0.023	-0.027	1		
time	5	-0.14	-0.037	0.023	-0.062	1	
KP	6	-0.108	-0.242	0.053	-0.103	0.088	1
		1	2	3	4	5	6

variance	d.f.	s.s.	m.s.	v.r.	F pr.
$b^*$ initial	1	174.193 (27.6%)	174.193	109.54	<0.001
$a_w$	1	62.749 (9.96%)	62.749	39.46	<0.001
temperature	1	271.598 (43.1%)	271.598	170.79	<0.001
time	1	30.638 (4.9%)	30.638	19.27	<0.001
KP	1	6.635 (1.0%)	6.635	4.17	0.046
Residual	53	84.285 (13.4%)	1.59		
Total	58	630.099	10.864		

Figure 4.20 Graphical representation of regression prediction equation of sultana  $b^*$ .  $b^*$  as a function of initial  $b^*$ ,  $a_w$ , temperature, time and initial KP. Statistical data for regression: calculated constant and regression coefficients with their respective standard errors (s.e.), t test values ( $t=53$ ) level of statistical significance and cumulative variance.

The previous data indicated that the use of either the free-arginine term or the KP term as predictors of either  $L^*$  or  $b^*$ , was statistically valid—further equations were developed using the 1996 storage trial II data combined with soil nitrogen storage data ( $n=16$  samples) from the next chapter. Again, samples flagged as outliers or samples with large residuals were removed to obtain an optimised data set.

Models using the free-arginine term together with temperature, time,  $a_w$  and initial  $L^*$  or  $b^*$  were performed. The graphical representation of predicted (fitted)  $L^*/b^*$  values vs actual  $L^*/b^*$  using the skin free-arginine term and the statistical data are shown in Figure 4.21 and Table 4.14. It can be seen that the arginine term was significant ( $p < 0.001$ ) in both models.

Similar regression models were performed using the KP term. Figure 4.22 shows graphically predicted (fitted)  $L^*/b^*$  values vs actual  $L^*/b^*$  using the KP term: the statistical data for model terms are shown in Table 4.15. It can be seen that in both models the use of the KP term was statistically justified.

It should be noted that it was attempted to use both the KP and free-skin arginine terms in the same equation. Because both variates were highly correlated (aliased) only one of the two nitrogen terms, usually the skin free-arginine term, was significant. Pre-storage substrate PPO activity was also used as a possible term in  $L^*$  and  $b^*$  models however it was not statistically significant; i.e. PPO for the  $L^*$  model ( $p=0.92$ ) and for the  $b^*$  model ( $p=0.115$ ).

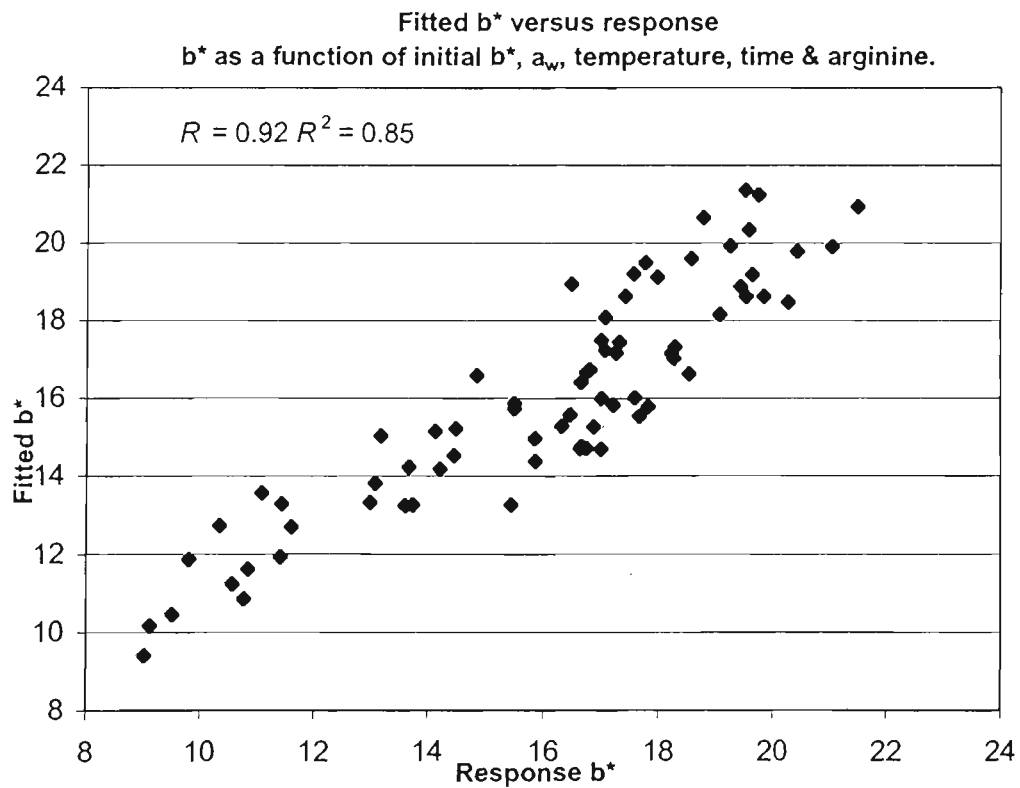
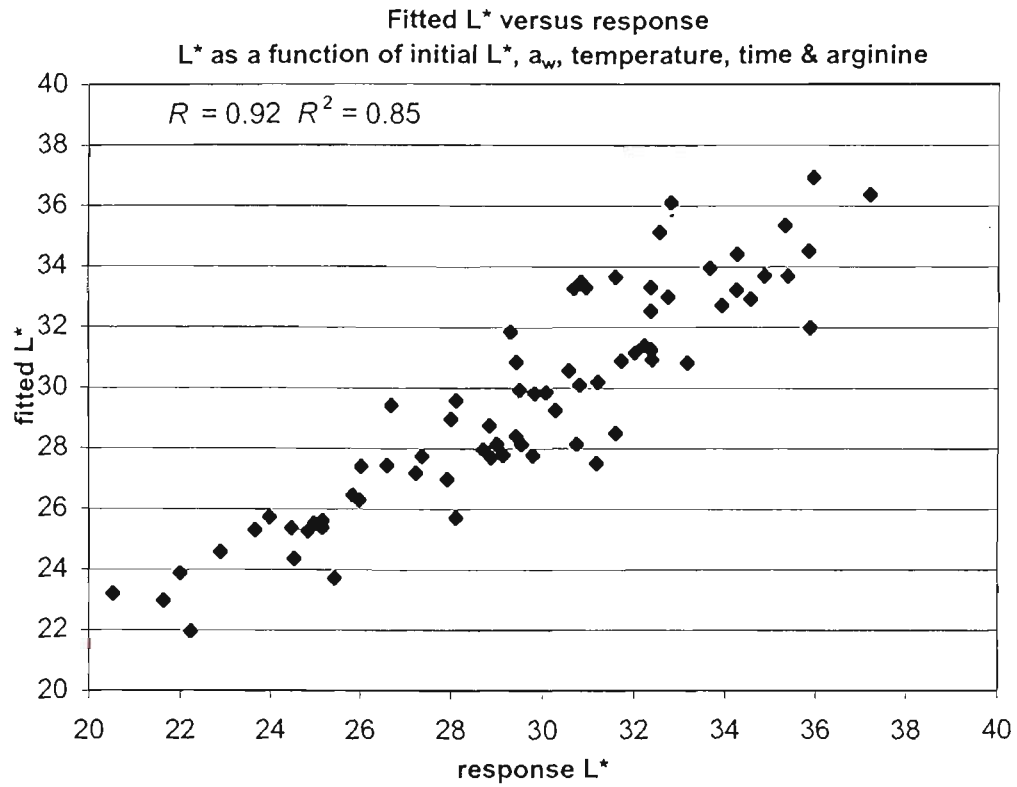


Figure 4.21 Graphical representation of fitted (predicted) L\* (above) and b\* (below) tristimulus values. Using MLR equations using initial L\* or b\* values, initial a<sub>w</sub>, initial skin-free-arginine, temperature and time. Data for sultanas from the 1996 storage trial (n=64) and the soil nitrogen storage trial (n=16) were used.

Source of variation	Coefficient	s.e.	t(67)	t pr.
Constant	41.55	5.22	7.95	<.001
L* initial	0.2367	0.0938	2.52	0.014
a <sub>w</sub>	-16.41	4.200	-3.9	<.001
temperature	-0.2769	0.0194	-14.29	<.001
time	-0.4835	0.0775	-6.24	<.001
arginine	-0.735	0.117	-6.26	<.001

estimate	ref	correlations					
Constant	1	1					
L* initial	2	-0.941	1				
a <sub>w</sub>	3	-0.9	0.739	1			
temperature	4	-0.08	0.008	0.012	1		
time	5	-0.127	0.006	0.028	-0.043	1	
arginine	6	-0.24	0.178	0.166	-0.027	0.062	1
		1	2	3	4	5	6

Variance	d.f.	s.s.		m.s.	v.r.	F pr.
L* initial	1	191.005	(16.18 %)	191.005	70.24	<0.001
a <sub>w</sub>	1	17.598	(1.49%)	17.598	6.47	0.013
temperature	1	589.819	(50.0%)	589.819	216.91	<0.001
time	1	93.438	(7.91%)	93.438	34.36	<0.001
arginine	1	106.446	(9.0%)	106.446	39.15	<0.001
<b>Residual</b>	<b>67</b>	<b>182.182</b>		<b>2.719</b>		
<b>Total</b>	<b>72</b>	<b>1180.489</b>		<b>16.396</b>		

Source of variation	coefficient	s.e.	t(66)	t pr.
Constant	25.93	3.84	6.76	<0.001
b* initial	0.349	0.115	3.03	0.004
a <sub>w</sub>	-16.05	3.59	-4.47	<0.001
temperature	-0.1956	0.016	-12.26	<0.001
time	-0.2907	0.0639	-4.55	<0.001
arginine	-0.611	0.106	-5.74	<0.001

estimate	ref	correlations					
Constant	1	1					
b* initial	2	-0.927	1				
a <sub>w</sub>	3	-0.923	0.759	1			
temperature	4	-0.062	-0.009	-0.02	1		
time	5	-0.131	-0.008	0.019	-0.036	1	
arginine	6	0.082	-0.168	-0.112	-0.072	0.065	1
		1	2	3	4	5	6

Variance	d.f.	s.s.		m.s.	v.r.	F.pr
b* initial	1	148.13	(20.8%)	148.136	81.55	<.001
a <sub>w</sub>	1	52.53	(7.4%)	52.534	28.92	0.004
temperature	1	298.87	(42.2%)	298.873	164.54	<.001
time	1	29.98	(4.2%)	29.989	16.51	<.001
arginine	1	59.87	(8.4%)	59.878	32.96	<.001
<b>Residual</b>	<b>66</b>	<b>119.88</b>		<b>1.816</b>		
<b>Total</b>	<b>71</b>	<b>709.29</b>		<b>9.99</b>		

Table 4.14 Statistical data for L\* and b\* tristimulus regression models.

Top: calculated constant and regression coefficients with their respective standard errors (s.e.), t test values (t66) and level of statistical significance. Bottom: table of accumulated analysis of variance for the regression.

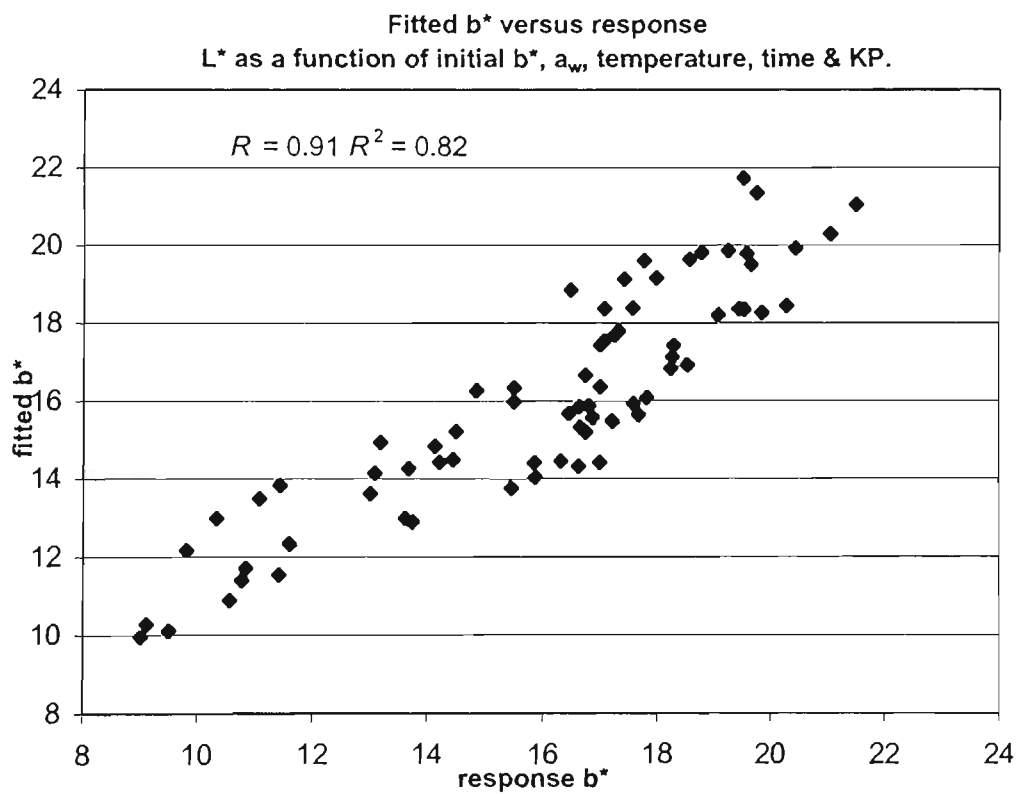
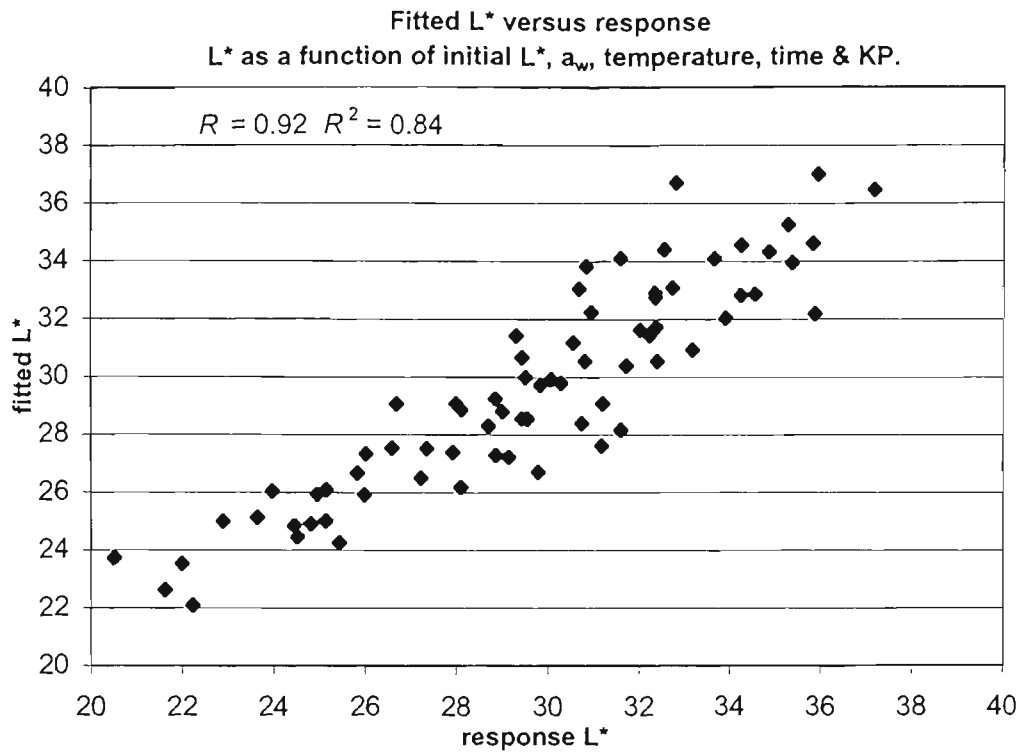


Figure 4.22 Graphical representation of fitted (predicted)  $L^*$  (above) and  $b^*$  (below) tristimulus values. Using MLR equations using initial  $L^*$  or  $b^*$  values, initial  $a_w$ , KP, temperature and time. Data from the 1996 storage trial ( $n = 64$ ) and the soil nitrogen storage trial ( $n=16$ ) were used.

Source of variation	coefficient	s.e.	t(67)	t pr.
Constant	49.18	5.74	8.56	<0.001
L* initial	0.1858	0.097	1.91	0.06
a <sub>w</sub>	-22.26	4.53	-4.91	<0.001
temperature	-0.2765	0.0196	-14.08	<0.001
time	-0.4745	0.0784	-6.05	<0.001
KP	-0.2047	0.0339	-6.03	<0.001

estimate	ref	correlation					
Constant	1	1					
L* initial	2	-0.93	1				
a <sub>w</sub>	3	-0.913	0.753	1			
temperature	4	-0.066	0.004	0.003	1		
time	5	-0.123	0.007	0.034	-0.043	1	
KP	6	-0.447	0.265	0.374	-0.032	0.045	1
		1	2	3	4	5	6

Change	d.f.	s.s.		m.s.	v.r.	F pr.
L*initial	1	191.00	(16.2%)	191.005	68.41	<0.001
a <sub>w</sub>	1	17.59	(1.5%)	17.598	6.3	0.014
temperature	1	589.81	(49.9%)	589.819	211.25	<0.001
time	1	93.43	(7.9%)	93.438	33.47	<0.001
KP	1	101.56	(8.6%)	101.564	36.38	<0.001
<b>Residual</b>	<b>67</b>	<b>187.065</b>		<b>2.792</b>		
<b>Total</b>	<b>72</b>	<b>1180.489</b>		<b>16.396</b>		

	estimate	s.e.	t(66)	t pr.
Constant	31.5	4	7.87	<0.001
b* initial	0.294	0.117	2.5	0.015
water	-20.74	3.7	-5.6	<0.001
temperature	-0.1966	0.0164	-11.98	<0.001
time	-0.2867	0.0657	-4.36	<0.001
KP	-0.1544	0.0295	-5.24	<0.001

estimate	ref	correlations					
Constant	1	1					
b* initial	2	-0.894	1				
a <sub>w</sub>	3	-0.922	0.736	1			
temperature	4	-0.044	-0.015	-0.036	1		
time	5	-0.151	-0.001	0.038	-0.035	1	
KP	6	-0.179	-0.091	0.123	-0.064	0.082	1
		1	2	3	4	5	6

Change	d.f.	s.s.		m.s.	v.r.	F pr.
b* initial	1	148.13	(20.9%)	148.136	77	<0.001
a <sub>w</sub>	1	52.53	(7.4%)	52.534	27.31	<0.001
temperature	1	298.87	(42.2%)	298.873	155.34	<0.001
time	1	29.98	(4.2%)	29.989	15.59	<0.001
KP	1	52.78	(7.4%)	52.784	27.44	<0.001
<b>Residual</b>	<b>66</b>	<b>126.98</b>		<b>1.924</b>		
<b>Total</b>	<b>71</b>	<b>709.296</b>		<b>9.99</b>		

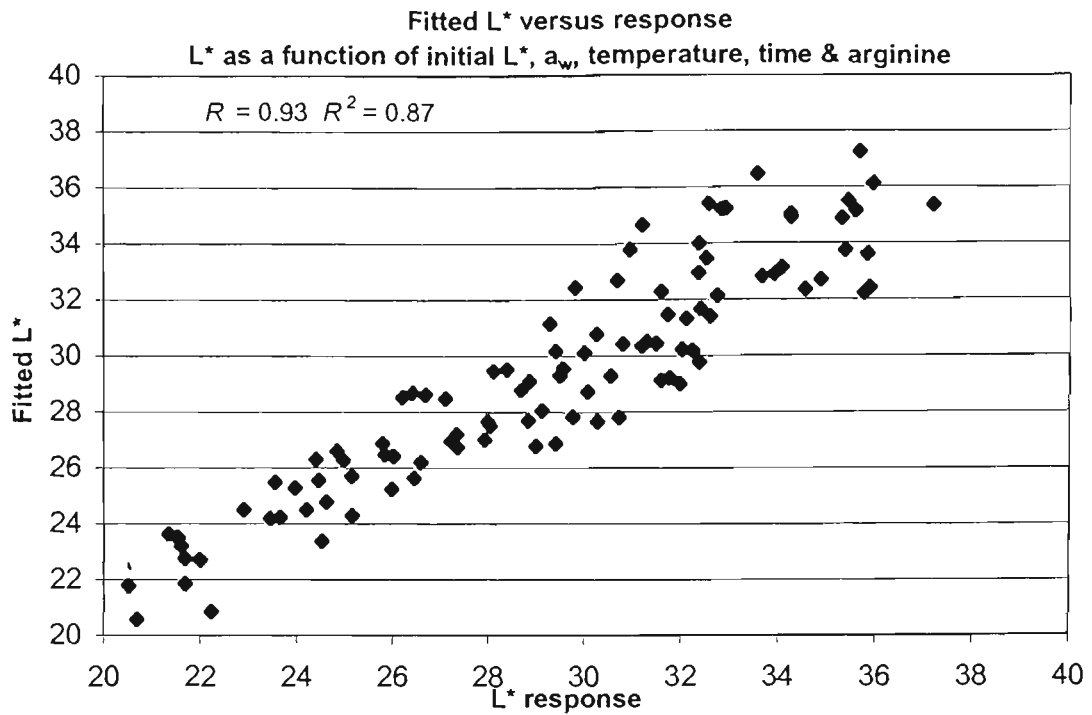
Table 4.15 Top: calculated constant and regression coefficients with their respective standard errors (s.e.), t test values (t65) and level of statistical significance. Bottom: table of accumulated analysis of variance for the regression.

#### 4.34 Regression model of storage browning using combined 1995 and 1996 data

The large amount of data accumulated during the 1995 and 1996 storage trials were used to generate a multiple linear regression model using initial  $L^*$  or  $b^*$ , initial  $a_w$ , initial skin free-arginine, storage temperature and time to predict sultana colour ( $L^*$  and  $b^*$ ). KP was not used as a predictor as it was not measured for 1995 samples. The data from the soil nitrogen experiments (see chapter 5) were also incorporated in the prediction model. The model was only performed for sultanas stored in the presence of oxygen, as this reflects typical storage conditions.

Figure 4.23 shows the regression model for prediction of  $L^*$  together with the statistical significance of the terms used in the model together with the accumulated ANOVA table. It can be seen that both initial  $L^*$  and the initial arginine are both significant ( $p < 0.001$ ) and valid predictors in the equation. The regression prediction model for  $b^*$  (Figure 4.24) indicated that the inclusion of the arginine term was statistically valid, however the initial  $b^*$  term was not. Because the initial  $b^*$  term was not valid it was not included in the final model shown in Figure 4.24.

In order to estimate how different the data were for each year, ANOVA was performed with the two seasons coded as 1 (1995 data) and 2 (1996 data). The ANOVA data is shown in Table 4.16. It can be seen that for the  $L^*$  data, there was a significant difference ( $p < 0.001$ ), although the season term accounted for only a small portion of the total SS variance. In contrast, there was found to be no significant difference data between the two years for the  $b^*$  data. Interestingly the  $a_w \times$  year interaction was significant ( $p < 0.001$ ); the fact that there was a much greater range of  $a_w$  values in the 1996 seasons may have accounted for this.

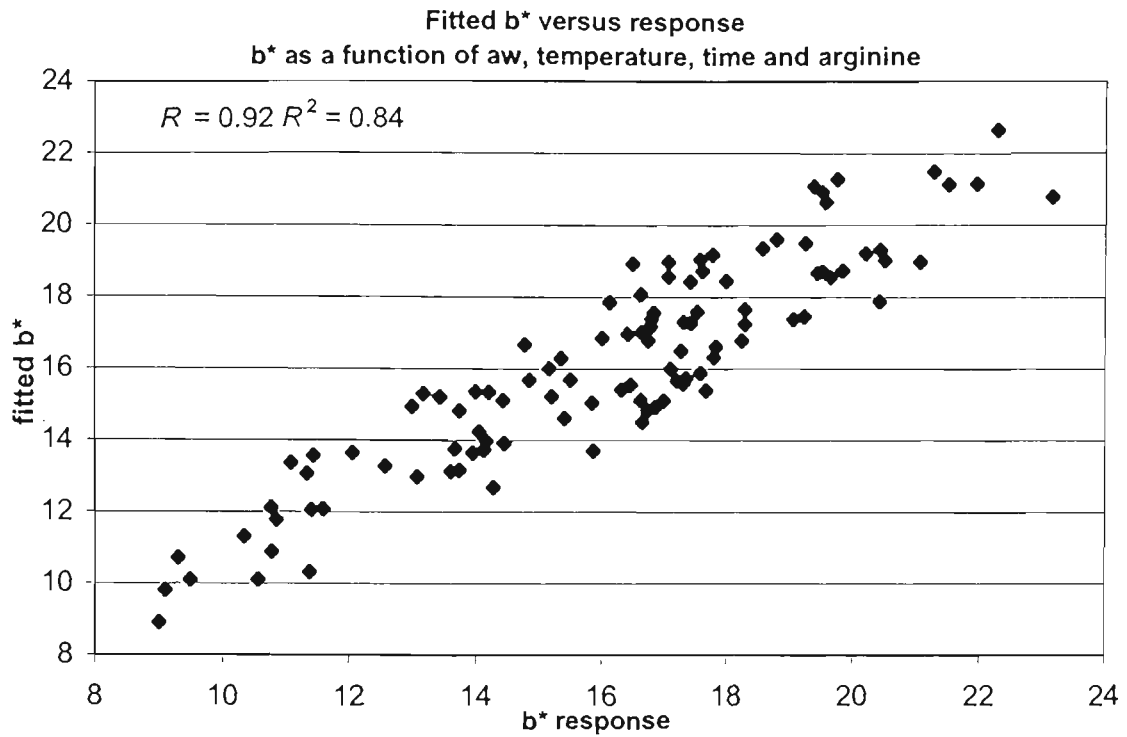


Source of variation	coefficient	s.e.	t(100)	t pr.
Constant	76.25	5.15	14.82	<0.001
L* initial	-0.469	0.108	-4.36	<0.001
a <sub>w</sub>	-35.89	3.45	-10.41	<0.001
temperature	-0.2965	0.0160	-18.51	<0.001
time	-0.5037	0.0504	-9.99	<0.001
arginine	-0.996	0.109	-9.10	<0.001

estimate	ref	correlations					
Constant	1	1					
L* initial	2	-0.963	1				
a <sub>w</sub>	3	-0.883	0.750	1			
temperature	4	-0.061	0.015	-0.019	1		
time	5	-0.034	-0.066	0.017	-0.074	1	
arginine	6	-0.161	0.076	0.151	-0.033	0.015	1
		1	2	3	4	5	6

variance	d.f.	s.s.	m.s.	v.r.	F pr.
L* initial	1	50.26 (2.4%)	50.265	18.94	<0.001
a <sub>w</sub>	1	227.54 (11.1%)	227.547	85.75	<0.001
temperature	1	1019.44 (50.0%)	1019.443	384.194	<0.001
time	1	257.81 (12.65%)	257.810	97.16	<0.001
arginine	1	219.85 (10.79%)	219.853	82.86	<0.001
<b>Residual</b>	<b>99</b>	<b>262.693</b>	<b>2.653</b>		
<b>Total</b>	<b>104</b>	<b>2037.612</b>	<b>19.592</b>		

Figure 4.23 Graphical representation of the multiple term linear regression equation. For the prediction of L\* under oxygen exposed conditions using combined data from 1995, 1996 and nitrogen experiments. The middle table shows the statistical significance of the terms used and the bottom table shows the accumulated ANOVA table for the regression equation.



Source of variation	coefficient	s.e.	t(100)	t pr.
Constant	38.11	1.1	34.54	<0.001
a <sub>w</sub>	-25.98	1.8	-14.45	<0.001
temperature	-0.1809	0.0127	-14.27	<0.001
time	-0.3909	0.0395	-9.91	<0.001
arginine	-0.6115	0.0889	-6.87	<0.001

estimate	ref	correlations					
Constant	1	1					
a <sub>w</sub>	2	-0.902	1				
temperature	3	-0.175	-0.05	1			
time	4	-0.401	0.146	-0.052	1		
arginine	5	-0.299	0.093	-0.024	0.042	1	
		1	2	3	4	5	1

variance	d.f.	s.s.	m.s.	v.r.	F pr.	
a <sub>w</sub>	1	294.08	27.5%)	294.085	175.85	<.001
temperature	1	373.93	(34.9%)	373.933	223.59	<.001
time	1	154.94	(14.5%)	154.949	92.65	<.001
arginine	1	79.03	(7.3%)	79.039	47.26	<.001
<b>Residual</b>	<b>100</b>	<b>167.24</b>		<b>1.672</b>		
<b>Total</b>	<b>104</b>	<b>1069.247</b>		<b>10.281</b>		

Figure 4.24 Graphical representation of the multiple term linear regression equation. For the prediction of b\* under oxygen exposed conditions using combined data from 1995, 1996 and nitrogen experiments. The middle table shows the statistical significance of the terms used and the bottom table shows the accumulated ANOVA table for the regression equation.

Change L*	d.f.	s.s.	m.s.	v.r.	F pr.
L* initial	1	50.265 (2.4%)	36.052	16.49	<.001
a <sub>w</sub>	1	227.54 (11.3%)	139.347	63.73	<.001
temp	1	1019.44 (50.49%)	315.133	144.12	<.001
time	1	257.81 (12.8%)	987.744	451.71	<.001
arg	1	219.85 (10.9%)	268.737	122.9	<.001
year	1	19.64 (0.97%)	43.279	19.79	<.001
L*initial.year	1	0.010	1.002	0.46	0.500
a <sub>w</sub> .year	1	2.835	2.835	1.3	0.258
temp.year	1	15.658	15.658	7.16	0.009
time.year	1	0.281	0.281	0.13	0.721
arg.year	1	0.723	0.723	0.33	0.567
<b>Residual</b>	<b>95</b>	<b>207.734</b>	<b>2.187</b>		
<b>Total</b>	<b>106</b>	<b>2018.526</b>	<b>19.043</b>		

Change b*	d.f.	s.s.	m.s.	v.r.	F pr.
b* initial	1	200.72 (15.6%)	200.721	82.49	<0.001
arg	1	87.35 (6.8%)	87.357	35.9	<0.001
a <sub>w</sub>	1	128.42 (9.9%)	128.427	52.78	<0.001
temp	1	405.06 (31.5%)	405.065	166.46	<0.001
time	1	172.73 (13.4%)	172.735	70.99	<0.001
year	1	0.616	0.616	0.25	0.616
b* initial.year	1	0.015	0.015	0.01	0.938
arg.year	1	0.698	0.698	0.29	0.593
a <sub>w</sub> .year	1	29.022 (2.3%)	29.022	11.93	<0.001
temp.year	1	6.622	6.622	2.72	0.102
time.year	1	1.984	1.984	0.82	0.369
<b>Residual</b>	<b>104</b>	<b>253.073</b>	<b>2.433</b>		
<b>Total</b>	<b>115</b>	<b>1286.334</b>	<b>11.186</b>		

Table 4.16 ANOVA data showing the effect of season in the combined equation for L\* tristimulus values (above) and b\* tristimulus values (below).

#### 4.35 Discussion of data

The various field treatments, such as exposure and harvest date, provided a range of chemico-physical characteristics in the sultanas which could be related to storage browning. The caveat applies once again that the effects of field treatments exposure and harvest must be interpreted in the context that they were not replicated within the season, and hence cannot be considered as anything more than preliminary observations, until multi-season trials are performed.

Anecdotal and literature evidence (Uhlig and Clingeleffer 1998) indicate that grape maturity may play a critical role in sultana colour stability; late-harvest fruit can often be less colour stable. Uhlig and Clingeleffer (1998) found that lightest L\* values were obtained for sultanas produced from H5 Sultana grapes with TSS between 21 and 23° Brix. None of the Brix values in this trial fell into this category however, it was observed that the maturity had a significant effect on the

physico-chemical characteristics of pre-storage sultanas viz, free-arginine and proline, 5-HMF (via HPLC analysis),  $a_w$  and the relative concentration of *trans*-caftaric acid. Differences in the initial PPO activity were generally not significant between harvest (maturity) dates. Other chemical characteristics, such as KP, iron and copper were not significantly different on each of the two harvest dates.

Late-harvest, higher maturity sultanas underwent significantly greater browning than their early harvest counterparts under comparable storage conditions. The significantly higher pre-storage  $a_w$  values in late harvest sultanas made it difficult to separate the true effects of other factors, such as higher free-arginine. Sultana  $a_w$  is undoubtedly a very important determinant of sultana browning, as was observed in this storage trial, the ANOVA data and the MLR regression model. The single effect of high  $a_w$ , i.e. non-sunfinished sultanas, was strong regardless of the presence or absence of oxygen. Clearly oxygen enhanced the rates of browning regardless of the  $a_w$ , however, exclusion of oxygen retarded, but did not prevent browning at 30°C. It was seen in Figure 4.9 and Figure 4.13 that low  $L^*$  and  $b^*$  values were observed for non-sunfinished sultanas regardless of their storage oxygen exposure. The lack of significance ( $p=0.05$ ) of the 'oxygen×sunfinishing' interaction (for  $L^*a^*b^*$ )—especially for the late harvest sultanas—offered important information in the interpretation of the nature of the browning processes. If the storage browning reactions were primarily due to  $a_w$ -sensitive PPO reactions, this term would be expected to be highly significant. The lack of significance of this interaction strongly implied oxygen sensitive, but non-oxygen dependent reactions, i.e. Maillard reactions.

In contrast, only a small amount of browning was observed at 10°C storage, showing that the browning processes that occurred were activated at higher temperature. It has been shown that the grape PPO enzyme has an optimal temperature for activity (25°C–40°C), however complete inhibition of activity at 10°C storage would not be expected. It was observed from HPLC data that late harvest sultanas had already undergone significant oxidation of *trans*-caftaric acid before storage, yet little further browning was observed even after 10 months of storage at 10°C in the presence of oxygen. In contrast, the same sultanas stored at 30°C underwent intense browning, even in the absence of oxygen. It was previously discussed that dark PPO pigments are largely the result of interactions of quinones with other phenolics and other compounds such as amino acids and proteins. This process, however, occurs rapidly, as quinones are highly reactive. These non-enzymatic quinone reactions would be expected to occur fairly rapidly at 10°C (days to weeks). It is proposed that most PPO-related browning had already occurred in late-harvest non-sunfinished sultanas before the storage trial (evinced through the low concentration of *trans*-caftaric acid in pre-storage sultanas) and that subsequent browning reactions were mainly non-enzymatic in nature and, importantly, not inherently oxygen dependent. Whether the subsequent reactions

which occurred were dependent on previous oxidation of *trans*-caftaric acid is not known; this would be, however, difficult to demonstrate. It is certain that the reactions were not inherently oxygen-dependent which indicated Maillard-type reactions. The greater degree of browning observed in oxygen exposed fruit might have been due to interactions of further oxidative reactions of phenolics with other browning substrates, such as MRPs, or interactions of MRPs with lipid oxidation products leading to coloured pigments. There is mounting evidence that lipids and their oxidation products interact with and enhance the colour of basic Maillard compounds (Whitfield 1992, Hidalgo and Zamora 2000 and Mastrocola *et al.* 2000).

It was also seen that the relative concentration of 5-HMF and the MRP eluting at 5.3 min. (Figure 4.8) in pre-storage, non-sunfinished, late-harvest sultanas was lower than concentrations measured in sunfinished late-harvest sultanas, providing some evidence that Maillard browning systems are also  $a_w$  sensitive. It is important to reiterate that many early Maillard reaction products are in themselves colourless; it is only after polymerisation that coloured pigments are formed. It is also known that the rates of formation and polymerisation of MRPs are oxygen sensitive. Maillard reactions occur more rapidly in the presence of oxygen and trace metals (Saltmarsh and Labuza 1982 and Yalayan and Huyghues-Despointes 1994). Oxygen sensitivity of Maillard reactions in sultanas was indicated by the often significantly lower concentrations of 5-HMF in fruit stored at 30°C in the presence of oxygen.

Previous investigations showed that organic nitrogen steadily increased in grapes during maturation (Peynaud 1947, Peynaud and Maurie 1953 and Kliewer 1968) with synthesis of amino acids and proteins occurring mainly in the last six to eight weeks of berry ripening after veraison. Concentrations of proline can differ from ten- to twelve-fold and those of arginine two- to six-fold respectively, between early and late harvest fruit for a given cultivar (Kanellis and Roubelakis-Angelakis 1993). Higher concentrations of both free-proline and free-arginine in the higher maturity late-harvest sultanas compared to early harvest fruit, which generally supported these previous observations. The effect of vine solar exposure had a significant effect on the pre-storage concentration of free-arginine and proline, with higher concentrations of these amino acids in shaded fruit. The free-amino acid data was also supported by the KP data. It was seen that the vine solar exposure had a significant effect on the colour of early-harvest sultanas, with high shaded grapes producing darker fruit, although the magnitude of this effect was small. This trend was, however, not apparent for late harvest fruit. It was shown that the pH was higher in late harvest grapes (and presumably in late harvest sultanas) which together with higher initial  $a_w$  values may have had a combined effect on browning reactions. In the case of the early harvest sultanas it would be tempting to ascribe the higher browning in shaded fruit as being a result of higher pre-storage free-amino acids, however this can only be considered as speculative in the absence of multi-season trials.

Previous investigations have found that most grape and sultana PPO activity is localised in the skin (Radler 1964 and Rathjen and Robinson 1992a). Table 4.2 shows that skin PPO potential activity was at least 4 to 10 times higher on a fresh weight basis in grape skins compared to flesh, which is in broad agreement with their findings. Uhlig (1998) found no significant difference in PPO levels between shade and sun exposed berries, which is generally supported by the lack of significant difference in PPO activity observed between EX and GR grapes harvested on both dates. Interestingly, the lowest skin activity fruit was in the MS fruit on both harvest dates. In summary only small differences in soluble PPO activity existed between shading levels or between fruit of the same shading level harvested on both dates, and it is probably reasonable to assume that those differences contributed little to differences in storage browning.

Both copper and iron are well known for their catalytic roles in many chemical processes, especially as catalysts in Maillard browning reactions (Kawakishi *et al.* 1990 and Rendleman and Inglett 1990). The effect of both copper and iron on rates of product formation in model Maillard systems is well documented in the literature (Cheng and Kawakishi 1994, Yaylayan and Huyghues-Depointes 1994, Hayase *et al.* 1996 and Birlouez-Aragon *et al.* 1997). In addition iron has been shown to be incorporated in high-molecular weight, dark, end-products, causing enhanced absorbance in the visible region. Interactions of iron with quinones also intensify the colour of brown chromophores (Guyot *et al.* 1995, Garcia *et al.* 1996, and Ozmianski *et al.* 1996). Whether these post-oxidation interactions require oxygen has not been shown. It was shown in this trial that there were only small differences in the concentration of iron and copper in the sultanas used, thus differences in browning rates could not be ascribed to differences in these elements. In addition to catalytic roles, copper, which is an essential component of the PPO enzyme, has been correlated with plant PPO activity (Mayer 1987). The copper concentration was higher in shaded sultanas as was PPO activity, in accordance with Mayer (1987), although in contrast to the previous season's data.

## 5.0 SOIL NITROGEN AND SULTANA BROWNING

---

### 5.01 Soil nitrogen and sultana colour—introduction

The possible effect of soil nitrogen on the short and *long-term* browning potential of sultanas has not been investigated widely in the literature. Keller *et al.* (1999) noted that high rates of nitrogen fertilisation of vines decreased the colour stability of *Pinot Noir* grapes used in wine-making. In addition there are anecdotal reports (pers. comm. Hayes 1995 and Nagarajah 1995) that over-fertilised soils produce darker dried fruit which tends to be less colour-stable during storage. In a limited experiment, the effect of soil nitrogen on long-term sultana colour was examined through a storage trial and chemical analysis. In addition arginine-glucose Maillard reactions were further examined in sultanas and model systems using HPLC and UV spectral characterisation.

It is known that the application of nitrogen containing fertilisers to grape-vines is mirrored by a high concentration of free-amino acids in berries (Williams 1946 and Kliewer 1977). If the hypothesis that a significant portion of storage browning in sultanas is due to Maillard reactions (at 30°C storage temperature) is to be credible, sultanas with higher pre-storage concentrations of free-arginine would be expected to undergo browning more rapidly than sultanas with lower pre-storage arginine, other factors—storage temperature, oxygen exposure,  $a_w$  etc.—being equal. It was expected that sultanas produced from (genetically identical) grape-vines receiving different nitrogen fertiliser regimes would provide a comparable set of sultanas which varied only in their nitrogen and free-amino acid concentration. Such samples would allow further characterisation of storage-Maillard reactions.

### 5.02 Experimental aims

The aims of these experiments were to:

- establish whether soil nitrogen fertilisation has a significant effect on sultana PPO activity, HPLC phenolic profiles, free-amino acids and pre-storage colour;
- test the hypothesis that higher levels of free-amino acids (specifically arginine) predispose sultanas to more rapid browning; and finally
- further characterise sultana Maillard reactions using HPLC and UV spectral analysis.

### 5.03 Source of sultana material

The sultanas used in this trial were produced in a separate experiment by Dr Nagarajah and colleagues at the SHC. Ten-year-old H5 sultana vines were transferred from the nursery at SHC

to cement pots (60 cm diameter and 60 cm high) in August 1995. The soil used in the pots was sandy and had a low concentration of nitrate and a low oxidisable carbon content (0.4–0.5%). Four levels of nitrogen application were used: 0, 8.5, 17.0 and 25.5 g of nitrogen were randomly added to the pots in the form of ammonium nitrate on 10 September each year (1995 and 1996). The application of nitrogen containing fertilisers increased the soil nitrate concentration to ca. 0, 80, 100 and 140 ppm. The grapevines were placed outside at the SHC in a fully sun-exposed position and were irrigated using micro-jets in such a manner as to minimise leaching losses of nitrate. On days of rainfall the pots were covered with plastic sheets. Grapes were harvested on 10 February 1996 and were dipped and dried down to about 18% moisture as described previously. The dried sultanas were placed on black polyethylene sheets and sunfinished on consecutive days until the moisture level was reduced to around 12%. The sultanas produced from vines at each of the levels of soil fertiliser application were coded as N<sub>0</sub> (0 added fertiliser), N<sub>1</sub> (8.5 g added fertiliser), N<sub>2</sub> (17.0 g added fertiliser) and N<sub>3</sub> (25.5 g added fertiliser). The sultanas will be referred to by these codes henceforth. These levels of nitrogen were chosen to mimic soil nitrogen concentrations commonly found within vineyards, corresponding to the following conditions: N<sub>0</sub> severely deficient, N<sub>1</sub> deficient to marginal, N<sub>2</sub> adequate to high and N<sub>3</sub> high.

Table 5.1 shows analytical data for the fresh grapes at harvest. Chemical analyses performed by Dr Nagarajah and colleagues at the SHC. The grape petiole nitrate and total nitrogen were determined for each level of fertiliser application, using the methods outlined previously by Nagarajah (1999). Juice from 100 grapes from vines for each nitrogen treatment level was used. TSS was determined using an Atago hand-held refractometer (Atago Co. Ltd. Japan) and TA was determined via titration with NaOH (0.1 M) and phenolphthalein end-point determination.

ANOVA was performed using Genstat. The effect of the fertiliser was significant ( $p < 0.001$ ) for both the petiole nitrate content and the percent nitrogen. The effect of the fertilisers on TSS, TA and sultana yield was not significant for the 1996 season's harvest. The fertiliser regime did have a significant effect on yield only in subsequent years (data not shown). Dr Nagarajah provided approximately 1.5 kg of sultanas from each of the nitrogen treatments for use in the following storage experiment. Sultanas were stored at 4°C until being transported to VUT for the storage trial and chemical analyses.

Nitrogen code	Petiole Nitrate $\mu\text{g.g}^{-1}$ DW	% Nitrogen fresh grape	TSS °Brix	TA $\text{g.L}^{-1}$	Sultana yield $\text{kg.vine}^{-1}$ DW
N <sub>0</sub>	10	0.60	19.7	5.36	1.4
N <sub>1</sub>	20	0.67	19.1	5.49	1.6
N <sub>2</sub>	180	0.89	19.7	5.31	1.5
N <sub>3</sub>	2000	1.31	20.3	5.34	1.7

Table 5.1 Analytical data for grape petiole nitrate, percent nitrogen, total soluble solids (TSS), titratable acidity (TA) and sultana yield. Grapes harvested on 10 February 1996. Source: Nagarajah et al. unpublished data.

Sultanas not used in the storage trial were frozen at  $-80^{\circ}\text{C}$  until further chemical analyses could be performed. For all chemical analyses, two portions of twenty-five sultanas were prepared and at least two duplicate chemical analyses were performed on each sub-sample i.e. a total of four determinations for each treatment level. The data for experiments were arranged in spreadsheet format and imported into Genstat for statistical analyses.

#### 5.04 Experimental-storage trial

Free-amino acids, total phenolics, KP,  $L^*a^*b^*$  tristimulus data, PPO substrate activity, iron and copper were determined as described previously. Sultanas from each of the four soil nitrogen applications were packaged at the same time and in the same manner as for the 1996 storage trial II. Sultana samples were removed at 5 and 10 months and subjected to physico-chemical analyses.

#### 5.05 HPLC diode-array analysis of Maillard model system and sultana extracts

In order to characterise the peaks which appeared on HPLC profiles (320 nm) in the previous section, a diode-array detector (DAD, Varian 9065-Polychrom) was connected to the HPLC system in series with the UV fixed wavelength detector at 320 nm (Varian 9050). For the DAD, the 'peak-sense' function was set to detect peaks at 320 nm and the 'peak-scan' function was set to scan between 190 and 370 nm, the maximum range. The following settings were employed: scan rate 10.851 Hz, bunch rate 4, data rate 2.71 Hz. Quantification was performed on the data output from the fixed wavelength module channel and qualitative spectral data were obtained from the DAD module. Data were examined using the Varian proprietary spectral analysis software, 'Polyview®' (Version 5.0) and the Star Chromatography Software ® (Version 5.34). The HPLC system used was identical to that previously described. All sultana, grape and Maillard model systems were run under identical conditions.

#### 5.06 Pre-storage sultana chemical data

Pre-storage analytical data for the soil-nitrogen treated sultanas are shown in Table 5.2. Pre-storage substrate PPO activity was lower in the lowest soil nitrogen sultanas ( $N_0$ ), however PPO activities in sultanas from higher soil nitrogen application ( $N_1$ ,  $N_2$ ,  $N_3$ ) were not significantly different, ranging from  $6.03\text{-}6.38 \mu\text{mole.O}_2\text{.min}^{-1}\text{.g}^{-1}$ . Pre-storage  $a_w$  values were similar for all the samples, ranging between  $0.496$  to  $0.501 \mu\text{g.g}^{-1}$ . Copper and iron concentrations were not significantly different, although the concentration of copper was notably higher than the typical concentrations measured in sultanas from the previous trial. Sultana KP increased with soil fertiliser: the relationship between the soil nitrogen and sultana KP did not appear to be linear: the relationship appeared to approximate sigmoidal. The difference in KP values for the two lowest soil nitrogen sultanas ( $N_0$  and  $N_1$ ) was around  $5 \text{mg.g}^{-1}$  and that between the two highest soil

nitrogen sultanas ( $N_2$  and  $N_3$ ) was also approximately  $5 \text{ mg.g}^{-1}$ , while the difference between the low and high groups was around  $10 \text{ mg.g}^{-1}$ . Pre-storage  $L^*a^*b^*$  tristimulus data indicated that all the fruit was light golden to light amber in colour; low soil nitrogen sultanas ( $N_0$ ) were noticeably lighter than the highest soil-nitrogen samples ( $N_3$ ). Total phenolics were similar for all soil nitrogen treatments, indicating that the fertiliser level did not significantly affect pre-storage concentrations.

### 5.07 Pre-storage free-amino acid profiles

Free-amino acid profiles were determined using F-moc pre-column derivatisation and HPLC in the manner described previously. In agreement with the data from the preceding trials, proline, arginine and the unidentified compound dominated the free-amino acid profiles. Only trace amounts of other amino acids were present. Sultana skins and flesh were separated and analysed. Figure 5.1 shows the pre-storage concentrations of free-arginine and proline in sultana skins and flesh.

It can be seen that significantly higher concentrations of arginine and proline were present in sultana skins than flesh, with increasing concentrations of each amino acid observed for increasing soil nitrogen application. The concentration of the unidentified compound ranged from  $1.3$  to  $3.5 \text{ mg.g}^{-1}$  in sultana skins and from  $1.4$  to  $1.9 \text{ mg.g}^{-1}$  in sultana flesh; this compound did not show any obvious relationship with soil nitrogen. The concentration of skin free-arginine and proline tended to increase with the level of soil nitrogen addition.

	PPO $\mu\text{mole.O}_2$ $\cdot \text{min}^{-1} \cdot \text{g}$ $\text{DW}^{-1}$	Total phenols $\text{mg.g}^{-1}$ $\text{DW}$	$a_w$	Copper $\mu\text{g.g}^{-1}$ $\text{DW}$	Iron $\mu\text{g.g}^{-1}$ $\text{DW}$	KP $\text{mg.g}^{-1}$ $\text{DW}$	$L^*$	$a^*$	$b^*$
<b>LSD</b> <b>p=0.05</b>	<b>1.015</b>	<b>ns</b>	<b>0.002</b>	<b>ns</b>	<b>ns</b>	<b>1.613</b>	<b>3.85</b>	<b>1.01</b>	<b>1.67</b>
$N_0$	4.62	0.91	0.496	25.50	19.89	14.91	36.01	6.51	20.07
$N_1$	6.03	0.94	0.501	20.80	21.95	19.84	35.02	4.23	17.62
$N_2$	6.10	0.85	0.494	22.02	23.59	30.87	35.10	4.49	18.20
$N_3$	6.38	0.88	0.500	20.73	20.73	36.01	31.01	4.30	16.60

Table 5.2 Pre-storage analytical data for soil nitrogen sultanas. Substrate PPO activity, total phenolics (Folin-Ciocalteu method),  $a_w$ , copper, iron, Kjeldahl protein (KP) and the Minolta tristimulus coordinates ( $L^*a^*b^*$ ). All values are the means of two determinations of  $2 \times 20$  sultanas (4 measurements). LSD calculated from the mean measurement for the two sub-samples for each nitrogen application level.

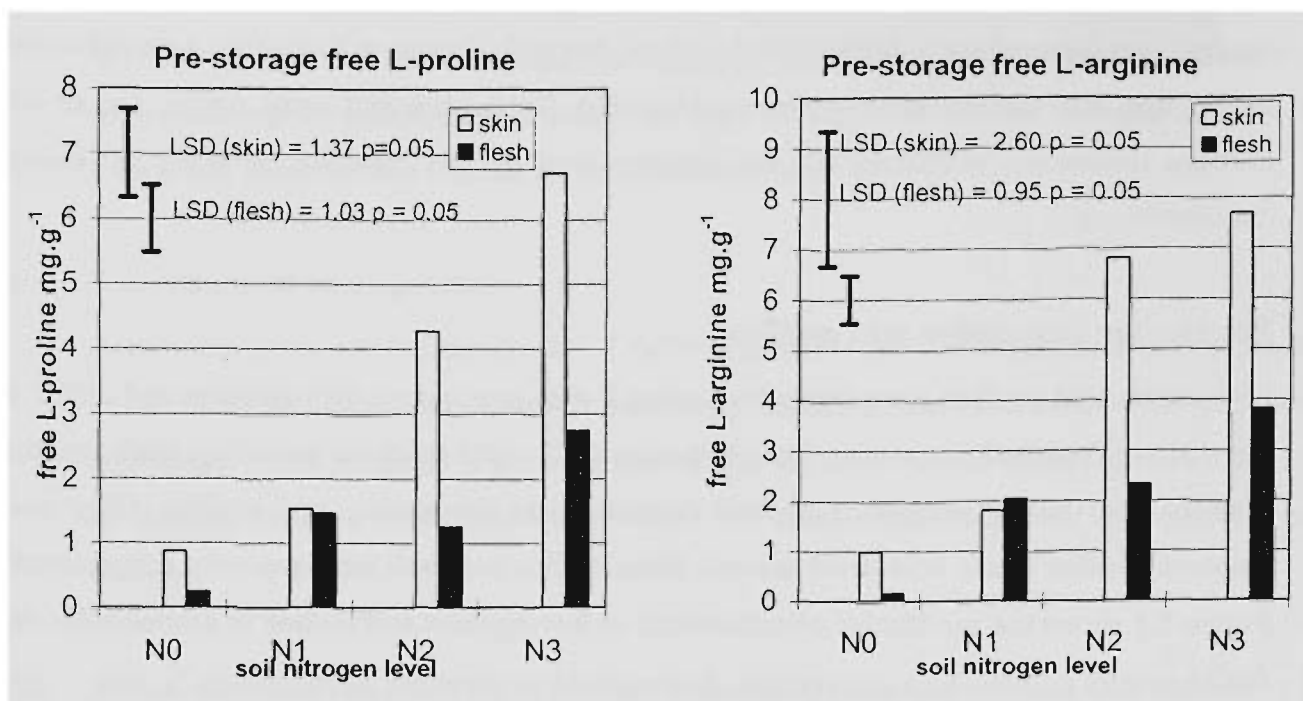


Figure 5.1 Pre-storage free-proline and arginine in sultanas from vines given four amounts of nitrogen fertiliser.

Each value is the mean of two instrumental determinations performed on two sub-samples of 25 sultanas. The mean data for each of the replicate sub-samples were used to determine LSD data for the nitrogen treatment.

## 5.08 Storage trial

Sultanas from each of the soil nitrogen application levels were packaged for storage under the same conditions as for the 1996 storage trial. Approximately 1.5 kg bulk sample from each of the four soil nitrogen levels was divided in such a way that ca. 200 g of sultanas were packaged into individual sachets containing air or in the absence of air as described in section 3.22. These were stored at either 10°C or 30°C and removed from storage after 5 or 10 months. There were thus eight such lots for each nitrogen application level, namely 2 (temperature) × 2 (oxygen) × 2 (time).

## 5.09 Storage colour changes

Changes in L\*a\*b\* tristimulus values were measured after 5 and 10 months storage. L\*a\*b\* data were arranged in a spreadsheet format and imported into Genstat 5 for ANOVA analysis. The treatment factors were coded as follows: added soil 'nitrogen' (0, 8.5, 17.0, 25.5), 'oxygen' exposure (0, 1), storage 'temperature' (10, 30) and 'time' (0, 5, 10). Tables of mean data were used to generate the graphical data.

## 5.10 Changes in the L\* tristimulus coordinate

The ANOVA data for the L\* tristimulus coordinate (lightness) is shown in Table 5.3. The single effects of time, soil nitrogen and temperature were highly significant as well as the temperature×time interaction. The nitrogen×time accounted for large variance ( $p < 0.007$ ) highlighting the time dependence of the decreases in L\*. As shown by the ANOVA table, the oxygen effect accounted for a small portion of the variance and was less significant ( $p < 0.011$ ) than other effects.

The effect of soil nitrogen, oxygen and temperature are shown for average L\* values in Figure 5.2. There was not a significant difference in pre-storage L\* values, except for the highest soil nitrogen samples (N<sub>3</sub>). At 10°C storage in the presence and absence of oxygen small decreases in L\*, compared to pre-storage values, were observed for most samples. Significant decreases in average L\* were observed for all samples stored at 30°C. It can be seen that generally there was not a significant difference between average L\* values of sultanas stored either in the presence or absence of oxygen. It can also be seen that average L\* values decreased significantly with increasing soil nitrogen. The effect of time on average L\* values is shown in Figure 5.2 (bottom). After 5 and 10 months storage at 30°C, L\* values decreased significantly, compared to pre-storage values, as soil nitrogen was increased. Small changes in average L\* values were observed at 10°C.

## 5.11 Changes in a\* tristimulus coordinate

ANOVA data for the a\* tristimulus data (redness) (Table 5.3) indicated that the highly significant effects in decreasing importance were: nitrogen, time, the nitrogen×time interaction and temperature. The nitrogen×time interaction was also important. The effect of oxygen was not significant ( $p = 0.085$ ).

The a\* tristimulus data increased for all storage conditions, compared to the pre-storage values (Figure 5.3). Pre-storage a\* values were significantly higher for the lowest soil nitrogen sultanas (N<sub>0</sub>) compared to the sultanas from higher soil nitrogen treatments. Lowest nitrogen sultanas maintained this difference for all storage conditions. At 30°C storage a\* values were lowest in the highest soil nitrogen sultanas (N<sub>3</sub>).

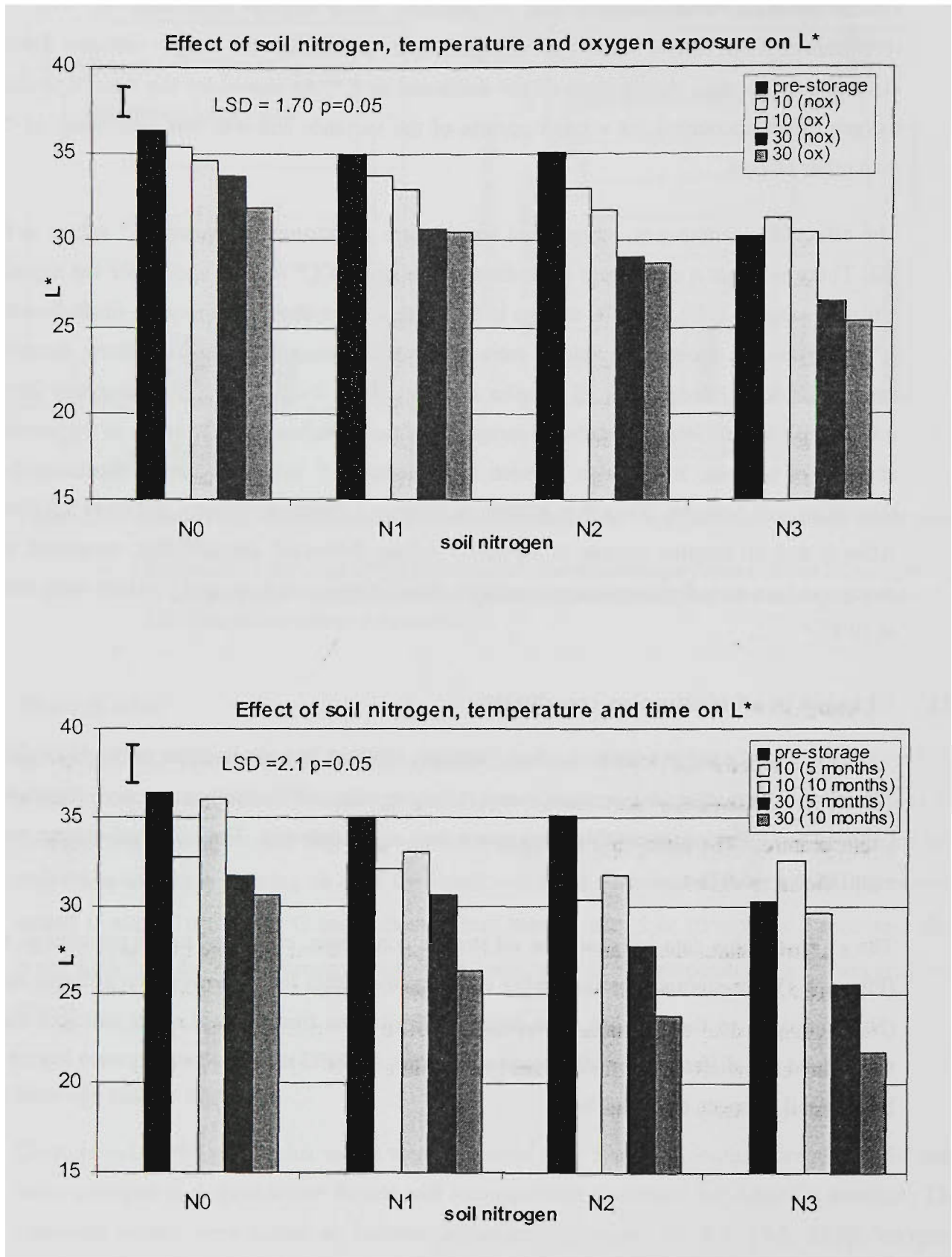


Figure 5.2 Change in L\* values for soil nitrogen sultanas stored for 10 months. Top: effect of soil nitrogen, temperature and oxygen. Bottom: effect of soil nitrogen, storage temperature and time. LSD values generated by ANOVA for all samples and interactions.

(L*) Source of variation	d.f.	s.s.	m.s.	v.r.	F pr.
nitrogen	3	199.95	66.65	91.35	<0.001
oxygen	1	9.72	9.72	13.32	0.011
temperature	1	132.93	132.93	182.20	<0.001
time	2	219.98	109.99	150.76	<0.001
nitrogen.oxygen	3	0.95	0.31	0.44	0.734
nitrogen.temperature	3	12.89	4.29	5.89	0.032
oxygen.temperature	1	0.0065	0.0065	0.01	0.928
nitrogen.time	6	42.36	7.06	9.68	0.007
oxygen.time	2	6.74	3.37	4.62	0.061
temperature.time	2	97.00	48.52	66.51	<0.001
<b>Pooled non-significant three-way terms</b>					
Residual	6	4.37	0.72		
<b>Total</b>	<b>47</b>	<b>747.92</b>			
(a*) Source of variation	d.f.	s.s.	m.s.	v.r.	F pr.
nitrogen	3	41.68	13.89	68.68	<0.001
oxygen	1	0.85	0.85	4.24	0.085
temperature	1	9.90	9.90	48.94	<0.001
time	2	25.00	12.50	61.79	<0.001
nitrogen.oxygen	3	1.19	0.39	1.96	0.221
nitrogen.temperature	3	2.15	0.71	3.55	0.087
oxygen.temperature	1	0.90	0.90	4.46	0.079
nitrogen.time	6	10.94	1.82	9.02	0.009
oxygen.time	2	1.04	0.52	2.58	0.155
temperature.time	2	5.03	2.51	12.45	0.007
oxygen.temperature.time	2	4.42	2.21	10.94	0.01
<b>Pooled non-significant three-way terms</b>					
Residual	6	1.21	0.20		
<b>Total</b>	<b>47</b>	<b>110.80</b>			
(b*) Source of variation	d.f.	s.s.	m.s.	v.r.	F pr.
nitrogen	3	156.36	52.120	34.99	<0.001
oxygen	1	14.08	14.083	9.46	0.022
temperature	1	55.68	55.685	37.39	<0.001
time	2	55.50	27.753	18.63	0.003
nitrogen.oxygen	3	3.02	1.008	0.68	0.597
nitrogen.temperature	3	8.06	2.690	1.81	0.246
oxygen.temperature	1	4.91	4.915	3.30	0.119
nitrogen.time	6	19.23	3.206	2.15	0.187
oxygen.time	2	7.97	3.987	2.68	0.148
temperature.time	2	42.69	21.347	14.33	0.005
<b>Pooled non-significant three-way interactions</b>					
Residual	6	8.93	1.489		
<b>Total</b>	<b>47</b>	<b>393.09</b>			

Table 5.3 ANOVA table for the effects of nitrogen, oxygen, temperature, time on L\*a\*b\* tristimulus values.

## 5.12 Changes in $b^*$ tristimulus coordinate

ANOVA data for  $b^*$  (yellowness) are shown in Table 5.3. Significant effects, in order of decreasing importance, were nitrogen, temperature, time, the temperature×time interaction and oxygen. No other interactions were significant ( $p < 0.05$ ).

In Figure 5.4 (top), the effect of soil nitrogen, storage temperature and oxygen on average  $b^*$  values is graphically shown. Pre-storage  $b^*$  values were highest in the low soil nitrogen sultanas, and were lowest for the highest soil nitrogen fruit. At 10°C storage,  $b^*$  values either did not change or decreased slightly. Although sultanas stored under oxygen had slightly lower average  $b^*$  values, in the higher soil nitrogen samples ( $N_2$  and  $N_3$ ) the differences were not significant. At 30°C storage average  $b^*$  values were lower for sultanas stored in the presence of oxygen; all oxygen exposed samples had significantly lower average  $b^*$  values. For sultanas stored at 30°C in an oxygen free environment, significantly lower  $b^*$  values were measured only in the two highest soil nitrogen samples ( $N_2$  and  $N_3$ ). The effect of time on average  $b^*$  values is shown in Figure 5.4 (bottom). Largest decreases in  $b^*$  were observed at 30°C, with increasing significance over time. The strong effect of soil nitrogen on average  $b^*$  values at 5 and 10 months was apparent.

All sultanas stored at 10°C remained essentially light golden or light amber in colour up until 10 months with no evidence of internal sugaring. Photographs of soil nitrogen samples after 5 and 10 months storage at each of the four storage conditions are shown in Figure 5.5 and Figure 5.6.

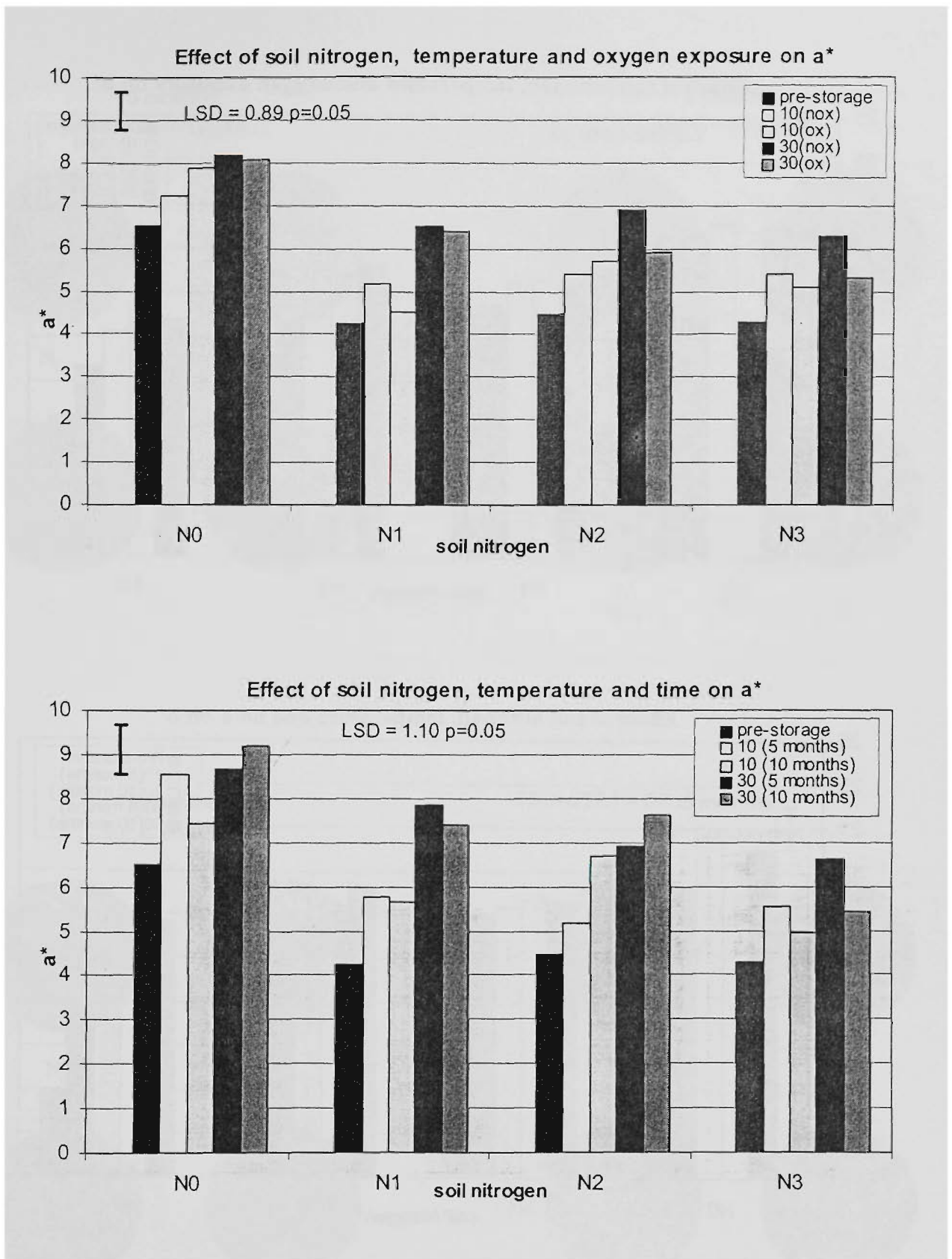
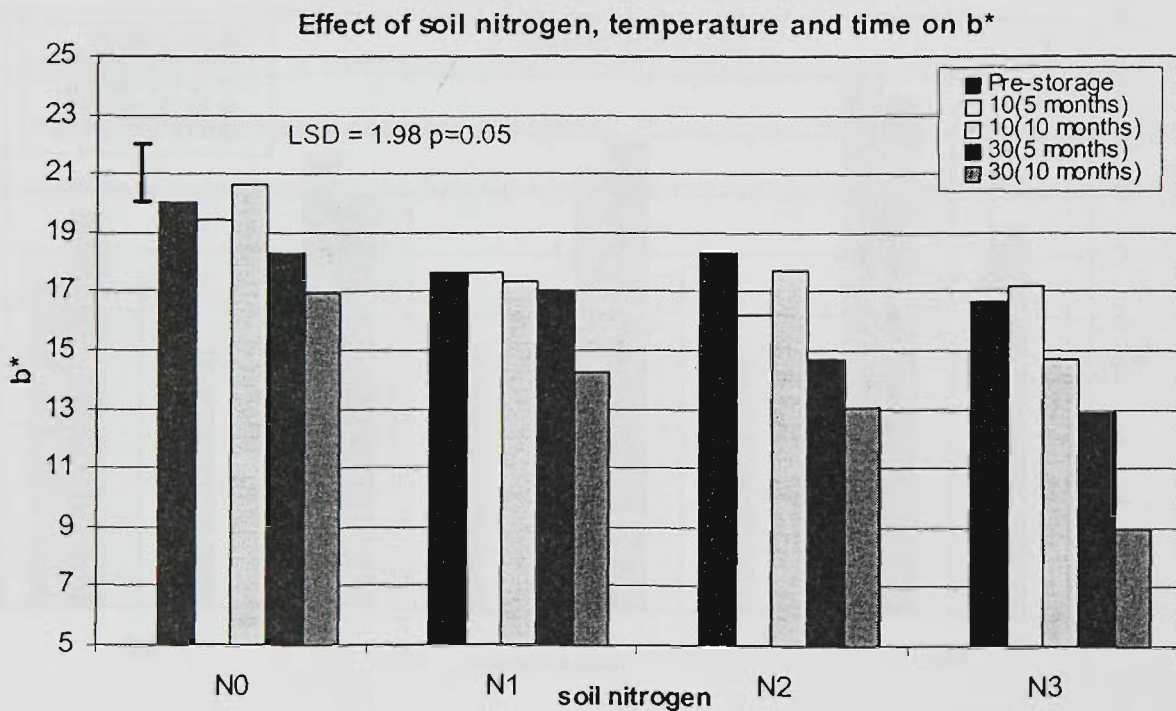
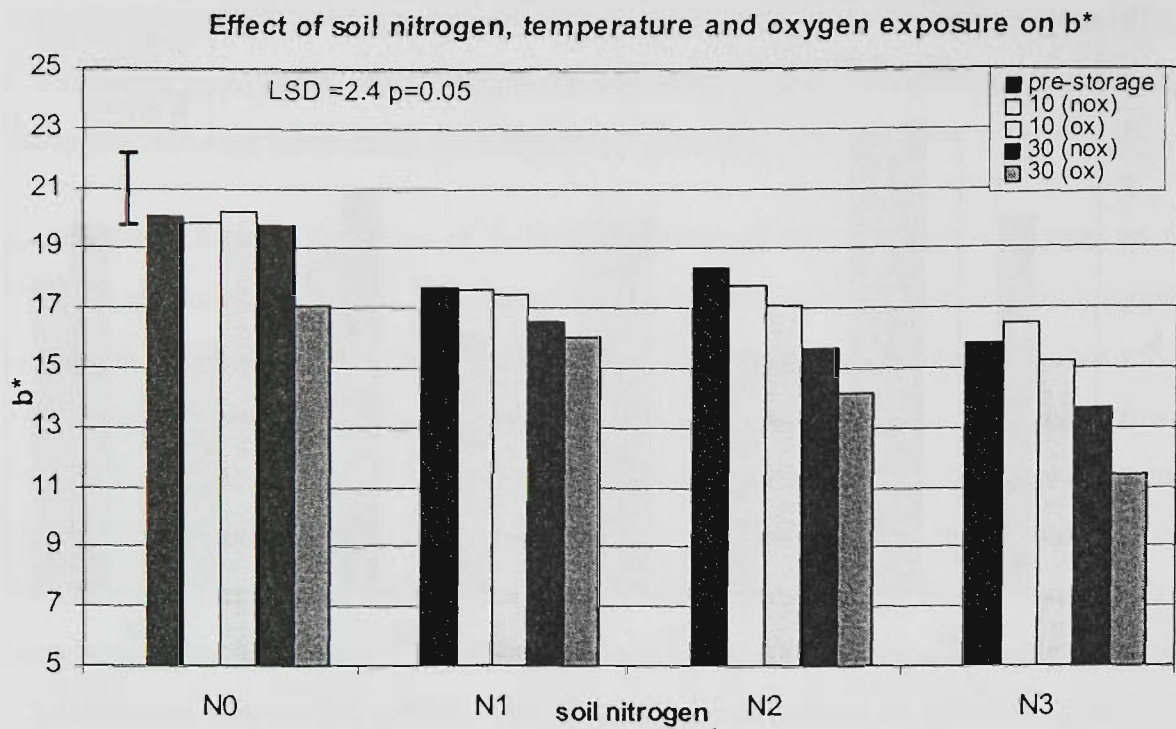
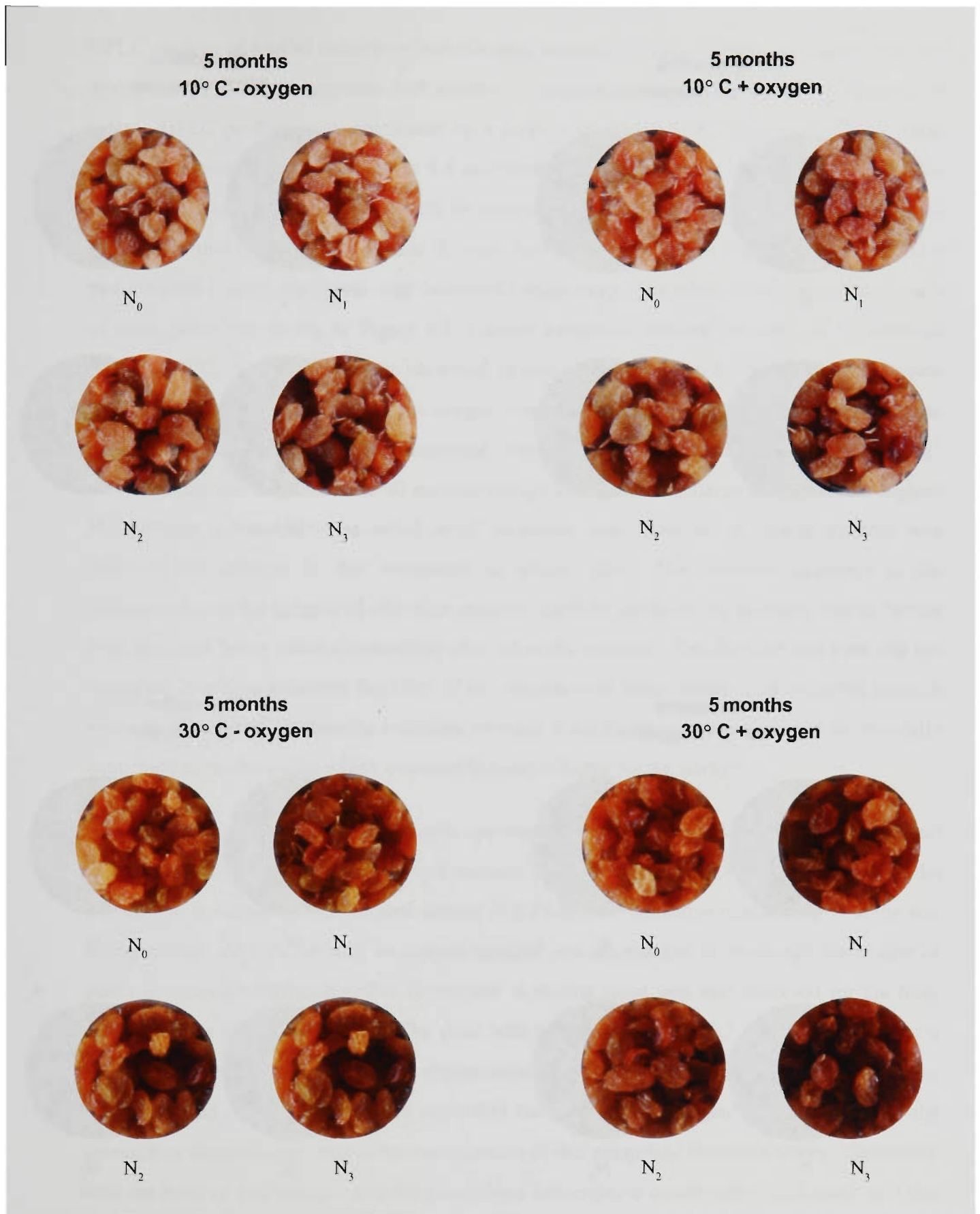


Figure 5.3 Change in  $a^*$  (Lightness) values for soil nitrogen sultanas stored for 10 months. Top – effect of soil nitrogen, temperature and oxygen. Bottom – effect of soil nitrogen, storage temperature and time. LSD values generated by ANOVA for all samples and interactions.



**Figure 5.4** Change in b\* (Lightness) values for soil nitrogen sultanas stored for 10 months. Top: effect of soil nitrogen, temperature and oxygen. Bottom: effect of soil nitrogen, storage temperature and time. LSD values generated by ANOVA for all samples and interactions.



*Figure 5.5 Colour of soil nitrogen experiment sultanas after 5 months at each of the storage conditions: Top (left): 10°C no oxygen, (right): 10°C with oxygen. Bottom (left): 30°C no oxygen, (right): 30°C with oxygen.*

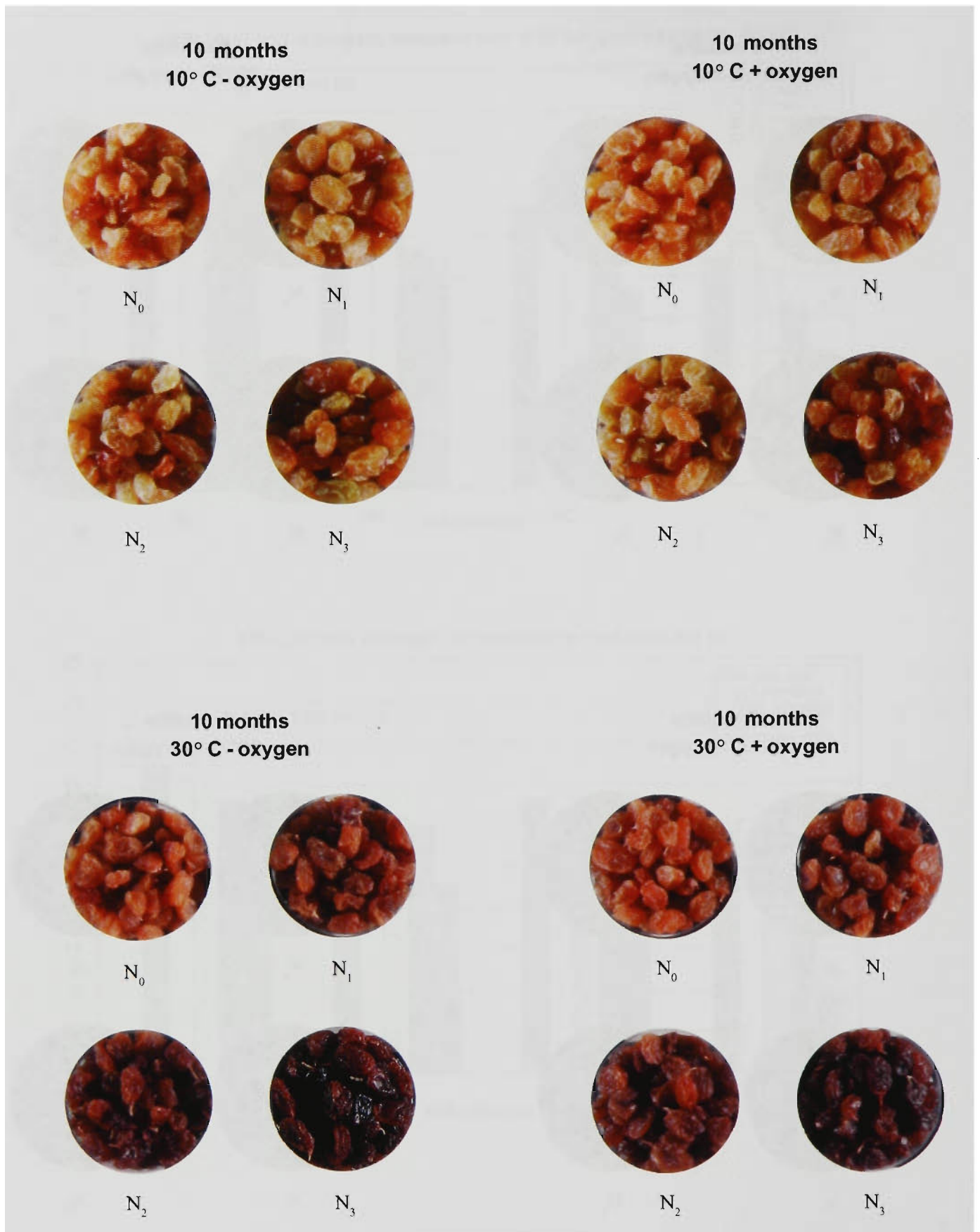


Figure 5.6 Colour of soil nitrogen experiment sultanas after 10 months at each of the storage conditions: Top (left): 10 °C no oxygen, (right): 10 °C with oxygen. Bottom (left): 30 °C no oxygen, (right): 30 °C with oxygen.

### 5.13 Changes in HPLC Profiles of sultana MeOH extracts

HPLC profiles of MeOH extracts of soil-nitrogen sultanas (skins) at 0 time and after 10 months storage at 30°C in the presence and absence of oxygen are shown in Figure 5.7. Pre-storage sultana HPLC profiles were dominated by a large peak eluting at 8.3 min., a cluster of peaks eluting at around 2.7 min., a peak at 6.5 min. and some smaller peaks eluting at 10.5 and 13.4 min. There was also a small peak with an elution time of 5.3 min. After storage at 30°C, both with and without oxygen, the peak at 6.5 min. had decreased to trace levels on chromatograms and the peak eluting at 5.3 min. had increased considerably. The relative concentrations of each of these peaks are shown in Figure 5.8. Despite medium to intense browning in the sultanas stored at 30°C, the peak tentatively identified as *trans*-caftaric acid ( $t_R$  8.3 min) did not disappear from HPLC profiles, regardless of the oxygen condition. It can be seen (Figure 5.8) that the pre-storage skin concentration of this compound was similar in all sultanas ( $230\text{--}250 \text{ IAC} \times 10^{-3} \cdot \text{g}^{-1} \text{ DW}$ ), and did not decrease after 10 months storage in any of the sultanas except for the highest soil nitrogen sultanas ( $N_3$ ), in which small decreases were observed. A similar situation was observed for changes in this compound in sultana flesh. The observed increases in the concentration of the compound over time could be partially explained by moisture loss in berries over time and hence relative concentration of phenolic substrate. The fact that this peak did not disappear over time indicated that little, if any, oxidation of *trans*-caftaric acid occurred; hence it was assumed that PPO phenolic oxidation or other autoxidation processes did not substantially contribute to the browning which occurred in these sultanas during storage.

The peaks eluting at 2.7 min. and 5.3 min. appeared to be related to the level of soil nitrogen and were hence suspected as being Maillard reaction products. In Figure 5.8 it can be seen that the pre-storage concentration of the peak cluster at 2.7 min. had a positive relationship with the soil nitrogen level. At 30°C in both an oxygen-exposed and oxygen-free environment, the cluster of peaks decreased significantly after 10 months. A similar trend was also observed for the flesh concentrations of this compound. The peak with an elution time of 5.3 min. was present at a relatively low concentration in all pre-storage sultanas. After storage at 30°C, the concentration of this compound increased more than eight-fold for the highest nitrogen fruit regardless of the presence or absence of oxygen. The concentration of this compound showed a strong relationship with the level of soil nitrogen and the pre-storage free-arginine concentration indicating that this compound was likely to be a Maillard reaction product, rather than a phenolic oxidation product.

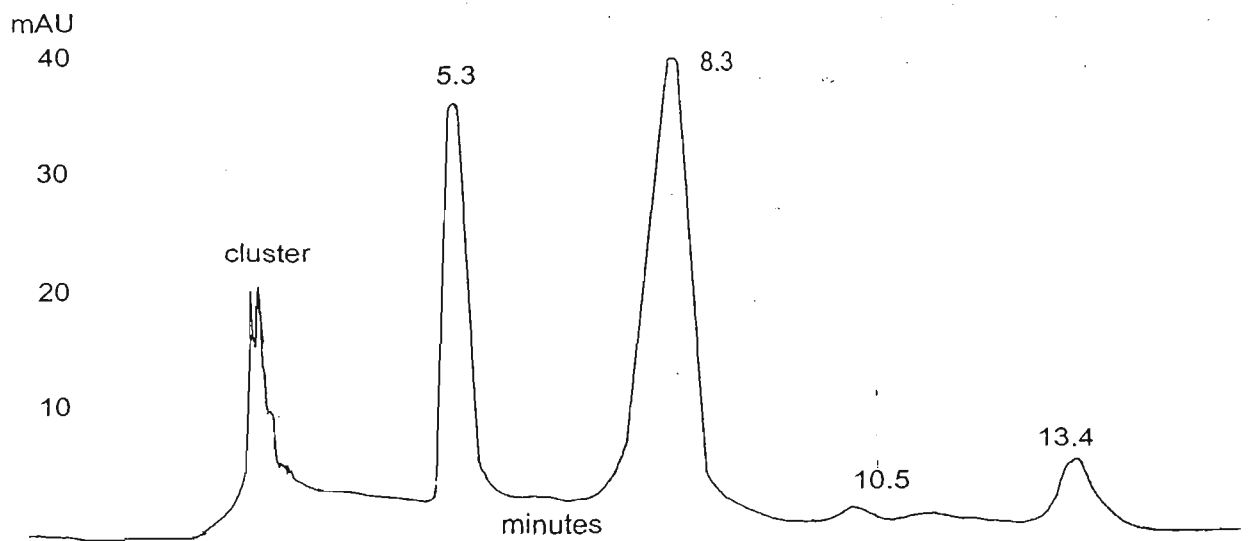
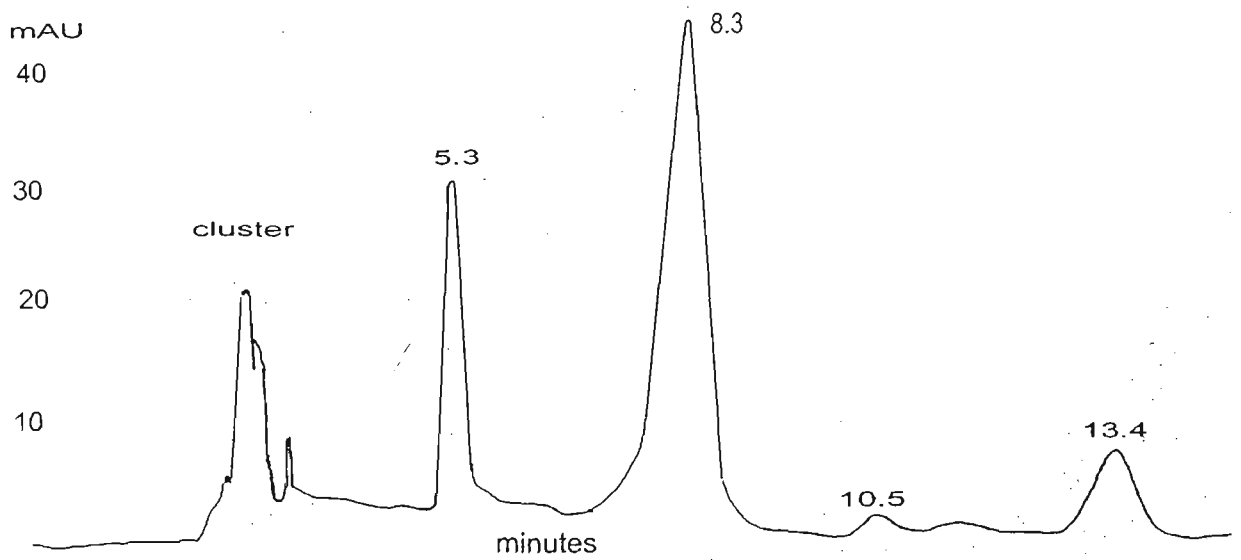
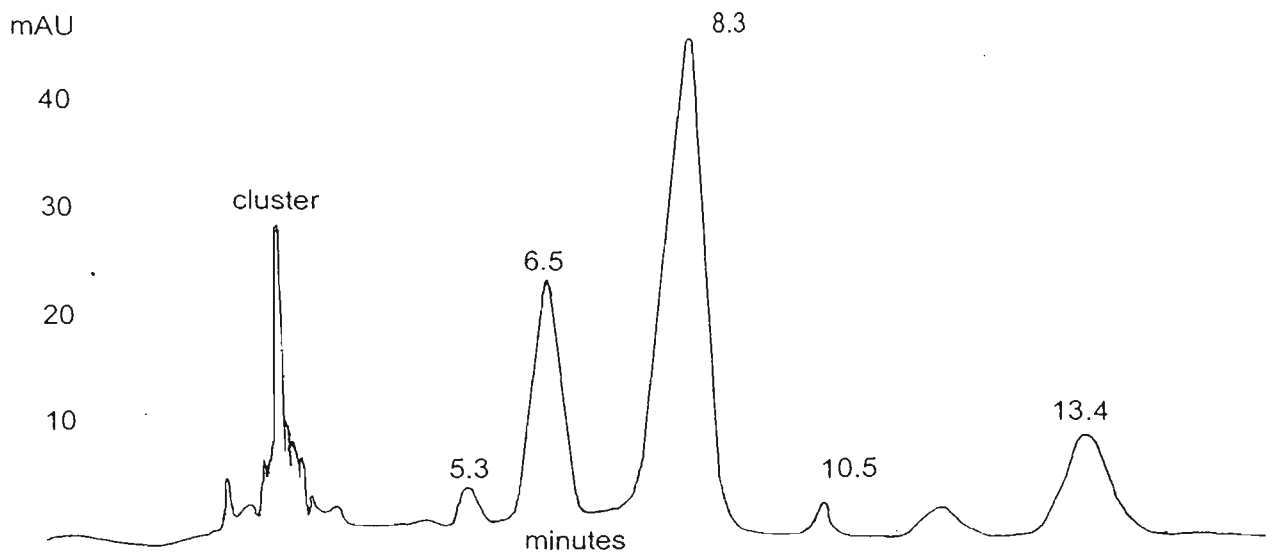


Figure 5.7 Changes in HPLC profiles of sultana MeOH extracts.  
 Top: pre-storage, middle: after 10 months storage at 30°C with oxygen and bottom: after 10 months 30°C no oxygen

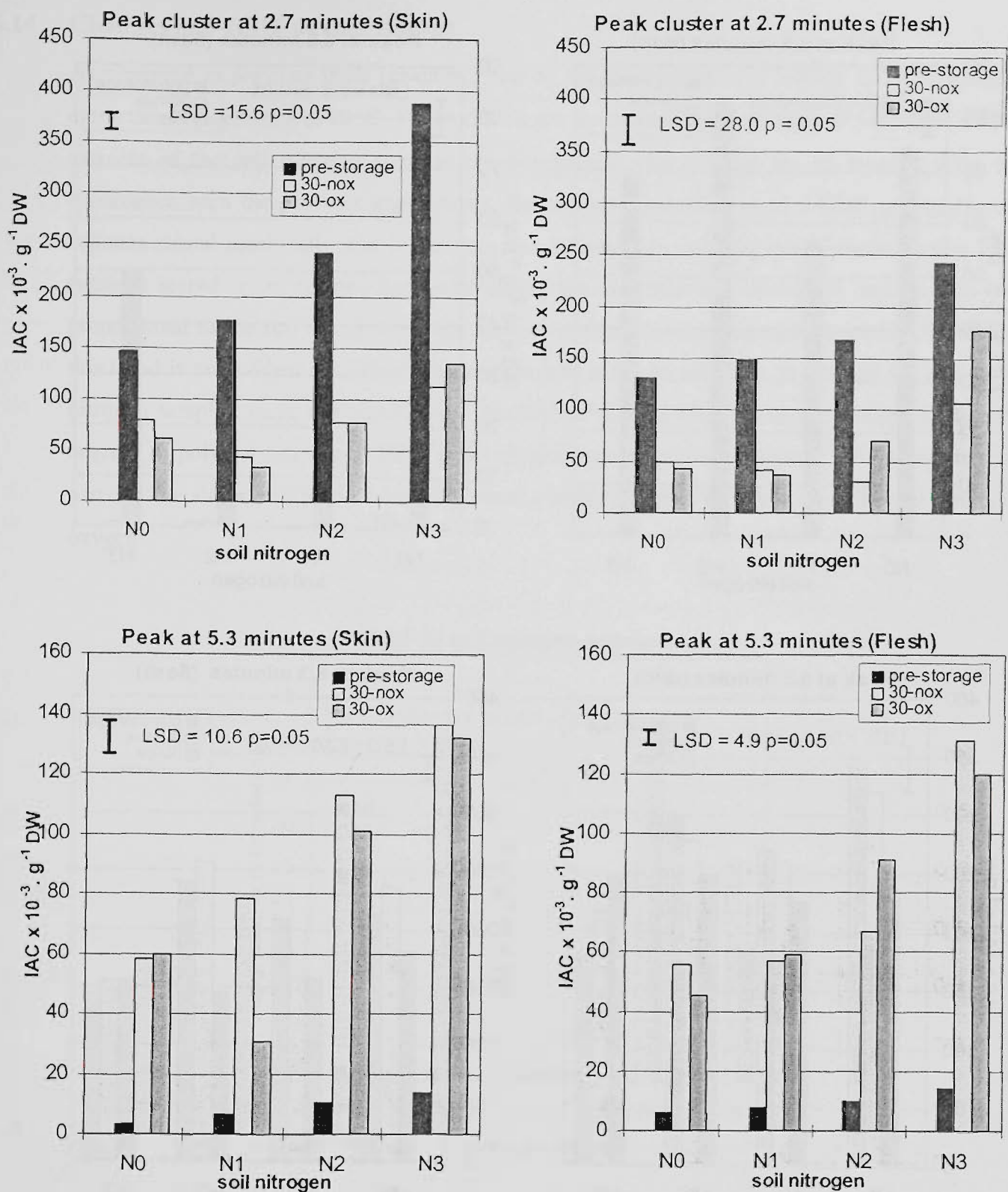
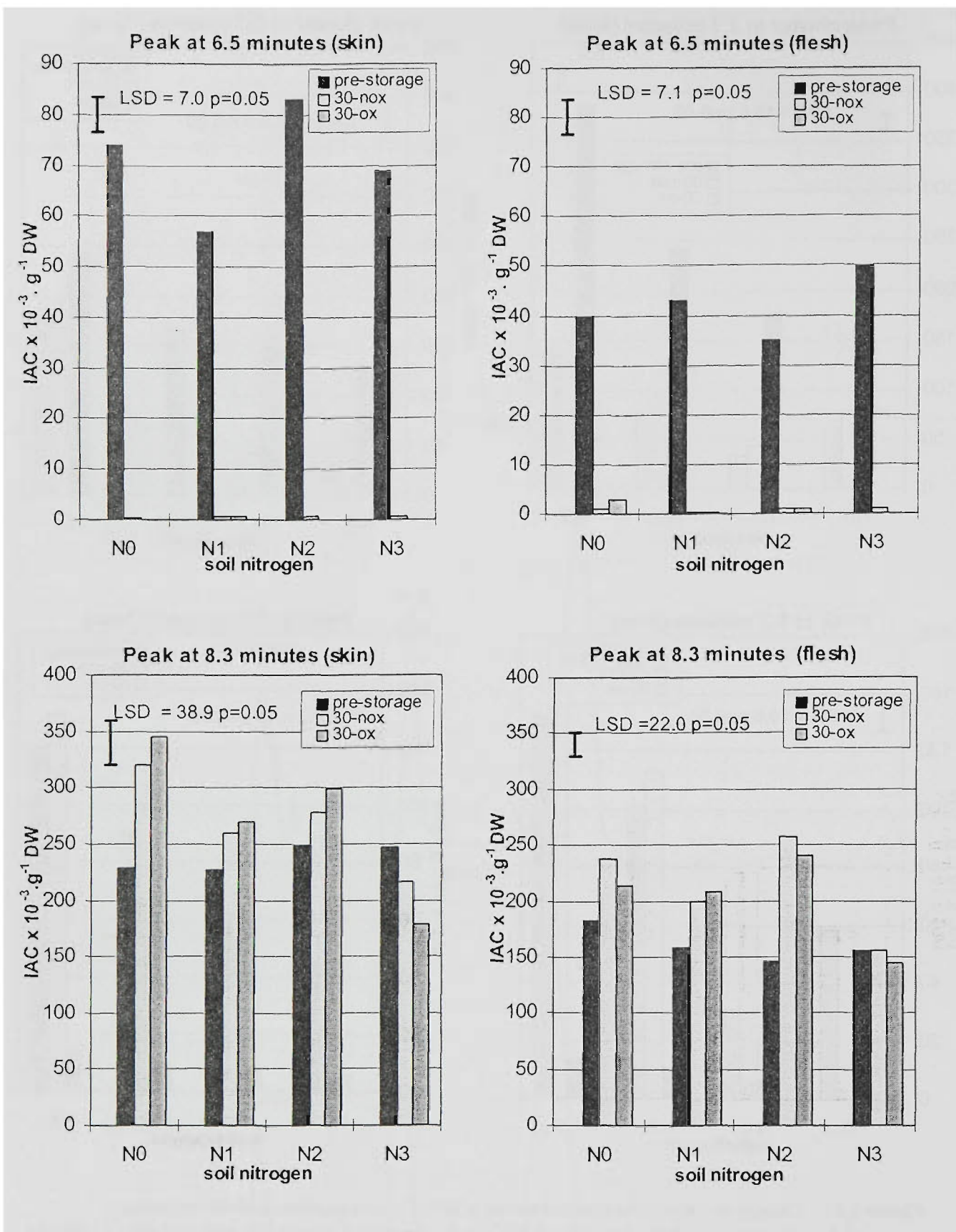


Figure 5.8 Change in the relative concentrations of HPLC peaks in sultana MeOH extracts. Pre-storage, after 10 months at 30°C in the absence of oxygen (30-nox) and after 10 months storage at 30°C in the presence of oxygen (30-ox). Top: peak cluster eluting at around 2.7 min. Bottom: peak eluting at 5.3 min. Relative concentrations of peaks are expressed as integrated area counts/1000 ( $IAC \times 10^{-3} \cdot g^{-1} DW$ ). Each value was the mean of two determinations on two sub-samples of 25 sultanas. LSD values were determined for the effects of nitrogen  $\times$  oxygen  $\times$  time using ANOVA.



**Figure 5.8** (Continued) Change in the relative concentrations of HPLC peaks in sultana MeOH extracts Pre-storage, after 10 months at 30 °C in the absence of oxygen (30-nox) and after 10 months storage at 30 °C in the presence of oxygen (30-ox). Top: peak eluting at 6.5 min. (5-HMF). Bottom: peak eluting at 8.3 min. (*trans*-caftaric acid). Relative concentrations of peaks are expressed as integrated area counts/1000 ( $IAC \times 10^{-3} \cdot g^{-1} DW$ ). Each value was the mean of two determinations of two sub-samples of 25 sultanas. LSD values were determined for the effects of nitrogen  $\times$  oxygen  $\times$  time.

## 5.14 Changes in 5-HMF during storage

As observed in previous trials (chapter 2 and 4), the concentration of 5-HMF in DCM sultana extracts increased only at 30°C. Figure 5.9 shows the relative concentration of 5-HMF in DCM extracts of the soil nitrogen sultanas pre-storage and after storage for 10 months. Also in accordance with the previous experiments, the relative concentration of 5-HMF in extracts of sultanas stored aerobically was lower than that measured in sultanas stored anaerobically. For sultanas stored in an oxygen-free environment the concentration of 5-HMF appeared to be proportional to the soil nitrogen content and pre-storage free-arginine concentrations. Although this trend is not evident in sultanas stored in oxygen it can be seen that, at least for the high soil nitrogen samples, there was significantly less 5-HMF present after 10 months storage. Different degrees of polymerisation of 5-HMF in an oxygen-exposed environment may have accounted in part for the slightly different rates of browning in 30°C stored fruit, compared to that without oxygen.

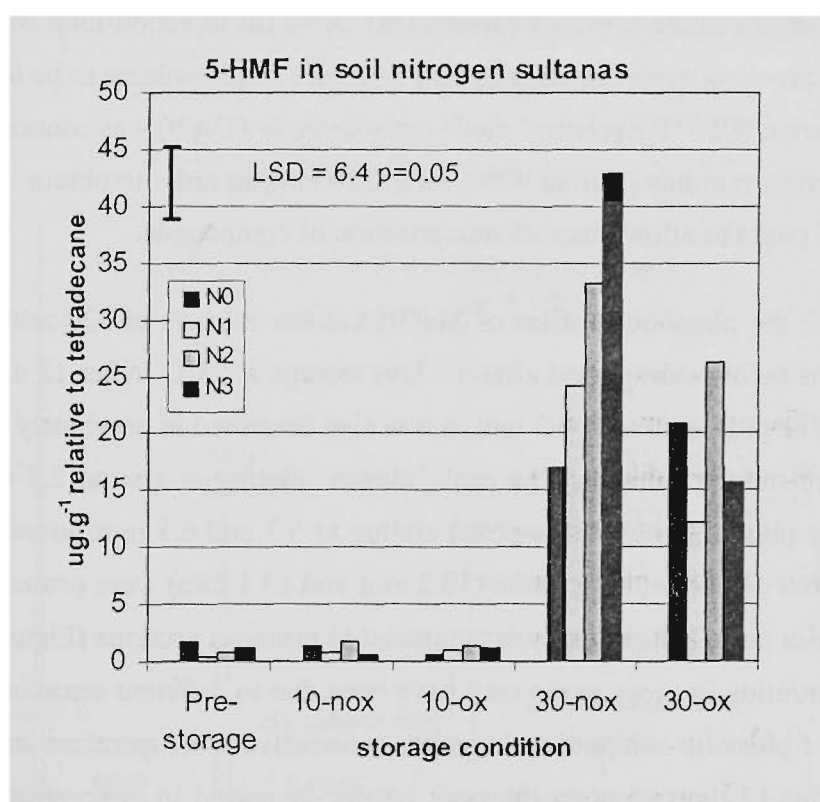


*Figure 5.9* 5-HMF measured in DCM extracts of the soil nitrogen sultanas pre-storage and after 10 months storage. 10°C no oxygen (10-nox), 10°C + oxygen (10-ox), 30°C no oxygen (30-nox) and 30°C + oxygen (30-ox). LSD was determined using the mean of the determinations on the two subsamples of sultanas for the interaction of nitrogen × oxygen × temperature.

## 5.15 Conformation experiment

In the above and previous sections it was assumed that the large peak dominating chromatograms ( $t_R$  8.3 min.) was *trans*-caftaric acid and that the peak cluster (2.7 min.) and the peak eluting at 5.3 min. were of Maillard origin. The finding that there was no significant decrease in the relative concentration of the putative major grape phenolic browning substrate—even after storage for 10 months at 30°C in the presence of oxygen—would seem difficult to support without any further confirmatory evidence. To confirm the previous findings, two lots (200 g) of light-amber dipped sultanas ( $a_w$  0.48) were sourced from packing sheds (1999/2000 season). Both samples were stored under ‘accelerated’ browning conditions: 12 days at 55°C in a Memmert® thermostatically controlled heating cabinet at VUT. Sultanas were removed after 3, 6 and 12 days storage at this temperature. After 6 days storage the sultanas had undergone appreciable browning and after 12 days they were dark brown. A 25-gram sample of every sultana sample was prepared for HPLC analysis in a similar manner as in the previous section. However the final extract volume of samples was made up to 10 mL and only one extraction step was performed (*cf.* 30 mL and multiple extractions in the previous experiment). A 50  $\mu$ L injection-loop was used instead of the 20  $\mu$ L used in previous experiments, allowing a larger sample volume to be loaded onto the HPLC column. A Varian 9065 ‘Polychrom’ diode array detector (DAD) was connected in series with the single wavelength monitor (Varian 9050, set at 320 nm), in order to obtain individual UV spectra for the HPLC peaks to allow quasi-characterisation of compounds.

In Figure 5.10 the phenolic profiles of MeOH sultana extracts at 320 nm are shown for light-amber sultanas before storage and after 12 days storage at 55°C. After 12 days the sultanas were dark brown. The peak eluting at 8.3 min as was also described in previously dominated the HPLC profiles of pre-storage sultanas. The peak ‘cluster’ eluting at around 2.7 min., also previously observed, was present, as were the peaks eluting at 5.3 and 6.5 min. In addition to these major peaks, a number of later eluting peaks (10.2 min and 13.1 min) were present in relatively higher concentration in these sultana extracts compared to previous sections (Figure 5.7). The relatively higher concentration in these peaks may have been due to different seasonal conditions; the rate of synthesis of phenolic compounds in grapes is sensitive to temperature and UV factors as well as others. After 12 days storage, the peak cluster increased in concentration, and a new peak appeared at 4.1 min. The previously described peaks eluting at 5.3 and 6.5 min. were also present. In contrast, the concentration of the peaks at 8.3 min, 10.2 min. and 13.1 min. did not decrease compared to their pre-storage concentration. The same phenomenon was measured on both sets of sultanas. In Figure 5.12 the relative concentration of each of the peaks measured at intervals over the 12 days storage period are shown graphically. It can be seen that whilst the peak ‘cluster’, the peak at 4.1 min. and the peak at 5.3 min. and the peak at 6.5 min. all increased, the relative concentration of other peaks did not change to any extent. The peak eluting at 5.3 min had been observed in the previous experiments to increase significantly over time. The peak tentatively identified as *trans*-caftaric acid was again shown not to decrease over time.

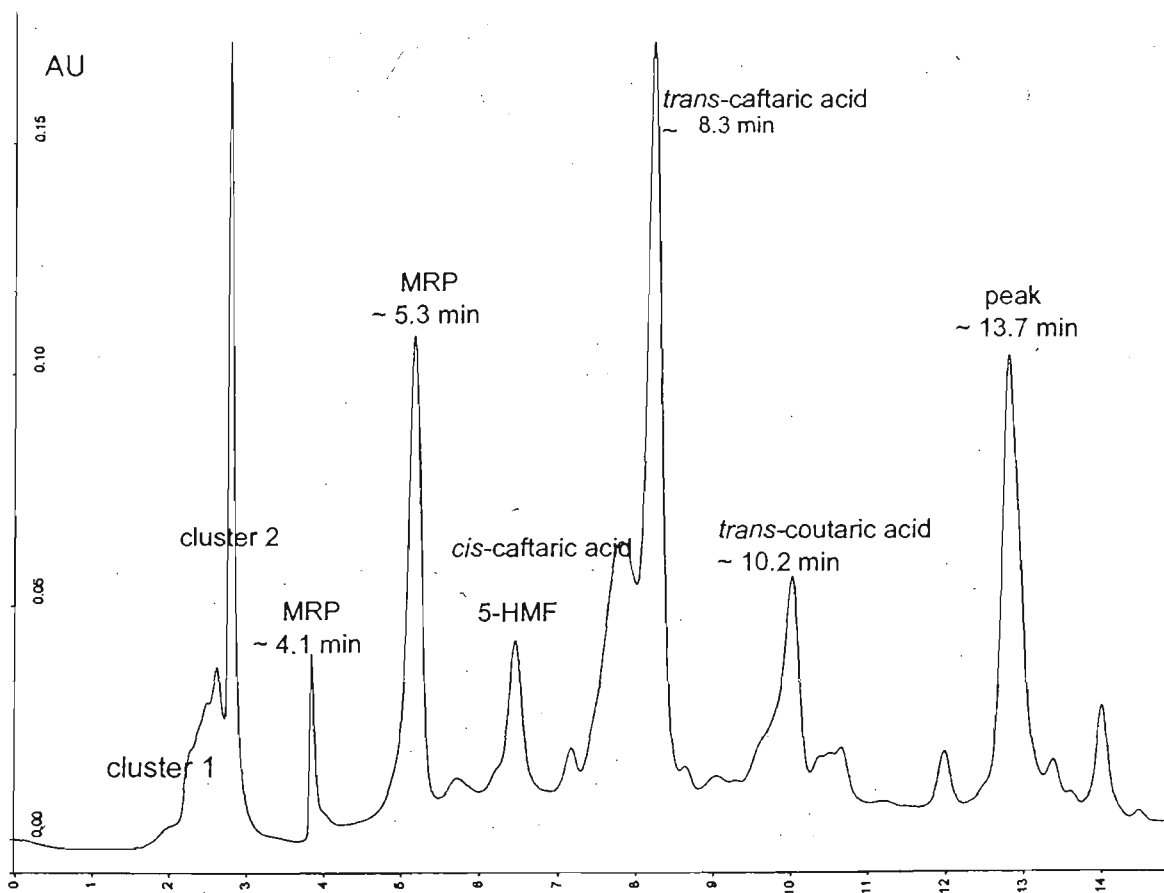
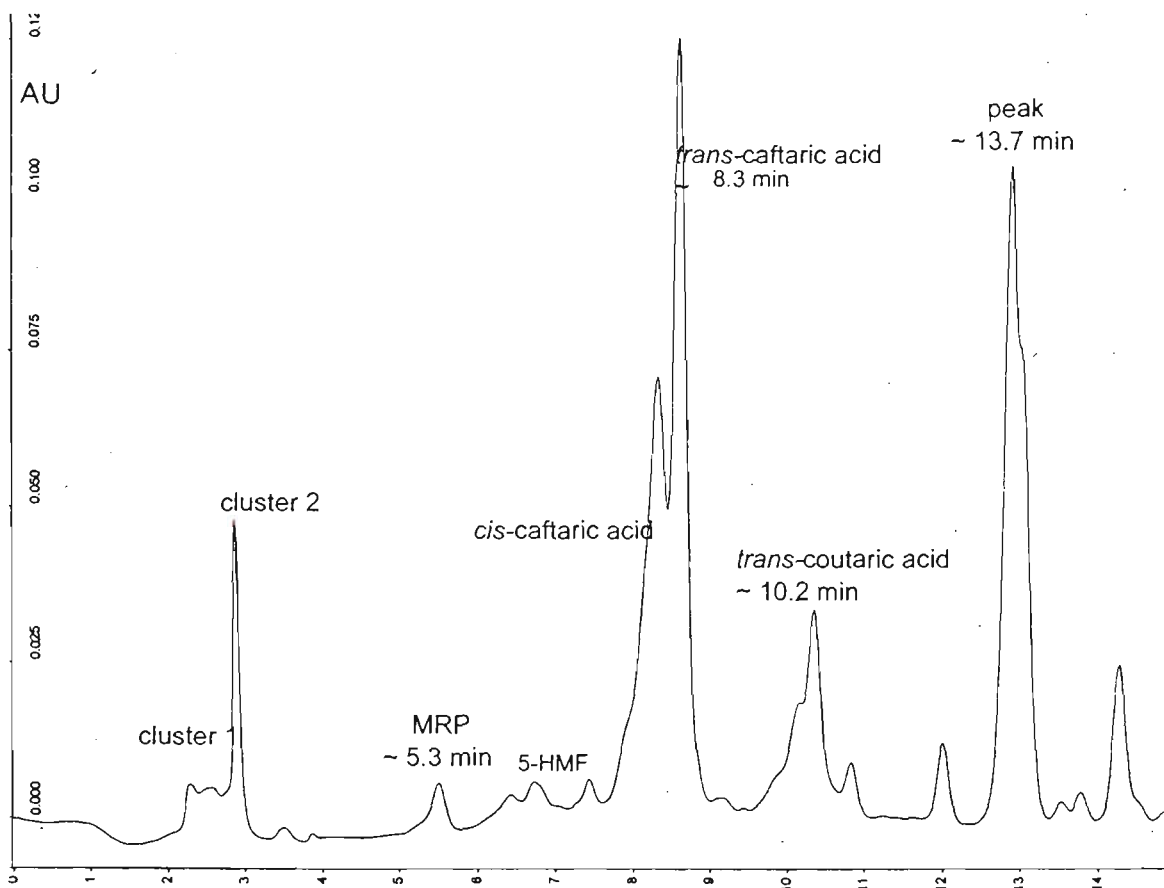


Figure 5.10 HPLC profiles at 320 nm of MeOH sultana extract before storage (top) and after storage for 12 days at 55°C

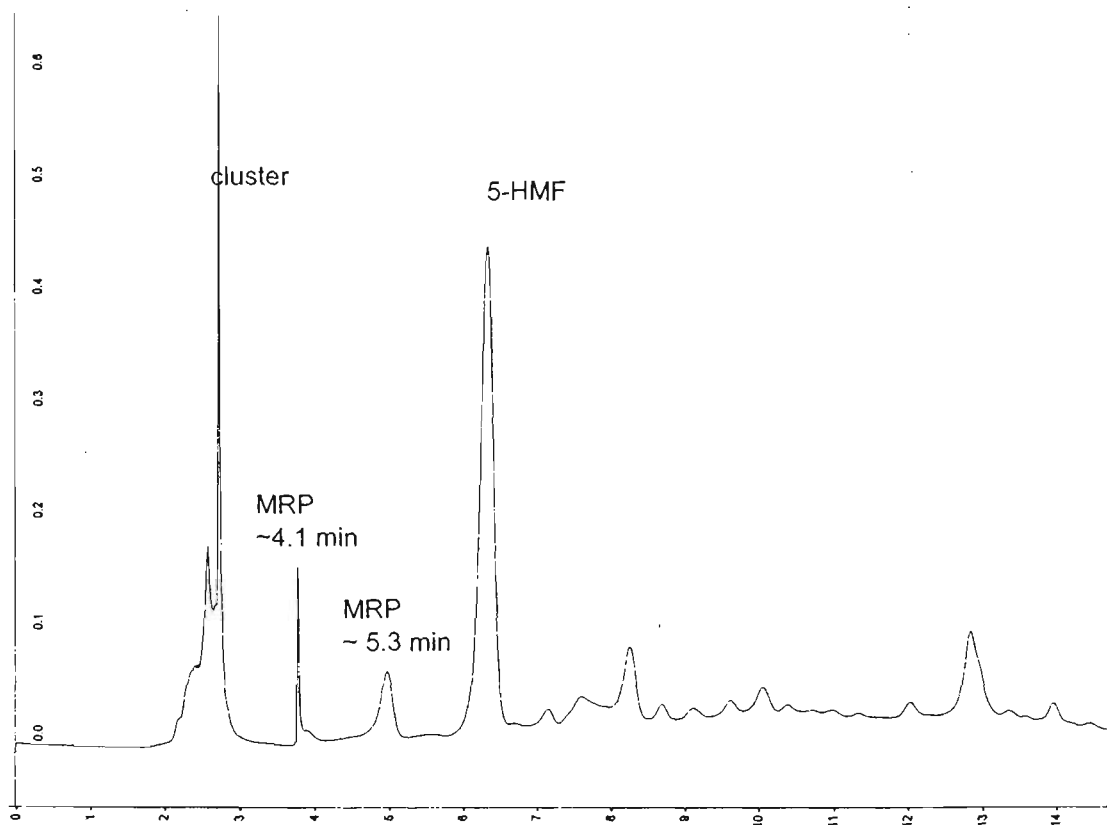


Figure 5.11 HPLC profile at 280 nm of a typical MeOH sultana extract.  
 Note peak at 8.3 min is barely visible at 280 nm, and 5-HMF is the dominant peak (6.5 min).

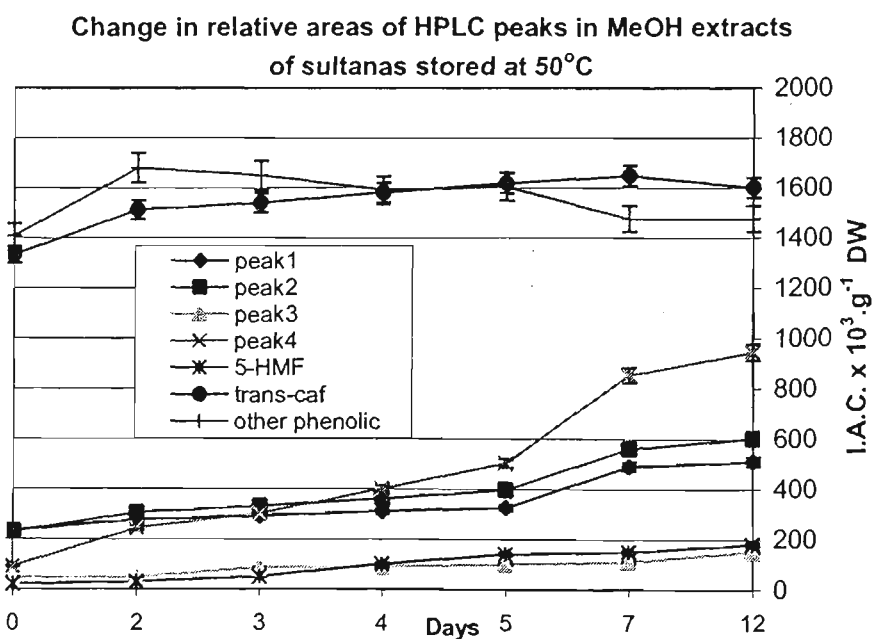


Figure 5.12 Areas of the major compounds evolving in MeOH extracts of sultanas stored at 55°C over 12 days. Peak 1 and 2 are 'cluster 1' and 'cluster 2' respectively, peak 3 is the peak eluting at 4.1 min and peak 4 is the peak eluting at 5.3 min., 5-HMF is the peak for 5-hydroxymethyl-furfural, trans-caf for the peak eluting at 8.3 min, tentatively identified as trans-caftaric acid and other phenolic for the peak eluting at 13.1 min. Every value is the mean of 3 HPLC determinations for an extract of 25g of sultanas. Error bars are the SD of the triplicate determinations.

In addition to the sultana MeOH extracts, fresh Sultana grape MeOH extracts were also prepared and run under the same conditions. The grape extracts had a large peak eluting at 8.3 min., a small coeluting peak at 8.2 min., a peak at 10.2 min. and a peak at 13.1 min. (chromatogram not shown). In addition there was a cluster of peaks at 2.7 min. and a small isolated peak at 4.2 min. The grape extract was left for 4 days at ambient temperature and then subjected to HPLC analysis (chromatogram not shown). Although the MeOH extract had apparently not undergone any noticeable browning, the three later eluting peaks had almost disappeared from HPLC profiles, indicating that they were oxygen sensitive and hence in accordance with the assumption that the compounds in question were phenolics. In contrast, the peaks at 2.7 min. and 4.2 min. did not change in concentration.

The UV spectra for the putative *trans*-caftaric acid, the peak eluting slightly before the former (8.2 min.), the peaks eluting at 10.2 min. and 13.1 min. from both fresh grapes and sultanas are shown in Figure 5.13 and Figure 5.14.

The peak eluting at 8.3 min. and the peak eluting slightly before (8.2 min.) had almost identical UV spectra, and the grape and sultana UV spectra were also almost identical. Both spectra had a maximum absorption ( $\lambda$  max) at approximately 328 nm, a shoulder peak at approximately 290 nm and a minimum ( $\lambda$  min) at approximately 260 nm. There was also high absorbance at approximately 215 nm. After 12 days of sultana storage at 55 °C, despite considerable browning, the UV spectrum of this peak had not changed, compared to the fresh grape spectrum.

The spectral characteristics of this peak at 8.3 min. were compared to reports in the literature. The UV data were consistent with those reported by Somers *et al.* 1987 and Singleton *et al.* 1978 for *trans*-caftaric acid. Somers *et al.* (1987) described a  $\lambda$  max at 329 nm, with a medium intensity shoulder at  $\lambda$  301 nm and a  $\lambda$  min at 263 nm for *trans*-caftaric acid in 10% aqueous ethanol. Singleton *et al.* 1978 described the *trans*-caftaric peak with a  $\lambda$  max at 325 nm and 217 nm in water. After consideration of this data it was assumed that the peak eluting at 8.3 min. on the chromatograms was in fact *trans*-caftaric acid. Cheynier *et al.* (1986) showed the UV spectrum of 2-*S*-glutathionylcaftaric acid (GRP) compared to that of *trans*-caftaric acid. On the UV-spectrum of the former compound there is a shift in the position of  $\lambda$ -max to 324 nm and a clear shift in the position of  $\lambda$ -min to around 280 nm. In addition, GRP eluted more than a minute after *trans*-caftaric acid. None of the sultana peaks were consistent with GRP, further indicating that *trans*-caftaric acid was unlikely to have undergone reaction at any stage in the drying or storage period.

The UV spectra for the peaks eluting 10.2 min. in grapes and sultanas are shown in Figure 5.14. The grape peak had a  $\lambda$  max at 313.6 nm a  $\lambda$  min at ~250 nm and another  $\lambda$  max at 230.8 nm. In sultanas the UV spectra were similar:  $\lambda$  max at 315.5 nm, and  $\lambda$  min approximately 250 nm. The

UV spectrum differed to that from the fresh grape in that there was high absorbance at around  $\lambda$  220 nm and a medium intensity shoulder apparent at around 285 nm. The spectral differences relative to the fresh grape could be interpreted as either indicating some kind of subtle chemical change that may have occurred during drying, or that the higher absorption at approximately 220 nm was due to the higher glucose concentration in these samples. Glucose and glucose degradation products absorb strongly in this spectral region. The shoulder may have become more pronounced simply due to a concentration effect. In any case, if substantial oxidation of phenolics had taken place, a large shift in the UV  $\lambda$  max at 314 nm would have been observed; as this was not the case, it was assumed that the phenolic in question had not undergone substantial oxidation in the grape to sultana transition. After 12 days storage, the UV spectrum for this peak remained essentially unchanged:  $\lambda$  max 314.4 nm and 220 nm and  $\lambda$  min 250 nm. Somers *et al.* (1987) reported similar UV spectral data for the *trans*-isomer of *p*-coumaroyl tartaric acid  $\lambda$  max 315 nm,  $\lambda$  min 250 nm with no shoulders on peaks. This peak also eluted after *trans*-caftaric acid on the chromatograms described in Somer's paper. It is reasonable to assume that this peak was *trans-p*-coumaroyl tartaric acid.

The peak eluting at 13.1 min (Figure 5.14) did not have UV spectral characteristics which were consistent with those described for other white grape phenolics in the literature (Ong and Nagel 1978, Singleton *et al.* 1978, Somers *et al.* 1987). The UV spectrum was characterised by a  $\lambda$  max at approximately 220 nm, 255.2 nm and 355.5 nm and a  $\lambda$  min at 280 nm. In pre-storage sultana MeOH extracts the UV spectrum was essentially the same:  $\lambda$  max approximately 220 nm, 255.9 nm and 355.2 nm and  $\lambda$  min 280 nm. After 12 days storage, the UV spectra appeared to have slightly changed:  $\lambda$  max approximately 220 nm, 252.5 nm and 354.9 nm and  $\lambda$  min 280 nm. The relative concentration of these peaks, however, did not decrease compared to their initial values, indicating that extensive oxidation had not taken place. Escarpa and González (1998) reported the UV absorption spectra of series of flavonol glycosides from apple skins with  $\lambda$  max 255.3 nm and  $\lambda$  max 357.6 nm. It is likely that this peak was a flavonol glycoside; such compounds are known to be present in white grapes (Spanos and Wrolstad 1990).

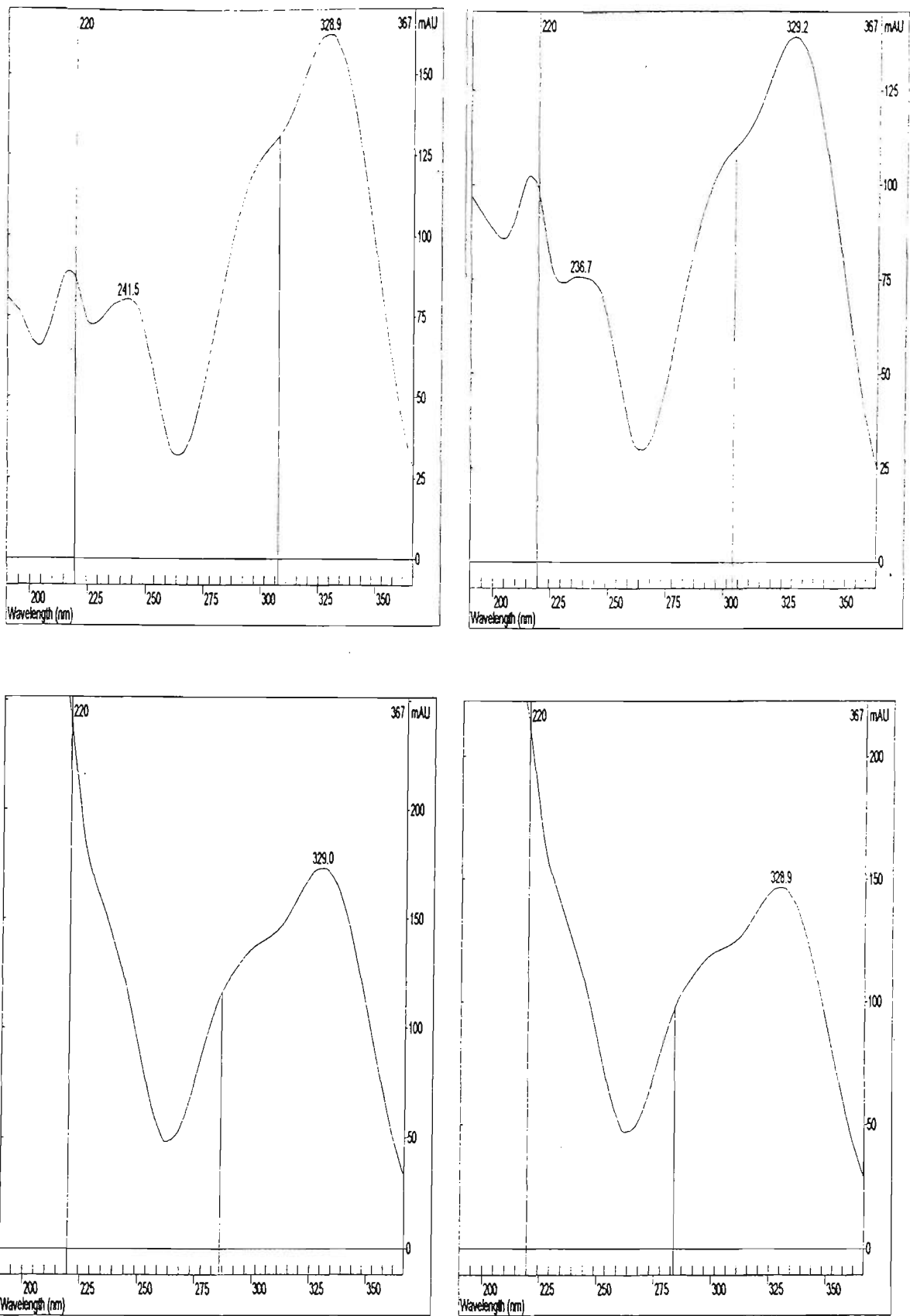


Figure 5.13 Diode array UV-spectra of peaks eluting at 8.2 min. (top) and 8.3 min. (bottom) in MeOH extracts.  
 Left: fresh Sultana grapes. Right: sultanas after storage at 55°C for 12 days. The peak at 8.2 was consistent with *cis*-caftaric acid and the peak at approximately 8.3 min. consistent with *trans*-caftaric acid.

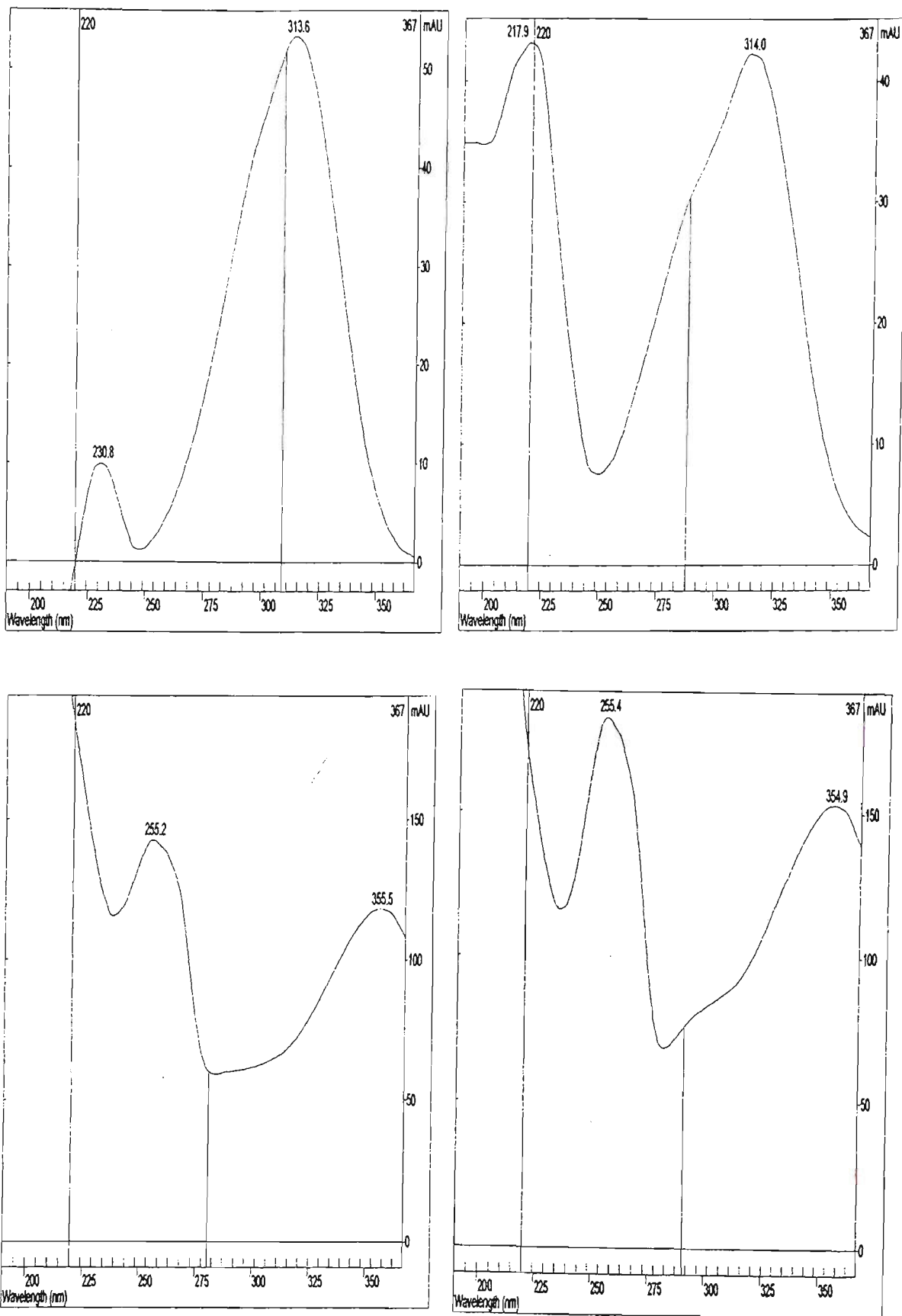


Figure 5.14 Diode array UV-spectra of peaks eluting at 10.2 min. (top) and 13.07 min. (bottom) in MeOH extracts. Left: fresh Sultana grapes. Right: sultanas after storage at 55°C for 12 days. The peak at 10.2 min. was tentatively identified as *trans-p-coumaroyl tartaric acid*. The compound eluting at 13.1 min. was not identified.

## 5.16 Maillard reaction products

To test the hypothesis that the peaks eluting at approximately 2.7 and 5.3 min. were of Maillard origin, model arginine-D-glucose Maillard browning solution material was diluted in Milli-Q water and run through the HPLC and DAD under the same conditions as sultana and grape extracts. The Maillard model solution was made up as follows. D-glucose (200 g AnalaR) was made into a thick paste with the addition of Milli-Q water (~200 mL). Arginine (Sigma-Aldrich, Australia) was added at a concentration of  $10 \text{ mg.g}^{-1}$  and iron was added in the form of  $\text{FeCl}_2 \cdot \text{H}_2\text{O}$  (BDH Chemicals) to give a final concentration of  $10 \text{ }\mu\text{g.g}^{-1}$ . After thorough mixing, the solution was stored in a Schott bottle at  $60^\circ\text{C}$  in an oven for 5 days. Samples were removed when the solution was light orange-brown (2 days), dark red-brown (4 days) and dark brown (5 days). A  $500 \text{ }\mu\text{L}$  aliquot was diluted in 10 mL of Milli-Q water and injected onto the HPLC column. The HPLC profiles of typical Maillard arginine-glucose model system at 320 nm and 280 nm are shown in Figure 5.15.

At 320 nm (top) the HPLC profile was dominated by three main peaks: a cluster of peaks eluting at approximately 2.7 min., a single peak eluting at 4.1 min. and a peak at 5.3 min. There were also various trace levels of peaks eluting up until 8 min. The peak 'cluster' actually appeared to be partially resolved into two separate groups of peaks, very similar to the shape of the cluster observed in grape and sultana samples. The shapes and retention times of the peaks matched exactly with the peaks from grape and sultana extracts. In order to eliminate the possibility that the peaks were solvent artefact peaks or due to ascorbic acid, free-arginine or D-glucose, pure, diluted samples of each of these compounds were run under the same conditions. None of these compounds absorbed strongly at 320 nm, hence it was established that the peaks were *bona fide* Maillard reaction products.

The UV spectrum of the peak eluting at approximately 5.3 min. was identical in both sultana and model systems (Figure 5.16) The peak was symmetrical with a  $\lambda \text{ max}$  at 295 to 296.5 nm and a  $\lambda \text{ min}$  at ~240 nm. There was also some absorption  $< 220 \text{ nm}$  with a shoulder at approximately 210 nm. The intensity of the shoulder peak varied both within different sultana samples and model samples, however the  $\lambda \text{ max}$  at approximately 295 was remarkably consistent, indicating that the product was a Maillard reaction intermediate of reasonable purity.

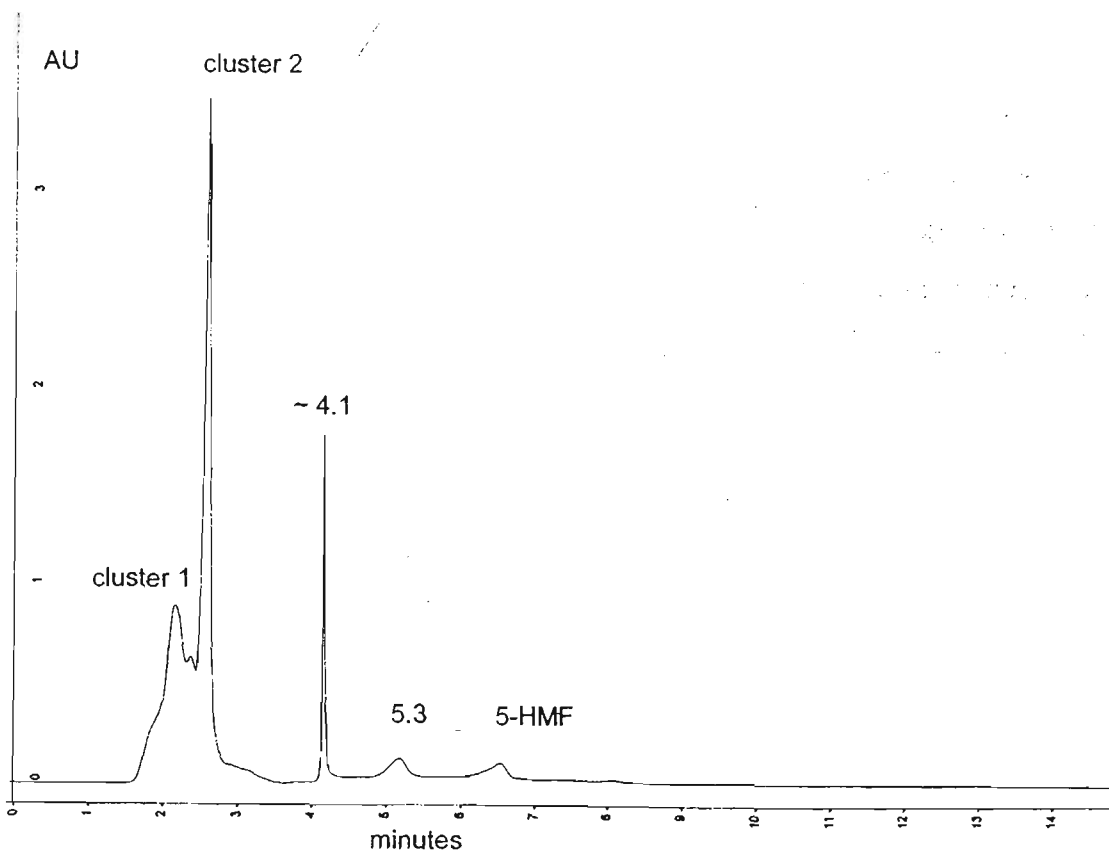
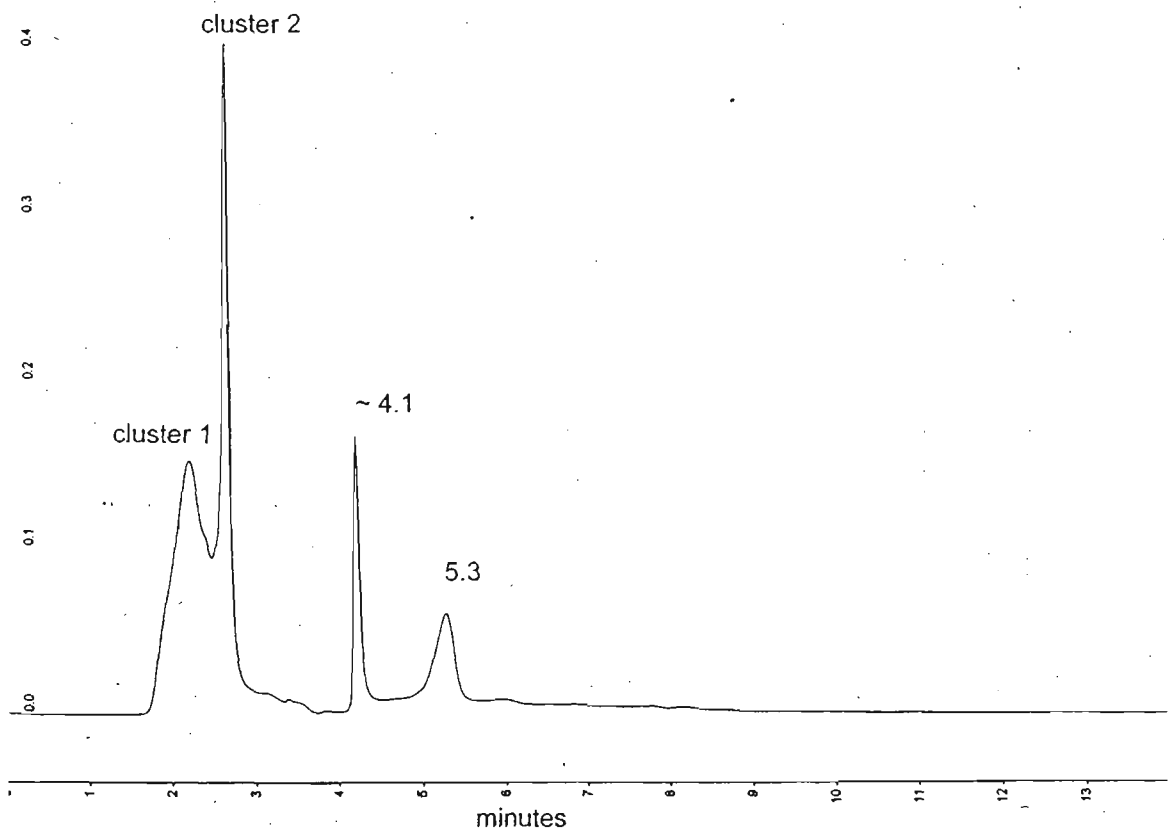


Figure 5.15 Typical HPLC profile of arginine-glucose model system.  
 Top: profile at 320 nm. Bottom: profile at 280 nm.

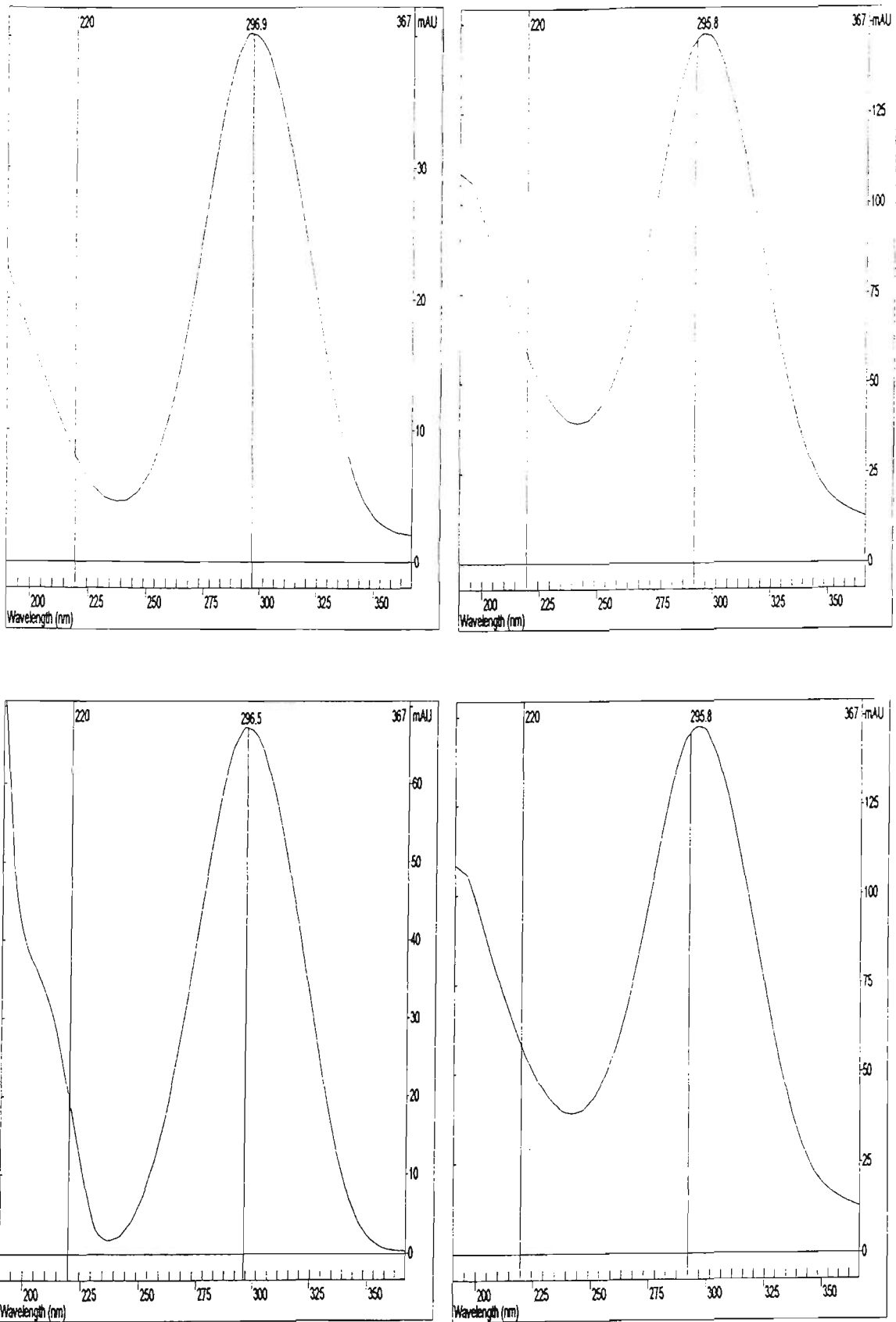


Figure 5.16 UV spectrum of Maillard peak eluting at 5.3 min.  
 Top: from arginine-glucose Maillard model systems. Bottom: from sultana extracts.

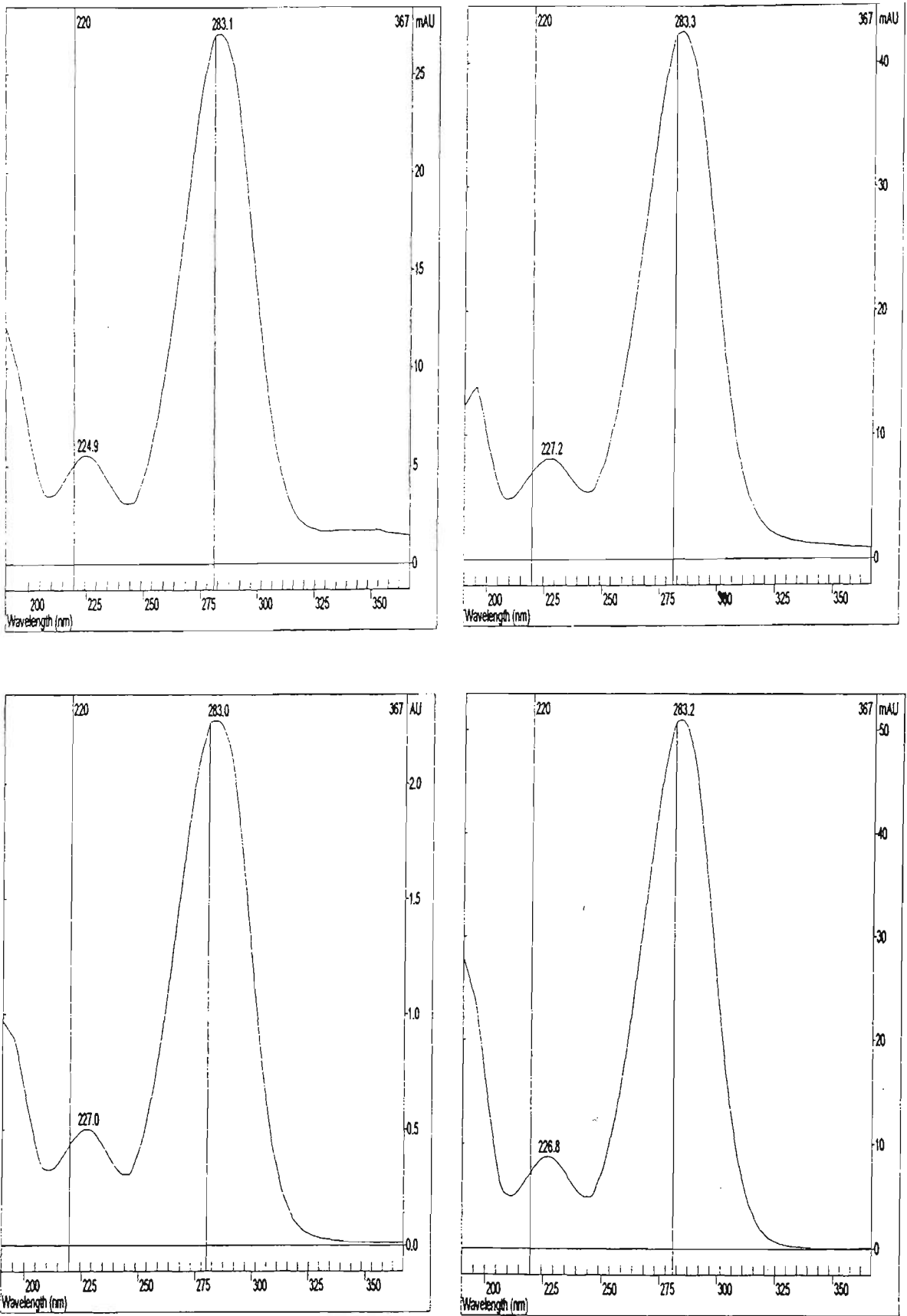


Figure 5.17 UV-spectra for the peak eluting at 6.5 min. (5-Hydroxymethyl furfural).  
 Top: from sultana extracts. Bottom (left): from Maillard model system. Bottom (right): 5-HMF standard (Sigma Chemical company).

	Peak 'cluster' 1				Peak 'cluster' 2			Between		Peak 3 ~ 4.1min	
	1	2	3	4	1	2	3	after	before	1	2
S initial	272	266	250	242	241	220	220	238	220	271	277
S initial	269	261	243	243	242	220	220	220	220	265	271
S 2days	273	267	257	242	242	238	220	241	265	270	285
S 5 days	273	267	242	240	242	237	220	239	259	269	282
S 5 days	274	262	242	242	242	240	242	242	239	275	286
S 7 days	274	263	242	241	242	239	220	237	247	281	288
S 7 days	288	264	242	242	243	220	220	236	246	261	291
S 12 days	291	288	242	244	243	232	282	239	294	292	291
S 12 days	290	271	241	241	242	220	220	237	250	279	282
M light	290	295	296	293	271	262	240	239	241	242	291
M light	297	295	296	241	265	265	244	242	241	244	291
M med	302	295	293	242	271	271	244	237	241	245	289
M med	291	292	295	275	247	249	244	242	243	241	291
M dark	291	292	242	241	249	249	241	241	241	289	291
M dark	274	262	242	242	242	240	241	242	238.9	275	286

Table 5.4  $\lambda$  max for the Maillard HPLC peaks.  
Peak 'cluster 1' was divided into 4 sections, the last peak in the cluster was divided into 3 parts and peak 3 was divided into 2 parts. S = sultana and M = Maillard model system.

Table 5.4 shows the  $\lambda$  max for UV spectra corresponding to the peaks in the 'cluster' and the peak eluting at approximately 4.1 min. The 'cluster' was divided into two sections: the earlier eluting wide peak ('cluster 1') and the later eluting peak ('cluster 2'). Because of the high variability of UV absorption in these peaks, each peak was divided into sections. The UV absorption  $\lambda$  max in the area after the cluster (between 'after' on table) peaks and before the peak eluting at 4.1 min (between 'before' on table) were also tabulated. Although the general peak shapes in both sultanas and models were often the same (see Figure 5.18 and Figure 5.19), there was considerable variation in the position(s) of maximum absorbance, both within sultana and model systems. Small differences in physico-chemical conditions at the various stages of the Maillard reaction can have a large affect on the rates of formation of the various browning precursors. Hence it was not surprising that there were some differences in UV data between model systems and sultana extracts. The sultana extracts also contained other matrix compounds (other than arginine-glucose MRPs), which may have co-eluted with the MRPs and absorbed in the UV region. Examination of the Table 5.4 shows that the absorption  $\lambda$  max had a tendency to move to a longer wavelength with increasing storage time and increased browning (12 days); nearly all models absorbed close to 290 nm. For the second part of peak cluster 1, the model

absorbed strongly at approximately 295 nm, whereas the  $\lambda$  max for sultana extracts was at a shorter wavelength. For the third position of the peak, the lighter model system extracts absorbed once again strongly at approximately 295 nm, however the darker model extracts had a  $\lambda$  max at 242 nm. Most sultana extracts also absorbed strongly at 242 nm. At position 4, within the first part of the cluster, all sultana extracts absorbed strongly at approximately 240-244 nm and nearly all model extracts had a  $\lambda$  max at the same wavelength.

The second part of the cluster was also divided into three sections. All sultana extracts had a  $\lambda$  max at 242 nm, whereas there was a considerable amount of variability within model peaks. At the edge of the cluster, both model and sultana systems generally had a characteristic  $\lambda$  max at approximately 240 nm. The peak eluting at approximately 4.1 min. had a similar appearance in both model and sultanas, however there was variability in the position of  $\lambda$  max.

On sultana HPLC-traces the peak eluting at approximately 6.5 min increased over time at 50°C storage. The UV spectrum of the peak is shown in Figure 5.17. The peak had maximum absorbance at  $\lambda$  283 nm and a small  $\lambda$  max at 229 nm. An authentic sample of 5-HMF (Sigma chemical company 99% purity), also run under the same conditions, eluted at that time (6.5 min). Its UV spectrum was almost identical with that in sultana extracts:  $\lambda$  max at 283.2 and a smaller  $\lambda$  max at 227 nm. Examination of HPLC profiles of the model system revealed that there was a small peak eluting at the position corresponding to the position of 5-HMF. The UV spectrum at this position was identical with that of 5-HMF, with a  $\lambda$  max at 283.2 and a smaller  $\lambda$  max at 227 nm. The UV absorption of 5-HMF was consistent with that reported by Bailey *et al.* 1998 ( $\lambda$  max 285 and 231 nm) and Ho *et al.* 1999 ( $\lambda$  max 283 nm; but no report of a second  $\lambda$  max). The peak eluting at this time in soil-nitrogen sultanas (Figure 5.7) was also identified as 5-HMF.

Although there was a high degree of similarity in HPLC profiles and UV data for model arginine-glucose systems and sultana extracts, the relative proportions of the peaks were sometimes different, especially in the case of 5-HMF (*cf* Fig 5.11 with Fig 5.15 bottom). The different  $a_w$ , pH and temperature conditions in the sultanas *viz* models would account for much of this difference. The sensitivity of Maillard reactions to  $a_w$ , relative concentration of reactants, pH and temperature is well known. The kinetics of formation and degradation of 5-HMF were apparently different in model systems compared to sultanas; this is discussed further in the next section.

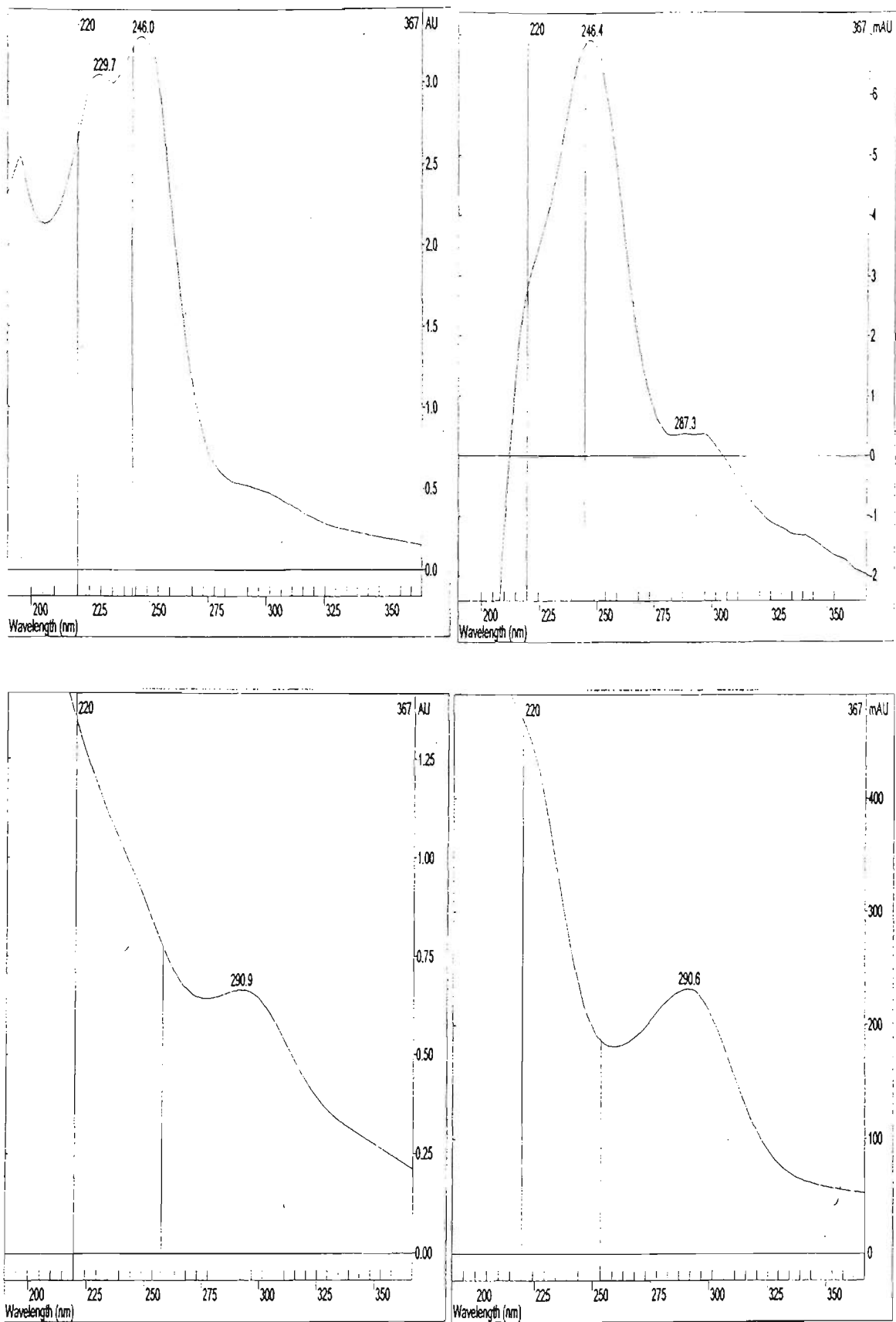


Figure 5.18 Characteristic UV spectra for the peak eluting at 4.1 min. (see Table 5.4). Top: spectrum of the first part of the peak: model (left) and sultana (right). Bottom: spectrum occurring in the second part of the peak: model (left) and sultana (right). Note that there was variation in the position of the shoulder peak at approximately 290 nm in both model and sultana extracts.

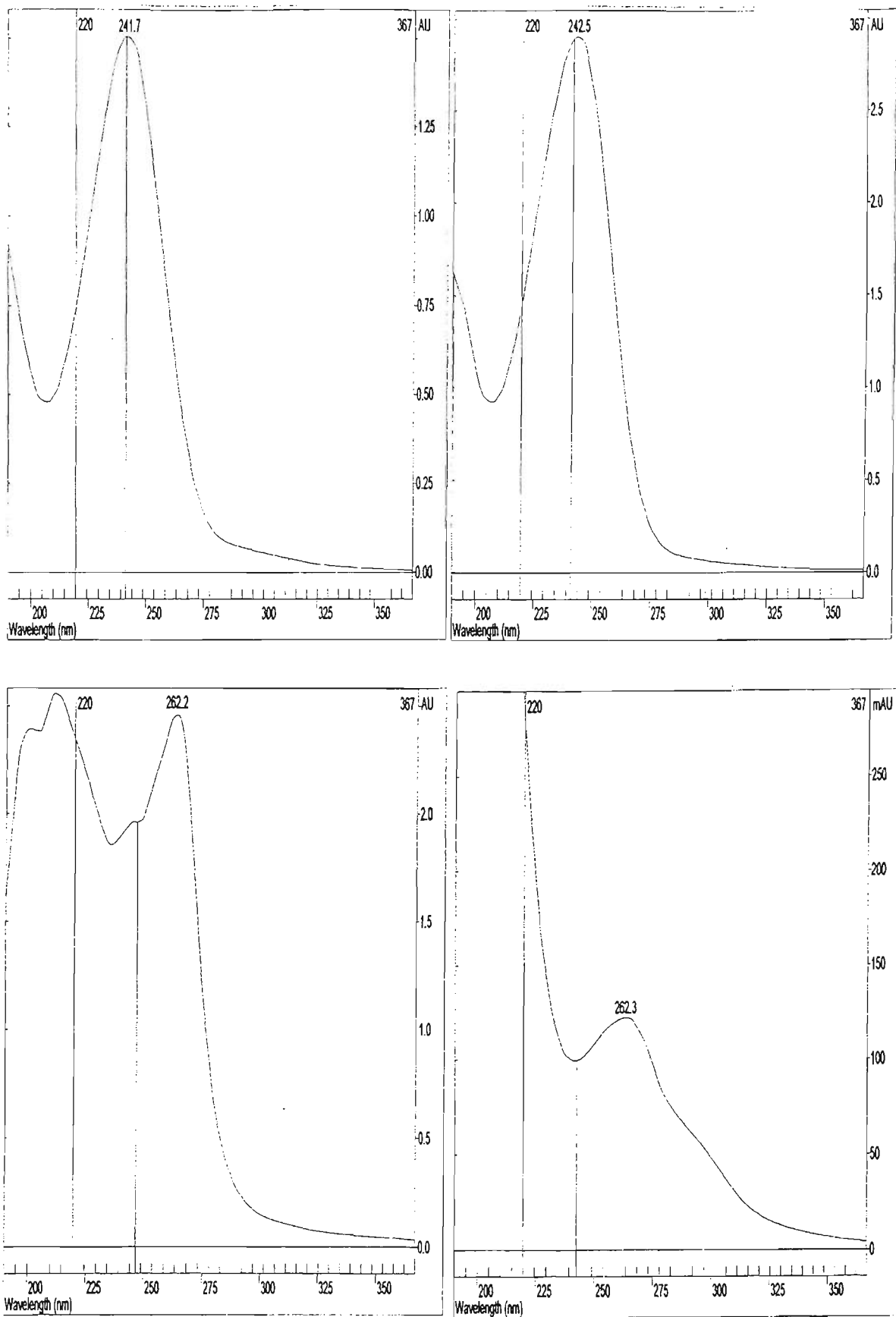


Figure 5.19 Typical UV spectra for characteristic peaks discussed in Table 5.4. Top: characteristic UV spectrum found in 'cluster 1 and 2' in model (left) and sultana (right). Note that the position of the  $\lambda$  max. varied from approximately 239 – 247 nm in both systems. Bottom: characteristic UV spectrum occurring in MRP peaks: model (left) and sultana (right). Note that there was large variation in the position of the shoulder peak at approximately 262 nm: the position of  $\lambda$  max varied from approximately 260 – 275 nm.

## 5.17 Discussion

HPLC analysis of initial phenolics indicated that the concentration of the peak identified as *trans*-caftaric acid was similar for all sultanas regardless of the soil nitrogen level. After storage at 30°C, in the presence and absence of oxygen, a significant increase in this compound was observed in all samples, except the highest soil nitrogen fruit, for which a decrease was observed. The increase may be explained by the loss of moisture from sultanas and relative concentration of this compound. After storage at 30°C, much of the sultana skin ultrastructural integrity would have degraded, possibly releasing phenolics. It was discussed previously that grape phenolics are compartmentalised in vacuoles mainly in the skins of healthy grape tissue. There is some indication in the literature that high soil nitrogen produces fruit with lower phenolics (Kliewer 1977 and Keller *et al.* 1999a). Kliewer (1977) conducted a comprehensive study of the effect of solar exposure and nitrogen on coloration of the red grape cultivar 'Emperor', and found a negative relationship between soil nitrogen and anthocyanin phenolic concentration in grapes. Kliewer suggested two reasons for lower anthocyanin phenolic levels: high soil nitrogen promotes vegetative growth and delays fruit maturation and thus synthesis of phenolics, or high soil nitrogen diverts synthetic activity towards nitrogen and grape protein synthesis at the expense of sugar accumulation and phenolic synthesis. Williams (1946) and Artyunayan *et al.* (1964) previously reported this general trend. Kliewer (1977) found a positive correlation between anthocyanin phenolics in grape skins and glucose in grape juice and Creasy *et al.* (1965) found that addition of glucose to strawberry leaf disks increased the synthesis of anthocyanins. Faust (1965) found that both sugar and anthocyanin synthesis was higher when chemical inhibitors were used to divert flux into the pentose phosphate pathway, away from amino acid synthesis. Hence the highest level of nitrogen administration may have resulted in suppression of phenolic synthesis, largely supported by the previous literature investigations. The relative decreases in this phenolic in the highest nitrogen sultanas may also have been due to an interaction occurring between Maillard reaction products and *trans*-caftaric acid. The reason decreases were observed only in these samples is unknown, however free radicals and reactive intermediates formed via Maillard reactions may have reacted with phenolics, especially when present at high concentration.

It is well known that high grape amino nitrogen, specifically high free L-proline and L-arginine mirror high soil nitrogen. Kliewer (1977) showed that the free-arginine concentration increased in 'Emperor' grapes with increased soil nitrogen, however the free-proline concentrations did not increase linearly with added soil nitrogen. Recently Keller *et al.* (1999) and Keller and Hrazdina (1999) examined the effects of soil nitrogen on grape growth and quality for *Cabernet Sauvignon*, and found that grape yield was affected by soil nitrogen and quality was determined more strongly by level of sun exposure. The same authors verified that high soil nitrogen retarded

synthesis of phenolics, however low light had a more critical effect on rates of phenolic accumulation. Näsholm and McDonald (1990) investigated nitrogen accumulation in birch seedling roots and leaves, and found that concentrations of citrulline, glutamine and arginine increased with soil nitrogen. Arginine has the highest nitrogen/carbon ratio of all the amino acids, making arginine a prime nitrogen storage compound. Stewart and Larher (1980) found that high concentrations of arginine are a common stress response in plants where nitrogen availability exceeds rate of usage and growth: this was found to be especially true when other soil nutrients such as phosphorus were growth limiting (Rabe and Lovatt 1986).

Other pre-storage chemical parameters measured in the sultanas did not indicate a natural predisposition towards higher browning. Although slightly lower levels of pre-storage substrate PPO was measured in the lowest soil nitrogen samples, in the light of HPLC phenolic data and the statistically minor role of oxygen played during the storage trial, it was assumed that PPO played a minor role in the browning processes observed. An increase in the level of soil nitrogen application did not result in higher levels of the elements copper or iron in the sultana samples, with similar concentrations of both elements measured in each of the sultanas. It was interesting that the copper concentration was higher ( $20.5\text{-}25.5\ \mu\text{g.g}^{-1}$ ) in these sultanas compared to sultanas in the previous trial ( $5.64\text{-}9.45\ \mu\text{g.g}^{-1}$ ). Despite the large difference in copper concentrations, the substrate PPO activity was comparable in both sets of sultanas. Mayer (1987) indicated that the bioavailability of soil copper had an important effect on the synthesis and absolute activity of functional PPO in plants because copper atoms are an essential component of the PPO active site. From the data in this and the previous section it would seem that soil copper content had no bearing on final PPO activity in sultanas. The concentration of iron in contrast was comparable for both groups of sultanas. It should be noted that the copper and iron determinations were performed on both groups of sultanas at the same time; hence the differences in copper measured were unlikely to be due to instrumental or analytical error. Copper and particularly iron are both known to have a profound effect on the rate of Maillard browning reactions (Yaylayan and Huyghues-Despointes 1994) and autoxidation of phenolics (Valero 1988). It was important to check for any differences in the concentrations of these elements, as a higher concentration may have pre-disposed sultanas to more rapid browning.

Pre-storage  $a_w$  values were similar for the sultanas and were all under  $a_w$  0.5. In the preceding chapters, the important effect of  $a_w$  on browning was observed. The  $a_w$  values were slightly higher than the  $a_w$  values of sunfinished fruit used in the previous trials, however well under the typical values of non-sunfinished sultanas. The skin free-arginine and KP concentrations measured in the highest soil nitrogen samples (approximately  $7.5\ \text{mg.g}^{-1}$  and  $36\ \text{mg.g}^{-1}$  respectively) were higher than comparable concentrations in the preceding chapter. The other nitrogen samples had, however, comparable concentrations of both free-arginine and KP to the

sultanas used in the 1995 and 1996 storage trials. The second highest nitrogen administration ( $N_2$ ) was rated as adequate to high. Substantial browning occurred in these samples indicating that a lower level of soil nitrogen administration would be a means to lighter sultanas; however lower soil nitrogen may have a negative effect on sultana yield.

This soil nitrogen storage experiment showed that significant decreases in the tristimulus  $L^*a^*b^*$  data were only observed in sultanas stored at 30°C. The temperature dependence of browning, also observed in previous trials, strongly indicated that Maillard browning was the major route to browning in these samples. PPO mediated and phenolic autoxidation browning occur readily at low temperatures, i.e. 10°C. PPO type browning is known to occur in grapes damaged during frozen storage. The fact that little browning was observed at 10°C, would preclude PPO processes as a major contributor to storage browning.

Analysis of the phenolic profiles of sultanas using DAD analysis provided strong evidence that very little if no oxidation of sultana phenolics occurred in these sultanas during the storage trial, regardless of the oxygen condition. It should be noted that some of the sultanas stored at 10°C (with and without oxygen) were also analysed (results not shown) and virtually no changes were observed in both phenolics or the MRP compared to pre-storage samples. These samples provided convincing evidence of the large role of Maillard browning processes during storage. The large agreement of many of the sultana extract peaks with arginine-glucose model extracts also further implicated arginine as the main amino acid in sultana browning reactions. The UV spectra of the Maillard model system are discussed further in the following.

A number of researchers have examined Maillard model systems using HPLC and UV detection (Bailey *et al.* 1996, Ames 1998, Royle *et al.* 1998, Monti *et al.* 1998 and Yaylayan and Kaminsky 1998). Although these authors did not examine arginine-glucose systems specifically, they found in general that specific amino acids resulted in both generic peaks and some amino acid-specific peaks. Yaylayan and Kaminsky (1998) reported some of the absorption maxima of glycine-glucose melanoidin polymers; polymer B1 was reported to have an absorption  $\lambda$  max at 295 nm and 209 nm and polymer B2 at 293 nm. Monti *et al.* (1998) reported the  $\lambda$  max for some unknown peaks from a lysine-glucose Maillard model system, which did not match any of the peaks found in sultanas or arginine-glucose model system extracts. Bailey *et al.* (1996) listed spectral characteristics of  $\lambda$  maxima for pure compounds commonly encountered in Maillard systems. Of the compounds listed, a number of low molecular weight retro-aldol sugar degradation products such as acrolein ( $\lambda$  max 227 nm and 193 nm) and glyoxal (249 nm) had absorption maxima at shorter wavelengths, perhaps partially accounting for some of the UV absorption found within the peaks in Table 5.4. Other peaks described by the same author did not really match any peaks observed in sultana and arginine-glucose model systems. Lederer *et al.*

(1998) reported interestingly that  $\alpha$ -acetyl-arginine-glyoxal intermediates (i.e. imidazolone type structures) had a  $\lambda$  max at 243 nm.; the many peaks with  $\lambda$  max close to this wavelength in sultana and model extracts may be compounds containing imidazolone moieties.

Monti *et al.* (1998) described peaks from xylose-lysine and glucose-lysine model systems, two of which had peaks with a  $\lambda$  max at 297 nm, similar to the peak eluting at 5.3 min. found in sultana and arginine-glucose model systems extracts. The peaks described by them also had a strong shoulder peak at ~271 nm, which was not found in the arginine-glucose model system. The authors gave no further information on the likely structure of the compound in question, however since the shoulder peak was absent in the arginine-glucose system peak, it was probably a different compound. Henle *et al.* (1994) described the lysine derived Maillard product pyrrolidine as having a strong  $\lambda$  max at 297 nm. As lysine has a nitrogen containing side group, similar to the guanidino functionality of arginine, it may be that the compound in sultanas is a similar arginine analogue.

Comparison of Maillard model system extracts and sultana extracts contributed further evidence that a number of the peaks occurring on sultana HPLC profiles were of Maillard origin. Furthermore, the peak eluting at 5.3 min. appeared to be a unique compound generated in arginine-glucose Maillard systems. Proline-glucose Maillard model systems were also made up in a similar manner to the arginine-glucose model systems. After storage at 60°C for 12 days the proline model systems, with and without catalytic iron, had not undergone any colour change. Proline model systems were also run through the HPLC system (results not shown) and there was only one large peak present, which was identified as 5-HMF from retention time data and the UV DAD spectrum.

There are considerable problems encountered in analysing Maillard systems and the limitations of current analytical techniques are well known (Ledl and Schleicher 1990, Bailey *et al.* 1996, Ames 1998, Monti *et al.* 1998, and Royle *et al.* 1998). As was discussed in section 2.09, the initial phase of Maillard reactions result in the generation of a complex array of sugar degradation products and heterocyclic compounds; most of which have no inherent colour (i.e. 5-HMF). Colour changes occur in samples as condensation of these initial products occurs to form Melanoidins, the chemical nature of which still remains relatively undefined (Yaylayan and Kaminsky 1998). As Bailey *et al.* (1996) and Monti *et al.* (1998) reported, a large amount of the material from Maillard browning systems passes through a reverse phase HPLC column without retention within a short amount of time. The same researchers also reported a characteristic unresolved broad band of background absorbance for Maillard systems. In both sultana extracts and Maillard model systems there was UV absorbing material between the peak cluster and peak 3 consistent with an 'unresolved' band of melanoidin type material (see Table 5.4).

The HPLC data for 5-HMF (Figure 5.8) appeared to contradict the GC data for the same compound in DCM sultana extracts (Figure 5.9). Via HPLC analysis, 5-HMF levels decreased to trace levels relative to pre-storage values (after 10 months at 30°C). The GC data indicated that the relative concentration of 5-HMF increased significantly for samples stored only at 30°C (see also storage trial I & II) after storage. Polymerisation of 5-HMF occurs rapidly in browning systems to produce an important component of melanoidin (Kroh 1994 and Yaylayan and Kaminsky 1998). A polymer of a number of 5-HMF units would behave differently on a HPLC column, compared to free, non-polymerised 5-HMF. It is proposed that the 5-HMF polymer would either not be resolved by the column or it would be eluted earlier on chromatograms, together with other melanoidin material. In contrast, injection of such polymeric material into a hot GC injector (250°C) would probably result in some breakdown of the polymer into individual units of 5-HMF. In any case, sultana DCM extract samples for GC analyses were all performed in an identical manner. Pre-storage sultanas and those stored at 10°C, with and without oxygen, either had trace or zero levels of 5-HMF on GC profiles. It was therefore unlikely that the 5-HMF detected in GC DCM samples stored at 30°C was an experimental artefact, as it was not detected in samples stored at 10°C.

In the conformation experiment, a 5-HMF peak was observed in HPLC profiles; these sultanas were stored at 50°C for 12 days and were prepared and analysed immediately. The storage sultanas were stored at 30°C for 10 months and stored at -20°C for a number of weeks before HPLC analyses. An alternative explanation for the discrepancy in data analysed by the two techniques may be that the free 5-HMF polymerised during the refrigeration period.

## 6.0 SULTANA SURFACE LIPID OXIDATION DURING STORAGE

---

### 6.01 Introduction

Sultanas stored at 30°C in the presence of oxygen were generally darker than comparable fruit stored in an oxygen-free environment (Chapters 3.0, 4.0 and 5.0). The difference in browning in sultanas stored at 30°C in the presence of O<sub>2</sub> may have been due to oxidation of lipid components in the surface wax of sultanas. Lipid oxidation products may have subsequently interacted with other browning systems to increase browning potential: lipid oxidation can cause colour changes through interactions with other common food components such as amino acids, proteins and phenolic compounds.

### 6.02 Experimental aims

This investigation aimed to:

- ascertain whether oxidation of sultana surface lipid material occurred during storage, and if so,
- investigate possible effects of various field treatments: harvest date, sunfinishing and vine solar exposure on lipid oxidation.

### 6.03 Gas chromatography-mass spectrometry (GC-MS)

Sultanas from the 1996 storage trial II were used in this experiment; fruit was stored in the absence and presence of oxygen at 10°C and 30°C in the manner previously described. Pre-storage sultanas were held at -80°C in plastic bags until the end of the storage trial (10 months). Samples from the storage trial (after 10 months) were prepared for chemical analysis within a few days from being removed from oxygen-free environments. Sultanas were extracted into dichloromethane (DCM) and analysed via gas chromatography-mass spectrometry (GC-MS) as described in the following section.

### 6.04 Sample preparation

Duplicate sub-samples of 25 g of sultanas from each treatment were broken up with a mortar and pestle by hand in a small amount of Milli-Q water and placed into 250 mL round bottom flasks. A 100 mL volume of HPLC grade DCM (HyperSolv) was added to the sultana suspension and then reflux-extracted at 40°C for 60 minutes. After cooling to ambient temperature, approximately 22°C, the aqueous-DCM liquid was decanted into a 500 mL separating funnel. The DCM fraction was collected into 200 mL storage bottles and 2 g portions of anhydrous sodium sulphate was

added to the samples to absorb any residual H<sub>2</sub>O. After two hours, the DCM extract was reduced in volume under vacuum at 40°C in a rotary evaporator (Eyela Co. Japan) to a final volume of approximately 3 mL and was then filtered through individual disposable teflon filters via a 5 mL plastic syringe into a 10 mL graduated glass cylinder. High purity nitrogen gas (BOC Gases Australia) was used to further evaporate the volume to approximately 2.8 mL. A 20µL aliquot of tetradecane internal standard solution (1.00 g tetradecane made up volumetrically to 100 mL in DCM) was added to the sultana extracts. DCM was added to make the samples up to a final volume of 3 mL.

Chromatography was performed on a Varian Star 3400-X gas chromatograph (Varian Instruments, Mulgrave, Australia). Separation was achieved on a DB-1 100% dimethylsiloxane fused silica capillary column (J&W Scientific, Folsom, CA, USA) with a 30 m. length, 0.32 mm internal diameter, and a 0.25 µm film thickness. The carrier was ultra high purity helium gas (BOC Gases Australia). A sample volume of 1 µL was injected onto the column by a Varian 8200 CX autosampler (0.5 µL air gap with 0.5 µL solvent plug). The universal 1078 Varian injector was used in split mode, with a vent flow to give a split ratio of 1:100. The instrument was run in constant pressure mode; the column head pressure was maintained at 12 psi throughout the run, to give a calculated flow rate of 2.8 mL.min<sup>-1</sup> at 50°C. The injector port was held isothermal at 280°C throughout injection and separation. The temperature program for the GC was as shown in Table 6.1.

Temperature Segment	Start Temperature (°C)	End Temperature (°C)	Rate (°C.min <sup>-1</sup> )	Time (min.)
1	35	35	0.0	1.00
2	35	100	32.0	2.00
3	100	280	4.5	40.00
4	280	280	0.0	5.00

Table 6.1 Temperature program for the gas chromatograph—DB-1 column.

Detection for quantitative work was achieved with a flame ionisation detector (FID). The attenuation was set at two and the detector range at twelve. For qualitative characterisation of individual peaks, key samples were analysed with a Varian Saturn II ion trap mass spectrometer (ITMS) as a detector. The ITMS was connected directly via a heated transfer line to the GC column, and analytical runs were performed under the GC conditions described in Table 6.1. The ITMS was conditioned overnight to eliminate water and air from the system.

Ionisation Mode	EI-70 eV	Transfer line temperature	260°C
Scan range	15 – 400 amu	Multiplier Set Voltage	2200 V
Filament delay time	120 s	Manifold Set Temperature	220°C
Segment acquire time	48 min	Emission Set Current	15 $\mu$ A

Table 6.2 The Varian Saturn II instrument settings used in the analysis of sultana DCM extracts.

Optimal instrument settings were determined using the Varian Saturn II software auto-tune program. The ITMS was calibrated with perfluorotributylamine (FC-43) prior to use to ensure correct calibration of  $m/z$  values. Table 6.2 shows a summary of the ITMS instrument settings used. Total ion chromatograms and mass spectra were analysed in the Varian proprietary spectral analysis software SaturnView™ (Version 5.41). Peaks present on GC-MS total ion chromatograms were tentatively assigned into a specific lipid class from mass spectral matches with compounds present in the NIST-98 mass spectral search data base (Version 1.6 d), which includes combined mass spectral data from the United States National Institute of Standards and Technology (NIST), the United States Environmental Protection Agency (EPA) and the United States National Institute of Health (NIH) spectral databases.

## 6.05 Experimental results

Figure 6.1. shows typical GC chromatograph profiles of sultana DCM extracts after 10 months storage at 30°C: anaerobically (top) and aerobically (bottom). Some differences in the chromatograms were immediately obvious: the large peak at around 7.1 min., identified as 5-HMF, was present in sultanas stored under oxygen-free conditions in higher concentration than oxygen-exposed sultanas (see Chapter 3.0, 4.0 and 5.0). The large peak at 11.8 min. was the internal standard peak (tetradecane). Conspicuous peaks at 25.48 min, 28.85 min., 35.77 min., 37.16 min. and 38.8 min. were present in relatively higher concentration in oxygen-free compared to oxygen-exposed samples. Changes in peaks at 42.10 min., 42.15 min. and 44.35 min. were less obvious. The small peaks present at the beginning of the chromatograms, eluting approximately 2 to 7 min., were consistent with Maillard reaction intermediates. Sultana Maillard reaction products are examined in detail in the following chapter.

Lipid and 5-HMF peaks were semi-quantitatively measured against the internal standard (IS). The IS was present in samples at a concentration of approximately  $6.6 \text{ pmole.}\mu\text{L}^{-1}$ , which is within the recommended range for quantitative GC analysis.

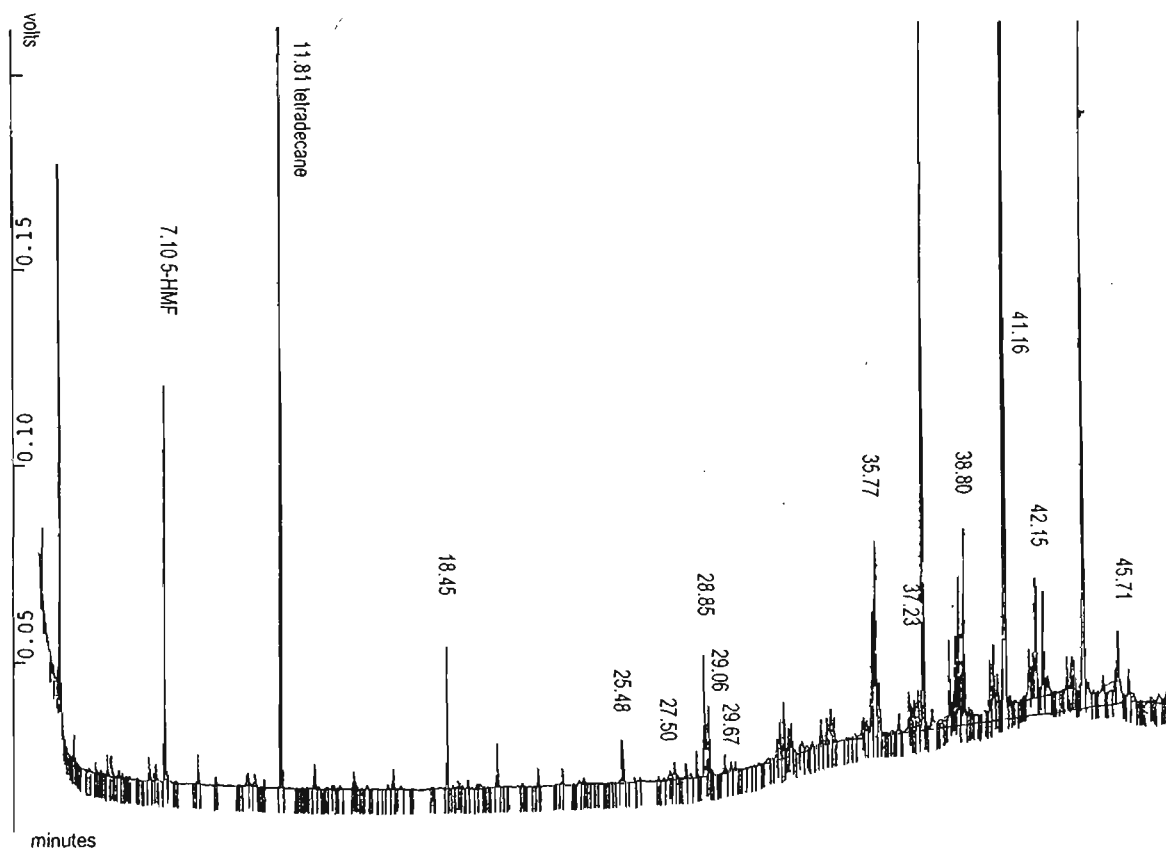
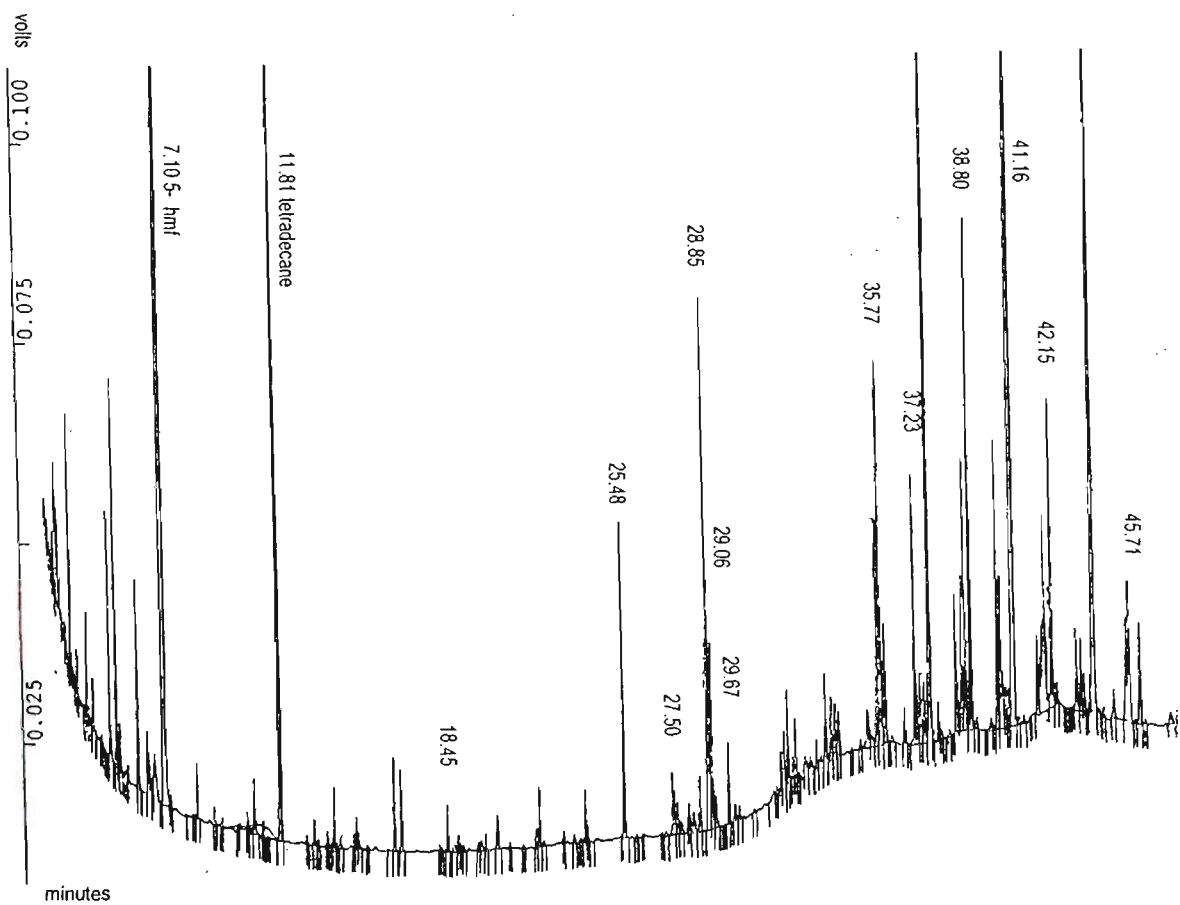


Figure 6.1 GC profiles of DCM extracts of sultanas after 10 months storage at 30°C. Top: stored without oxygen. Bottom: stored with oxygen.

Mass spectra for the peaks are shown in Figure 6.2, and a tentative classification of the type of lipid, based on matches with spectra in the NIST-98 data base in Table 6.4. In most cases, there was a good match with library spectra. Close matches are given together with their Chemical Abstracts Service (CAS) number. The lipid material was not treated with any chemical agents to facilitate conversion into free fatty acids and subsequent fatty acid methyl esters. Under these relatively non-aggressive extraction conditions it was expected that a realistic picture of possible oxidation processes would be obtained, with minimal introduction of chemical artefacts.

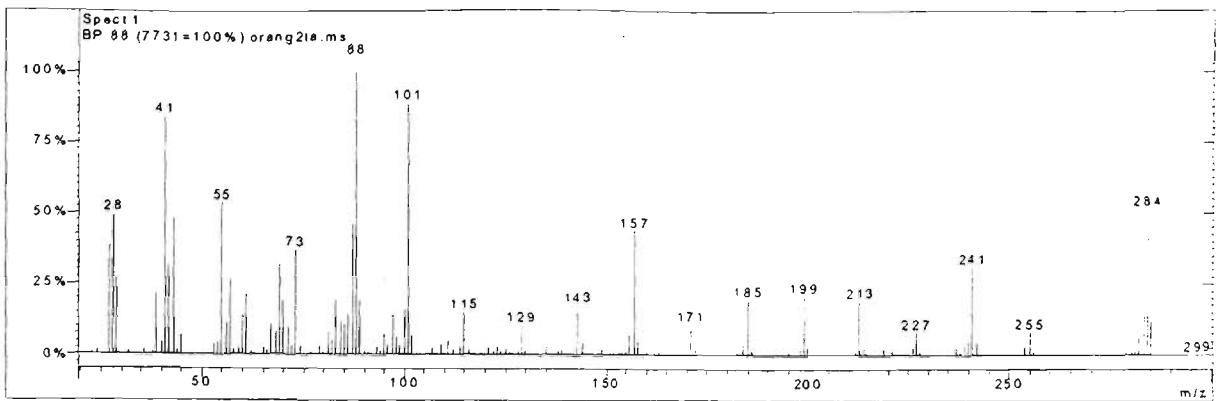
## 6.06 Mass spectra of lipid peaks and statistical analysis

The mean concentrations of each peak for each sample were arranged in spreadsheet format for ANOVA analysis using Genstat 5. The field and storage treatments—solar ‘exposure’, ‘harvest’ date, ‘sunfinishing’, storage ‘oxygen’ exposure and storage ‘temperature’—were coded in the manner previously described. None of the four-way interactions were statistically significant for any of the peaks so all LSD values were calculated at the three-way interaction level. Changes in relative concentrations of peaks are shown in Figure 6.3 and Figure 6.4.

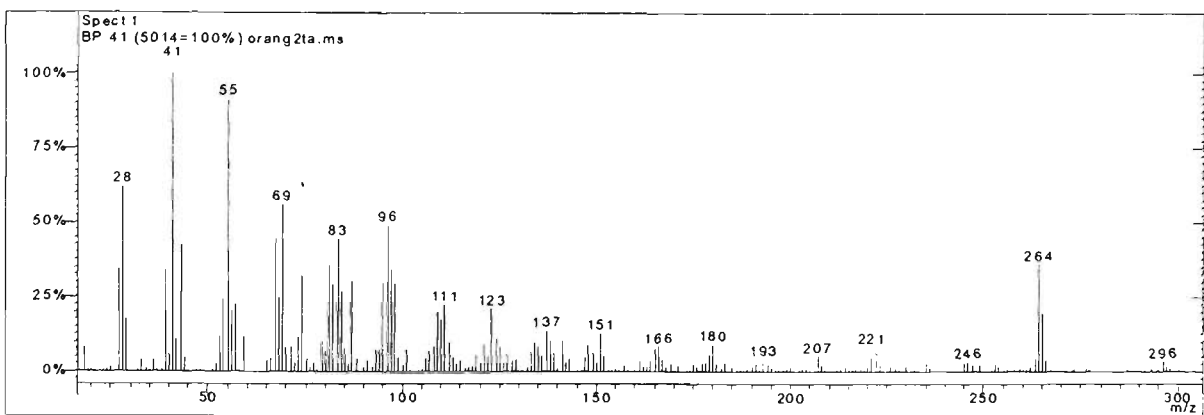
## 6.07 Saturated fatty acid esters

The peaks eluting at 25.48 min., 29.68 min. 37.23 min. and 38.80 min. were characterised as a homologous series of ethyl esters of saturated fatty acids. The presence of prominent ions with  $m/z$  88 ( $\text{CH}_3\text{CH}_2\text{OOCHCH}_2^+$ ) and  $m/z$  101 ( $\text{CH}_3\text{CH}_2\text{OOCHCH}=\text{CH}_2^+$ ), are diagnostic ions for ethyl esters of long chain fatty acids. Both methyl and ethyl-esters of fatty acids yield a stable  $\text{M}^+$  ion, as well as a number of regularly spaced peaks corresponding to successive fragmentation of carbon chains by one methylene unit (i.e. 14 amu). The peak with  $t_R$  25.48 min. matched closely with the mass spectrum of the ethyl ester of unsaturated palmitic acid (C16 hexadecanoic acid ethyl ester). The peak with  $t_R$  29.68 min. matched with the mass spectrum of the ethyl ester of stearic acid (C18 octadecanoic acid ethyl ester). The peak with  $t_R$  37.23 min. matched with the ethyl ester of docasanoic acid (C22). and the peak with  $t_R$  38.80 min was tentatively identified as the ethyl ester of tetracosanoic acid (C24). The elution order and  $t_R$  values agreed well with Kovat’s law: the plot of the number of carbons in the series of homologous long chain ethyl esters versus  $t_{RS}$  yielded a straight line with a correlation coefficient of 0.99.

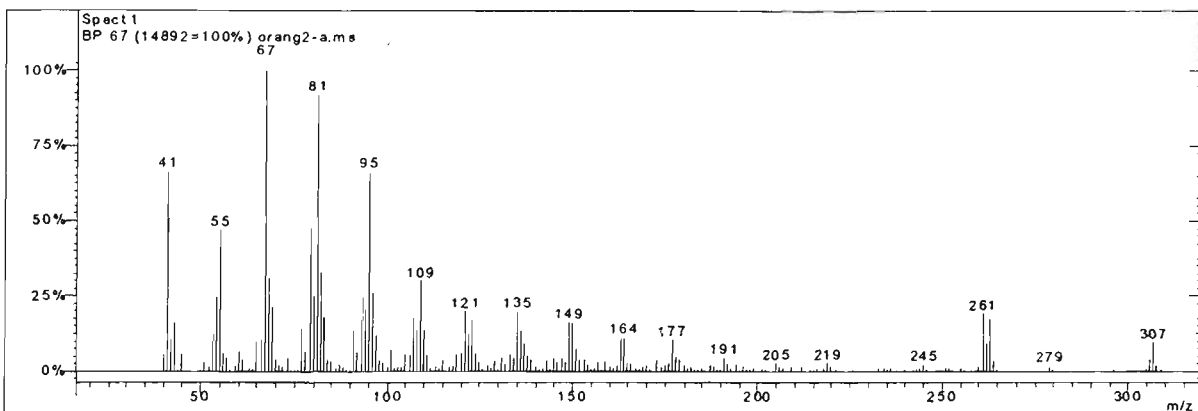
Storage changes in concentration of these ethyl ester compounds are shown in Figure 6.3. Free ethyl esters do not normally account for a large portion of natural grape/sultana surface lipid material, while commercial dipping oils contain ethyl esters in the C14, C16 and C18 range (Fogerty and Burton 1981). Plant waxes are typically composed of two long chain saturated and unsaturated hydrocarbon chains joined by an ester linkage. Hence the presence of an ethyl ester fatty acid would indicate either residual dipping oil esters or breakdown of endogenous waxes through enzymatic or non-enzymatic processes.



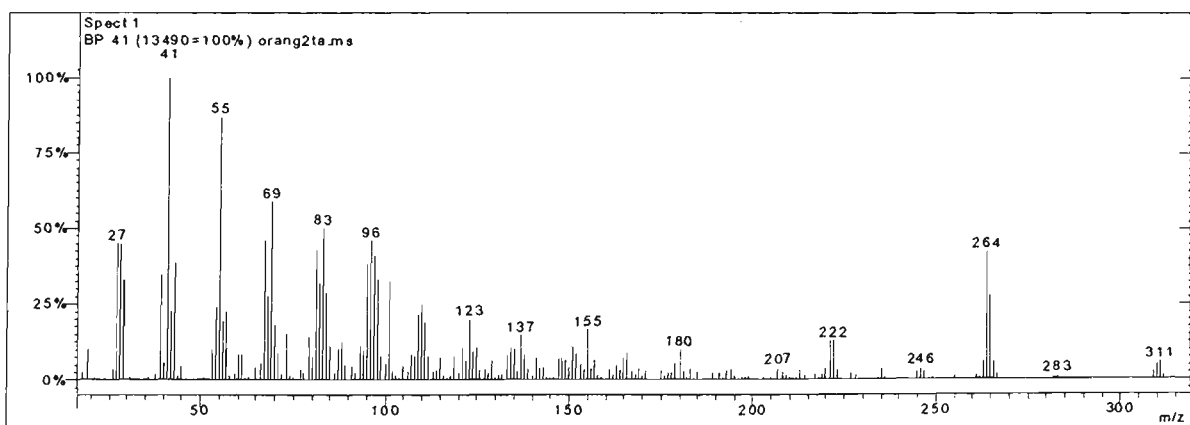
Peak at 25.48 minutes



Peak at 27.50 minutes

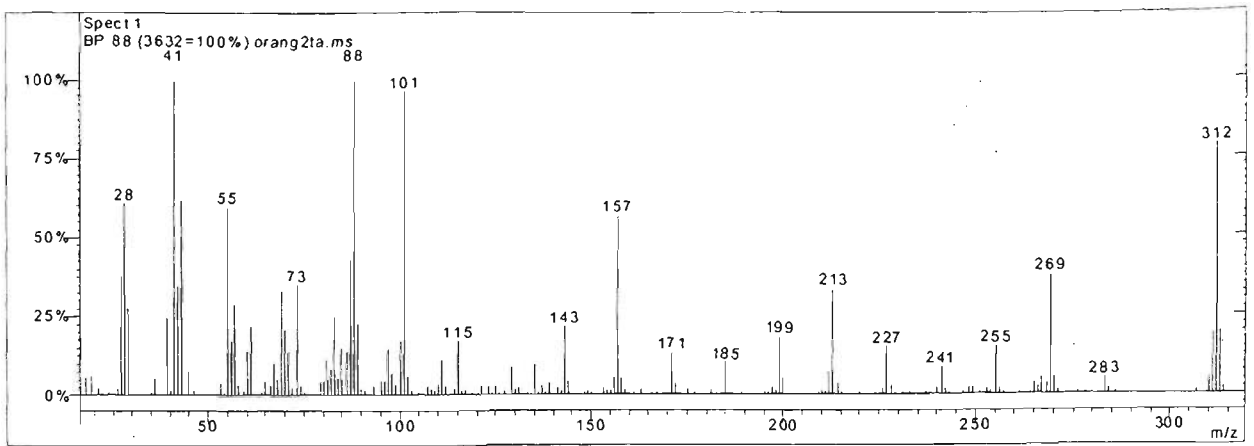


Peak at 28.85 minutes

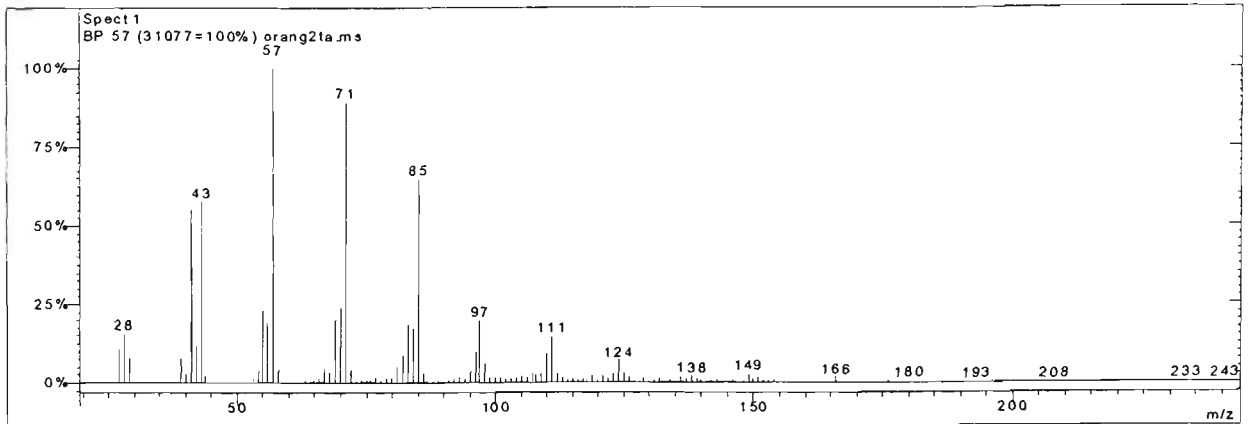


Peak at 29.09 minutes

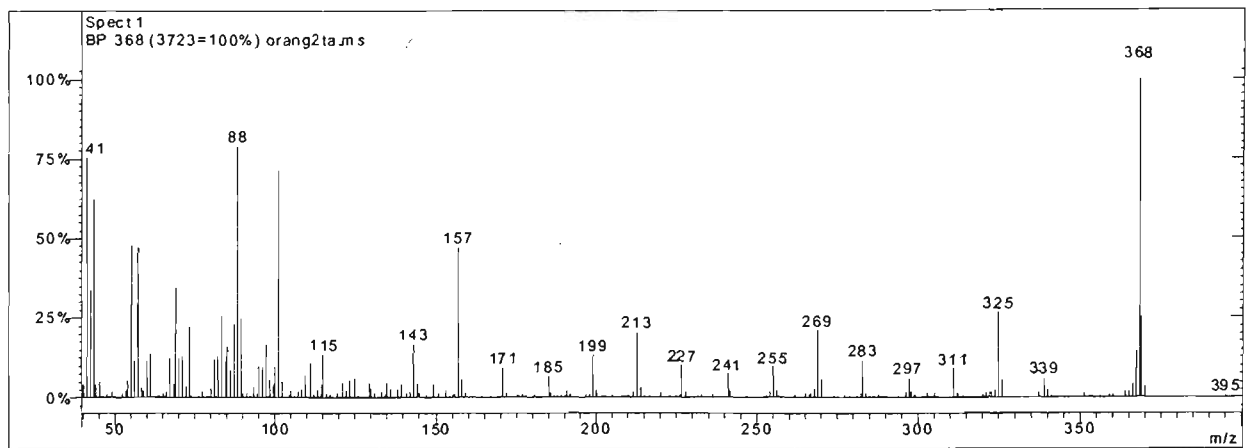
Figure 6.2 Mass spectra for peaks described in Table 6.3.



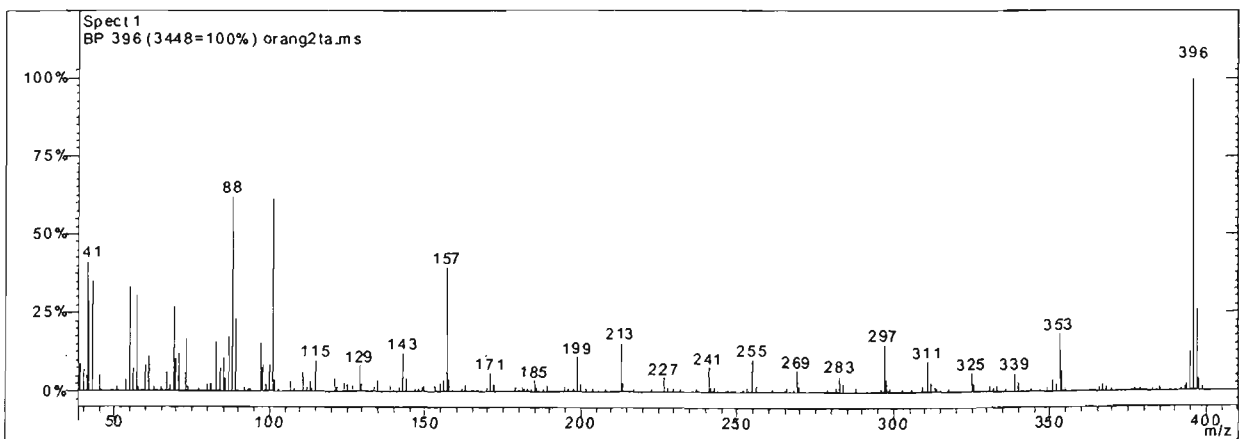
Peak at 29.67 minutes



Peak at 35.77 minutes

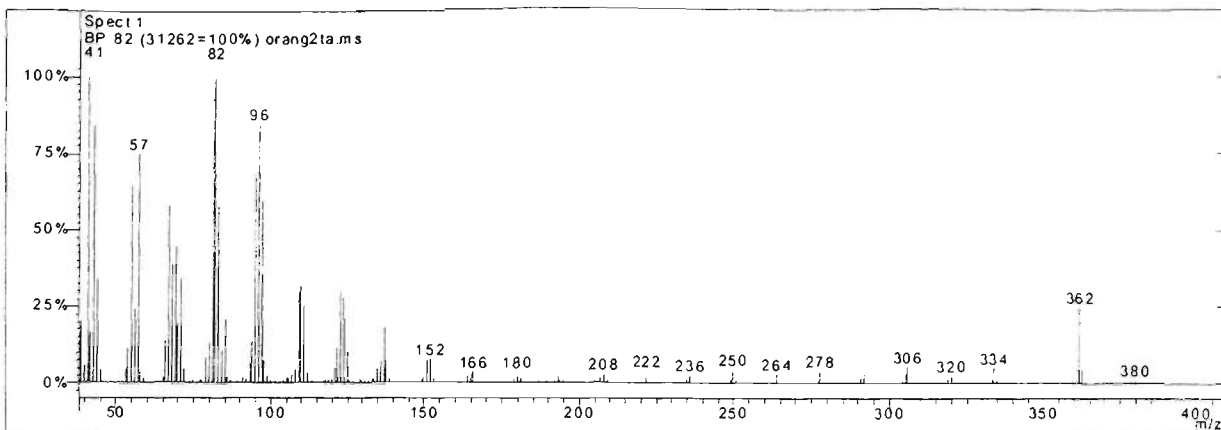


Peak at 37.23 minutes

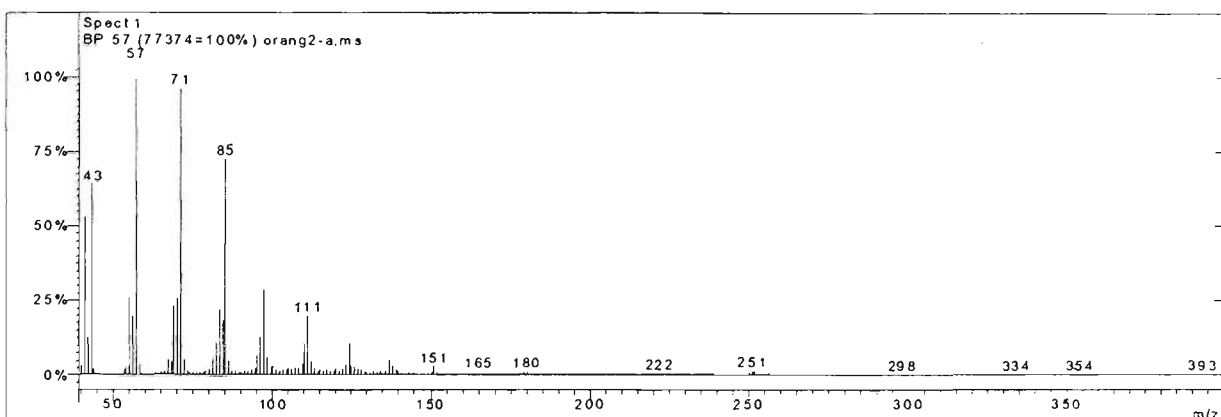


Peak at 38.80 minutes

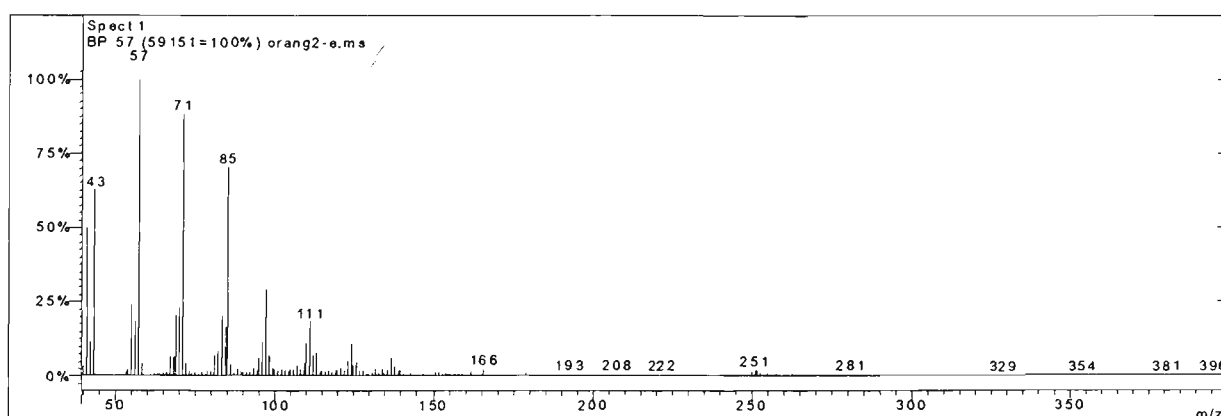
Figure 6.2 Mass spectra for peaks described in Table 6.3 (Continued).



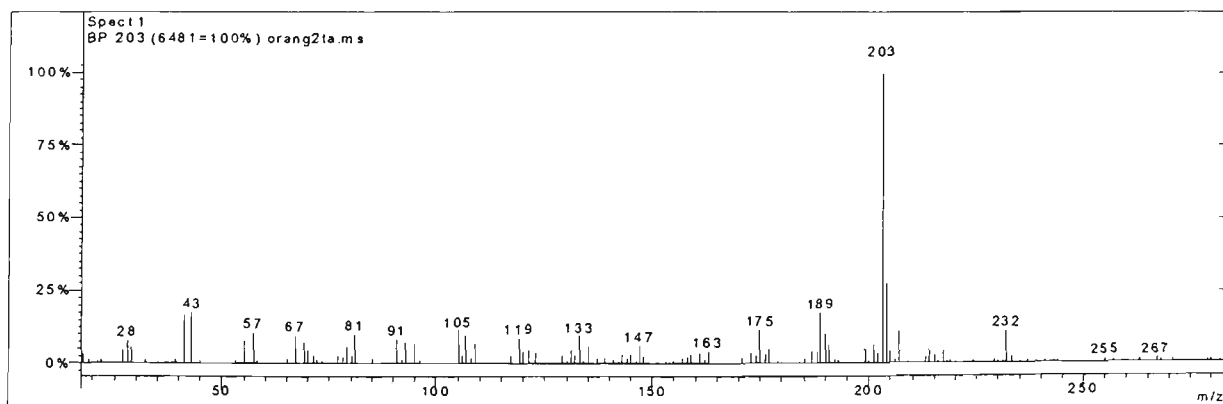
Peak at 41.16 minutes



Peak at 42.15 minutes



Peak at 44.35 minutes



Peak at 45.71 minutes. Possibly a breakdown product of oleanolic acid.

Figure 6.2 Mass spectra for peaks described in Table 6.3. (Continued).

The peak with  $t_R$  25.48 min. (tentatively identified as palmitic acid ethyl ester) was present in DCM extracts from pre-storage sultanas in trace amounts. Negligible changes were measured in extracts of sultanas stored at 10°C either aerobically or anaerobically. After storage at 30°C in the absence of oxygen, a large increase in the relative concentration was observed; in contrast only trace levels of the peak were measured after storage at 30°C in the presence of oxygen.

The concentration of the peak with  $t_R$  29.68 min. (tentatively identified as stearic acid ethyl ester) did not change appreciably in 10°C stored sultanas (aerobically and anaerobically) compared to pre-storage. The concentration of this lipid compound increased relative to pre-storage in most anaerobically stored sultanas at 30°C. Only traces of this compound were measured in extracts of sultans stored aerobically for 10 months at 30°C.

The minor peak with  $t_R$  37.23 min. was tentatively identified as docasanoic acid ethyl ester. Relative to pre-storage concentrations, this lipid did not decrease for any of the storage conditions except at 30°C in the presence of oxygen. The ethyl ester with  $t_R$  38.80 min., tentatively tetracosanoic acid ethyl ester, followed the general pattern observed for the peak eluting at 25.48 min; higher concentrations were measured at 30°C in the absence of oxygen. After 10 months storage at 10°C, the compound was present at a relatively high concentration in extracts of sultanas which were stored anaerobically compared to aerobically, implying oxidation may have also occurred in these samples. ANOVA analysis of the data for these peaks (25.48 min., 29.68 min., 37.23 min. and 38.80 min.) (Table 6.5) indicated that the difference in oxygen exposure had a significant effect on the concentration of each of the unsaturated ethyl esters ( $p < 0.001$ ) and the significant interaction of oxygen  $\times$  temperature ( $p < 0.001$ ) supported the observation that the most significant changes occurred only at 30°C.

The ANOVA data also supported the observation that late-harvest fruit appeared to have a higher content of the liberated lipid material; the significance level for the harvest effect ranged from  $p < 0.1$  to  $p < 0.001$  (See Table 6.5). The effect of grape exposure was rated as significant for the peaks  $t_R$  37.23 min and  $t_R$  38.80. The effect of sunfinishing did not have a statistically significant effect ( $p < 0.1$ ) for any of these samples

## 6.08 Mono-unsaturated fatty acid esters

A number of peaks, which changed over time in DCM extracts, were tentatively identified as mono-unsaturated fatty acid esters. The peaks with  $t_R$  27.50 min,  $t_R$  29.09 min. and  $t_R$  41.16 min. had mass spectra typical of fatty acid esters. The peak  $t_R$  27.50 min. had a very high match with the mass spectrum of the methyl ester of oleic acid (octadecenoic acid methyl ester) and the peak  $t_R$  29.09 min. was tentatively identified as the ethyl oleate ((Z)-9-octadecenoic acid ethyl ester). Fragmentation of unsaturated fatty acids preferentially occurs at the double bond and involves complex rearrangement sequences. The diagnostic ions at  $m/z$  88 and  $m/z$  101 for saturated ethyl esters tend to be fairly weak in unsaturated fatty acid ethyl esters.

Peak Retention Time	Parent ion	Major ions in order of decreasing intensity (m/z)	Lipid class (based on mass spectral data) and match with spectra in the NIST-98 mass spectral library §	Approximate concentration range ( $\mu\text{g}\cdot\text{g}^{-1}$ )
25.48	284	88, 101, 41, 55, 28, 284, 157, 73, 241, 86, 43, 69, 57, 143, 185, 199, 213, 143, 115, 129, 171, 227, 255	Hexadecanoic acid, ethyl ester (CAS 628-977) Palmitic acid, ethyl ester (CAS 2490-531)	40-140
27.50	296	41, 55, 28, 69, 83, 96, 264, 43, 67, 79, 81, 87, 98, 110, 124, 137, 151, 165, 180, 221, 223, 296	10-Octadecenoic acid, methyl ester (CAS 13481-95-3)	5-16
28.86	308	67, 81, 95, 41, 55, 79, 28, 109, 263, 121, 135, 149, 163, 178, 307, 191, 205, 220, 279	Linoleic acid ethyl ester (CAS 544-35-4) 9-12-Octadecenoic acid, ethyl ester (CAS 7619-08-1)	50-200
29.09	311	41, 28, 55, 69, 83, 96, 67, 81, 264, 265, 110, 123, 155, 222, 180, 311, 246	10-Octadecanoic acid, methyl ester (CAS 13481-95-3) 9-octadecanoic acid, methyl ester (CAS 112-629)	10-80
29.68	370	88, 101, 41, 312, 28, 43, 55, 157, 269, 213, 69, 57, 29, 143, 199, 227, 255, 355, 115, 171, 185, 241	Octadecanoic acid, ethyl ester (CAS 111-61-5)	1-6
35.77	—	57, 71, 85, 43, 97, 111, 125, 138, 193	Long chain unsaturated alcohol (CAS 2425-77-6)	1-6
37.23	368	368, 88, 41, 101, 28, 55, 157, 69, 213, 269, 325, 143, 199, 283, 129, 185, 241, 297, 339, 399	Docasanoic acid, ethyl ester (CAS 5908-87-2)	1-5
38.80	396	396, 88, 101, 41, 43, 28, 55, 157, 57, 69, 73, 325, 269, 213, 369, 199, 283, 115,	Pentacosanoic acid, methyl ester (CAS 55373-89-2)	1-5
41.16	501	41, 82, 96, 43, 79, 94, 55, 83, 97, 110, 124, 362, 137, 152, 306, 334, 250, 180, 222, 379, 501	alcohol fatty acid ester oleyl alcohol (CAS 143-282) octadecen-1-ol (CAS 506 423)	20-90
42.15	—	57, 71, 85, 43, , 97, 111, 124, 138, 153, 179, 208, 278, 300, 359, 395	Long chain unsaturated alcohol (CAS 2425-77-6)	15-60
44.35	—	57, 71, 85, 43, 97, 111, 125, 138, 193	Long chain unsaturated alcohol (CAS 2425-77-6)	20-35

Table 6.4 Retention times and most intense ion fragments in mass spectra (decreasing intensity). § NIST 98. Version 1.6d of the National Institute of Standards and Technology/ Environmental Protection Agency/National Institute of Health Spectral data Library- United States of America. Tentative assignments are related to spectral data in the NIST/EPA/NIH library by Chemical Abstracts Service (CAS) Registry number.

The peak eluting at  $t_R$  27.50 min. was not present in DCM extracts of pre-storage sultanas or sultanas stored at 10 °C. Those stored at 30° C showed low concentration or complete absence of this compound after aerobic storage, but somewhat higher concentrations after anaerobic storage, which were of the order of 3-4  $\mu\text{g}\cdot\text{g}^{-1}$  in February-harvested fruit and 4-16  $\mu\text{g}\cdot\text{g}^{-1}$  in March-harvested fruit. Harvest date was found to have an overall significant effect on the concentration of this lipid ( $p < 0.001$  see Table 6.5).

The lipid peak eluting at 29.09 min. was generally significantly higher in extracts of pre-storage late-harvest sultanas ( $p < 0.001$ ) compared to early harvest fruit. Large decreases of this lipid (octadecenoic acid methyl ester) were measured consistently in extracts of sultanas stored at 30°C in the presence of oxygen; only small changes were observed for the other storage conditions.

An exact match for the mass spectrum of the peak at  $t_R$  41.16 min. was not found in the NIST 98 library. The mass spectrum up to  $m/z$  268 matched closely to that of oleyl alcohol ((Z)-9-

octadecen-1-ol), however from the retention time and the prominent ions present at  $m/z$  362 and  $m/z$  380, this compound was clearly a longer-chain molecule. It was assumed that this lipid was some kind of mono-unsaturated long chain alcohol (~C26). In Figure 6.3 it can be seen that this lipid was present at around 20 to 88  $\mu\text{g.g}^{-1}$  in pre-storage sultanas. The relative concentration of this peak generally increased for all storage conditions. The lowest values of this lipid were present on surfaces of sultanas stored at 30°C in the presence of oxygen implying that some oxidation of this peak had taken place.

### 6.09 Polyunsaturated lipid material

The peak with  $t_R$  28.86 min. matched closely with the mass spectrum of the ethyl ester of linoleic acid (C18: 9-12-octadecenoic acid ethyl ester). Large increases in the concentration of this compound were measured in extracts of sultanas stored anaerobically at 30°C compared to pre-storage concentrations. In contrast only low concentrations of these peaks were measured after aerobic storage at 30°C. Sultanas stored at 10°C had similar concentrations of this compound compared to pre-storage concentrations. ANOVA data indicated that the harvest effect was significant ( $p < 0.01$ ). It can be seen in Figure 6.3 that the concentration of this lipid compound was in most cases higher for late harvest sultanas stored at 30°C without oxygen, compared to the early harvested fruit.

### 6.10 Saturated hydrocarbon material

The peaks with  $t_R$  35.77 min., 42.15 min. and 44.35 min. had similar spectra (Figure 6.3). Their carbon number dictates the elution order of long chain hydrocarbons. Assuming the compound eluting at 35.77 min. was a C18 hydrocarbon chain, the two later eluting compounds contained longer carbon chains. Given that unsaturated hydrocarbons generally do not yield  $M^+$  ions tentative identification was not possible. From NIST-98 database these compounds are most likely long-chain saturated hydrocarbons or long-chain alcohols.

Changes in the peak eluting at 35.77 min. did not show the clear-cut trend, seen for other lipid peaks. In many cases significantly higher concentrations of this compound were measured in extracts of anaerobically stored sultanas at 30°C, compared to aerobically stored. This lipid was present only at low concentration in pre-storage samples: after storage at 10°C differing concentrations were measured. The single effect of oxygen (Table 6.5) was not significant ( $p < 0.1$ ), however the single effect of temperature ( $p < 0.001$ ) and the combined effect of oxygen $\times$ temperature ( $p < 0.01$ ) were both significant. This can be interpreted as meaning that the effect of oxygen was enhanced at higher temperature (e.g. 30°C).

The concentration of the lipid with  $t_R$  42.15 min. was significantly higher in extracts of sultanas stored anaerobically-at 30°C, compared to pre-storage. Although there were small increases in 10°C anaerobically stored samples, generally there were only small changes in samples stored under other conditions. In all cases the concentration of this compound was lower in extracts of 30°C aerobically-stored sultanas (compared to anaerobically-stored), implying oxidation of this compound took place. The effects of oxygen, temperature and the interaction of oxygen×temperature were all significant at the  $p<0.001$  level. The data also indicated that there was a statistically significant harvest effect ( $p<0.05$ ), which was apparent for HS and MS sultanas but not for EX fruit.

The peak eluting at 44.35 mins. was present in pre-storage DCM extracts at ~5-8  $\mu\text{g.g}^{-1}$  and increased in concentration for all storage conditions. Highest concentrations of this peak were measured in samples stored at 30°C in the absence of oxygen. Lowest concentrations of this peak were measured in samples, which had been stored at 30°C aerobically. Both the effect oxygen and the interaction oxygen×temperature were significant at the  $p<0.001$  level. There was not a significant harvest effect observed for this peak.

The latest eluting peak at 45.71 min. (see Figure 6.2) had to a large extent a reasonable match with the mass spectrum of oleanolic acid ( $\text{C}_{30}\text{H}_{48}\text{O}_3$  CAS 508-02-1). The NIST-98 mass spectrum had the following fragments in decreasing intensity: 248, 203, 69, 41, 55, 81, 133, 95, 119, 189, 175, 233, 147, 161. Whilst the sultana spectrum clearly lacked the intense ion at  $m/z$  248, nearly all of the other peaks were present indicating that it may be a degradation product of oleanolic acid. This peak did not appear to undergo clear changes during storage however (data not shown).

	lipid peaks from gas chromatograph — $t_R$ minutes										
Effects	25.48	27.50	28.86	29.09	29.68	35.77	37.23	38.80	41.16	42.15	44.35
exposure	ns	ns	ns	ns	ns	ns	****	***	ns	ns	ns
harvest	**	****	***	****	****	ns	****	*	***	***	ns
sunfinishing	ns	**	ns								
oxygen	****	****	****	***	****	ns	****	****	****	****	****
temperature	****	****	****	ns	**	****	****	****	****	****	ns
oxygen× temperature	****	****	****	***	****	***	****	****	****	****	****
harvest×oxygen	**	****	***	ns	**	ns	*	ns	**	**	ns
sunfinish×oxygen	ns	****	ns								

Table 6.5 Table of significance of effects on lipid peaks in DCM extracts. Significance levels were determined by ANOVA at the level of three-way interaction. \* ( $p < 0.1$ ), \*\* ( $p < 0.05$ ), \*\*\* ( $p < 0.01$ ) and \*\*\*\* ( $p < 0.001$ )

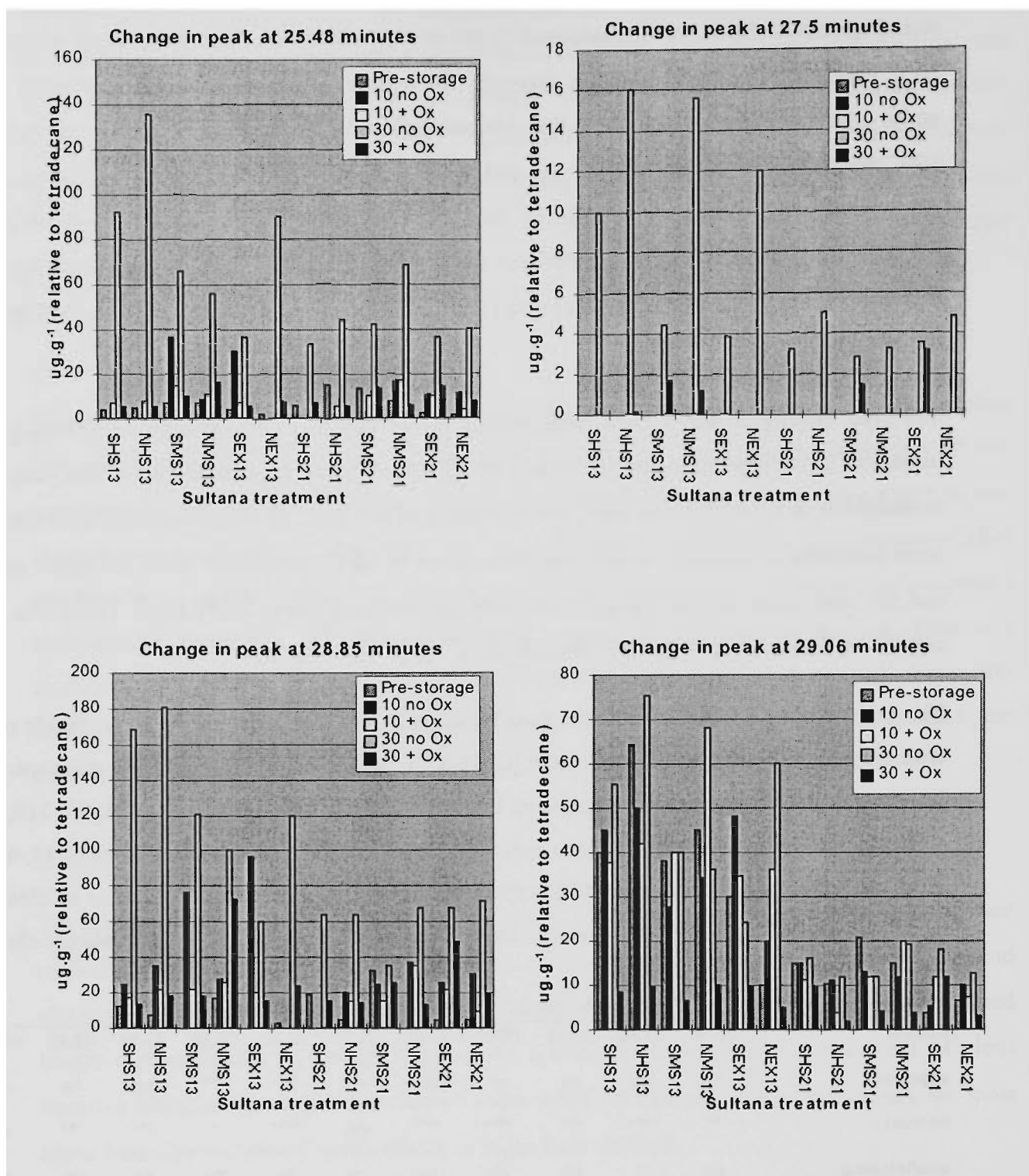


Figure 6.3 Quantitative changes in individual lipids after 10 months storage at 10°C and 30°C. Pre-storage (before storage trial), 10°C no oxygen (10-no ox), 10°C with oxygen (10 + ox), 30°C no oxygen (30-no ox), 30°C with oxygen (30 + ox). The probable class and tentative identities of peaks are listed below. For codes of sultana samples see Table 4.4.

- Peak at 25.48 min.: unsaturated ethyl ester (2-methyl hexadecanoic acid ethyl ester)
- Peak at 27.50 min.: unsaturated methyl ester (10-octadecanoic acid methyl ester)
- Peak at 28.86 min.: poly-unsaturated ethyl ester (linoleic acid ethyl ester)
- Peak at 29.09 min.: mono-unsaturated ethyl ester (ethyl oleate)

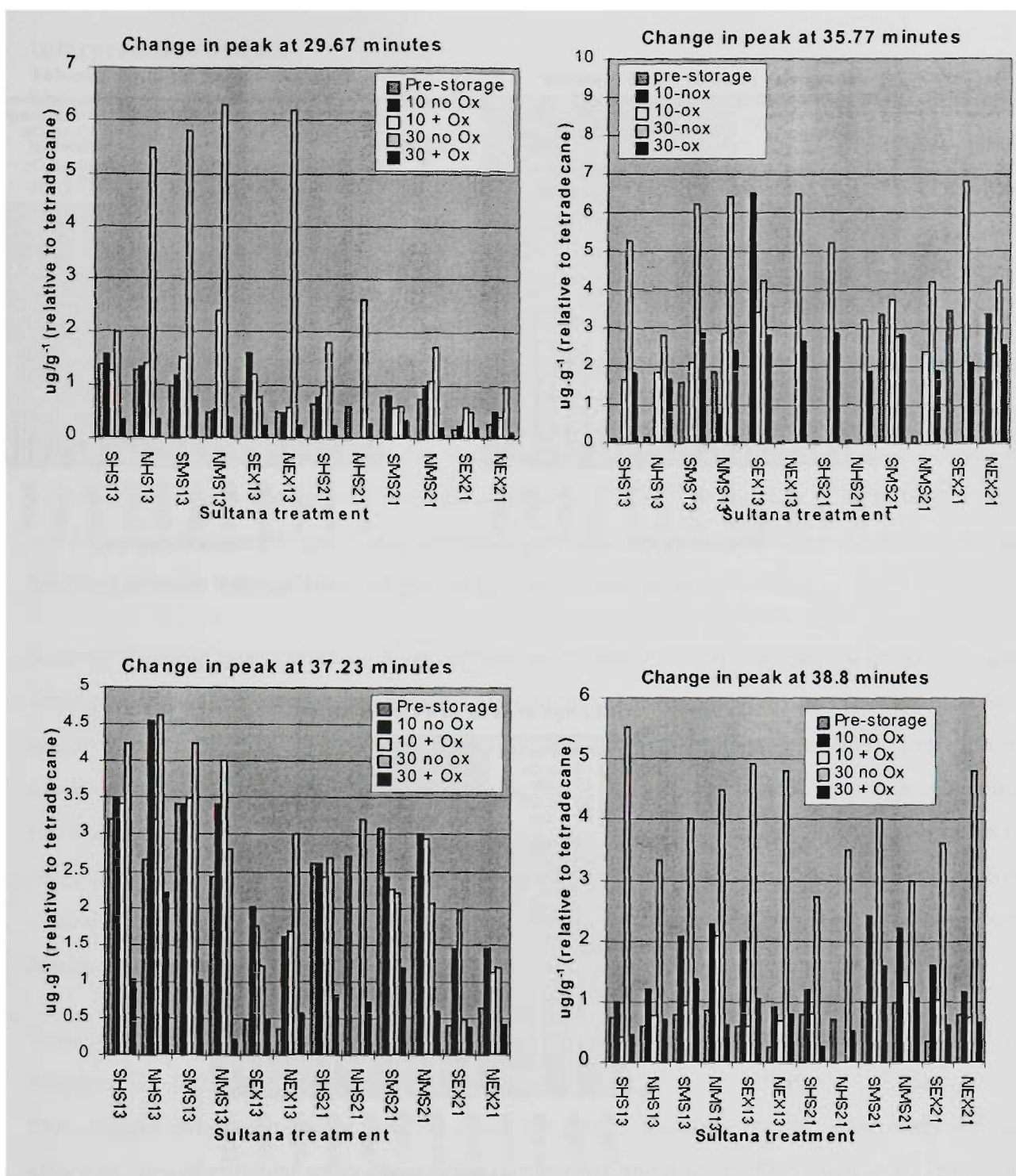


Figure 6.3 (cont'd). Quantitative changes in individual lipids after 10 months storage at 10°C and 30°C. Pre-storage (before storage trial), 10°C no oxygen (10-no ox), 10°C with oxygen (10 + ox), 30°C no oxygen (30-no ox), 30°C with oxygen (30 + ox) The probable class and tentative identities of peaks are listed below. Refer Table 4.4 for codes of sultana samples.

Peak at 29.68 min.: saturated ethyl ester ((Z)-9-octadecanoic acid ethyl ester)

Peak at 35.77 min.: saturated long chain alcohol

Peak at 37.23 min.: saturated ethyl ester (docasanoic acid ethyl ester)

Peak at 38.80 min.: saturated methyl ester (pentacosanoic acid methyl ester)

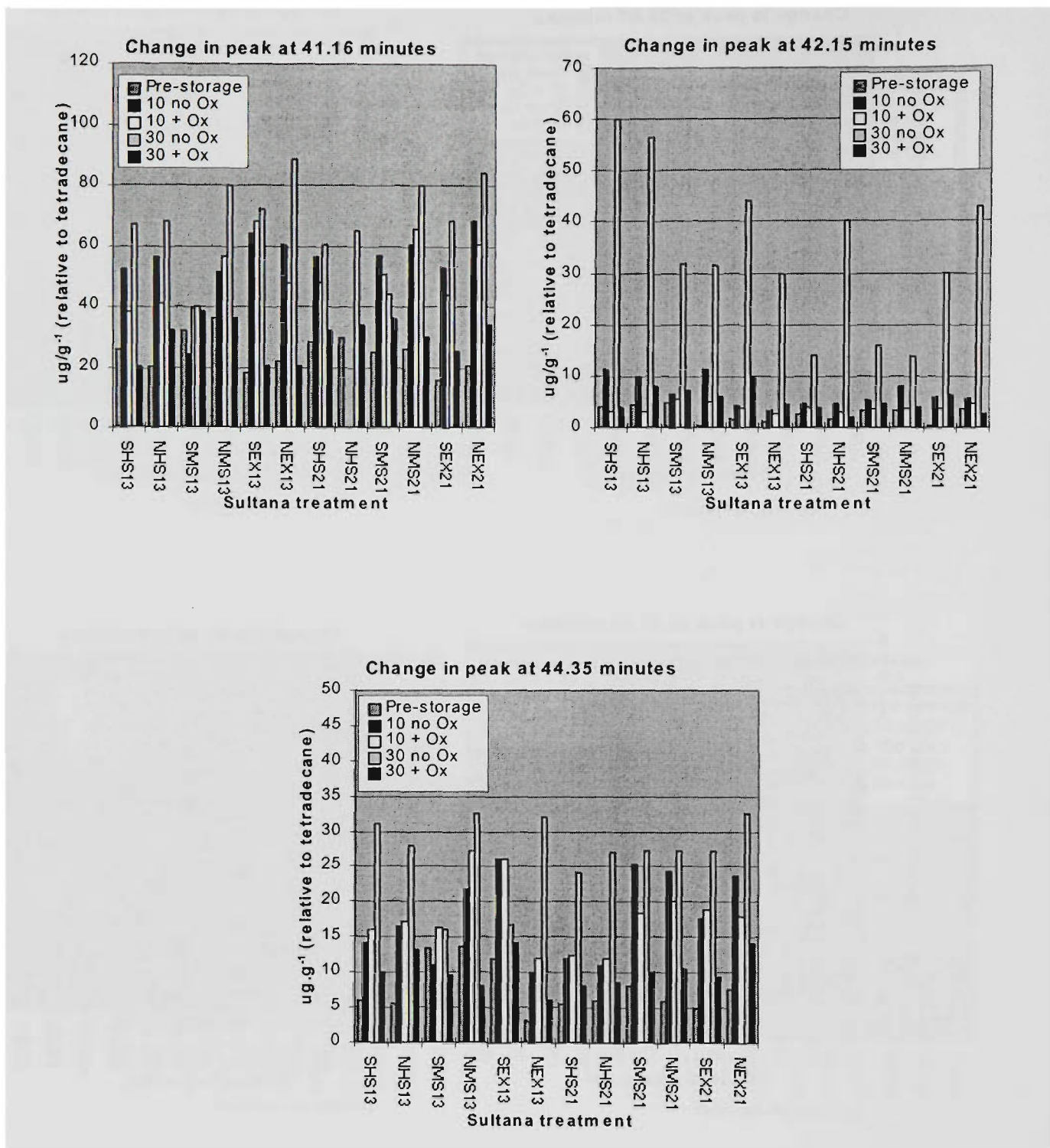


Figure 6.4 Quantitative changes in individual lipids after 10 months storage at 10°C and 30°C. Pre-storage (before storage trial), 10 °C no oxygen (10-no ox), 10°C with oxygen (10 + ox), 30 °C no oxygen (30-no ox), 30°C with oxygen (30 + ox). The probable class and tentative identities of peaks are listed below. For codes of sultana samples see Table 4.4.

Peak at 41.16 min.: mono-unsaturated alcohol (oleyl alcohol)

Peak at 42.15 min.: saturated long chain alcohol

Peak at 44.35 min.: saturated long chain alcohol

## 6.11 Interpretation of data

The mass spectra of the peaks, which changed during storage, were consistent with lipid type material. The data indicated that certain lipid-type compounds were degraded via temperature sensitive oxidative reactions during storage. During plant tissue senescence, free radical induced lipid peroxidation and increased lipoxygenase activity (Wilhelm and Wihelnova 1981, Pauls and Thompson 1984, Wolff and Dean 1986 and Thompson *et al.* 1987) accompany loss of cellular compartmentalisation. Linoleic and linolenic acids released during senescence are thought to be the primary substrates for lipoxygenase. Release of fatty acids through de-esterification processes during senescence have been shown to be due to the activities of three membrane associated lipases: phospholipase D, phosphatidic acid phosphatase and lipolytic acyl-hydrolase (Mayak *et al.* 1983, Lynch and Thompson 1984 and Lynch *et al.* 1985). The activity of these lipases does not require molecular oxygen. Lipid oxidation products may react with other substrates such as Maillard reaction intermediates and phenolics to accelerate storage browning.

Auto-oxidation of unsaturated lipids constitutes an important route to textural and quality changes during food storage. Reaction mechanisms are complex, but can generally be classified into four major steps: initiation, propagation, branching and termination (Frankel 1984). Initiation is catalysed by heat, light and trace metals and the loss of a hydrogen radical. During propagation, the lipid radical reacts with oxygen to form peroxy free-radicals, which react with further lipids to form hydroperoxides. Decomposition of hydroperoxide molecules produces further reactive radical intermediates which react with other radicals, proteins, membranes and intermediates from Maillard sugar degradation reactions (Ullrich and Grosch 1987 and Whitfield 1992).

Total waxy substances extracted from sultana grape skins have been determined to amount to between 125-140  $\mu\text{g}\cdot\text{cm}^{-2}$  (Dudman and Grncarevic 1962) or 90 to 110  $\mu\text{g}\cdot\text{cm}^{-2}$  (Radler 1965). The cuticular overlapping waxy platelets create a highly hydrophobic barrier on the berry surface affecting rates of cuticular water penetration (Grncarevic and Radler 1971, Noga *et al.* 1987, and Riederer and Schneider 1990). Radler and Horn (1965) identified components of light petroleum extracts of fresh sultana grapes and found that free aldehydes (C16-C32 range), free alcohols (C20-C32) and oleanolic acid (C30) made up 12, 40 and 22 % of total extractable components respectively. Hydrocarbons, ester alcohols, free acids and ester acids made up the remaining waxy substances. The major fatty acid components include oleic (mono-unsaturated C-18), stearic (saturated C-18) and oleanolic (poly-unsaturated C-30) acids. Breakdown of wax fatty acid esters via de-esterification reactions generally precedes oxidation of lipids. Dipping solutions are typically composed of C14, C16 and C18 fatty acids, some of which are also retained on sultana surfaces (Fogerty and Burton 1981).

As discussed in section 2.13, there are numerous studies in the literature showing that there are interactions with lipid oxidation products and Maillard intermediates. Aliaz and Barragan (1995) described a facile interaction of an analogue lysyl residue with E-(2)-octenal and Farag *et al.* (1978) described a model system in which oxidation of linoleic acid was catalysed by amino acids and copper. Riisom *et al.* (1980) described a pro-oxidant effect of amino acids on safflower oil auto-oxidation under ambient conditions. Although none of these types of reactions were proven by the data in this section, it is feasible that they may have occurred and contributed to browning processes and also in part to more rapid sultana browning in an oxygen-exposed environment.

Whilst the data did show that significantly different processes occurred at 30°C in the absence and presence of oxygen it is difficult to reach a conclusive interpretation of the processes which were at hand. The data might be interpreted as evidence that higher temperature (30°C) favoured the release of lipid material from sultana surface waxes (non-oxygen dependent reactions i.e. lipases): in the absence of oxygen these compounds simply accumulated and were subsequently oxidised in sultanas stored aerobically. Further trials with more frequent measurements over time would provide further understanding. The statistical analysis (Table 6.5) indicated that for a number of peaks there was a significant harvest effect. It was seen (Figure 6.3) that there was generally significantly more lipid compounds present at 30°C oxygen-free stored samples in late harvest sultanas. It was seen earlier that late harvest fruit tended to be less colour stable. It is feasible that greater oxidation of wax lipid material in late harvest fruit contributed to their darker colour. A future more comprehensive study, in which changes in free fatty acids in the form of FAME derivatives are also performed, would provide valuable further insight into these processes. The effects of sunfinishing and vine exposure were generally not found to have a significant effect on changes in lipids.

## 7.0 MAILLARD REACTION INTERMEDIATES IN SULTANAS AND ARGININE-GLUCOSE MODEL SYSTEMS

---

### 7.01 Introduction

Arginine as an amino acid initiator of Maillard browning has not received as much attention in the literature as other amino acids, such as lysine or proline. Typically, Maillard browning model studies are conducted on systems in which the amino acid is present at a high concentration; this is useful if the objective is to isolate large amounts of MRPs, however such systems do not reflect normal physiological conditions. In this section some aspects of glucose-arginine Maillard processes were examined in sultanas and models with concentrations of arginine similar to those found in sultanas.

### 7.02 Experimental aims

The general aims of this section of this work was to obtain further understanding of Maillard browning in sultanas using GC-MS. Specific aims were:

- to employ a number of sample preparation techniques such as solvent extraction, Maillard extract dilution and headspace gas analysis to further characterise Maillard type reactions in sultanas and glucose-arginine model systems from mass spectral data,
- to compare both sultana and arginine-glucose model mass spectral data as a means of furthering the hypothesis that arginine is the main amino acid involved in sultana Maillard reactions, and
- to attempt to identify some arginine-specific Maillard compounds in model systems and sultanas.

### 7.03 Sample preparation—sultana and model systems

Maillard model systems were made up with arginine (10 mg.g<sup>-1</sup>, Sigma 99% purity) and saturated D-glucose (BDH AnalaR) solutions (100g.100mL<sup>-1</sup>) and the pH was adjusted to pH 5.0 with orthophosphoric acid. A catalytic amount of Fe was added in the form of FeCl<sub>2</sub> solution to give a final concentration of 10 µg.g<sup>-1</sup>. Samples were stored until browning had occurred, i.e. at 37°C for 4 weeks, 50°C for 5 days and 60°C for 4 days. Sultanas were also stored under similar temperature conditions—30°C (10 months aerobic storage, derived from the 1996 storage trial II), 50°C (4 days) and 60°C (2 days)—and removed. These higher temperatures (50°C and 60°C) were used because during sun-drying and dehydrator drying it is not uncommon for sultanas to be subjected to such temperatures for an extended period. It has been shown that rapid browning of sultanas occurs above 60°C (ADFM 1998).

#### 7.04 Ethyl acetate (EtAc) and methanol (MeOH) extracts

Brown sultanas (25 g) which had been stored at either 30°C, 50°C or 60°C were soaked in 50 mL of alkaline Milli-Q water (pH 9 adjusted with 0.05 M NaOH) for 1 h and homogenised with the Polytron. Sultana alkaline suspensions were transferred into a 500 mL separating funnel and a 50 mL volume of ethyl acetate (HyperSolv) was added. The sultana-EtAc solution was vigorously inverted,  $\times 20$ , and the EtAc phase was removed. Subsequent 50 mL portions of EtAc were added ( $4 \times 50$  mL) and extracted. All EtAc volumes (ca. 200 mL) were pooled and dried over anhydrous sodium sulphate to remove any water in the samples. Dried extracts were reduced in volume at 40°C using a rotary evaporator to a final volume of 3 mL. Extracts were passed through teflon filters. Undiluted filtered EtAc extracts were subjected to GC-MS analysis. This solvent extraction methodology was adapted from that reported by Shu and Lawrence (1994).

The brown model systems were made alkaline with 0.05 M NaOH to a final pH of 9 and then extracted into  $5 \times 50$  mL EtAc in a separating funnel. EtAc volumes were pooled, dried and concentrated to a final volume of 3 mL in the rotary evaporator. Filtered undiluted extracts were analysed directly via GC-MS under the same conditions as described in the following section. MeOH samples were prepared by diluting (1:200) the brown water-soluble material from alkaline extracts in an appropriate volume of MeOH (HyperSolv HPLC grade). A volume of 1  $\mu$ L of the diluted material was injected in split mode (1:100).

#### 7.05 Maillard reaction products GC-MS

Samples were manually introduced into the Varian 1077 split-splitless injector in split mode with a split ratio of 1:100. Separation was achieved on a DB-1701 moderately polar 14% cyanopropyl-phenylsilicone fused silica capillary column (J & W Scientific, Folsom, CA, USA). The column specifications were as follows: length 30 m, internal diameter 0.32 mm, film thickness 0.25  $\mu$ m. The carrier gas was ultra high purity helium gas (BOC Gases Australia). Analyses were performed on a Varian 3400 Gas Chromatograph connected to a Varian Saturn II-ITMS. The GC conditions were as follows. The injector and transfer line were held at 280°C. The initial column temperature was 40°C and then ramped to 100°C in 4.0 min. The temperature was then ramped to 200°C over 30 min. and then held at 200°C for 5 min. (total run time 39 min.). The GC was run in constant pressure mode, with a head pressure of 12 psi, resulting in a flow rate of 2.8 mL.min<sup>-1</sup> at 50°C. The ITMS operation conditions were as outlined in Table 7.1.

Ionisation Mode	EI-70 eV	Transfer line temperature	280°C
Scan range	15 – 400 amu	Multiplier Set Voltage	1750 V
Filament delay time	240 s	Manifold Set Temperature	220°C
Segment acquire time	35 min	Emission Set Current	27 $\mu$ A

Table 7.1 Varian Saturn II ITMS settings used in the analysis of EtAc and MeOH extracts.

## 7.06 Analysis of EtAc extracts

Mass spectra were analysed with the Varian proprietary software 'Saturn View ®' (Version 5.4). Model system extracts were run consecutively and then followed by sultana extracts to avoid any possibility of cross-contamination from each system. Blank runs of either EtAc or MeOH solvent were run between samples to confirm that there was no contamination between model system and sultana extracts. In order to eliminate the possibility of spontaneous formation of glucose pyrolysis products in the injector, a sample of D-glucose or arginine dissolved in 95 % MeOH was run through the system; no significant peaks were found on total ion chromatograms. The mass spectra of the small peaks present were different to the large peaks found in sultana and model system extracts (results not shown). Furthermore, the mass spectra for compounds present in the Maillard model systems and sultana extracts were checked against mass spectra of known D-glucose pyrolysis products. As identified by Heyns *et al.* (1966) and Heyns and Klier (1968); none of the mass spectra in sultana extracts or arginine-D-glucose model system extracts corresponded with the glucose pyrolysis products listed in their report.

Typical total ion chromatograms for EtAc extracts of sultana and model systems are shown in Figure 7.1 to Figure 7.3. There was a high degree of match in peak retention times for corresponding peaks in sultana extracts and model systems. Although there was generally a difference in the relative abundance of peaks in model and sultana extracts, there was a high match in terms of mass spectral data. The mass spectra of the main peaks from sultana and model system extracts are shown in Appendix I. In Table 7.2 each of the peaks is listed together with the closest credible match in the NIST-98 library. The main ion fragments for the compound from the spectral library are also shown. Many of the mass spectra agreed with typical Maillard intermediates, and in most cases it was possible to make a tentative match. In the following section the possible identity of some peaks is discussed.

In addition, some of the fractions from HPLC analysis of sultana extracts (Section 5.07) were collected from multiple runs and injected (1 $\mu$ L) without concentration onto the GC-MS for analysis. HPLC peaks 1 and 2 were collected together and analysed via GC-MS. A typical total ion chromatogram is shown in Figure 7.4. Most of the peaks present were also observed in the EtAc extracts. The other HPLC fractions did not give any clear peaks on total ion chromatograms, indicating that the compounds were most probably not sufficiently volatile for GC analysis.

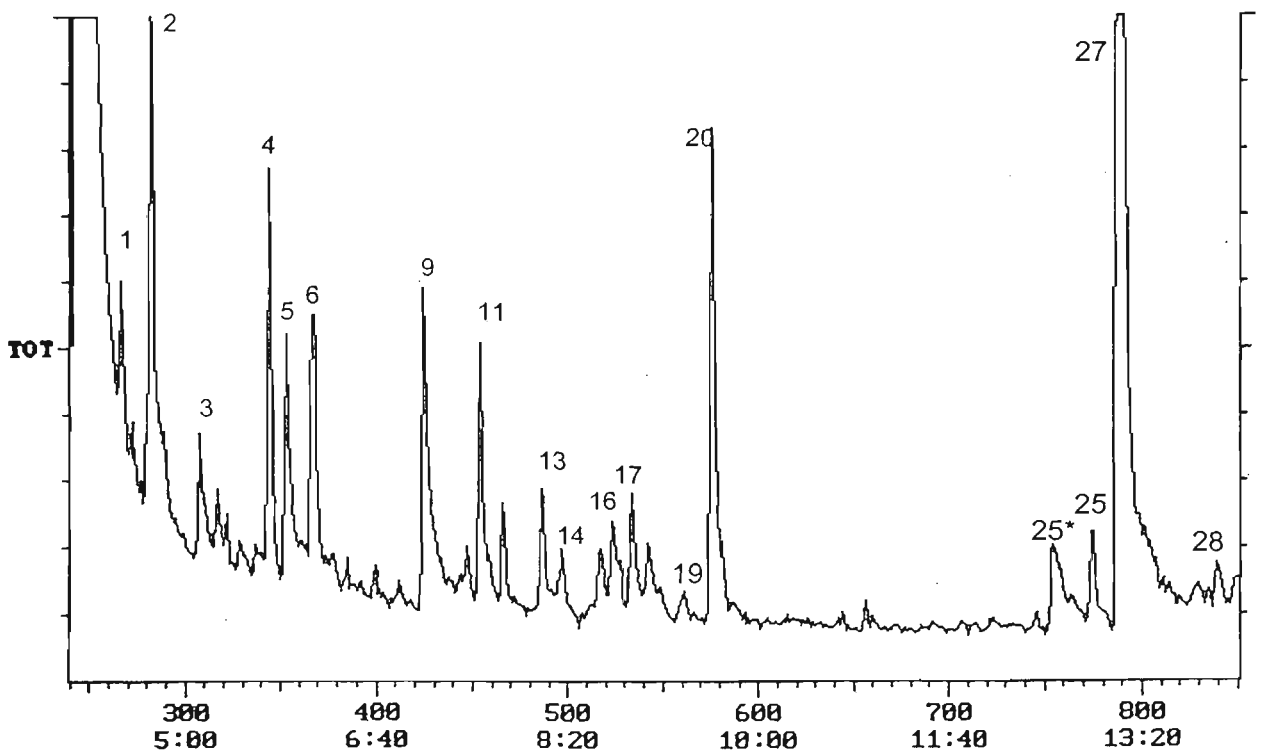
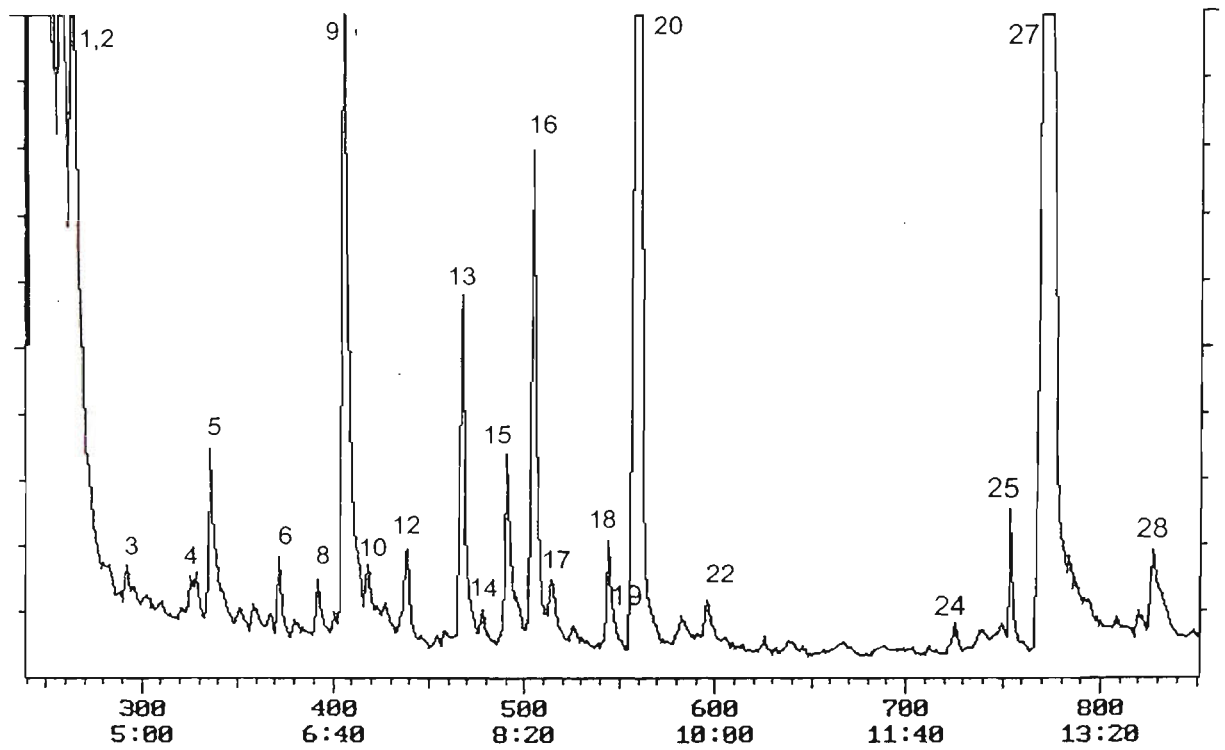


Figure 7.1 Total ion chromatogram of EtAc extract of sultanas (30°C) and model systems (37°C). Sultanas stored 10 months (top) and arginine-glucose model stored for 4 weeks (below).

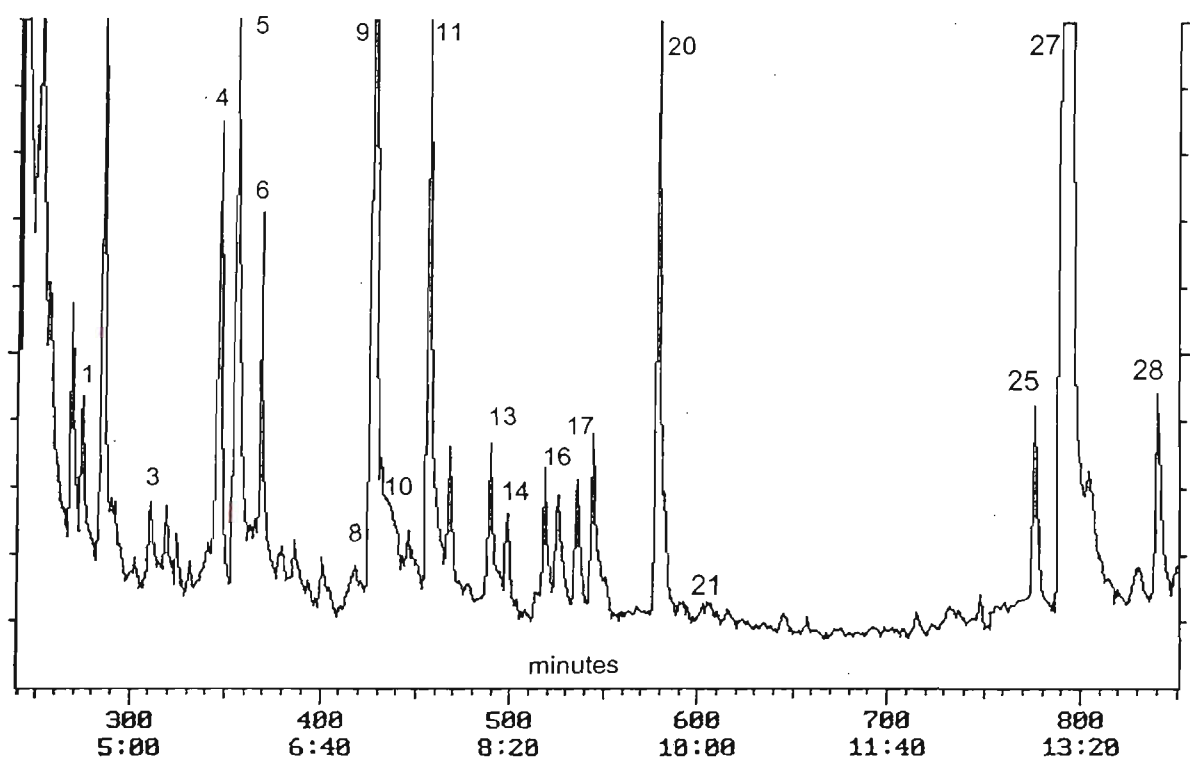
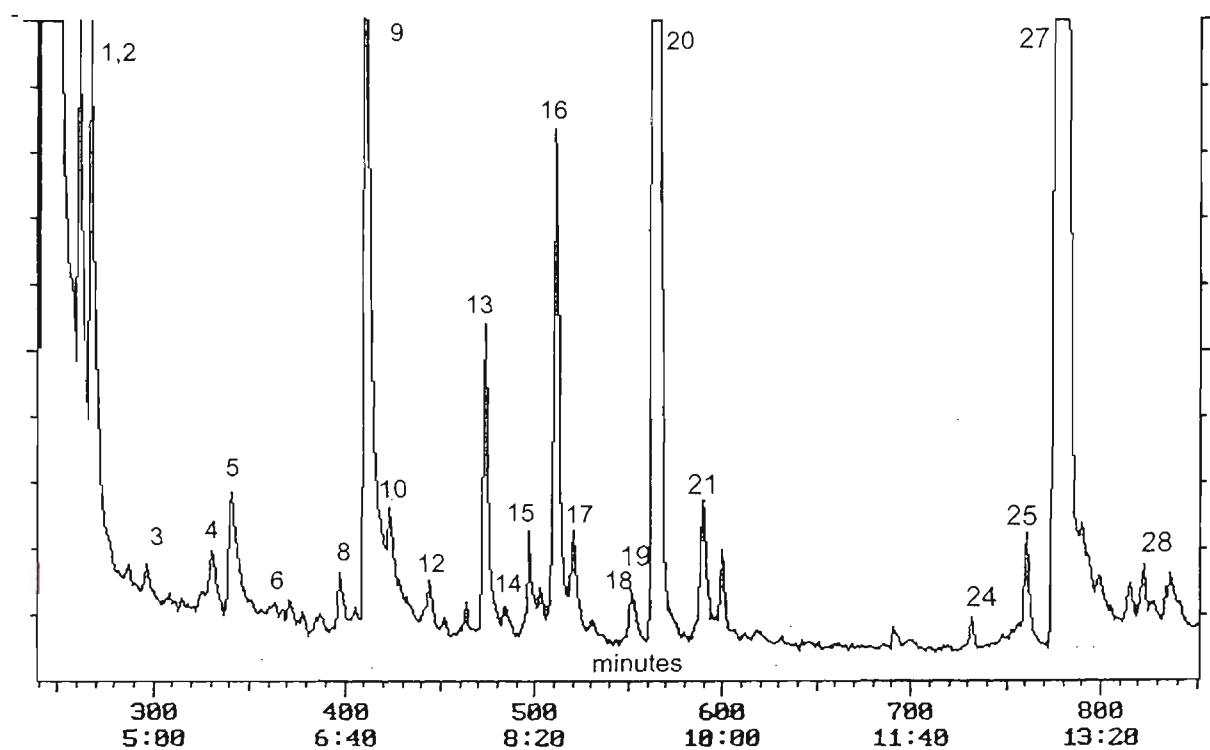


Figure 7.2 Total ion chromatograms of EtAc extracts of sultanas (50 °C) and model system (50 °C). Sultanas stored 4 days (top) arginine-glucose model systems stored 5 days (bottom).

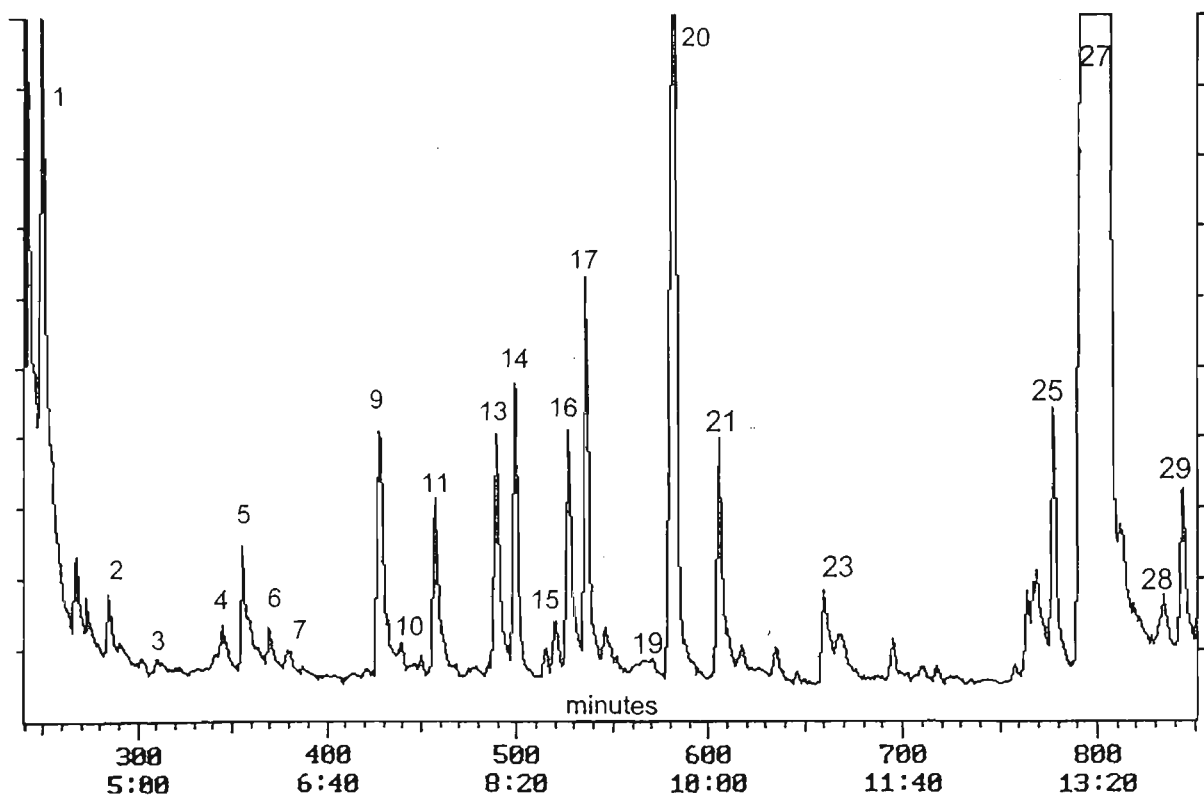
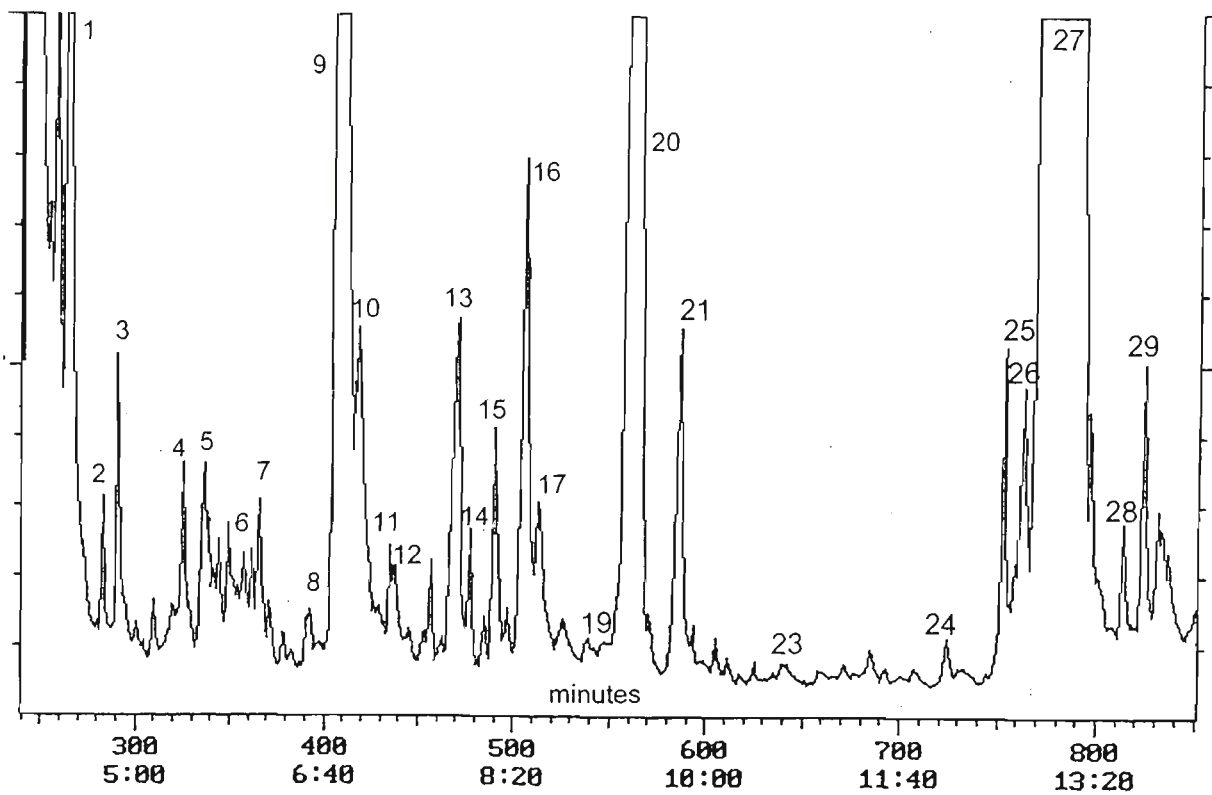


Figure 7.3 Total ion chromatograms of EtAc extracts of sultanas (60°C) and model system (60°C). Sultanas stored 2 days (top) arginine-glucose model systems stored for 4 days (bottom).

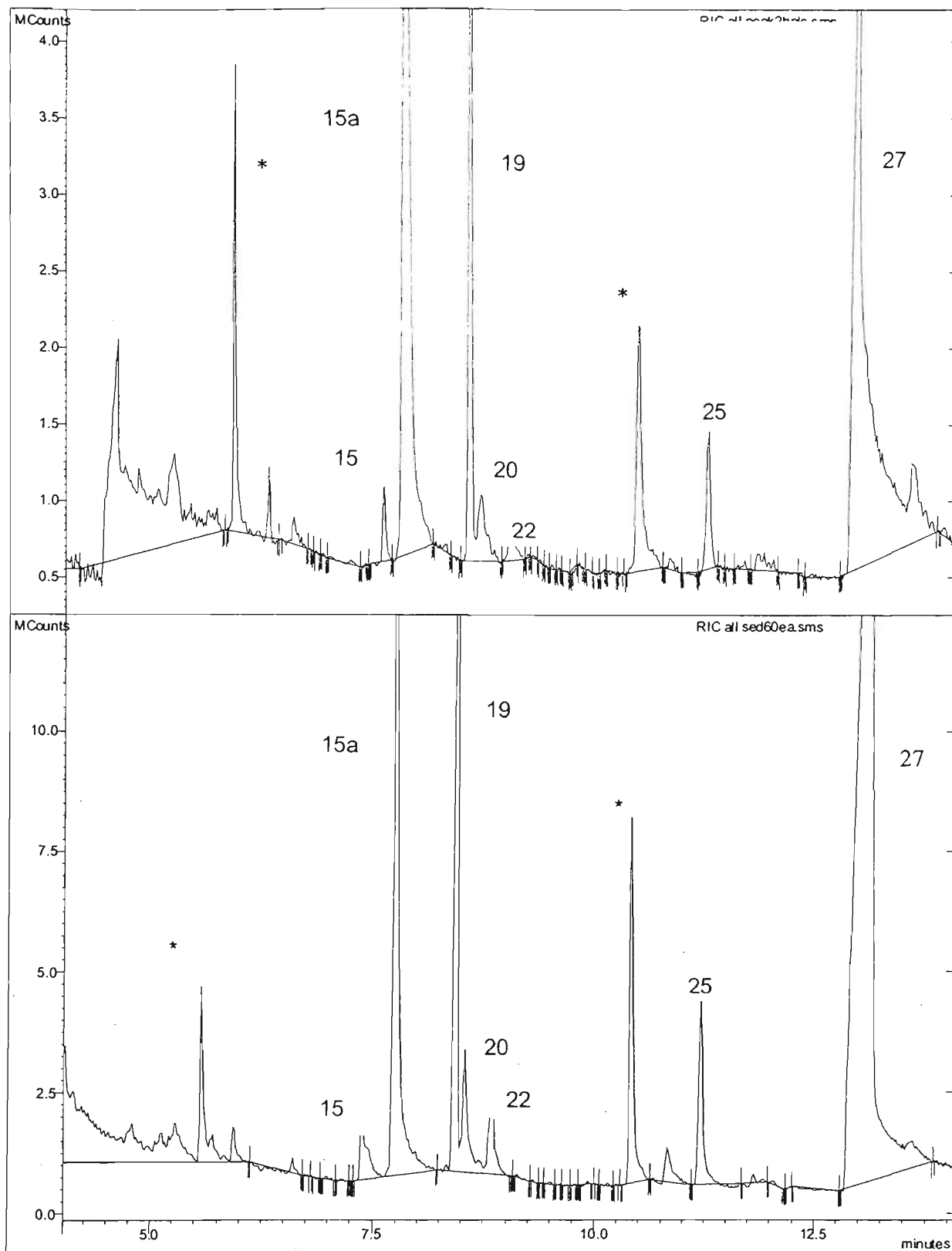


Figure 7.4 Total ion chromatogram of HPLC separated MeOH extract. (peak cluster 1 & 2-see section 5.15 and Fig. 5.10) sultana extract (top) and model (bottom: see section 5.0). See Appendix I for mass spectra\* denotes column or septum bleed peaks.

Peak N°.	t <sub>R</sub> (min)	Mass spectral fragments Sultana	Mass spectrum NIST 98 Library	Tentative ID Most likely match CAS number
1	4.4	72 (100), 43, 88, 29, 55		Most likely an arginine guanidine derivative see-N-methyl guanididne (CAS 471-29-4) or a derivative of a dihydro-2-methyl 3(2H)-furanone (CAS 3188-00-9)
2	4.5	95,97, 39, 29, 51,66	* 96, 95, 39, 29, 67, 42, 51	* Furfural (CAS 9801-1) MW 96
3	4.8	81, 97, 41, 53,68	97, 42, 69, 81, 54, 40 *98, 41, 97, 81, 53, 70, 69	Imidazole-4-hydroxymethyl (CAS 822-55-9) MW 98 * Furfuryl alcohol (CAS 98-00-00) MW 98
4		43, 101, 143, 55, 127, 72		No reasonable match in NIST library —
5	5.6	90, 61, 29, 43, 72, 31	42, 90, 43, 44, 30, 60, 74	Methanamine (CAS 4164-28-7) MW 90
6	5.9	109, 110, 53, 27, 50, 81, 39, 43	110, 109, 53, 27, 39, 51, 43, 29, 95	5-methylfurfural (CAS 620-02-0) MW 110
7		41, 86, 28, 61	42, 41, 86, 56	dihydro-2(3H)-furanone (CAS 96-48-0 MW 86)
8		43, 55, 99, 72, 27, 85		3-ethyl, 2,5-dihydrofuran
9	6.78	90, 61, 29, 43, 72, 31	42, 90, 43, 44, 30, 60, 74	Methanamine (CAS 4164-28-7) MW 90
10	6.96	91, 112, 39, 29, 41, 54, 68, 83, 84	27, 39, 112, 43, 41, 55, 83, 84	Pyridazinone (contaminated with previous compound) CAS (5157-08-4) MW 112
11		43, 115, 29, 69, 72		No reasonable match in NIST library —
12	7.31	108, 77, 91, 79, 43, 29, 50, 62, 80, 90		No reasonable match in NIST library — Probably a substituted phenol
13	7.8	43, 115, 113, 129, 55, 29, 84		No reasonable match in NIST library —
14	7.96	94, 109, 65, 39, 43, 65, 80	*94, 109, 66, 39, 43, 67, 80 ** 94, 109, 67, 53,77, 80	* 2-acetyl pyrrole (CAS 1072-83-9) MW 109 ** Ethyl methyl pyrrole (CAS 5690 960) MW 109
15	8.2	95, 39, 127, 81, 29, 108, 153	95, 126, 39, 38, 29, 67, 81, 53	Methyl furoate (CAS 13129-23-2) MW 126
16	8.43	126, 43, 55, 69, 82, 39, 103, 110	126, 55, 83,42, 45, 68, 69, 39, 111	3H-Pyrazole-3-one-2,4-dihydro-2,4,5-trimethyl (CAS 17826-82-3) MW126
17	8.58	123, 124, 95, 39, 53, 66, 108	*124, 123, 95, 94, 54, 68, 56, 66, 81, 109 ** 123, 96, 95, 43, 67, 39, 28, 82, 66, 81, 108	Pyrazine- 2-methoxy-6-methyl MW 124 (CAS 2882-21-5) 2-amino-4,6-dimethyl pyrimidine MW 123 (CAS 767-15-7)
18	9.33	86, 28, 30, 39, 41, 55, 69	86, 30, 28, 42, 58, 56	2-imidazolidinone(CAS 120-934) MW 86
19	9.10	98, 97, 68, 39, 53, 81, 42, 69	98, 41, 69, 97, 81, 39, 53, 70, 29	Furan methanol (CAS 441-2-91-3) MW 98
20	9.24	43, 144, 101, 29 55, 71, 114, 127	43, 44, 144, 101, 55, 72, 115, 126	4-H-pyran-4-one, 2,3-dehydro , 3,5-dihydroxy-6-methyl (CAS 27564-83-2 and CAS 2856483-2) MW 144 DDMP
21	9.90	142, 28, 42, 53, 67, 84, 113, 100	142, 43, 68, 55, 85, 71, 113, 96	4-H-pyran-4-one,3,5-dihydroxy-3-methyl (CAS 1073-96-7) MW 142
22	9.80	99, 43, 56,55, 71, 39	99, 43, 71, 56, 55, 69	4H-imidazole-4-one-2-amino, 1,5-dihydro CAS (503-86-6)
23	10.70	80, 109, 39, 53, 26, 91, 67, 63, 81	109, 80, 53, 29, 91, 29, 81, 63, 65	2-hydroxy-3-methylpyridine (CAS 1003-56-1) MW 109
24	12.1	120, 91, 65, 39, 53, 77, 107, 135		No reasonable match in NIST library — Probably a substituted phenol
25	12.58	126, 109, 43, 78, 81, 53, 69, 39, 96	126, 43, 79, 109, 53, 81, 97, 69, 39	5-acetoxy-methyl-2-furaldehyde (CAS 10551-1-58-3)
26		85, 43, 61, 103, 73, 31		No reasonable match in NIST library —
27	12.78	97, 126, 39, 41, 109, 69, 81, 53, 29	97, 41, 126, 39, 69, 28, 53, 109, 81	5-hydroxymethyl furfural (CAS 67-47-0) * also identified with an authentic standard
28	13.66	43, 103, 85, 68, 94, 127, 145, 110	43, 85, 103, 127, 145, 187	1,2,3-tri-O-acetyl-d-glycero-tetrolucose (CAS 78215664)
29	15.68	15, 124, 68, 136, 108, 80, 39, 53, 96		No reasonable match in NIST library — Dihydroxybenzoic acid derivative

Table 7.2 Mass spectral fragments for the peaks in EtAc sultana and model system extracts. Tentative matches are based on similarity of spectra to reference spectra in the NIST 98 spectral database. The sultana and model spectra are shown in Appendix I.

## 7.07 Interpretation of mass spectral data

It has been shown that in the initial phase of arginine-mediated Maillard reactions arginine does not react with glucose via the guanidine moiety, but rather through the  $\alpha$ -amino group (see section 2.15). Hence in the initial phase of arginine Maillard reactions 'generic' glucose degradation intermediates would be expected, i.e. furan- and pyranone- based molecules. During the Maillard reaction of sugars, retroaldol-cleavage of the sugar chain occurs to produce a large array of reactive dicarbonyl compounds, retroaldol-cleavage products, which can then undergo numerous condensation reactions (Namiki *et al.* 1973 and Weenen 1998). In the early phases of sugar fragmentation 2-carbon intermediates, such as glyoxal, predominate (Ledl and Schleicher 1990). The guanidine moiety of arginine can not initiate Maillard browning, in contrast to the  $\alpha$ -amino group. However, many of the reactive  $\alpha$ -dicarbonyl fragmentation products formed through other reactions, are known to undergo facile reaction with the guanidine group to form Maillard heterocycles unique to arginine browning systems, such as N-substituted amino pyrimidines and imidazolone compounds.

The most abundant compounds present on total ion chromatograms of both model systems and sultana extracts were peaks 9, 20 and 27. Peak 27 was identified as 5-hydroxymethylfurfural (5-HMF) from mass spectral data and coelution with standard 5-HMF (Sigma-Aldrich, Australia.). 5-HMF has been found in a large number of foods, however, it was significant that it was also the most dominant compound in aged-*sweet* red wine (Cutzach *et al.* 1999). Peak 20 was consistent with the mass spectrum of 2,3-dihydro-3,5-dihydroxy-6-methyl 4-(H)-pyran-4-one (DDMP) which is a common product formed through the degradation of glucose by primary or secondary amines, identified in many model and food systems at relatively high concentration (Ledl and Schleicher 1990, Pischetsrieder and Severin 1994, Ames 1998 and Yalayan and Kaminsky 1998). DDMP can also be formed through the degradation of Amadori intermediates under MS electron impact conditions (Yalayan and Huyghues-Despointes 1994). Cutzach *et al.* (1999), also found that very high concentrations of this compound were present in aged, sweet red wine. Peak 9, with a dominant peak at  $m/z$  90, was present at high concentration in both model and sultana EtAc extracts. There was no close match in the NIST library allowing even tentative identification, however it is suspected that the compound is a breakdown product of a guanidine residue which has undergone interaction with a sugar fragmentation product.

Of the relatively less abundant compounds in EtAc extracts, peak 1, which had a dominant fragment with  $m/z$  72, was consistent with methylene guanidine ( $C_2H_6N_3^+$ ). The peak at 44  $m/z$  is characteristic of the loss of  $CH_4N_2^+$ : this product may have been a guanidine containing breakdown product of arginine. Peak 2, present at a relatively high concentration in most samples, had a mass spectrum matching closely that of furfural. Furfural has been previously identified in a number of food systems including wine products (Cutzach *et al.* 1999). The mass spectral data for

peak 3 was consistent with a hydroxymethyl imidazole derivative or furfuryl alcohol; many imidazoles have been reported in Maillard model systems, however their reaction pathway is not well known (Vernin and Párkányi 1982). The mass spectrum of peak 4 was similar to that of peak 20 (DDMP), a common pyranose Maillard degradation product. Peak 5 was almost identical to peak 9, indicating that this moiety is likely to be an important reactive intermediate, which reacts with a number of other compounds. The mass spectrum of peak 6 had a high match with 5-methylfurfural, a common Maillard reaction product (Vernin and Párkányi 1982) which has a characteristic 'grape sweet spicy aroma' (Vernin and Vernin 1982) and has also been identified in sweet red wine (Cutzach *et al.* 1999). Structures of some of these Maillard intermediates are shown in Figure 7.5.

Peak 7 had a mass spectrum consistent with dihydro-2-(3*H*)-furanone ( $\gamma$ -butyrolactone); this unsaturated furanone has been found in nearly all foods (Vernin and Vernin 1982). Peak 8 was detected only in sultana extracts and had a mass spectrum close to that of 3-ethyl-2,5-dihydro furan. Peak 10 and peak 11, present in both sultana and model extracts, were not readily identifiable from mass spectral data. Peak 12 was only detected in sultanas. The mass spectrum of the peak was consistent with a benzyl alcohol structure; probably a grape phenolic breakdown product. Peak 13 was present both in sultana and model system extracts, however no close matches were found in the NIST-98 library. Peak 14 had a high match with the mass spectrum of either 2-acetyl pyrrole or ethyl methyl pyrrole. 2-Acetyl pyrrole has been widely identified in a large number of foods (Vernin and Vernin 1982 and Ames 1998).

Peak 15 was tentatively identified as methyl-3-furoate from mass spectral likeness to that in NIST-98 library. However, there are a number of ions present which are not in the reference spectrum; the compound in question may co-elute with another another compound or may be a part of a condensation product of two or more units. Methyl-3-furoate is described as having a 'pleasant, fruity' aroma and has been identified in cocoa and coffee (Vernin and Vernin 1982).

Peak 16, present in both sultana extracts and model, did not match completely with any compounds in the NIST-98 library. Whilst the key ions ( $m/z$  126, 127, 43 and 55) were present in a number of Maillard library compounds, library spectra also contained additional major ions.

Peak 17 was not readily identified in the NIST library, however a number of pyrazine type compounds gave possible matches such as 2-methoxy-6-methyl-pyrazine or 2-amino-4,6-dimethyl pyrimidine. Amino pyrimidine derivatives are known products of arginine (guanidine) specific Maillard reactions (Vernin and Shaffei 1982 and Ledl and Schleicher 1990).

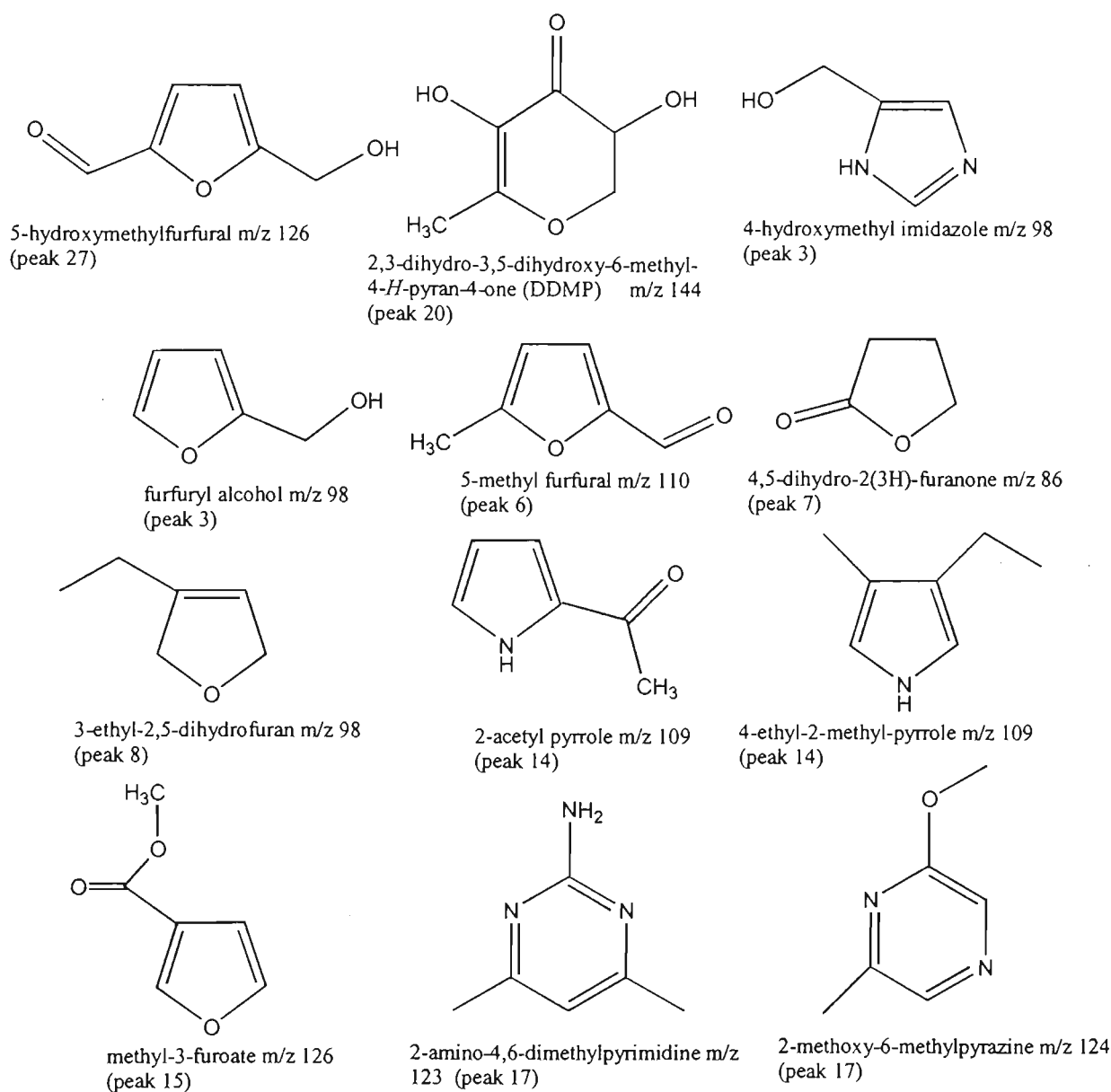


Figure 7.5 Structures of some of the Maillard intermediates tentatively identified in EtAc extracts. Compounds detected in both sultana and glucose-arginine model system extracts.

Peak 18 with an intense ion at 86 m/z possessed a mass spectrum close to that of 2-imidazolidinone (imidazolid-2-one) in the NIST-98 library. Whilst the former is unlikely, the condensation of a reactive two-carbon sugar cleavage product (i.e. glyoxal) across the guanidine moiety, and subsequent cleavage (or decomposition in the MS ion source), could conceivably result in the imidazolidinone isomeric structures a or b pictured in Figure 7.7. The former hypothesis is consistent with the fragmentation of the arginine (guanidine) specific imidazolone cited by a number of researchers (Ledl and Schleicher 1990, Henle *et al.* 1994, Lo *et al.* 1994 and Lederer *et al.* 1998.). Peak 19 gave a high match with furan methanol, also previously isolated from Maillard systems.

Peak 21, with an intense ion at  $m/z$  99 gave high match with 2-amino-1,5-dihydro-4H-imidazole-4-one (glycocyanidine) another guanidine imidazole derivative. This peak was present in relatively low concentration in both sultana and model system extracts, and was generally obscured by peak 21, however it was clearly separated in the HPLC fraction 1 & 2 of the arginine-glucose Maillard system (Figure 7.4). Peak 22 had a mass spectrum consistent with that of 3,5-dihydroxy-2-methyl-4-H-pyran-4-one (5-hydroxymaltol) which is also a well-established Maillard glucose breakdown product resulting directly from the degradation of Amadori intermediates (Vernin and Párkányi 1982); it has also been found in wine (Cutzach *et al.* 1999). Peak 23 matched closely with the mass spectrum of 2-hydroxy-3-methylpyridine; methylpyridine derivatives are abundant Maillard reaction products identified primarily in model systems (Vernin and Vernin 1982 and Ledl and Schleicher 1990).

Peak 24 was present only in sultana extracts and had a fragmentation pattern consistent with that of a phenolic type compound. Peak 25 was present in small amounts eluting just before 5-HMF on total ion chromatograms. The mass spectrum of this compound was close to that of 5-acetoxy-methyl-2-furaldehyde or 3-methyl-2-furan carboxylic acid. Peak 28 had spectral characteristics similar to that of a 'Melanoidin-like' fragment such as 1,2,3-tri-O-acetyl-d-glycero-tetrol. Whilst it is unlikely that this peak is exactly the aforementioned compound, it might be assumed many melanoidin complexes of this type would fragment in a similar manner. Peak 29 was not readily identifiable from mass spectral data.

Overall the mass spectra were consistent with previously identified Maillard intermediates. As the model and sultana extracts were not subjected to any separation or purification prior to GC-MS analysis, it was probable that for some peaks there was co-elution of compounds and hence a degree of background contamination.

### 7.08 Semi-quantification of Maillard intermediates in sultanas

Maillard reaction intermediates in EtAc extracts of sultanas were semi-quantitatively assessed by comparing the integrated ion currents of major peaks. It can be seen in Figure 7.6 that there was a large difference in the concentration of the dominant Maillard intermediates in extracts from sultanas which had been stored at 60°C; both 5-HMF (peak 27), DDMP (peak 20) and the unidentified compound (peak 9) were present at higher concentration compared to sultanas stored at 30°C or 50°C. A number of the minor MRPs were also present at a higher concentration in the extract of 60°C stored sultanas. The temperature sensitivity of Maillard reactions is well known, with increased browning rates observed at higher temperatures in model systems. The very large difference in the concentration of the major MRP in the 60°C stored samples would explain the very rapid browning observed in sultanas subjected to high temperatures, whether caused by hot-boxing or dehydrator drying.

## 7.09 Methanol extracts

As both sultana and model system extracts were completely soluble in MeOH, a small volume of the browning extracts were diluted in MeOH and subjected to GC-MS analysis. This crude method of sample preparation was expected to provide limited chromatographic separation, however it was anticipated that it may provide a 'fingerprint' of the more water-soluble browning pigments in both sultana and model systems. Figure 7.8 to Figure 7.10 show total ion chromatograms for MeOH dilutions of browning material stored at a number of temperature conditions. The individual mass spectra are shown in Appendix I. Compared with EtAc extracts, the separation of components was inferior, with a degree of peak overlap. Due to lack of separation of many peaks exhaustive spectral analysis was not attempted, as in many cases poor matches were found in the NIST-98 library. The profiles of both sultana and model extracts were similar in terms of the general shape and mass spectral data. Many of the mass spectra were the same as those found in EtAc extracts and some new peaks were present which were generally consistent with typical Maillard compounds. The dominant peaks in the MeOH dilutions were: peak 9, with the principal ion at  $m/z$  90 (EtAc peak 9), peak 12 (EtAc peak 20) and peak 20 (EtAc peak 27, which was identified as 5-HMF). A number of other peaks showed some similarity with those found in EtAc extracts such as: peak 1 (EtAc peak 3), peak 4 (EtAc peak 4), peak 5 (EtAc 21). Peak 10 from MeOH extracts had a number of fragments which were consistent with furaneol (MW 128) and norfuraneol (MW 114) coeluting together; both of these compounds are known to have very similar retention times (Buttery *et al.* 1994) The remaining peaks defied easy identification with NIST-98 spectral data. Overall, however, peak retention times and mass spectral data were similar in both sultana and model systems.

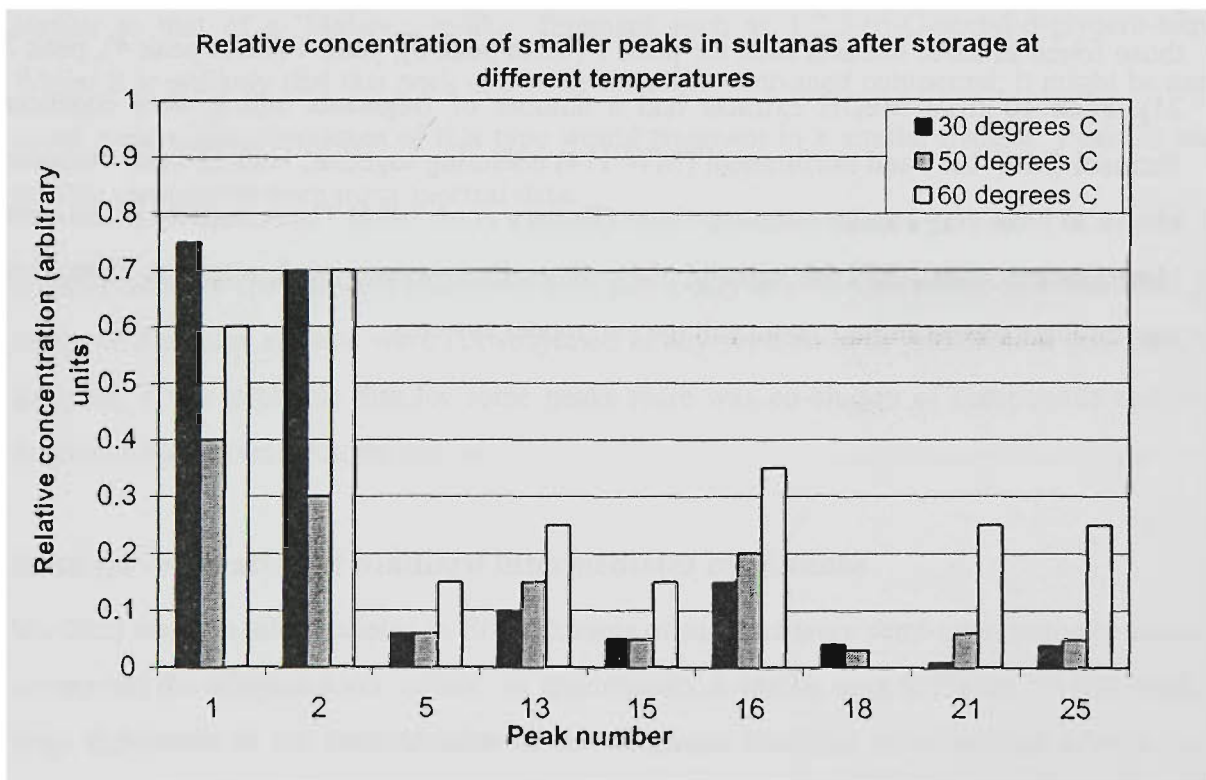
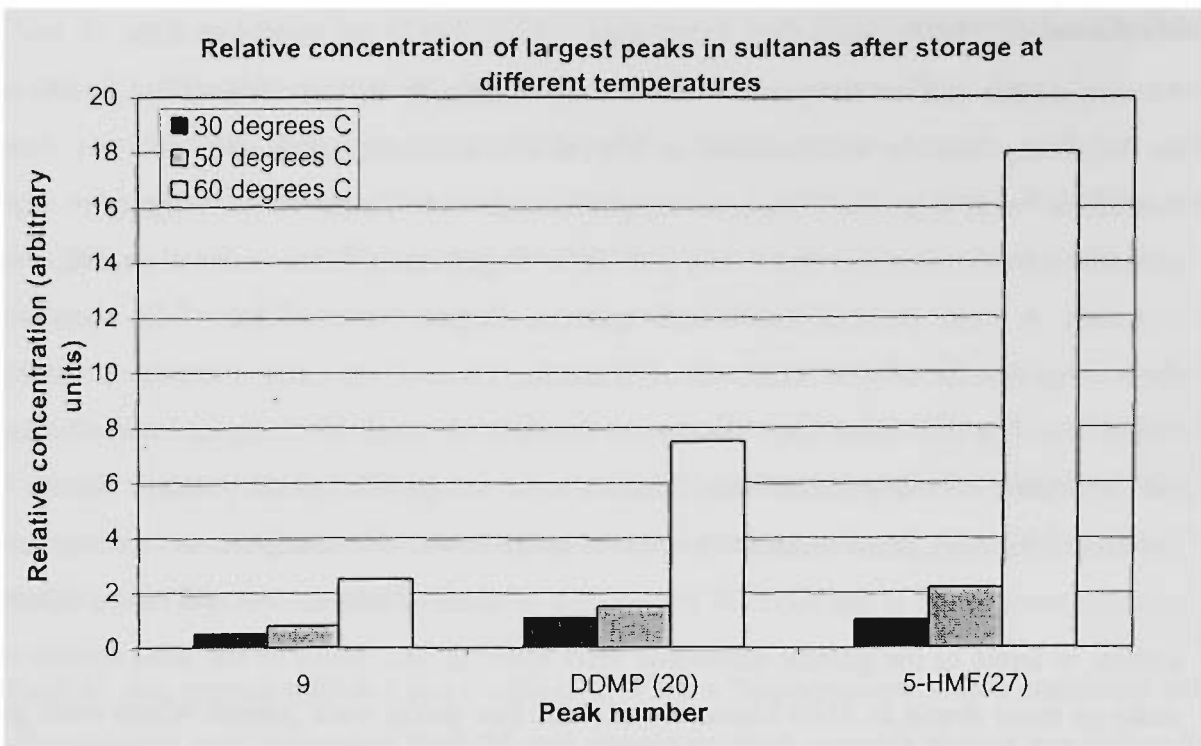


*Figure 7.6* Relative concentration of Maillard intermediates in EtAc extracts from sultanas. Stored at 30°C (10 months), 50°C (4 days) and 60°C (2 days)

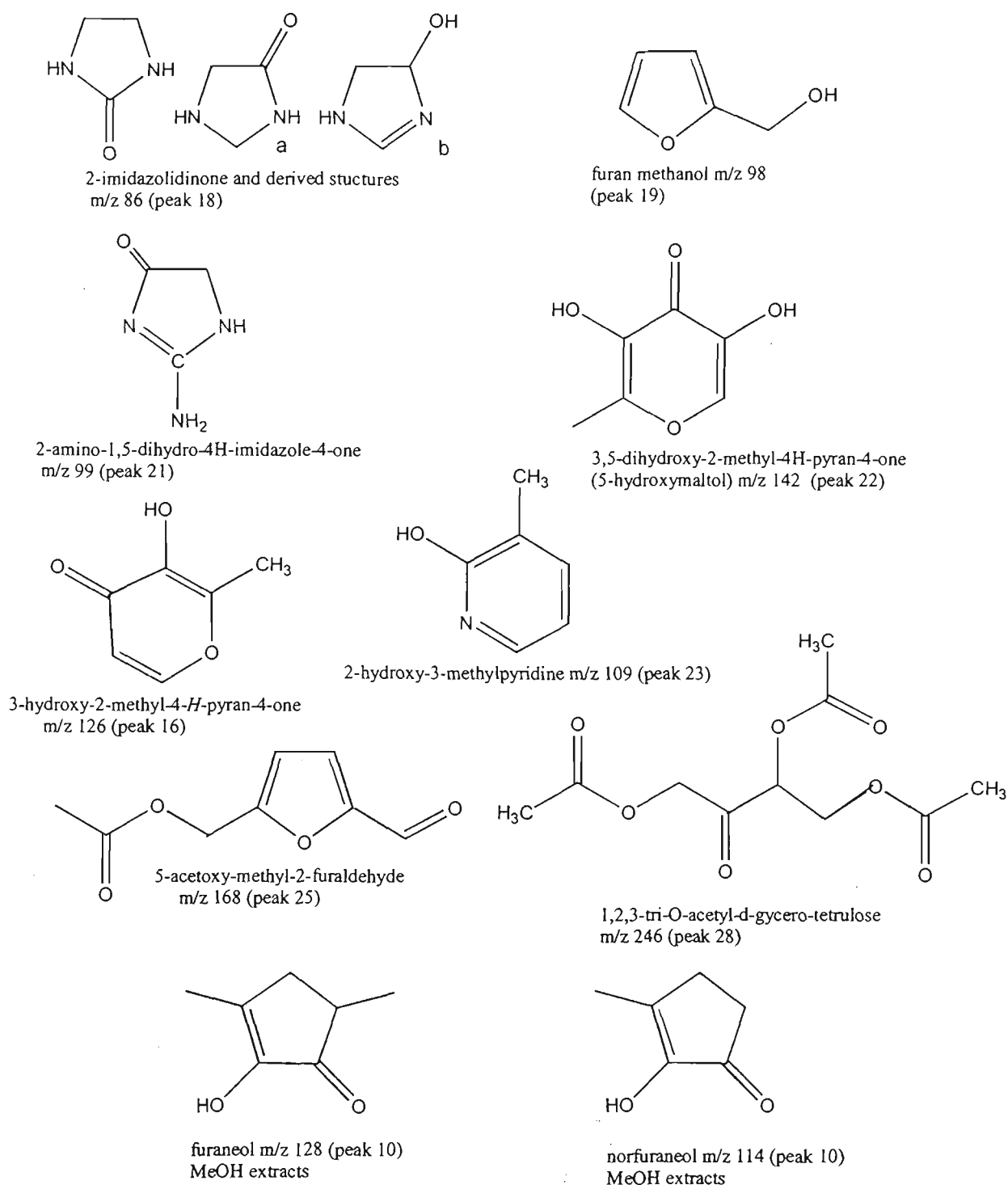


Figure 7.7 Structures of some of the Maillard intermediates tentatively identified in EtAc extracts. Compounds detected in both sultana and glucose-arginine model systems. Structures of furaneol and norfuraneol (bottom) identified in MeOH extracts.

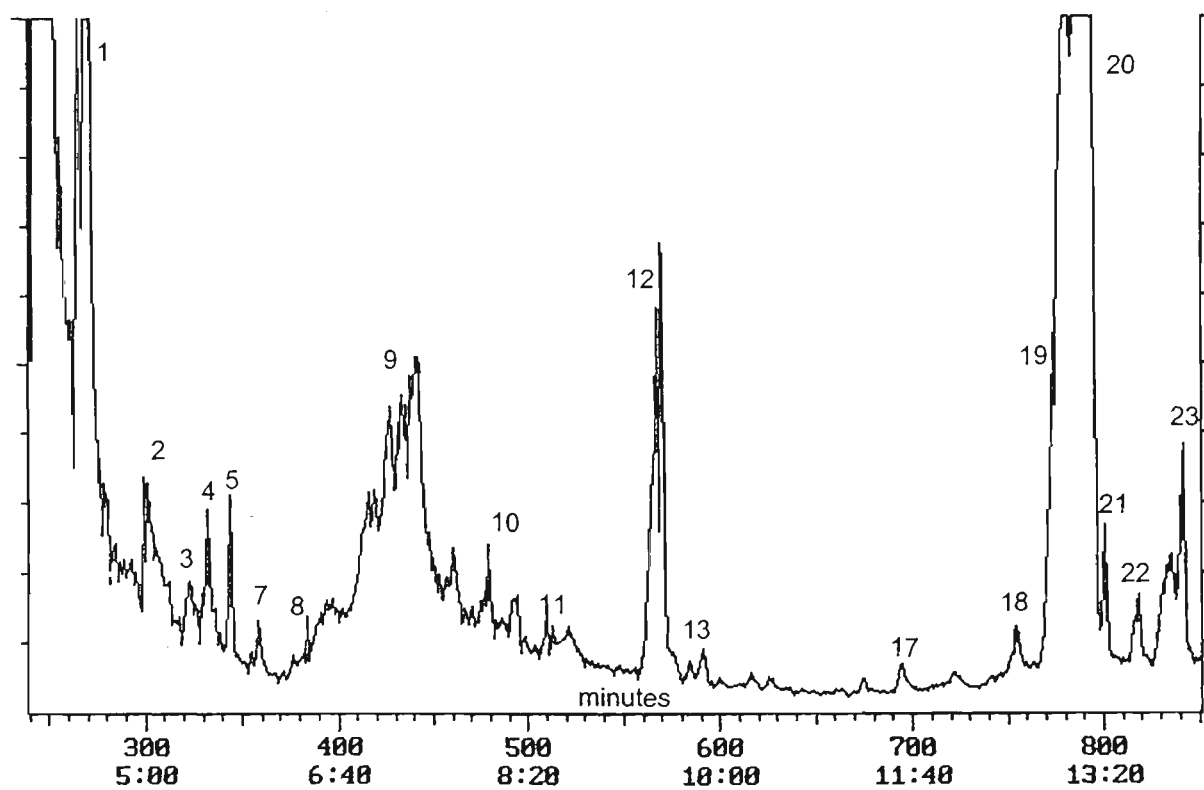
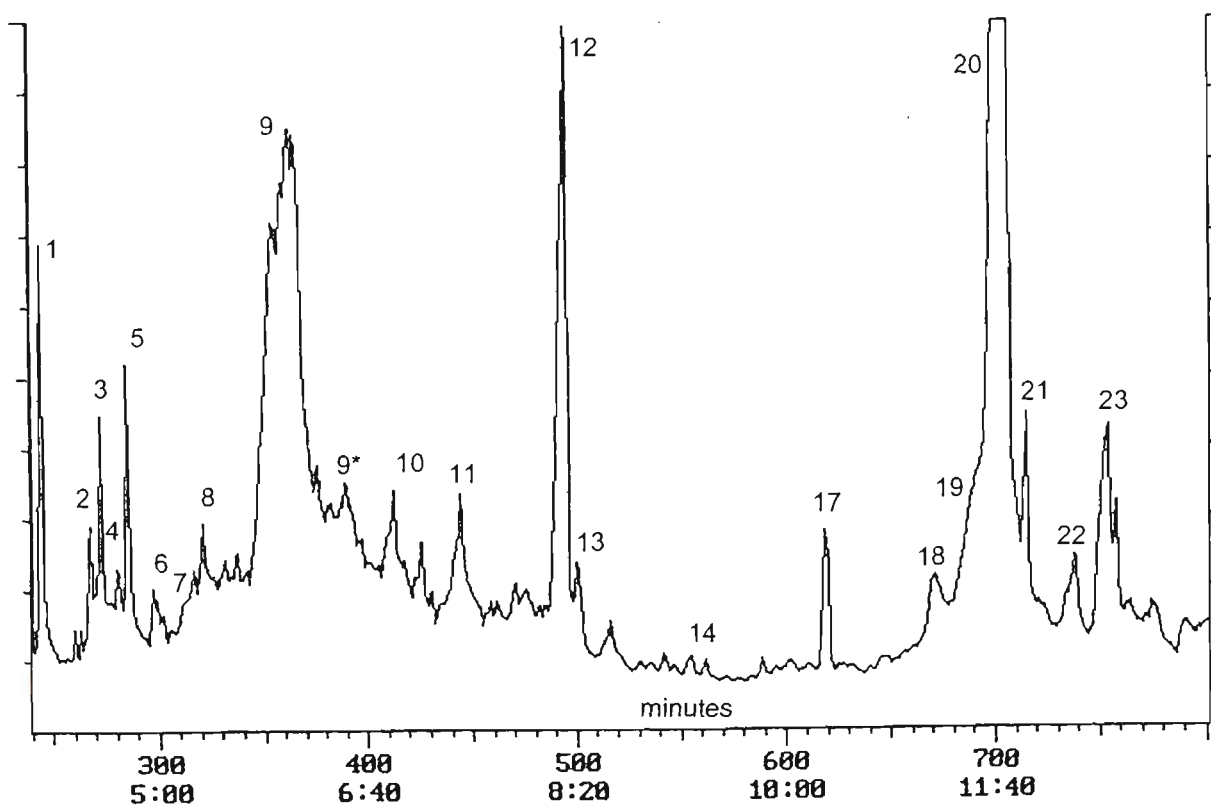


Figure 7.8 Total ion chromatograms of MeOH extracts of sultanas stored at 30°C (top) and arginine-glucose model stored at 37°C (bottom).

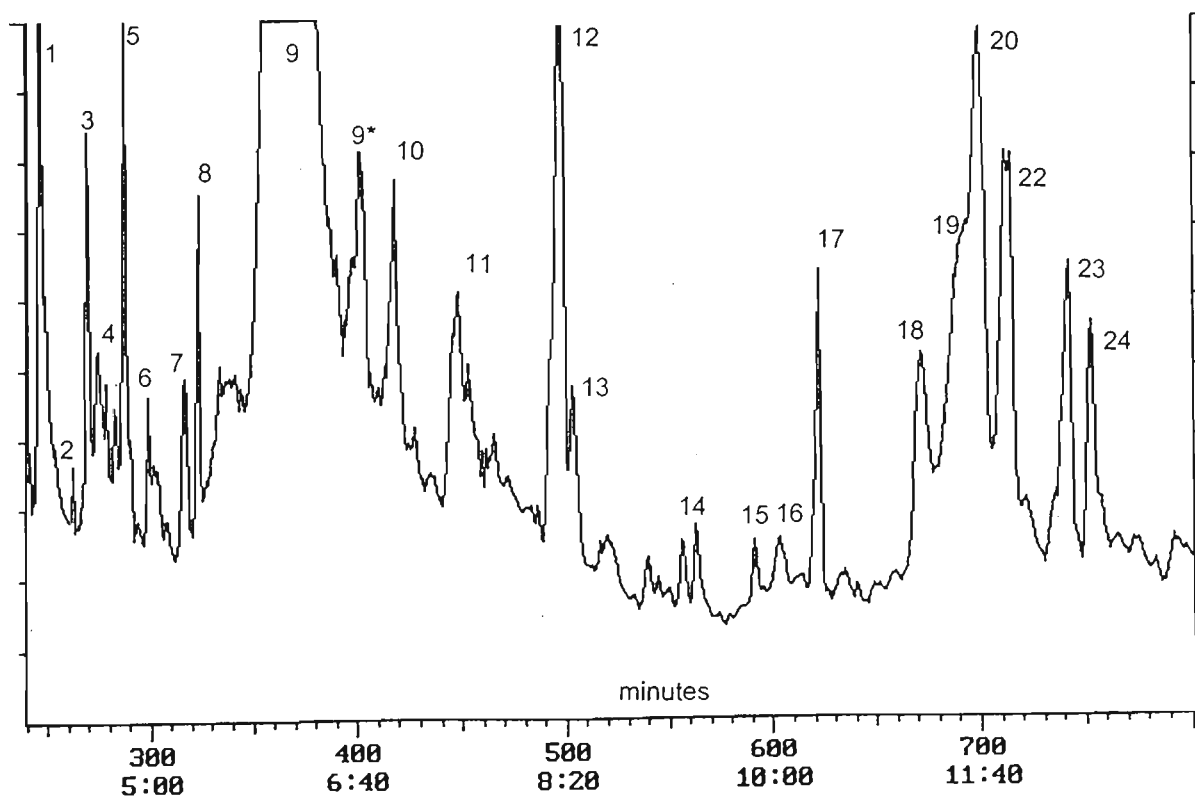
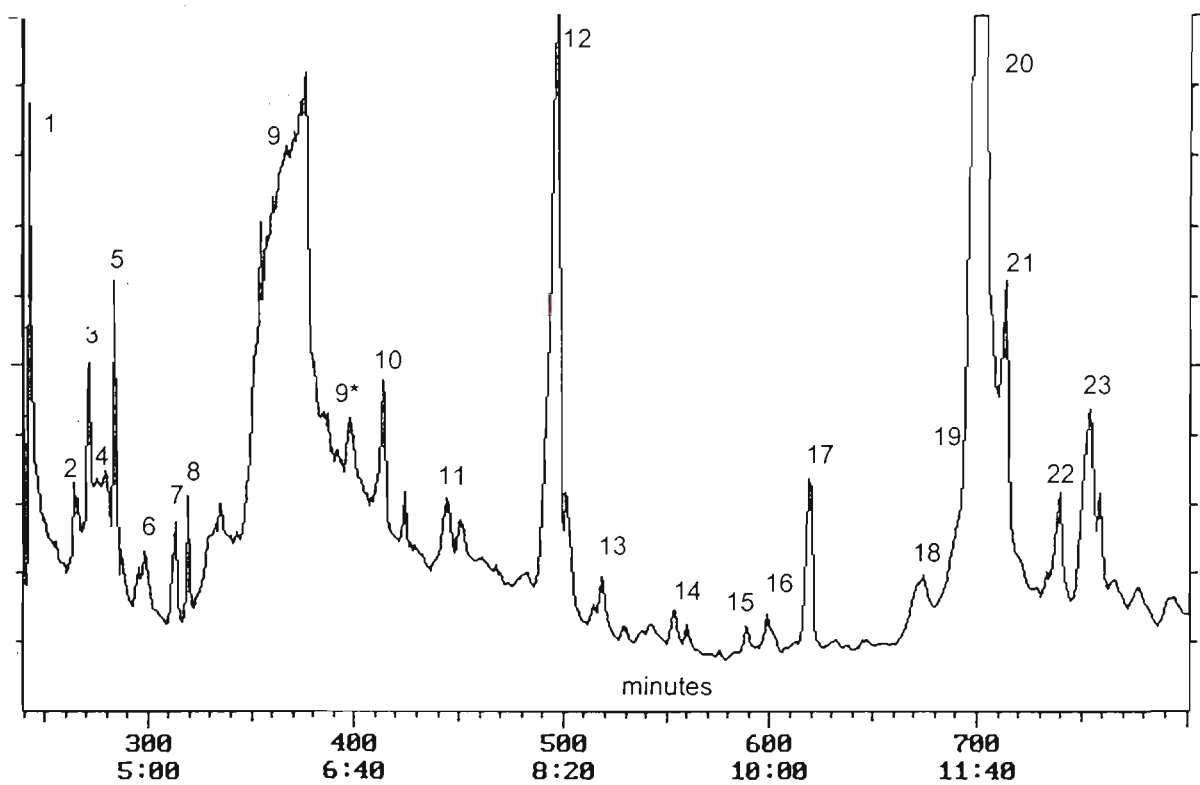


Figure 7.9 Total ion chromatograms of MeOH extracts of sultanas (top) and arginine-glucose model (bottom) stored at 50°C

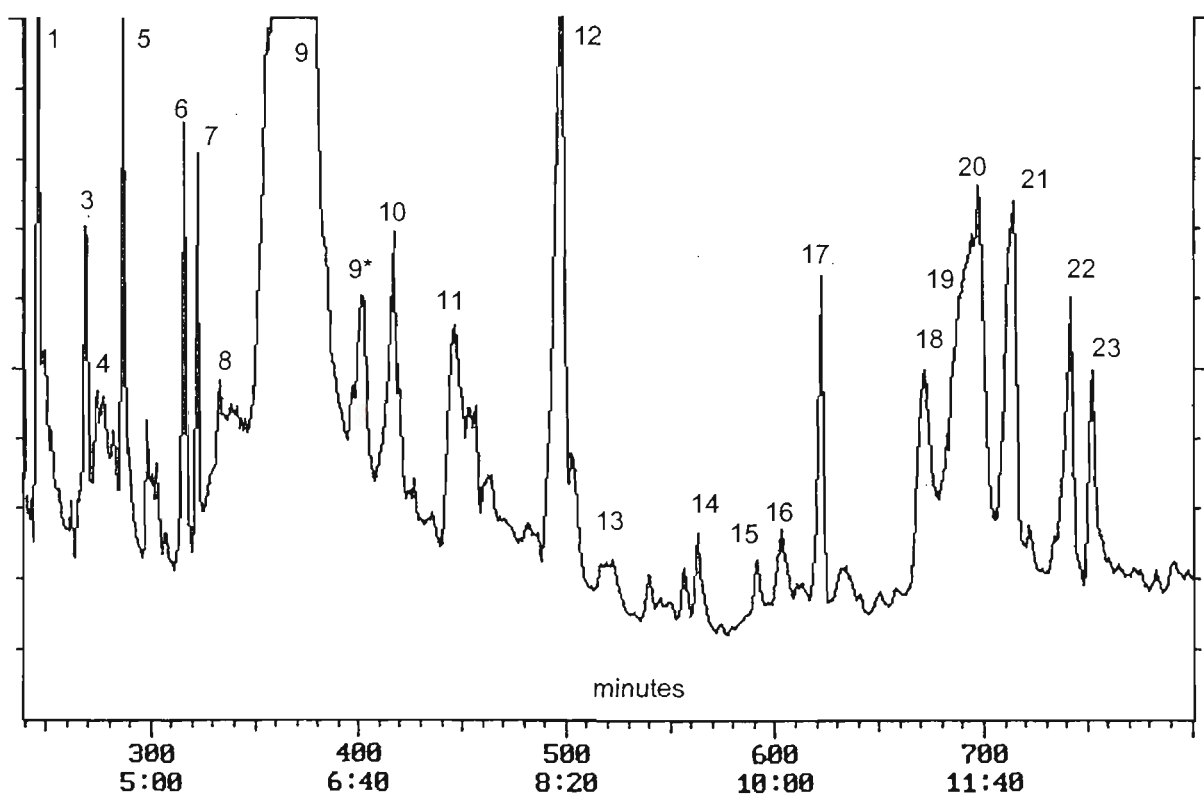
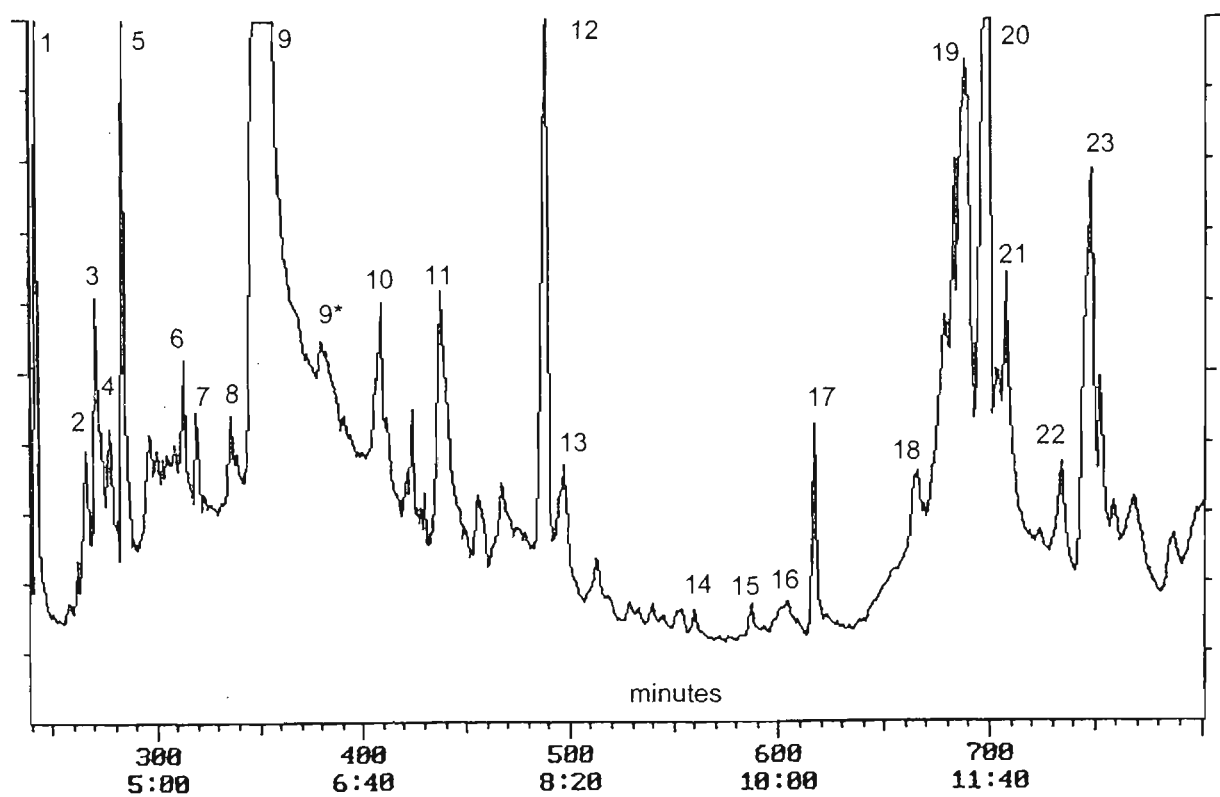


Figure 7.10 Total ion chromatograms of MeOH extracts of sultanas (top) and arginine-glucose model (bottom) stored at 60°C

## 7.10 Solid-phase micro-extraction (SPME)–GC-MS

Solid-phase micro-extraction (SPME) is a relatively new solventless sample preparation technology developed by Pawlitzyn and co-workers (Górecki *et al.* 1999) at the University of Waterloo (Ontario, Canada). The technology has been commercialised and marketed by Supelco Inc. (Bellefonte, PA, USA). The SPME fibre consists of a 1cm length of fused silica fibre coated with a polymer, which is bonded onto a stainless steel plunger. The plunger is housed inside a hollow needle barrel. The needle pierces the septum of a closed headspace sample vial and the plunger is depressed so that the fibre is exposed to the headspace gas. The fibre is left for a nominal time period to adsorb/absorb the headspace volatiles and is withdrawn back into the needle barrel. The needle is immediately transferred into a hot GC port and desorbed onto the GC column for routine GC or GC-MS analysis. SPME is claimed to be more sensitive than many other extraction concentration techniques, with an ability to concentrate volatile compounds present in the parts-per-trillion range. The main advantage of this technology is that no solvent extraction phase is needed eliminating any problems of introduction of chemical artefacts. SPME is also especially suitable for volatile analysis, as only those compounds volatile enough to exist in gas phase at the sampling temperature will be taken up by the fibre. It is important to realise that the material collected in this manner only represents the most volatile compounds from sultanas and model systems. Many of compounds isolated in this manner would be of no direct consequence to browning, however since Maillard reactions also generate many volatile odour compounds, SPME provided one further method for fingerprinting Maillard type intermediates in sultana and model systems.

## 7.11 SPME sampling

Carboxen® SPME fibres (Supelco, Bellefonte, PA, USA) and a manual SPME fibre holder (Supelco) were purchased from Sigma-Aldrich, Australia. The fibre was prepared according to the manufacturer's instructions: 40 min. in the GC injector port set at 280°C, with a He flow of 1.7 mL.min<sup>-1</sup> in split mode (1:100). The fibres were desorbed and run through the GC temperature gradient to remove any fibre bleed artefacts from the column until a clean flat baseline was present.

Sultanas, which had been stored at 30°C for 10 months and subsequently held at -20°C storage, were used. A model arginine-glucose Maillard mixture was made up using a saturated glucose Milli-Q water paste and adding arginine to attain a final concentration of 10 mg.g<sup>-1</sup> arginine. The browning mixture was held at 55°C for 48 h until red-brown colour was obtained. An aliquot of

FeCl<sub>2</sub> was added to the browning mixture to give a final Fe concentration of 10 µg.g<sup>-1</sup> and the mixture was held for a further 24 h at 50°C until the Maillard mixture was dark red brown.

Sultanas were macerated with a mortar and pestle in a small amount of Milli-Q water. GC headspace sampling vials with a nominal volume of 20 mL (Alltech Australia) were filled with either sultanas or Maillard solution such that a 2 mL deep headspace remained in the vials. The vials were made air tight with an aluminium crimp closure with a silicone-teflon coated septum (Alltech Australia) ready for SPME extraction as described above. The fibre remained in position to concentrate the headspace material through equilibrium 'adsorption' for 20 hours at ambient temperature (approximately 25°C) or at 65°C for 1 hour. After adsorption the fibre was immediately inserted into the GC injector port for GC-MS analysis. The fibre was desorbed for 5 minutes before retraction and subsequent re-use.

A Varian Star 3400 gas chromatograph connected to a Varian Saturn 2000-ITMS were used to obtain data. A polar Econowax-TM (Alltech, Australia) ethylene glycol phase capillary column was used for the separation: (30 m, 0.32 i.d., 0.5 µm phase). The GC injector (Varian 1077) was held isocratic at 200°C for all injections. A suitable deactivated glass injector insert sleeve with a narrow i.d. (0.7 mm) for SPME work was used. The split vent valve was activated to splitless mode for the first minute of fibre desorption and then programmed to split mode for the remainder of the run (split ratio 1:50). The GC oven was temperature programmed as follows: the initial column temperature of 45°C was held for 8 min and the temperature was increased at 5°C. min<sup>-1</sup> to a final temperature of 190 °C and held at that temperature for 5 min. The He column linear flow rate was set at approximately 1.7 mL. min<sup>-1</sup> at a column temperature of 45°C. The Saturn ITMS module was operated with the parameters shown in Table 7.3.

Ionisation Mode	EI-70 eV	Transfer line temperature	200 °C
Scan range	15 – 400 amu	Multiplier Set Voltage	1650 V
Filament delay time	30 s	Manifold Set Temperature	60 °C
Segment acquire time	42.00 min	Emission Set Current	10 µA

Table 7.3 *Varian Saturn 2000-ITMS instrument settings for SPME analyses*

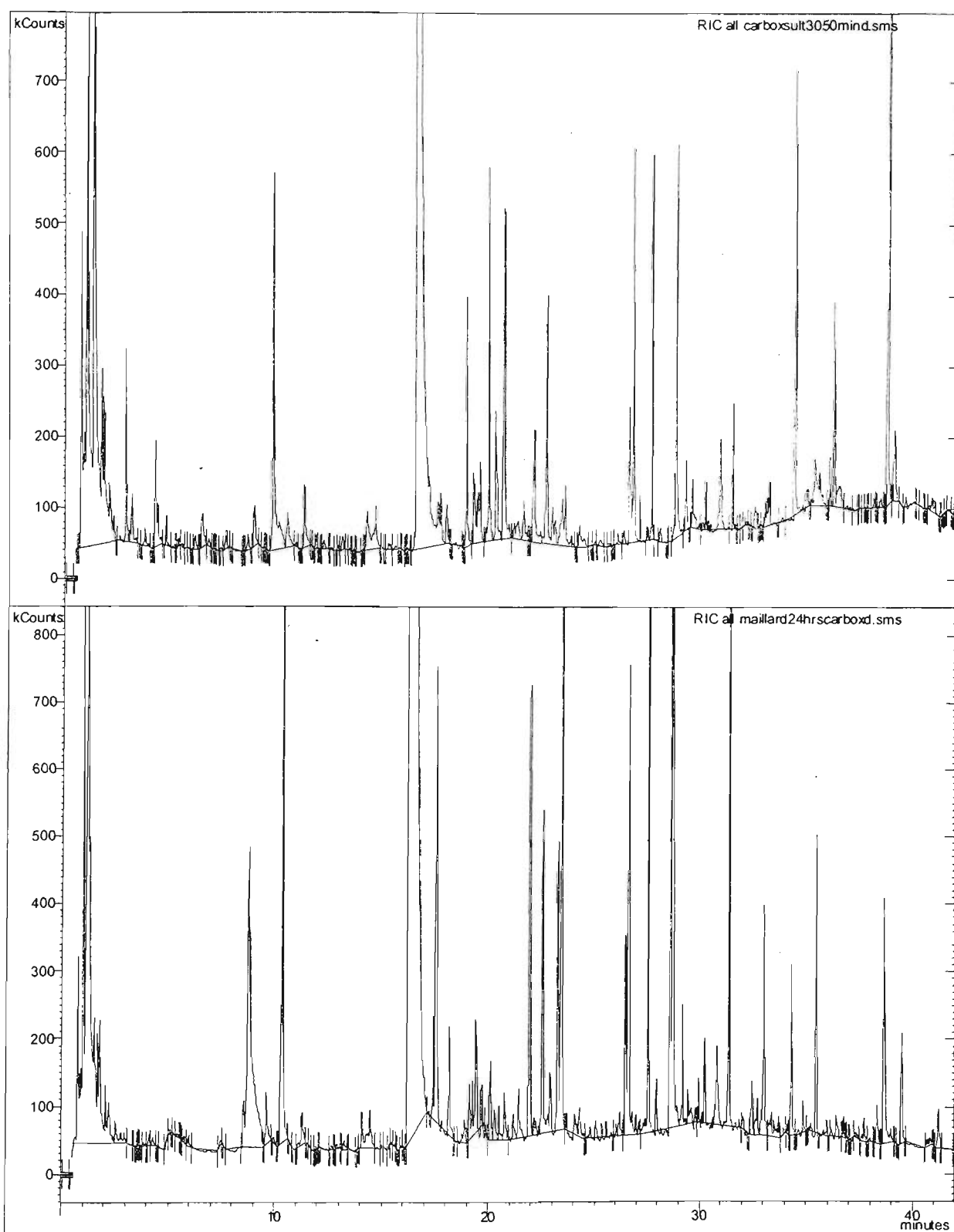


Figure 7.11 Total ion chromatogram for SPME analysis of sultana and arginine-glucose model headspace.  
 Top: sultanas stored at 30°C for 10 months. Bottom: arginine-glucose browning model headspace (72 h at 50°C).

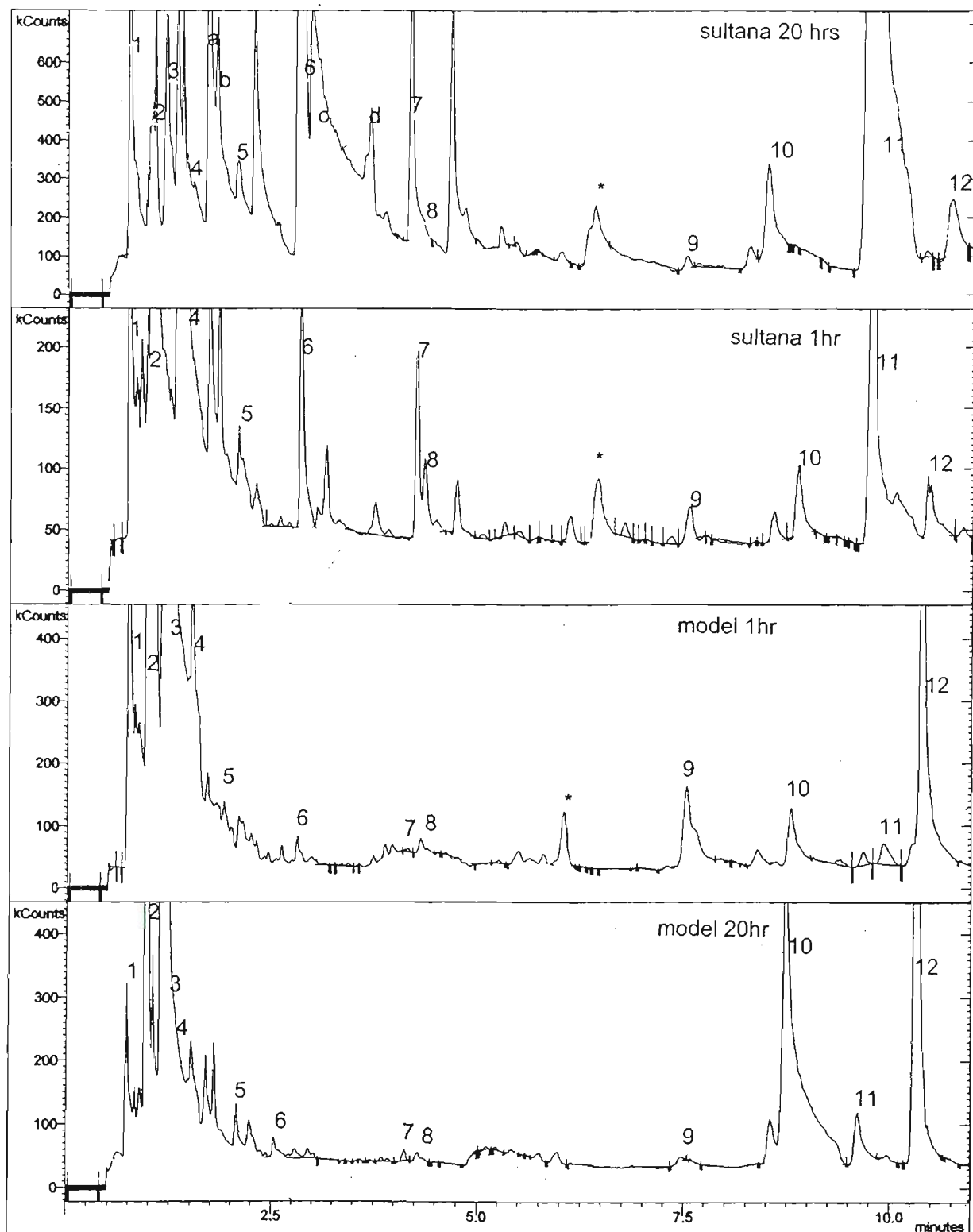


Figure 7.12 Expanded view of total ion chromatogram for Carboxen fibre sampling (0.5-12 minutes) Peaks with an asterisk are column bleed. Peaks marked by a letter were in sultanas only.



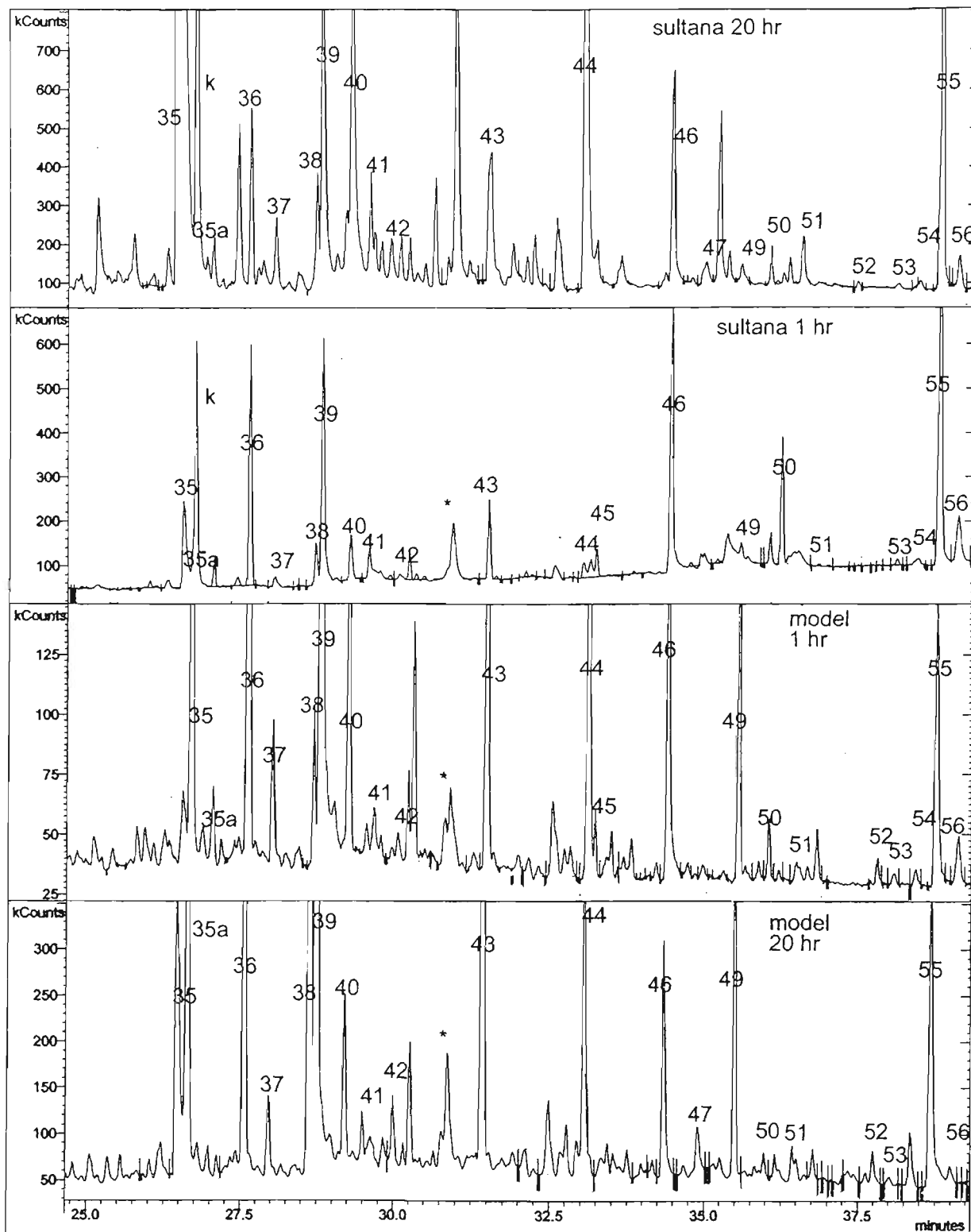


Figure 7.14 Expanded view of total ion chromatogram for Carboxen fibre sampling (25-41 minutes). Peaks with an asterisk are column bleed. Peaks marked by a letter were in sultanas only.

Peak N°.	t <sub>R</sub> min	Mass spectral fragments	Tentative ID Most likely match CAS Number
1	0.711	44, 32	dimethylamine (CAS 124-40-3) MW 44
2	0.96	68, 39	furan (CAS 110-00-9 ) MW 68
3	1.2	44, 82, 81, 53, 39	2-methyl furan (CAS- 534-22-5)
4	1.50	44, 57, 81, 82, 71	3-cyclopentene 1,2-diol, cis (CAS 694-29-1)
5	1.52	44, 57, 81, 39, 53, 82, 50	
6	2.83	41, 39, 56, 67, 82, 71	
7	4.12	41, 56, 55, 70,	2 (3H)-furanone-dihydro-4-methyl (CAS 167-9-49-8)
8		57, 41, 71, 109, 83	
9	6.78	67, 97, 109, 57, 39, 81, 123, 137	
10	8.8	43, 72	Methyl glyoxal (CAS 78-98-8)
11	9.7	45, 43, 89, 88, 71	3-hydroxy butanone (CAS 513-86-0)
12	10.27	44, 75, 43	
13	11.15	44, 73, 58	butanamine (CAS 33966-50-6) N,N-dimethyl formamide (CAS 68-12-2)
14	11.27	108, 42, 52, 66, 80, 93	2,6-dimethyl pyrazine (CAS 694-81-5) 4,5-dimethyl pyrimidine (CAS 694-81-5) 2-H-pyranone derivative (CAS 3720-22-7)
15	12.99	56, 55, 41, 69, 40, 75, 82	
16	14.08	41, 67, 55, 81, 96, 122, 109	
17	15.45	97, 109, 123, 137, 69, 81, 66, 41	
17a		43, 61, 87	isopropyl acetate (CAS 108-214)
18	16.54	43, 61, 97, 96, 95, 69	furfural (CAS 98-01-1)
19	17.44	95, 39, 43, 96, 67, 55, 81	1H-pyrazole-3,5-dimethyl (CAS 67-51-6)
20	17.59	95, 110, 39, 67, 81	acetyl furan (CAS1192-62-7)
21	17.92	105, 77, 51, 50	3-ethenyl pyridine (CAS 1121-55-7)
22	19.16	73, 74, 45, 55, 56, 57	hexanediol (CAS 82360-67-6)
23	19.42	109, 110, 53, 81, 39	5-methyl furan carboxaldehyde (CAS 620-02-0)
24	19.68	68, 96, 42, 39, 50, 54	2H-pyran-2-one (CAS 504-31-4)
25	20.16	109, 124, 103,	2-acetyl-5-methyl furan
26	20.37	57, 71, 43, 41, 85, 84	
27	20.53	41, 42, 39, 87, 56	
28	21.66	111, 55, 67, 43, 83, 98, 126	
29	22.01	97, 81, 98, 69, 39, 42, 53	3-furan methanol (CAS 98-00-0)
30	22.56	97, 57, 55, 123, 137, 81, 67, 109	
31	22.98	57, 97, 67, 148, 146, 71, 123, 109, 163, 136	
32	23.27	57, 70, 41, 39, 97, 83, 143, 159	
33	23.36	95, 112, 111, 43, 50, 55, 69, 83	5-methyl-1H imidazole-4-methanol(CAS 29636-87-1)
34	23.68	55, 84, 39	2(3H) furanone (CAS 20825-71-2)
35	26.48	60, 73, 55, 41, 89, 45, 87	butanoic acid (CAS 107-92-6)
36	27.58	205, 220, 177, 145, 57, 91, 105, 121	butylated hydroxytoluene (CAS 128-37-0) probably contamination
37	28.01	135, 108, 219, 40, 69, 82	
38	28.59	94, 109, 66, 39, 53, 80	2-acetyl pyrrole (CAS 1072-83-9)
39	28.73	69, 55, 41, 53, 97, 111, 124	
40	29.16	95, 55, 69, 39, 23, 113, 123	
41	29.55	94, 66, 65, 39	5-methyl pyrimidine (CAS 2036-41-10)
42	30.06	57, 128, 97, 39, 69, 83, 107	
43	31.42	165, 180, 137, 57, 123, 193, 109, 151	probably fibre artefact
44	33.01	60, 73, 39, 115, 129, 87, 97	
45	33.10	221, 143, 91, 128, 77, 105, 115	
46	34.32	43, 144, 101, 55, 115, 72	2,3-dihydro-3,5-dihydroxy-6-methyl-4H-pentanone (CAS 28564-83-2)
47	34.80	73, 129, 60, 55, 41, 87, 142, 115, 101, 163	
48	35.55	191, 57, 163, 206, 175, 91, 107	
49	35.65	43, 102, 56, 70, 191	
50	36.22	149, 177, 176, 105, 65	
51	36.82	143, 221, 236, 91, 128, 105, 115, 193	
52	37.74	136, 107, 91, 77, 57, 41	
53	38.01	85, 57, 39	2-H-pyran derivative (CAS 1927-63-5) (CAS694-54-2)
54	38.36	219, 191, 175, 214, 91, 57, 115, 147	
55	38.65	97, 69, 39, 126, 53, 81, 109	5-hydroxymethyl-2-furancarboxaldehyde (CAS 67-47-0)
56	39.44	149, 173, 55, 104, 76	probably fibre artefact

Table 7.5 Most abundant mass spectral fragments for the peaks from 'Carboxen' - SPME fibre. Peaks found in both sultana and arginine-glucose model system headspace. Tentative matches are based on similarity of spectra to reference spectra in the NIST 98 spectral database. The sultana and model spectra are shown in Appendix I.

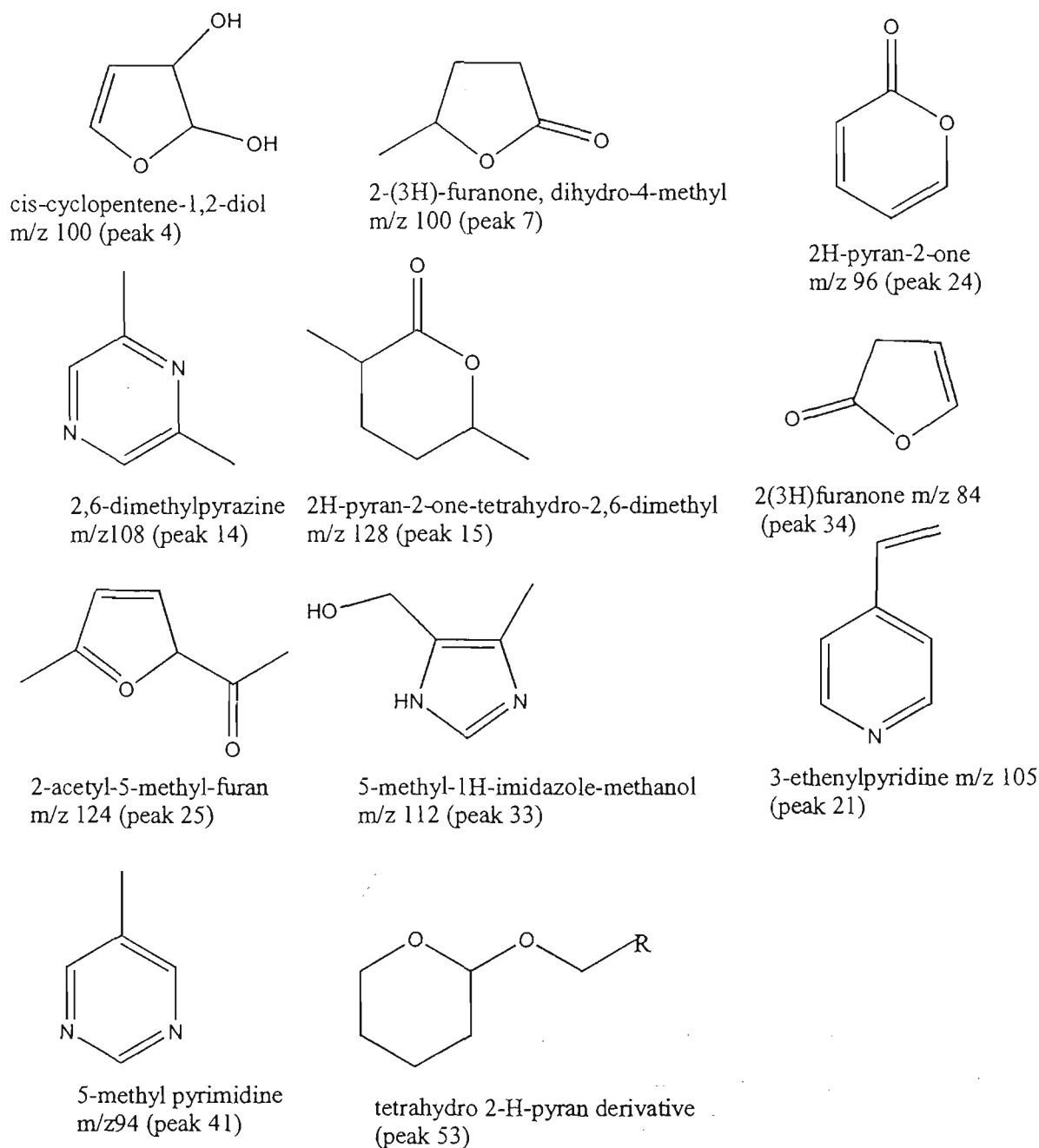


Figure 7.15 Structures of some of the Maillard compounds present in SPME extracts. Tentatively identified from spectral likeness with spectra in the NIST-98 library.

## 7.12 Interpretation of mass spectral data

The SPME fibre was able to absorb at least 56 similar compounds from both sultana and arginine-glucose model headspace, but the relative concentration of some peaks was quite different. Only a few of the compounds analysed by more conventional methods (EtAc and MeOH extraction) were present in the fibre extracts. The major peaks 5-HMF (peak 55) and DDMP (peak 46) were present in SPME samples as well as some other peaks such as 5-methyl furfural (peak 23), furan methanol (Peak 29), 2-acetyl-pyrrole (peak 38).

Many peaks not present in either EtAc or MeOH extracts were not easily characterised by reference to NIST-98 library data. Peaks, which had close matches to library mass spectra, were given tentative identification (Table 7.5). The most dominant peak (peak 18) had a mass spectrum very close to furfural (2-furaldehyde) or 3-furaldehyde; it has been identified in many foods and is described as having a caramel-like flavour (Vernin and Vernin 1982). Furfural was the one of the most concentrated Maillard compounds isolated from sweet red wine after six-months aging (Cutzach *et al.* 1999). Other typical Maillard compounds included furan (Peak 2) found in a number of foods and described as having an ethereal sickly smell (Vernin and Vernin 1982), 2-methyl furan (peak 3), peak 4 (3-cyclopentene-1,2-diol), tetrahydro-3,6-dimethyl-2-H-pyranone (peak 7), 2,6-dimethyl-pyrazine (peak 14) 3,5-methyl-pyrazole (peak 19), acetyl furan (peak 20), 2H-pyran-2-one (24), 2-acetyl-5-methyl furan (peak 25), an imidazole derivative (peak 33), a 2-(5H)-furanone (peak 34), butanoic acid (peak 36) and a 2-H-pyran derivative at peak 53. Other peaks may have been some non-heterocyclic Maillard intermediates such as: peak 12 (1,2-propane-diol, 2 acetate), 17a (acetic acid methyl ethyl ester), peak 22 (hexanediol), peak 35 (butanoic acid) and peak 37 (perhaps some kind of adenine derivative). In addition there were a number of peaks which were almost definitely fibre artefacts: peak 21 (acetophenone), peak 36 (butylated hydroxy toluene), peak 43 and peak 56; these peaks were also present in blank fibre runs. None of the Maillard compounds were particularly arginine-specific; many arginine-derived heterocycles are water-soluble and probably were not sufficiently volatile to be picked up by the fibre. There were a number of peaks present only in sultana samples which could not be identified from their mass spectra: peaks a and b ( $m/z$  43, 57, 69, 85), peak c (41, 56, 69, 83, 98  $m/z$ ), peak d (56, 41, 63, 69  $m/z$ ), peak f (73, 45  $m/z$ ) peak g (87, 41, 39  $m/z$ ) and peak h (69, 81, 95, 57, 41  $m/z$ ). Peak k (79, 77, 107, 108, 91, 51  $m/z$ ) had a mass spectrum consistent with benzyl alcohol. Often the sultana mass spectrum had additional material compared to the model peak (see Appendix I), indicating chromatographic coelution of peaks. The utility of using the model reference mass spectrum to filter out contaminant material is immediately apparent.

### 7.13 Conclusions

GC-MS analysis of EtAc, MeOH and SPME volatiles of sultana and arginine-glucose browning systems furnished further evidence of the existence of sultana storage Maillard reactions. Many of the compounds tentatively identified were furan- and pyran-derived compounds which are known to be ubiquitous glucose Maillard degradation products and important components of polymeric melanoidin material. The presence of a number of arginine specific compounds previously cited by other researchers was tentatively inferred via mass spectral data. Both imidazolone- and pyrimidine- type structures are formed directly through the reaction of guanidine with a reactive dicarbonyl fragment as cited by Tressl *et al.* (1990) and by Belitz and Grosch (1999). General imidazolone and pyrimidine structures and their formation are shown in Figure 7.16.

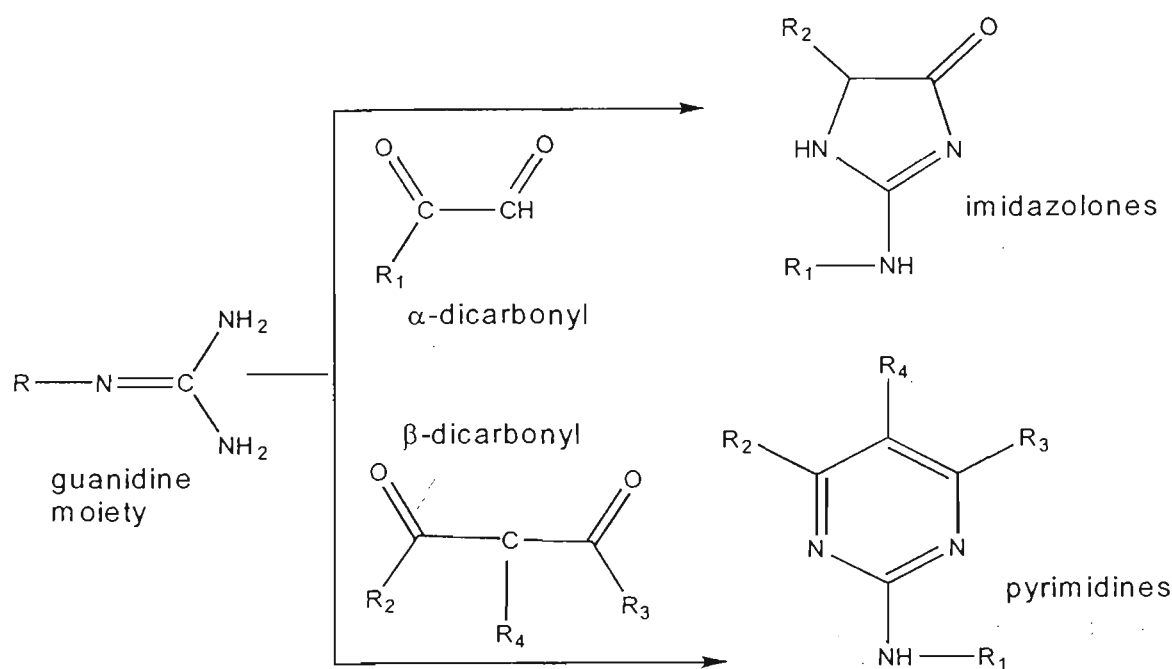
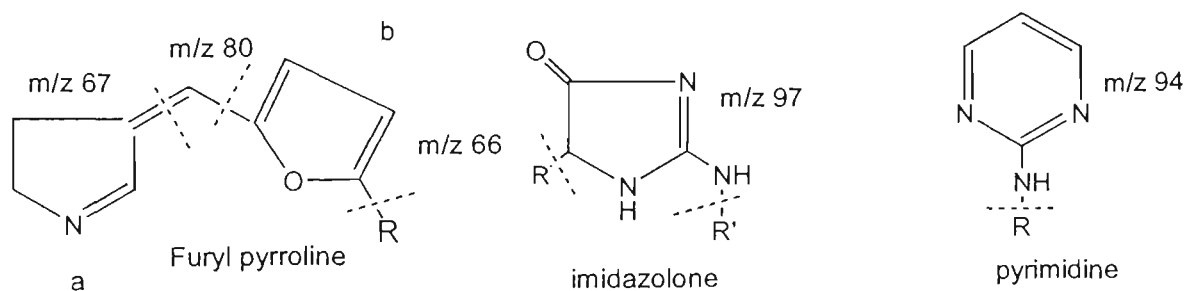


Figure 7.16 Typical arginine-specific Maillard products.  
 Top: identified by Tressl et al. (1990). Bottom: general reaction scheme for the guanidine moiety proposed by Belitz and Grosch (1999).

Imidazolone structure			pyrimidine structure				
R <sub>1</sub>	R <sub>2</sub>	m/z	R <sub>1</sub>	R <sub>2</sub>	R <sub>3</sub>	R <sub>4</sub>	m/z
H	H	99	H	H	H	H	95
H	CH <sub>3</sub>	113	H	H	CH <sub>3</sub>	H	109
CH <sub>3</sub>	CH <sub>3</sub>	127	H	CH <sub>3</sub>	CH <sub>3</sub>	H	123

Table 7.6 Expected  $m/z$  values for  $M^+$  fragment of imidazolone and pyrimidine structures. Showing the  $m/z$  with various R substituents. See Figure 7.16 above.

Table 7.5 shows expected  $M^+$   $m/z$  values for various R groups attached to the structures shown in Figure 7.16. It was shown that peak 21 in EtAc extracts had a mass spectrum consistent with the reaction product of glyoxal and guanidine: 2-amino-1,5-dihydro-4H-imidazole-4-one. The mass spectrum of this peak from both sultana and model extracts was very close to the mass spectrum of this compound in the NIST-98 spectral database (CAS 503-86-6). Peak 17 was consistent with 2-amino-4,6-dimethylpyrimidine (CAS 767-15-7), which could also be expected to form through the reaction of a sugar  $\beta$ -dicarbonyl with guanidine. Most of the compounds present were, however, not arginine-specific, which may be partially explained by the low volatility of guanidine derivatives.

The mass spectral profiles of sultana and arginine-glucose model systems did, however, provide evidence that Maillard reactions occur in sultanas and that much of the material was similar to that found in arginine-glucose model systems. The differences in relative concentration of compounds was not surprising given the sensitivity of Maillard reactions to factors such as  $a_w$ , pH, temperature etc. 5-HMF was the only positively identified compound present. The identity of the other peaks was not confirmed with authentic standards; their identity remains to be proven in further studies. Differences in compounds between MeOH and EtAc were partially explained by the different polarities of each solvent, and also that EtAc samples were extracted, whereas MeOH samples were simply diluted from alkaline solutions. Exhaustive identification of compounds would require separation into pure components via a semi-preparative method such as HPLC or thin layer chromatography with GC-MS and NMR investigations.

## 8.0 BROWNING MODEL SYSTEMS

---

### 8.01 Maillard model systems—introduction

Data from previous experiments indicated a significant contribution of Maillard type reactions (arginine mediated) to sultana storage browning. Arginine Maillard reactions were examined in a number of model systems, where the concentrations of arginine were close to those normally encountered in sultanas.

### 8.02 Experimental aims

Some basic information regarding glucose-arginine Maillard reactions was sought through model systems. The major objectives were:

- to establish whether arginine-glucose Maillard reactions generate brown pigments at a range of relatively low temperatures
- to partially characterise  $a_w$  sensitivity in these reactions, and
- to examine the effects of temperature, arginine concentration, catalytic iron and pH on these browning reactions.

### 8.03 Influence of arginine concentration, temperature and $a_w$ on Maillard browning systems

A multi-factorial experimental design was used to analyse the effects of  $a_w$ , arginine concentration, storage temperature and time on arginine-glucose Maillard reactions. The experiment involved three arginine concentrations (5, 10 and 15 mg.g<sup>-1</sup>), five  $a_w$  levels (0.2, 0.4, 0.55, 0.68, and 0.89) and three storage temperatures (37°C, 50°C and 60°C); a total of n=45 separate experimental units.

Browning pastes with varying  $a_w$  were made in the following manner: Milli-Q water was mixed with powdered D-glucose (~500 g AnalaR) and the humectant glycerol (AnalaR) was added to lower the  $a_w$  to a desired specific value—0.2, 0.4, 0.55, 0.68, or 0.89—in such a manner that all of the pastes had a similar solid gel-like consistency. The  $a_w$  values were checked using the Decagon  $a_w$  meter which had been calibrated prior to measurement. L-arginine (Sigma-Aldrich, Australia) was added to the pastes to give final concentrations of 5, 10 and 15 mg.g<sup>-1</sup> and thoroughly mixed. A 35 g sample of the glucose arginine paste was placed inside a transparent OPP/PVDC bag and flushed with nitrogen and then vacuum-heat sealed using the Multivac bag sealer. Any excess plastic was trimmed away from the bags (approximately 11×6 cm<sup>2</sup>) and this sealed bag was

placed into a second OPP/PVDC bag together with an Ageless oxygen scavenger and an Ageless Eye indicator and vacuum sealed. One bag at each of the  $a_w$  levels was stored at 37°C, 50°C and 60°C. The packaging not only ensured an oxygen-free storage environment but also provided a partial barrier to water mass-transfer. The Minolta Chromameter was used to determine the  $L^*a^*b^*$  values of the pastes over a 21-day period by placing the double layered pouch on a sheet of white paper and placing the reading head of the Chromameter flush with the surface. For each sample, 15 readings were taken in different positions by moving the reading head around the sample surface. The standard deviation of these readings was small, indicating homogeneous colour. The  $L^*a^*b^*$  readings and other data for each sample were arranged for ANOVA statistical analysis. The  $L^*a^*b^*$  values were the variates and the treatments were coded in the following manner: arginine concentration (5, 10 and 15),  $a_w$  (0.2, 0.4, 0.55, 0.68, and 0.89), storage temperature (37, 50 and 60) and time (0, 2, 3, 5, 9, 12, 14, 17 and 21).

#### 8.04 Results

At zero time the samples were bright white. All samples underwent browning, however the rate of colour change was dependent on  $a_w$ , temperature, time and to a lesser extent the arginine concentration. Changes in the tristimulus values are shown graphically in Figure 8.1, Figure 8.2 and Figure 8.3. Most importantly, the data indicated that significant colour changes occurred over time at relatively low temperatures (37°C to 60°C) with arginine concentrations at a physiologically similar concentration encountered in sultanas.

$L^*$  data (Figure 8.1) and ANOVA data (Table 8.1) show that all main effects were highly significant: time was the most important, followed by  $a_w$ , temperature and arginine concentration. All two-way interactions were highly significant, except for the arginine $\times$ temperature interaction. From the graphical data it can be seen that at 37°C and 50°C storage, regardless of the arginine concentrations, the samples with initial  $a_w$  values of 0.68 and 0.86 were significantly darker than samples with lower initial  $a_w$  values at all intervals. The strong effect of  $a_w$  on browning rates is illustrated by the data and is also reflected in the ANOVA analysis. At an  $a_w$  somewhere between 0.55 and 0.68 a critical change in the browning kinetics occurred. At higher temperature storage (60°C) the effect of  $a_w$  on  $L^*$  was not as strong, indicating that the water activity effect is temperature dependent, hence the relative importance of the  $a_w$  $\times$ temperature term. The arginine concentration also had a significant effect on the rate of decrease in  $L^*$ , however the effect was not as important as temperature and  $a_w$ . Generally, with increased temperature and  $a_w$ , the initial arginine concentration appeared to have less of a decisive effect; rates of change of  $L^*$  appeared to converge with increasing temperature regardless of arginine concentration and  $a_w$ .

Observation of data for  $a^*$  (Figure 8.2) and  $b^*$  (Figure 8.3) also showed similar apparent sensitivity to  $a_w$ , temperature and arginine. At 37°C storage it can be seen that  $a^*$  values increased over time and reached a higher maximum with increasing arginine concentration. With increased temperature,  $a_w$  had an important effect. At 50°C and 60°C it was apparent that the higher  $a_w$  samples (0.68 and 0.89) had significantly different  $a^*$  values, compared to the lower  $a_w$  samples. At higher  $a_w$  the samples rapidly reached a maximum  $a^*$  value (approximately 3 days) and then rapidly decreased. In contrast, samples of lower  $a_w$  attained a lower maximum  $a^*$  value and then proceeded to slowly decrease. Final  $a^*$  values (after 21 days) were significantly lower as temperature and arginine concentration increased. It should be noted that dark brown pigments were observed at the point where both  $a^*$  and  $b^*$  values began decreasing after reaching a maximum value. ANOVA analysis indicated that temperature was the most important effect after time. The temperature×time interaction was also important, highlighting the time dependence of Maillard reactions. Although the single effect of  $a_w$  was not statistically significant, the  $a_w$ ×temperature interaction was ( $p=0.004$ ), indicating that the  $a_w$  effect was temperature dependent. This can be seen in the data; there were only significantly different  $a^*$  values observed in some high  $a_w$  samples stored at 50°C and 60°C.

Changes in  $b^*$  (Figure 8.3) were also affected by  $a_w$ , temperature and arginine concentration. It can be seen that for all samples,  $b^*$  values increased to a maximum value and proceeded to decrease as brown pigments were formed. The maximum  $b^*$  value was reached after approximately 4 to 12 days for 37°C stored samples, whereas  $b^*$  maxima were reached within a few days for samples stored at the higher temperatures. The important effect of temperature is reflected in the ANOVA data where both temperature and the temperature×time interactions accounted for a large fraction of total variance. It can be seen that decreases in  $b^*$ , after reaching the maximum, were influenced by the  $a_w$ , especially at 37°C and 50°C storage. Once again, the highest  $a_w$  samples underwent significantly faster decreases in  $b^*$ . Although the arginine concentration was the least important main effect, it can be seen that for a given temperature, the rate of decrease in  $b^*$  increased with increasing arginine concentration.

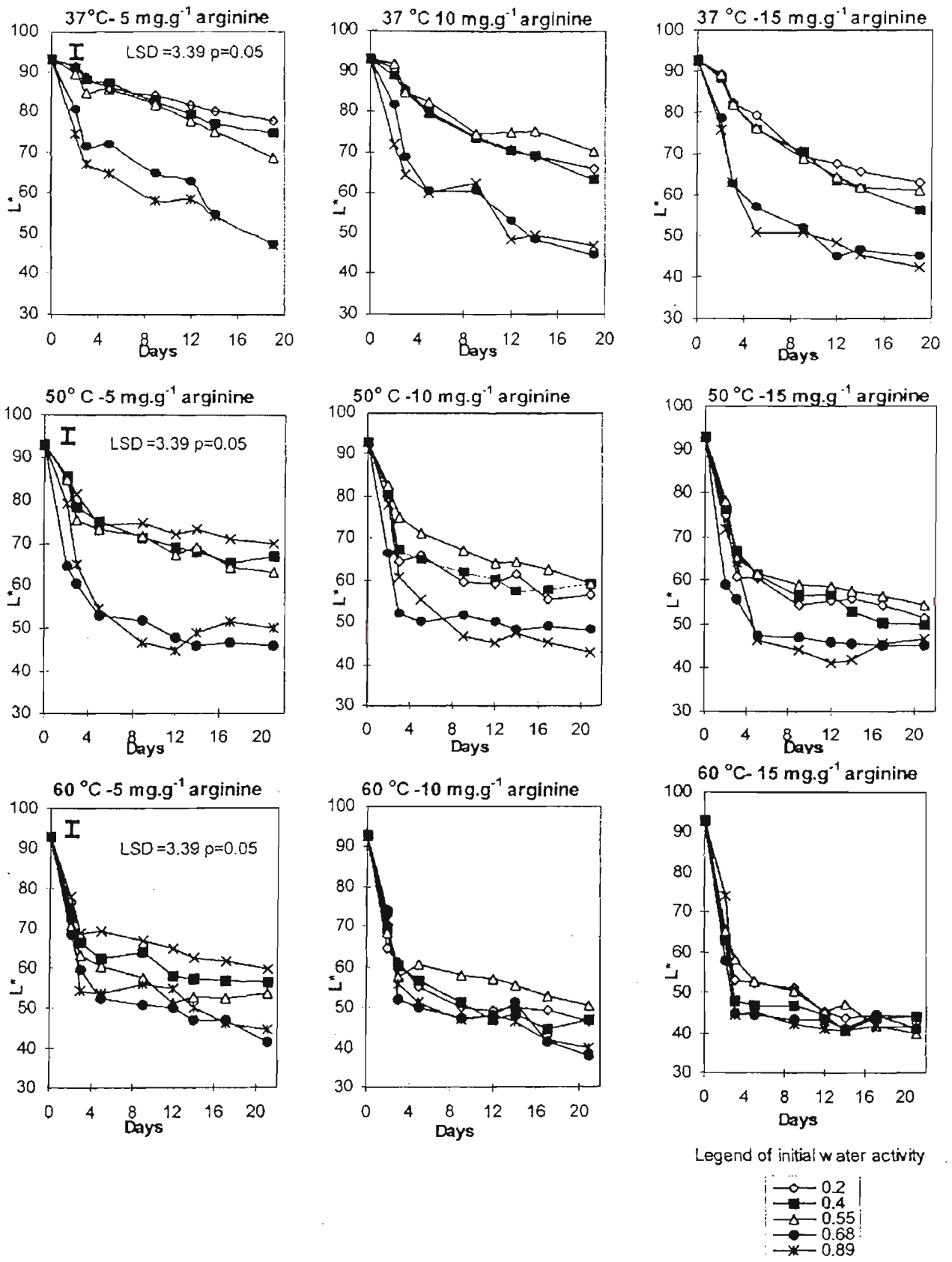


Figure 8.1 Time course for  $L^*$  values in arginine-glucose model systems with different initial  $a_w$  values. Arginine concentration 5, 10 and 15 mg.g<sup>-1</sup> and storage temperature 37°C, 50°C and 60°C. LSD calculated for the interaction of all treatments.

Source of variation in L*	d.f.	s.s.	m.s.	v.r.	F pr.
arg	2	4593.87 (5.4%)	2296.93	522.55	<0.001
aw	4	13776.32 (16.2%)	3444.08	783.53	<0.001
temp	2	11728.11 (13.7%)	5864.0	1334.08	<0.001
time	7	46281.63 (54.3%)	6611.66	1504.16	<0.001
arg.aw	8	449.58	56.19	12.78	<0.001
arg.temp	4	22.23	5.55	1.26	0.288
aw.temp	8	2170.12 (2.5%)	271.26	61.71	<0.001
arg.time	14	901.96	64.42	14.66	<0.001
aw.time	28	683.66	24.41	5.55	<0.001
temp.time	14	2226.80 (2.6%)	159.05	36.19	<0.001
arg.aw.temp	16	199.65	12.47	2.84	<0.001
arg.aw.time	56	376.49	6.72	1.53	0.029
arg.temp.time	28	251.09	8.96	2.04	0.005
aw.temp.time	56	1033.93 (1.2%)	18.46	4.2	<0.001
Residual	112	492.31	4.39		
<b>Total</b>	<b>359</b>	<b>85187.75</b>			

Source of variation in a*	d.f.	s.s.	m.s.	v.r.	F pr.
arg	2	859.58 (6.10%)	429.79	62.68	<0.001
aw	4	34.96	8.74	1.27	0.285
temp	2	2507.78 (17.08%)	1253.89	182.88	<0.001
time	6	5065.01 (35.9%)	844.17	123.12	<0.001
arg.aw	8	77.94	9.74	1.42	0.198
arg.temp	4	349.74	87.44	12.75	<0.001
aw.temp	8	171.36	21.42	3.12	0.004
arg.time	12	355.95	29.66	4.33	<0.001
aw.time	24	313.58	13.07	1.91	0.015
temp.time	12	2115.97 (15.0 %)	176.33	25.72	<0.001
arg.aw.temp	16	111.04	6.94	1.01	0.451
arg.aw.time	48	207.41	4.32	0.63	0.961
arg.temp.time	24	719.46 (5.1%)	29.98	4.37	<0.001
aw.temp.time	48	542.22	11.30	1.65	0.019
Residual	96	658.22 (4.7%)	6.86		
<b>Total</b>	<b>314</b>	<b>14090.21 (100%)</b>			

Source of variation b*	d.f.	s.s.	m.s.	v.r.	F pr.
arg	2	638.24 (1.2%)	319.12	22.05	<0.001
aw	4	5,018.86 (9.6%)	1254.72	86.7	<0.001
temp	2	1338.27	669.13	46.23	<0.001
time	6	20,851.69 (40.0%)	3475.28	240.13	<0.001
arg.aw	8	80.84	10.1	0.7	0.692
arg.temp	4	978.17	244.54	16.9	<0.001
aw.temp	8	720.17	90.02	6.22	<0.001
arg.time	12	1783.72	148.64	10.27	<0.001
aw.time	24	3521.73	146.74	10.14	<0.001
temp.time	12	12661.34 (24.3%)	1055.11	72.9	<0.001
arg.aw.temp	16	565.13	35.32	2.44	0.004
arg.aw.time	48	572.66	11.93	0.82	0.768
arg.temp.time	24	1026.54 (2.0%)	42.77	2.96	<0.001
aw.temp.time	48	980.99	20.44	1.41	0.077
Residual	96	1389.36 (2.6%)	14.47		
<b>Total</b>	<b>314</b>	<b>52127.69</b>			

Table 8.1 ANOVA table for L\* a\* b\* data for model systems.

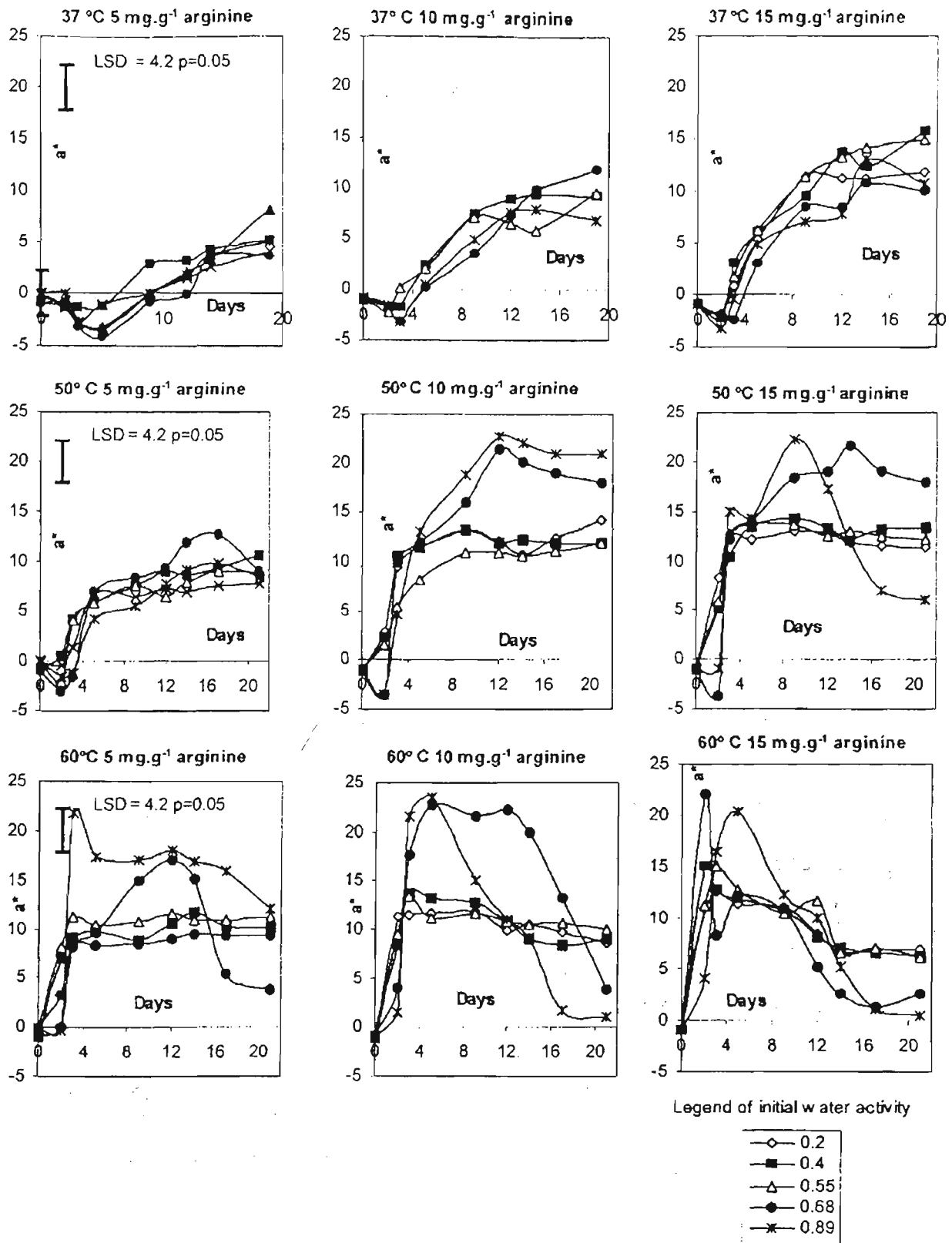


Figure 8.2 Time course for  $a^*$  values in arginine-glucose model systems with different initial  $a_w$  values. Arginine concentration 5, 10 and 15  $\text{mg.g}^{-1}$  and storage temperature 37°C, 50°C and 60°C. LSD calculated for the interaction of all treatments.

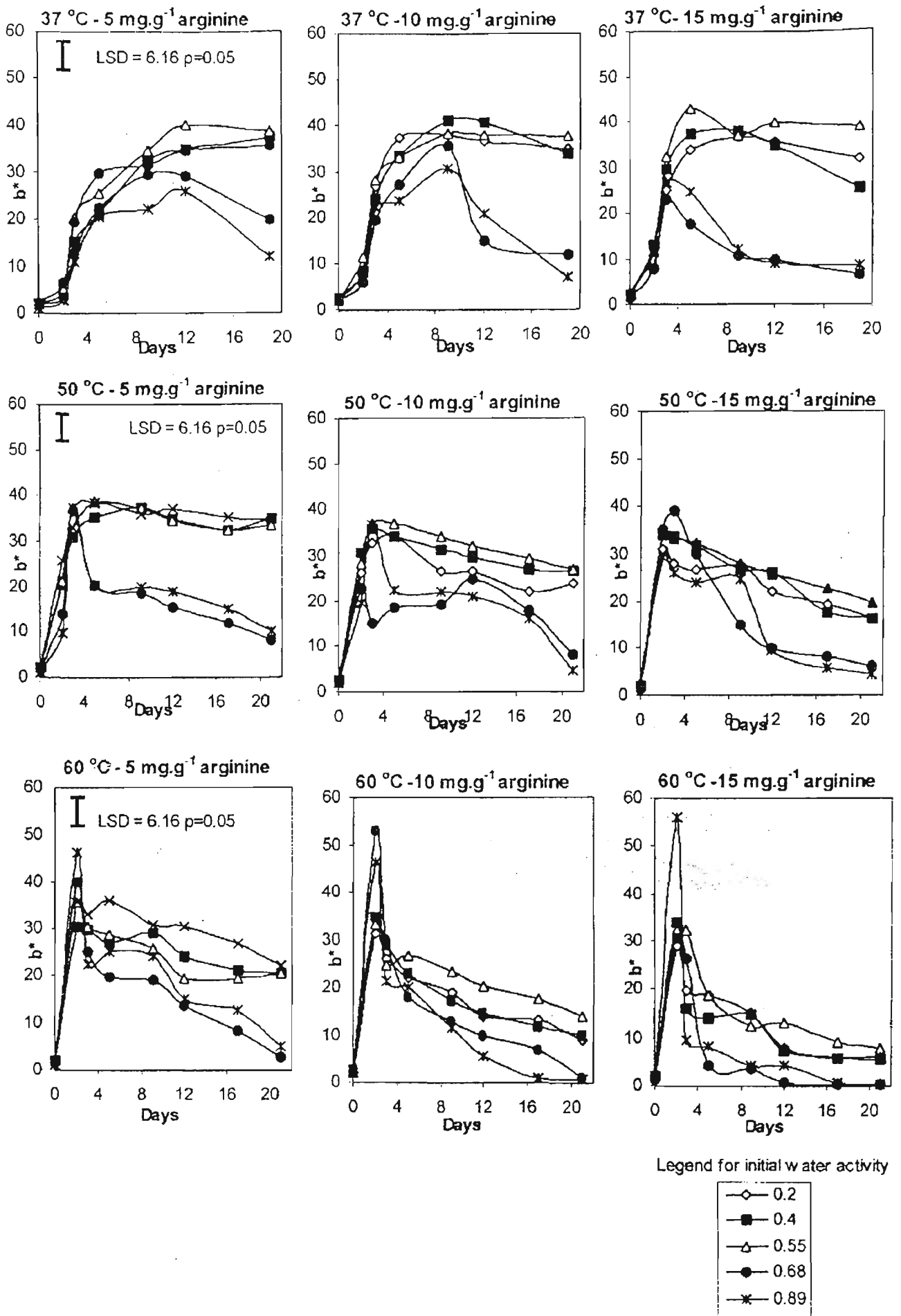


Figure 8.3 Time course for  $b^*$  values in arginine-glucose model systems with different initial  $a_w$  values. Arginine concentration 5, 10 and 15 mg.g<sup>-1</sup> and storage temperature 37°C, 50°C and 60°C. LSD calculated for the interaction of all treatments.

### 8.05 Influence of pH on arginine- glucose interaction

Arginine is the most basic of the amino acids, due to the guanidino nitrogen, with a  $pK_a$  of approximately 12.5. Addition of arginine into a chemical environment can markedly increase the pH. Maillard reactions are affected by pH, with different reactions and rates observed for acidic and alkaline solutions. Here the affect of pH on colour development was tested in arginine-D-glucose model systems. To a slurry of glucose in 0.05 M  $\text{NaH}_2\text{PO}_4$ , arginine was added to give a final concentration of  $10 \text{ mg.g}^{-1}$ . Iron was added in the form of  $\text{Fe(II)Cl}_2$  at a concentration of  $20 \text{ }\mu\text{g.g}^{-1}$  and dilute orthophosphoric acid was added to achieve specific pH values: 3.5, 5, 6 and 7. Glycerol was added and the  $a_w$  was adjusted to 0.80. Control samples without Fe were used. Samples were prepared in duplicate and were held at  $37^\circ\text{C}$  for 14 days and  $50^\circ\text{C}$  and  $60^\circ\text{C}$  for 5 days. Colour was measured using the Minolta chromameter (the mean of 15 separate measurements was used). The two mean colour values were used in the ANOVA analysis to calculate LSD values. Changes in  $L^*$ ,  $a^*$  and  $b^*$  values for the different pH arginine-D-glucose systems are shown in Figure 8.4.

Colour developed in the Maillard browning systems in the following manner:  $L^*$  decreased steadily,  $a^*$  (redness) increased to a maximum before decreasing as browning advanced. Yellowness ( $b^*$ ) increases initially, to a maximum, and decreased as browning proceeded. For samples stored at  $37^\circ\text{C}$ , it can be seen that decreases in  $L^*$  were observed at all pH levels, with most extreme decreases occurring at higher pH. Larger decreases were observed in the presence of the catalytic amount of iron. After 14 days at  $37^\circ\text{C}$ ,  $a^*$  values had increased for all samples stored with iron, reflecting the light to dark reddish brown colour of the samples. Only small  $a^*$  values were measured in samples stored without iron, as the samples without iron were yellow to light orange in colour. At  $37^\circ\text{C}$  storage, it can be seen that  $b^*$  values were much higher for samples without iron than those with iron, once again showing the strong effect of iron on Maillard browning rates. For samples stored at  $50^\circ\text{C}$  and  $60^\circ\text{C}$  without iron,  $b^*$  values increased with increasing pH, illustrating the pH dependence of the reactions. In the presence of iron, however, these samples had very low  $b^*$  values, reflecting the dark brown colour of these samples. Overall, the data showed that at low temperature ( $37^\circ\text{C}$ ), lowering the pH had the effect of slowing browning reactions, especially in the absence of iron. At higher temperature storage ( $50^\circ\text{C}$  and  $60^\circ\text{C}$ ), low pH was less effective at slowing the Maillard reaction, which once again, was especially true for samples stored with iron.

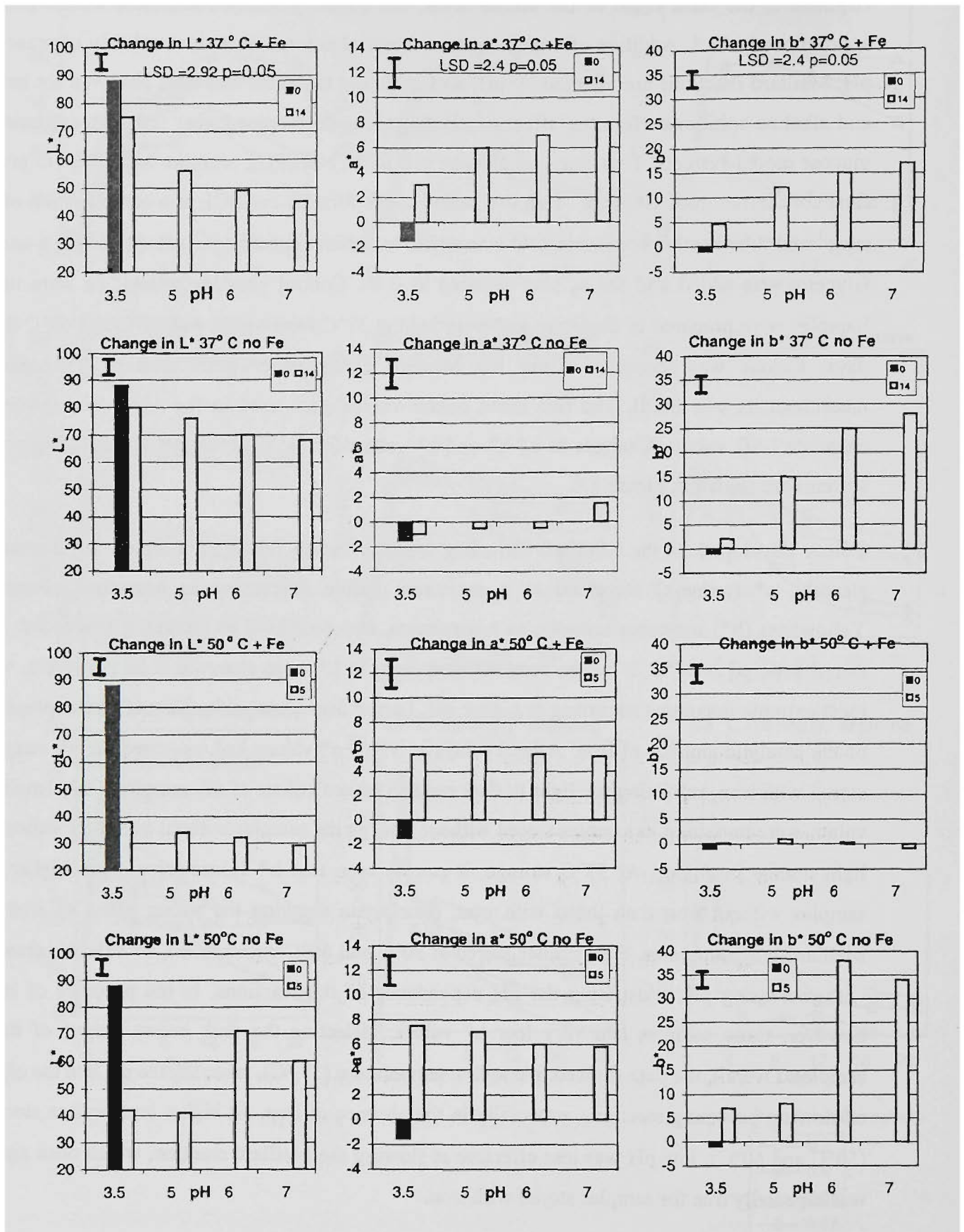


Figure 8.4 The effect of pH on rates of arginine-D-glucose Maillard browning at 37°C and 50°C. With and without catalytic Fe. LSD was calculated for the effect of pH, Fe and temperature (0=pre-storage, 14=after 14 days storage and 5=after 5 days storage).

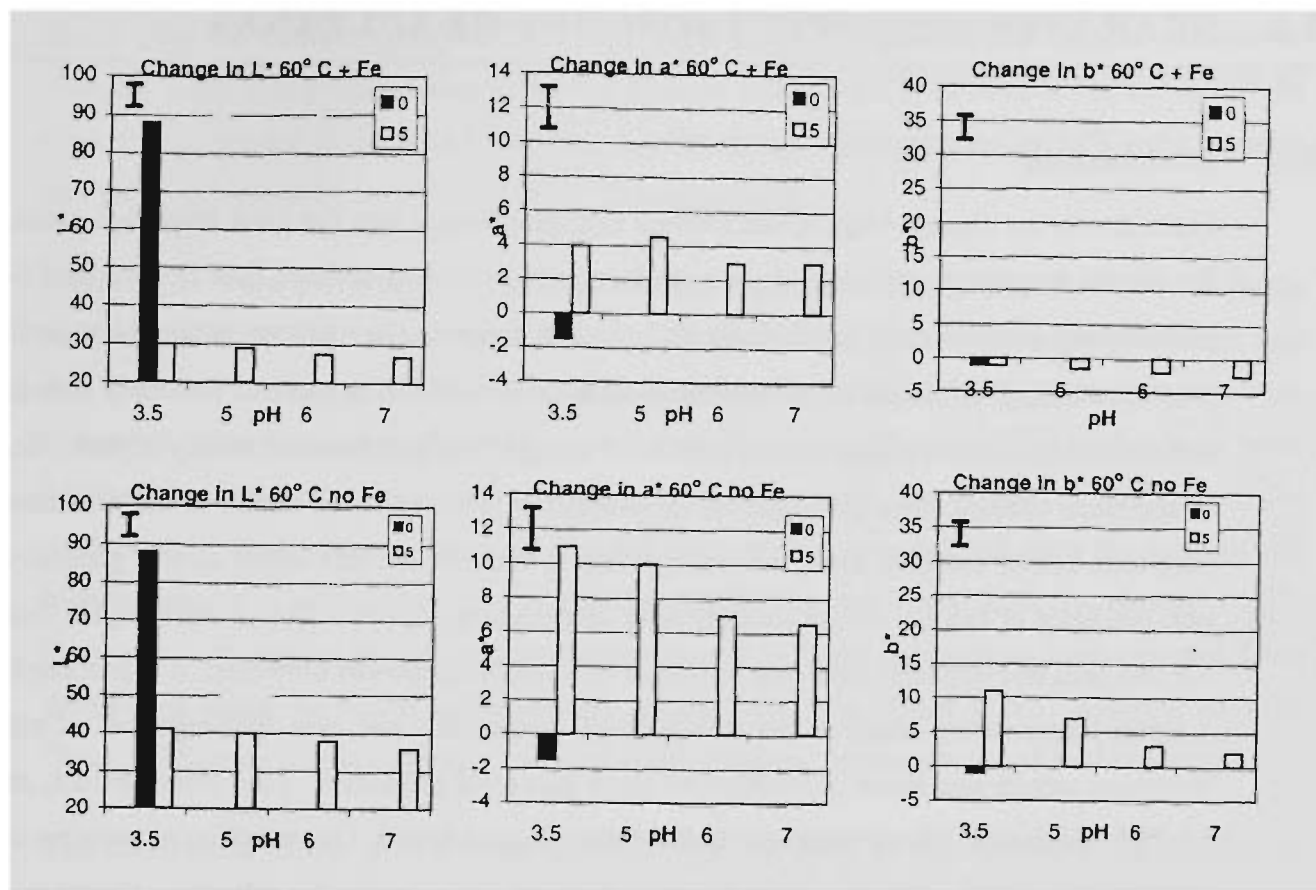


Figure 8.4 Continued. The effect of pH on rates of arginine-D-glucose Maillard browning at 60°C with and without catalytic Fe. LSD was calculated for the effect of pH, Fe and temperature.

### 8.06 Maillard model systems—discussion

The rate of browning in sultanas has been observed to increase rapidly with increasing temperature, i.e. above 30°C, strongly indicating Maillard type reactions rather than phenolic oxidation reactions. The temperature sensitivity of sultana storage browning was shown in previous storage trials (chapters 3, 4 and 5). The rate of browning in sultanas stored at 30°C was relatively slow (months). The Maillard model systems showed a strong temperature dependence and rates of browning were relatively slow at low pH at 37°C. In contrast at higher storage temperature (50°C and 60°C), the inhibitory effect of low pH was less. At lower  $a_w$  it would be expected that the effect of low pH would have slowed browning further.

Maillard model systems illustrated the critical effect of  $a_w$  and temperature on rates of Maillard browning. The model systems also demonstrated that arginine-glucose Maillard reactions are strongly affected by the presence of a catalytic concentration of iron in the presence of oxygen. Importantly, the model systems showed that arginine mediated Maillard browning occurred within a temperature range relevant to sultana storage.

## 9.0 NEAR INFRARED SPECTROSCOPY OF SULTANAS

---

### 9.01 Introduction

From the earlier storage trials it was evident that temperature was the most important parameter for sultana browning reactions. Large-scale temperature control of dried fruit storage facilities is probably not economically feasible; presently fruit is subjected to whatever ambient temperatures prevail in storage facilities, which may often be well above 30°C in summer and early autumn. In addition, temperatures reached in the middle of storage bins may be considerably higher. Short of temperature control, there are a number of parameters which may be useful in the prediction of long-term colour stability. From the storage trials it was evident that initial  $a_w$  was generally the best predictor of storage colour stability after temperature, all other factors being equal. Sultana KP and skin free-arginine were also shown to be valid predictors of browning. It is proposed that a much larger future study of the influence of sultana KP and skin free-arginine on sultana browning would rate these parameters as more powerful predictors. To a lesser extent, initial  $L^*a^*b^*$  tristimulus values were also useful browning predictors. On reception at packing sheds inspectors currently measure sultana moisture and rate colour using the subjective Crown system of classification; sultana KP and skin free-arginine are not measured, as to perform such analyses would be prohibitively expensive. It is highly likely that other physico-chemico parameters may be useful for assessing sultana quality, such as TA, maturity, sugars etc. It would be uneconomic to perform such tests in a traditional wet-chemical manner.

### 9.02 Experimental aims

A feasibility study was conducted with the Foss-NIRSystems 6500 spectrometer at VUT to see if the following parameters could be measured in whole sultanas:

- $a_w$ , using the Decagon dew-point device as the laboratory reference,
- $L^*a^*b^*$  tristimulus coordinates,
- KP and skin free-arginine, measured in the manner described previously.

### 9.03 Materials and methods

All data were collected on a Foss-NIRSystems 6500 spectrometer (Foss-NIRSystems, Silver Springs, MD, USA) at VUT Werribee. The instrument radiation source was a broad-band quartz halogen lamp. An oscillating concave holographic grating was used to disperse the radiation. A silica type photovoltaic detector was used in the visible to very near infrared range (400-1100 nm) and a lead sulphide crystal detector was utilized in the range 1100-2500 nm. Data was acquired

using the software NSAS® Version 3.5. Each sultana sample was scanned 64 times in reflectance mode, over the entire range (400-2500 nm) in the coarse sample cell and sample transporter. Samples were manipulated using either the N-point smooth (NPS) or second derivative (2<sup>nd</sup> D) algorithms provided in the NSAS software. A point size of 5 was selected for NPS and a segment and gap size both of 10 nm selected for 2<sup>nd</sup> D manipulation.

Calibrations were performed using both standard regression (MLR) and PLS options in the software. Generally calibrations were first performed on the whole spectral region 400-2500 nm, and then only on data from 700-2500 nm. For standard regressions, multi-term equations were generated with 4 wavelengths, which are listed for each calibration. PLS calibrations were performed using a cross validation technique, with 4 segments. The number of factors used for models were those recommended by the software, which corresponded with the ratio of the highest mean standard error of cross validation (MSECV) to the lowest MSECV, closest to 1.25. Outliers recommended by the software were removed and best calibrations were reported. Data determined using the NSAS software were imported into the Vision ® 2.11 software package (Foss-NIRSystems, Silver Springs, MD, USA) for graphical representation of calibrations.

The dimensions of the ground quartz glass sample cell were 17 cm×3.5 cm×2 cm, capable of holding around 250 g of whole sultanas. The automated sample transport unit moves the sample cell surface over the radiation source and detector, taking multiple acquisitions over the entire sample surface. For each sample 64 scans were performed and averaged by the software, to produce one final mean spectrum. Spectra were acquired over the entire visible and NIR range 400-2500 nanometres. All calibrations were performed on spectra which had either been processed with an NPS or 2<sup>nd</sup> D algorithm. The NSAS software allows calibrations to be performed using either visible region spectral data (400-700 nm) or the very near to near infrared region (700-2500 nm) or both regions together (400-2500 nm).

Calibration experimental results are listed for each component showing  $R^2$  values, SEP values (Standard Error of Prediction), sample range, sample SD (standard deviation) and SEP/SD ratios. For PLS calibrations SEP=SECV (standard error of cross validation) and MLR calibrations SEP=SEC (standard error of calibration). Sultanas from 1995 and 1996 experiments were used in

Samples for the  $L^*a^*b^*$  and  $a_w$  calibrations were selected to encompass a typical range of colour commonly encountered in Australian sultanas. Kjeldahl protein (KP) and skin free-amino acid analyses were conducted on 1996 sultanas (n=42) and a further KP determination was conducted on sultanas from the 1988 season. Samples were scanned in a constant temperature environment  $22.00^\circ\text{C} \pm 0.05^\circ\text{C}$ . Bulk sultana samples were also equilibrated to room temperature before scanning. Figure 9.1 shows typical raw NIR reflectance spectra of sultanas (top) and the same spectra after NPS and 2<sup>nd</sup> D processing. Figure 9.2 and Figure 9.3 show detail of spectral variation for NPS-2<sup>nd</sup> D spectra.

## 9.04 Water activity

The critical influence of water activity in the long-term storage potential of sultanas has been shown in previous chapters and has also been highlighted by a number of other researchers (Aguilera *et al.* 1987 and Cañellas *et al.* 1993). Due to the ease of measurement,  $a_w$  is an ideal method of moisture estimation in sultanas.  $A_w$  can also be easily related to percent moisture values from a number of reliable isotherms. The high sugar content of sultanas make them less than ideal for moisture estimation because of the tendency of sugars to undergo Maillard reactions and caramelisation processes upon heating, which produce a significant amount of water *de novo*. Oven moisture methods are also highly time-consuming. In contrast  $a_w$  measurement (via a benchtop dew-point device) obviates the need to heat samples and is rapid in comparison with other moisture determination techniques. Huxsoll *et al.* (1995) demonstrated that NIR transmittance technology could measure moisture and other parameters in raisins.

Sultana samples from the 1996 season were used for  $a_w$  calibrations. Sultanas ( $n=50$ ) were placed in a mortar and pestle and made to a homogeneous paste. A sample was placed in the Decagon water activity meter and  $a_w$  was measured. The mean of two  $a_w$  readings was used for the NIR experiment, with a population range of  $a_w$  from 0.42 to 0.72. Table 9.1 shows calibration information for  $a_w$  NIR experiments. Optimal calibrations were achieved using second derivative spectra using both NIR and vis-NIR ranges.  $R^2$  values of 0.95 and 0.96 were obtained using a three wavelength MLR model and a three factor PLS model respectively. Both models had low SEP/SD ratios indicated a high degree of prediction reliability. Figure 9.4 shows graphically the correlation between predicted values (Y axis) and laboratory measured values (X axis), with each solid sphere representing a sultana sample. Note that many samples overlapped; hence it appears that less than 94 samples were present in the calibration.

Table 9.1 shows the wavelengths chosen during the MLR calibration for  $a_w$ . The most strongly correlated wavelength ( $\lambda_1$  1276 nm) does not appear in the official tables of assigned water signals for 2<sup>nd</sup> D pure spectra of water (*Identification of Near Infrared Absorbers. Instrumentation Research Laboratory, United States Department of Agriculture, Beltsville, MD*).

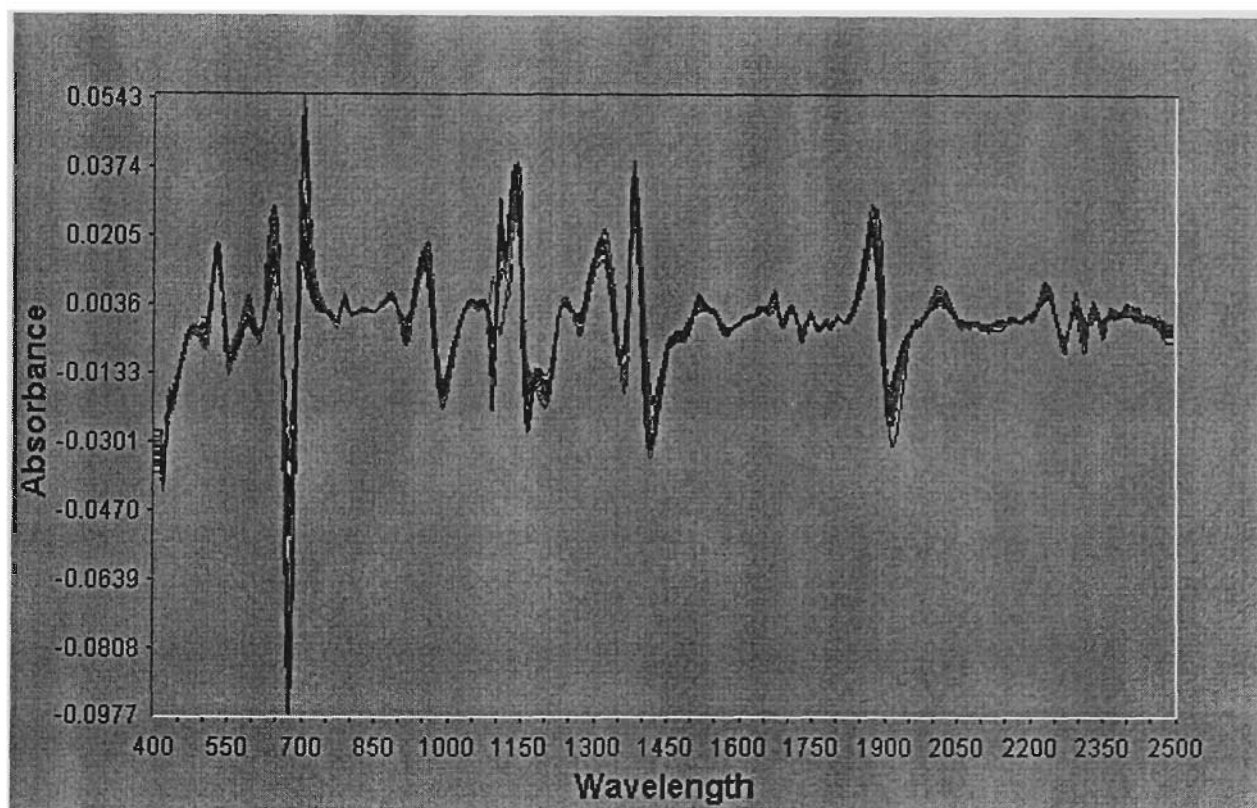
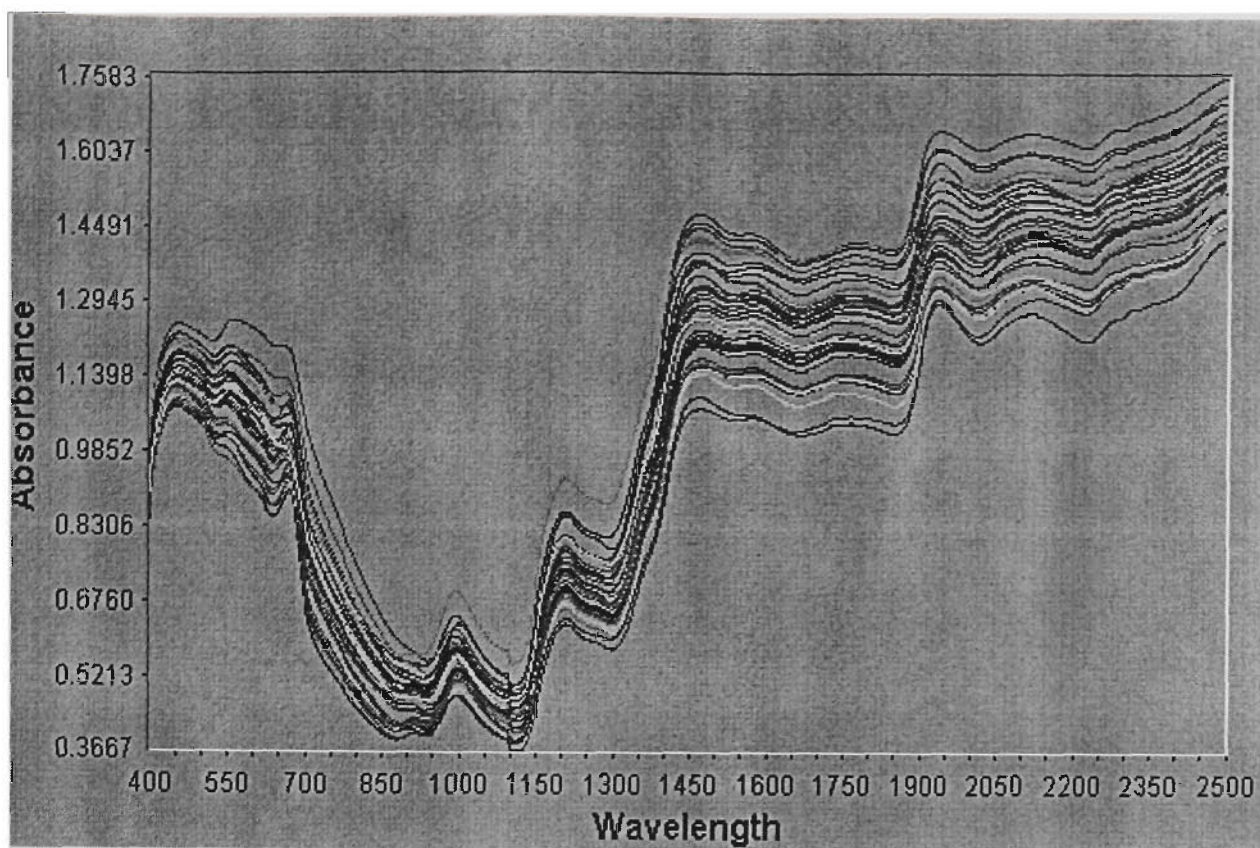


*Figure 9.1 Typical reflectance NIR spectra of sultanas.  
 Top: no processing. Bottom: the same spectra after NPS and second derivative processing.*

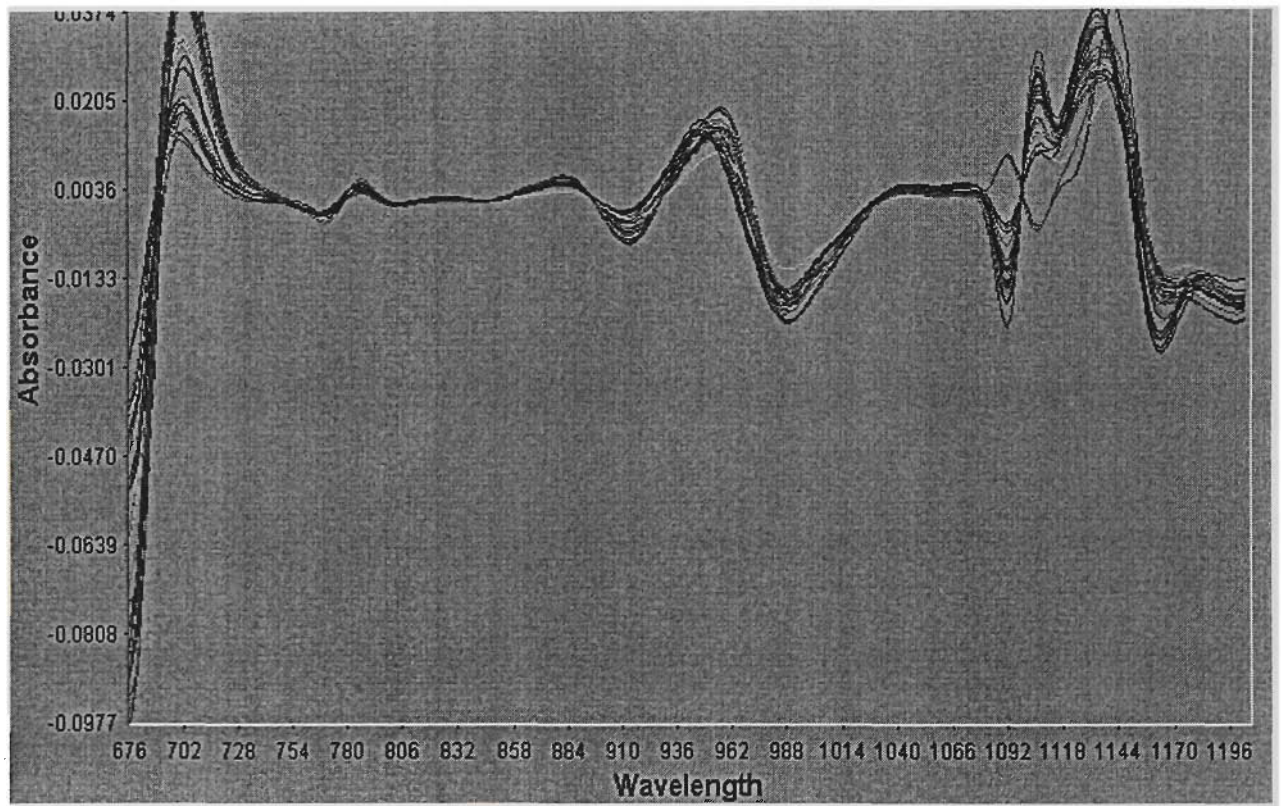
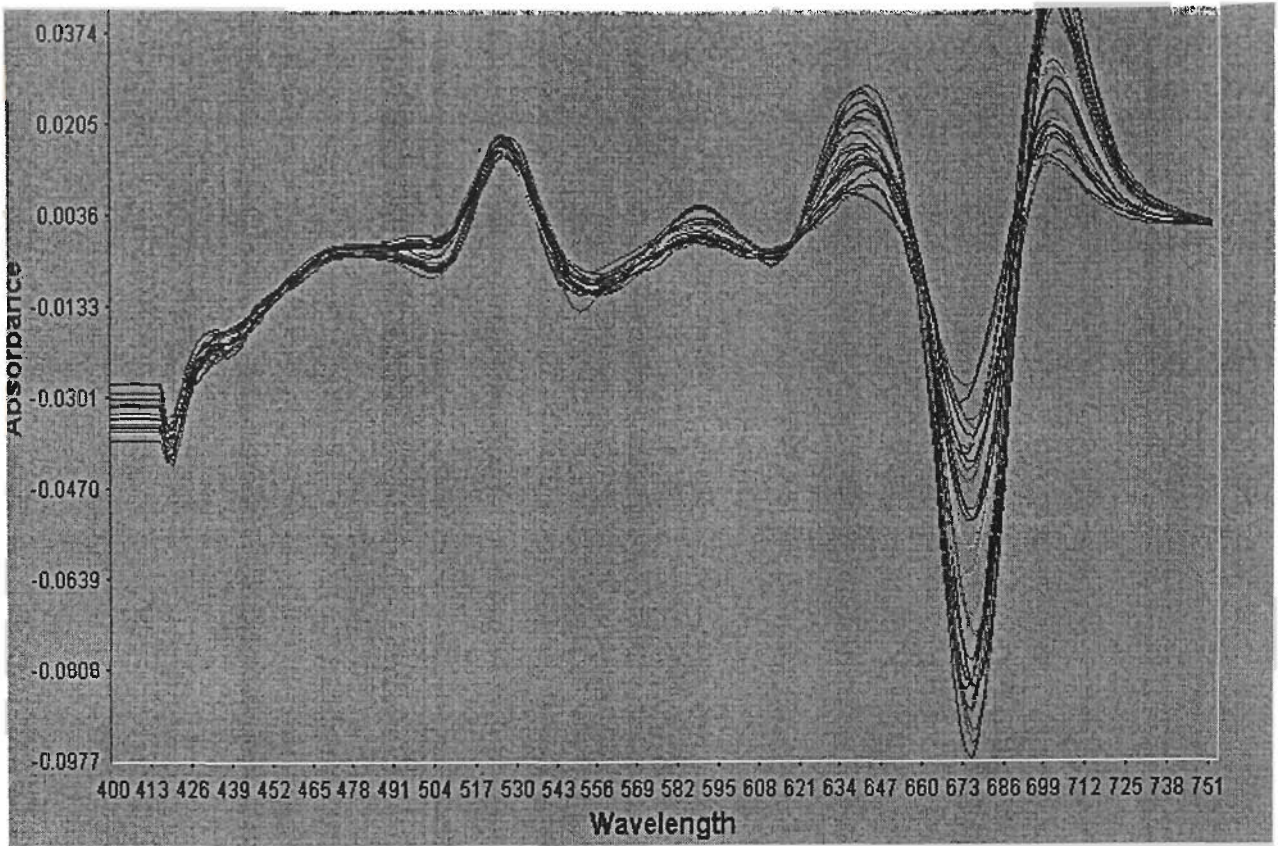


Figure 9.2 Detail of spectral variation of NPS 2<sup>nd</sup> D spectra.  
 Top: 400-700 nm. Bottom: 700-1100 nm.

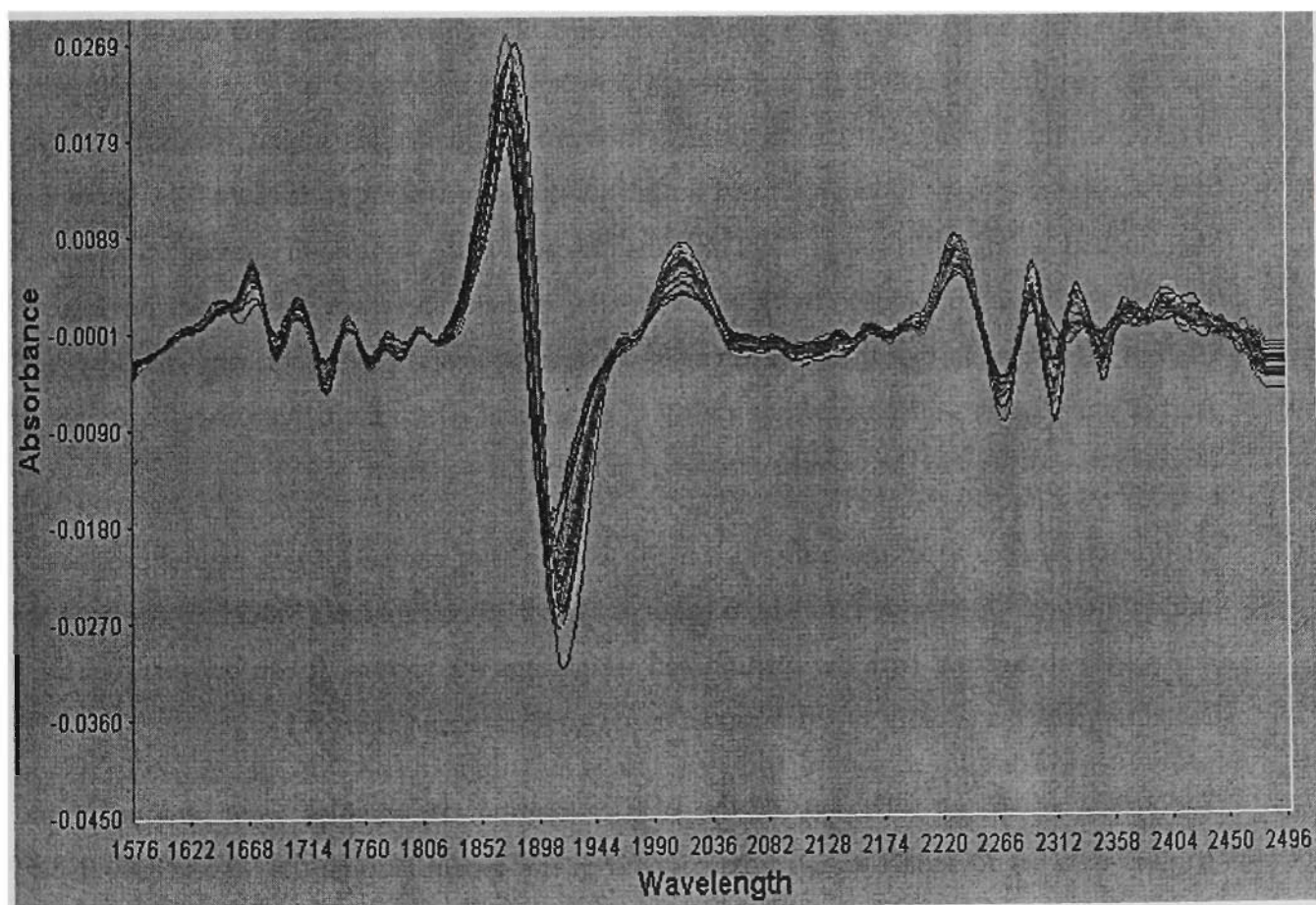
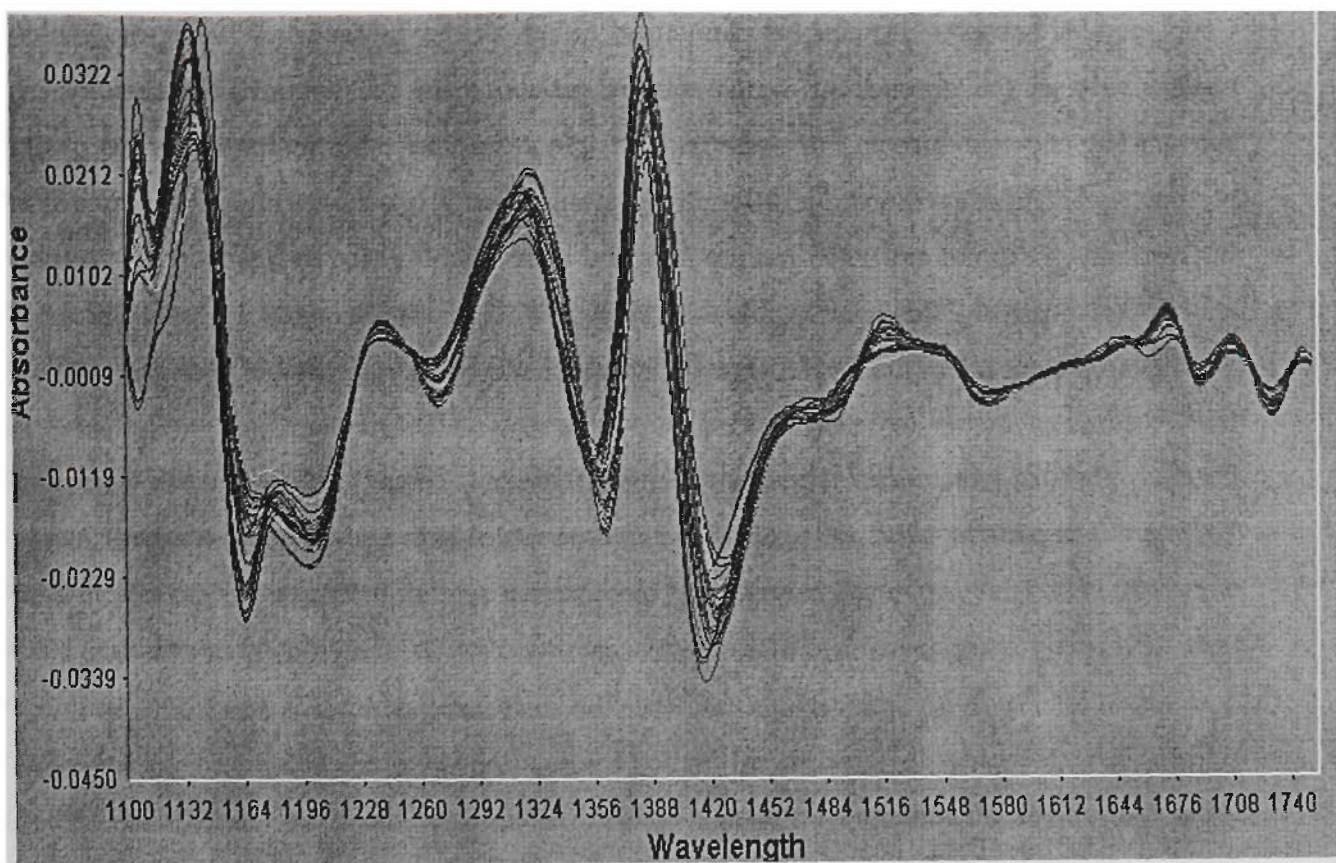


Figure 9.3 Detail of spectral variation of NPS 2<sup>nd</sup> D spectra  
 Top: 1100-1700 nm. Bottom: 1700-2500 nm.

Conceptually, however,  $a_w$  can be thought of either as the presence of water molecules, or alternatively as the absence of water and its influence on the overall all plasticity of the surrounding chemical matrix. For example hydrogen atoms and other molecular bonds in sugars, proteins and cellulose will exhibit different vibrational modes in a low or high water environment. Interestingly, 1276 nm and 1275 nm are assigned as reasonably strong signals from protein and cellulose respectively. It is conceivable that the principal calibration signal derives from a sultana matrix component rather than water directly, however it is often not possible to empirically assign NIR absorption bands to specific known pure chemical components or well characterised chemico-physical interactions. The absorption at 1026 nm is close to a known weak water band at 1030 nm. The peak at 1962 nm is not listed in data tables as a known band, however bands for water and cellulose have been characterised close to that region. In Figure 9.5 the salient data for each calibrating wavelength is shown graphically. For  $\lambda_1$  1276 nm (top) it can be seen that the correlation ( $R^2$ ) with  $a_w$  is very high and that the instrumental relative sensitivity is low; low sensitivity is desirable for a robust calibration as small absorbance changes do not have a large (negative) impact on constituent values. The distance between the absorbance of the highest  $a_w$  sample and the lowest  $a_w$  sample was large: this wavelength had by far the strongest correlation with  $a_w$  in MLR equations. This single wavelength alone accounted for >95% ( $R^2 = 0.95$ ) of the model. It can also be clearly seen that the condition of high correlation, low sensitivity and good spectral discrimination held for a number a wavelengths either side of 1276 nm, indicating that the use of this single wavelength would yield prediction models which would be stable and robust. Similar graphical data is shown for the additional wavelengths (Figure 9.5). It can be seen that for both  $\lambda_2$  1026 nm and  $\lambda_3$  1962 nm, that although there was a high correlation with  $a_w$  there was also relatively high sensitivity and a smaller distance between absorbance for lowest and highest  $a_w$  indicating that these wavelengths are less powerful predictors; they did however add further statistically valid predictive ability to the model. Only multi-season calibrations would attest to the stability of the wavelengths used in the MLR equation.

As previously described, generally PLS is the technique of choice for raw natural products. PLS calibrations were performed on whole sultanas. The PLS calibration (700-2500) for  $a_w$  is shown in Figure 9.4 together with the loading and weightings for factors. It can be seen that the PLS equation yielded a slightly superior model based on  $R^2$  criteria (Table 9.1).

To further assess the reliability of the PLS calibration, 10 samples were removed from the original data set to span the  $a_w$  range covered in the model (Range 0.41-0.68 SD 0.088). The remaining samples (n=84) were used to form a calibration model and the  $a_w$  values of the 10 unique samples were predicted. Results are shown in Table 9.1 (bottom). The high  $R^2$  value and low SEP/SD ratio for the validation samples indicated that the calibration model was accurate in its predictive ability for samples not in the original calibration set.

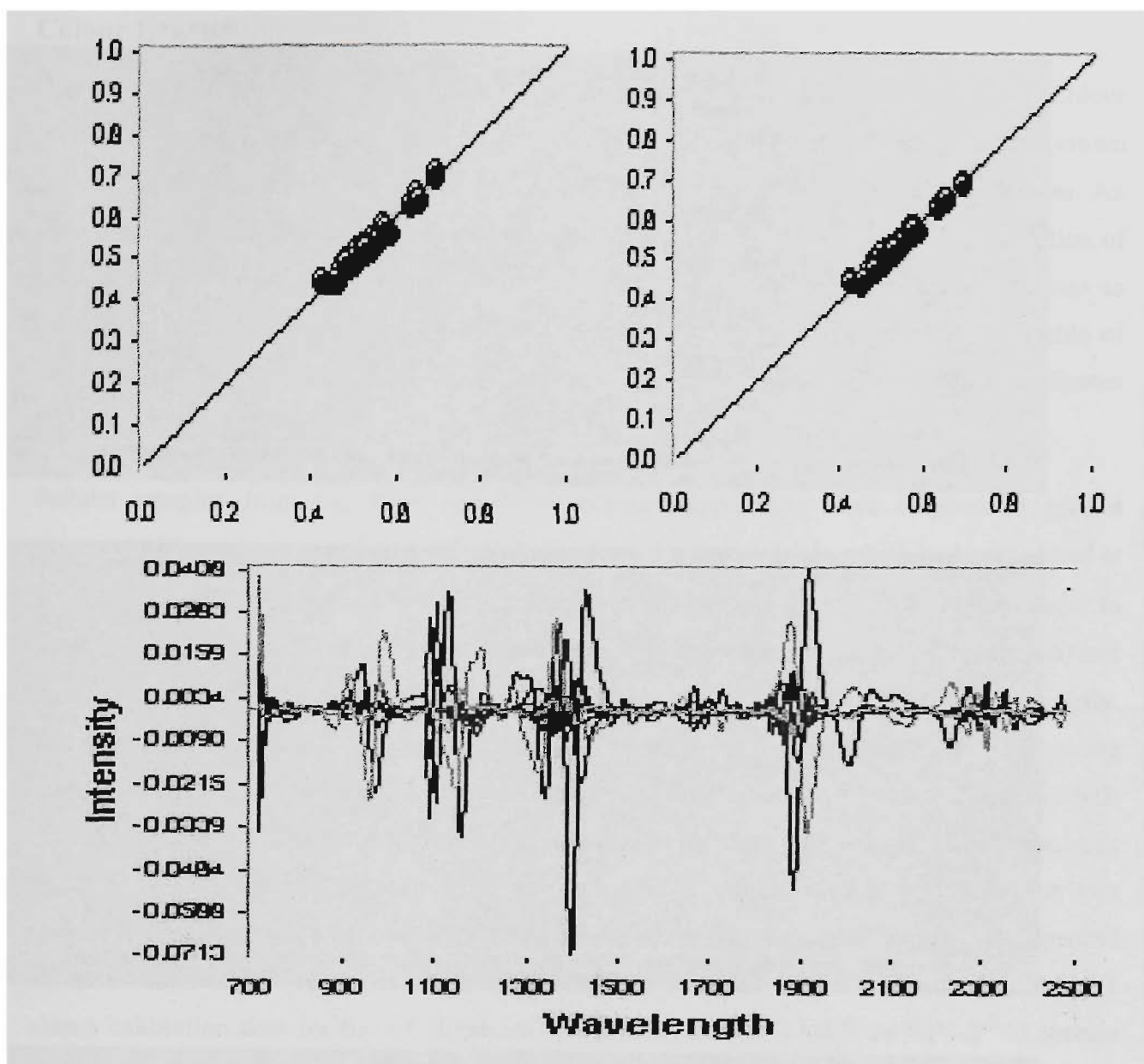


Figure 9.4 Plot of MRL predicted and PLS predicted water activity. Clockwise from top left: plot of MRL predicted vs laboratory  $a_w$ , plot of PLS predicted vs laboratory  $a_w$ , and weights and loadings at each wavelength for the first seven factors in the PLS  $a_w$  model.

$\lambda$ region nm	n	Math	Statistic	F	$R^2$	SEP	Range	SD	SEP / SD	$\lambda$ nm
700-2500	94	2 <sup>nd</sup> D	PLS	3	0.96	0.015	0.42-0.72	0.067	0.21	
400-2500	94	2 <sup>nd</sup> D	MLR	3	0.95	0.017	0.42-0.72	0.067	0.21	1276,1026,1962

Parameter	n	$R^2$ Cal	SEC	n	$R^2$ Val	SD	SEP	SEP / SD
$a_w$	83	0.95	0.015	10	0.98	0.088	0.01	0.011

Table 9.1 Calibration data for water activity. Top: calibration data for PLS and MLR models. Bottom: calibration data for prediction of  $a_w$  in 10 unique sultana samples with a calibration model using 83 samples

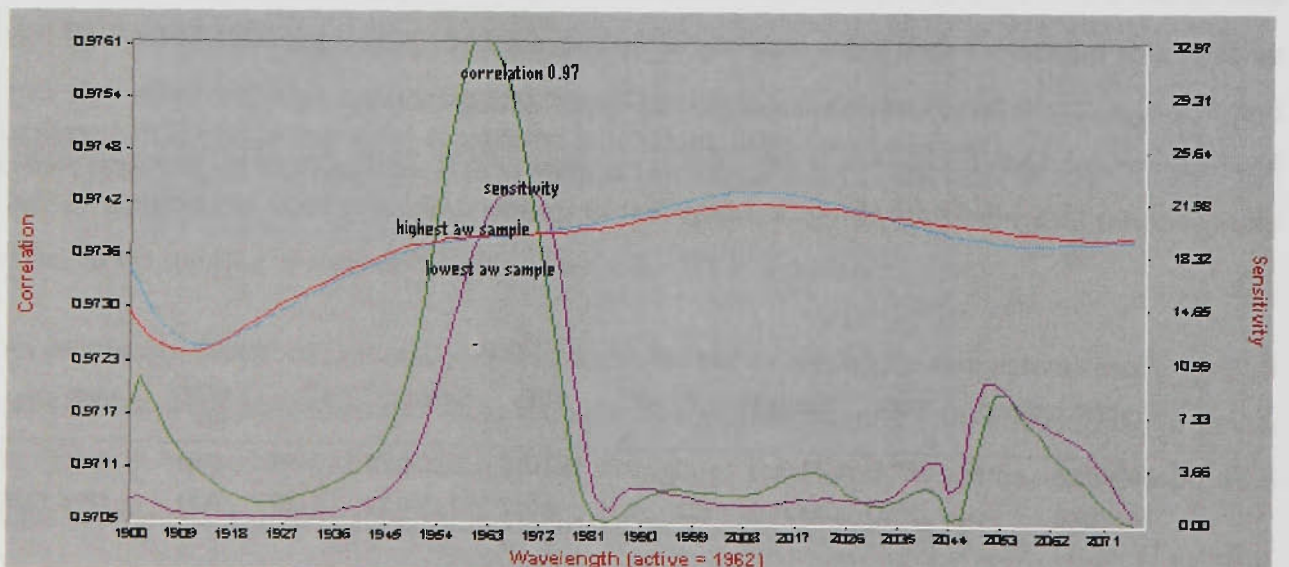
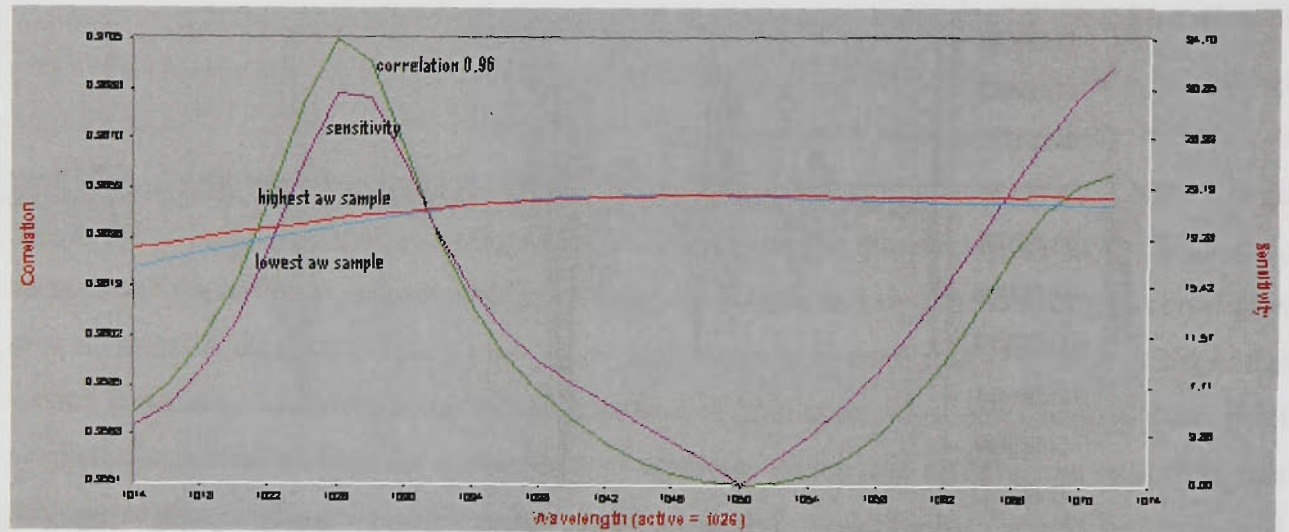
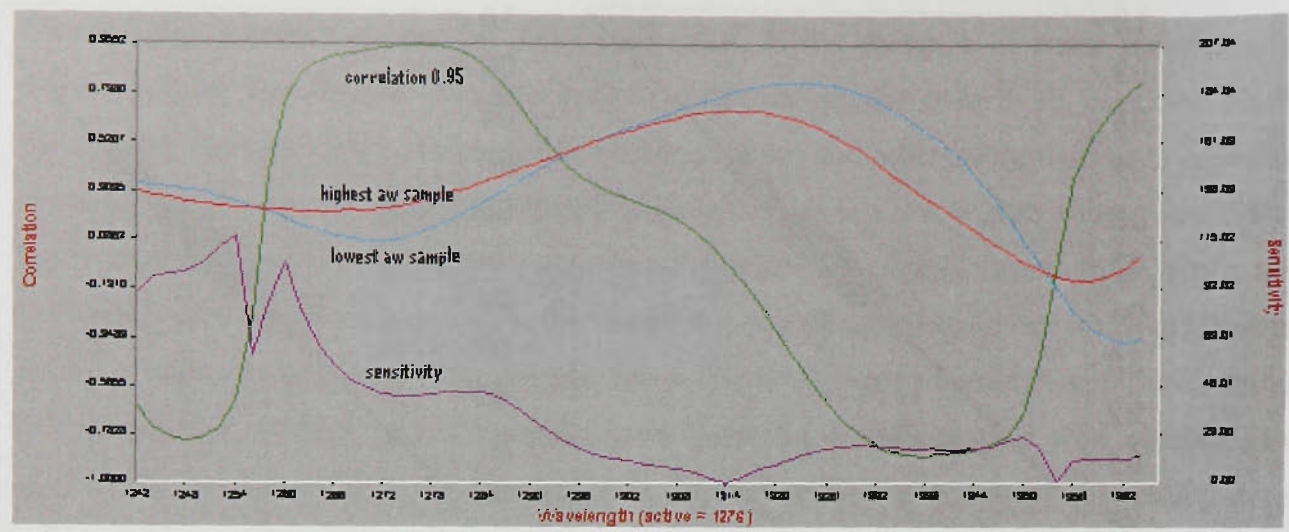


Figure 9.5 Calibration data for  $\lambda_1$  1276 nm,  $\lambda_2$  1026 nm and  $\lambda_3$  1962 nm. The green line represents the correlation coefficients ( $R^2$ ) with  $a_w$ , the dark blue line represents the relative sensitivity at a particular wavelength, the red line is the absorption of the highest  $a_w$  sample and the light blue line is the absorption of the lowest  $a_w$  sample.

## 9.05 Colour L\*a\*b\*

Objective colour measurement technology is of interest to the Australian sultana industry. Colour is currently graded by skilled fruit inspectors, who classify sultanas according to the crown system. Crown grades are seasonally varied, and higher crown fruit receives higher prices. An objective, easy colour measurement technology would allow for a more consistent definition of sultana colour, which could ultimately assist the industry in better allocation of sultanas to specific buyer requirements. As the FOSS-NIR Systems 6500-spectrophotometer is capable of acquiring spectral data in the visible region, calibration for the tristimulus colour coordinates L\*a\*b\* was investigated.

Sultana samples from the 1995 and 1996 storage experiments were selected to give a representative range of samples (n=80). Sultanas from the storage trials, which had been stored at 30°C for a period of time and had undergone significant browning, were also used. In order to obtain L\*a\*b\* values, sultanas were transferred to a sample cup (approximately 200 sultanas) and 2 × 50 scans were obtained with the Minolta Chromameter in the manner described previously. The mean value was used in NIR calibrations. Calibrations were performed on 2<sup>nd</sup> D spectra using both MLR and PLS techniques, within the visible and NIR range (400-2500 nm) and the NIR range only (700-2500 nm). Each sample was scanned three times with re-packing between each scan. Before data analysis, the three spectra were averaged using the NSAS software: this approach is recommended for natural products as it helps to eliminate some of the spectral artefacts inevitably introduced as a consequence of differences in sample-cell packing. Table 9.2 shows calibration data for the L\* (lightness) coordinate. PLS and MLR on NPS-2<sup>nd</sup> D spectra generated R<sup>2</sup> values of 0.93 with SEP/SD values of 0.23 and 0.24 respectively. Calibration graphs and spectral loading plots for PLS calibrations are shown in Figure 9.6.

The red-green tristimulus coordinate (a\*) was similarly used to form an NIR calibration. Results for calibration experiments are also shown below in Table 9.2. Calibration models for a\* were generally less precise than L\* models. Graphical representation of predicted versus measured values are shown in Figure 9.7 together with the weightings used for the first seven factors used in PLS models. Finally, calibrations were performed for the b\* tristimulus colour coordinate; models were achieved using both MLR and PLS algorithms as shown in Table 9.3. Graphical representations of predicted b\* values versus laboratory measured and weightings for PLS factors are shown in Figure 9.8.

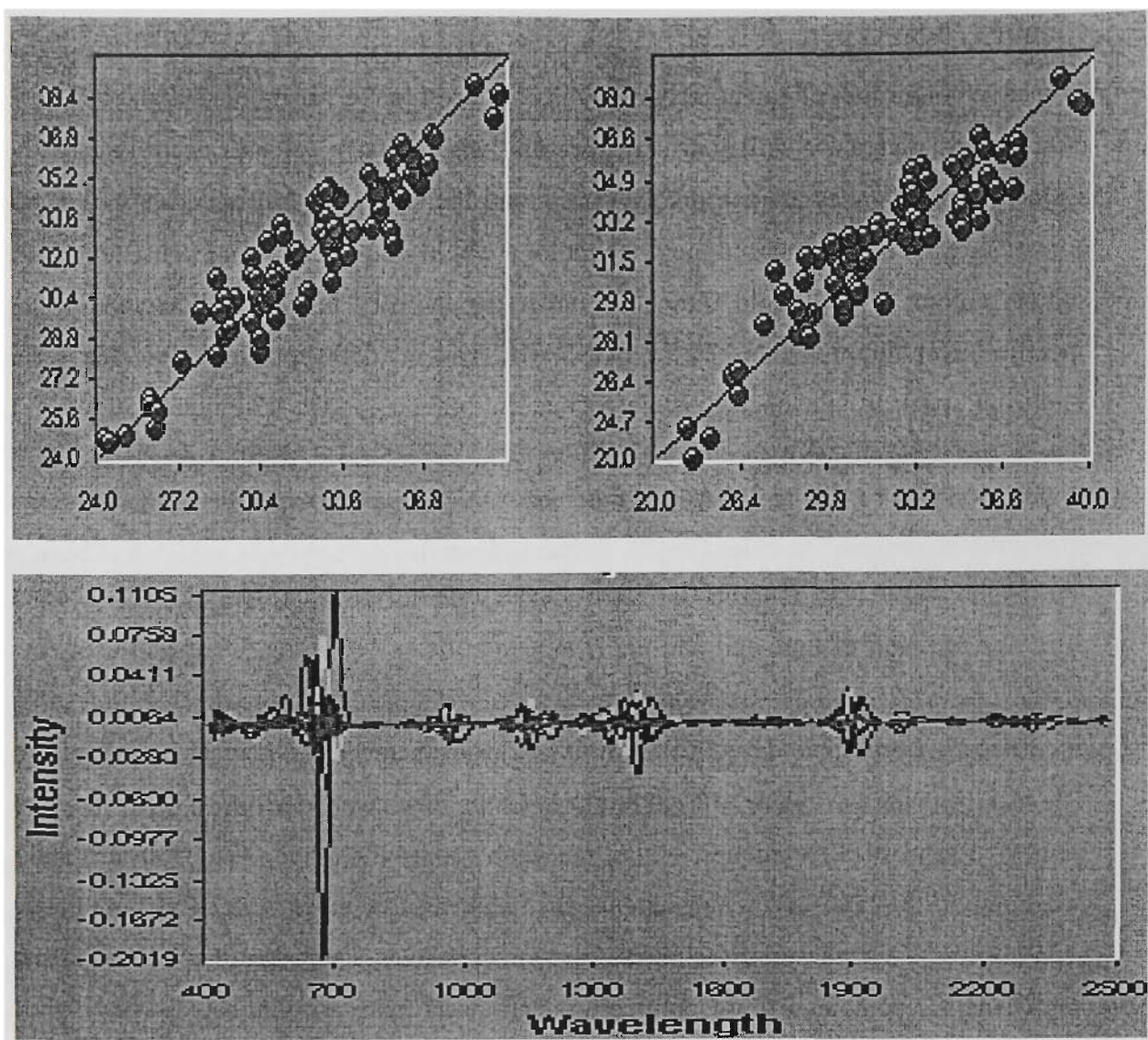


Figure 9.6 Plot of PLS predicted for  $L^*$   
 Clockwise from top left: plot of  $L^*$  PLS predicted vs laboratory 400 - 2500 nm, plot of  $L^*$  PLS predicted vs laboratory 700 - 2500 nm and weighting scores for factors 400 - 2500 nm.

$\lambda$ Region nm	n	Math	Statistic	F	$R^2$	SEP	Range	SD	SEP/SD
$L^*$ 400-2500	79	NPS-2 <sup>nd</sup> D	PLS	5	0.85	1.41	24-39	4.00	0.35
$L^*$ 400-2500	80	NPS-2 <sup>nd</sup> D	MLR	4	0.91	1.06	24-39	4.00	0.27
$L^*$ 700-2500	79	NPS-2 <sup>nd</sup> D	PLS	4	0.93	0.92	24-39	4.00	0.23
$L^*$ 700-2500	80	NPS-2 <sup>nd</sup> D	MLR	4	0.93	0.95	24-39	4.00	0.24

$\lambda$ Region nm	n	Math	Statistic	F	$R^2$	SEP	Range	SD	SEP/SD
$a^*$ 400-2500	80	NPS-2 <sup>nd</sup> D	PLS	3	0.86	0.57	2.9-9.3	1.44	0.40
$a^*$ 400-2500	79	NPS-2 <sup>nd</sup> D	MLR	4	0.93	0.40	2.9-9.3	1.44	0.28
$a^*$ 700-2500	80	NPS-2 <sup>nd</sup> D	PLS	4	0.82	0.67	2.9-9.3	1.44	0.47
$a^*$ 700-2500	83	NPS-2 <sup>nd</sup> D	MLR	4	0.88	0.56	2.9-9.3	1.44	0.39

Table 9.2 Calibration statistics for  $L^*$  and  $a^*$  tristimulus coordinates.

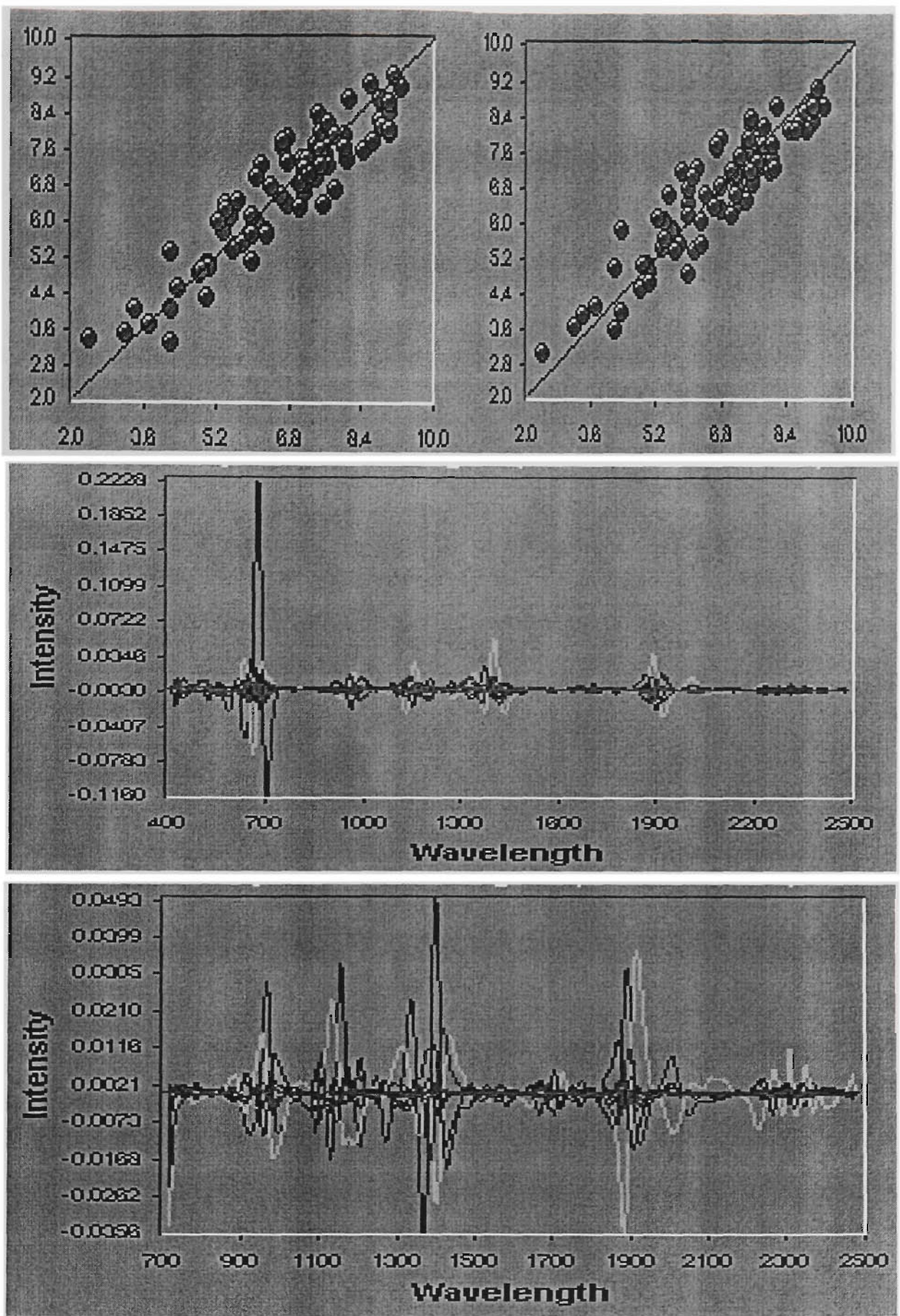


Figure 9.7 Plot of PLS predicted for  $a^*$   
 Clockwise from top left: plot of  $a^*$  PLS predicted vs laboratory 400 - 2500 nm, plot of  $a^*$  PLS predicted vs laboratory 700 - 2500 nm, weighting scores for factors 400-2500 nm and weighting scores for factors 700-2500 nm

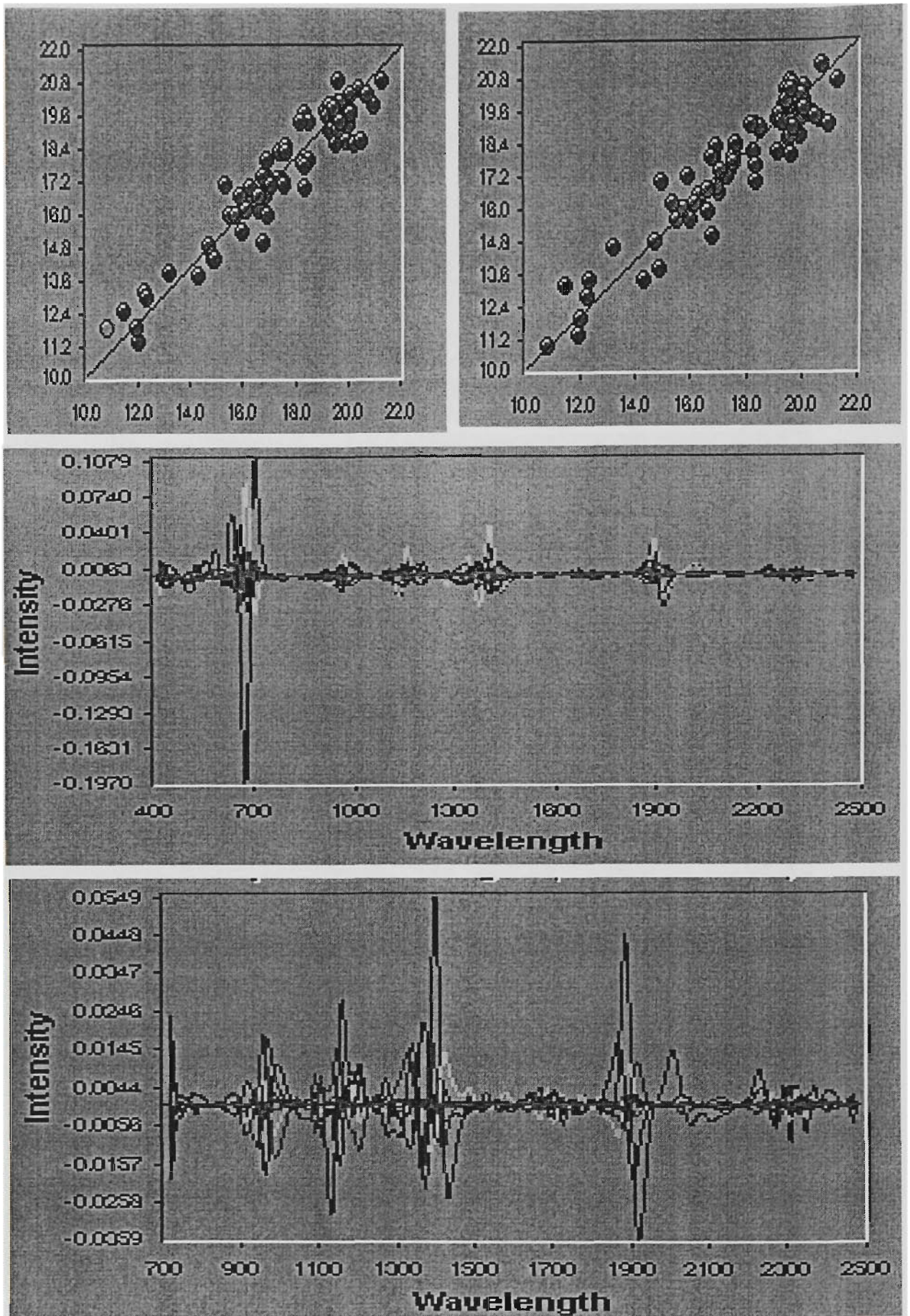


Figure 9.8 Plot of predicted PLS for  $b^*$   
 Clockwise from top left: plot of  $b^*$  PLS predicted vs laboratory 400 - 2500 nm, plot of  $b^*$  PLS predicted vs laboratory 700 - 2500 nm, weighting scores for factors 400-2500 nm and weighting scores for factors 700-2500 nm

$\lambda$ Region nm	n	Math	Statistic	F	R <sup>2</sup>	SEP	Range	SD	SEP/SD
b* 400-2500	86	2nd D	PLS	4	0.86	0.95	11.9-20.6	2.42	0.393
b* 400-2500	85	2nd D	MLR	4	0.913	0.95	11.9-20.6	2.42	0.393
b* 700-2500	82	2nd D	PLS	4	0.93	0.70	11.9-22.6	2.42	0.287

Table 9.3 Calibration statistics for b\* tristimulus coordinate

Spectral weighting scores show relative contributions of spectral regions to latent factors used in PLS models. Although impossible to unambiguously assign specific signals to chemical components, it is interesting to compare main spectral regions to known chemical assignment data. For example, in calibrations formed in the region 400-2500 nm region, major weighting are on the region around 700 nm, corresponding to electronic phenomena rather than pure NIR absorption, which is reasonable given that the calibration was performed on a colour component. PLS calibrations with visible data excluded generated models with a large emphasis on the region around 1900-1920 nm. This region is assigned to second overtone stretch phenomena of a carbonyl moiety either in COOH or CONH at 1900 and 1920 respectively, which is consistent with both a peptide bond and also various Maillard reaction intermediates and colour chromophores. The second major region, at around 1400 includes aromatic C-H combination signals (1417 and 1445 nm) which may be due to either Maillard heterocyclic aromatic chromophores or phenolic colour systems. The same relative spectral weighting used in b\* PLS calibration was observed for calibrations of L\* and a\* respectively, suggesting that compounds which are both aromatic and contain carbonyl groups are responsible for sultana coloured pigments. This would be consistent with a Maillard origin of colour in sultanas.

Table 9.4 shows the 4 wavelengths used to generate MLR calibrations for L\*a\*b\* values. As described previously in the text, calibrations were performed using both visible and NIR (400-2500 nm) and NIR data only (700-2500 nm). In the first instance, wavelengths in the visible region were selected as principal calibration data, and subsequently a number of NIR wavelengths were also included in the model. Calibration models with good to fair colour prediction ability using only NIR spectral material were achieved as was shown in preceding sections. Visible spectral data is due to electron transition phenomena, whereas NIR signals arise strictly from hydrogen bond vibrational modes. The exact end of the visible and commencement of the NIR portions of the electromagnetic spectrum is arbitrarily defined as occurring around 700 nm, with some overlap of both electronic and bond vibrational phenomena. Most calibration models used at least one or two wavelengths for colour calibration within the region defined as the very near infrared (700-1100) Colour chromophores also have a corresponding vibrational signature within the NIR region. Exact assignment of the chemico-physical origin of these signals would be difficult if not impossible, notwithstanding a general functional group assignment approach, as discussed previously. Most models include a wavelength around 1400 nm, which is a known region for various aromatic C-H combination signals, such as 1417 nm and 1440 nm, and an aromatic O-H first overtone vibration at 1420 nm.

Parameter	Spectral Region	$\lambda 1$	$\lambda 2$	$\lambda 3$	$\lambda 4$
L*	400-2500	510	1296	742	612
L*	700-2500	836	808	1422	2436
a*	400-2500	538	590	1762	526
a*	700-2500	712	1438	816	784
b*	400-2500	894	978	654	1460
b*	700-2500	894	978	1462	772

Table 9.4 Multiple Linear Regression wavelengths for L\* a\* b\* calibrations

Parameter	n cal	F	R <sup>2</sup> cal	SEC	n- val	R <sup>2</sup> val	SD	SEP	SEP/SD
L*	72	4	0.910	1.03	10	0.97	4.7	0.83	0.17
a*	72	4	0.86	0.393	10	0.96	2.01	0.50	0.25
b*	72	4	0.92	0.742	10	0.95	2.73	0.47	0.17

Table 9.5 Calibration validation data for L\*, a\* and b\* tristimulus values

As a final verification of colour prediction using NIR, ten samples were removed from the calibration sets over the calibration range and used to validate the optimised PLS prediction models. The range and SD for validation sets were as follows: L\* range 24.5-36.3 and SD 4.7, a\* range 4.3-9.1 and SD 2.01 and b\* range 11.4-21.60 with a SD of 2.75. As can be seen in Table 9.5 good predictions on new sultana spectra were obtained, indicating a stable predictive ability of colour models.

## 9.06 Free-arginine in sultanas

Skin free-arginine in sultanas was measured using F-moc HPLC analysis as previously described. A total of 36 samples was analysed and arginine data were used to create an NIR-calibration. Table 9.6 shows the calibration data. The broad range of skin free-arginine values in the small sultana population facilitated promising calibration models. Both MLR and PLS models indicated a reasonable predictive ability of models based on both R<sup>2</sup> and SEP/SD scores (Figure 9.9).

Spectral range	n	Math	Statistic	F	R <sup>2</sup>	Range & mean	SEP	Wavelength	SD	SEP/SD
400-2500	36	NPS, 2 <sup>nd</sup> D	PLS	6	0.91	0.451-8.69 3.38	0.79		2.12	0.37
400-2500	35	NPS, 2 <sup>st</sup> D	MLR		0.90	0.451-8.69 3.38	0.72	614, 1964, 2396, 602	2.12	0.34
700-2500	34	NPS, 2 <sup>nd</sup> D	PLS	7	0.90	0.451-8.69 3.38	0.81		2.12	0.38
700-2500	33	NPS, 2 <sup>nd</sup> D	MLR		0.90	0.451-8.69 3.38	0.56	898, 732, 2298, 1812	2.12	0.26

Table 9.6 Calibration statistics for skin free-arginine

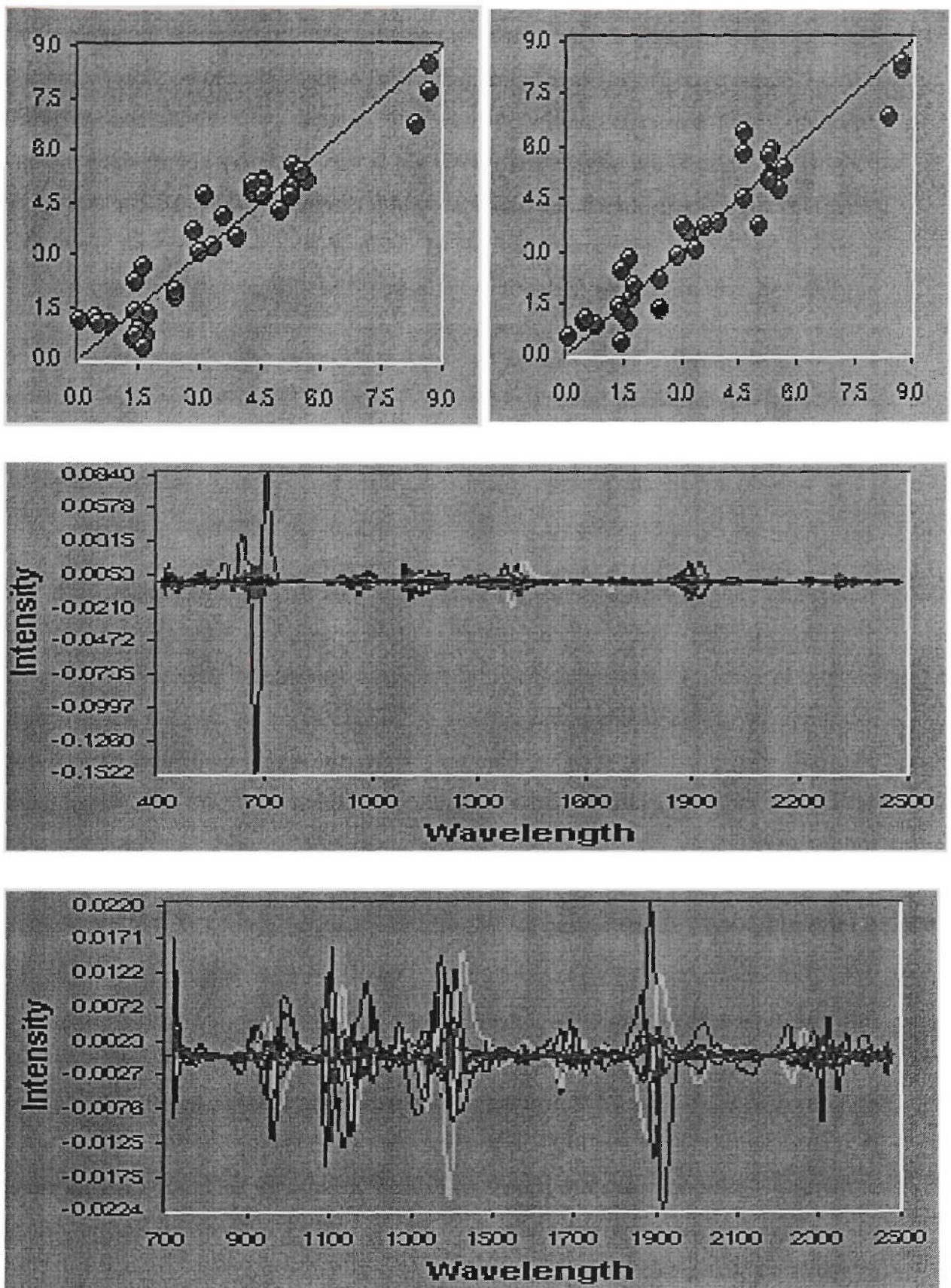


*Figure 9.9 Plot of predicted skin free-arginine  
 Clockwise from top left: plot of arginine PLS predicted vs laboratory 400 - 2500 nm, plot of arginine PLS predicted vs laboratory 700 - 2500 nm, weighting scores for factors 400-2500 nm and weighting scores for factors 700-2500 nm.*

The wavelengths used in MLR calibrations (400-2500 nm) (Table 9.6) are an unusual combination, because the primary wavelength used is in fact in the visible region, i.e. 614 nm. This absorption is clearly due to an electron transition requiring a visible frequency photon, rather than a vibrational overtone. Since arginine has been demonstrated to be a key factor in the colour potential of sultanas, the correlation may well coincide with an arginine-derived Maillard chromophore. Use of the wavelength at 1964 nm is very close to a known combination band due to an N-H asymmetric stretch and amide II band (Osborne *et al.* 1993). The absorption band at 2396 nm lies close to a characterised R-OH deformation second overtone signal at 2380 nm, however the chemical source of this absorption would be difficult to ascertain.

The MLR calibration for 700-2500 nm used a different set of wavelengths. The principal wavelength was at 898 nm, which lies close to a strong C-H third overtone from protein (Osborne *et al.* 1993.) and the second calibrating wavelength was 732 nm, which is close to a R-O-H strong overtone band at 738 nm. The absorption at 2298 nm may be due to the N-H and C=O stretches on amino acids listed as occurring at 2294 nm in assignment references.

Although a relatively large number of factors was used for PLS calibrations, both  $R^2$  and SEC/SD ratios indicated a reasonable predictive ability for the model. Because of the small number of samples used in the calibrations the results must be viewed as a preliminary indication of NIR measurement of the free-arginine content of sultana skins. A number of investigators have claimed to have obtained good calibrations for the amino acid content of various unprocessed agricultural materials, such as wheat and barley (Williams *et al.* 1984), supporting the merit of further investigation.

### 9.07 Kjeldahl protein in sultanas

Total Kjeldahl protein (KP) was measured in a small set of whole sultanas from the 1996 season ( $n=36$ ) and data were used to form a calibration with NIR spectra. The laboratory measured KP range was from 16.6 to 41.65  $\text{mg}\cdot\text{g}^{-1}$  DW with a standard deviation of 7.32. Calibrations were performed using Vision 2.1® Software, with redundant samples removed using the software recommendations. MLR and PLS calibrations were executed for the 400-2500 nm and 700-2500 nm ranges. Calibration data are shown in Table 9.7. Superior calibration results were obtained using a PLS modeling approach compared to MLR. Table 9.7 shows that PLS models had higher  $R^2$  values and lower SEP/SD ratios.

Figure 9.10 shows predicted versus laboratory values for the PLS calibration of these samples (1996 sultanas) and also the spectral loading data for the model equation. The plot of the predicted versus laboratory KP shows that the distribution of samples was not even over the protein concentration range, with relatively fewer high protein samples. The correlation for lower

protein samples, approximately in the range from 16 to 34 mg.g<sup>-1</sup>, was not, however, compromised by the inclusion of the high nitrogen samples. Removal of the five high nitrogen data resulted in calibration models with very similar  $R^2$  and SEP/SD values (results not shown). Thus it can be concluded that the inclusion of the high KP data did not falsely inflate the prediction capability of the model.

A further random set of sultana samples (1998) was collected from a packing shed, representing fruit from across the Sunraysia area. A total of 75 sultanas were analysed for KP and spectra were subjected to pre-calibration processing using the Vision 2.1 software. Redundant samples identified by the software algorithm were removed from the data set, before calibrations were performed. The range of nitrogen was from 11.7 to 31.8 mg.g<sup>-1</sup> DW, with a predominance of samples with nitrogen values around the mean value, 25.04. The lack of spread in the calibration set resulted in lower  $R^2$  values and higher SEP / SD ratios see (Table 9.8).

Data from 1996 and 1998 were added together and subjected to pre-calibration processing for removal of redundant samples by the software. PLS calibration yielded models with  $R^2$  values of 0.84 and reasonable SEP/SD ratios (>0.4). The extremely high nitrogen samples used in the 1996 trial generally had a negative effect on the model for combined 1996-1998 samples, so they were not used in the calibration process.

Model type	F	n	$R^2$	Range & Mean	SD	SEP	SECV	SEP /SD
Spectral math								
Spectral region								
PLS	5	34	0.95	41.6-16.6	7.32	1.76	2.43	0.24
NPS, 2 <sup>nd</sup> D				25.76				
400-2500 nm								
PLS	8	34	0.94	41.6-16.6	7.32	1.98	3.52	0.27
NPS, 2 <sup>nd</sup> D				25.76				
700-2500 nm								

Model type	n	$R^2$	Range & mean	SD	SEP	SEP/SD	Wavelengths Used
Spectral math							
Spectral region							
MLR	34	0.88	41.6-16.6	7.32	2.688	0.36	614, 1792, 560, 978
NPS, 2 <sup>nd</sup> D			25.76				
400-2500 nm							
MLR	34	0.87	41.6-16.6	7.32	2.92	0.39	788, 2236, 1226, 810
NPS, 2 <sup>nd</sup> D			25.76				
700-2500 nm							

Table 9.7 Calibration statistics for whole sultana Kjeldahl Protein for 1996 samples. Top: PLS data. Bottom: MLR data.

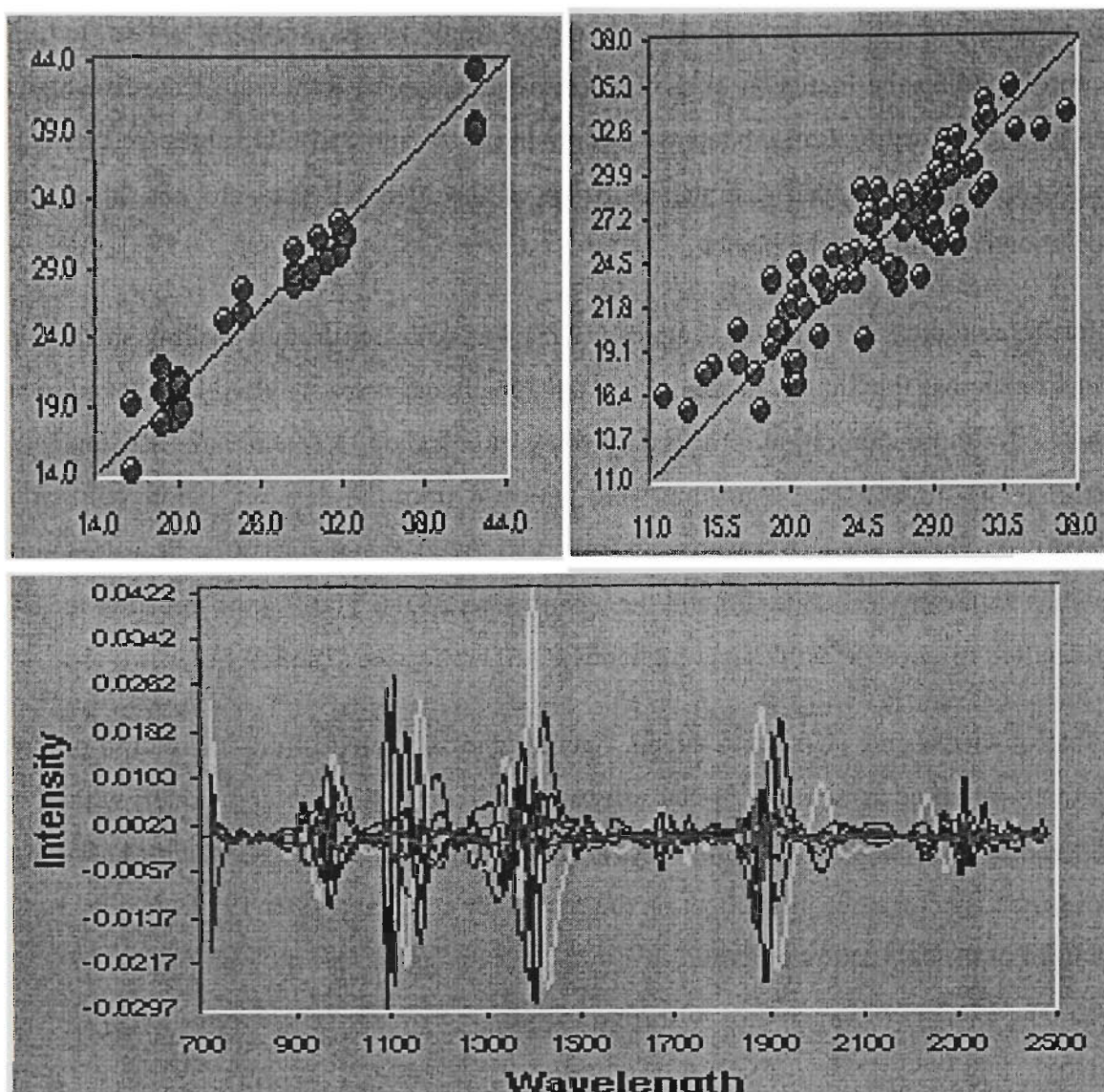


Figure 9.10 Plot of PLS predicted for Kjeldahl Protein (KP)  
 Clockwise from top left: plot of KP PLS predicted vs laboratory 700 - 2500 nm 1996 samples (n=34), plot of KP PLS predicted vs laboratory 700 - 2500 nm 1996&1998 (n=85) and weighting scores for factors 700-2500 nm.

Statistic	F	n	R <sup>2</sup>	Range & Mean	SD	SEP	SECV	SEP /SD
<b>1998 Sultanas</b>								
PLS	7	69	0.84	11.74-31.8	4.88	2.169	3.07	0.44
NPS, 2 <sup>nd</sup> D				25.04				
400-2500 nm								
PLS	7	69	0.82	11.74-31.8	4.88	2.26	3.28	0.46
NPS, 2 <sup>nd</sup> D				25.04				
700-2500 nm								
<b>1998 Sultanas</b>								
PLS	7	85	0.84	11.74-34.5	5.85	2.17	2.52	0.37
NPS, 2 <sup>nd</sup> D				24.14				
400-2500 nm								
PLS	7	85	0.84	11.74-34.5	5.85	2.23	3.28	0.38
NPS, 2 <sup>nd</sup> D				24.14				
700-2500 nm								

Table 9.8 Calibration data for 1998 and 1996 & 1998 PLS calibrations for KP.

## 9.08 Conclusions

NIR indicated an ability to measure  $a_w$ ,  $L^*$ ,  $a^*$   $b^*$  colour tristimulus values, KP and skin free-arginine in whole unprocessed sultanas. The data in this section were based on a limited number of samples, generally from only one season, i.e. 1996 ( $a_w$ , skin free-arginine and  $L^*a^*b^*$ ) and thus can only be considered as an initial investigation. Larger data sets with multi-season information would be required to improve calibration models to include more natural variation and increase model robustness.

The practical application of large-scale NIR calibrations for these and possibly other parameters could become the basis of a rapid test for overall sultana quality and an indicator of colour stability. An NIR calibration could be substituted for existing colour classification systems. Translation of NIR technology into a practical industry device would require collaboration with an NIR spectrometer manufacture, where an industry specific model could be constructed with only wavelengths pertinent to particular calibrations being included. Fibre optic measuring probes are available from NIR manufacturers, which could be used to sample sultanas as they arrive at packaging sheds. It is plausible that when a full calibration has been modelled and thoroughly validated, real time NIR spectra for incoming samples could be acquired and sent to a database with relevant information about the grower together with NIR measured quality indicators. An immediate computer feedback system could classify sultana bins on the basis of this data and print out a quality report with a quality indication score which could immediately be attached to the bin and facilitate further processing. Prices for growers' sultanas could also be determined via a quality algorithm based on NIR spectral information.

## 10.0 CONCLUSIONS AND FURTHER WORK

---

### 10.01 Summary of data

The storage trial data furnished evidence that Maillard reactions occurred during sultana storage and made a significant contribution to sultana browning. Significant colour change occurred mainly at 30°C in both aerobically- and anaerobically-stored sultanas: the lack of oxygen dependence was consistent with Maillard reactions rather than phenolic oxidation processes. The existence of storage-Maillard reactions was also indicated by increases in 5-HMF, measured only in 30°C stored samples. A number of lines of evidence implicated arginine as the principal amino acid catalysing Maillard sugar degradation reactions: the disappearance of free-arginine over time (storage trial I 1995), the direct relationship between soil-nitrogen, sultana free-arginine and storage browning in the nitrogen trial (chapter 5), the close match of HPLC-DAD profiles of sultana extracts and arginine-glucose model systems and, finally, the match of GC-MS profiles of sultana and model systems. In addition, model systems were used to examine arginine-glucose Maillard browning processes, such as their sensitivity to  $a_w$ , temperature, pH and initial arginine concentration: much of the model system browning behaviour was consistent with browning phenomena observed in sultanas.

Within the sultanas from each storage trial (1995 I, 1996 II and the nitrogen trial), there were only small differences in pre-storage PPO activity, indicating that differences in browning were not likely to be due to initial higher enzyme activity. Differences in grape and sultana PPO activity have been shown to have an important effect on final sultana colour; e.g. Bruce's Sport has low PPO and subsequently produces lighter dried sultanas. It has been demonstrated that PPO is substantially inhibited by high glucose concentration (Grcarevic and Hawker 1971) and it is generally assumed that PPO is not active in sultanas below a certain moisture content or  $a_w$ , although the precise  $a_w$  at which PPO becomes inactive in sultanas has not been identified. In this thesis it was initially hypothesised that higher  $a_w$  sultanas (non-sunfinished sultanas in the storage trials) may allow for PPO activity during storage and hence account for the greater browning observed in those samples. It was, therefore, essential that pre-storage PPO activity was measured to account for any differences in storage browning. Higher  $a_w$  sultanas invariably underwent significantly greater browning than lower  $a_w$  controls (storage trial I and II), which was observed for sultanas stored both aerobically and anaerobically. The fact that greater browning was observed in high  $a_w$  anaerobically stored sultanas (compared to anaerobically stored low  $a_w$  fruit) indicated that at least some of the storage browning must have been due to  $a_w$ -sensitive, non-oxygen dependent reactions i.e. Maillard processes. The significantly greater browning observed at 30°C in higher  $a_w$  aerobically-stored samples could then logically be attributed to PPO oxidation reactions, non-PPO dependent phenolic oxidation reactions (autoxidation), lipid free-radical

induced oxidation reactions and secondary, oxidative-Maillard reactions. Evidence of lipid oxidation was given in chapter 6 and differences in the rates of Maillard reactions in the presence of oxygen were indicated by lower concentrations of 5-HMF in aerobically stored sultanas. The measured skin pre-storage PPO activity in the 1995 sultanas ( $9.05\text{-}13.79 \mu\text{mole.O}_2\text{.g}^{-1}\text{.min}^{-1}$ ) was more than double that of the following year 1996 ( $3.25\text{-}5.2 \mu\text{mole.O}_2\text{.g}^{-1}\text{.min}^{-1}$ ), yet from the regression data in section 4.36 there was not a significant difference in browning between years. This would indicate that differences in pre-storage PPO activity within the range observed in the trials did not have an effect on the browning potential. The assumption that the process of sunfinishing may induce a positive effect on sultana colour by inactivating PPO could not be supported by the data. From the limited data in the nitrogen storage experiment it appeared that the application of high soil nitrogen did not significantly increase sultana PPO.

It has been suggested that higher concentrations of certain phenolic browning substrates may predispose aerobically-stored sultanas to greater browning. Total phenolics measurements for sultanas in 1995 indicated that there was a small difference between exposed ( $1.22\text{-}1.37 \text{mg.g}^{-1}$ ) and protected sultanas ( $1.57\text{-}2.01 \text{mg.g}^{-1}$ ). This difference was not found to be statistically useful as a browning predictor in regression models however. In the 1996 trial and the nitrogen experiment, total phenolics were slightly lower than the previous year ( $0.70\text{-}1.13$  and  $0.88\text{-}0.94$ ) respectively, however, as this term was not significant in the combined 1995 & 1996 regression model, differences of this magnitude would appear to be unimportant in terms of sultana browning and colour prediction. Data for the nitrogen sultana experiment indicated that the nitrogen application did not have a significant effect on total phenolics.

In the 1996 trial, the maturity of the grapes had an important effect on sultana browning; the late-harvest, more-mature sultanas were darker than comparable early-harvest controls. There was some evidence that these more mature sultanas may have undergone more extensive Maillard-type reactions, evidenced by (1) higher pre-storage concentrations of skin free-arginine (Fig 4.4), (2) by lower 5-HMF measured after 10 months storage compared to the early-harvest fruit (Fig 4.15). There was also evidence that lipid oxidation reactions may have contributed to the greater browning observed in these higher maturity samples (Table 6.4). The fact that these samples also had higher pre-storage  $a_w$  values may have somewhat confounded the data, as  $a_w$  was been shown to have a strong effect on storage browning. The higher free-amino acids in the more mature sultanas indicated that some kind of protein degradation had occurred, as there was not a difference in KP between harvest dates.

The important effect of sultana sunfinishing on sultana colour was largely supported by the data. Although in most cases sunfinishing did not decrease the PPO activity it had an important effect on  $a_w$  (Table 3.4 and 4.5). From the regression models of browning prediction it was seen that  $a_w$

was a strong predictor of sultana browning. It was found that high  $a_w$  promoted more rapid browning regardless of whether sultanas were stored in an oxygen-exposed or oxygen-free environment. It has long been known in the Sultana Industry that high moisture fruit undergoes rapid browning. It has not been shown whether this browning is due to active PPO oxidizing phenolics or non-enzymatic reactions, i.e. Maillard reactions. In chapter 4.0, it was demonstrated that oxidation of *trans*-caftaric acid had occurred in late-harvest non-sunfinished sultanas before storage although the immediate effect on initial sultana colour was not observed. After storage at 30°C, with and without oxygen, intense browning occurred, indicating that the nature of these processes was not inherently oxygen dependent, and thus was unlikely to be due to a high moisture reactivation of PPO during storage.

The strong effect of  $a_w$  on glucose-arginine Maillard model system browning was illustrated in chapter 8.0. The model systems demonstrated that arginine-glucose Maillard reactions occur at a significantly faster rate at an  $a_w$  level beyond about 0.60, which is, to an extent, consistent with observed browning behaviour in sultanas.

In most cases oxygen-free packaging was effective in retarding rates of browning. Higher relative concentrations of 5-HMF in extracts from sultanas stored in an oxygen-free environment indicated that Maillard reactions in sultanas were oxygen sensitive. The autoxidation of Amadori Products to produce reactive  $\alpha$ -dicarbonyl intermediates was discussed in section 2.09. It is proposed that oxidative Maillard routes were primarily responsible for the greater browning in aerobically-stored samples rather than phenolic oxidation phenomena. The adoption of oxygen-free packaging would be recommended to the industry as a means to slow but not eliminate storage browning processes.

Comparison of the relative importance of the various storage factors for each trial (1995, 1996 and the nitrogen experiment) allowed some general statements to be made regarding the nature of the browning that occurred. Table 10.1 shows the most important effects for the  $L^*$  and  $b^*$  tristimulus values in order of decreasing significance. For change in  $L^*$  (lightness), temperature was the most important single effect (in the nitrogen experiment the second most important) and that the temperature $\times$ time interaction was also significant. Extensive browning reactions occurred almost exclusively at 30°C over an extended time-frame, consistent with Maillard-type reactions rather than PPO mediated reactions. Although the PPO enzyme is temperature sensitive, it would not be expected that the enzyme was completely inactive at 10°C; the absence of significant aerobic browning at this temperature supports this statement. In addition, for all samples the temperature $\times$ time interaction was important, underlying the observation that the storage browning occurred mainly at 30°C and became more intense over time. The time dependence of the browning is more consistent with Maillard type processes than PPO browning; PPO browning occurs rapidly i.e. days to weeks (Grncarevic and Hawker 1963).

Year	1995	1996 early	1996 late	Nitrogen	1995	1996 early	1996 late	Nitrogen
Tristimulus coordinate	L*	L*	L*	L*	b*	b*	b*	b*
Effect 1	Temp	Temp	Temp	N	Sun	Temp	Temp	N
Effect 2	Sun	Ex	Sun	Temp	Ox	Time	Sun	Temp
Effect 3	Temp x Time	Time	Temp x Time	Time	Ox x Temp	Ox x Temp	Ox	Time
Effect 4	Time	Temp x Time	Ox	Temp x Time	Temp	Ox	Temp x Time	Temp x Time
Effect 5	Ox	Ox	Ex x Sunf		Temp x Time	Temp x Time	Sun x Temp	
Effect 6	Ox x Time	Sun				Ex		

*Table 10.1 Summary of the single effects and two-way interactions from the ANOVA analyses of the sultana storage trials (trials I, II and the soil-nitrogen experiment). The effects are listed in order of decreasing importance. Temp=temperature, Sun=sunfinishing, N=nitrogen, Ox=oxygen.*

For 1995 and 1996 samples the sunfinishing terms was significant, highlighting the  $a_w$  sensitivity of the reactions. Although the oxygen exposure had a significant effect on browning, the relative magnitude of its effect was small (see ANOVA data for each trial). The higher browning that occurred under oxygen-exposed conditions may have been due to different rates of Maillard browning and lipid oxidation reactions. Temperature and the interaction of temperature $\times$ time were similarly important effects for the  $b^*$  tristimulus value. Changes in  $b^*$  appeared most oxygen and  $a_w$  sensitive. In the time-course study of arginine-glucose browning model systems, the  $b^*$  term increased to reach maximum yellowness, and then declined as browning progressed (Fig 8.3). High  $b^*$  is a positive attribute for sultanas as it contributes to the golden colour. It is proposed that in the presence of oxygen (with iron present) the point at which this decline occurs is hastened. Once again, the temperature $\times$ oxygen interaction was in many cases important, indicating that the effect of oxygen was mainly significant at 30°C. If changes in  $b^*$  were mainly PPO-mediated, this interaction would not have been expected to be significant, as the effect of oxygen would have been important regardless of temperature. The importance of the temperature $\times$ oxygen interaction also indicated that the browning reactions required time at 30°C to occur; this was more consistent with Maillard reactions. Maillard reactions are heat sensitive, hence controlling temperatures of sultanas during storage and transportation, e.g. shipping, would be one effective method of browning minimisation. As internal crystallisation was observed to occur only at low temperatures in sultanas, i.e. 10°C, long-term cool storage at this temperature would not be recommended.

The soil nitrogen and confirmation experiment provided further evidence of the contribution of Maillard reactions to storage browning. The lack of oxidation of *trans*-caftaric acid in these experiments despite intense browning provided the strongest single piece of evidence of the important role of Maillard reactions in sultana storage browning reactions. The presence of Maillard peaks on HPLC profiles over time, also observed in the arginine-glucose models, was further indication of Maillard reactions and, importantly, arginine-mediated Maillard reactions.

GC-MS analysis of EtAc, MeOH and SPME extracts from sultanas and arginine-glucose models showed a high level of match indicating similar reactions. All major Maillard components in model systems were also present in sultana extracts. Most of the major Maillard intermediates were previously identified in aged sweet-wine products (Cutzach *et al.* 1999), however the major products were of a generic Maillard nature rather than arginine specific. There was some indication of the presence of arginine-specific compounds, however these compounds were present at relatively low concentration. There was a large quantitative difference in the amount of extractable MRPs from sultanas stored at 60°C (Fig 7.6), implying that at this temperature a critical change of Maillard kinetics occurred. It is well known that sultana browning is rapid at around 60°C (ADFM 1998). The arginine-glucose model systems in chapter 8.0 also exhibited a strong increase in browning at 60°C.

## 10.02 Further research

The data in this thesis provided evidence of Maillard browning in sultanas during storage. Arginine was implicated an important amino acid in the development of these reactions. Further research is required to better characterise these processes. Future research directions are outlined in point form:

- The role of arginine as a Maillard amino acid in food systems, specifically fruits and vegetables, warrants further investigation. Arginine mediated browning and flavour development may be relevant to fortified and aged sweet-wine products.
- Further characterisation of the kinetics of arginine Maillard reactions especially with respect to temperature,  $a_w$ , oxygen and pH would be important. Characterisation of specific arginine Maillard products, such as the HPLC peaks eluting at 4.1 min and 5.3 min (chapter 5) would be necessary to better understand these Maillard processes. HPLC-DAD analysis of MeOH extracts of sultanas would provide an excellent means to simultaneously monitor changes in both phenolic substrates and Maillard intermediates, during further storage trials.

- A strong anti-oxidant effect of the arginine-glucose Amadori Product, fructosyl-arginine, in aged garlic extract has been cited recently in the literature (Ide *et al.* 1997, 1999). If the anti-oxidant activity of this compound is in fact significantly higher than other common food antioxidants, it could add sultanas to the list of healthy anti-aging foods and could also be used as a sales pitch by the Australian Sultana Industry. Intentional high soil nitrogen application and special packaging and storage to maintain a reasonable colour could produce high fructosyl-arginine sultanas.
- NIR as a quality control tool for the sultana industry demonstrated high potential in preliminary experiments. It is essential, however, that further samples over multiple seasons be analysed, in order to obtain a robust universal calibration. Additional sultana quality parameters such as bulk density, TA, etc. are probably also measurable using NIR.

## BIBLIOGRAPHY

---

- Abd El Al, M., Abd-El-Fadeel, M., El-Samahy, S. and Askar, A. 1994. Application of microwave energy in the heat treatment of fruit juices, concentrates, and pulps. *Flussig. Obst.* 61(10): 307-312.
- Abney, W. and Festing, E. 1881. On the influence of the atomic grouping in the molecules of organic bodies on their absorption in the infra red region of the spectrum. *Philosophical. Trans Royal Soc.* 172: 887-918.
- Adams, J. 1991. Review: enzyme inactivation during heat processing of food-stuffs. *Int. J. Food Sci. Technol.*, 26: 1-22.
- Affleck, R., Xu, Z., Suzawa, V., Focht, K., Clark, D. and Dordick, J. 1992. Enzymatic catalysis and dynamics in low-water environments. *Proc. Natl. Acad. Sci. USA.* 89:1100-1107.
- Aguilera, J., Oppermann, K. and Sanchez F. 1987. Kinetics of browning in sultana grapes. *J. Food Sci.* 52(4): 990-993, 1025.
- Aliaz, M. and Barragan, S. 1995. Reaction of a lysyl residue analogue with (E)-2-octanol. *Chem. Phys. Lipids.* 75: 43-49.
- Aliaz, M., Zamora, R and Hidalgo, F. 1995. Natural antioxidants in oxidised lipid/amino acid browning reactions. *J. Am. Oil. Chem. Soc.* 72(12): 1571-1575.
- Aliaz, M., Zamora, R., and Hidalgo, F. 1996. Antioxidative activity of pyrrole, imidazole, dihydropyridine and pyridinium salt derivatives produced in oxidized lipid/amino acid browning reactions. *J. Agric. Food Chem.* 44: 686-691.
- Albanell, E., Caceres, P., Caja, G., Molina, E. and Gargouri, A. 1999. Determination of fat, protein, and total solids in ovine milk by near-infrared spectroscopy. *JAOAC Int.* 82(3):753-758.
- Ames, J., Apriyantano, A. and Arnoldi, A. 1993. Low molecular weight coloured compounds formed in xylose-lysine model systems. *Food Chem.* 46: 121-127.
- Ames, J. 1998. Applications of the Maillard reaction in the food industry. *Food Chem.* 62(4): 431-439.
- Ames, J., Bailey, R. and Mann, J. 1999. Analysis of furanone, pyranone and new heterocyclic colored compounds from sugar-glycine model Maillard systems. *J. Agric. Food. Chem.* 47: 438-443.
- Antcliff, A. and Webster, W. 1962. Bruce's Sport—a mutant of the Sultana. *Aust. J. Exp. Agric. Anim. Husb.* 2: 97-100.

- Artyunayan, A., Dzahnpoladyan, L., Samvelya, A. and Khachatryan, A. 1964. The effect of fertilizers on the increase on the content of anthocyanins and aromatic compounds in grapes and wines. *Tr. Armyansk. Nauchn. Tssled. Inst. Vingradarstva, Vinodeliya I Plodvadvsta.* (6-7): 455-469 in *Chem. Abstr.* 64: 20575 (1966).
- Ashie, I., Simpson, B. and Smith, J. 1996. Mechanisms for controlling enzymatic reactions in foods. *Crit. Rev. Food Sci. Nutr.* 36 (1/2): 1-30
- Australian Bureau of Statistics. 1999. Australian Grape and Wine Industry—Report 1329.0. Canberra, Australia, December 16.
- Ayranci, E., Ayranci, G. and Dogantan, Z. 1990. Moisture sorption isotherms of dried apricot, fig and raisins at 20°C and 36°C. *J. Food Sci.* 55: 1591-1593, 1625.
- Bagchi, D., Garg, A., Krohn, R., Bagchi, M., Balmoori, J. and Stohs, S. 1998. Protective effect of grape seed proanthocyanidins and selected antioxidants against TPA-induced hepatic and brain lipid peroxidation and DNA fragmentation and peritoneal macrophage activation in mice. *Gen. Pharmac.* 30(5): 771-776.
- Bailey, R., Ames, J. and Monti, S. 1996. An analysis of the non-volatile reaction products of aqueous Maillard model systems at pH 5, using reverse-phase HPLC with diode array detection. *J. Sci. Food Agric.* 72: 97-103.
- Balsberg, R. and Phalsson, A. 1989. Mineral nutrients, carbohydrates and phenolic compounds in leaves of Beech (*Fagus sylvatica* L.) in Southern Sweden as related to environmental factors. *Tree Physiol.* 5: 485-493.
- Baltes, W. 1990. Roast aroma formation: the role of amino acids during the Maillard reaction. In '*The Maillard Reaction in Food Processing Human Nutrition and Physiology*'. (Ed. P.A. Finot). Birkhäuser Verlag, Basel, Switzerland. pp. 42-60.
- Benzig-Purdie, L. and Ratcliffe, C. 1986. A study of the Maillard reaction by <sup>13</sup>C and <sup>15</sup>N CP-MAS-NMR: influence of time, temperature and reactants on major products. In '*Amino Carbonyl Reactions in Food and Biological Systems: Developments in Food Science. Vol 13.*' (Eds. M. Fujimaki, M. Namiki and H. Kato) Elsevier, New York, USA. Pp. 193-205.
- Berke, B., Cheze, C., Vercauteren, J. and Deffieux, G. 1998. Bisulfite addition to anthocyanins-revisited structures of colourless adducts. *Tetrahed. Letts.* 39(32): 5771-5774.
- Birch, E., Lelievre, J. and Richards, E. 1984. Influence of the amine moiety on the thermal degradation of N-substituted 1-amino-1-deoxyfructoses. *Carbohy. Research.* 128: 351-355.

- Bjørsvik, H and Martens, H. 1991. Data analysis: Calibration of NIR instruments by PLS regression. In 'Handbook of Near Infrared Spectroscopy'. (Eds. D. Burns and E. Ciurczak). Marcel Dekker Inc. New York, USA. pp. 159-179.
- Blank, I. and Fay, L. 1996. Formation of 4-hydroxy-2,5-dimethyl-3(2H)-furanone and 4-hydroxy-2-(or 5)-ethyl-5(or 2)-methyl-3(2H)-furanone through Maillard reactions based on pentose sugars. *J. Agric. Food Chem.* 44: 531-536.
- Bolin, H. 1980. Relation of moisture to water activity in prunes and raisins. *J. Food Sci.* 45: 1190-1191.
- Bolin, H. and Petrucci, V. 1985. Amino acids in raisins. *J. Food Sci.* 50: 1507.
- Bolliger, S., Zeng, Y. and Windhab E. 1999. In-line measurement of tempered cocoa butter and chocolate by means of near-infrared spectroscopy. *J. Am. Oil Chem. Soc.* 76(6): 659-667.
- Bone, S. 1987. Time domain reflectometry studies of water binding and structural flexibility in chymotrypsin. *Biochim. Biophys. Acta.* 916: 128-134.
- Bozkurt, H., Göğüç, F. and Eren, S. 1999. Nonenzymatic browning reactions in boiled grape juice and its models during storage. *Food Chem.* 64: 89-93.
- Bressa, F., Tesson, N., Mdalla, R., Sensidoni, A. and Tubaro, F. 1996. Antioxidant effect of Maillard reaction products: application to a butter cookie of a competition kinetics analysis. *J. Agric. Food Chem.* 44(3): 692-695.
- Brierly, E., Bonner, P. and Cobb, A. 1997. Aspects of amino acid metabolism in stored potato tubers (cv. Pentland Dell). *Plant Sci.* 127: 17-24.
- Brownlee, M., Vlassara, H., Kooney, A., Ulrich, P. and Cerami, A. 1986. Aminoguanidine prevents diabetes induced arterial wall cross-linking. *Science.* 232: 1629-1632.
- Buttery, R., Takeoka, G., Krammer, G. and Ling, L. 1994. Identification of 2,5-dimethyl-4-hydroxy-3(2H)-furanone (furanol) and 5-methyl-4-hydroxy-3(2H)-furanone in fresh processed tomato. *Lebensm. Wiss. u Technol.* 27: 592-594.
- Cabanes, J., García-Cánovas, F. and García-Carmona, F. 1987. Chemical and enzymatic oxidation of 4-methylcatechol in the presence and absence of L-serine. Spectrophotometric determination of intermediates. *Biochim. Biophys. Acta.* 914: 190-197.
- Campos, C., Souza, P., Coelho, J. and Gloria, M. 1996. Chemical composition, enzyme activity and effect of enzyme inactivation on flavour quality of green coconut water. *J. Food Proc. Pres.* 20(6): 487-500.

- Cañellas, J., Rossello, C., Simal, S., Soler, L. and Mulet, A. 1993. Storage conditions affect quality of raisins. *J. Food Sci.* 58(4): 805-809.
- Chambers, T. and Possingham, J. 1963. Studies of the fine structure of the wax layer of Sultana grapes. *Aust. J. Biol. Sci.* 16: 818-825.
- Chang, R. 1990. Physical Chemistry with applications to biological systems. *Second Edition*. Macmillan Publishing Co. Inc. New York.
- Chen, C. and Cerami, A. 1993. Mechanism of inhibition of advanced glycosylation by aminoguanidine *in vitro*. *J. Carbohyd. Chem.* 12: 731-742.
- Cheng, R. and Kawakishi, S. 1994. Novel decomposition of Amadori compound catalysed by copper ion. *J. Agric. Food Chem.* 42(3):700-703.
- Cheyrier, V. and Moutounet, M. 1992. Oxidative reactions of caffeic acid in model systems containing polyphenoloxidase. *J. Agric. Food Chem.* 40: 2038-2044.
- Cheyrier, V. and Van Hulst, M. 1988. Oxidation of *trans*-caftaric acid and 2-*S*-glutathionylcaftaric acid in model solutions. *J. Agric. Food Chem.* 36(1): 10-15.
- Cheyrier, V., Osse, C. and Rigaud, J. 1988. Oxidation of grape juice phenolic compounds in model systems. *J. Agric. Food Sci.* 53(6): 1729-1732, 1760.
- Cheyrier, V., Rigaud, J. and Moutounet, M. 1990. Oxidation kinetics of *trans*-caffeoyl tartrate and its glutathione derivatives in grape musts. *Phytochem.* 29(6): 1751-1753.
- Cheyrier, V., Trousdale, E., Singleton, V., Salgues, M. and Wilde, R. 1986. Characterisation of 2-*S*-glutathionyl caftaric acid and its hydrolysis in relation to grape wines. *J. Agric. Food Chem.* 34: 217-221.
- Chirife, J., Ferro-Fontan, C. and Favetto, G. 1981. The water activity of fructose solutions in the intermediate moisture range. *Lebens. Wiss. Technol.* 15:159-160.
- Chirife, J. and Buera, M. 1996. Water activity, water glass dynamics, and the control of biological growth in foods. *Crit. Rev. Food Sci. Nutr.* 36(5): 465-513.
- Chou, H. and Labuza, T. 1974. Antioxidant effectiveness in intermediate moisture content model system. *J. Food. Sci.* 39: 479-482.
- Cilliers, J. and Singleton, V. 1991. Characterisation of the products of nonenzymatic autoxidative phenolic reactions in a caffeic acid model system. *J. Agric Food Chem.* 39: 1298-1303.

Concise Encyclopedia of Foods and Nutrition. 1995. (Eds. A. Ensminger, M. Ensminger, J. Konlande and R. Robson). CRC Press, Boca Raton, FL, USA.

Coombe, B. 1987. The distribution of solutes within the developing grape berry in relation to its morphology. *Am. J. Enol. Vitic.* 38:127-129.

Cooper, T. 1982. Nitrogen metabolism in *Saccharomyces cerevisiae*. In 'The Molecular Biology of Yeasts. *Saccharomyces: Metabolism and Gene Expression*'. (Eds J. Strathern, E. Jones and J. Borach). Cold Springs Harbor Laboratory. Cold Springs, New York, USA.

Creasy, L., and Coffee, M. 1988. Phytoalexin production potential of grape berries. *J. Am. Soc. Hort. Sci.* 113: 230-234.

Creasy, L., Maxie, C. and Chichester, C. 1965. Anthocyanin production in strawberry leaf disks. *Phytochemistry.* 4: 517-521.

Crippen, D. and Morrison, J. 1986. The effects of sun exposure on the phenolic content of Cabernet Sauvignon berries during development. *Am. J. Enol. Vitic.* 37(4): 243-247.

Cunico, R., Mayer, A., Dimson, P. and Zimmerman, C. 1995. Pre-column derivatisation of amino acids using amino tag. Application note, Varian Instrument Group, Walnut Creek Division, Walnut Creek, CA, USA.

Cutzach, I., Chatonnet, P. and Dubourdieu, D. 1999. Study of the formation mechanisms of some volatile compounds during the aging of sweet fortified wines. *J. Agric. Food Chem.* 47(7): 2837-2846.

Del Castillo, D., Corzo, N. and Olano, A. 1999. Early stages of Maillard reaction in dehydrated orange juice. *J. Agric. Food Chem.* 47: 4388-4390.

Delwiche, S., Pierce, R., Chung, O. and Seabourn, B. 1998. Protein content of wheat by near infrared spectroscopy of whole grain. A collaborative study. *J. AOAC Int.* 81(3):587-603.

Di Cosmo, F. and Towers, G. 1984. Stress and secondary metabolism in cultured plant cells. *Recent Adv. Phytochem.* 18: 97-102.

Australian Dried Fruits Association. 1998. *Dried Vine Fruit Manual*, July 1998.

Dry, I. and Robinson, S. 1994. Molecular cloning and characterisation of grape berry polyphenol oxidase. *Plant Molec. Biology.* 26(1): 495-502.

Dry, P. and Gregory, G. 1988. Grapevine Varieties. In 'Viticulure: Volume 1-Resources,' (Eds. B.G. Coombe and P.R. Dry). Winetitles, Underdale, South Australia. pp. 119-138.

- Dudman, W. and Grncarevic, M. 1962. Determination of the surface waxy substances of grapes. *J. Food Sci. Agric.* 13(4): 2231-2241.
- Edwards, K., Cramer, C., Bolwell, G., Dixon, R., Schuch, W. and Lamb, C. 1985. Rapid transient induction of phenylalanine ammonia-lyase m-RNA in elicitor treated bean cells. *Proc. Natl. Acad. Sci USA.* 82: 6731-6735.
- Eichner, K. and Karel, M. 1972. The influence of water content and water activity on the sugar-amino browning reaction in model systems under various conditions. *J. Agric. Food Chem.* 20(2): 218-223.
- Elizalde, B., Dalla-Rosa, M. and Lericci, C. 1991. Effect of Maillard reaction volatile products on lipid oxidation. *J. Am. Oil Chemist. Soc.* 68(10): 758-762.
- Escarpa, A. and González, M. 1998. High-performance liquid chromatography with diode-array detection for the determination of phenolic compounds in peel and pulp from different apple varieties. *J. Chromatogr A.* 823: 331-337.
- Evershed, R. 1992a. Gas Chromatography of lipids. In '*Lipid Analysis: a Practical Approach.*' (Eds: Hamilton and S. Hamilton.). IRL Press (Oxford University Press Inc.) New York, USA. pp. 113-151.
- Evershed, R. 1992b. Mass Spectrometry of lipids. In '*Lipid Analysis: a Practical Approach.*' (Eds: J. Hamilton and S. Hamilton) IRL Press (Oxford University Press Inc.) New York, USA. pp. 263-308.
- Farag, R., Osman, S., Hallabo, S. and Nasr, A. 1978. Linoleic acid oxidation catalysed by various amino acids and cupric ions in aqueous media. *J. Am. Oil Chem. Soc.* 55: 703-707.
- Faust, M. 1965. Physiology of anthocyanin development in McIntosh apple I. Participation of pentose phosphate pathway in anthocyanin development. *Proc. Am. Soc. Hortic. Sci.* 87:1 201-215.
- Felton, J., Knize, M., Roper, M., Fultz, E., Shen, N. and Turteltaub, K. 1992. Chemical analysis, prevention and low level dosimetry of heterocyclic amines from cooked food. *Cancer Res.* 52: 2103-2107.
- Fennema, O. 1985. '*Food Chemistry*' - Second Ed. Marcel Dekker, Inc. New York, USA. pp. 99.
- Fernández-Zurbano, P., Ferreira, V., Escudero, A. and Cacho, J. 1998. Role of hydroxycinnamic acids and flavanols in the oxidation and browning of white wines. *J. Agric. Food Chem.* 4937-4944.
- Fernández-Zurbano, P., Ferreira, V., Peña, C., Escudero, A., Serrano, F. and Cacho, J. 1995. Prediction of oxidative browning in white wines as a function of their chemical composition. *J. Agric. Food Chem.* 43:2813-2817.

- Flanzy, G. and Poux, C. 1965. Sur la teneur en acides amine dans le raisin et la mout en relation aux conditions climatiques. *Anns of Technol. Agric.* 14: 87-91.
- Fobel, M., Lynch, D. and Thompson, J. 1987. Membrane deterioration in senescing carnation flowers; coordinated effects of phospholipid degradation of the action of membranous lipoxygenase. *Plant Physiol.* 85: 204-211.
- Fogerty, A. and Burton, D. 1981. Analysis of drying oils to reduce the drying time of vine fruits. *CSIRO Food Research Quart.* 41: 80-85.
- Fors, S. 1983. Sensory properties of volatile Maillard reaction products and related compounds. A literature review. In 'The Maillard Reaction in Foods and Nutrition' (Eds. G. Waller and M. Feather). ACS Symposium Series, American Chemical Society, Washington D.C., USA. pp. 183-286.
- Franke, S., Niwa, T., Deuther-Conrad, W., Sommer, M. and Stein, G. 2000. Immunochemical detection of imidazolone in uremia and rheumatoid arthritis. *Clin. Chim. Acta.* 300(1-2): 29-41.
- Frankel, E. 1984. Lipid oxidation: Mechanisms, products and biological significance. *J. Amer. Oil Chem. Soc.* 61: 521-528.
- Garcia, P., Romero, C., Brenes, M. and Garrido, A. 1996. Effect of metal cations on the chemical oxidation of olive *o*-diphenols in model systems. *J. Agric. Food Chem.* 44: 2101-2105.
- Gardner, H. 1979. Lipid hydroperoxide reactivity with proteins and amino acids. A review. *J. Sci. Food Chem.* 27: 220.
- Gardner, H. 1991. Recent investigations into the lipoxygenase pathway of plants. *Biochim. Biophys. Acta.* 1084: 221-239.
- Gershenzon, J. 1984. Changes in the level of plant secondary metabolites under water and nutrient stress. *Recent Adv. Phytochem.* 18: 273-281.
- Golan-Goldhirsh, A. and Whitaker, J. 1984. Effect of ascorbic acid, sodium bisulphite, and thiol compounds on mushroom polyphenol oxidase. *J. Agric. Food Chem.* 32: 1003-1009.
- Gómez-Sánchez, A., Hermosín, I. and Maya, I. 1992. Influence of Malondialdehyde on the Maillard degradation of Amadori compounds. *Carbohydr. Research.* 229(2): 307-322.
- Górecki, T., Yu, X. and Pawliszyn, J. 1999. Theory of analyte extraction by selected porous polymer SPME fibres. *The Analyst.* 124: 643-649.

- Gregory, G. 1988. Development and Status of Australian Viticulture. In 'Viticulture: Volume 1-Resources.' (Eds. B.G. Coombe and P.R. Dry). Winetitles, Underdale, South Australia. pp. 1-36.
- Gmrcarevic, M. 1963. Effect of various dipping treatments on the drying rate of grapes for raisins. *Am. J. Enol. Vitic.* 14: 230-234.
- Gmrcarevic, M. and Hawker, J. 1971. Browning of Sultana grape berries during drying. *J. Sci. Food Agric.* May (22): 270-272.
- Gmrcarevic, M. and Radler, F. 1971. A review of the surface lipids of grapes and their importance in the drying process. *Am. J. Enol. Vitic.* 22(2): 80-86.
- Guyot, S., Cheynier, V., Souquet, J. and Moutounet, M. 1995. Influence of pH on the enzymatic oxidation of (+)-catechin in model systems. *J. Agric. Food Chem.* 43: 2458-2462.
- Hahlbrock, K. and Scheel, 1989. Physiology and molecular biology of phenylpropanoid metabolism. *Ann. Rev. Plant Physiol. Plant Molec. Biol.* 40: 347.
- Haisman, D. 1974. The effect of sulfur dioxide on oxidizing enzyme systems in plant tissues. *J. Sci. Food Agric.* 25: 803-810.
- Hall, J., Flowers, T. and Roberts, R. 1984. The chloroplast. In 'Plant Cell Structure and Metabolism.' Second Edition, Longman Group Ltd. pp. 327-402.
- Haleva-Toledo, E., Naim, M. and Zehavi, U. 1997. 4-Hydroxy-2,5-dimethyl-3(2H)-furanone formation in buffers and model solutions of citrus juice. *J. Agric. Food Chem.* 45(4): 1314-1319.
- Hartel, R. and Shastry, A. 1991. Sugar crystallization in food products. *Crit. Reviews. Food Sci. Nutr.* 1(1): 49-112.
- Hayase, F., Koyama, T. and Konishi, Y. 1997. Novel dehydrofuro-imidazole compounds formed by the advanced Maillard reactions of 3-deoxy-D-hexos-2-ulose and arginine residues in proteins *J. Agric. Food Chem.* 45: 1137-1143.
- Hayase, F., Shibuya, T., Sato, J. and Yamamoto, M. 1996. Effects of oxygen and transition metals on the advanced Maillard reaction of proteins with glucose. *Biosci. Biotechnol. Biochem.* 60(11): 1820-1825.
- Hayashi, T. and Namiki, M., 1986. Role of sugar fragmentation in early stage browning of amino-carbonyl reaction of sugar with amino acid. *Agric. Biol. Chem.* 50: 1965-1971.
- Hayes, R., Johns, R., Mollah, M. and Morey, B. 1991. 'The Shaw Trellis- a new innovation in Trellis Dried Sultana Production'. Victorian Department of Agriculture, Technical Report Series No. 193.

- Helak, B., Kersten, E., Spengler, K., Tressl, R. and Rewicki, D. 1989. Formation of furylpyrrolidines and piperidines on heating L-proline with reducing sugars and furancarboxaldehydes. *J. Agric. Food Chem.* 37: 405-410.
- Henle, T., Walter, A. and Klostermeyer, H. 1994. Simultaneous detection of protein bound Maillard products by ion exchange chromatography and photodiode array detection. In '*Maillard Reactions in Chemistry, Food and Health*'. (Eds. T. Labuza, G. Reineccius, V. Monnier, J. O'Brien and J. Baynes). Royal Society of Chemistry. pp. 195-200.
- Henle, T., Walter, A., Haessner, R. and Klostermeyer, H. 1994. Detection and identification of a protein bound imidazolone resulting from the reaction of arginine residues and methylglyoxal. *Zeitschrift. Lebensmitt. Untersuch. Forsch.* 199: 55-58.
- Henschke, P.A. and Jiranek, V. 1993. Yeasts—metabolism of nitrogen compounds. In '*Wine Microbiology and Biotechnology*'. (Ed. G. Fleet). Harwood Academic Publishers. pp. 77-164.
- Hernandez-Orte, P., Guitart, A. and Cacho, J. 1999. Changes in the concentration of amino acids during the ripening of *Vitis vinifera* Tempranillo variety from the Denomination d'Origine Somontano (Spain). *Am. J. Enol. Vitic.* 50(2): 144-154.
- Heyns, K. and Klier, M. 1968. Bräunungsreaktionen und Fragmentierungen von Kohlenhydraten. Teil IV. Vergleich der flüchtigen Abbauprodukte der Pyrolyse von Mono-, Oligo- und Polysacchariden. *Carb. Research.*(6): 436-448.
- Heyns, K. and Noack, H. 1962. Die Umsetzung von D-Fructose mit L-Lysin und L-Arginin und deren Beziehung zu nichtenzymatischen Bräunungsreaktionen. *Chemische Berichte.* 95: 720-727.
- Heyns, K., Stute, R. and Paulsen, H. 1966. Bräunungsreaktionen und Fragmentierungen von Kohlenhydraten. Teil I. Die flüchtigen Abbauprodukte der Pyrolyse von D-glucose. *Carb. Research.*(2): 132-149.
- Hidalgo, F. and Zamora, R. 2000. The role of lipids in nonenzymatic browning. *Grassas y Aceites.* 51(1-2):35-49.
- Hidalgo, F., Aliaz, M., and Zamora, R. 1999. The effect of pH and temperature on comparative nonenzymatic browning of proteins produced by oxidised lipids and carbohydrates. *J. Agric. Food Chem.* 47(2): 742-747.
- Hildebrand, D., Hamilton-Kemp, C., Legg, C. and Bookjans. 1988. Plant lipoxygenases: occurrence, properties and possible functions. *Curr. Topics Plant Biochem. Physiol.* 7:201.

- Hirano, M., Miura, M. and Gomyo, T. 1996. Kinetic analysis of the inhibition by melanoidin of trypsin. *Biosci. Biotechnol. Biochem.* 60(3): 458-462.
- Hirsch, J., Petrakova, E. and Feather, M. 1992. The reaction of some dicarbonyl sugars with aminoguanidine. *Carb. Research.* 232: 125-130.
- Ho, P., Hogg, T. and Silva, M. 1999. Application of liquid chromatographic method for the determination of phenolic compounds and furans in fortified wines. *Food Chem.* 64: 115-122.
- Hodge, J. 1953. Chemistry of browning reactions in model systems. *J. Agric. Food Chem.* 1: 928-943.
- Hofmann, T. 1998a. Characterisation of the chemical structure of novel colored Maillard reaction products from furan-2-carboxaldehyde and amino acids. *J. Agric. Food Chem.* 46: 932-940.
- Hofmann, T. 1998b. 4-Alkylidene-2-imino-5-[4-alkylidene-5-oxo-1,3-imidazol-2-ynyl]aza-methylidene-1,3-imidazoline—a novel coloured substructure in melanoidins formed by Maillard reactions of bound arginine with glyoxal and 2-furan-2-carboxaldehyde. *J. Agric. Food Chem.* 46: 3896-3901.
- Hofmann, T. 1998c. Application of site specific <sup>13</sup>C enrichment and C-13 NMR spectroscopy for the elucidation of the formation pathway leading to a red 1H-pyrrol-3(2H)-one during the Maillard reaction of furan-2-carboxaldehyde and L-alanine. *J. Agric. Food Chem.* 46: 941-945.
- Hofmann, T., Bors, W., and Stettmaier, K. 1999a. Studies on radical intermediates in the early stages of the nonenzymatic browning reaction of carbohydrates and amino acids. *J. Agric. Food Chem.* 47: 379-390.
- Hofmann, T., Bors, W. and Stettmaier, K. 1999b. Radical assisted melanoidin formation during thermal processing of foods as well as under physiological conditions. *J. Agric. Food Chem.* 47: 391-396.
- Hrazdina, G., Parsons, G. and Mattick, L. 1984. Physiological and biochemical events during the development and maturation of grape berries. *Am. J. Enol. Vitic.* 35: 220-227.
- Huxsoll, C. Bolin, H. and Mackey, B. 1995. Near Infrared Analysis potential for grading raisin quality and moisture. *J. Food Sci.* 60 (1): 176-180.
- Huyghues-Despointes, A. and Yaylayan, V. 1996. Retro-aldol and redox reactions of Amadori compounds: mechanistic studies with variously labeled D-[13C]glucose. *J. Agric. Food Chem.* 44(3): 672-681.
- Hwang, H., Hartmann, T. and Ho, C. 1995. Relative reactivities of amino acids in the formation of pyridines, pyrroles and oxazoles. *J. Agric. Food Chem.* 43: 2917- 2921.
- Ide, N., Lau, B., Ryu, K., Matsuura, H. and Itakura Y. 1999. Antioxidant effects of fructosyl arginine—a Maillard reaction product in aged garlic extract. *J. Nutr. Biochem.* 10: 372-376

- Ide, N., Nelson, A. and Lau, B. 1997. Aged garlic extracts and its constituents inhibit Cu<sup>2+</sup>-induced oxidative modification of low density lipoprotein. *Planta Med.* 63: 263-264.
- Ingledeu, W. and Kunkee, R. 1985. Factors influencing sluggish fermentations of grape juice. *Am. J. Enol. Vitic.* 36: 65-76.
- Ishizuka, M., Yamada, F., Tanaka, Y., Takeuchi, Y. and Imaseki, H. 1991. Sequential induction of mRNAs for phenylalanine ammonia-lyase in slices of potato tuber. *Plant Cell Physiol.* 32(1):57-64.
- Jacobs, G. 1981. *Comparative Color Vision: Academic Press Series in Cognition and Perception.* Academic Press, New York, USA.
- Jägerstad, M., Skog, K., Grivas, S. and Olsson, K. 1991. Formation of heterocyclic amines using model systems. *Mutation Research.* 259: 219-233.
- Jaworski, A. and Lee, C. 1987. Fractionation and HPLC determination of grape phenolics. *J Agric. Food Chem.* 35: 257-259.
- Jayathilakan, K., Vasundahra, T., and Kumudavally, K. 1997. Effects of spices and Maillard reaction products on rancidity development in precooked refrigerated meat. *J. Food Sci. Tech. India.* 34(2): 128-131.
- Jerums, G., Soulis-Liparota, T., Panagiotopoulos, S. and Cooper, M. 1994. In vivo effects of amino-guanidine. In '*Maillard Reactions in Chemistry, Food and Health.*' (Eds. T. Labuza, G. Reineccius, V. Monnier, J. O'Brien and J. Baynes). Royal Society of Chemistry, Cambridge, U.K. 319-324.
- Jiranek, V., Langridge, P. and Henschke, P. 1991. Yeast nitrogen demand: selection criteria for wine yeasts for fermenting low nitrogen musts. In '*Proceedings of the International Symposium on Nitrogen in Grapes and Wine.*' (Ed. Rantz, J.). Seattle, WA. American Society of Enology and Viticulture. pp. 266-269.
- Jürgen, F. and Horst, H. 1980. Light absorption of organic colorants-reactivity and structure. Vol 12. Springer Verlag, Berlin, Germany. pp. 1-245.
- Kanellis, A. and Roubelakis-Angelakis, K. 1993. Grape. In '*Biochemistry of Fruit Ripening.*' (Eds. G. Seymour, J. Taylor and G. Tucker). Chapman and Hall, London, England. pp. 190-234.
- Kanner, J. 1992. Mechanism of nonenzymatic lipid peroxidation in muscle foods. In '*Lipid Oxidation in Food*' (Ed. A. St. Angelo) American Chemical Society. New York, USA. pp. 55-73.
- Kanner, J., Frankel, E., Granit, R., German, B. and Kinsella, J. 1994. Natural antioxidants in grapes and wines. *J. Agric. Food Chem.* 42: 64-69.

- Karadeniz, F., Durst, R. and Wrolstad, R. 2000. Polyphenolic composition of raisins. *J. Agric. Food Chem.* 48: 5343-5350.
- Karel, M. 1980. Lipid Oxidation, secondary oxidation, secondary reactions, and water activity of foods. In 'Autoxidation in Food and Biological Systems'. (Eds: M. Simic and M. Karel) Plenum Press. London, England.
- Katakoa, I., Yasutaka, K., Sugiura, A. and Tomana, T. 1983. Changes in L-phenylalanine ammonia lyase activity and anthocyanin synthesis during berry ripening of three grape cultivars. *J. Japan. Soc. Hort. Sci.* 52: 273-279.
- Kawakishi, S., Okawa, Y. and Uchida, K. 1990. Oxidative damage of protein induced by the Amadori compound—copper ion system. *J. Agric. Food. Sci.* 38: 13-17.
- Kays, S., Barton, F. and Windham, W. 2000. Predicting protein content by near infrared reflectance spectroscopy in diverse cereal products. *J. Near Infrared Spectrosc.* 8: 35-43.
- Keller M., Arnink K. and Hrazdina G. 1999. Interaction of nitrogen availability during bloom and light intensity during veraison I. Effects on grapevine growth, fruit development and ripening. *Am. J. Enol Vitic.* 49(3): 333-340.
- Keller, M. and Hrazdina, G. 1999a. Interaction of nitrogen availability during bloom and light intensity during veraison II. Effects on anthocyanin and phenolic development during grape ripening. *Am J Enol Vitic.* 49(3): 341-349.
- Kenten, R. and Mann, P. 1953. The oxidation of certain dicarboxylic acids in the presence of manganese. *Biochem. J.* 53: 498-505.
- Kidron, M., Harel, E. and Mayer, A. 1978. Catechol oxidase activity in grapes and wine. *Am. J. Enol. Vitic.* 29: 30-36.
- Kim, M., Saltmarch, M. and Labuza, T. 1981. Non-enzymatic browning of hygroscopic whey powders in open versus sealed pouches. *J. Food Proc. Pres.* 5: 49-57.
- Kirsch, J. and Drennen, J. 1999. Nondestructive tablet hardness testing by near-infrared spectroscopy: a new and robust spectral best-fit algorithm. *J. Pharmaceut. Biomed. Anal.* 19 (3-4): 351-362.
- Klein, B., King, D. and Grossman. 1985. Cooxidation reactions of lipoxygenase in plant systems. *Free Radical Biol. Med* 1: 309-315.
- Kliwer, W. 1968. Changes in the concentration of free-amino acids in grape berries during maturation. *Am. J. Enol. Vitic.* 19: 166-174.

- Kliewer, W. 1977. Influence of temperature, solar radiation and nitrogen on coloration and composition of emperor grapes. *Am. J. Enol. Vitic.* 28(2): 96-103.
- Kliewer, W. and Torres, R. 1972. Effect of controlled day and night temperatures on grape colouration. *Am. J. Enol. Vitic.* 23: 71-77.
- Koch, R. and Alleweldt, G. 1978. Der Gaswechsel reifender Weinbeeren. *Vitis*. 17: 30-44.
- Kohn, R., Cerami, A. and Monnier, V. 1984. Collagen aging *in vitro* by nonenzymatic glycosylation and browning. *Diabetes* 33: 57-59.
- Kroh, L. 1994. Caramelisation in food and beverages. *Food Chem.* 51: 373-379.
- Kostaropoulos, A. and Saravacos, G. 1995. Microwave pre-treatment for sun-dried raisins. *J. Food Sci.* 60(2): 344-347.
- Labuza, T. 1975. Oxidative changes in foods at low and intermediate moisture levels. In 'Water Relations of Foods.' (Ed: R. Duckworth). Academic Press, New York, USA. pp. 455.
- Langcake, P. 1981. Disease resistance of *Vitis* spp. and the production of the stress metabolites resveratrol,  $\epsilon$ -viniferin,  $\alpha$ -viniferin and pterostilbene. *Physiol. Plant. Path.* 18: 213-226.
- Lea, P., Wallsgrave, R. and Mifflin, B. 1985. The biosynthesis of amino acids in plants. In 'Chemistry and Biochemistry of Amino Acids.' (Ed. G. Barret). Chapman and Hall, London, England.
- Lederer, M. and Buhler, H. 1999. Cross-linking of proteins by Maillard processes—characterization and detection of a lysine-arginine cross-link derived from D-glucose. *Bioorg. Med. Chem.* 7: 1081-1088.
- Lederer, M., Gerum, F. and Severin, T. 1998. Cross linking of proteins by Maillard processes—model reactions of D-glucose or methylglyoxal with butylamine and guanidine derivatives. *Bioorg. Med. Chem.* 6: 993-1002.
- Ledl, F. and Schleicher, E. 1990. New aspects of the Maillard reaction in foods and the human body. *Angew. Chem.* 6: 565-706.
- Ledl, F. and Severin, T. 1978. Bräunungsreaktionen von Pentosen mit Aminen. *Z. Lebensm. Unters. Forsch.* 193: 119-122.
- Lee, C. and Jaworski, A. 1989. Major phenolic compounds in ripening white grapes. *Am. J. Enol. Vitic.* 40: 43-48.
- Lester, M. 1995. Sulfite sensitivity-significance in human health. *J. Am. College Nutr.* 14(3): 229-232.

- Levine, H. and Slade, L. 1992. Glass transitions in foods. In '*Physical Chemistry of Foods.*' (Eds: H. Schwarzbarg and R. Hartel). Marcel Dekker. New York, USA. pp. 83-220.
- Li, S. and Parish, J. 1998. The chemistry of waxes and sterols. In '*Food Lipids: Chemistry, Nutrition and Biotechnology.*' (Eds: A. Casimir and D. Min). Marcel Dekker Inc. New York, USA. pp. 89-114.
- Liswidowati, M., Hohmann, F., Burkhardt, S. and Kindl, H. 1991. Induction of stilbene synthase by *Botrytis cinerea* in cultured grapevine cells. *Planta*. 18: 307-314.
- Lo, T., Westwood, M., McLellan, A., Selwood, T. and Thornalley, P. 1994. Binding and modification of proteins by methylglyoxal under physiological conditions. *J. Biol. Chem.* 269(51): 32299-32305.
- Lynch, D. and Thompson J. 1984. Lipoxygenase-mediated production of superoxide anion in senescing plant tissue. *FEBS Letts.* 173: 251-254.
- Lynch, D., Sridhara, J. and Thompson J. 1985. Lipoxygenase-generated from 1-amino-cyclopropane-1-carboxylic acid by microsomal membranes of carnations. *Planta* 164: 121-125.
- Macheix, J., Fleuriet, A. and Bilot, J. 1990. '*Fruit Phenolics*'. CRC Press, Boca Raton FL, USA.
- Macheix, J., Sapis, J. and Fleuriet, A. 1991. Phenolic compounds and polyphenoloxidase in relation to browning in grapes and wine. *Crit. Rev. Food Sci. Nutr.* 30 (3): 441-486.
- Maillard, L. 1912 Action des acides amines sur les sucres: formation des melanoidines par voie Methodique. *C.R. Hebd. Seances Acad. Sci.* 154: 66-68.
- Malley D., Yesmin L., Wray, D. and Edwards S. 1999. Application of near-infrared spectroscopy in analysis of soil mineral nutrients. *Comm. Soil Sci. Plant Anal.* 30(7-8): 999-1012.
- Maloney, J., Labuza, T., Wallace, D. and Karel, M. 1966. Autoxidation of methyl linoleate in a freeze-dried model system. I. Effect of water on the autocatalyzed oxidation. *J. Food. Sci.* 31:878-883.
- Mark, H. 1992. Data analysis: multilinear regression and principal component analysis. In '*Handbook of Near Infrared Analysis.*' (Eds: D. Burns and E. Ciurczak). Marcel Dekker Inc. New York, USA. pp. 107-158.
- Marquez, G., and Anon, M. 1999. Influence of reducing sugars and amino acids in the colour development of fried potatoes. *J. Food Sci.* 51: 157-160.
- Martens, H. and Naes, T. 1991. *Multivariate Calibration*. John Wiley and Sons Ltd. New York, USA.

- Martin, C. and Thimann, K. 1972. The role of protein synthesis in the senescence of leaves-I. The formation of protease. *Plant Physiol.* 49: 64-71.
- Mason, H. and Peterson, E. 1965. Melanoproteins. I. Reactions between enzyme generated quinones and amino acids. *Biochim. Biophys. Acta.* 111: 134-146.
- Mastrocola, D., Munari, M., Cioroi, M. and Lerici, C. 2000. Interaction between Maillard reaction products and lipid oxidation in starch-based model systems. *J. Sci. Food. Agric.* 80: 684-690.
- Mathews, C., and Van Holde, K. 1990. '*Biochemistry*'. Benjamin-Cummings Publishing Company, Redwood City, CA, USA.
- Mavandad, M., Edwards, R., Liang, X., Lamb, C. and Dixon, A. 1990. Effects of *trans*-cinnamic acid on expression of the bean phenylalanine ammonia lyase gene family. *Plant Physiol.* 94: 671-680.
- Mayak, S., Legge, R. and Thompson, J. 1983. Superoxide radical production by microsomal membranes from senescing carnation flowers: an effect on membrane fluidity. *Phytochem.* 22: 1375-1380.
- Mayer, A. 1987. Polyphenol oxidases in plants: recent progress. *Phytochem.* 26(1): 11-20.
- Mayer, A. and Harel, E. 1979. Polyphenol oxidase in plants. *Phytochem.* 18: 193-215.
- Mc Bride, R., Mc Bean, D. and Kuskis, A. 1984. The shelf life of Sultanas: a sensory assessment. *Lebens. Wiss. Technol.* 17: 134-136.
- Molnar-Perl, I. and Friedman, M. 1990a. Inhibition of browning by sulfur amino acids. I. Heated amino acid-glucose systems. *J. Agric. Food Chem.* 38: 1642-1647.
- Molnar-Perl, I. and Friedman, M. 1990b. Inhibition of browning by sulfur amino acids. II. Fruit juices and protein containing foods. *J. Agric. Food Chem.* 38: 1648-1651.
- Molnar-Perl, I. and Friedman, M. 1990c. Inhibition of browning by sulfur amino acids. III. Apples and potatoes. *J. Agric. Food Chem.* 38: 1652-1657.
- Monnier, V. and Cerami, A. 1981. Nonenzymatic browning *in vivo*: possible process for aging of long-lived proteins. *Science.* 211: 491-494.
- Monnier, V., Kohn, R., and Cerami, A. 1984. Accelerated age related browning of human collagen in diabetes mellitus. *Proc. Natl. Acad. Sci. USA.* 81: 583-587.
- Monti, S., Bailey, R. and Ames, J. 1998. The influence of pH on the non-volatile reaction products of aqueous Maillard model systems by HPLC with diode array detection. *Food Chem.* 62(3): 369-375.

- Moskowitz, A. and Hrazdina, G. 1981. Vacuolar contents of fruit subepidermal cells from *Vitis* species. *Plant Physiol.* 68: 686-692.
- Nagarajah, S. 1999. A petiole sap test for nitrate and potassium in Sultana grapevines. *Aust. J. Grape Wine Res.* 5(2): 56-60.
- Nakamura, K., Amano, Y. and Kagami, M. 1983. Purification and some properties of a polyphenol oxidase from Koshu grapes. *Am. J. Enol. Vitic.* 34(2): 122-127.
- Namiki, M. 1988. Chemistry of Maillard reactions: recent studies on the browning reaction mechanism and development of antioxidants and mutagens. *Adv. Food Res.* 32:115-184.
- Namiki, M., Hayashi, T. and Kawakishi, S. 1973. Free radicals developed in the amino-carbonyl reactions of sugars with amino acids. *Agric. Biol. Chem.* 37: 2935-2937.
- Näsholm, T. and McDonald, A. 1990. Dependence of amino acid composition upon nitrogen availability in birch (*Betula pendula*). *Physiol. Plant.* 80: 507-514.
- Nassau, K. 1983. *The Physics and Chemistry of Color*. John Wiley and Sons, Inc. New York. USA.
- Nicolas, J., Richard-Forget, F., Goupy, P., Amiot, M., and Aubert, S. 1994. Enzymatic browning reactions in apple and apple products. *CRC. Crit. Rev. Food Sci. Nutr.* 34(2): 109-157.
- Nicoli, M., Elizalde, B., Pittoti, A. and Lericci, C. 1991. Effect of sugars and Maillard reaction products on polyphenoloxidase and peroxidase activity in food. *J. Food Biochem.* 15(3): 169-184.
- Nienaber, U. and Eichner, K. 1995. The antioxidative effect of Maillard reaction products in model systems and roast hazelnuts. *Fett. Wiss. Technol.* 97(12): 435-444.
- Noga, G., Knoche, M., Wolter, M. and Barthlott, W. 1987. Changes in leaf micromorphology induced by surfactant application. *Angew. Bot.* 61: 521-528.
- Nursten, H. and O'Reilly, R. 1986. Coloured compounds formed by the interaction of glycine and xylose. *Food Chem.* 20: 45-60.
- NSAS Version 3.50. 1996. Reference Manual, Perstop Analytical, NIRSystems, Silver Spring, Maryland, USA.
- O'Brien, J. and Morrissey, P. 1997. Metal ion complexation by products of Maillard reaction. *Food Chem.* 58(1/2): 17-27.

- Okuda, T., Pue, A., Fujiyama, K. and Yokotsuka, K. 1999. Purification and characterization of polyphenol oxidase from Muscat Bailey A grape juice. *Am. J. Enol. Vitic.* 50(2): 137-143.
- Olmo, H. 1993. Grapes. In, 'Encyclopedia of Food Science Food Technology and Nutrition' (Eds: R. MacCrae, R. Robinson, and M. Sadlers) Academic Press, London, England. pp. 2252.
- Ong, B. and Nagel, C. 1978a. High pressure liquid chromatographic analysis of hydroxycinnamic acid-tartaric acid esters and their glucose esters in *Vitis vinifera*. *J. Chrom.* 157: 345-355.
- Ong, B. and Nagel, C. 1978b. Hydroxycinnamic acid tartaric acid ester in mature grapes during the maturation of white Riesling grapes. *Am J. Enol Vitic.* 29, 277-281.
- Osborne, B., Fearn, T. and Hindle, P. 1993. *Practical NIR Spectroscopy-with Applications in Food and Beverage Analysis (second edition)*. Longman Group, UK.
- Ough, C. 1968. Proline content of California grapes. *Am J. Enol. Vitic.* 7: 321-331.
- Oya, T., Hattori, N., Mizuno, Y., Miyata, S., Maeda S., Osawa, T. and Uchida K. 1999. Methylglyoxal modification of protein- chemical and immunochemical characterization of methylglyoxal-arginine adducts. *J. Biol. Chem.* 274(26):18492-18502.
- Ozmianski, J., Cheynier, V. and Moutounet, M. 1996. Iron catalyzed oxidation of (+)-catechin in model systems. *J. Agric. Food Chem.* 44: 1712-1715.
- Patil, V., Chakrawar, P., Narwadkar, P. and Shinde, G. 1995 Grape. In 'Handbook of Fruit Science and Technology. Production, Composition, Storage and Processing'. (Eds. D. Salunkhe and S. Kadam). Marcel Dekker, Inc. New York, USA. pp. 7-38.
- Pauls, K. and Thompson, J. 1984. Evidence of the accumulation of peroxidised lipids in membranes of senescing cotyledons. *Plant Physiol.* 75: 1152-1157.
- Peynaud, E and Maurie, A. 1953. Sur l'évolution de azote dans les differentes parties du raisin au cours de la maturation. *Ann. Technol. Agr.* 2: 12-35.
- Peynaud, E. 1947. Contribution a l'étude biochemique de la maturation du raisin et de la composition des vins. *Bulletin O.I.V.* 20, 34-51.
- Peynaud, E. and Riberaeu-Gayon, G. 1971. The Grape. In 'The Biochemistry of Fruits and their Products'. Vol 2. (Ed. A. Hulme). Academic Press, London, England. pp. 179-205.
- Pierpont, W. 1969. O-quinones formed in plant extracts. Their reaction with amino acids and peptides. *Biochem. J.* 112: 609-616.

- Pischetsrieder, M. and Severin, T. 1994. The Maillard reactions of disaccharides. In *'Maillard Reactions in Food Chemistry and Health'* (Eds. T. Labuza, G. Reineccius, V. Monnier, J. O'Brien and J. Baynes.) Royal Society of Chemistry Publishers, Cambridge, England. pp. 37-42.
- Pischetsrieder, M., Schoetter, C. and Severin, T. 1998. Formation of an aminoreductone during the Maillard reaction of lactose with N $\alpha$ -Acetylsine or proteins. *J. Agric. Food Chem.* 46: 928-931.
- Pittoti, A., Dal Bo, A. and Stecchini, M. 1993. Effect of Maillard reaction products on proteases activity *in vitro*. *J. Food Qual.* 1: 211-220.
- Pont, V. and Pezet, R. 1990. Relation between the chemical structure and the biological activity of hydroxystilbenes against *Botrytis cinerea*. *J. Phytopathol.* 130: 1-8.
- Possingham, J. 1972. Surface wax structure in fresh and dried Sultana grapes. *Ann. Bot.* 36: 993-996.
- Possner, D. and Kliewer, W. 1985. The localisation of acids, sugars, potassium and calcium in developing grape berries. *Vitis.* 24: 229-240.
- Qiu P., Ding H., Tang, Y. and Xu, R. 1999. Determination of chemical composition of commercial honey by near-infrared spectroscopy. *J. Agric. Food Chem.* 47(7):2760-2765.
- Rabe, E. and Lovatt, C. 1986. Increased arginine biosynthesis during phosphorus deficiency. *Plant Physiol.* 81: 774-779.
- Radler, F. 1964. The prevention of browning during drying by the cold dipping treatment of Sultana grapes. *J. Sci. Food Agric.* 15(12): 864-869.
- Radler, F. 1965. The surface lipids of fresh and processed raisins. *J. Sci. Food Agric.* 16: 638-643.
- Radler, F. and Horn, D. 1965. The composition of grape cuticle wax. *Aust. J. Chem.* 18: 1059-1069.
- Rathjen, A. and Robinson, S. 1992a. Characterisation of a variegated grapevine mutant showing reduced polyphenol oxidase activity. *Aust. J. Plant Physiol.* 19: 43-54.
- Rathjen, A. and Robinson, S. 1992b. Aberrant processing of polyphenol oxidase in a variegated grapevine mutant. *Plant Physiol.* 99: 1619-1625.
- Reed, D. and Tuckey, H. 1982. Light intensity and temperature effects on epicuticular wax morphology and internal cuticle ultrastructure of carnation and brussel sprout leaf cuticles. *J. Am. Soc. Hort. Sci.* 107(3): 417-420.

- Rendelman, J. and Inglett, G. 1990. The influence of  $\text{Cu}^{2+}$  on the Maillard reaction. *Carbohydrate Research*. 201: 311-326.
- Richard-Forget, F., Goupy, P. and Nicolas, J. 1992. Cysteine as an inhibitor of enzymatic browning. II. Kinetic studies. *J. Agric. Food Chem.* 40(11): 2108-2113.
- Richard-Forget, F., Goupy, P., Nicolas, J., Lacombe, J. and Pavia, A. 1991. Cysteine as an inhibitor of enzymatic browning I. Isolation and characterisation of addition compounds formed during oxidation of phenolics by apple polyphenol oxidase. *J. Agric. Food Chem.* 39: 841-847.
- Richardson, S., Baianu, I. and Steinberg, M. 1987. Mobility of water in sucrose solutions determined by deuterium and oxygen-17 nuclear magnetic resonance measurements. *J. Food. Sci.* 52(3), 806-810.
- Riederer, M. and Schneider, G. 1990. The effect of the environment on the permeability and composition of citrus leaf cuticles. III. Composition of soluble cuticular lipids and correlation with transport properties. *Planta*. 180: 154-165.
- Riisom, T., Sims, R. and Fioriti, J. 1980. Effect of amino acids on the autoxidation of safflower oil in emulsions. *J. Am. Oil Chem. Soc.* 57: 354-359.
- Roe, M., Faulks, R. and Belsten, J. 1990. The role of reducing sugars and amino acids in fry colour of chips from potatoes grown under different nitrogen regimes. *J. Sci. Food Agric.* 52(2): 207-214.
- Romeyer, F., Sapsis, J. and Macheix, J. 1985. Hydroxycinnamic esters and browning potential in mature berries of some grape varieties. *J. Sci. Food Agric.* 36: 728-732.
- Romeyer, F., Macheix, J., Goiffon, J., Reminiac, C. and Sapis, J. 1983. The browning capacity of grapes. III. Changes and the importance of hydroxycinnamic acid-tartaric esters during development and maturation of the fruit. *J. Agric. Food Chem.* 31: 346-349.
- Roos, Y. 1987. Effect of moisture on the thermal behaviour of strawberries studied using differential scanning calorimetry. *J. Food Sci.* 52: 146-149.
- Roos, Y. 1993. Water activity and physical state effects on amorphous food stability. *J. Food Process. Prec.* 16: 433-447.
- Roubelakis-Angelakis K. and Kliewer, W. 1978 c. Enzymes of Krebs-Henseleit Cycle in *Vitis vinifera* L. III. *In vivo* and *in vitro* studies of arginase. *Plant Physiol.* 62: 344-347.
- Roubelakis-Angelakis, K. and Kliewer, W. 1978 a. Enzymes of Krebs-Henseleit Cycle in *Vitis vinifera* L. I. Ornithine carbamoyl transferase: isolation and some properties. *Plant Physiol.* 62: 337-339.

- Roubelakis-Angelakis, K. and Kliewer, W. 1978 b. Enzymes of Krebs-Henseleit Cycle in *Vitis vinifera* L. II. Arginosuccinate synthetase and lyase. *Plant Physiol* 62: 340-344.
- Roubelakis-Angelakis, K. and Kliewer, W. 1981. Influence of nitrogen fertilisation on activities of ornithine transcarbamoylase and arginase in *Chenin-blanc* berries at different stages of development. *Vitis*. 20: 130-135.
- Roubelakis-Angelakis, K. and Kliewer, W. 1985. Phenylalanine ammonia lyase in berries of *Vitis vinifera* L. Extraction and possible sources of error during assay. *Am. J. Enol. Vitic.* 36: 314-315.
- Roubelakis-Angelakis, K. and Kliewer, W. 1986. Effects of exogenous factors on phenylalanine ammonia lyase activity and accumulation of anthocyanins and total phenolics in grape berries. *Am. J. Enol. Vitic.* 37: 275-280.
- Royle, L., Bailey, R. and Ames, J. 1998. Separation of Maillard reaction products from xylose-glycine and glucose-glycine model systems by capillary electrophoresis and comparison to reverse phase HPLC. *Food Chem.* 62(4): 425-430.
- Saltmarch, M. and Labuza, T. 1982. Nonenzymatic browning via the Maillard reactions in foods. *Diabetes*. Vol.31. Suppl. 3. June. 29-36.
- Sánchez-Ferrer, A., Bru, R., Valero, E. and García-Carmona, F. 1989. Changes in pH-dependent grape polyphenoloxidase activity during maturation. *J. Agric. Food Chem.* 37: 1242-1245.
- Sapis, J., Macheix, J. and Cordonnier, R. 1983. The browning capacity of grapes. 1. Changes in polyphenol oxidase activities during the development and maturation of the fruit. *J. Agric. Food Chem.* 31: 342-345.
- Satue-Gracia, M., Andres-Lacueva, C., Lamuela-Raventos, R. and Frankel, E. 1999. Spanish sparkling wines (cavas) as inhibitors of *in vitro* human low-density lipoprotein oxidation. *J. Agric. Food Chem.* 47(6): 2198-2202.
- Saravacos, G., Tsiourvas, D. and Tsami, E. 1986. Effect of temperature on the water adsorption isotherm of sultana raisins. *J. Food Sci.* 51: 381-383, 387.
- Schaller, K., Lohnertz, O., Oswald, D. and Sprengart, B. 1985. Nitratanreicherung in Reben. 3 Mitteilung: Nitratdynamik in Reben und Beeren während einer Vegetationsperiode in verschiedenen Rebsorten. *Wein Wissenschaft.* 40: 147-159.
- Severini, C. and Lerici, C. 1995. Interaction between the Maillard reaction and lipid oxidation in model systems during high temperature treatment. *Italian. J. Food Sci.* 7(2): 189-196.

- Sharma, H., Kilpatrick, K. and Burns, L. 2000. On Herschel's paper—Herschel. W. XIV. Experiments on the refrangibility of the visible rays of the sun. *J. Near Infrared Spectr.* 8(2): 75-86.
- Shibamoto, T. and Bernhard, A. 1976. Effect of time, temperature and reaction ratio on pyrazine formation in model systems. *J. Agric. Food Chem.* 24(4): 847-851.
- Shibamoto, T., Akiyama, T., Sakaguchi, M., Enomoto, Y. and Masuda, H. 1979. A study of pyrazine formation. *J. Agric. Food Chem.* 27(5):1027-1031.
- Shu, C. and Lawrence, B. 1994. Temperature effect on the volatiles formed from the reaction of glucose and ammonium hydroxide: a model system. In '*Maillard Reactions in Chemistry, Food and Health*'. (Eds: T. Labuza, G. Reineccius, V. Monnier, J. O'Brien and J. Baynes). Royal Society of Chemistry Publishers, Cambridge, England. pp140-146.
- Simal, S., Rosselló, C., Sánchez, E. and Cañellas, J. 1996. Quality of raisins treated and stored under different conditions. *J. Agric. Food Chem.* 44: 3297-3302.
- Singleton, V. 1987. Oxygen with phenols and related reactions in musts, wines and model systems: observations and practical implications. *Am J. Enol. Vitic.* 38: 69-77.
- Singleton V., Timberlake, C. and Lea, A. 1978. The phenolic cinnamates of white grapes and wine. *J. Sci. Food. Agric.* 29: 403-410.
- Singleton, V. and Trousdale, E. 1983. White wine phenolics: varietal and processing differences as shown by HPLC. *Am. J. Enol. Vitic.* 34: 27.
- Singleton, V., Trousdale, E. and Zaya, J. 1985. One reason sun-dried raisins brown so much. *Am. J. Enol. Vitic.* 36(2): 111-113.
- Singleton, V., Zaya, J., Trousdale, E. and Salgues, M. 1984. Caftaric acid in grapes and conversion to reaction product during processing. *Vitis.* 23: 113-120.
- Smith, J., Abe, Y. and Hoshino, J. 1995. Modified atmosphere packaging – present and future uses of gas absorbents and generators. In '*Principles of Modified-Atmosphere and Sous-Vide Product Packaging*' (Eds. J. Farber and K. Dodds). Technomic Publishing Company, Inc., Lancaster, PA, U.S.A. pp. 287-323.
- Soleas, G., Diamandis, E., and Goldberg, D. 1997. Resveratrol: a molecule whose time has come? And gone? *Clin. Biochem.* 30(2): 91-113.
- Somers, T., Vérette, E. and Pocock, K. 1987. Hydroxycinnamate esters of *Vitis vinifera*: changes during white vinification, and effects of exogenous enzymatic hydrolysis. *J. Sci. Food Agric.* 40: 67-78.

- Sondermann, N. and Kovar, K. 1999. Identification of ecstasy in complex matrices using near-infrared spectroscopy. *Forens. Sci. Int.* 102(2-3): 133-147.
- Sorenson L. and Jepsen R. 1998 Assessment of sensory properties of cheese by near-infrared spectroscopy. *Int. Dairy J.* 8(10-11): 863-871.
- Spanos, G. and Wrolstad, R. 1990. Influence of processing and storage on the phenolic composition of Thompson Seedless grape juice. *J. Agric. Food. Chem.* 38(7) 1565-1571.
- Sparvoli, F., Martin, C., Scienza, A., Gavazzi, G. and Tonelli, C. 1994. Cloning and molecular analysis of structural genes involved in flavanoid and stilbene biosynthesis in grape (*Vitis vinifera* L.). *Plant Molec. Biol.* 24: 743-755.
- Steinman H., Leroux M. and Potter, C. 1993. Sulphur dioxide sensitivity in South African asthmatic children. *Sth. Afric. Med. J.* 83(6):387-390.
- Stewart, G. and Larher, F. 1980. Accumulation of amino acids and related compounds in relation to environmental stress. In 'The Biochemistry of Plants. A Comprehensive Treatise'. (Ed. B. Mifflin). Academic Press, New York. USA. Vol 5. pp. 609-635.
- Stines, A., Grubb, J., Gockowiak, H., Henschke, P., Høj, P. and Van Heeswijk, R. 2000. Proline and arginine accumulation in developing berries of *Vitis vinifera* L. in Australian vineyards: influence of vine cultivar, berry maturity and tissue type. *Aust. J. Grape Wine Res.* 6(2): 150-158.
- Stines, A., Naylor, D., Høj, P. and Van Heeswijk R. 1999. Proline accumulation in developing grapevine fruit occurs independently of changes in the levels of delta(1)-pyrroline-5-carboxylate synthetase m-RNA or protein. *Plant Phys.* 120(3): 923-931.
- Tamaoka, T., Itoh, N. and Hayashi, R. 1991. High pressure effect on Maillard reaction. *Agric. Biol. Chem. (Tokyo)*. 55: 2071-2074.
- Tan, B. and Harris, N. 1995. Maillard reaction products inhibit apple polyphenoloxidase. *Food Chem.* 53(3): 267-273.
- Täufel, K. and Voigt, J. 1964. Zur inhibierenden Wirkung von Ascorbinsäure gegenüber der Polyphenoloxidase des Apfels. *Z. Lebens. Unters. Forsch.* 126: 19-24.
- Taylor, A. and Clydesdale F. 1987. Potential of oxidised phenolics as food colorants. *Food Chem.* 24: 301.
- Taylor, S., Higley, N., and Bush, R. 1986. Sulfites in foods: uses, analytical methods, residues, fate, exposure assessment, metabolism, toxicity, and hypersensitivity. *Adv. Food Res.* 30, 1.

Thayer, S., Choe, H., Tang, A. and Huffaker. 1987. Protein turnover during senescence. In, '*Plant Senescence: Its Biochemistry and Physiology.*' *Proceedings of the Tenth Annual Symposium in Plant Physiology (Jan 8-10, 1987).* University of California Publishers, Riverside, CA, USA.

Thimann, K. 1987. Plant senescence: a proposed integration of the constituent processes, in "*Plant Senescence: its Biochemistry and Physiology*" *Proceedings of the Tenth Annual Symposium in Plant Physiology (Jan 8-10, 1987).* University of California Publishers, Riverside, CA, USA.

Thompson, J., Paliyath, G., Brown, J. and Duxbury, C. 1987. The involvement of activated oxygen in membrane deterioration during senescence, in '*Plant Senescence: its Biochemistry and Physiology*' *Proceedings of the Tenth Annual Symposium in Plant Physiology (Jan 8-10, 1987).* University of California Publishers, Riverside, CA, USA.

Todd, J. 1995. Ion trap theory, design, and operation. In '*Practical Aspects of Ion Trap Mass Spectrometry Vol III*' (Eds. R. March and J. Todd.) CRC Press Inc. Boca Raton, FL, USA.

Tome, D., Nicolas, J. and Drapron, R. 1978. Influence of water activity on the reaction catalysed by polyphenoloxidase from mushrooms in organic liquid media. *Lebensm. Wiss. Tech.* 11: 38-41.

Traverso-Rueda, S. and Singleton, V. 1973. Catecholase activity in grape juice and its implications in winemaking. *Am. J. Enol. Vitic.* 24:103

Treeby, M. T., Holzapfel, B.P., Walker, R.R. and Nicholas, P.R. 1998. Profiles of free amino acids in grapes of grafted Chardonnay grapevines. *Aust. J. Grape Wine Res.* 4(3): 121-126.

Tressl, R., Helak, B., Kersten, E. and Rewicki, D. 1990. Related ring enlargement reactions of proline, azetidinic acid, arginine and lysine with reducing sugars. In '*The Maillard Reaction in Food Processing, Human Nutrition and Physiology*' (Advances in Life Sciences) (Eds. P. Finot, H. Aeschbacher, R. Hurrell and R. Liardon). Birkhäuser Verlag, Basel, Switzerland. 121-132.

Tressl, R., Helak, B., Köppler, H. and Rewicki, D. 1985. Formation of 2-(1-pyrrolidinyl)-2-cyclopentenones and cyclopent(b)azepin-8(1H)-ones as proline specific Maillard reaction products. *J. Agric. Food Chem* 33(6): 1132-1137.

Tressl, R., Wondrak, G., Garbe, L., Krüger and Rewicki, D. 1998. Pentoses and hexoses as sources of new melanoidin-like Maillard polymers. *J. Agric Food Chem*, 46: 1765-1776.

Troller, J. and Christian, J. 1978. Water activity-basic concepts. In '*Water Activity and Food.*' Academic Press, Inc. New York. USA. pp. 1-12.

- Tsami, E., Marinos-Kouris, D., and Maroulis, Z.B. 1990. Water sorption isotherms of raisins, currants, figs, prunes and apricots. *J. Food Sci.* 50: 961-965.
- Tseng, Y. and Mau, J. 1999. Contents of sugars, free-amino acids and free 5'-nucleotides in mushrooms, *Agaricus bisporus*, during post-harvest storage. *J. Sci. Food. Agric.* 79: 1519-1523.
- Uhlig, B. 1998. Effects of solar radiation on grape (*Vitis vinifera L*) composition and dried fruit colour. *J. Hort. Sci Biotech.* 73(1): 111-123.
- Uhlig, B. and Clingeffer, P. 1998. The influence of grape (*Vitis vinifera L*) berry maturity on dried fruit colour. *J. Hort. Sci Biotech* 73(3): 329-339.
- Uhlrich, F. and Grosch, W. 1987. Identification of the most intense volatile flavor compounds formed during the autoxidation of linoleic acid. *Z. Lebensm. Unters. Forsch.* 184: 277-282.
- Umagat, H., Kucera, P. and Wen, L. 1982. Total amino acid analysis using pre-column fluorescence derivatization. *J. Chromatography.* 239: 463-474.
- Valero, E., Escribano, J. and Garcia-Carmona, F. 1988. Reaction of 4-methyl-*o*-benzoquinone, generated chemically or enzymatically, in the presence of L-proline. *Phytochem.* 7: 2055-2061.
- Valero, E., Sanchez-Ferrer, A., Varon, R. and Garcia-Carmona, F. 1989. Evolution of grape polyphenoloxidase activity and phenolic content during maturation and vinification. *Vitis.* 28: 85.
- Valero, E., Varon, R., and Garcia-Carmona, F. 1990. Inhibition of grape polyphenol oxidase by several aliphatic alcohols. *J. Agric Food Chem.* 38: 1097.
- Vamos-Vigyazo, L. 1981. Polyphenoloxidases and peroxidases in fruits and vegetables. *CRC Crit. Rev. Food Sci. Nutr.* 15: 49-127.
- Ventura M., Dejager, A., Deputter, H. and Roelofs, F. 1998. Non-destructive determination of soluble solids in apple juice by near infrared (NIRS). *Postharvest Biology Technology.* 14(1): 21-27.
- Vernin, G. and Vernin, G. 1982. Heterocyclic aroma compounds in foods: occurrence and organoleptic properties. In '*Chemistry of Heterocyclic Compounds in Flavours and Aromas*' (Ed: G. Vernin). Ellis Horwood Limited, Chichester, England. pp. 72-149.
- Vernin, G. and El-Shaffei, A. 1982. General synthetic methods for heterocyclic compounds used for flavouring. In '*Chemistry of Heterocyclic Compounds in Flavours and Aromas*'. (Ed: G. Vernin). Ellis Horwood Limited, Chichester, England. pp. 208-248.

- Vernin, G. and Parkányi, C. 1982. Mechanism of formation of heterocyclic compounds in Maillard and pyrolysis reactions. In '*Chemistry of Heterocyclic Compounds in Flavours and Aromas*' (Ed: G. Vernin). Ellis Horwood Limited, Chichester, England. pp. 151-207.
- Wan, M, Hill, S., Blanshard, J. and Derbyshire, W. 1998. Maillard reactions: do the properties of liquid matrices matter? *Food Chem.* 62(4): 441-449.
- Weaver, R. and Singh, I. 1978. Occurrence of endogenous ethylene and effect of plant regulators on ethylene production in the grapevine *Am. J. Enol. Vitic.* 29: 282-285.
- Weenen, H. 1998. Reactive intermediates and carbohydrate fragmentation in Maillard chemistry. *Food Chem.* 62(4): 393-401.
- Whitfield, F. 1992. Volatiles from interactions of Maillard reactions and lipids. *Crit. Rev. Food Sci. Nutr.* 31(1/2):1-58.
- Whiting, J. 1992. Harvesting and drying of grapes. In '*Viticulture: Volume 2. Practices*', (Eds. B. Coombe and P. Dry.). Winetitles, Underdale, South Australia. pp. 328-358
- Wilhelm, J. and Wihelnova, J. 1981. Accumulation of lipofuscin-like pigments in chloroplasts from senescent leaves of *Phaseolus vulgaris*. *Photosynthetica.* 15: 55-60.
- Williams, P. Preston, K., Norris, K. and Starkey, P. 1984. Determination of amino acids in wheat and barley by near infrared reflectance spectroscopy. *J. Food Sci.* 49: 17-20.
- Williams, W. 1946. California vineyard fertilizer experiment. *Proc. Am. Soc. Hortic. Sci.* 48: 269-278.
- Wissemann, K. and Montgomery, M. 1981. Characterisation of polyphenoloxidase from Ravat 51 and Niagra grapes. *J. Food Sci.* 46: 506-508, 514.
- Wolfe, W. 1976. Identification of grape varieties by isoenzyme banding patterns. *Am. J. Enol. Vitic.* 27(2): 244-250.
- Wolff, S. and Dean, R. 1986. Fragmentation of proteins by free radicals and its effect on their susceptibility to enzymatic hydrolysis. *Biochem. J.* 234: 399-403.
- Xia, J., Allenbrand, B. and Sun, G. 1998. Dietary supplementation of grape polyphenols and chronic ethanol administration on LDL oxidation and platelet function in rats. *Life Science.* 63(5): 383-390.
- Yaylayan, V. and Huyghues-Despointes, A. 1994. Chemistry of Amadori rearrangement products: analysis, synthesis, kinetics, reactions and spectroscopic properties. *Crit. Rev. Food Sci. Nutr.* 34(4):321-369.

Yaylayan, V. and Kaminsky, E. 1998. Isolation and structural analysis of Maillard polymers: caramel and melanoidin formation in glycine/glucose model system. *Food Chem.* 63(1): 25-31

Zagory, D. Principles and practice of modified atmosphere packaging of horticultural commodities. In 'Principles of Modified-Atmosphere and Sous Vide Product Packaging' (Eds. J. Farber and K. Dodds). Technomic Publishing Company, Inc., Lancaster, PA, U.S.A. pp. 189-206.

Zamora, R., Alaiz, M., and Hidalgo, F. 2000. Contribution of pyrrole formation and polymerisation to the nonenzymatic browning produced by amino-carbonyl reactions. *J. Agric. Food Chem.* 48: 3152-3158.

Zamora, R., Maynar, J. and Mesias, J. 1985. Lipoxygenase activity in grapes (cv. Maelaleo): I. Evidence and partial purification. *Am. J. Enol. Viticult.* 36: 316-322.

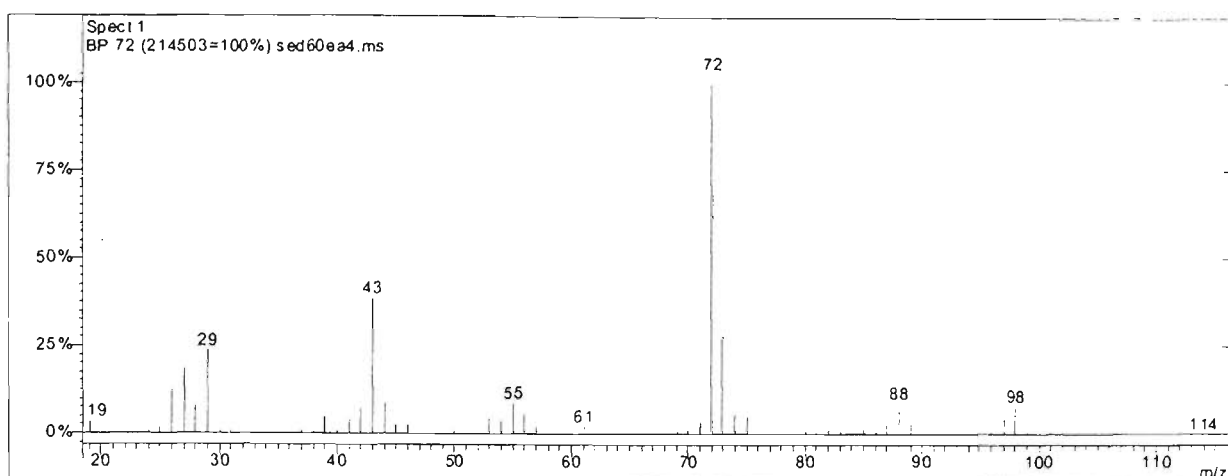
Zapata, J., Calderon, A. and Ros-Barcelo, A. 1995. Actual browning and peroxidases level are not correlated in red and white berries from grapevines (*Vitis vinifera*) cultivars. *Fruit Var. J.* 49(2): 82-84.

Zhuang, H., Barth, M. and Hildebrand, D. 1998. Fatty acid oxidation in plant tissues. In 'Food Lipids, Chemistry, Nutrition and Biotechnology'. (Eds. C. Akoh and D. Min). Marcel Dekker, Inc. New York, USA. pp. 351-375.

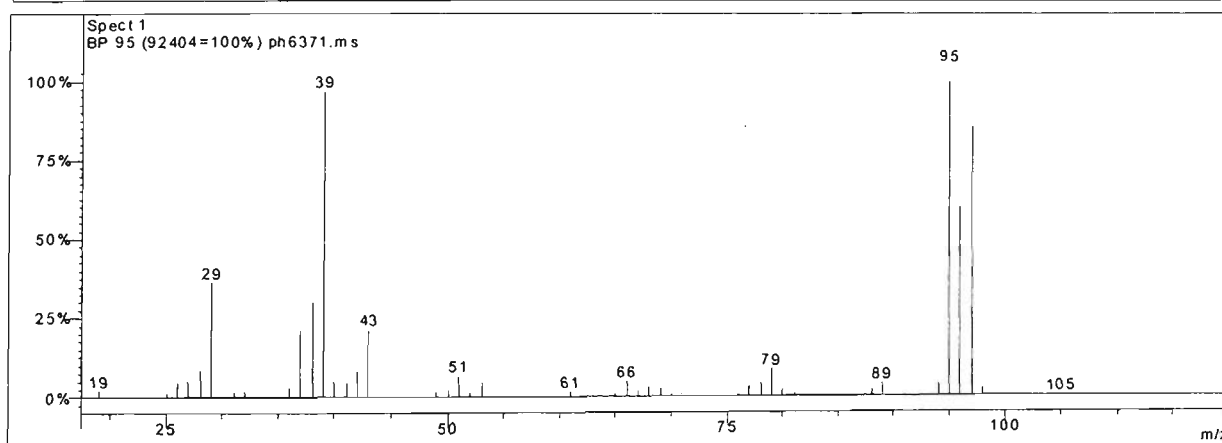
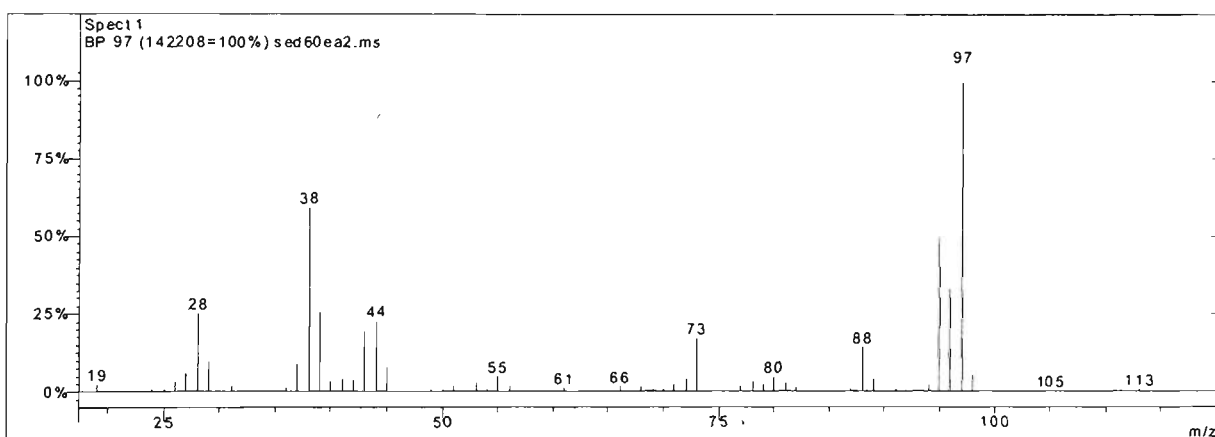
Zhuang, H., Hildebrand, D. and Barth, M. 1995. Senescence in broccoli buds is related to changes in lipid peroxidation. *J. Agric. Food. Chem.* 42: 2585-2591.



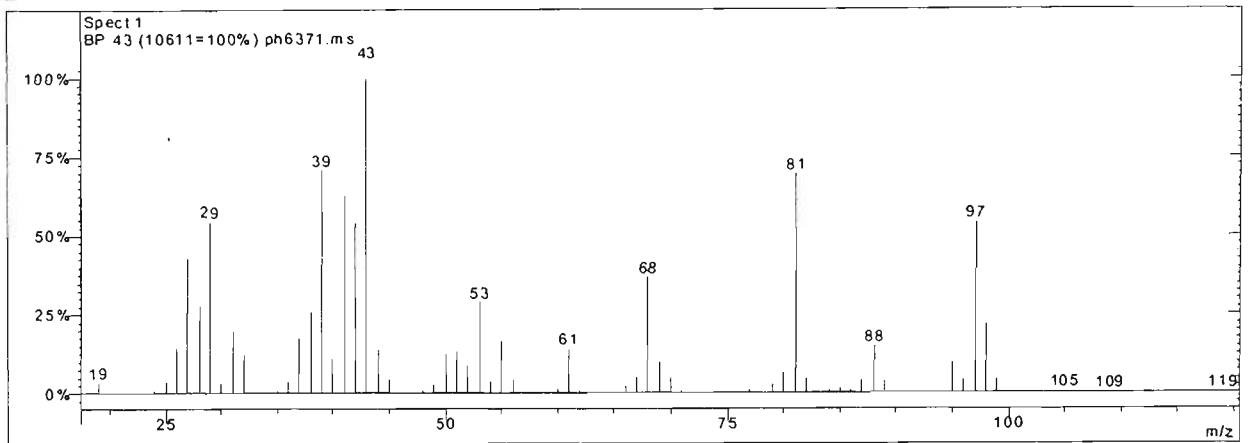
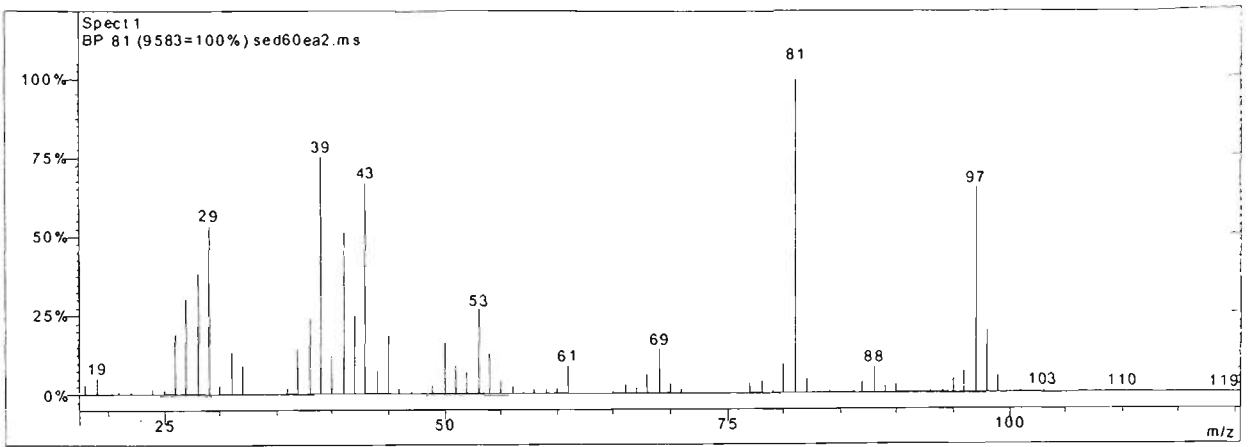
## Ethyl acetate spectra



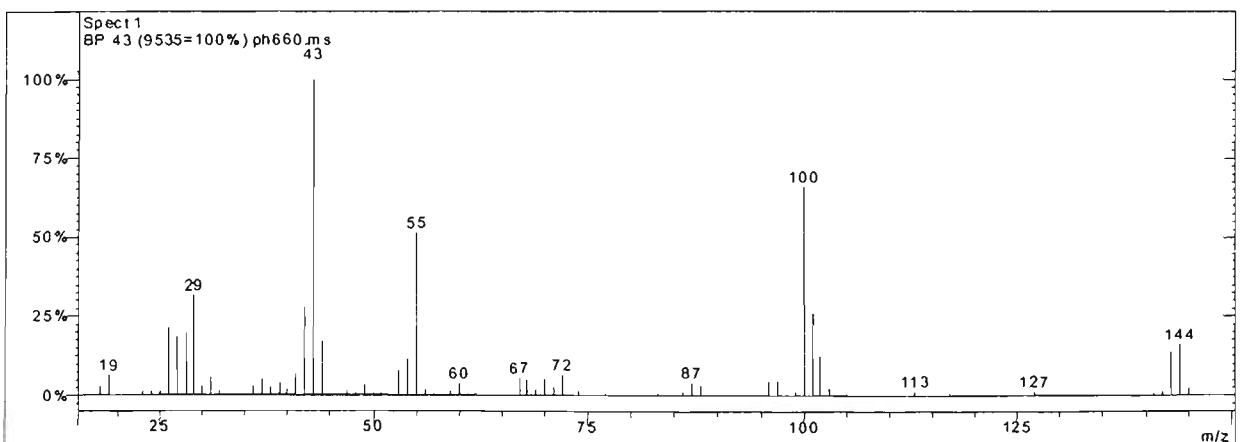
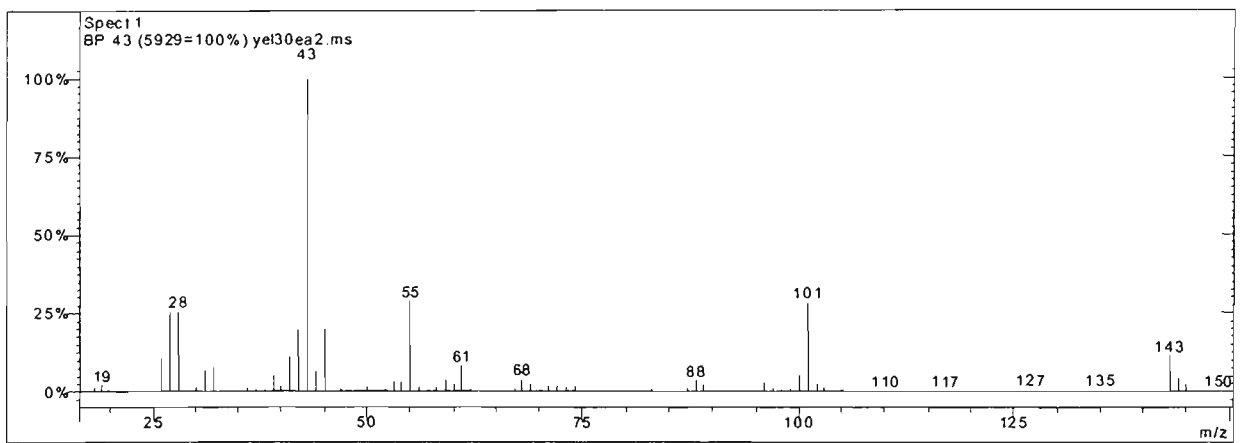
Peak 1 *EtAc extract sultana only*



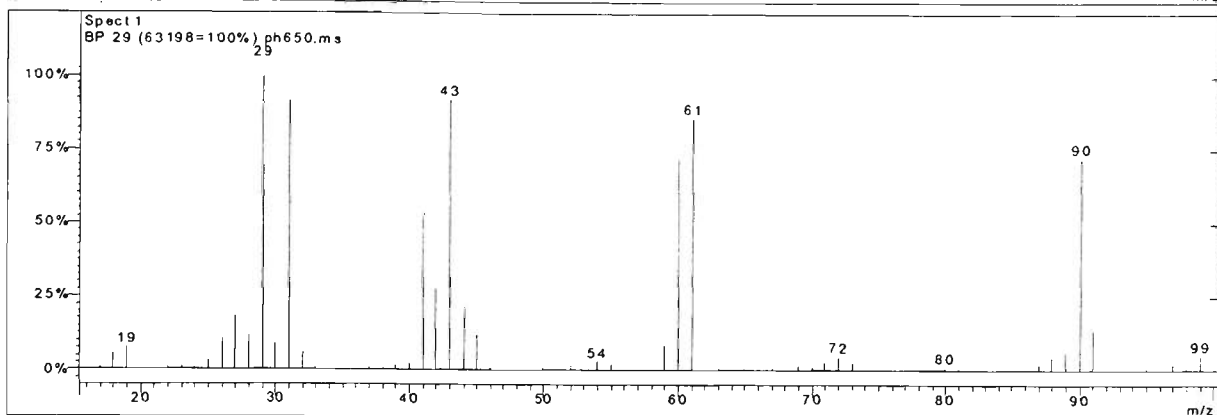
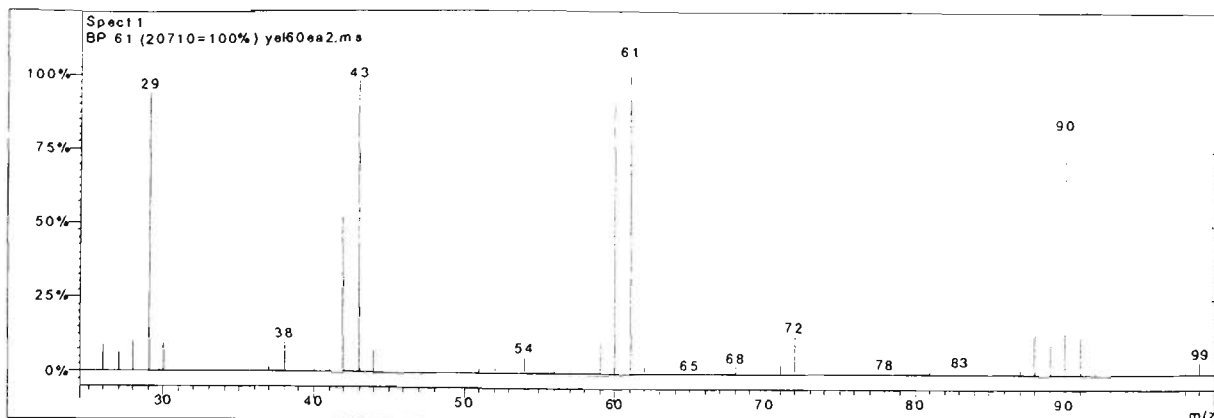
Peak 2 *From sultana EtAc extract (top) and arginine-glucose model EtAc extract (bottom)*



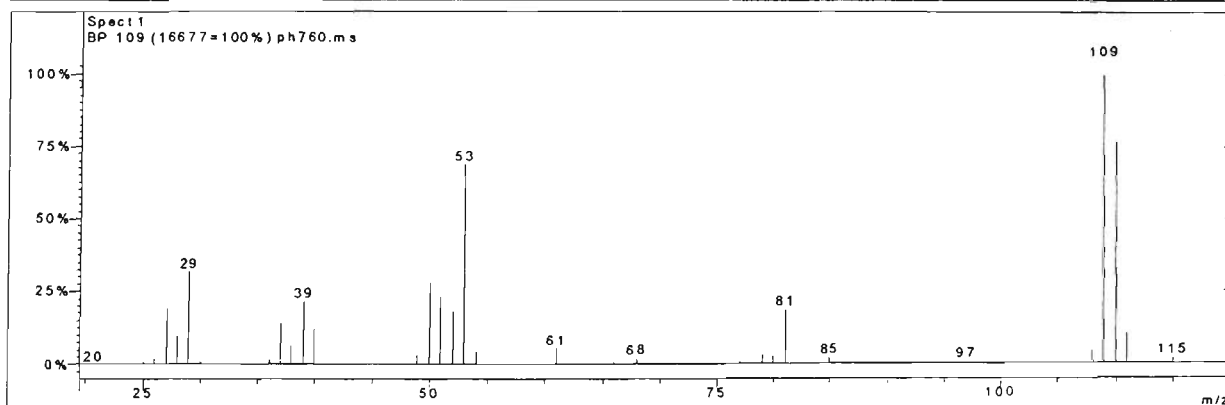
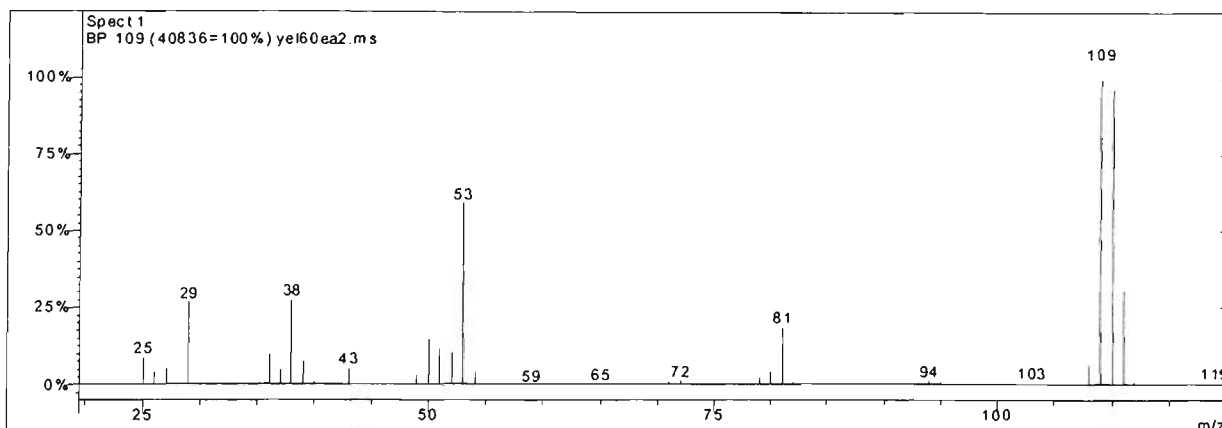
Peak 3 From sultana EtAc extract (top) and arginine-glucose model EtAc extract (bottom)



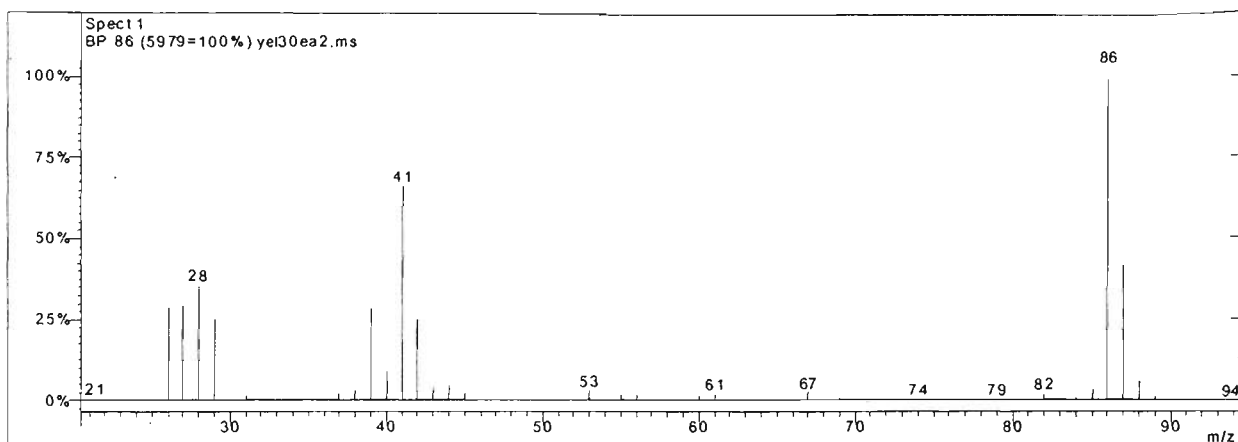
Peak 4 From sultana EtAc extract (top) and arginine-glucose model EtAc extract (bottom)



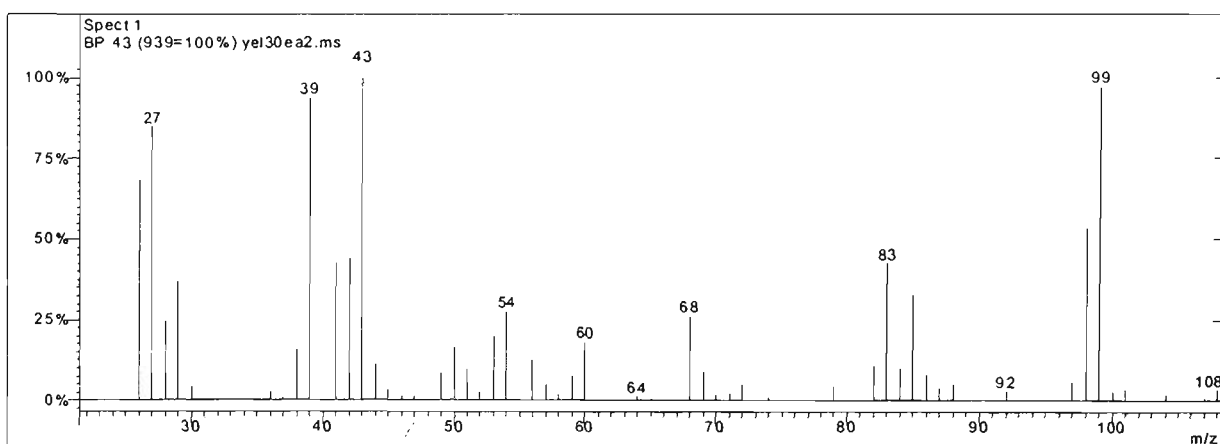
Peak 5 From sultana EtAc extract (top) and arginine-glucose model EtAc extract (bottom)



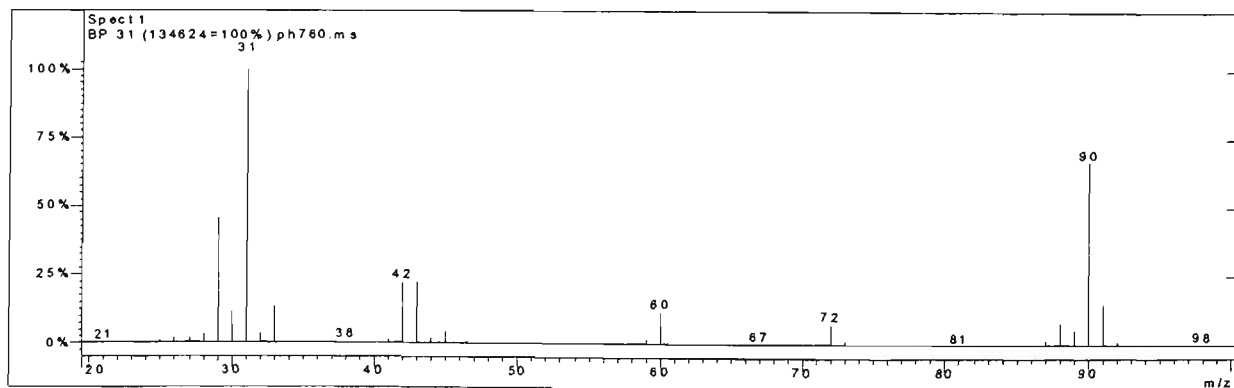
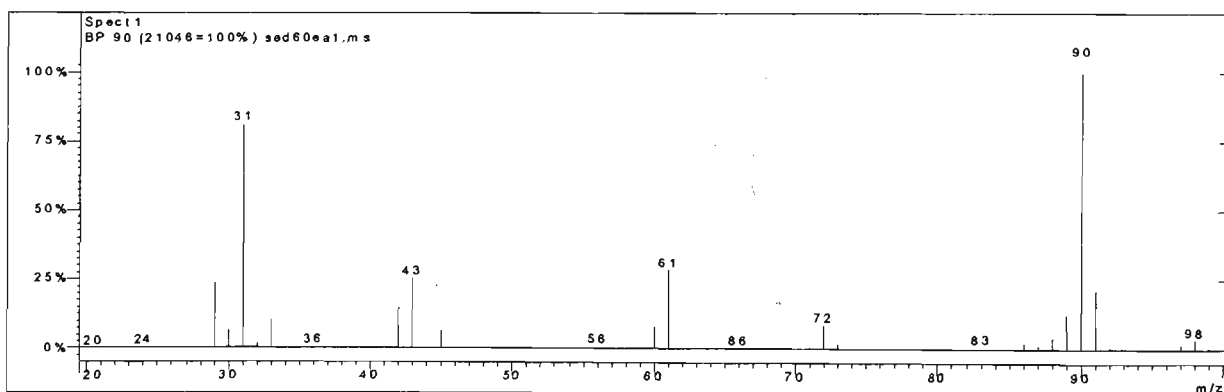
Peak 6 From sultana EtAc extract (top) and arginine-glucose model EtAc extract (bottom)



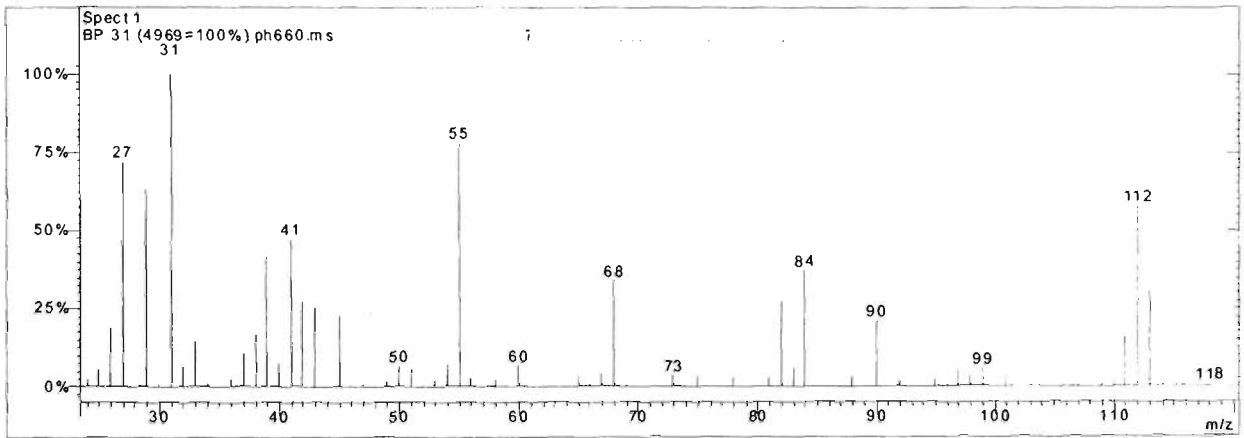
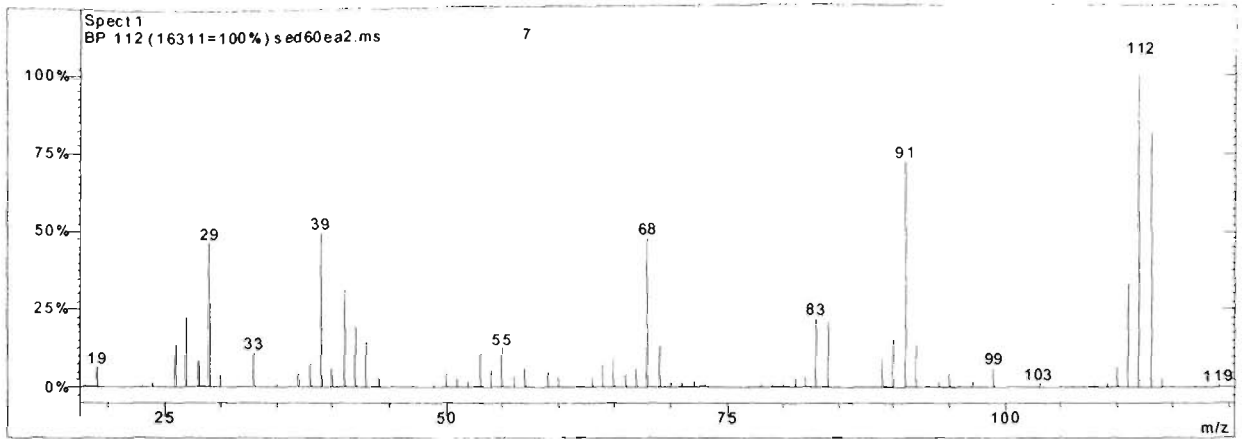
Peak 7 From sultana EtAc extract only



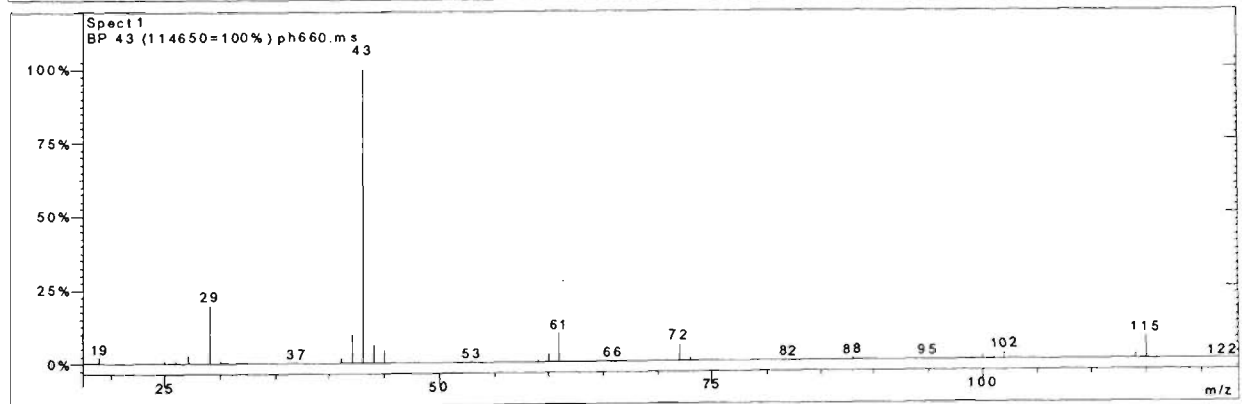
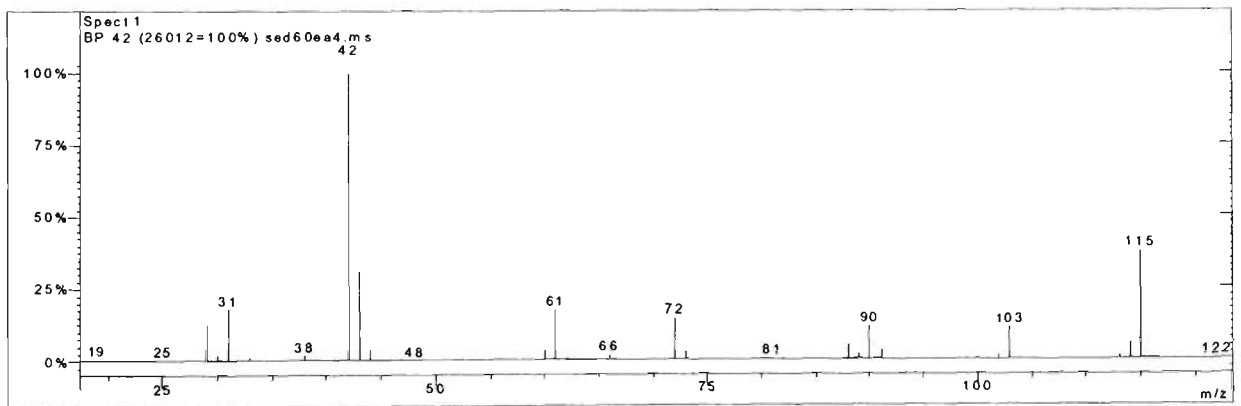
Peak 8 From sultana EtAc extract only



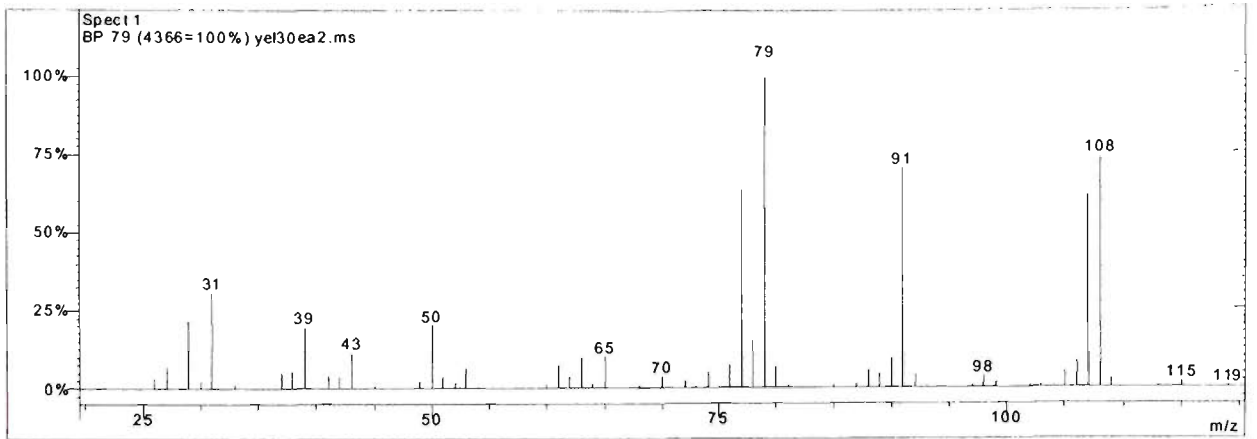
Peak 9 From sultana EtAc extract (top) and arginine-glucose model EtAc extract (bottom)



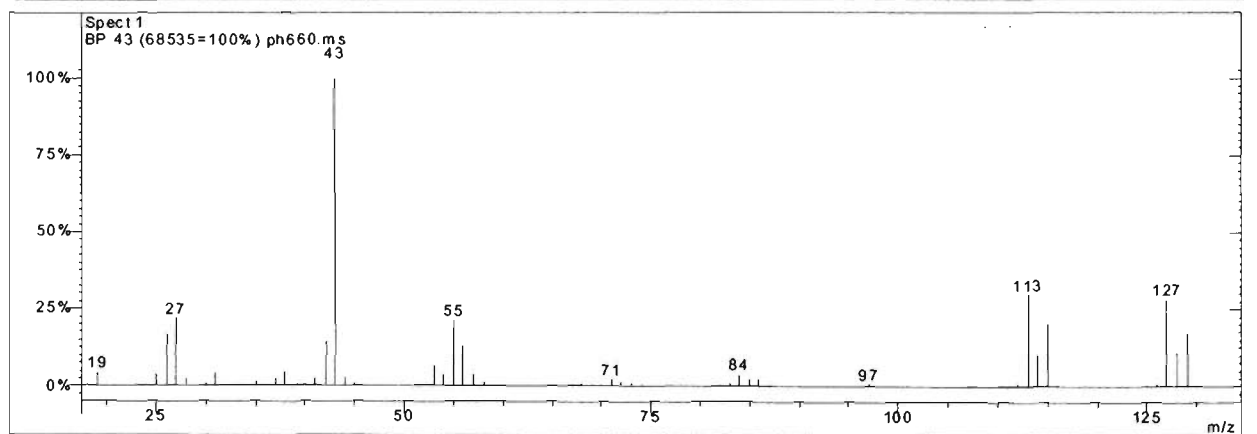
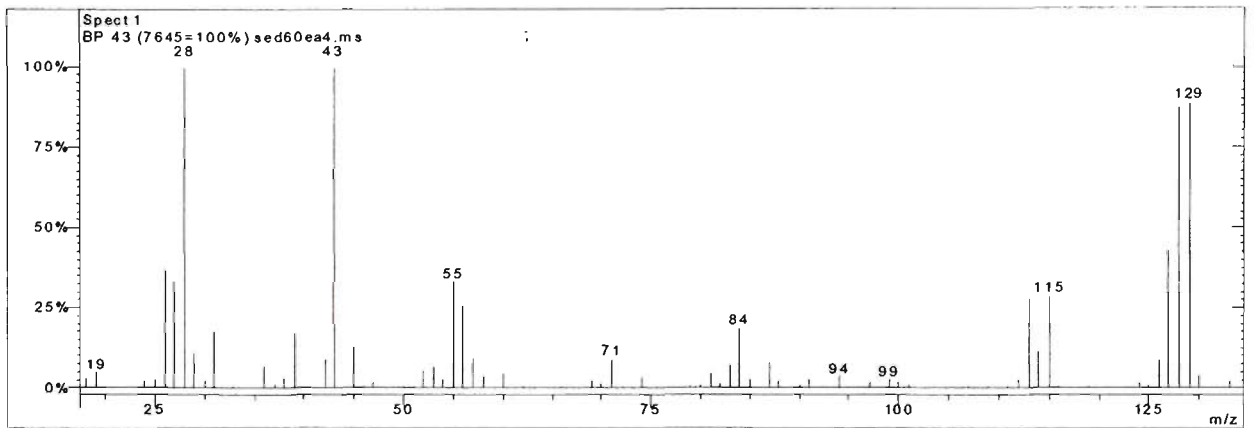
Peak 10 From sultana EtAc extract (top) and arginine-glucose model EtAc extract (bottom)



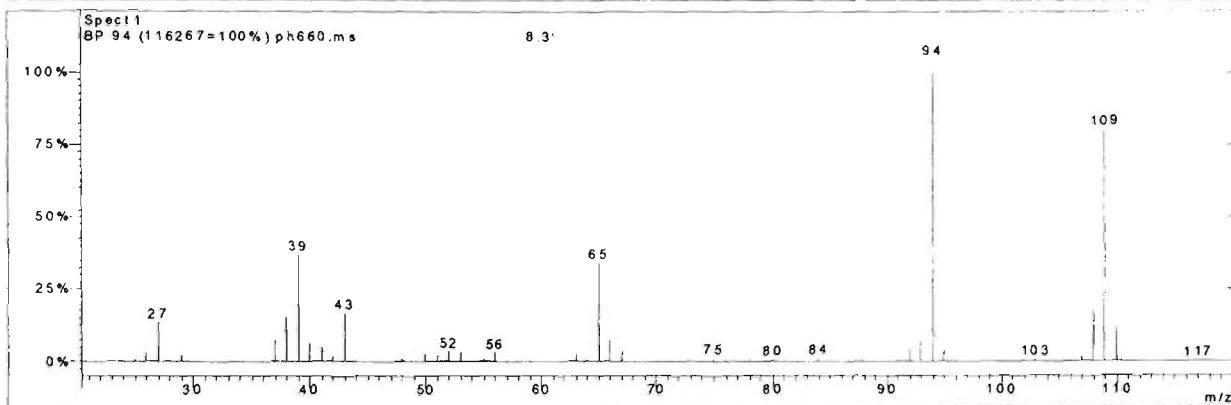
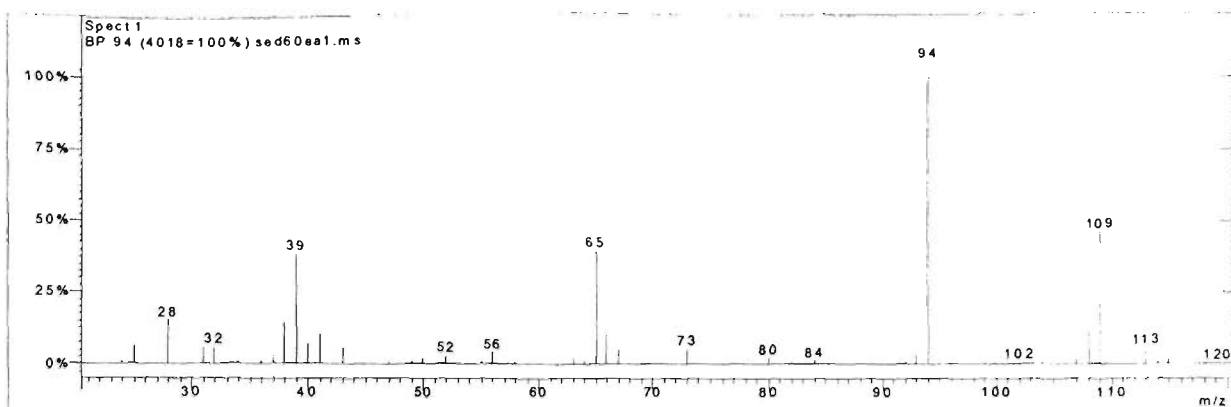
Peak 11 From sultana EtAc extract (top) and arginine-glucose model EtAc extract (bottom)



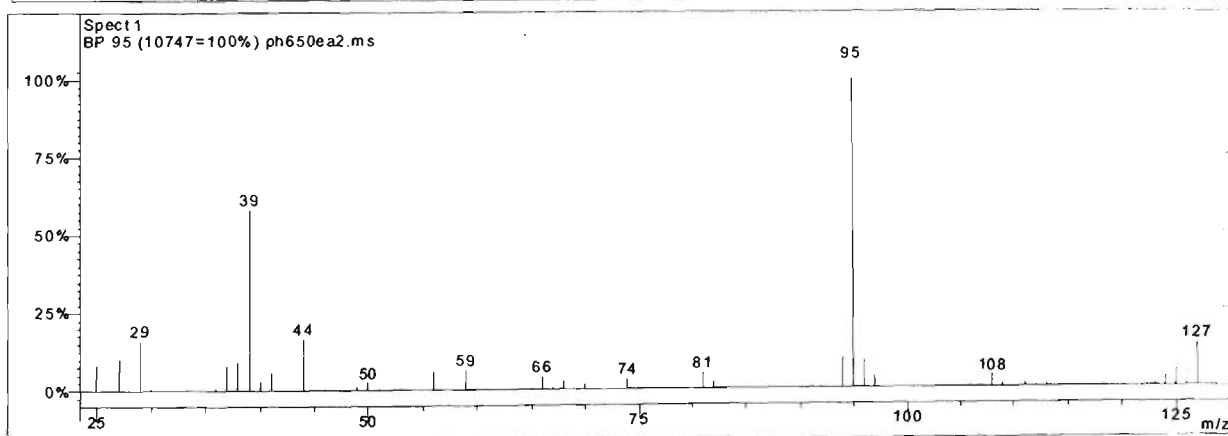
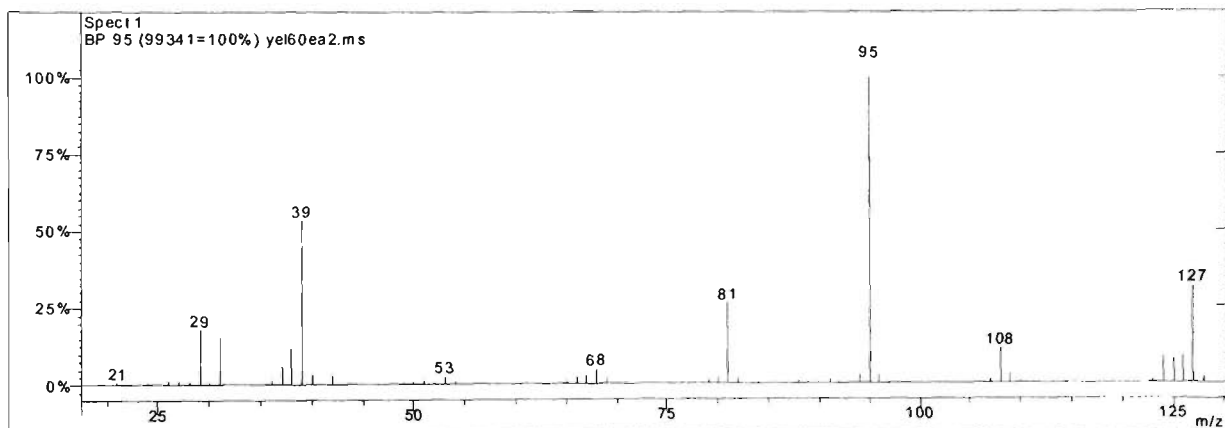
Peak 12 From sultana EtAc extract only



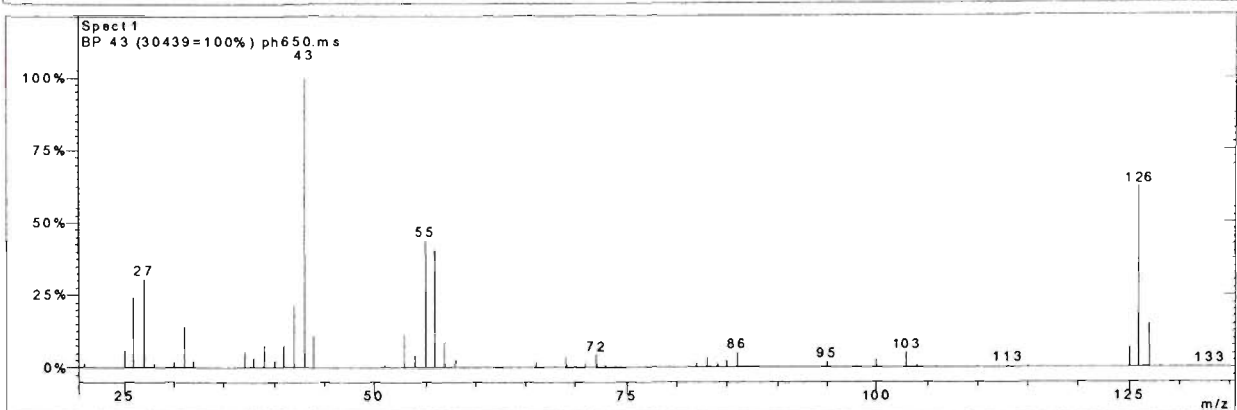
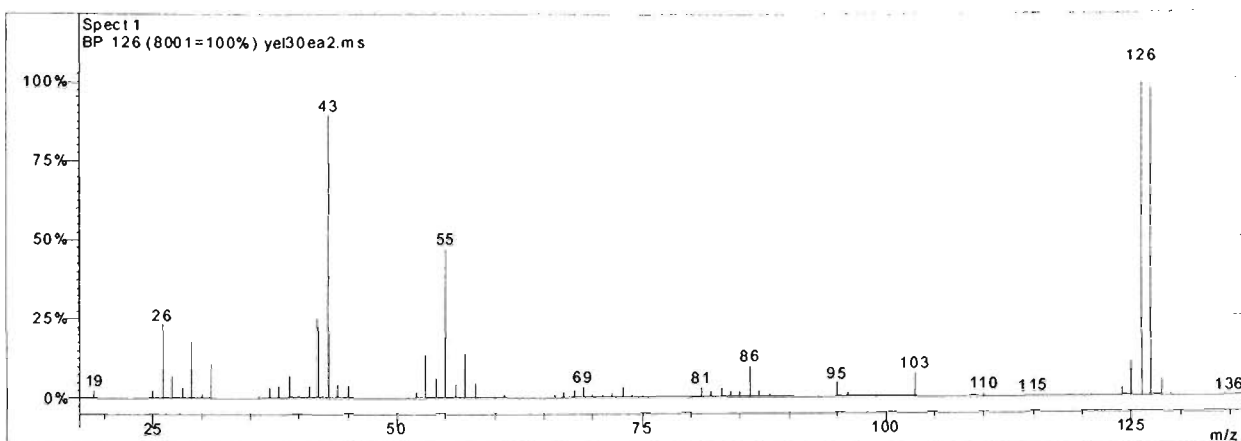
Peak 13 From sultana EtAc extract (top) and arginine-glucose model EtAc extract (bottom)



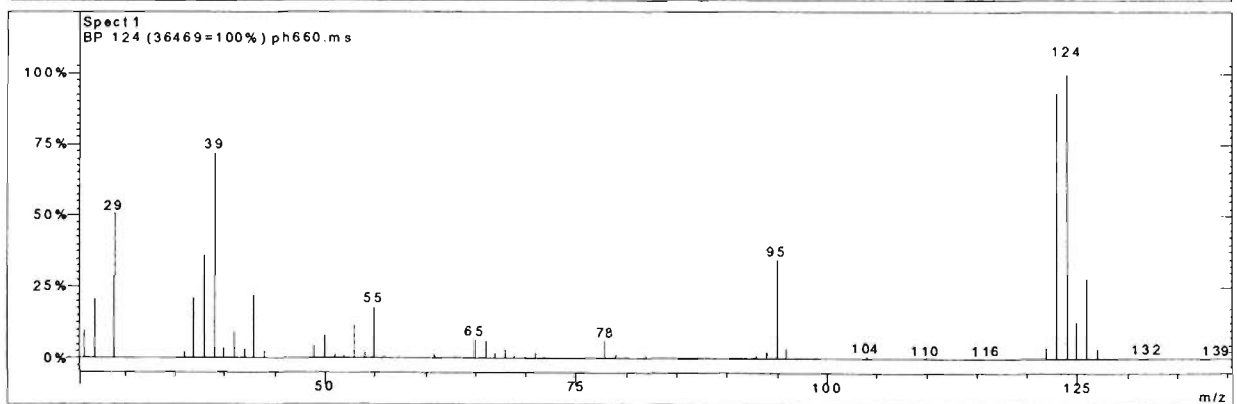
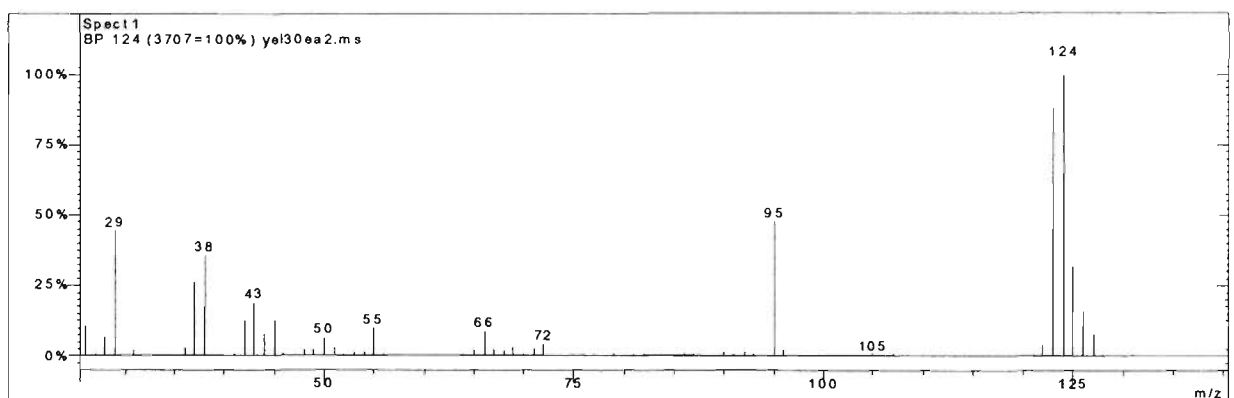
Peak 14 From sultana EtAc extract (top) and arginine-glucose model EtAc extract (bottom)



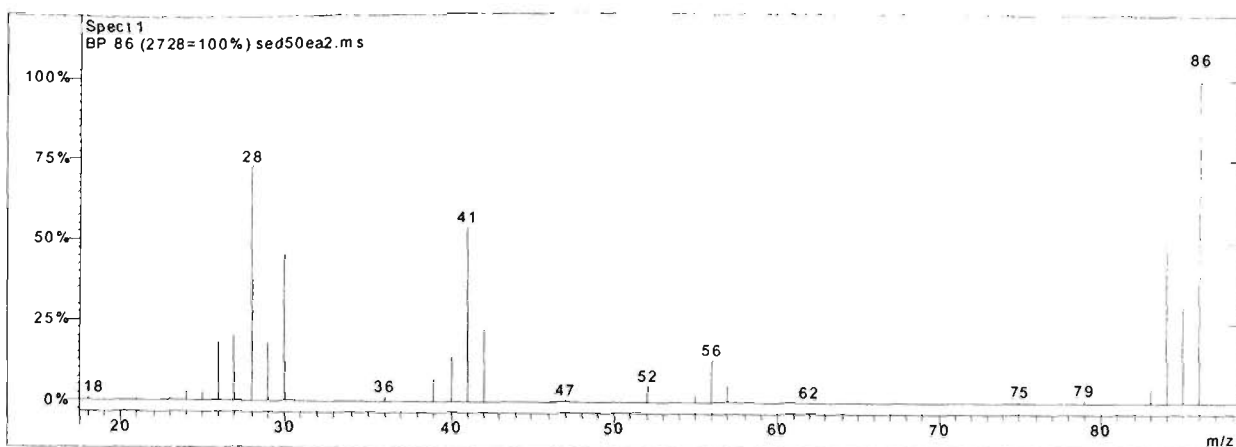
Peak 15 From sultana EtAc extract (top) and arginine-glucose model EtAc extract (bottom)



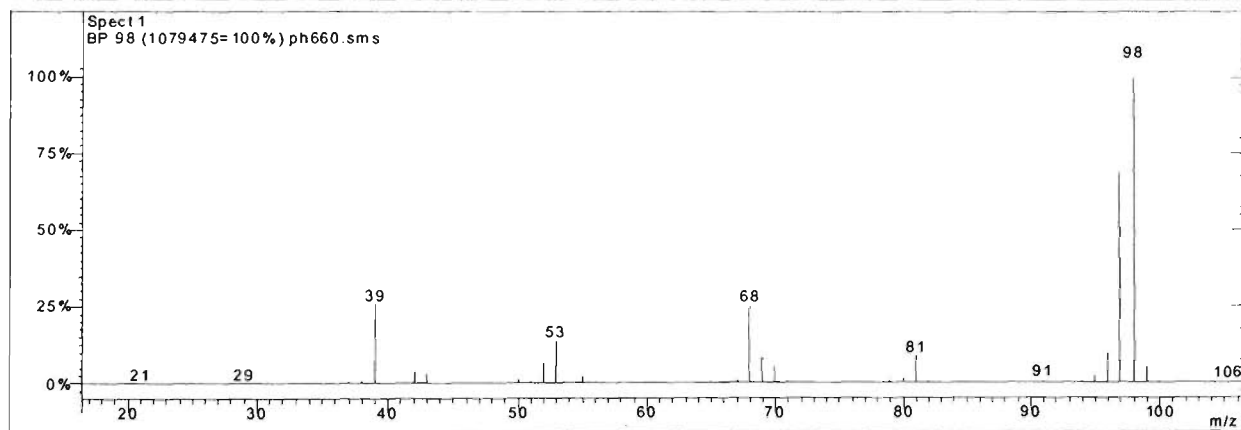
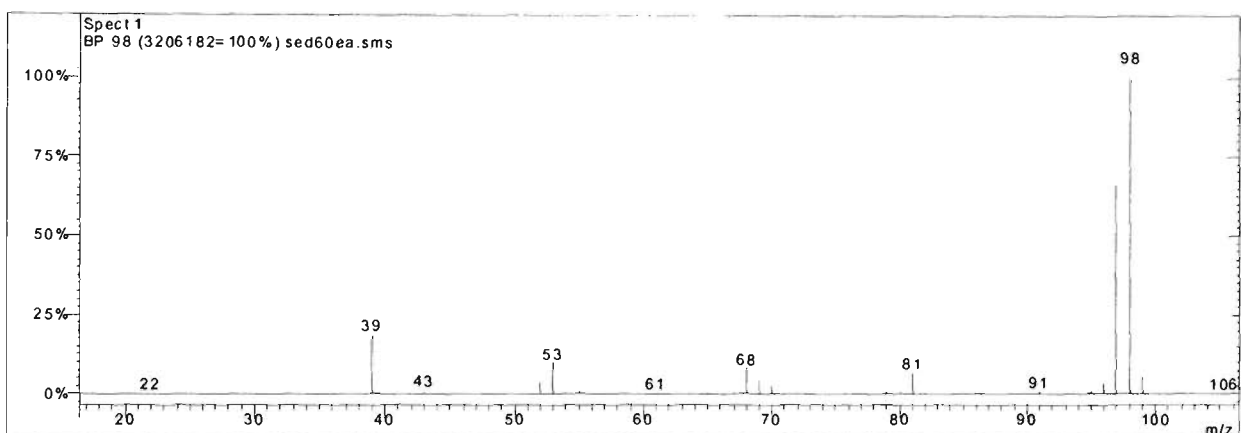
Peak 16 From sultana EtAc extract (top) and arginine-glucose model EtAc extract (bottom)



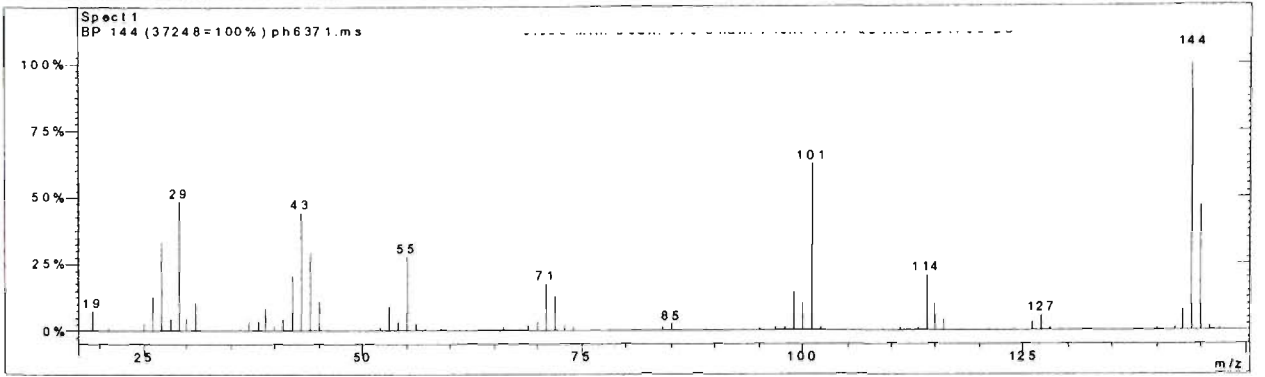
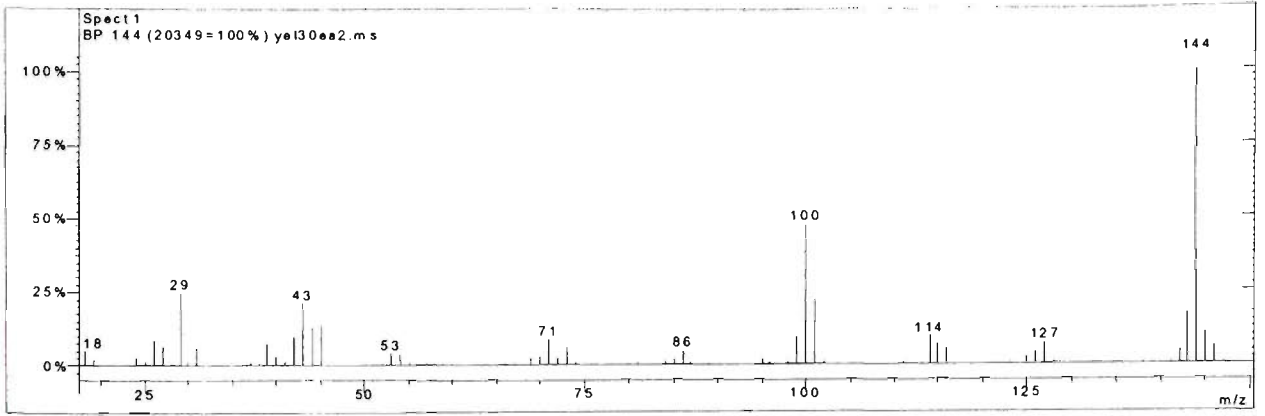
Peak 17 From sultana EtAc extract (top) and arginine-glucose model EtAc extract (bottom)



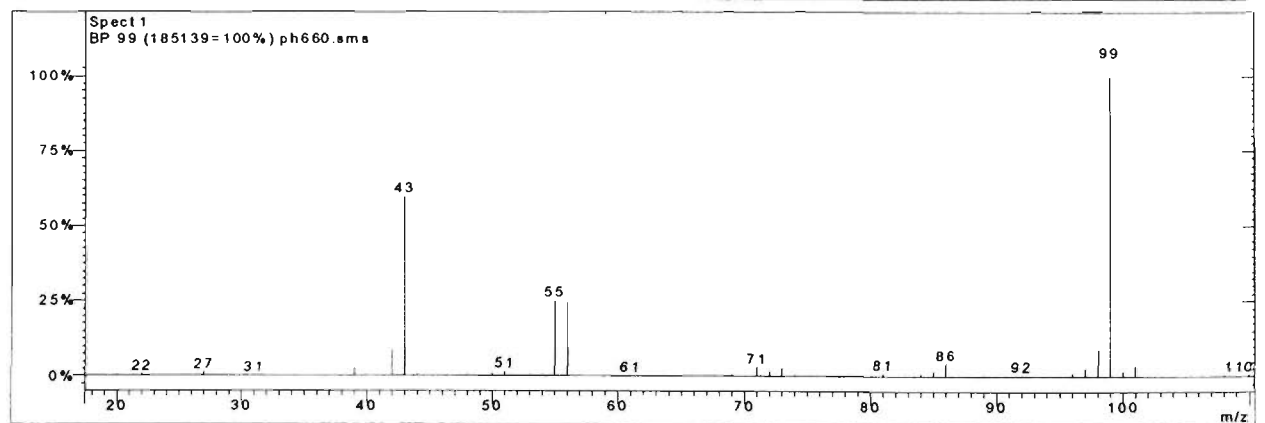
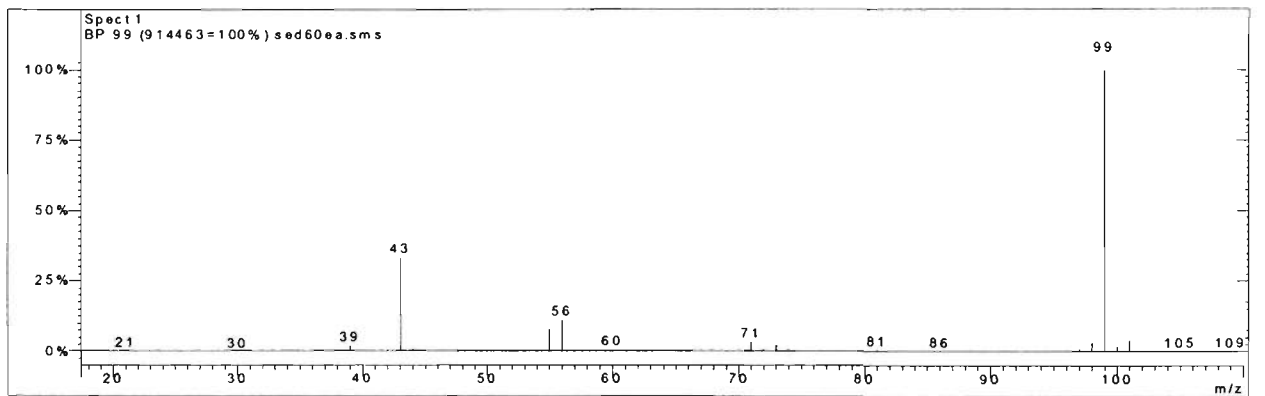
Peak 18 From sultana EtAc extract only



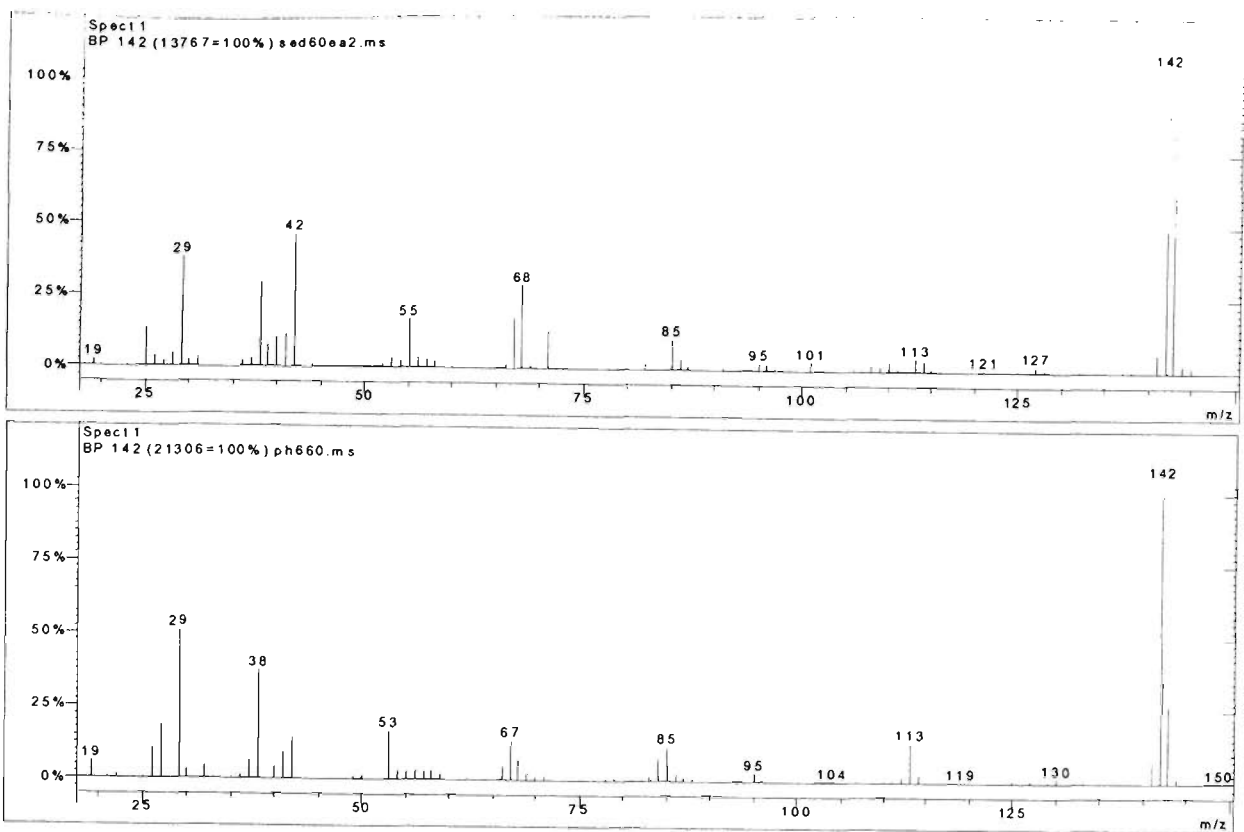
Peak 19 From sultana EtAc extract (top) and arginine-glucose model EtAc extract (bottom)



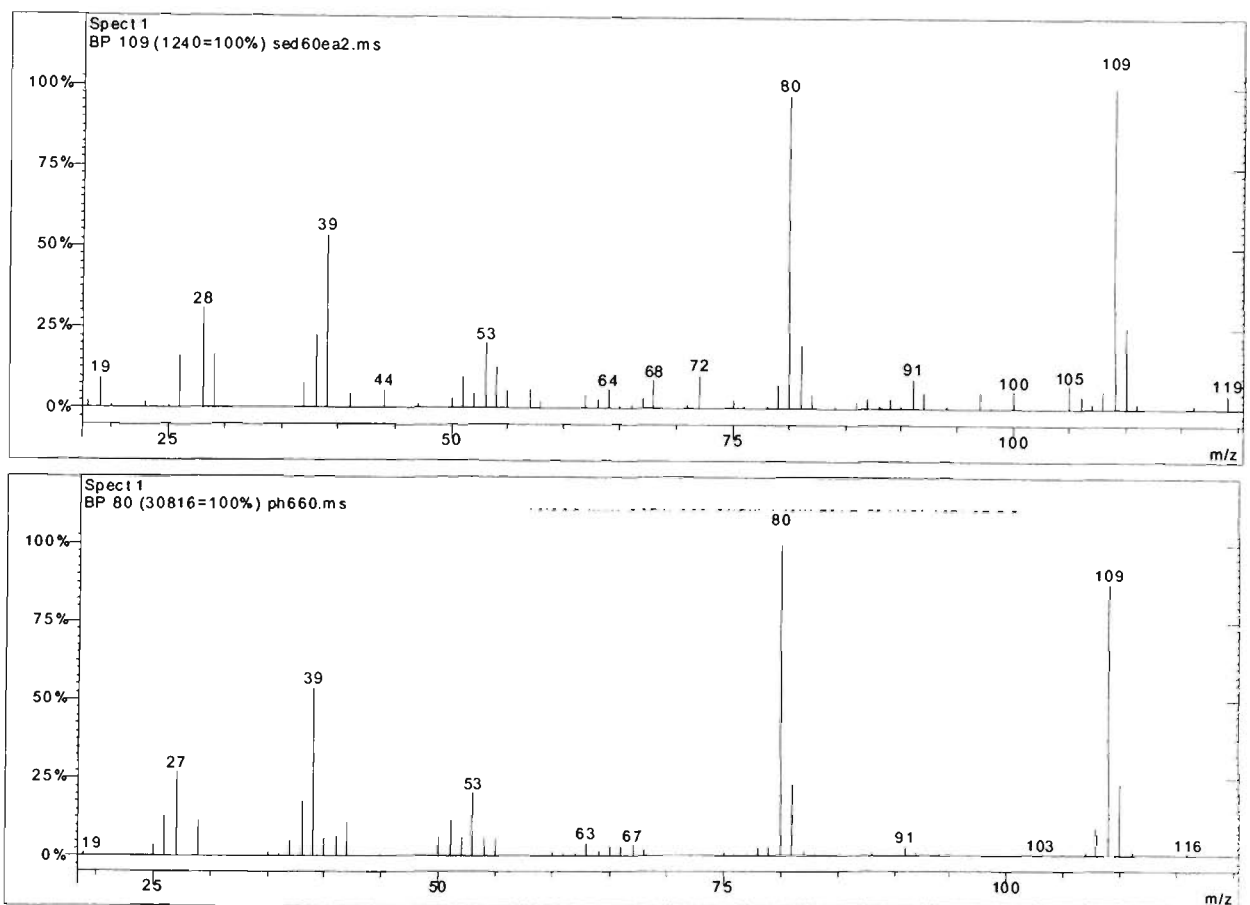
Peak 20 From sultana EtAc extract (top) and arginine-glucose model EtAc extract (bottom)



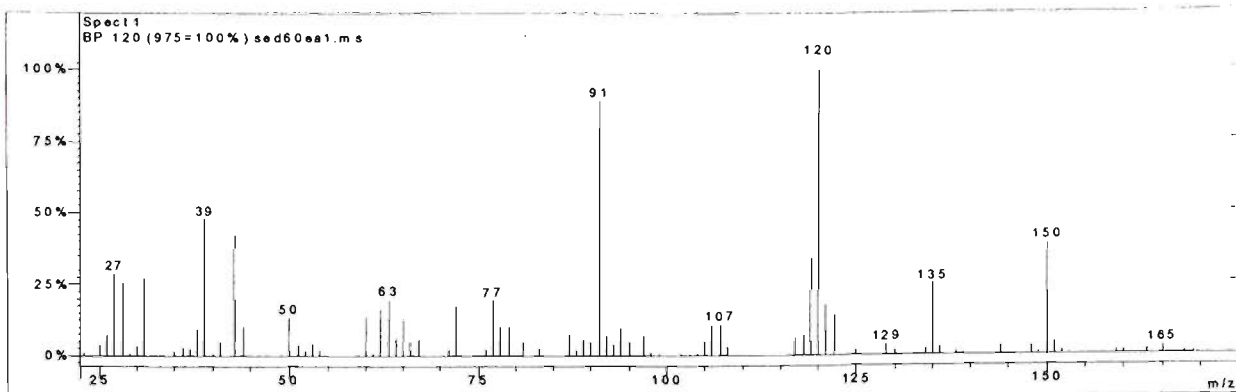
Peak 21 From sultana EtAc extract (top) and arginine-glucose model EtAc extract (bottom)



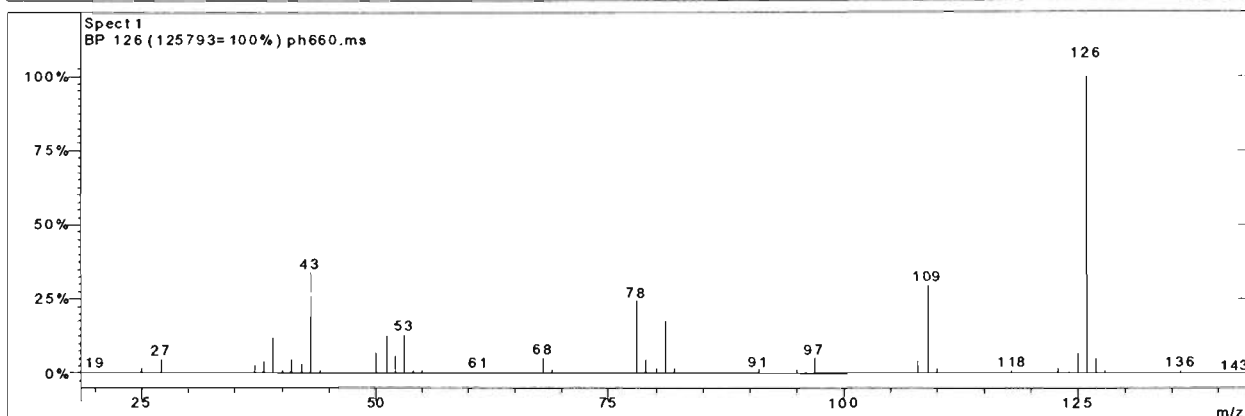
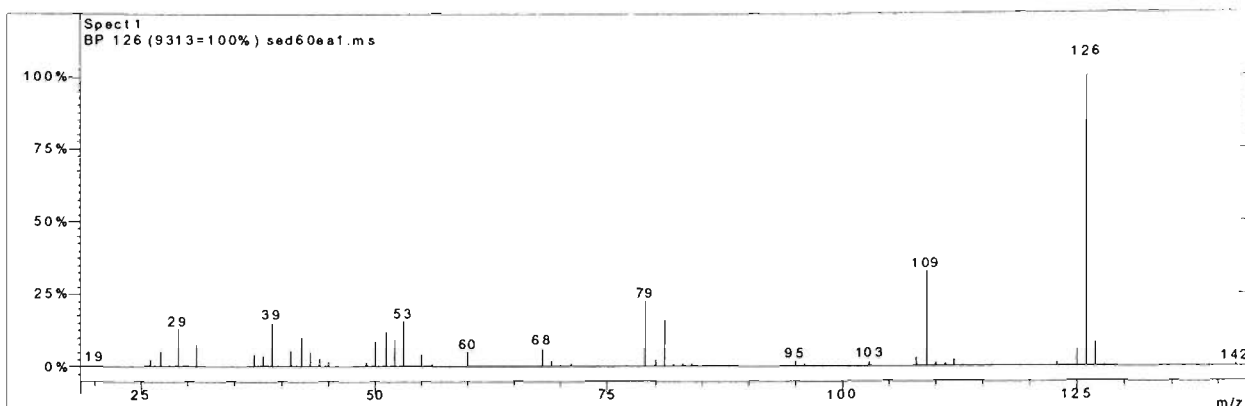
Peak 22 From sultana EtAc extract (top) and arginine-glucose model EtAc extract (bottom)



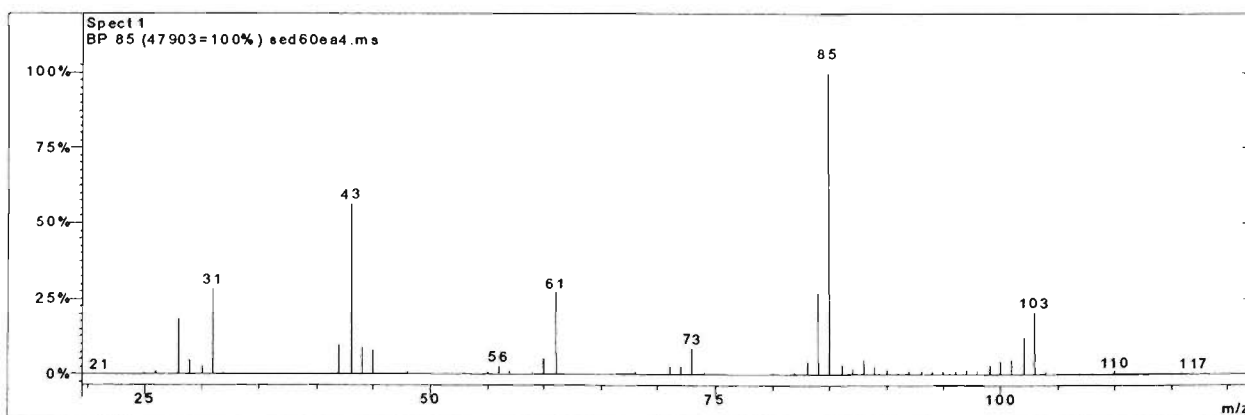
Peak 23 From sultana EtAc extract (top) and arginine-glucose model EtAc extract (bottom)



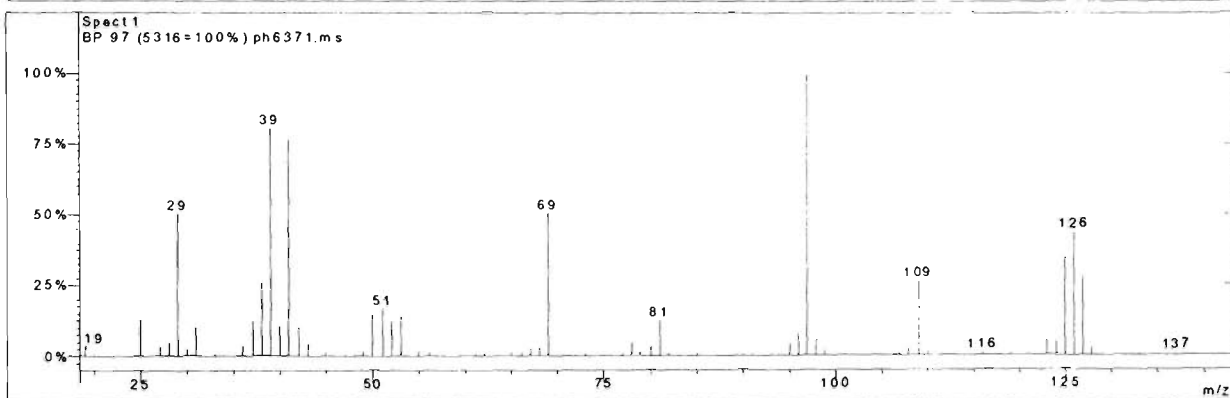
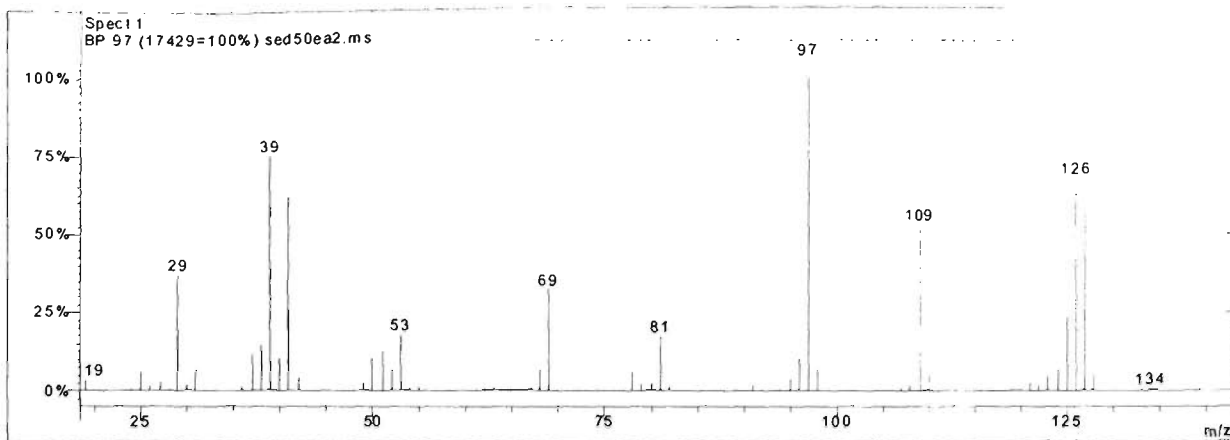
Peak 24 From sultana EtAc extract only



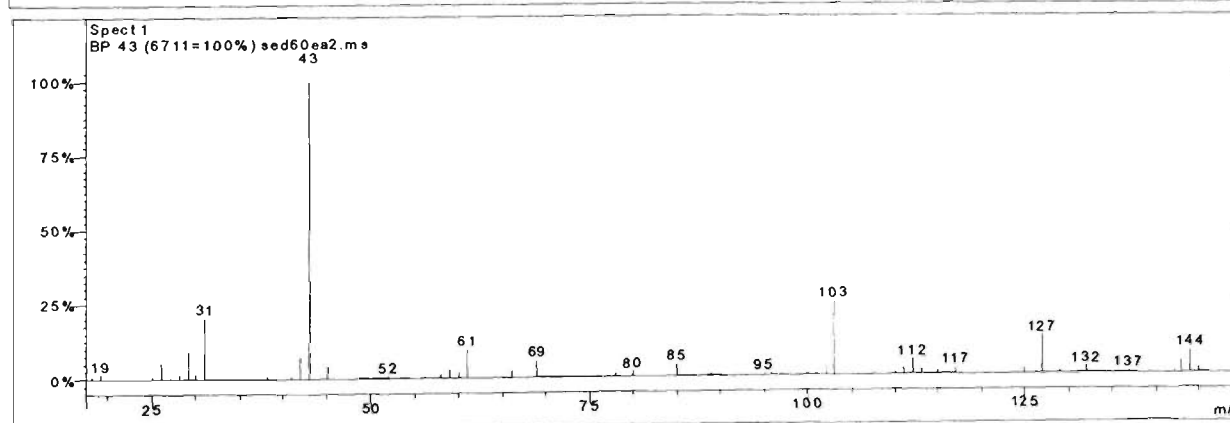
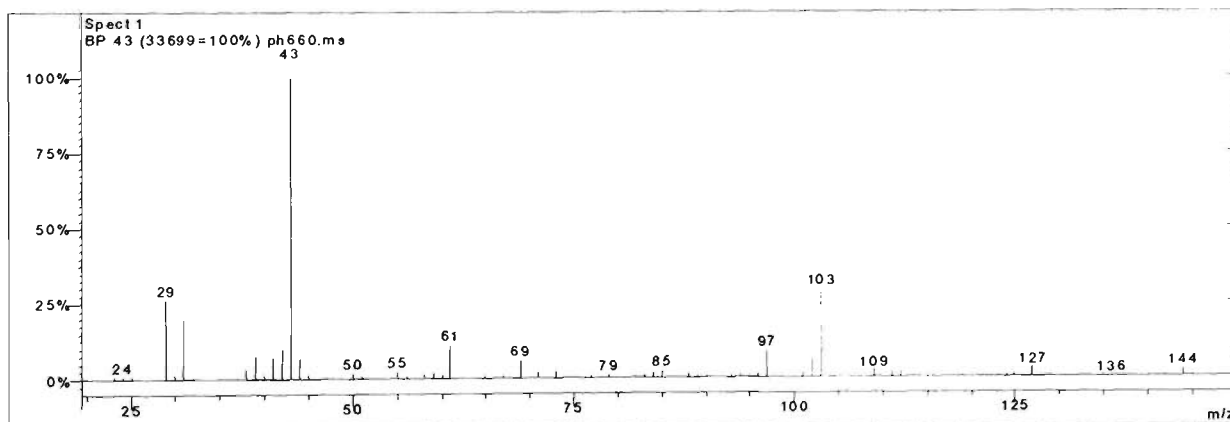
Peak 25 From sultana EtAc extract (top) and arginine-glucose model EtAc extract (bottom)



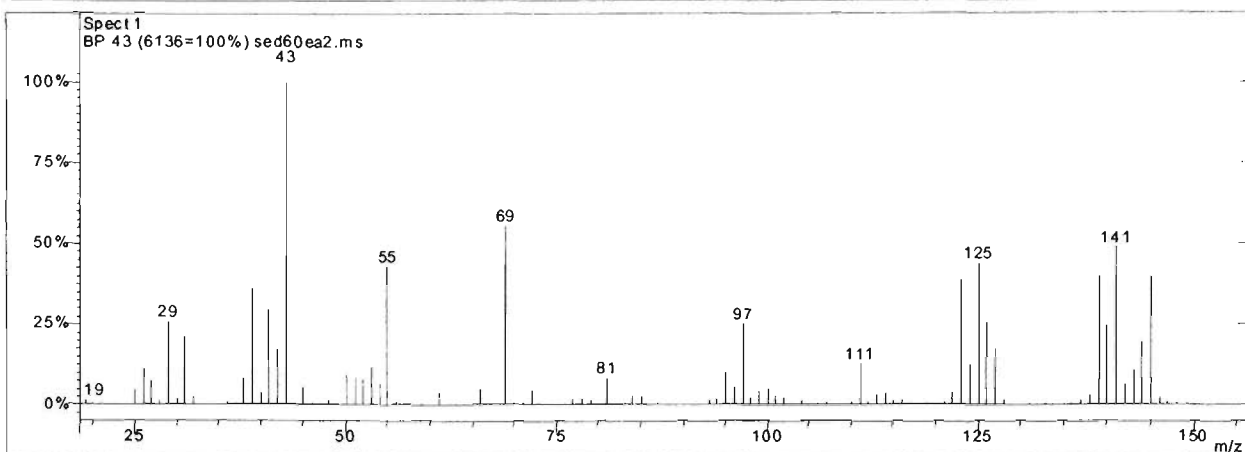
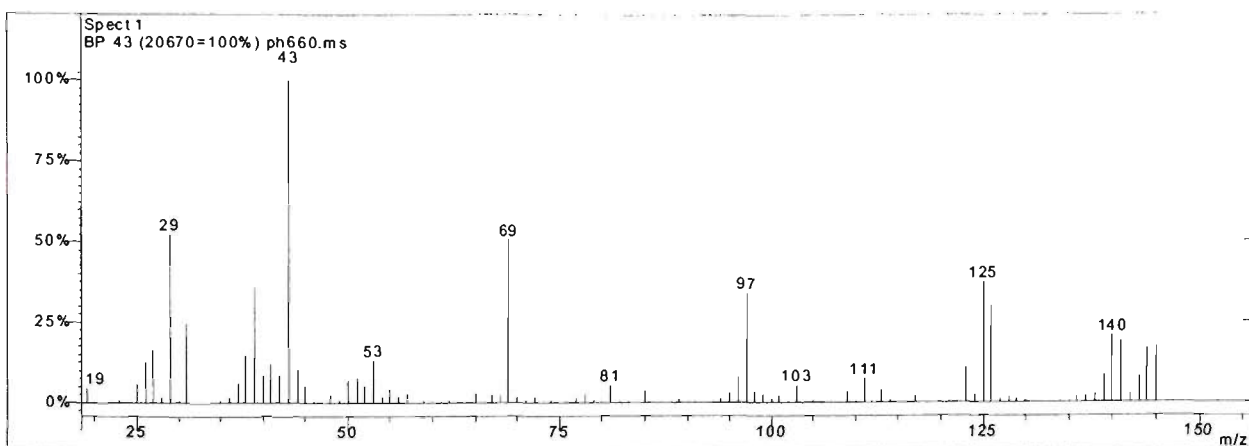
Peak 26 From sultana EtAc extract only



Peak 27 From sultana EtAc extract (top) and arginine-glucose model EtAc extract (bottom)

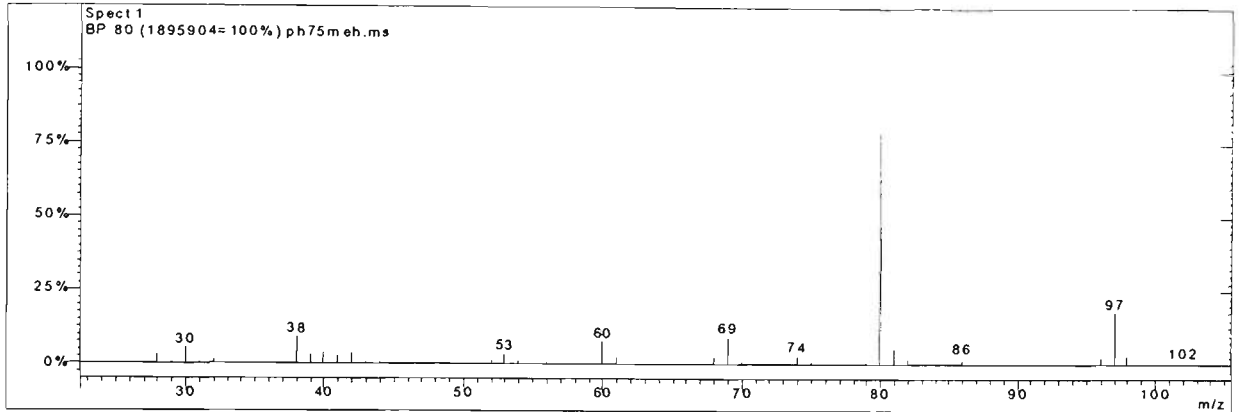
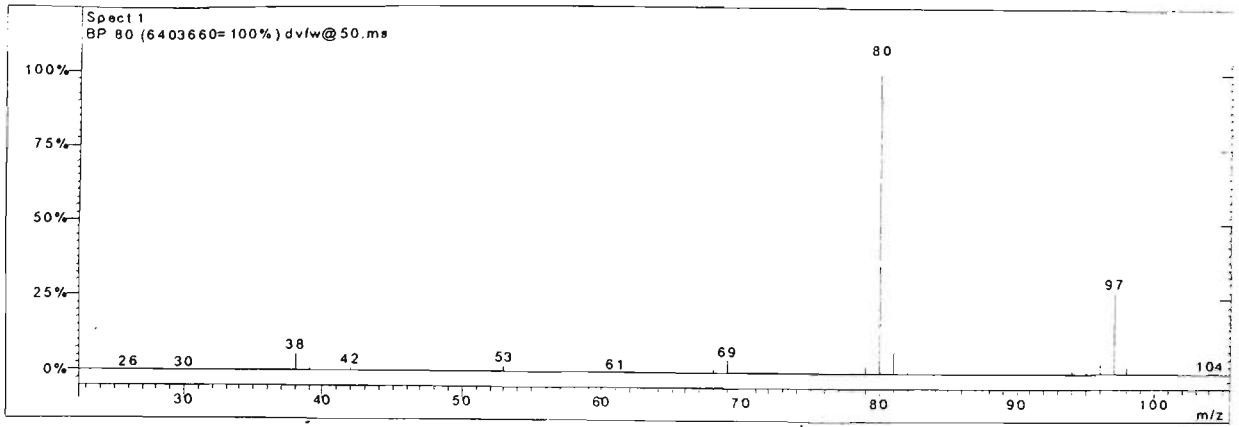


Peak 28 From sultana EtAc extract (top) and arginine-glucose model EtAc extract (bottom)

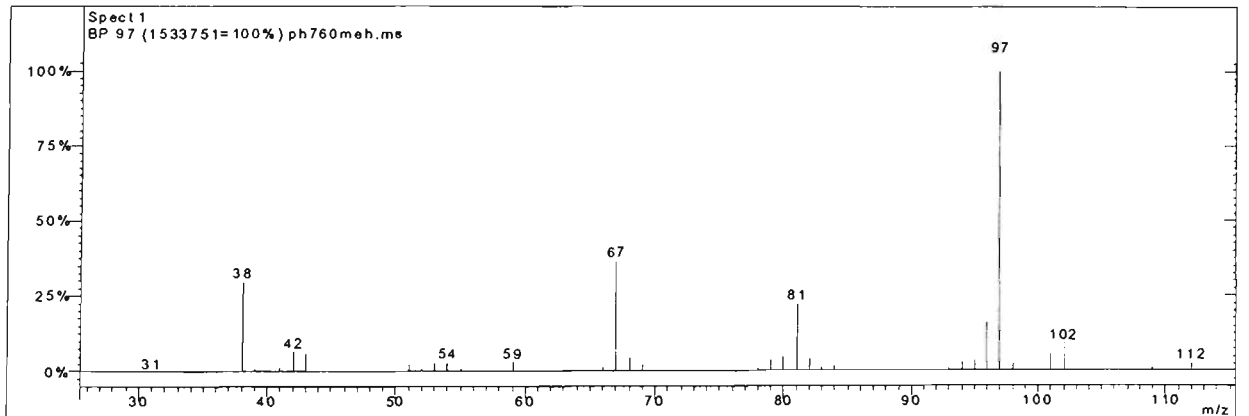
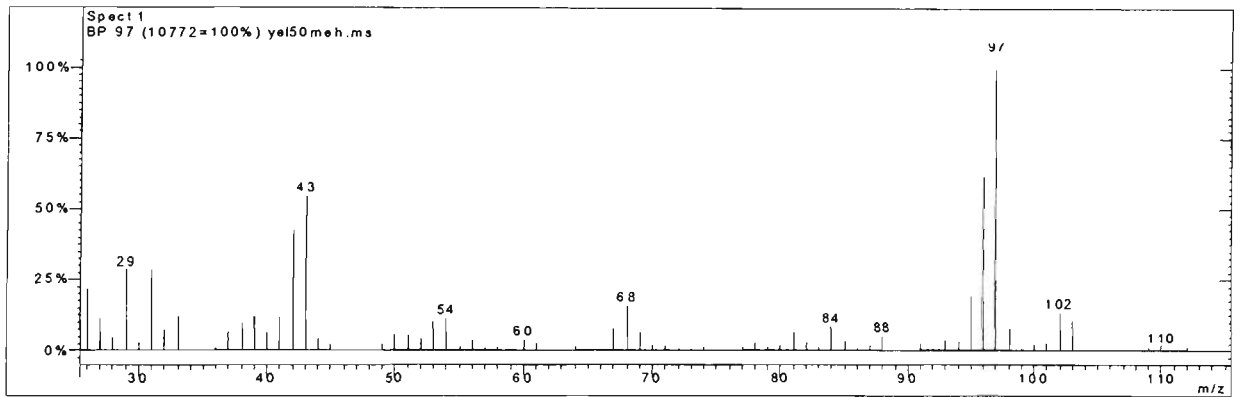


Peak 29 From sultana EtAc extract (top) and arginine-glucose model EtAc extract (bottom)

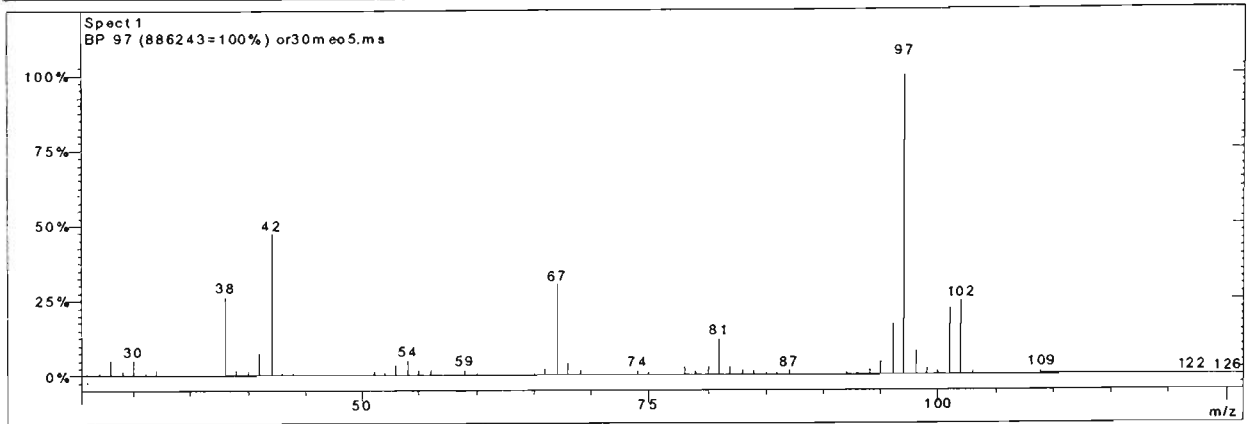
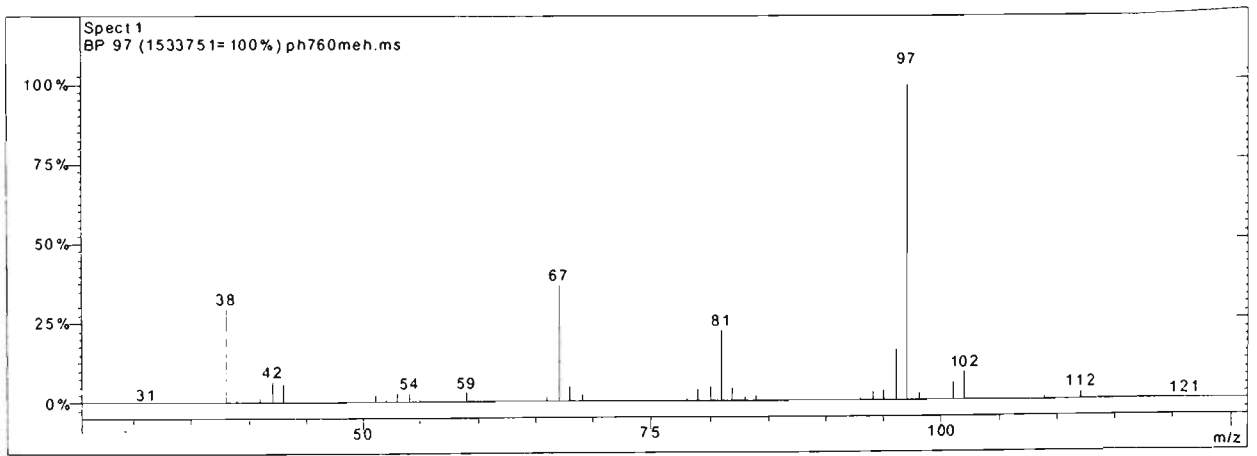
# Methanol spectra



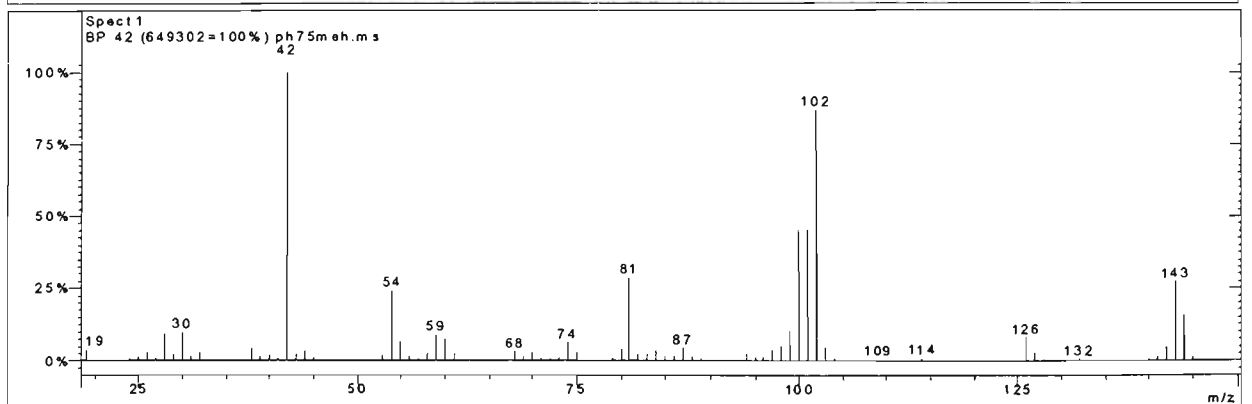
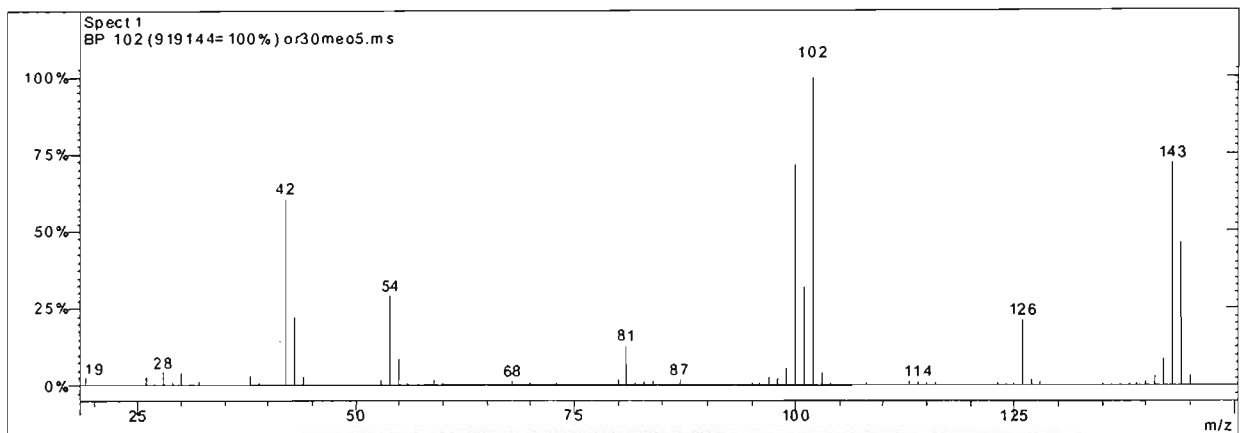
Peak 1 From sultana MeOH extract (top) and arginine-glucose model MeOH extract (bottom)



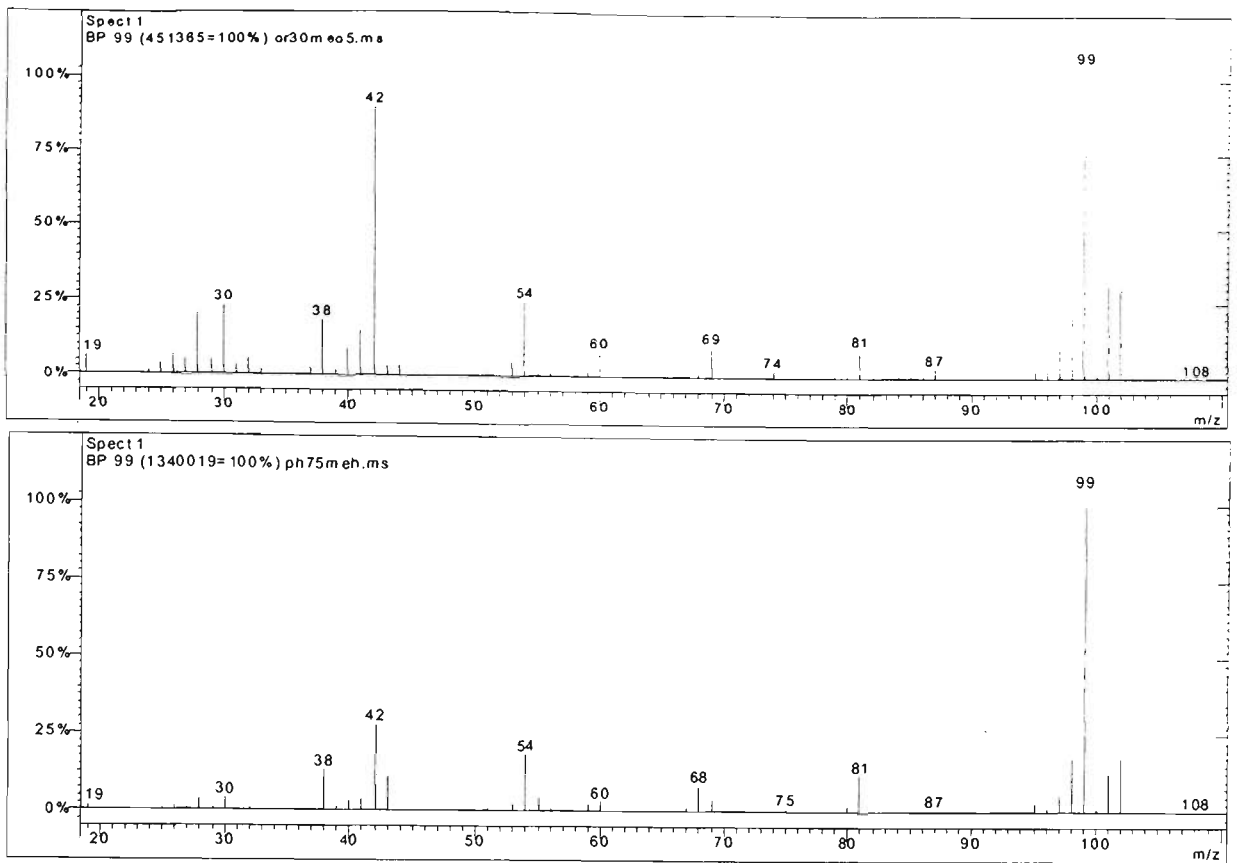
Peak 2 From sultana MeOH extract (top) and arginine-glucose model MeOH extract (bottom)



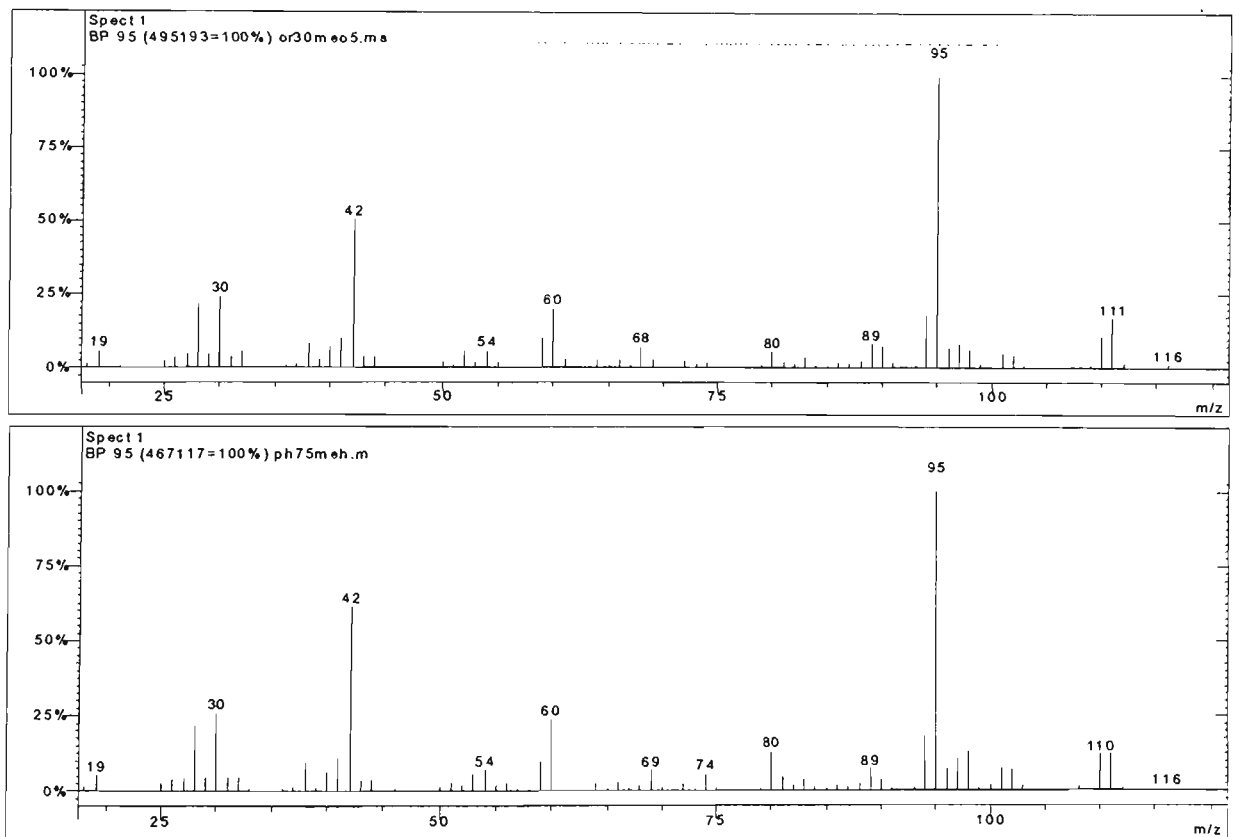
Peak 3 From sultana MeOH extract (top) and arginine-glucose model MeOH extract (bottom)



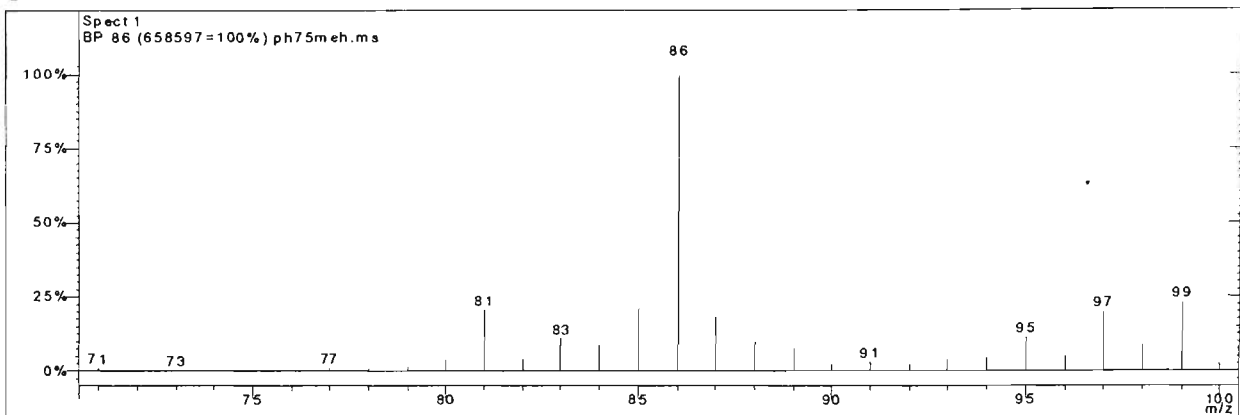
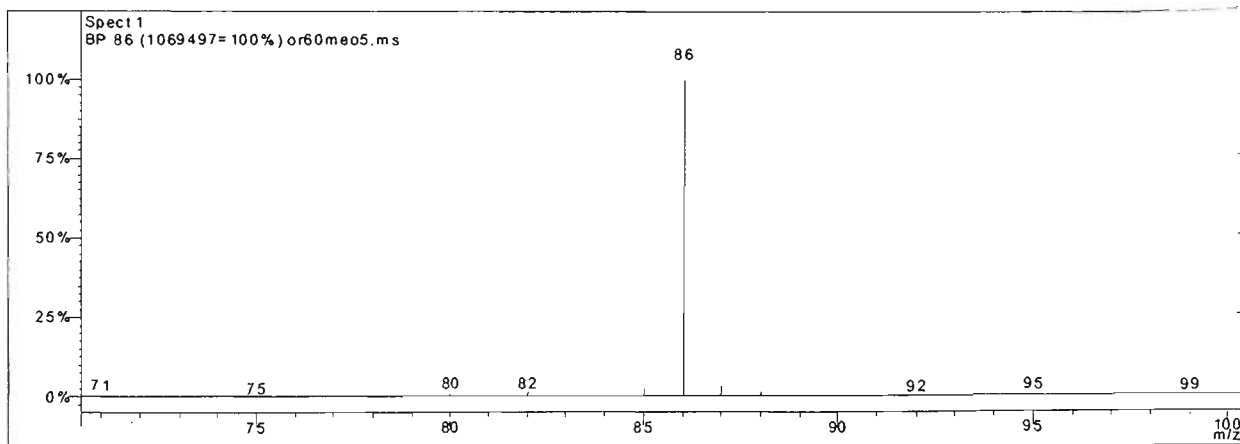
Peak 4 From sultana MeOH extract (top) and arginine-glucose model MeOH extract (bottom)



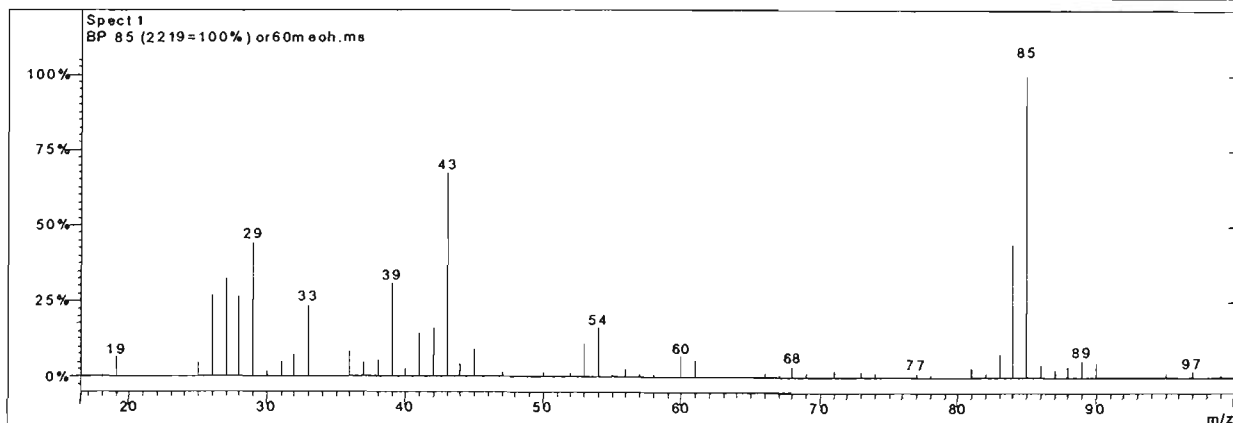
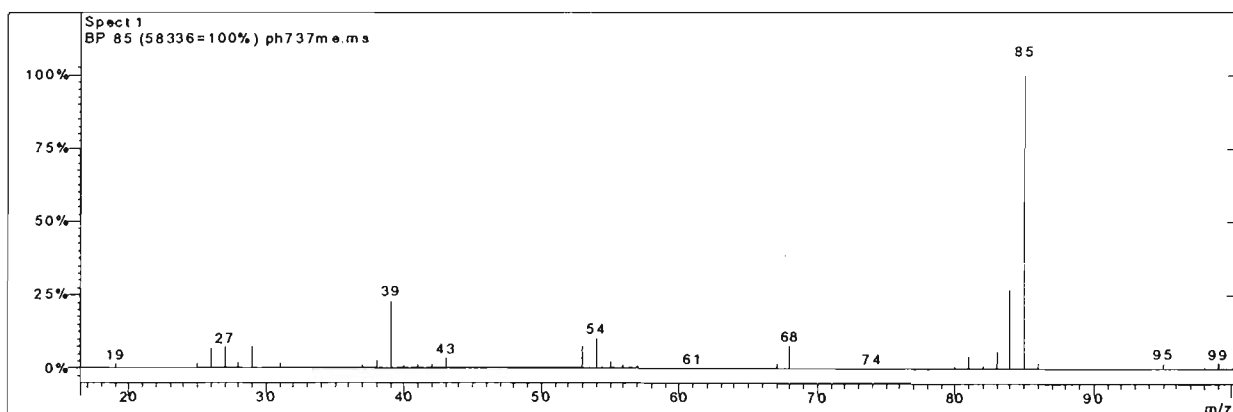
Peak 5 From sultana MeOH extract (top) and arginine-glucose model MeOH extract (bottom)



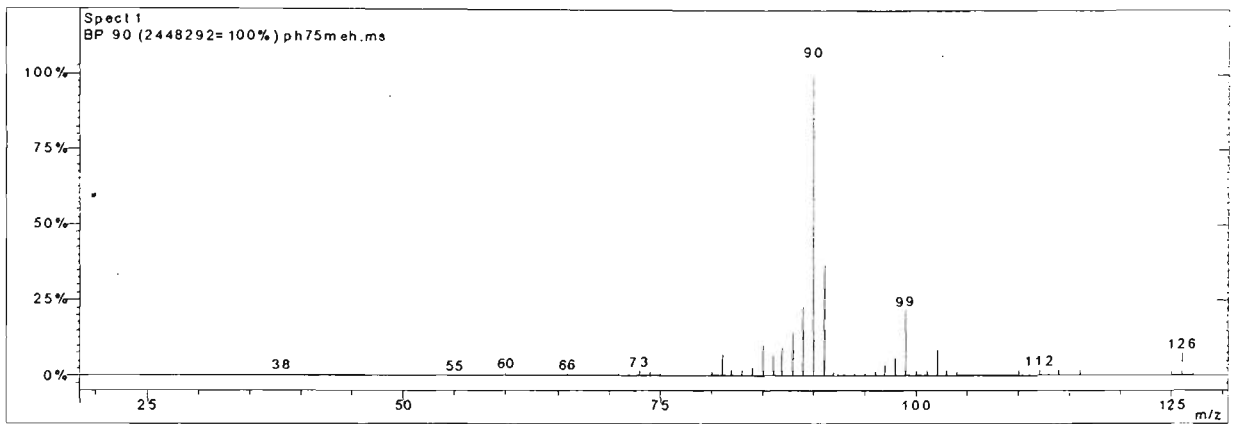
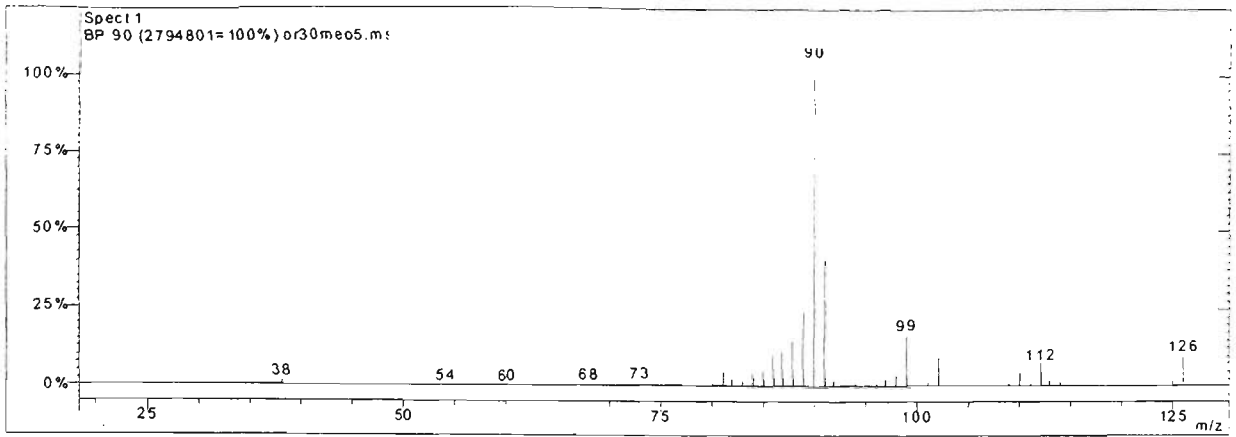
Peak 6 From sultana MeOH extract (top) and arginine-glucose model MeOH extract (bottom)



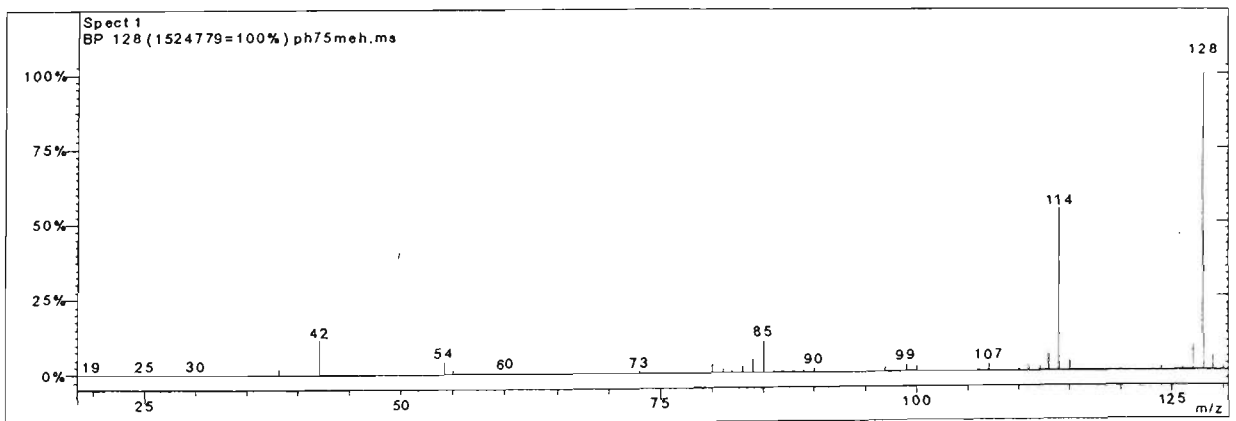
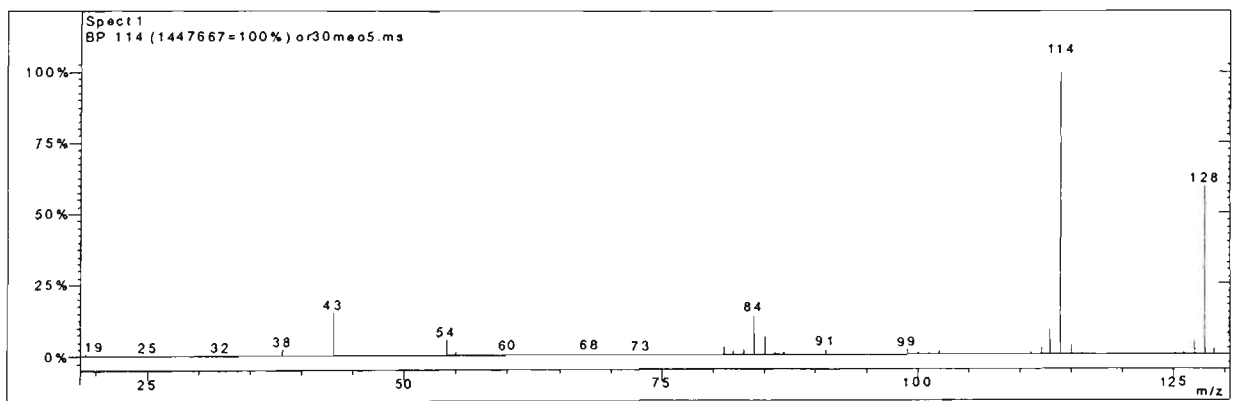
Peak 7 From sultana MeOH extract (top) and arginine-glucose model MeOH extract (bottom)



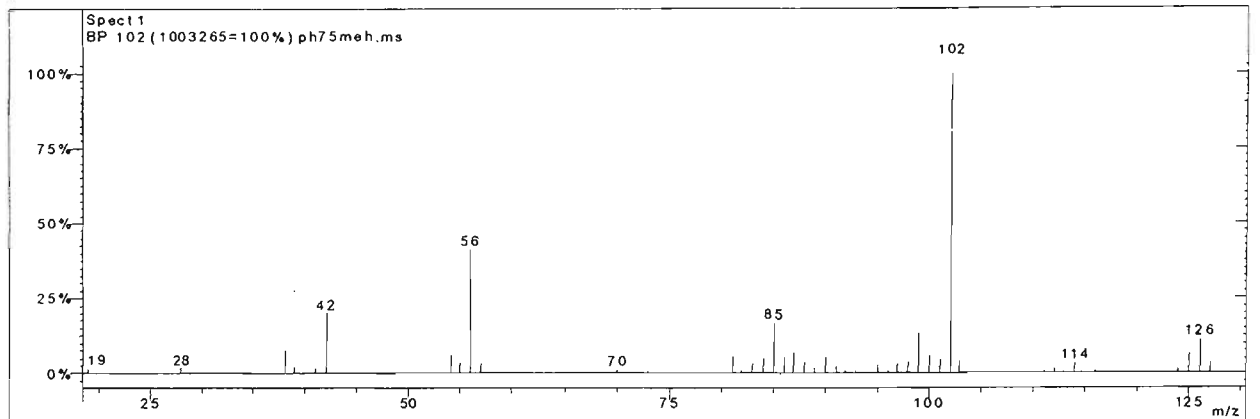
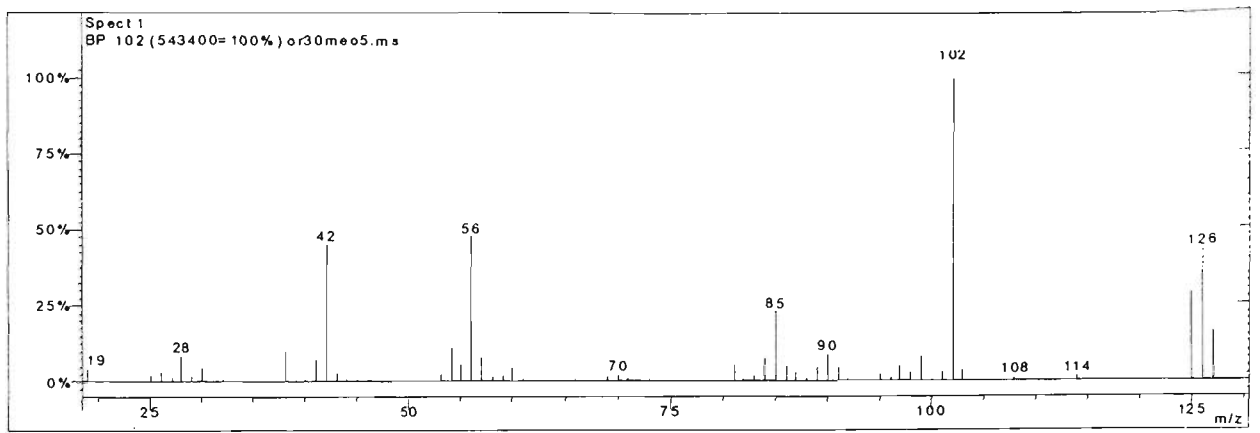
Peak 8 From sultana MeOH extract (top) and arginine-glucose model MeOH extract (bottom)



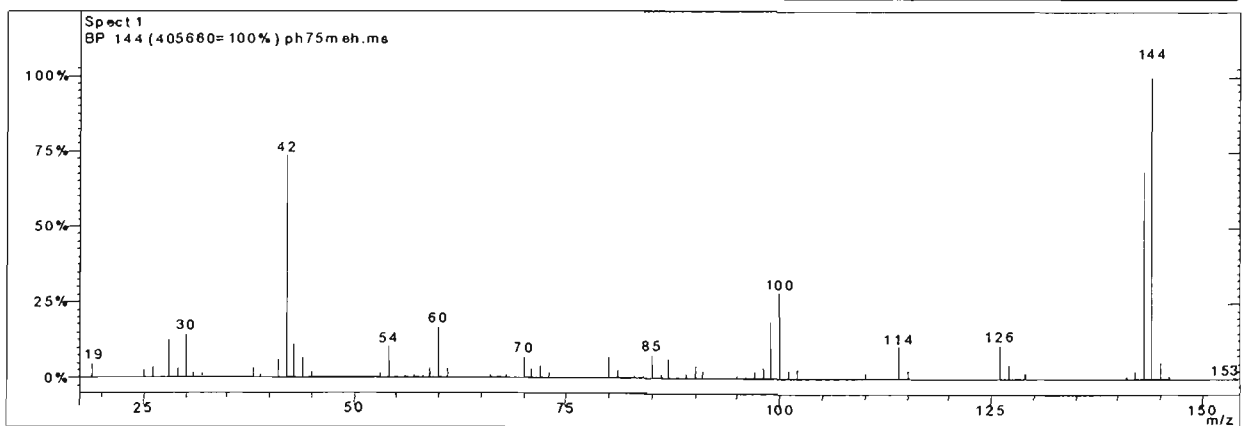
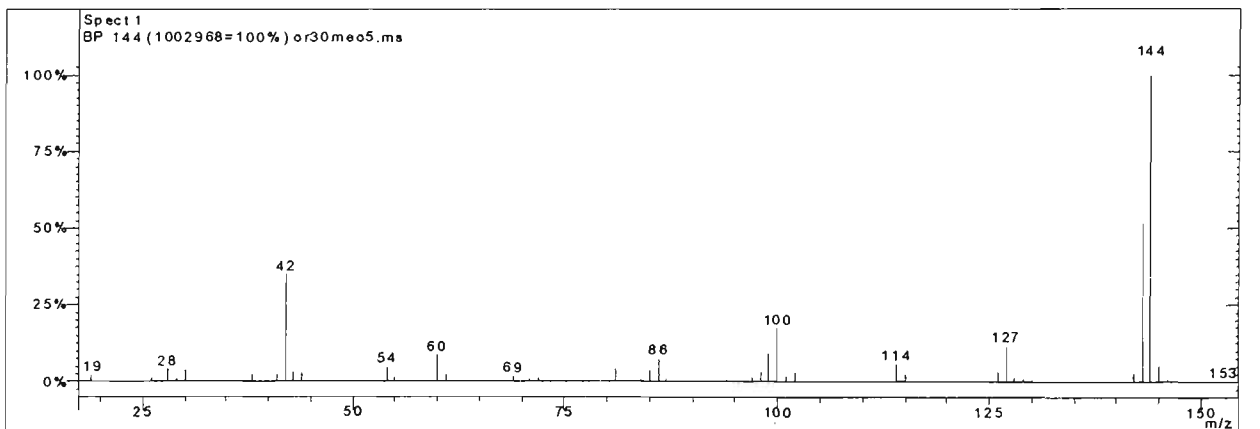
Peak 9 From sultana MeOH extract (top) and arginine-glucose model MeOH extract (bottom)



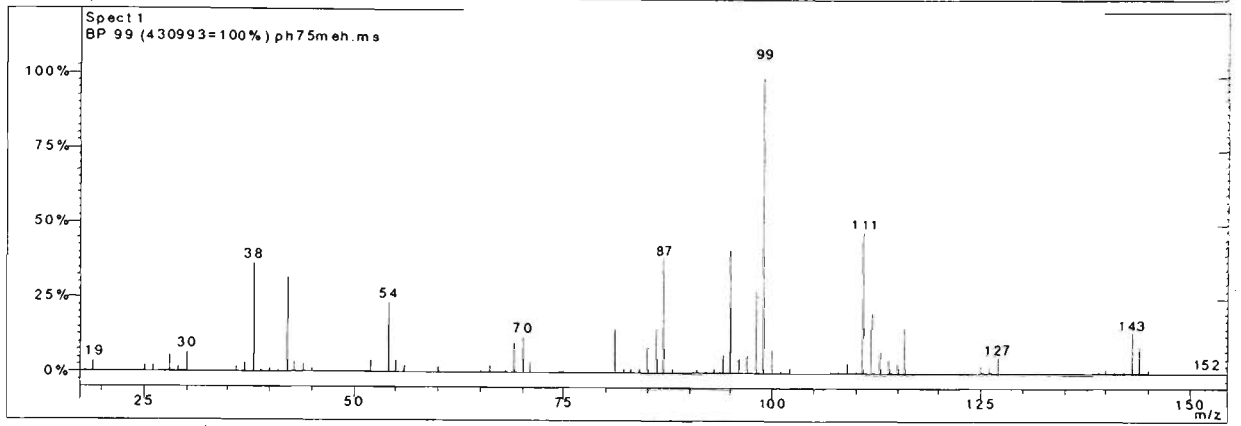
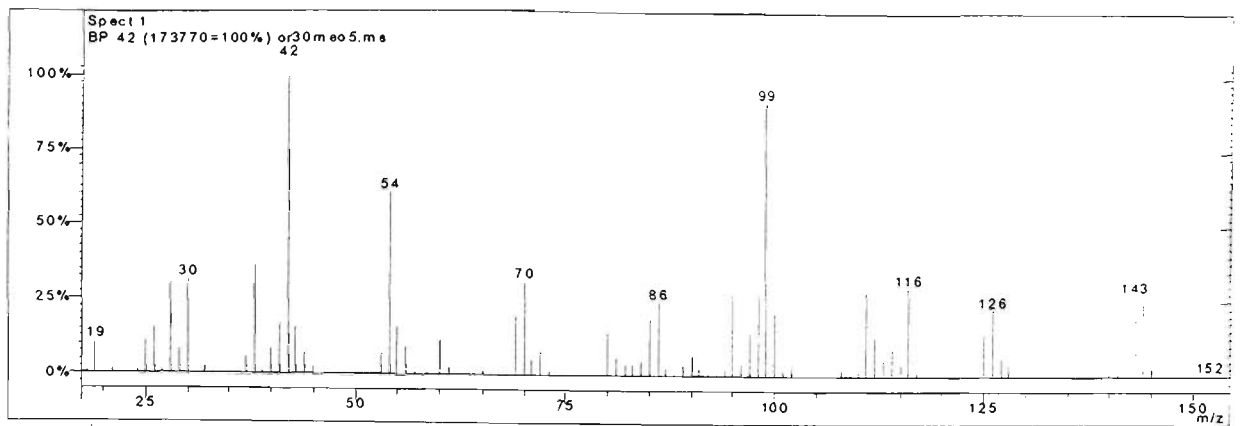
Peak 10 From sultana MeOH extract (top) and arginine-glucose model MeOH extract (bottom)



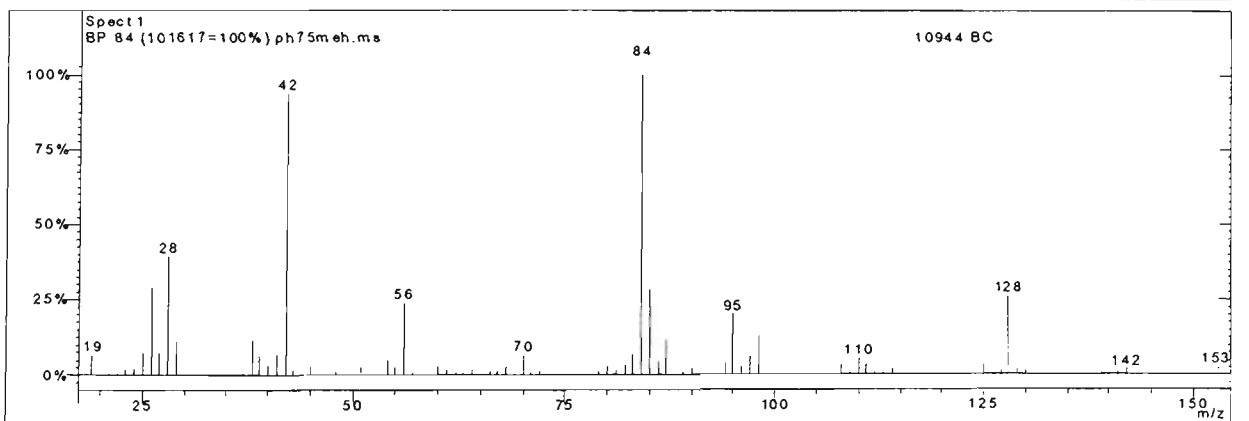
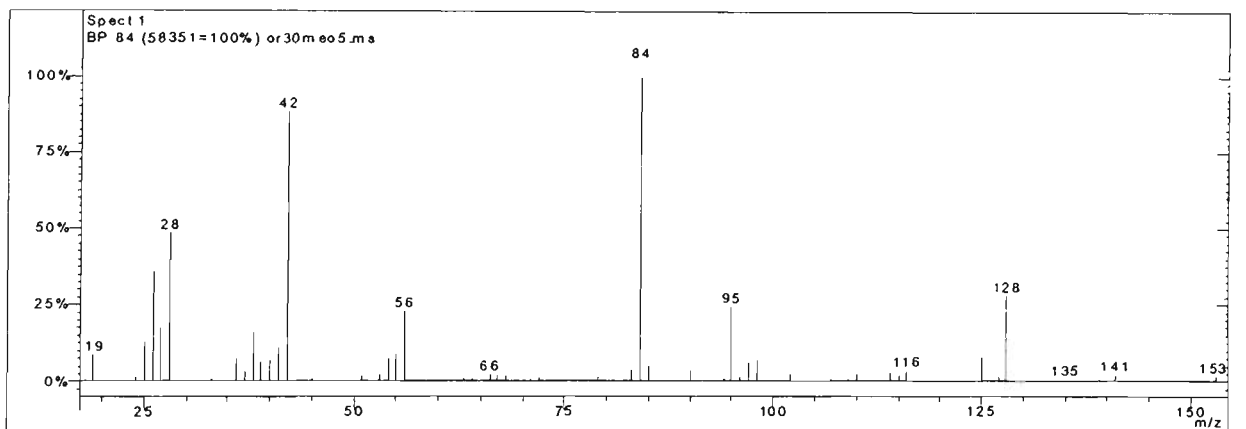
Peak 11 From sultana MeOH extract (top) and arginine-glucose model MeOH extract (bottom)



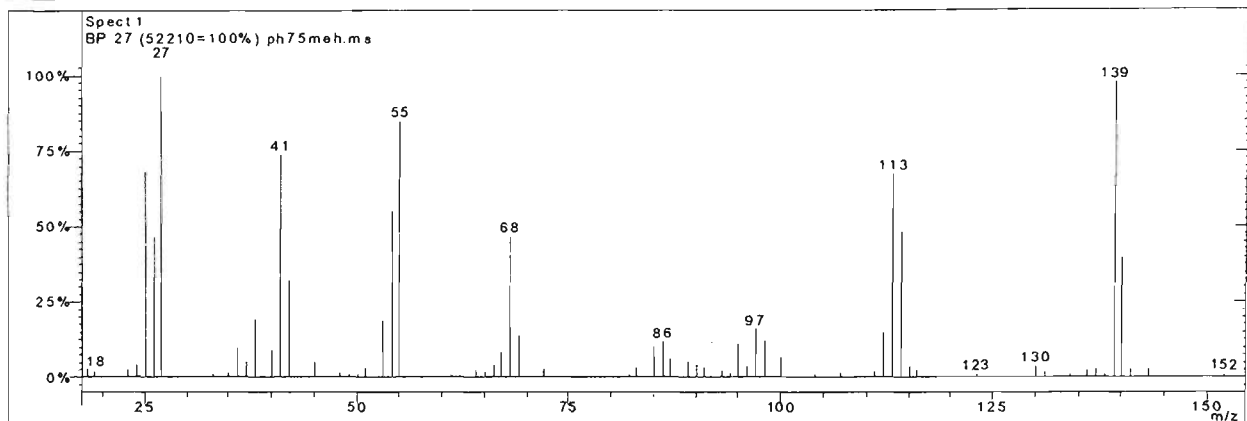
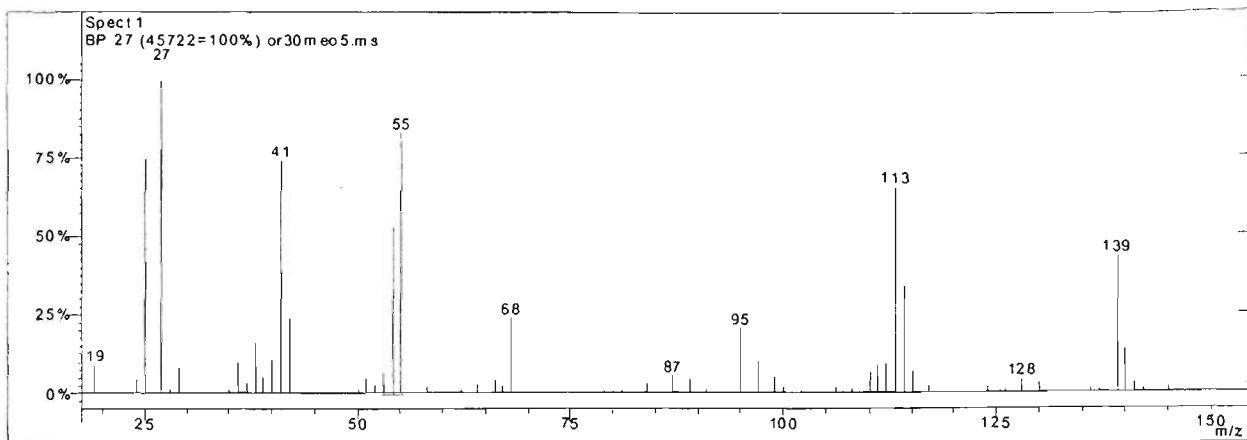
Peak 12 From sultana MeOH extract (top) and arginine-glucose model MeOH extract (bottom)



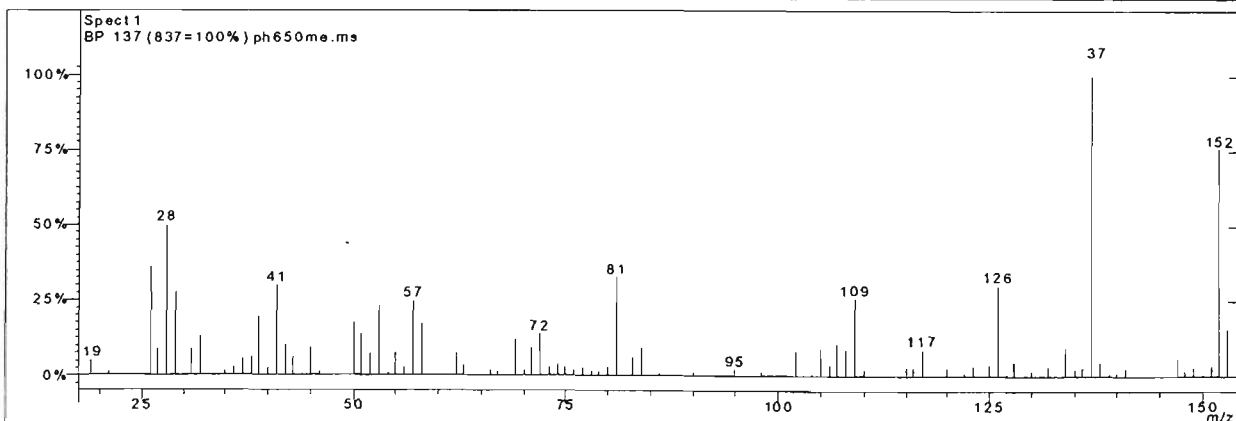
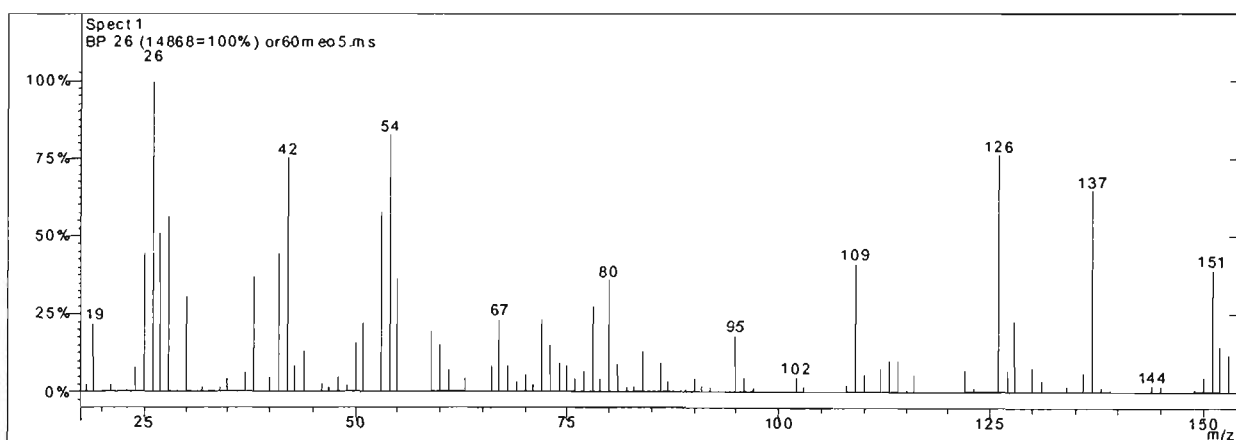
Peak 13 From sultana MeOH extract (top) and arginine-glucose model MeOH extract (bottom)



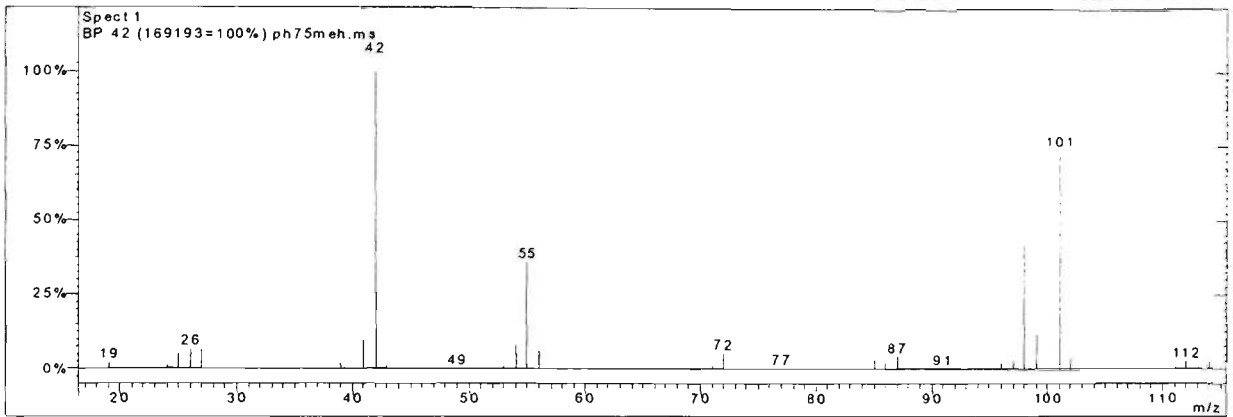
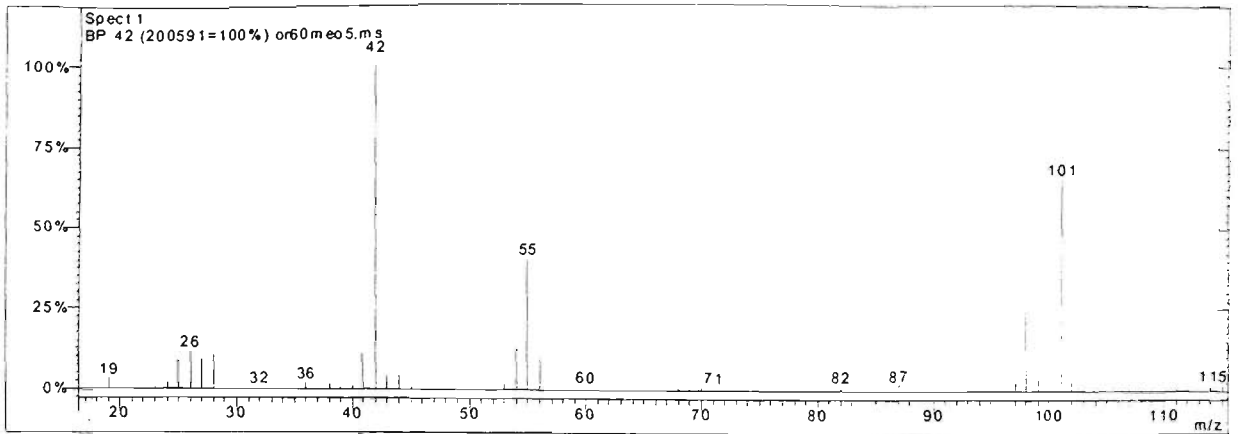
Peak 14 From sultana MeOH extract (top) and arginine-glucose model MeOH extract (bottom)



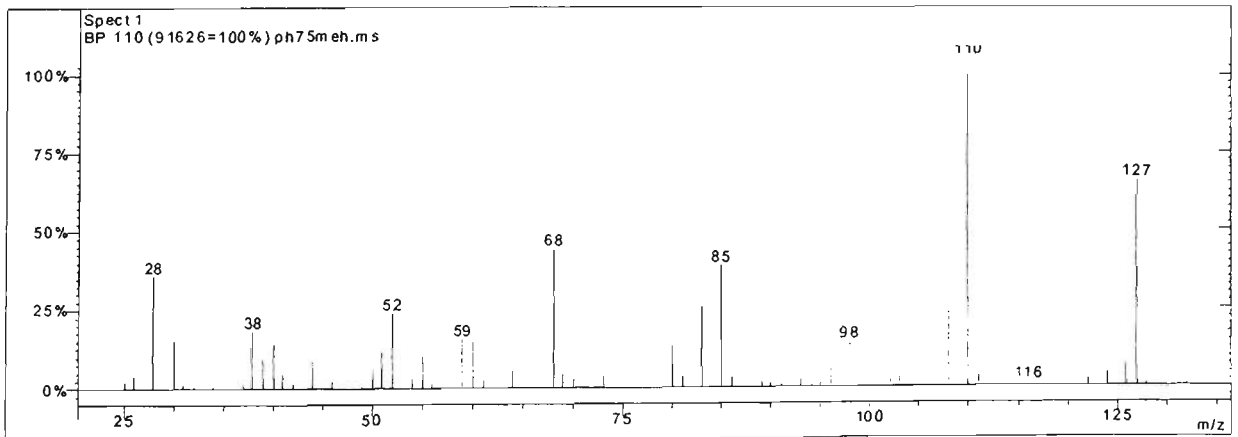
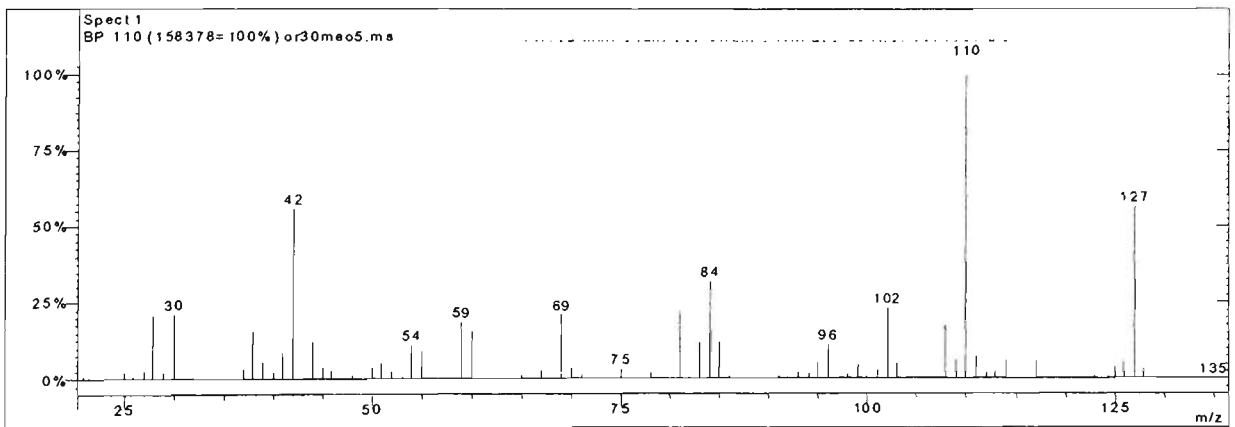
Peak 15 From sultana MeOH extract (top) and arginine-glucose model MeOH extract (bottom)



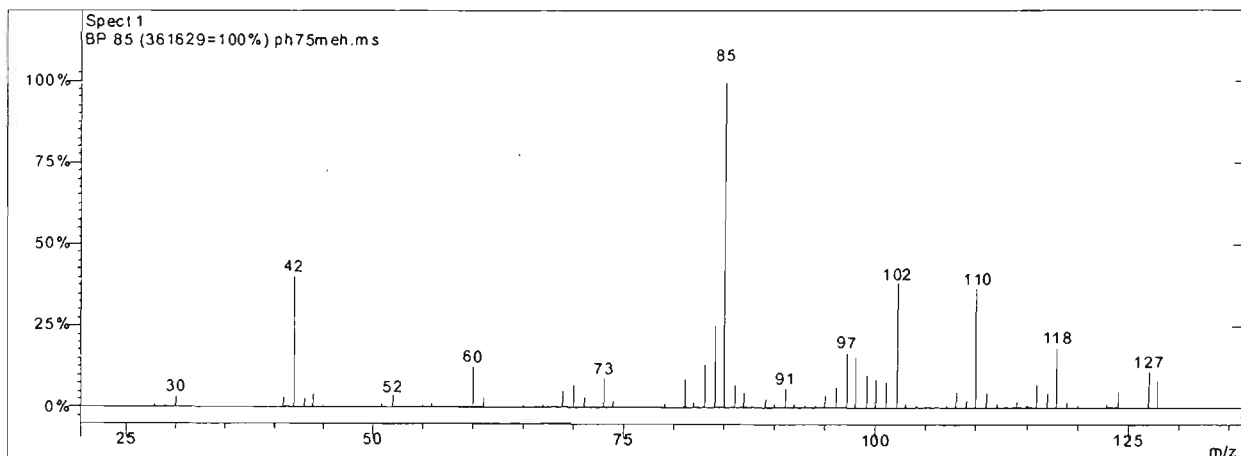
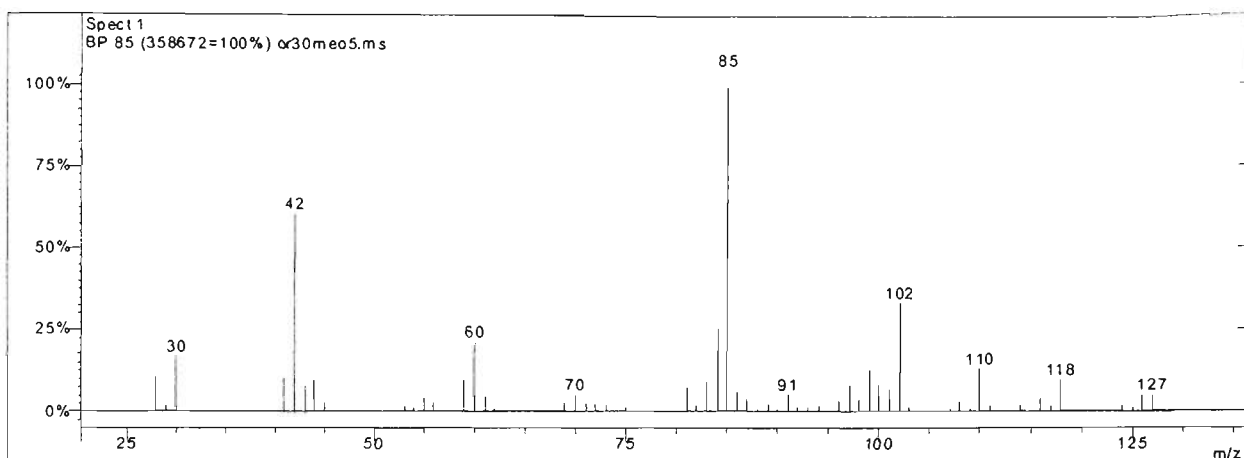
Peak 16 From sultana MeOH extract (top) and arginine-glucose model MeOH extract (bottom)



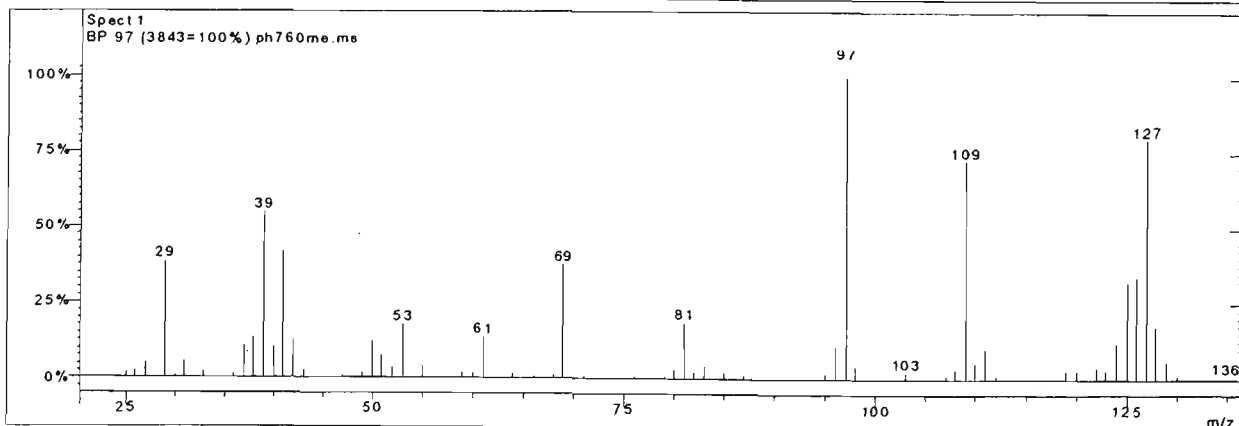
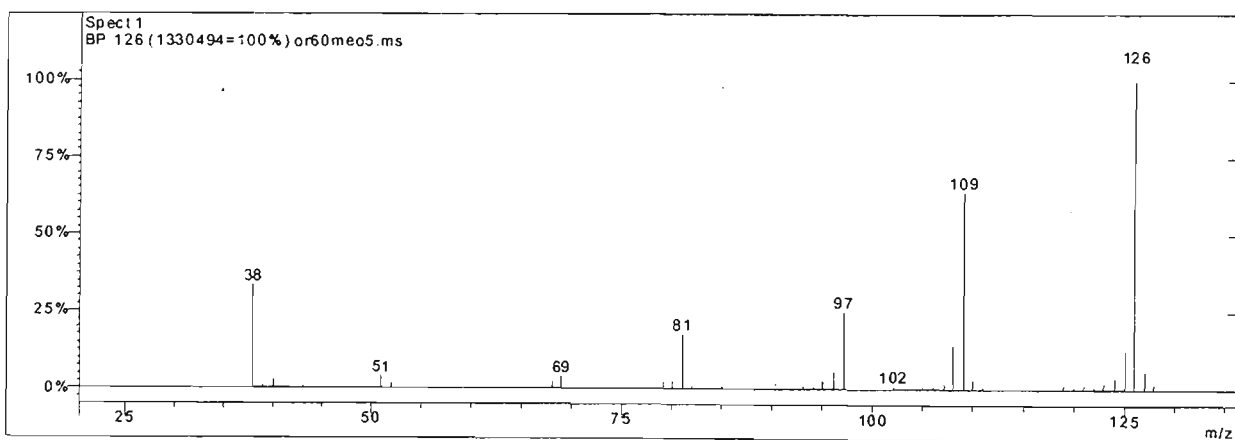
Peak 17 From sultana MeOH extract (top) and arginine-glucose model MeOH extract (bottom)



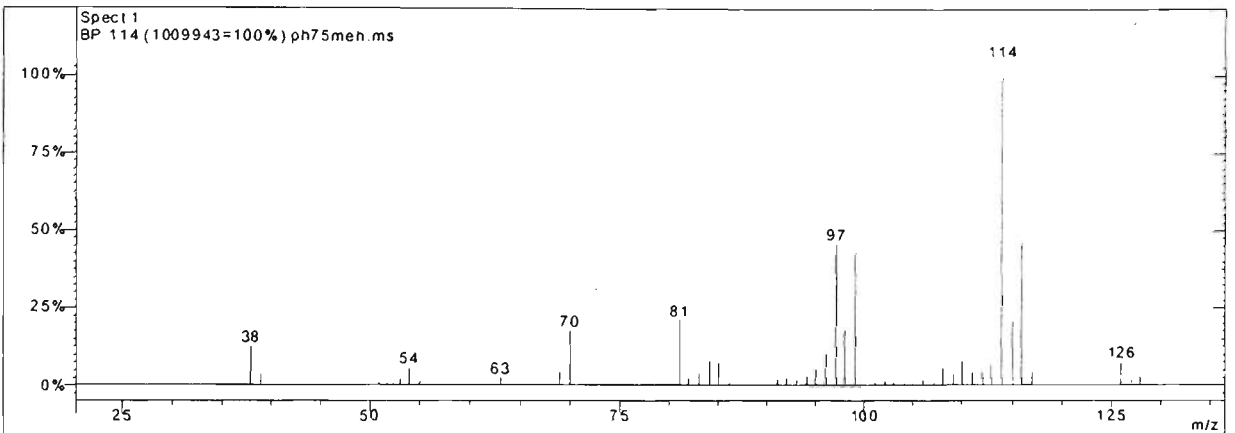
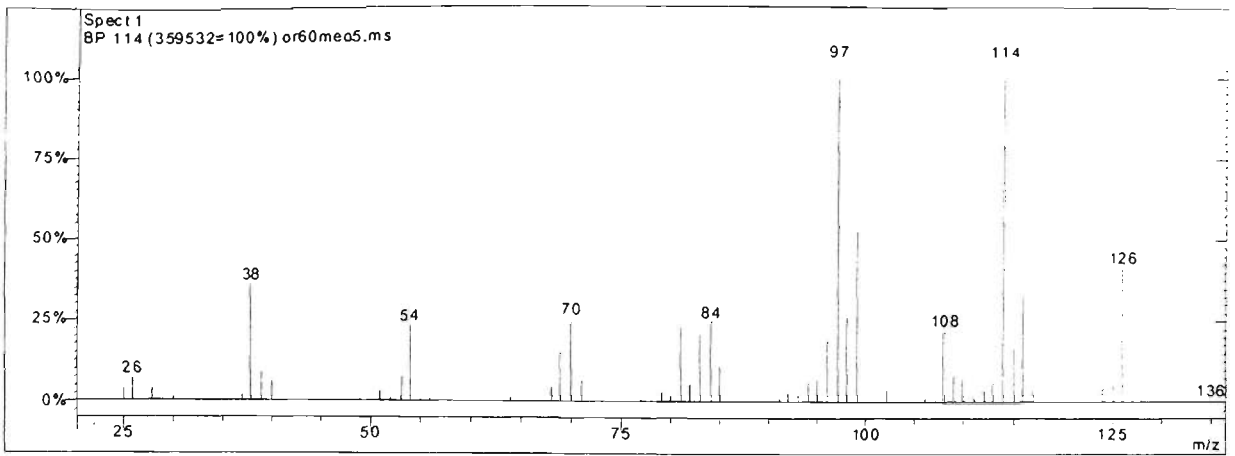
Peak 18 From sultana MeOH extract (top) and arginine-glucose model MeOH extract (bottom)



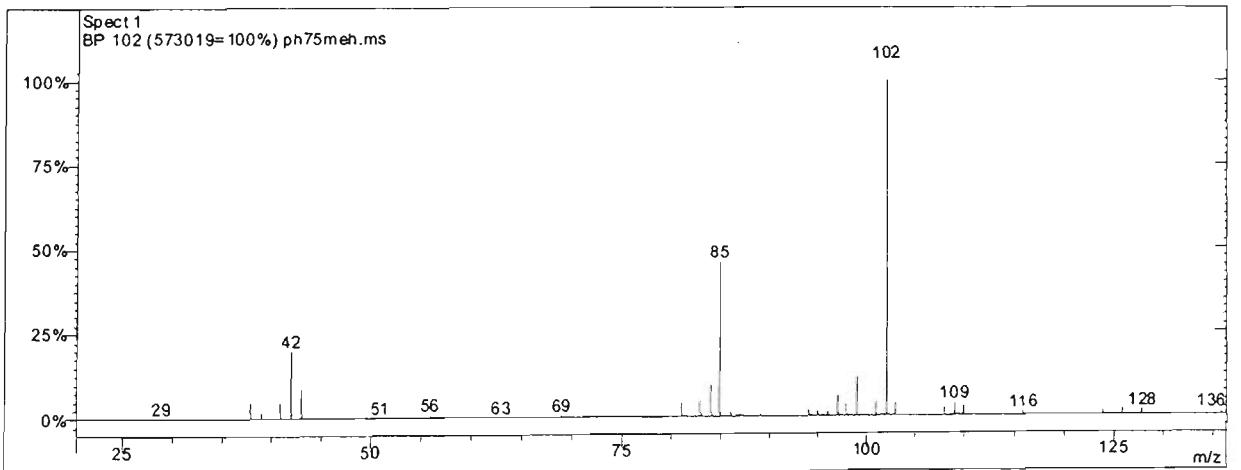
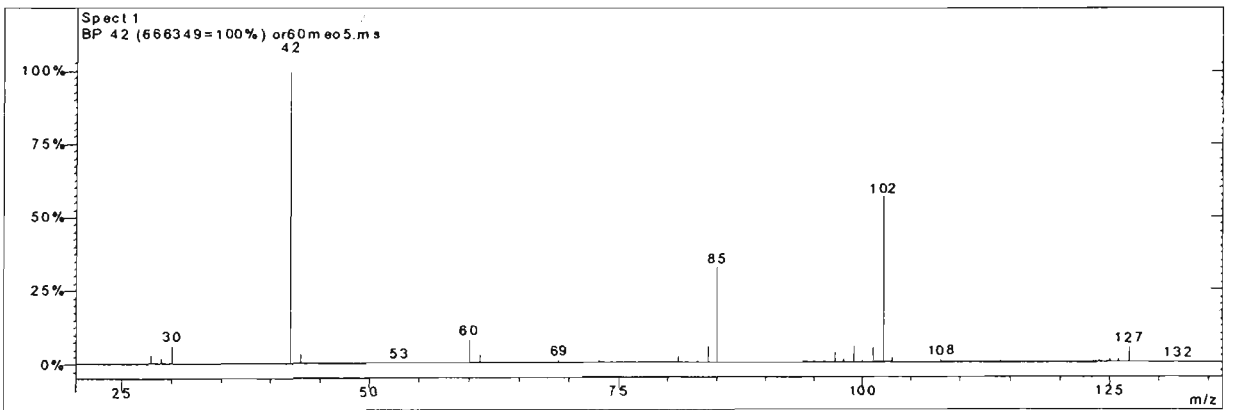
Peak 19 From sultana MeOH extract (top) and arginine-glucose model MeOH extract (bottom)



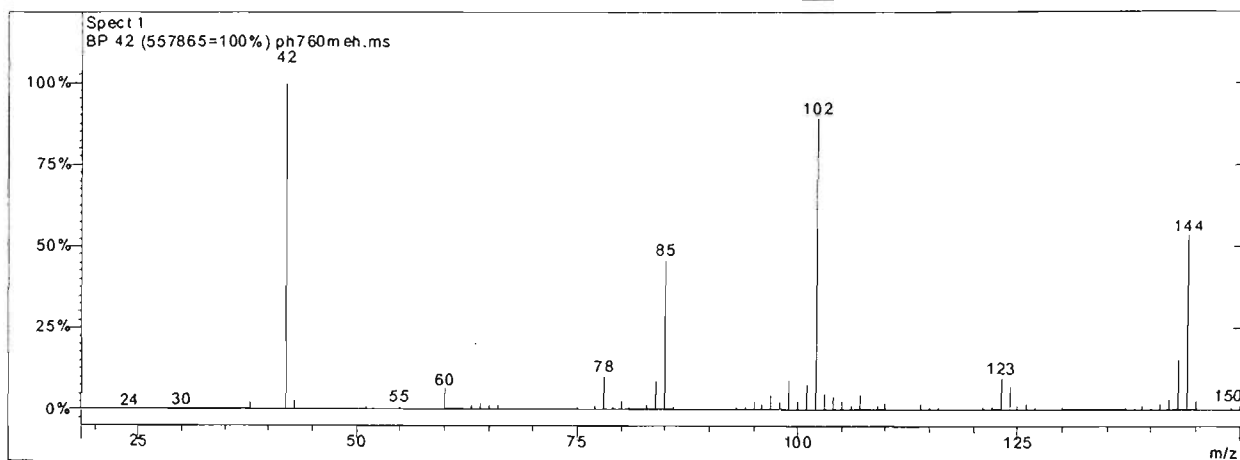
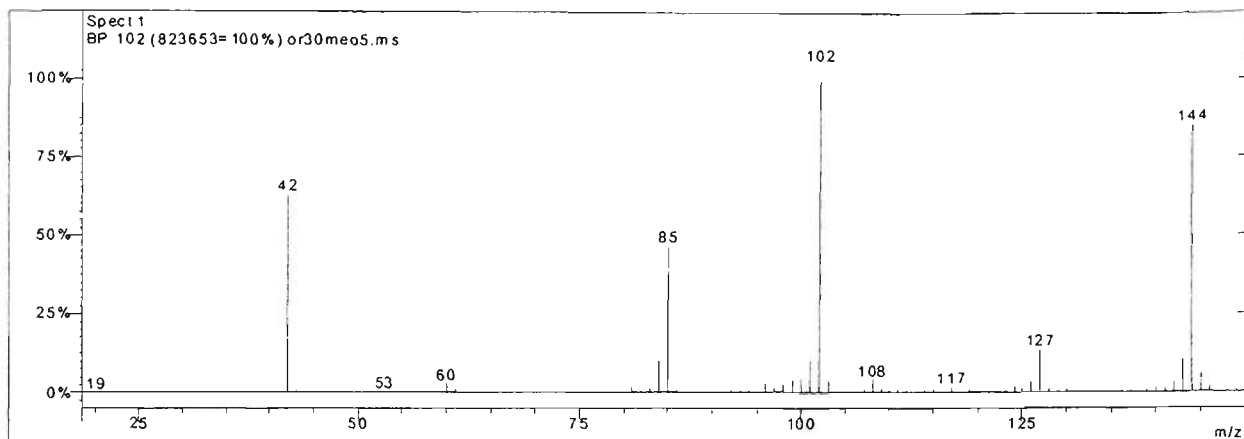
Peak 20 From sultana MeOH extract (top) and arginine-glucose model MeOH extract (bottom)



Peak 21 From sultana MeOH extract (top) and arginine-glucose model MeOH extract (bottom)

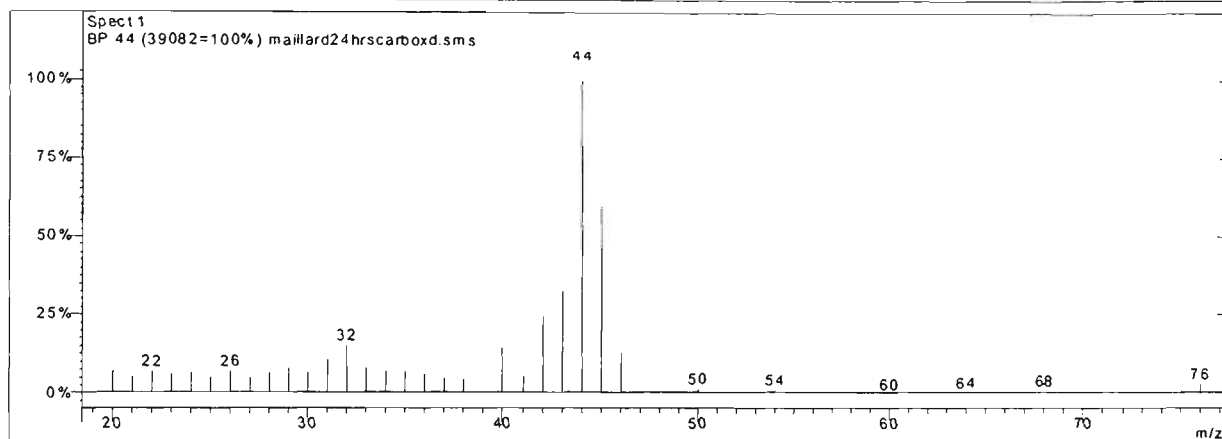
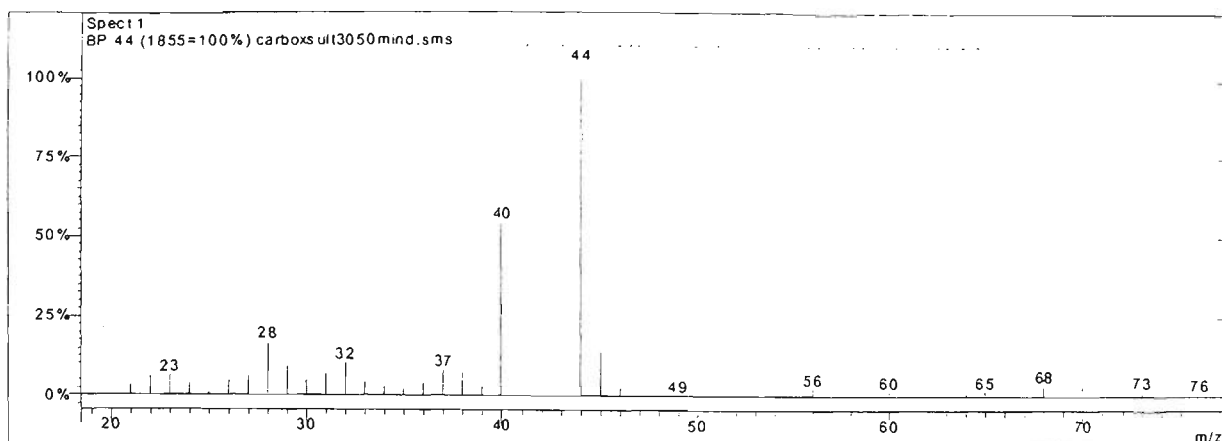


Peak 22 From sultana MeOH extract (top) and arginine-glucose model MeOH extract (bottom)

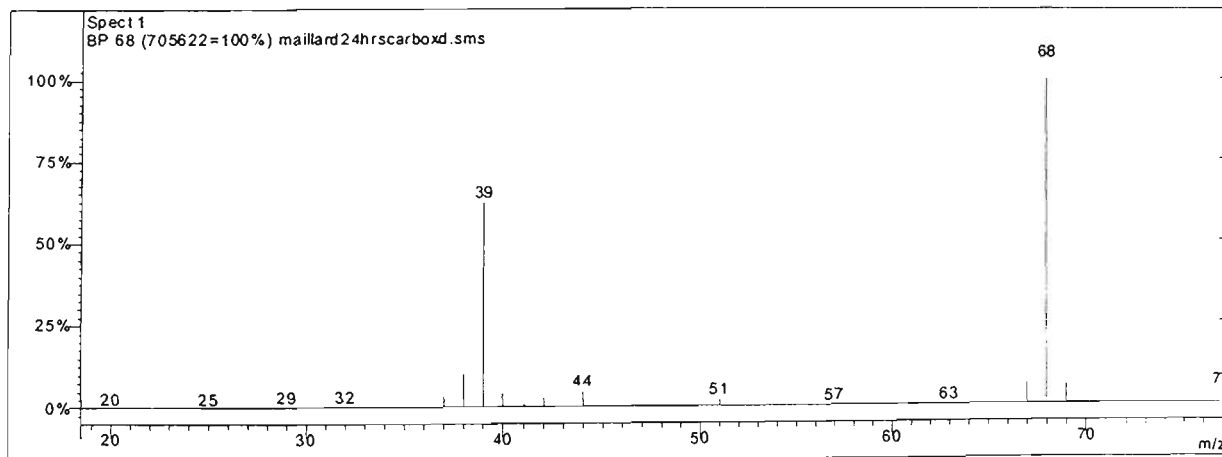
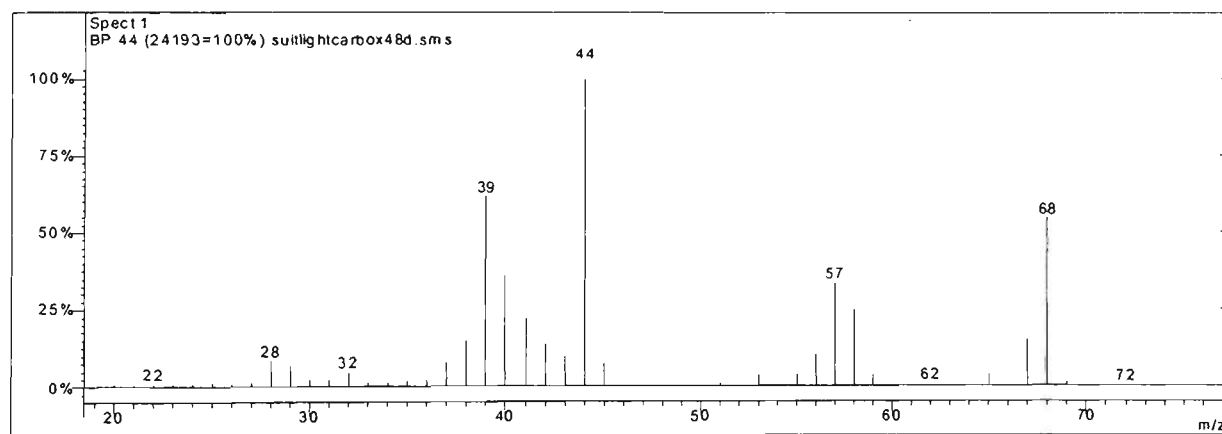


Peak 23 From sultana MeOH extract (top) and arginine-glucose model MeOH extract (bottom)

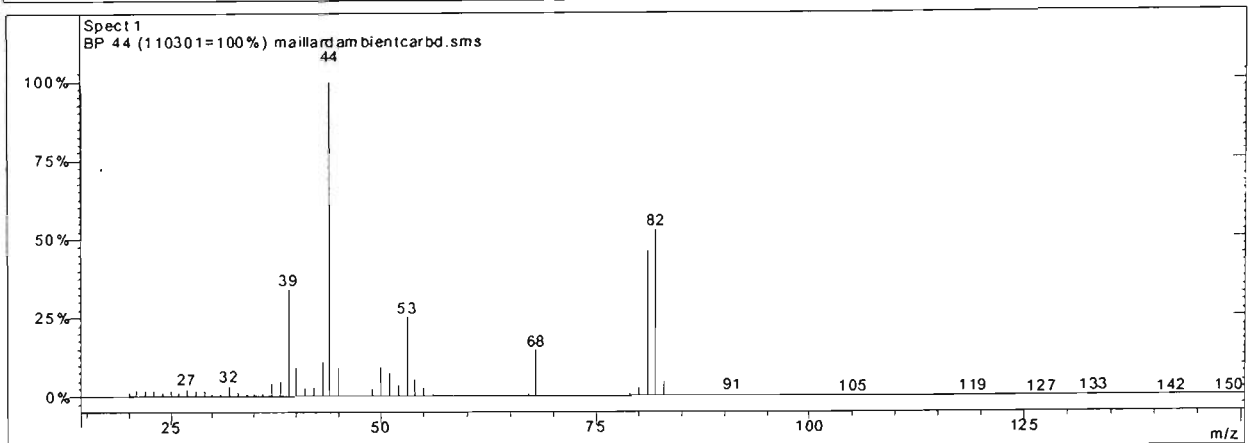
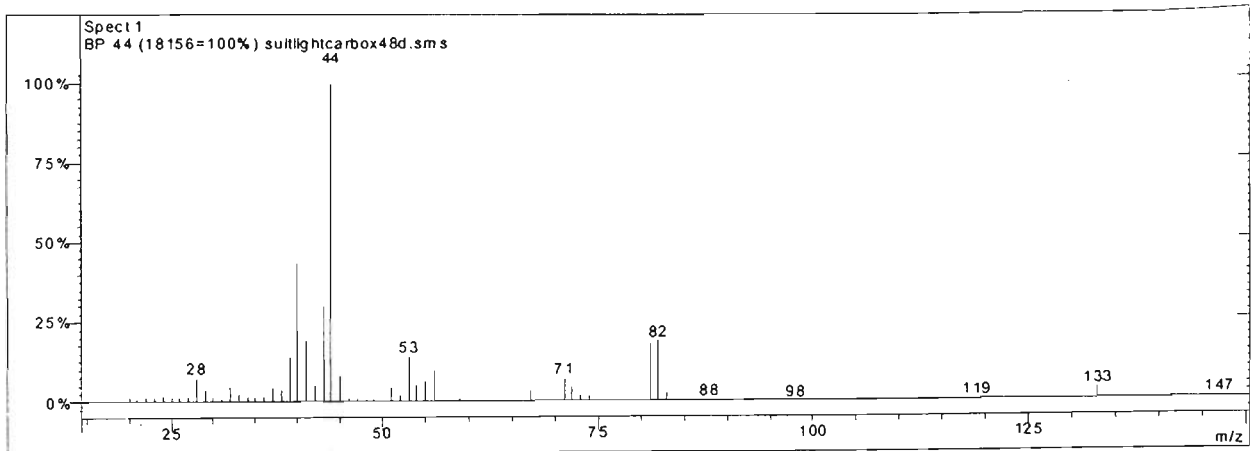
# SPME spectra



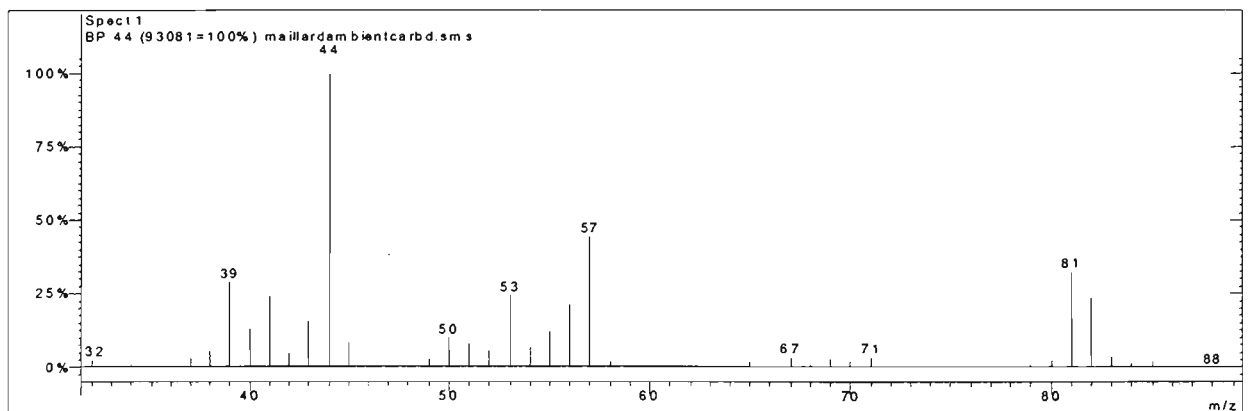
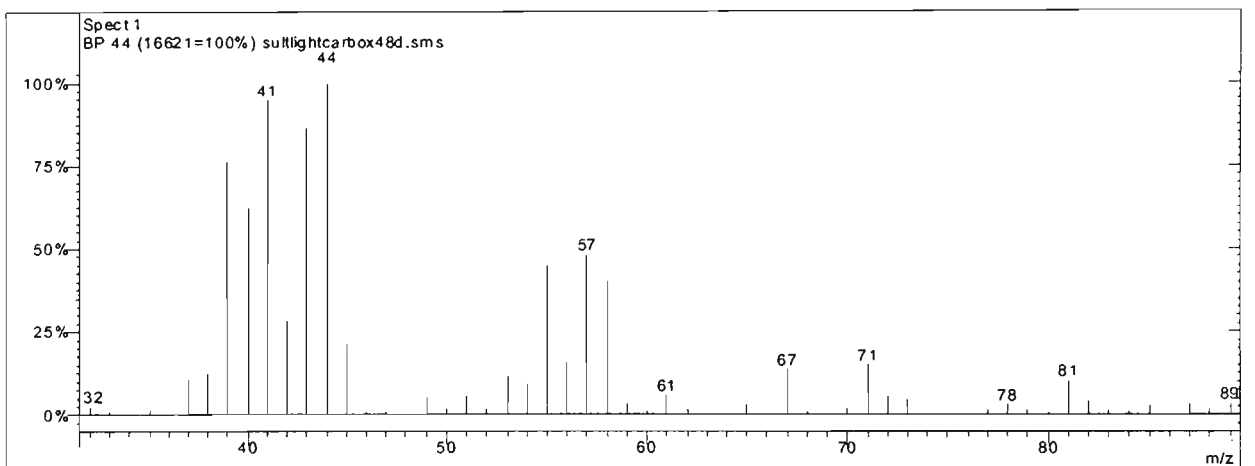
Peak 1 From Carboxen fibre sultana (top) and Carboxen fibre model (bottom)



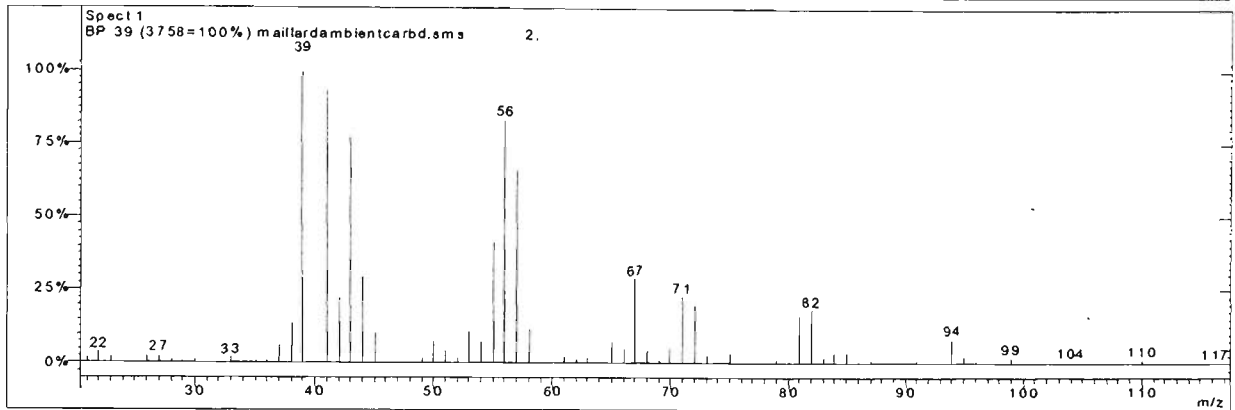
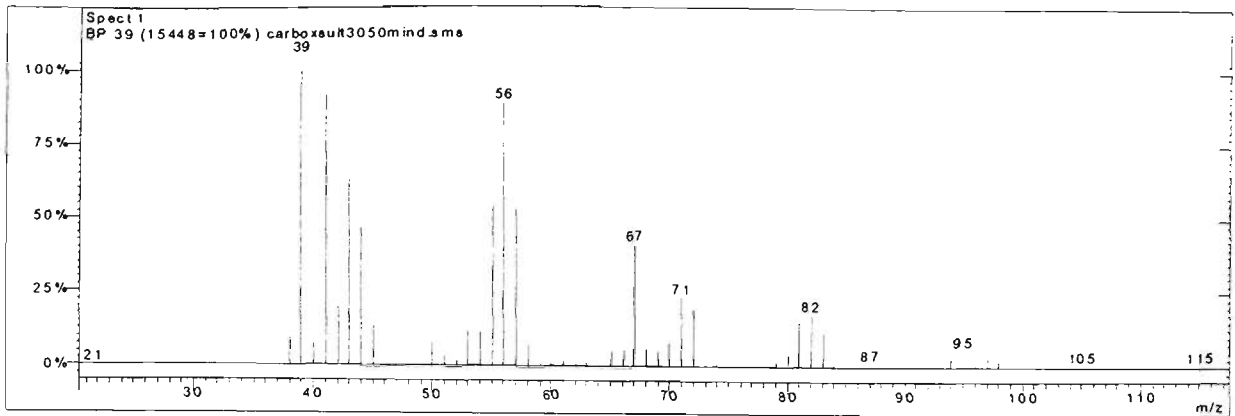
Peak 2 From Carboxen fibre sultana (top) and Carboxen fibre model (bottom)



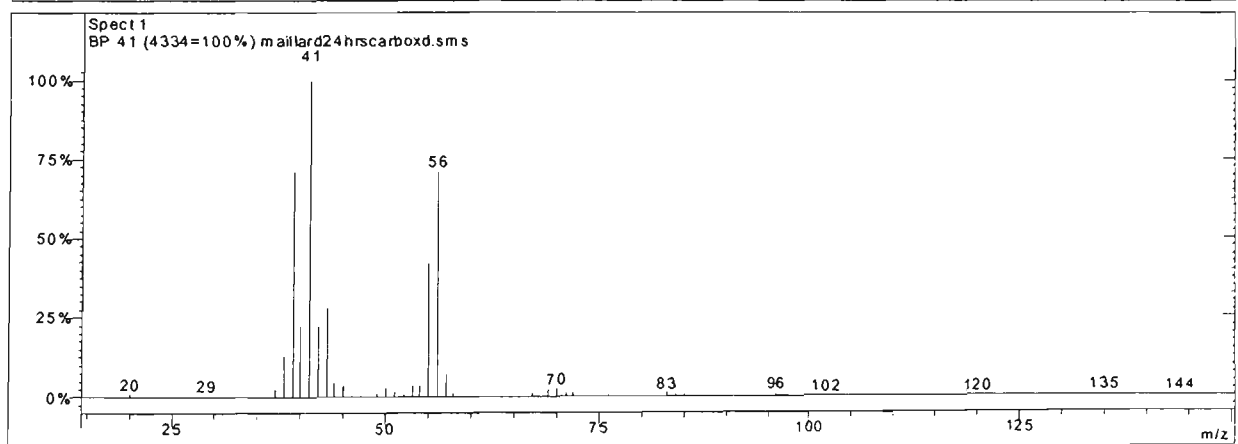
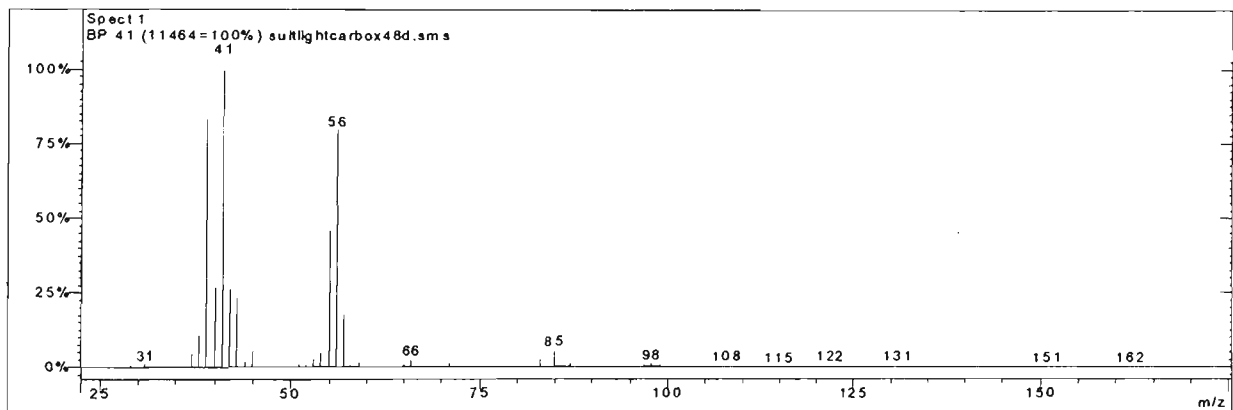
Peak 3 From Carboxen fibre sultana (top) and Carboxen fibre model (bottom)



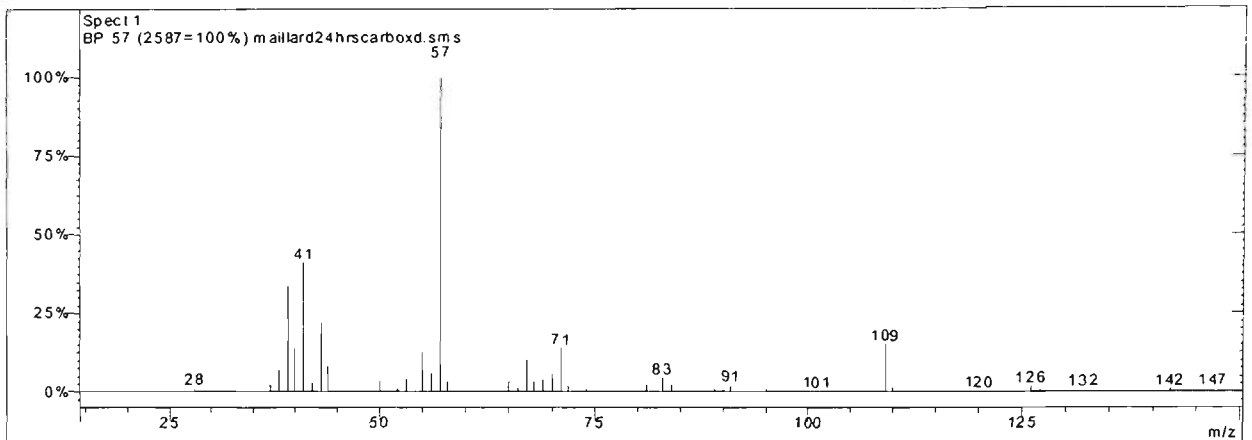
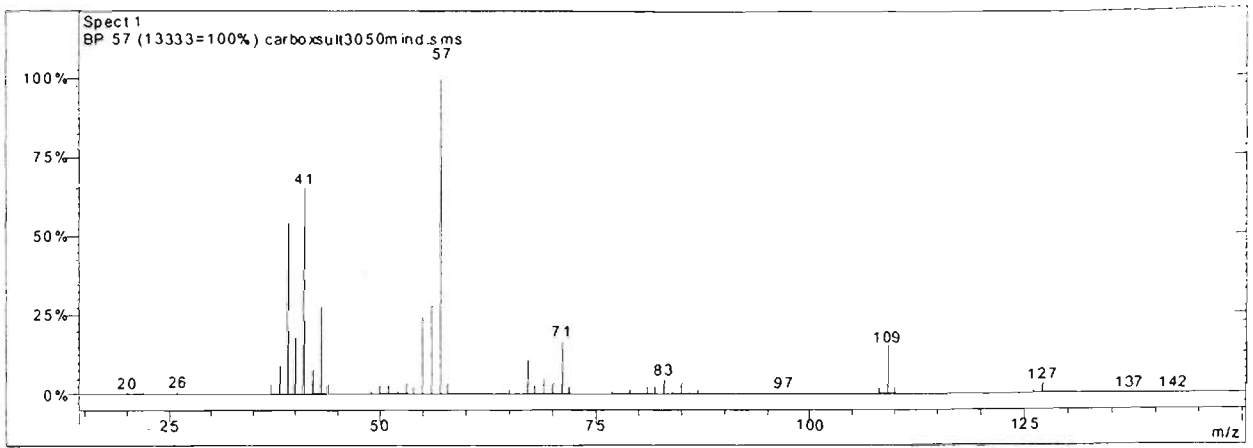
Peak 5 From Carboxen fibre sultana (top) and Carboxen fibre model (bottom)



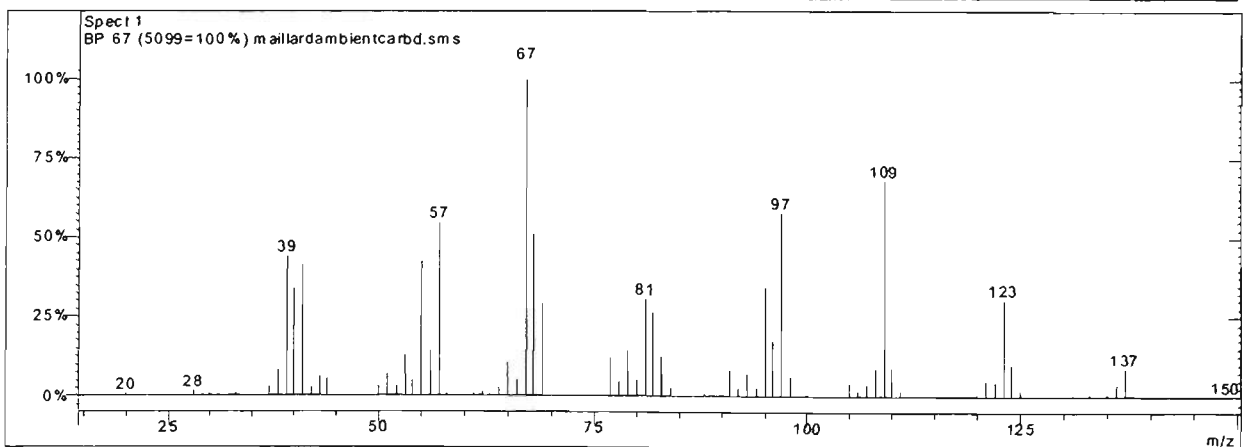
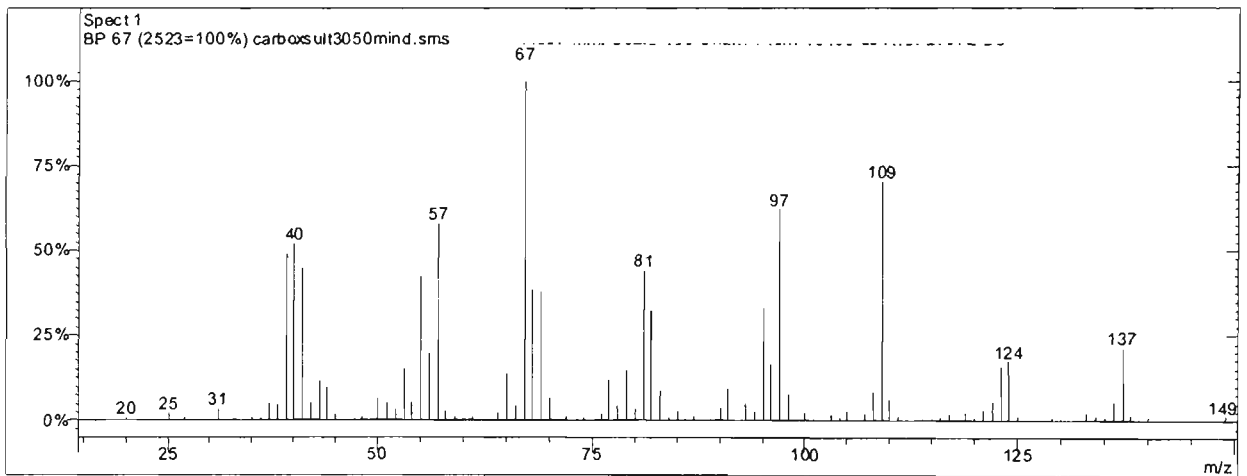
Peak 6 From Carboxen fibre sultana (top) and Carboxen fibre model (bottom)



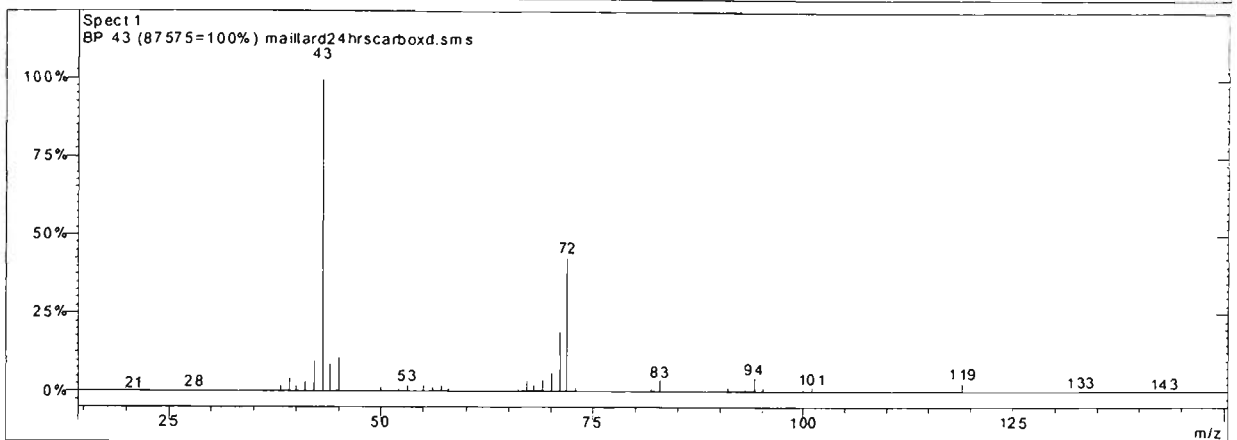
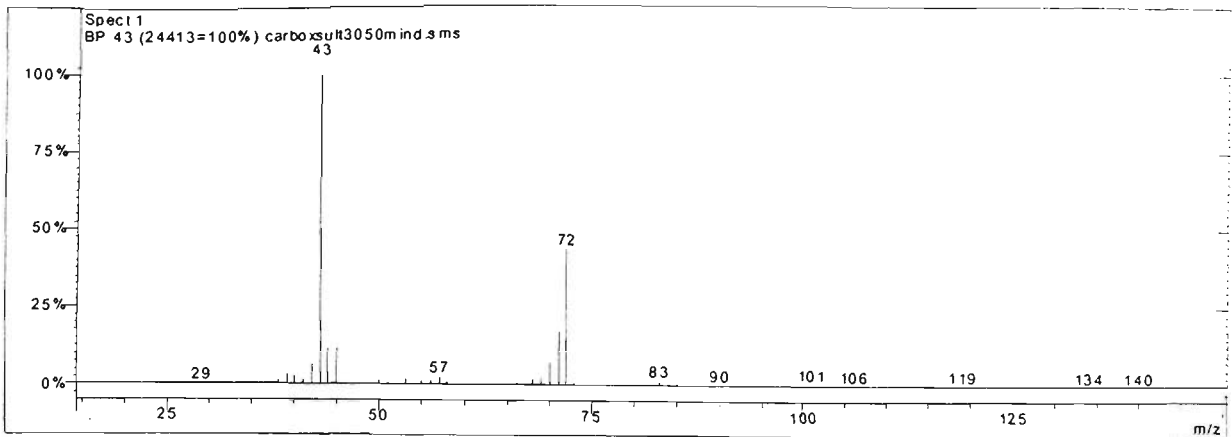
Peak 7 From Carboxen fibre sultana (top) and Carboxen fibre model (bottom)



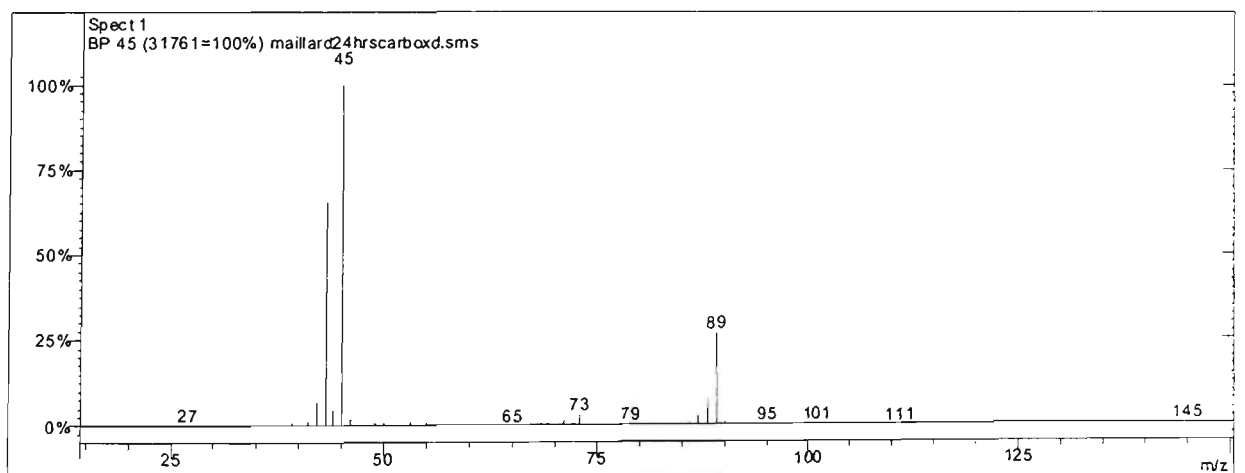
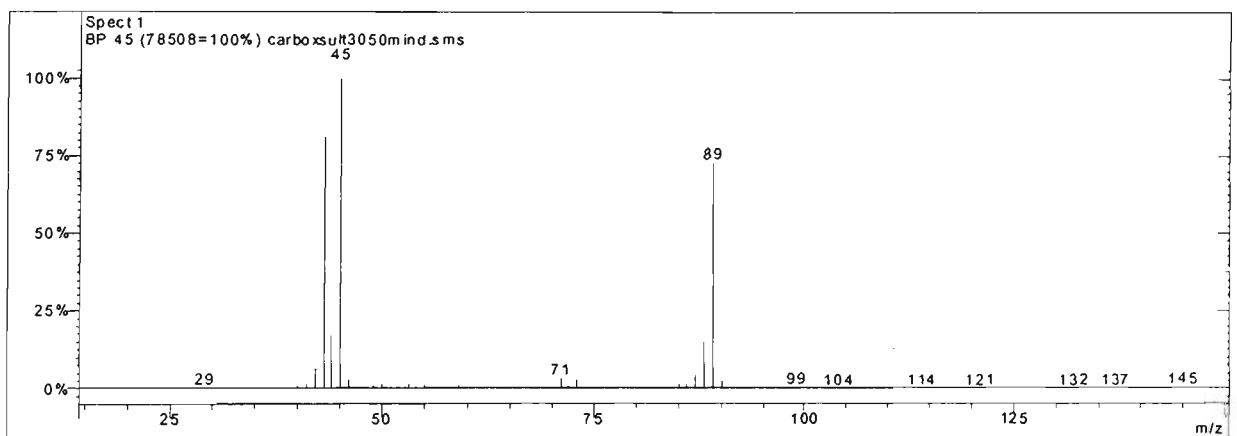
Peak 8 From Carboxen fibre sultana (top) and Carboxen fibre model (bottom)



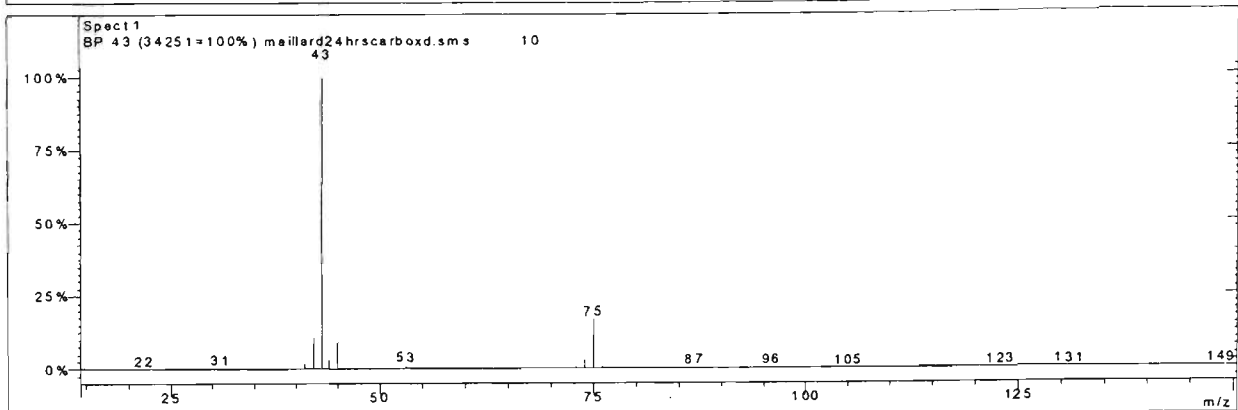
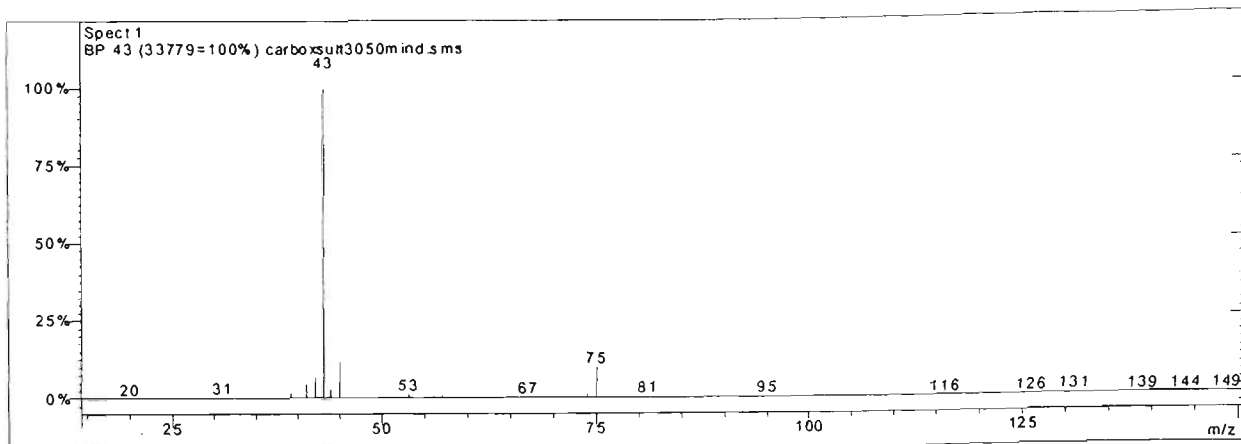
Peak 9 From Carboxen fibre sultana (top) and Carboxen fibre model (bottom)



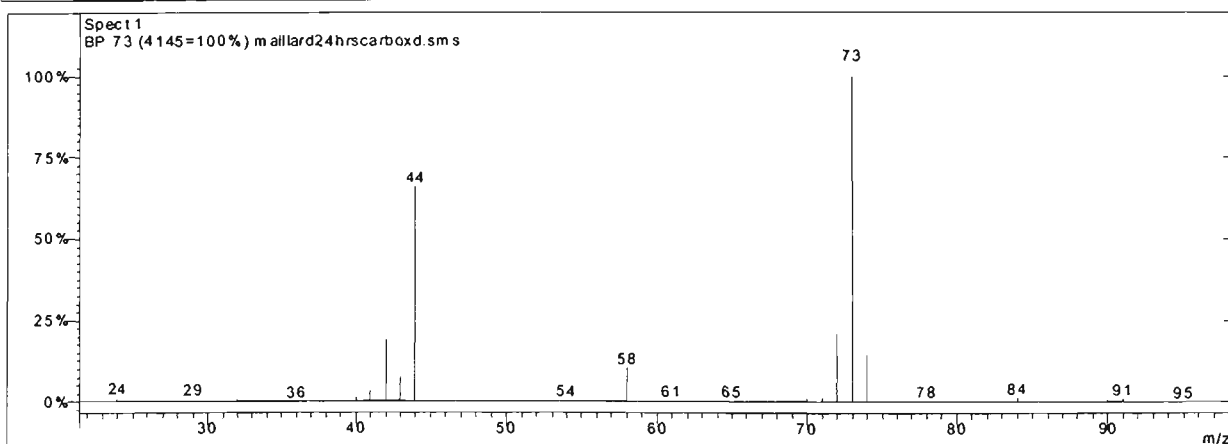
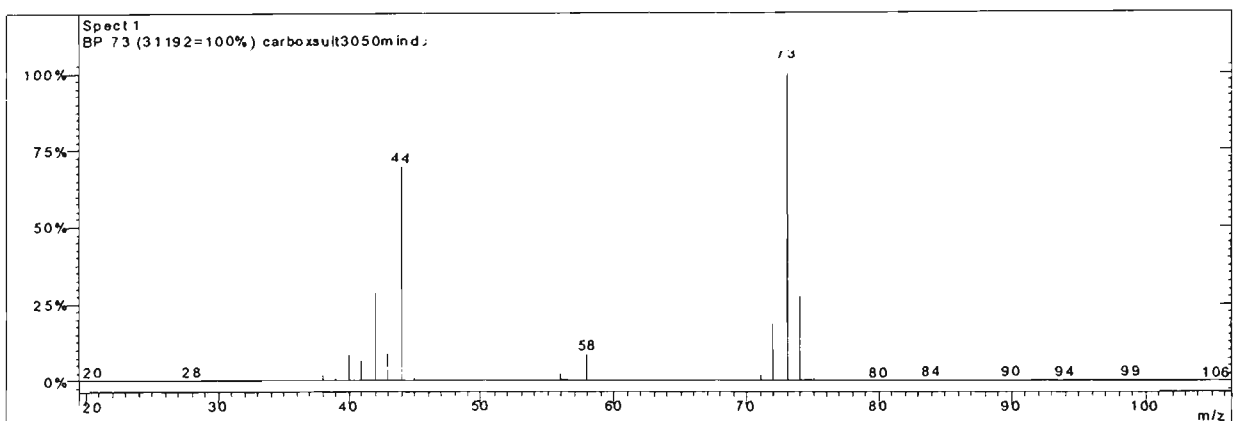
Peak 10 From Carboxen fibre sultana (top) and Carboxen fibre model (bottom)



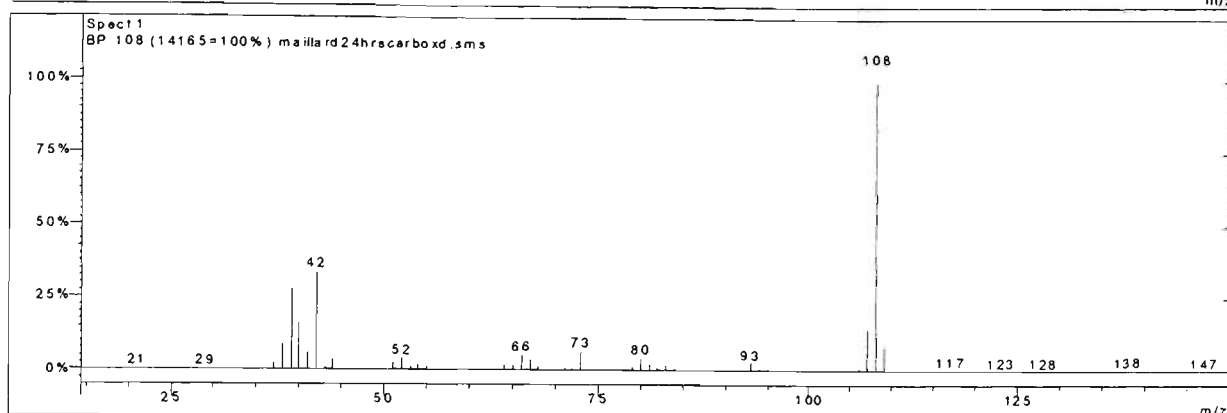
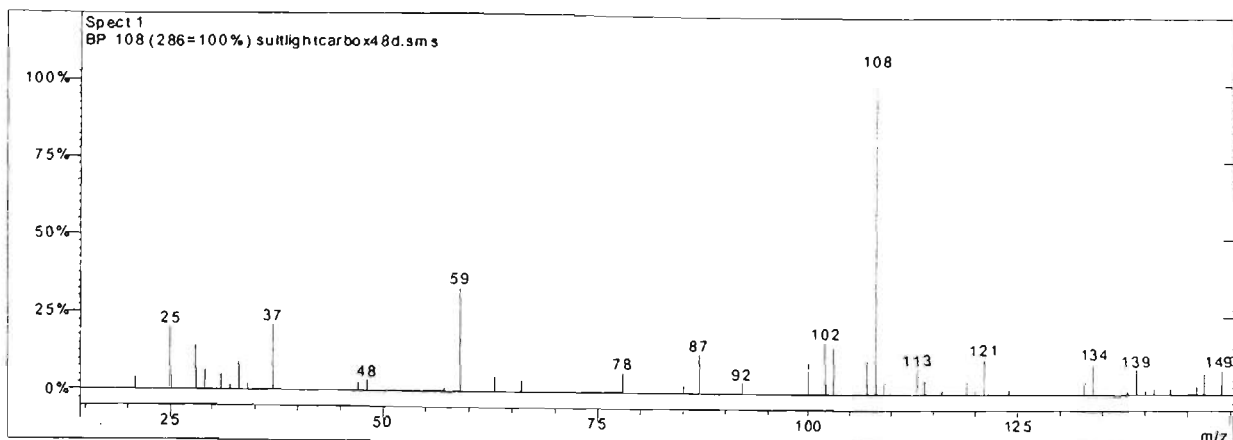
Peak 11 From Carboxen fibre sultana (top) and Carboxen fibre model (bottom)



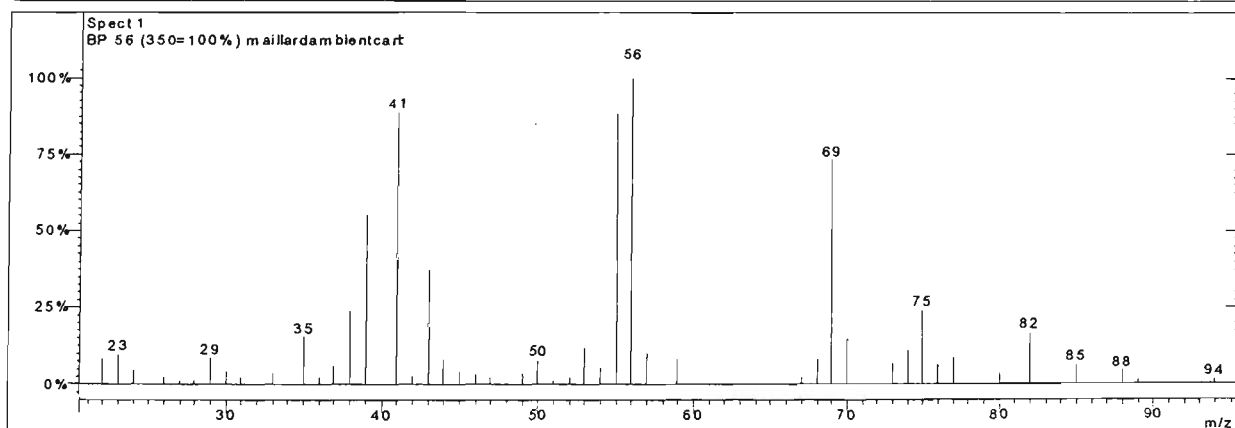
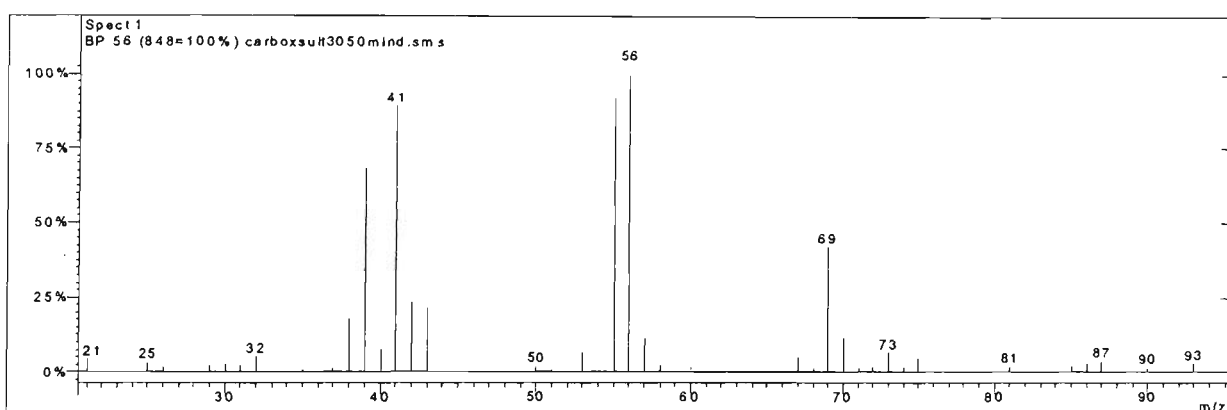
Peak 12 From Carboxen fibre sultana (top) and Carboxen fibre model (bottom)



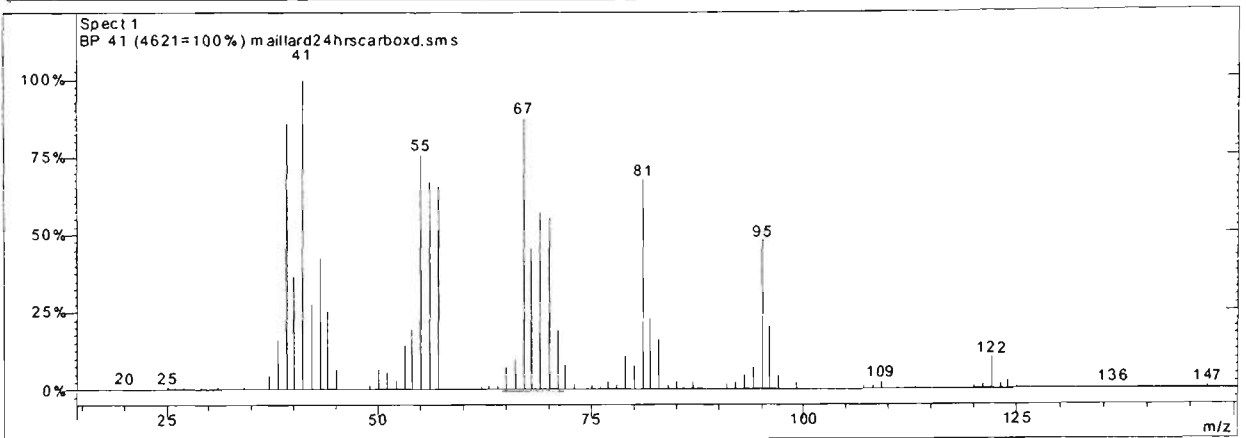
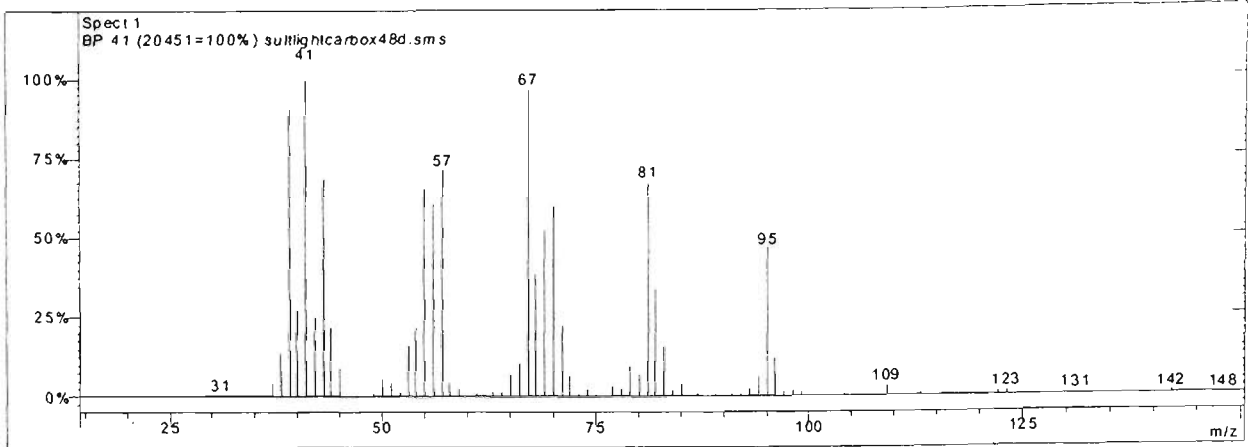
Peak 13 From Carboxen fibre sultana (top) and Carboxen fibre model (bottom)



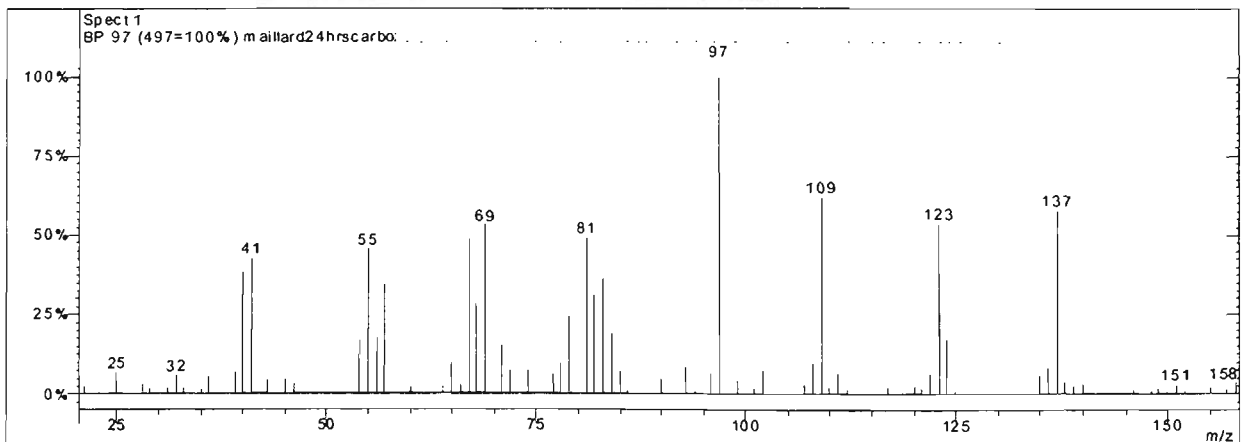
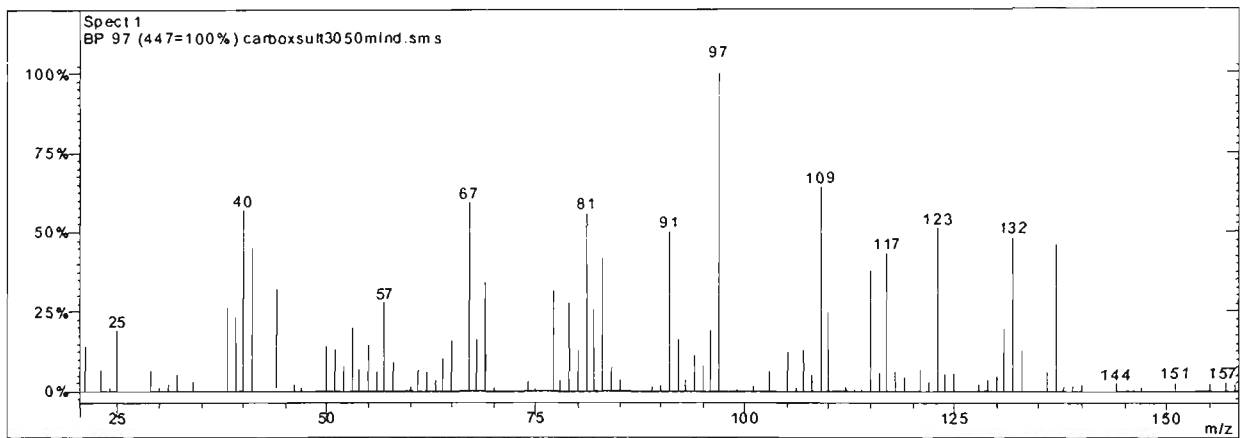
Peak 14 From Carboxen fibre sultana (top) and Carboxen fibre model (bottom)



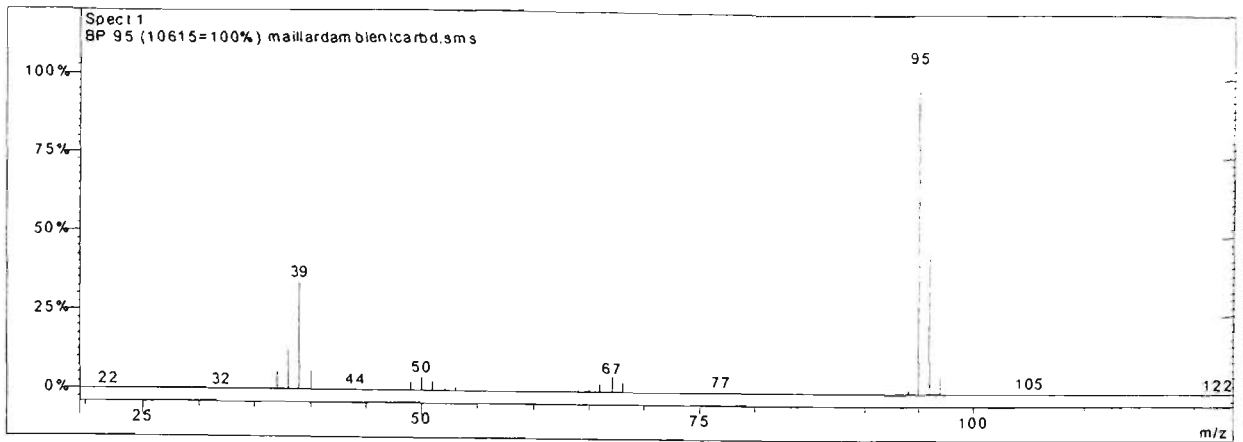
Peak 15 From Carboxen fibre sultana (top) and Carboxen fibre model (bottom)



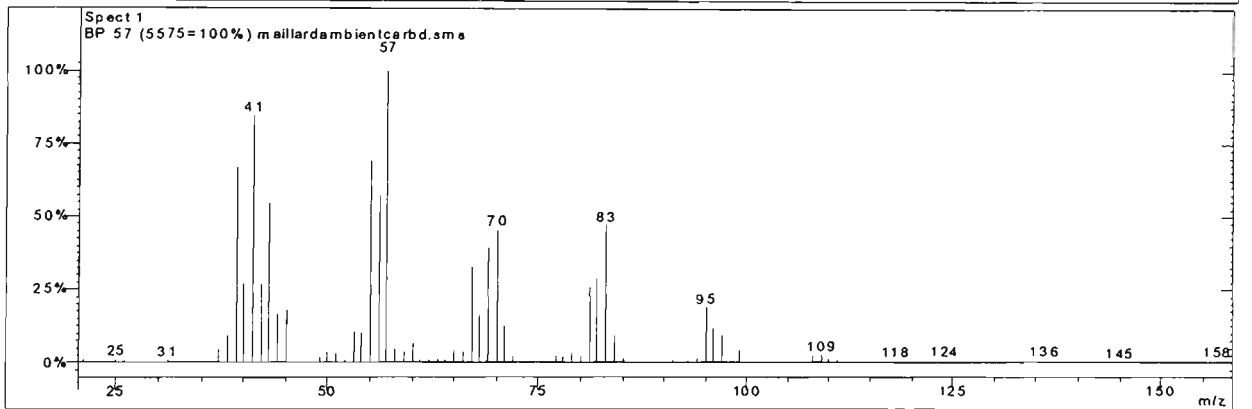
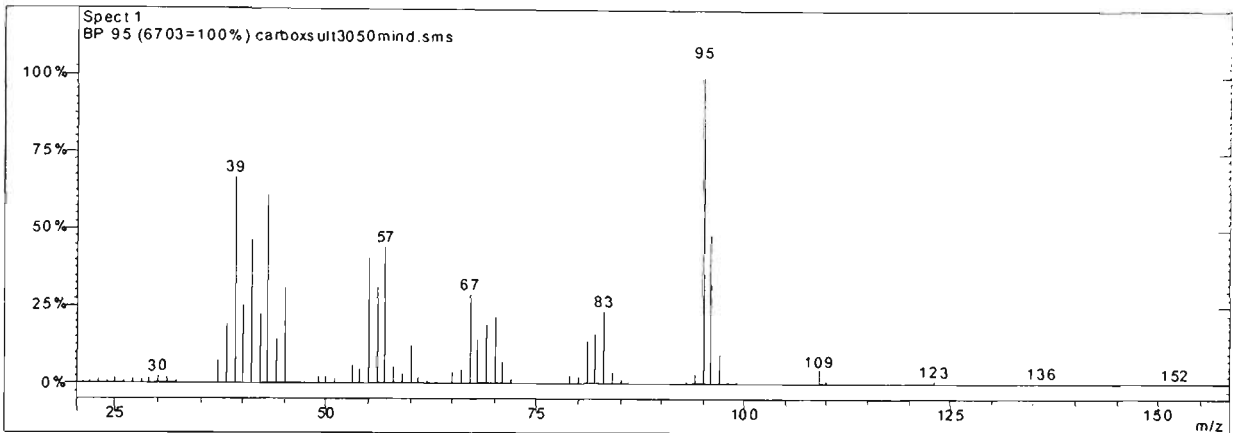
Peak 15 From Carboxen fibre sultana (top) and Carboxen fibre model (bottom)



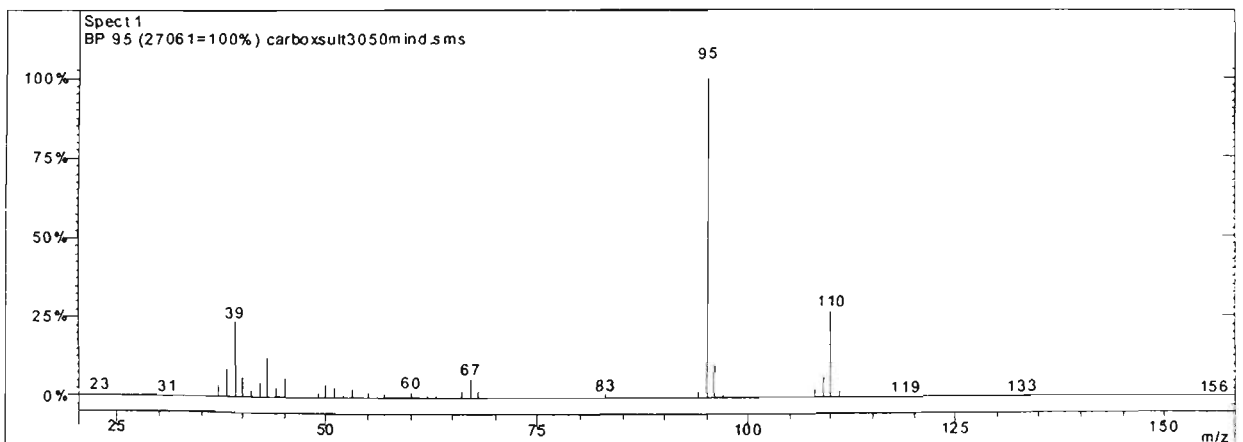
Peak 17 From Carboxen fibre sultana (top) and Carboxen fibre model (bottom)

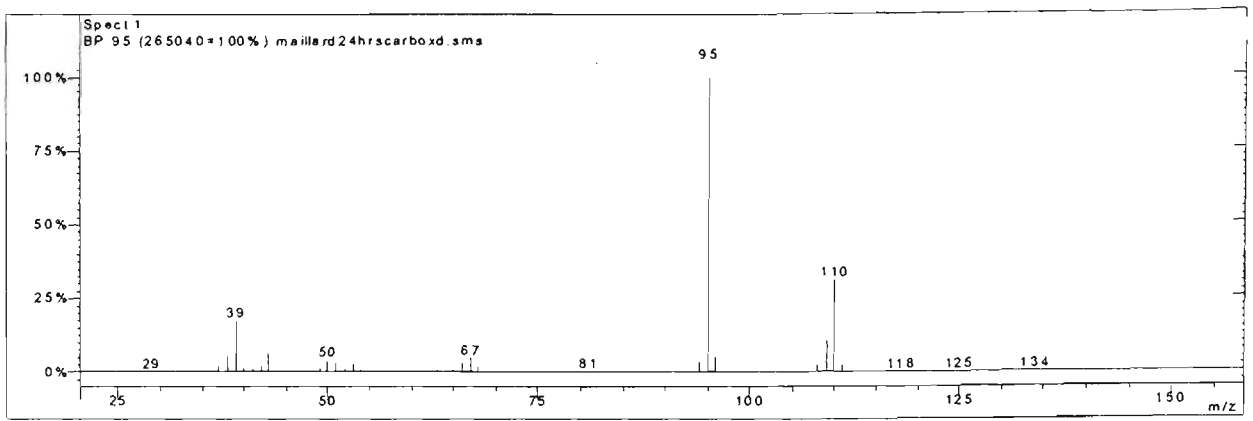


Peak 18 From Carboxen fibre sultana (top) and Carboxen fibre model (bottom)

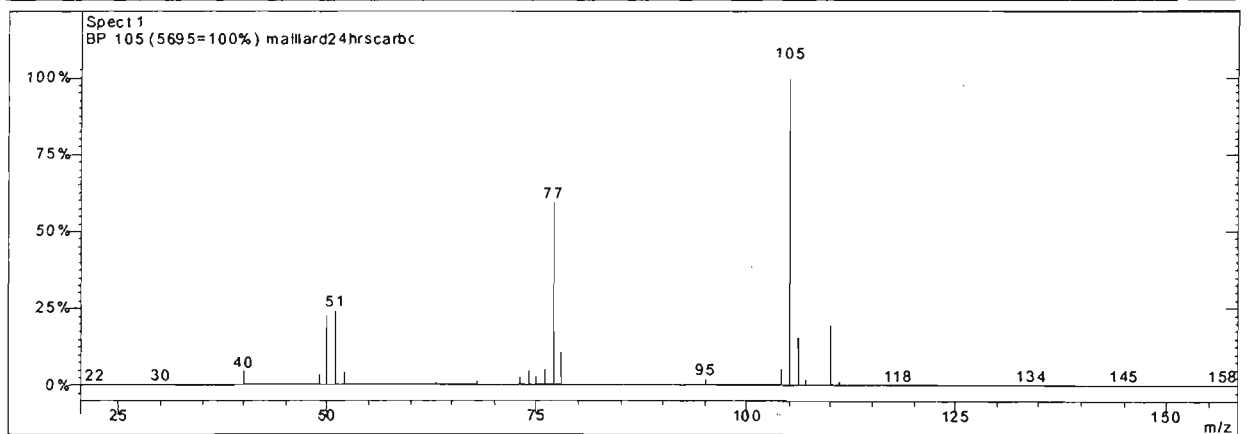
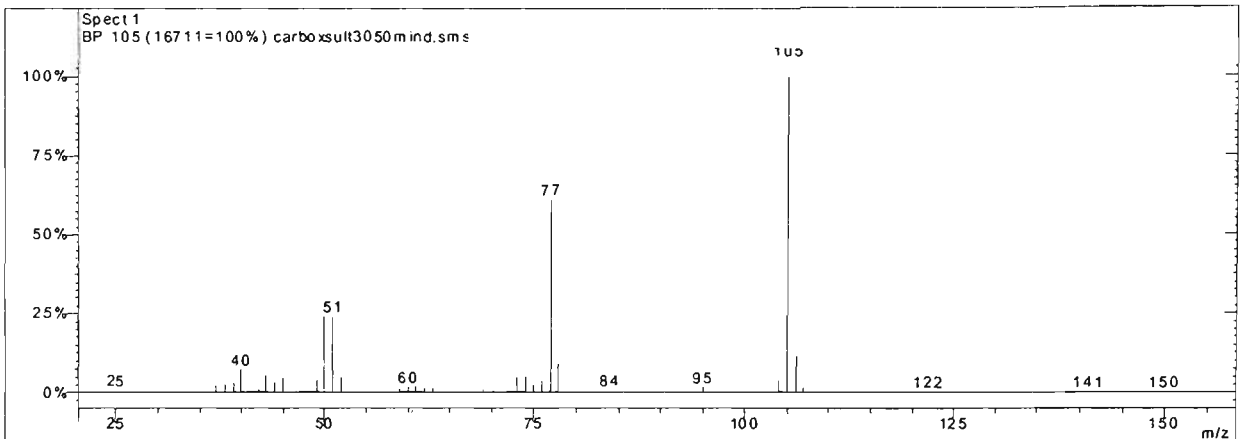


Peak 19 From Carboxen fibre sultana (top) and Carboxen fibre model (bottom)

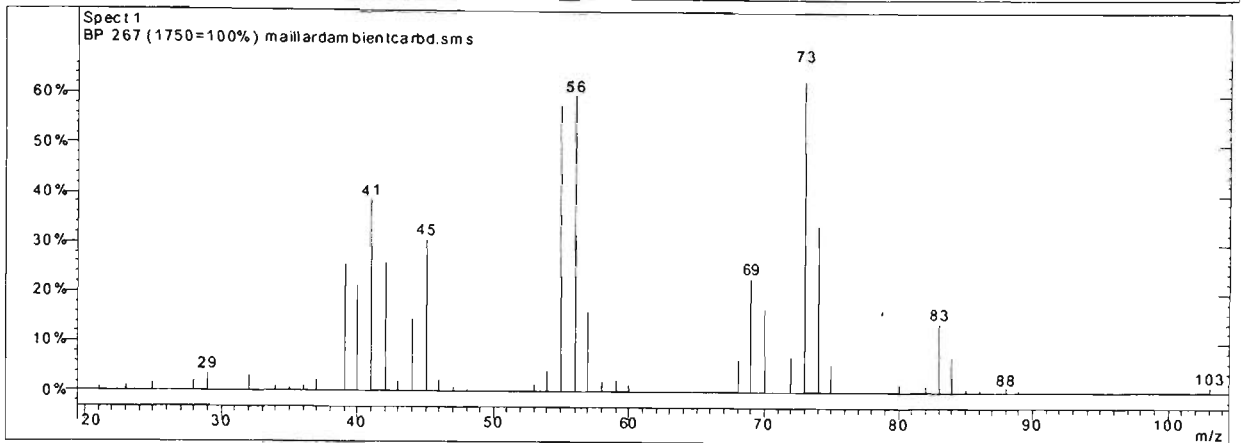
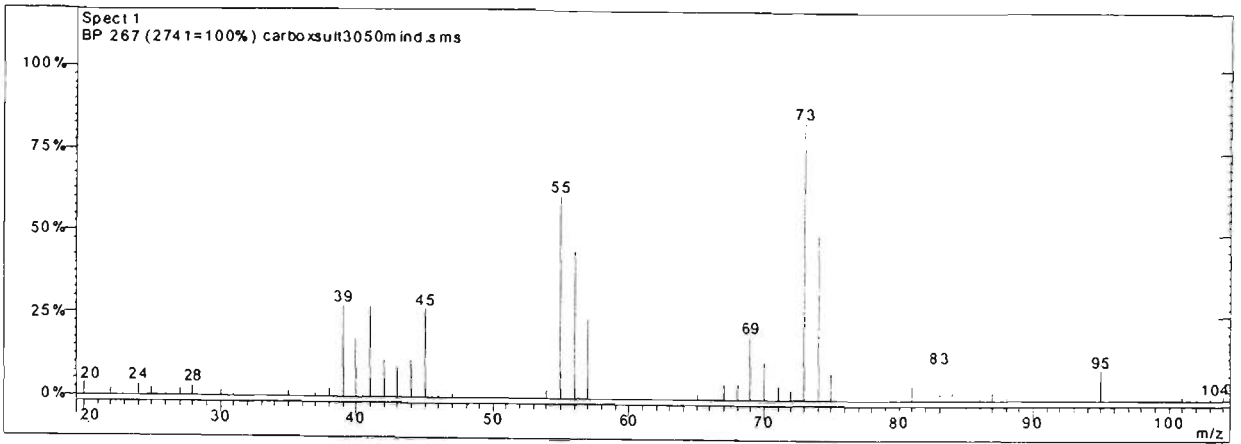




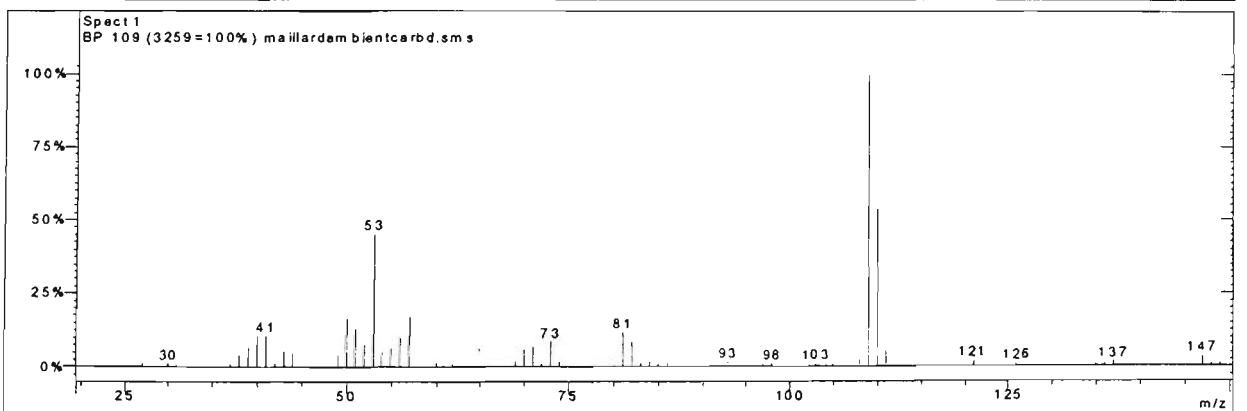
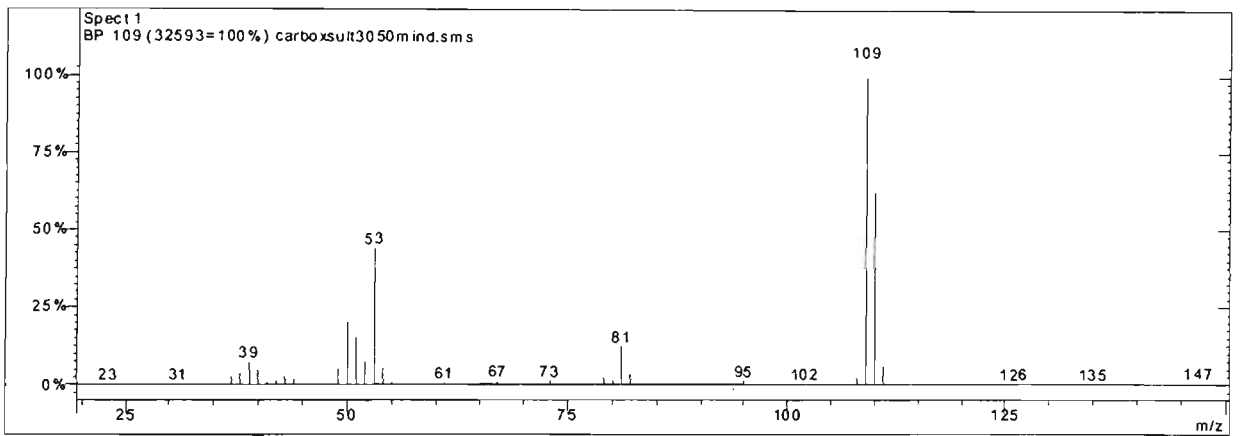
Peak 20 From Carboxen fibre sultana (top) and Carboxen fibre model (bottom)



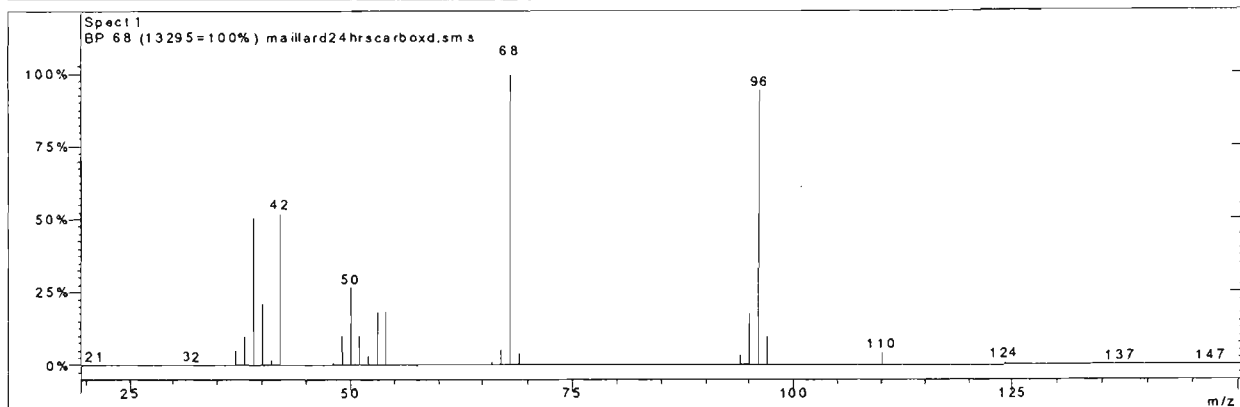
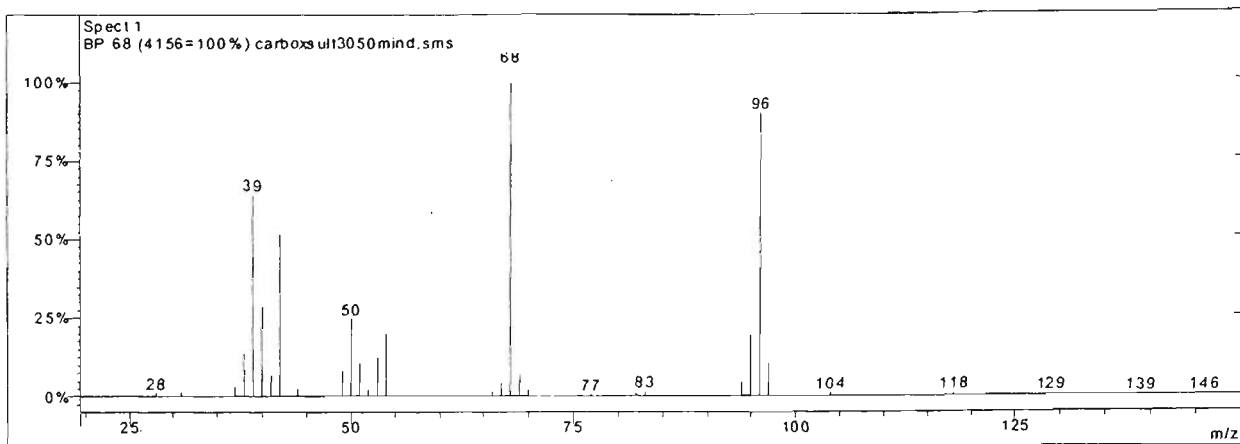
Peak 21 From Carboxen fibre sultana (top) and Carboxen fibre model (bottom)



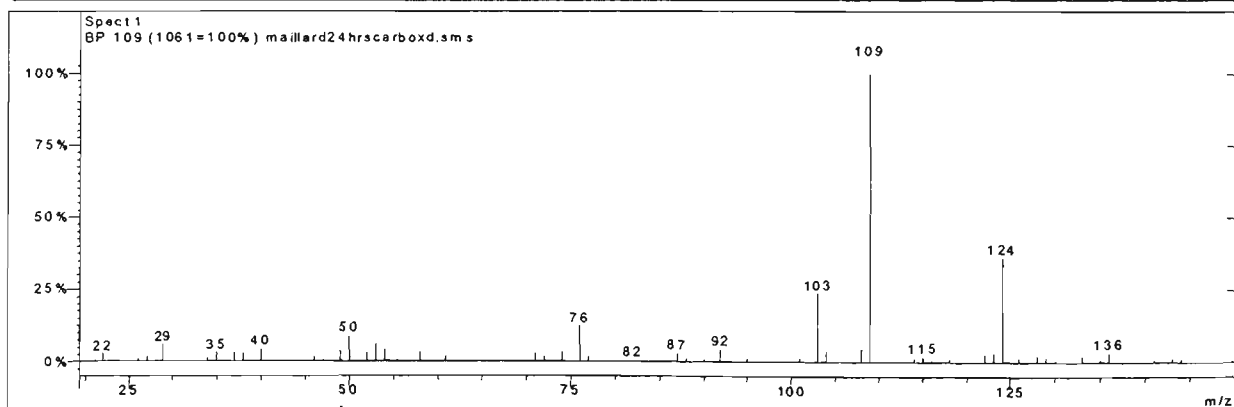
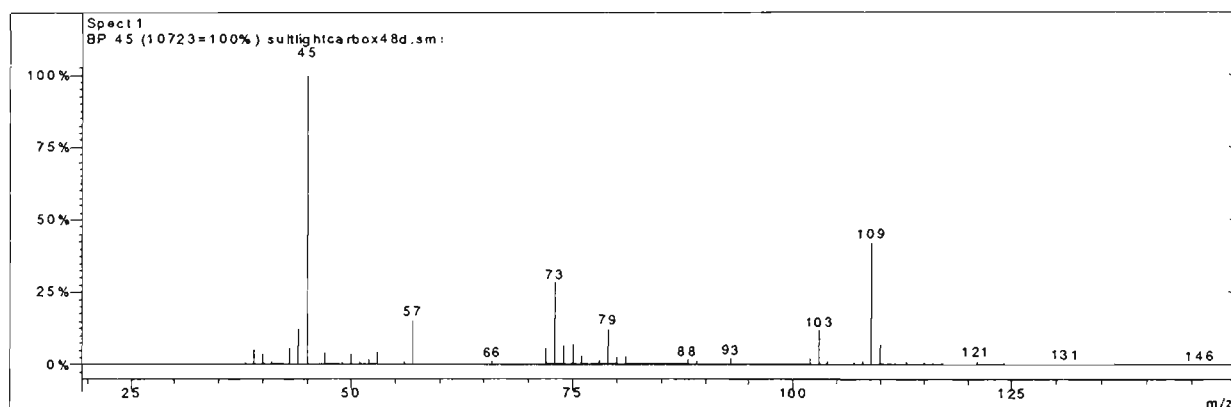
Peak 22 From Carboxen fibre sultana (top) and Carboxen fibre model (bottom)



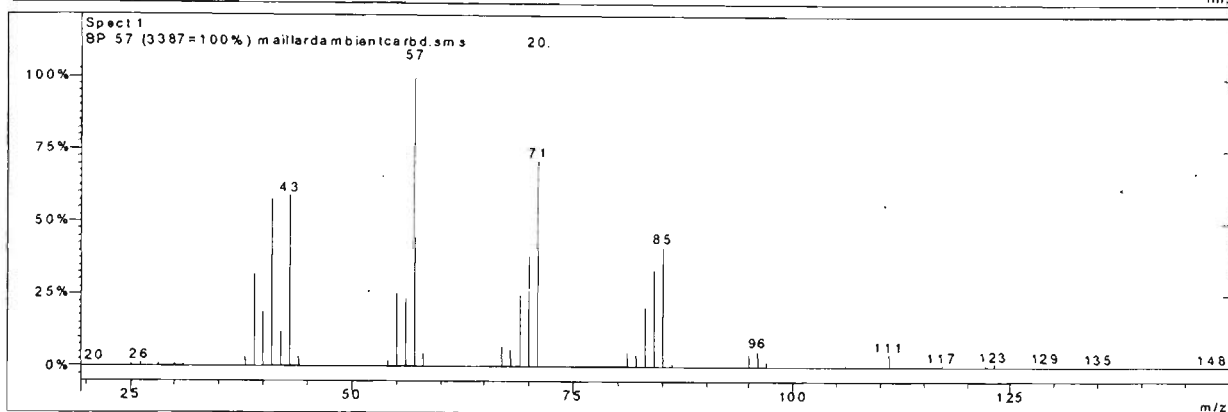
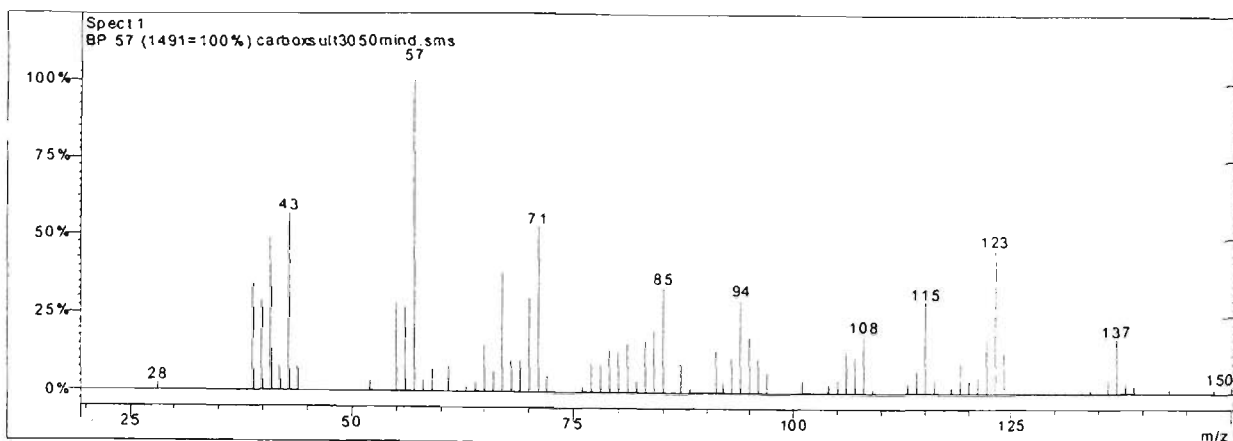
Peak 23 From Carboxen fibre sultana (top) and Carboxen fibre model (bottom)



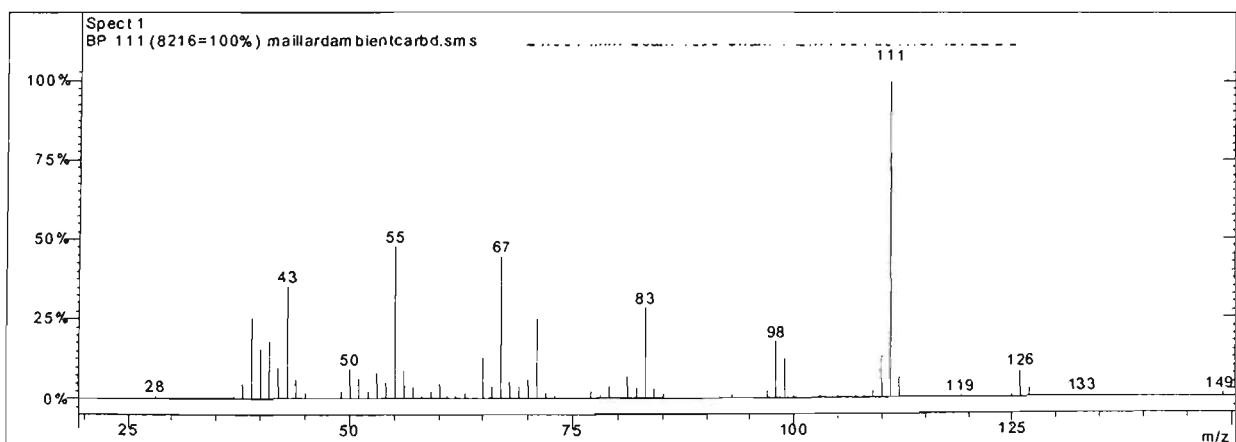
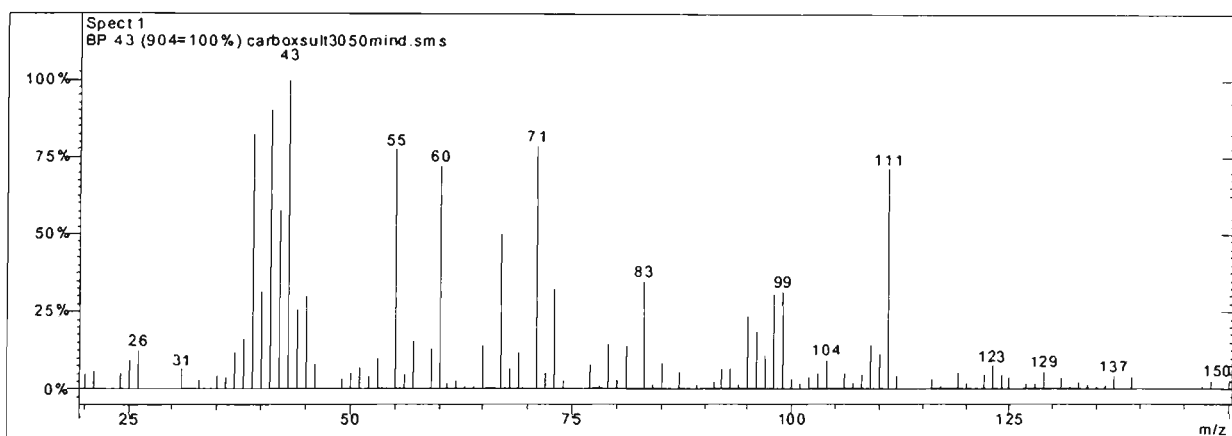
Peak 24 From Carboxen fibre sultana (top) and Carboxen fibre model (bottom)



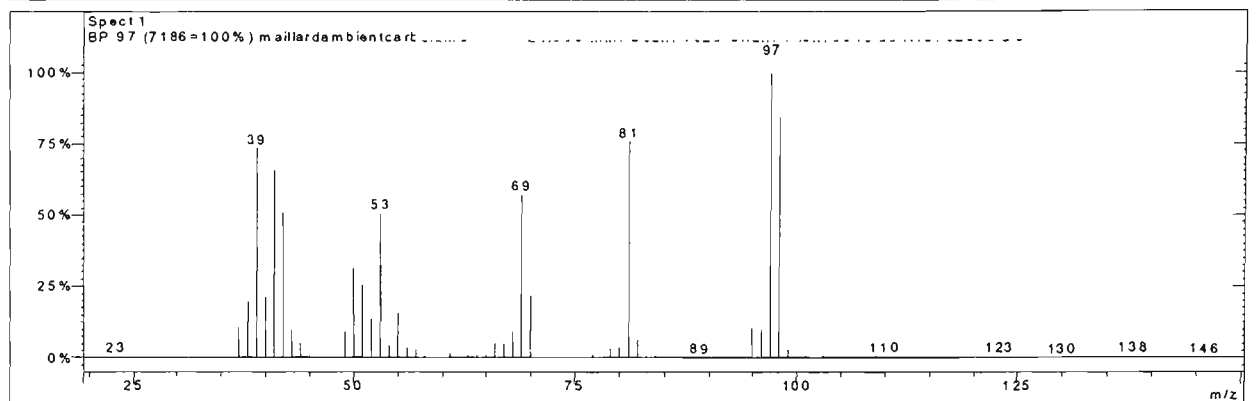
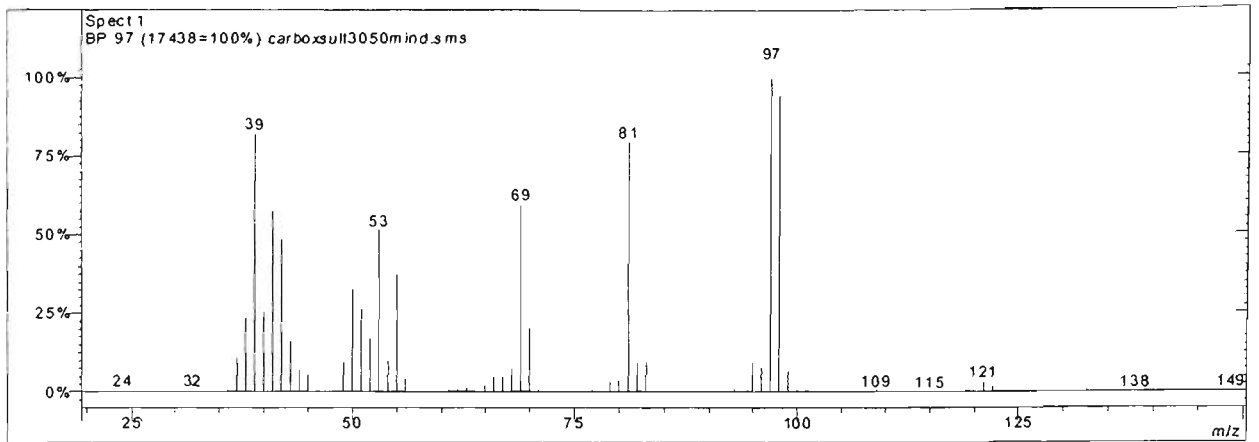
Peak 26 From Carboxen fibre sultana (top) and Carboxen fibre model (bottom)



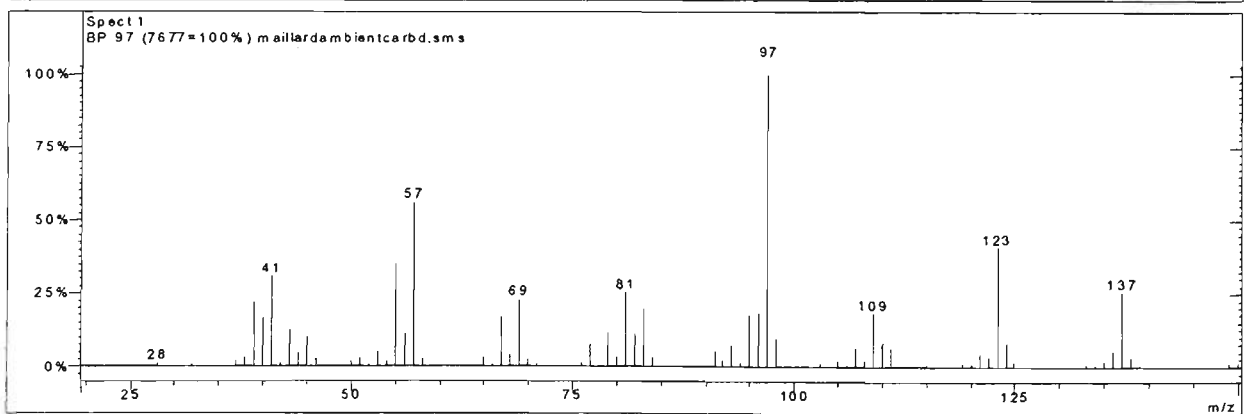
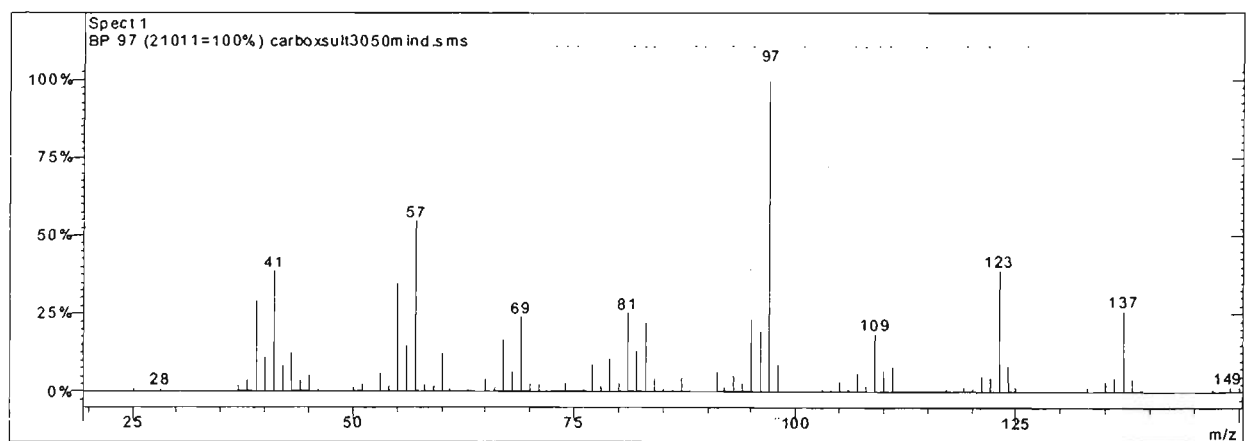
Peak 27 From Carboxen fibre sultana (top) and Carboxen fibre model (bottom)



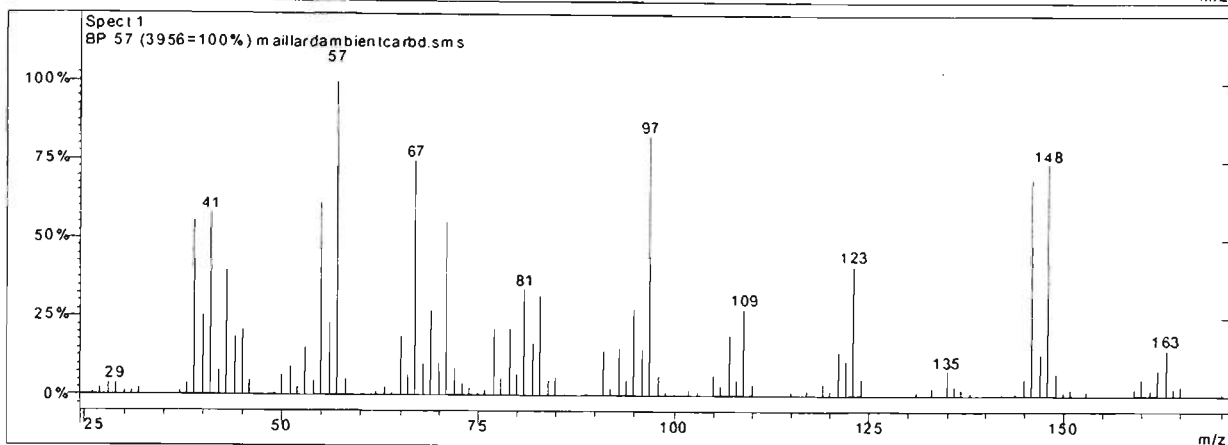
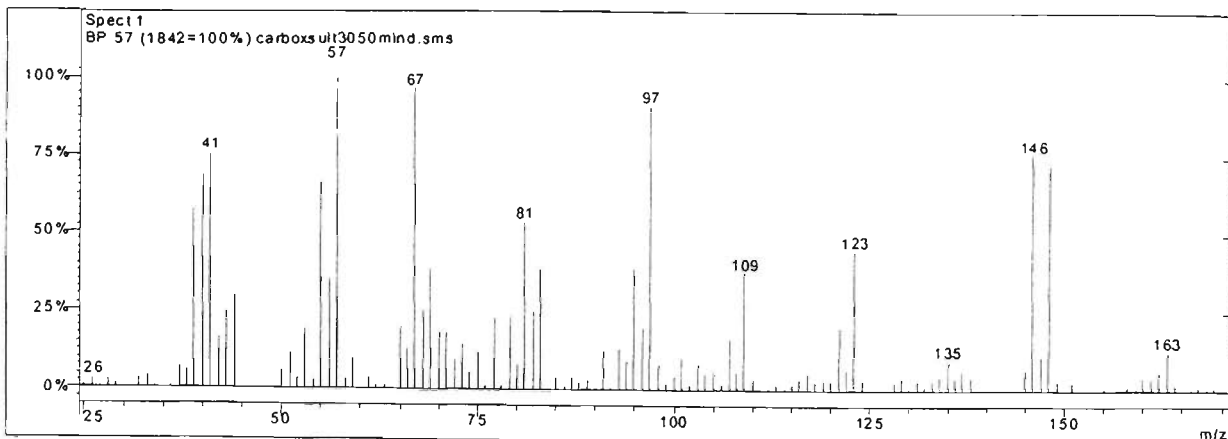
Peak 28 From Carboxen fibre sultana (top) and Carboxen fibre model (bottom)



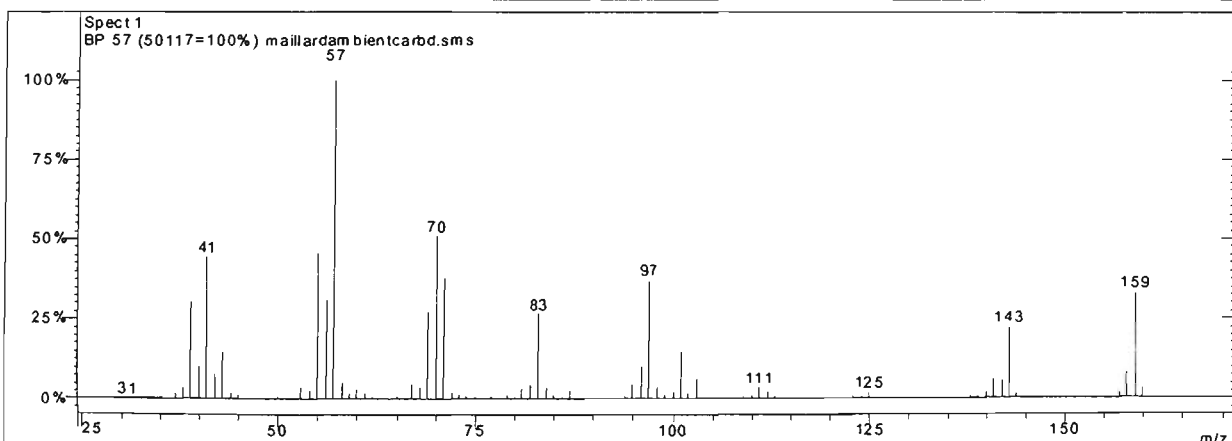
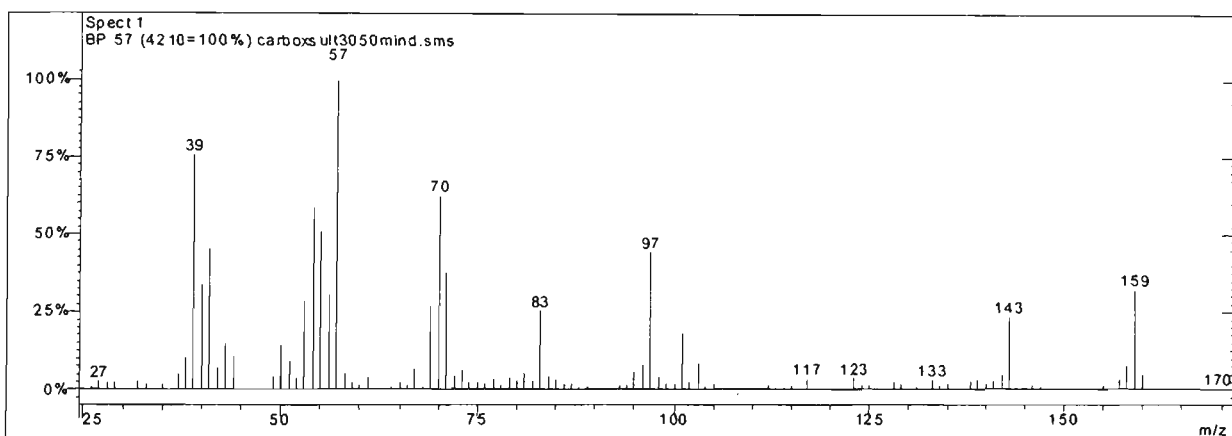
Peak 29 From Carboxen fibre sultana (top) and Carboxen fibre model (bottom)



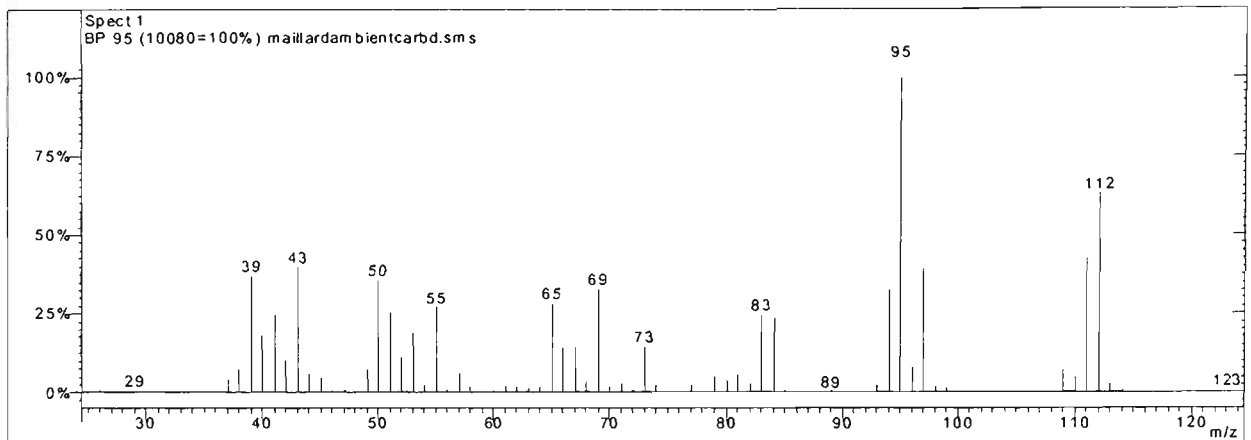
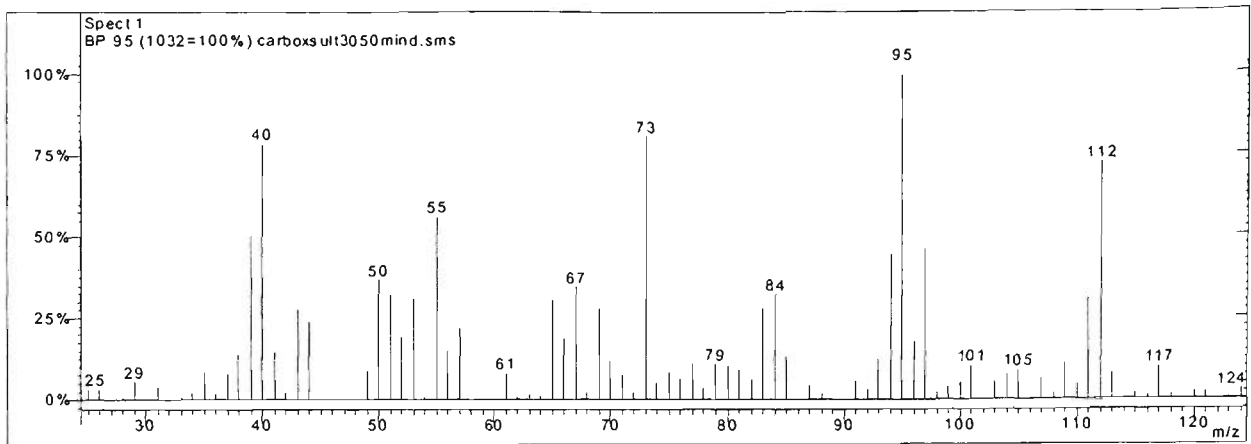
Peak 30 From Carboxen fibre sultana (top) and Carboxen fibre model (bottom)



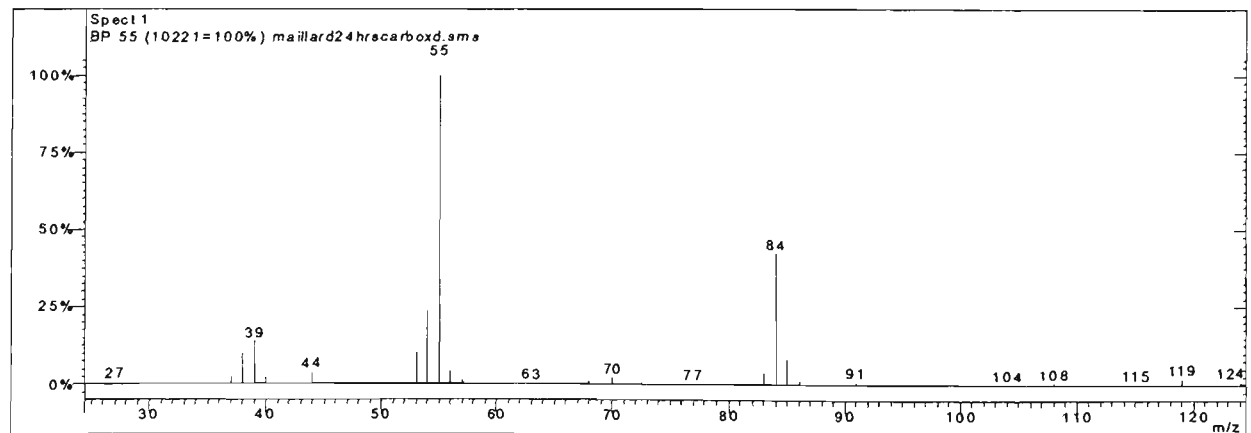
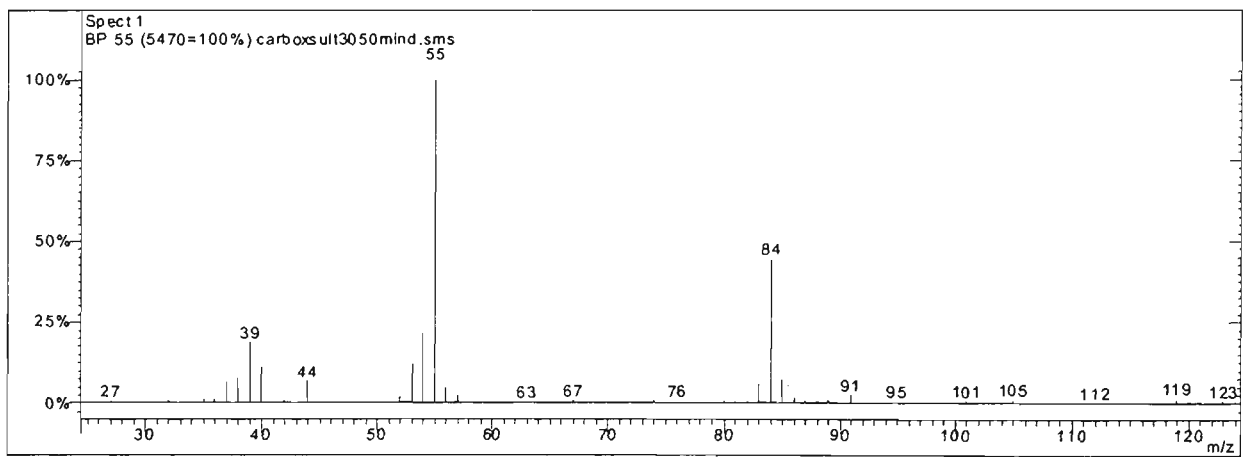
Peak 31 From Carboxen fibre sultana (top) and Carboxen fibre model (bottom)



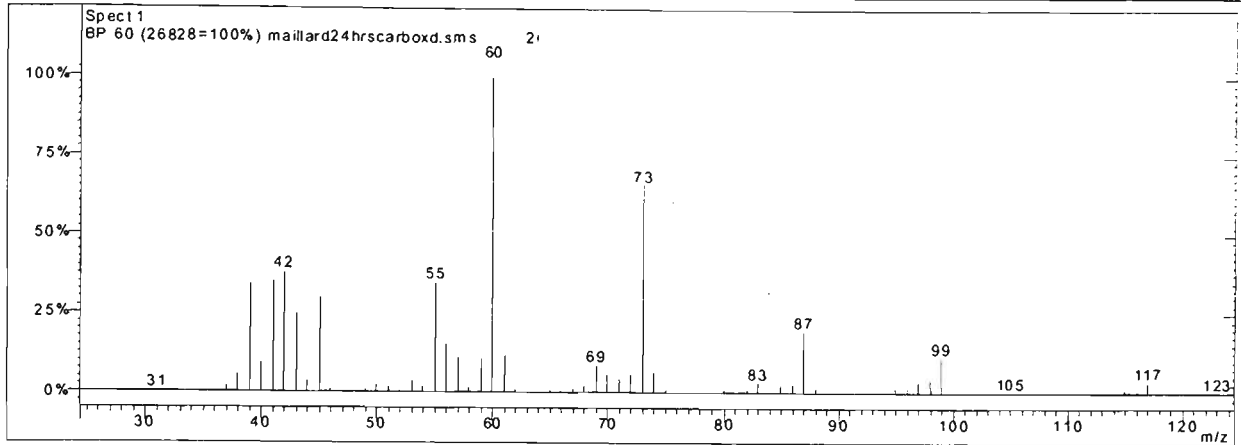
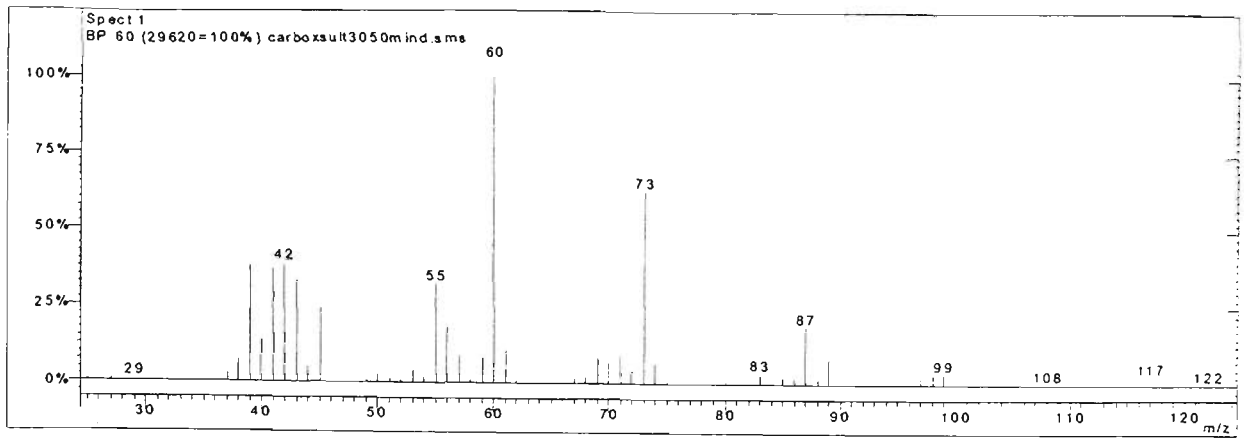
Peak 32 From Carboxen fibre sultana (top) and Carboxen fibre model (bottom)



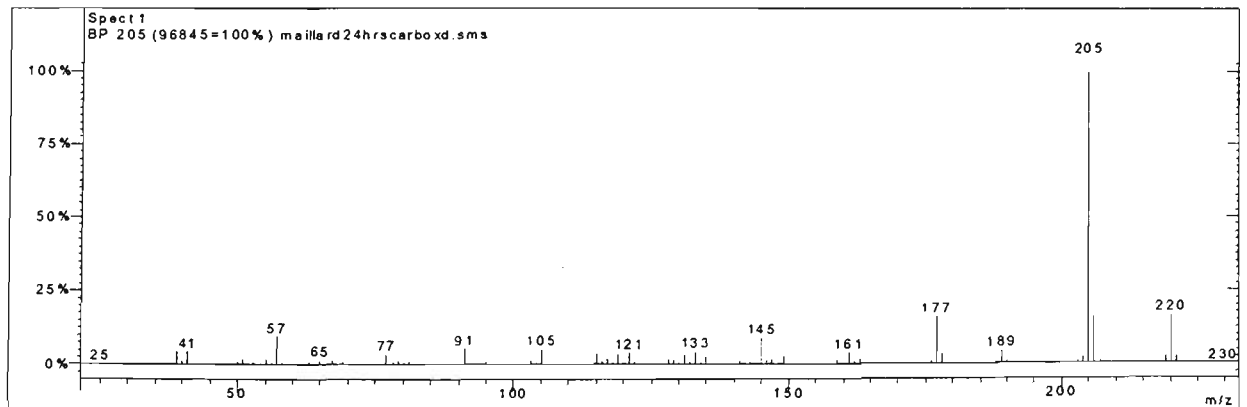
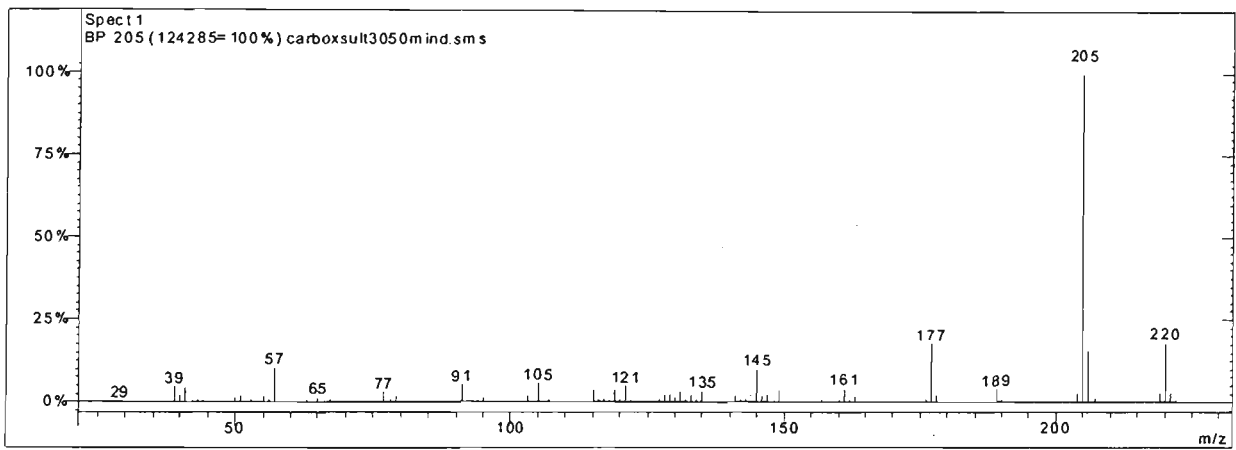
Peak 33 From Carboxen fibre sultana (top) and Carboxen fibre model (bottom)



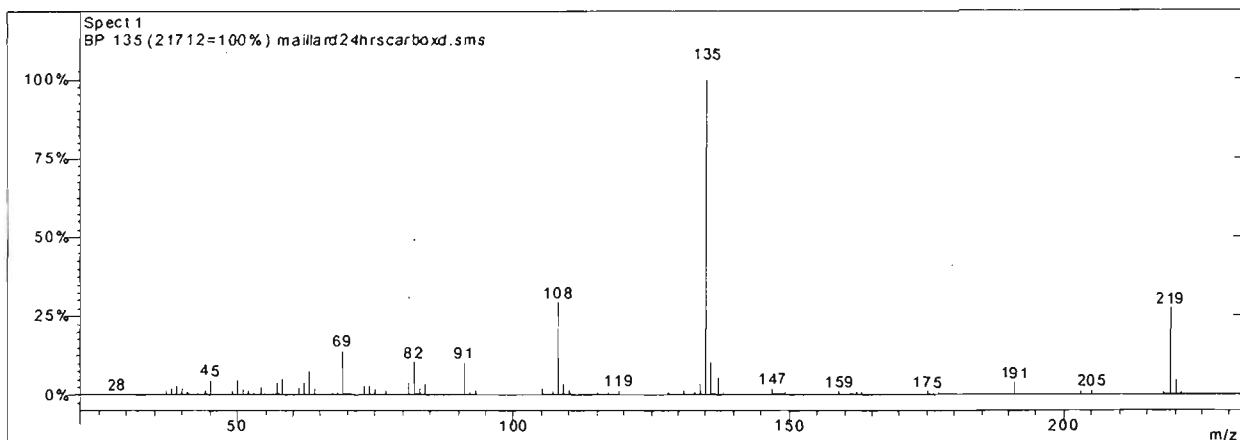
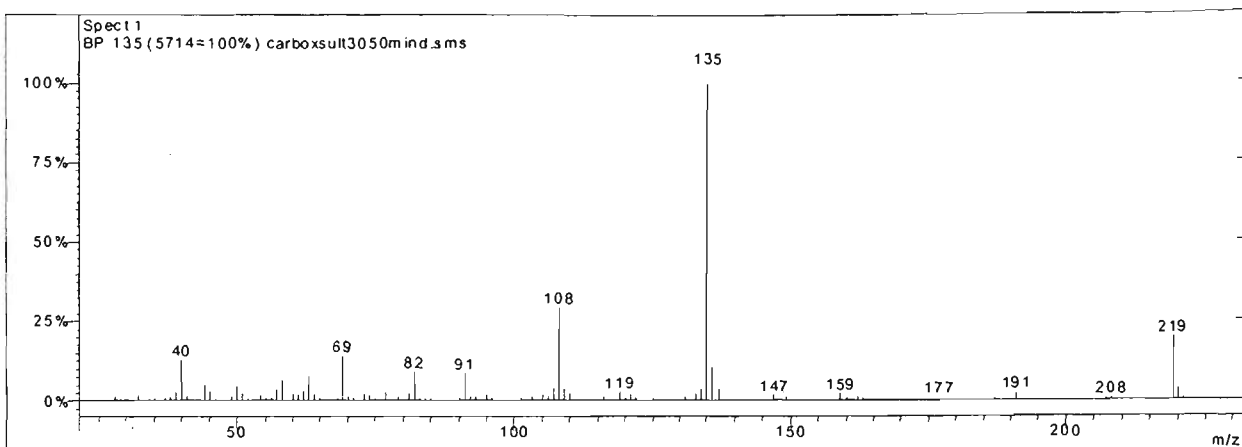
Peak 34 From Carboxen fibre sultana (top) and Carboxen fibre model (bottom)



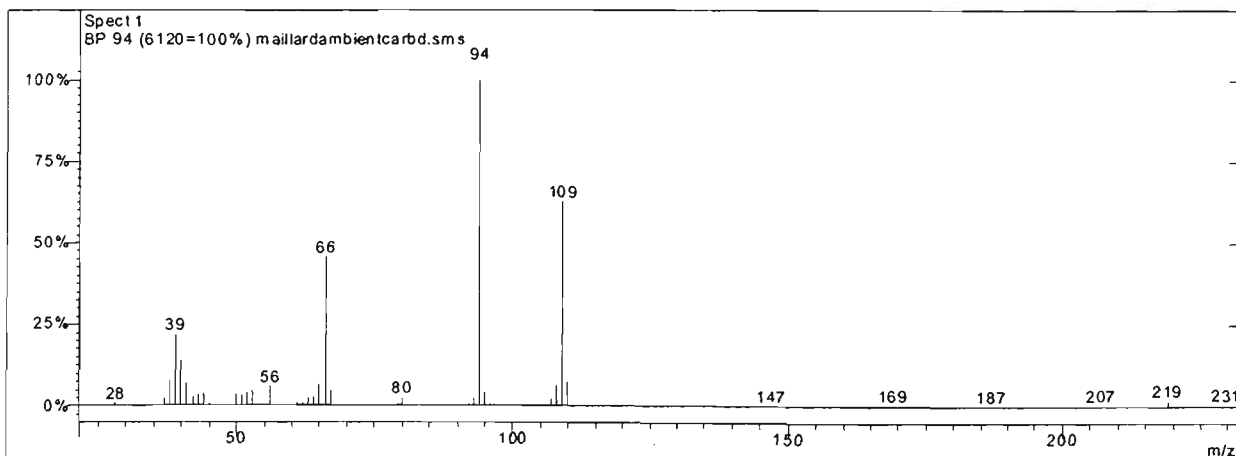
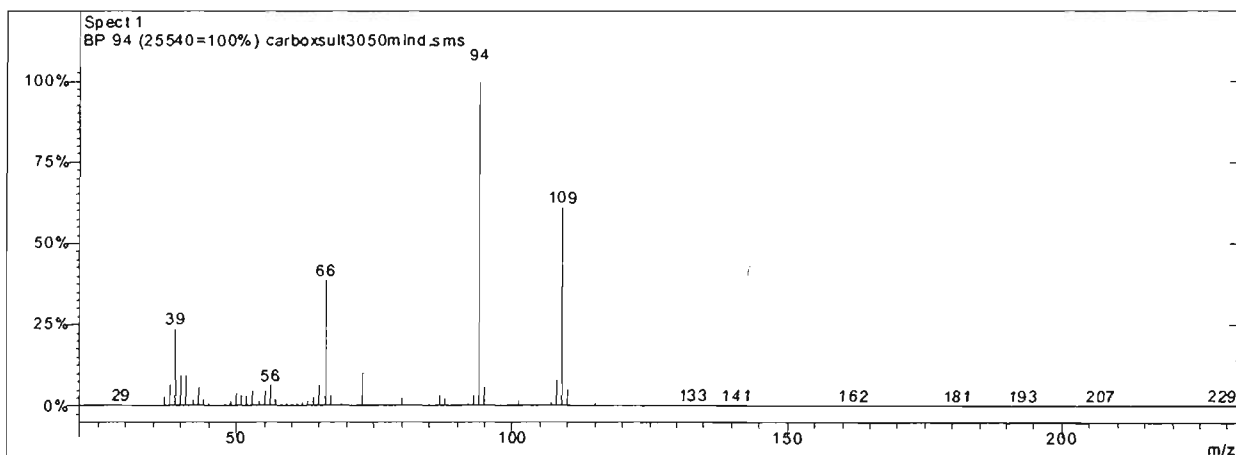
Peak 35 From Carboxen fibre sultana (top) and Carboxen fibre model (bottom)



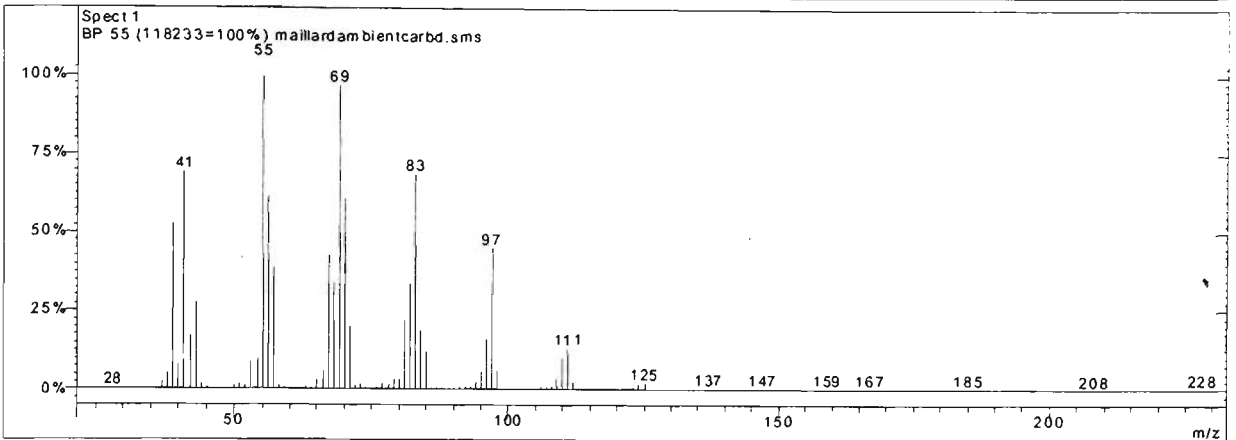
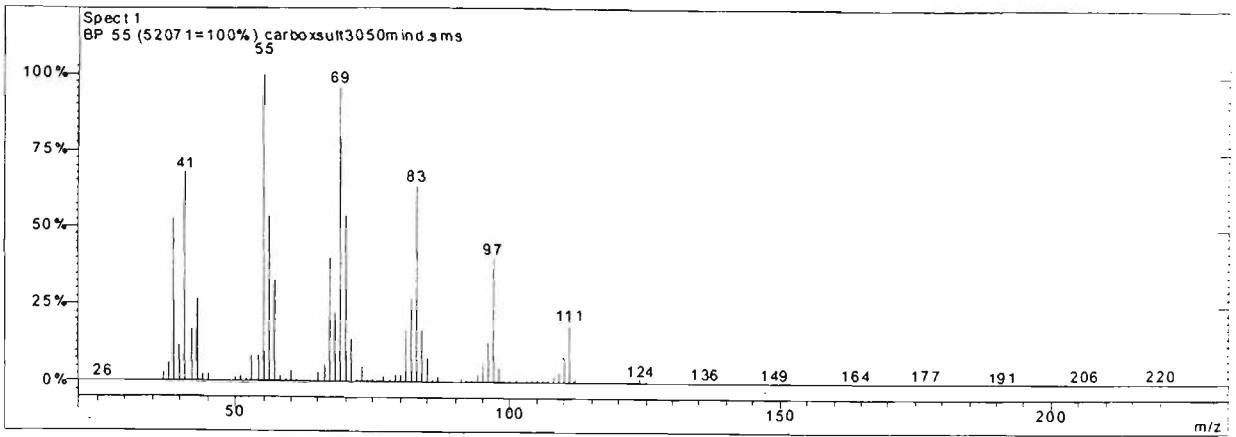
Peak 36 From Carboxen fibre sultana (top) and Carboxen fibre model (bottom)



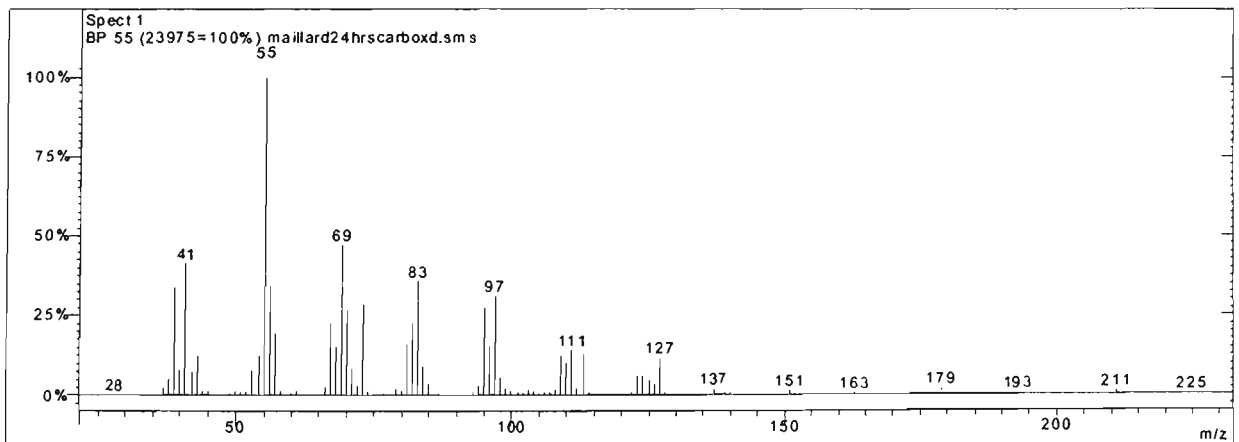
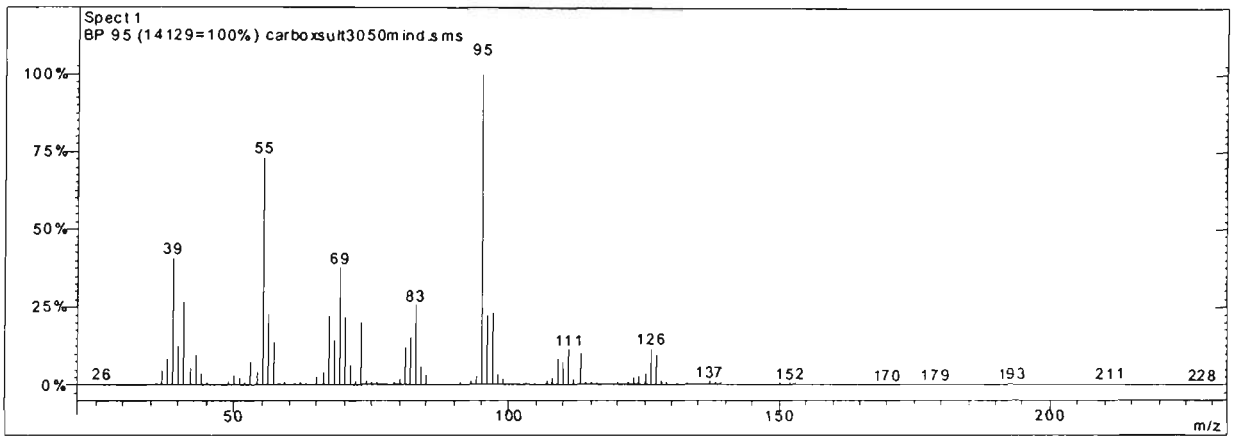
Peak 37 From Carboxen fibre sultana (top) and Carboxen fibre model (bottom)



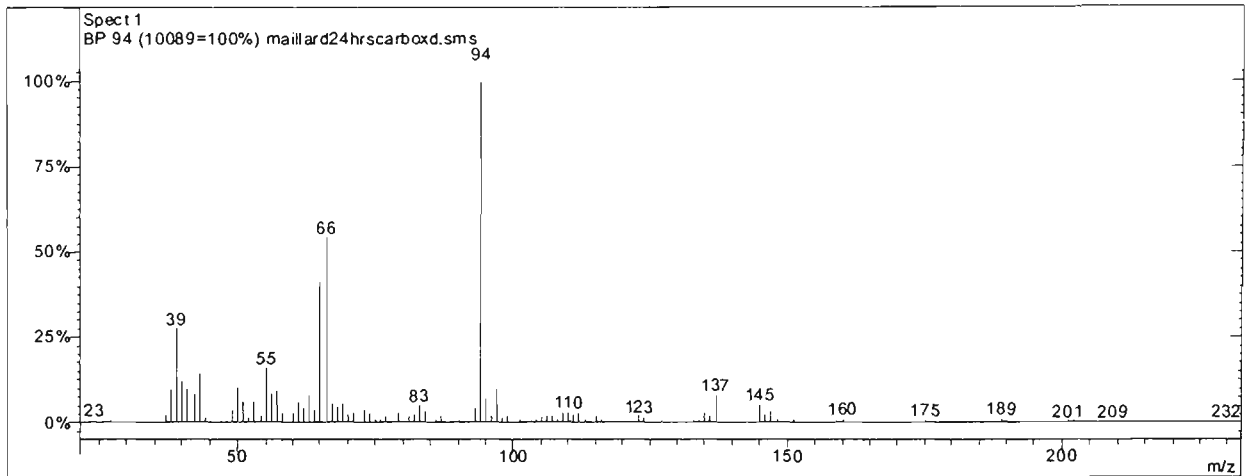
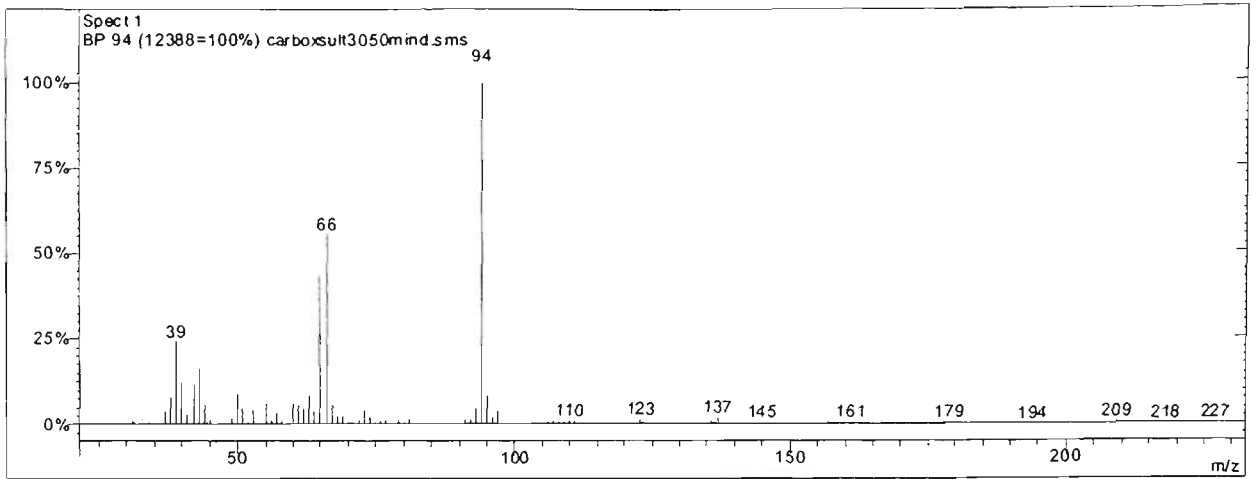
Peak 38 From Carboxen fibre sultana (top) and Carboxen fibre model (bottom)



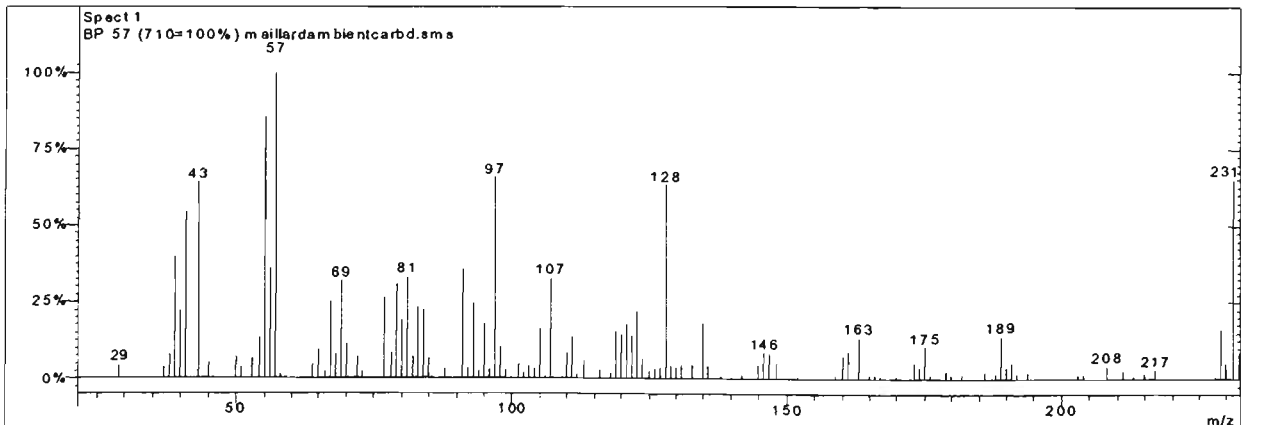
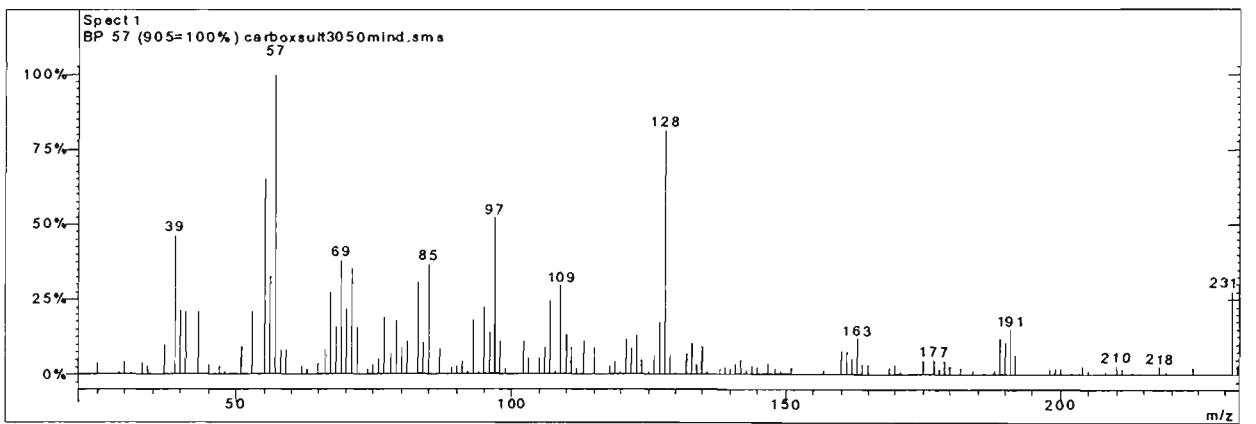
Peak 39 From Carboxen fibre sultana (top) and Carboxen fibre model (bottom)



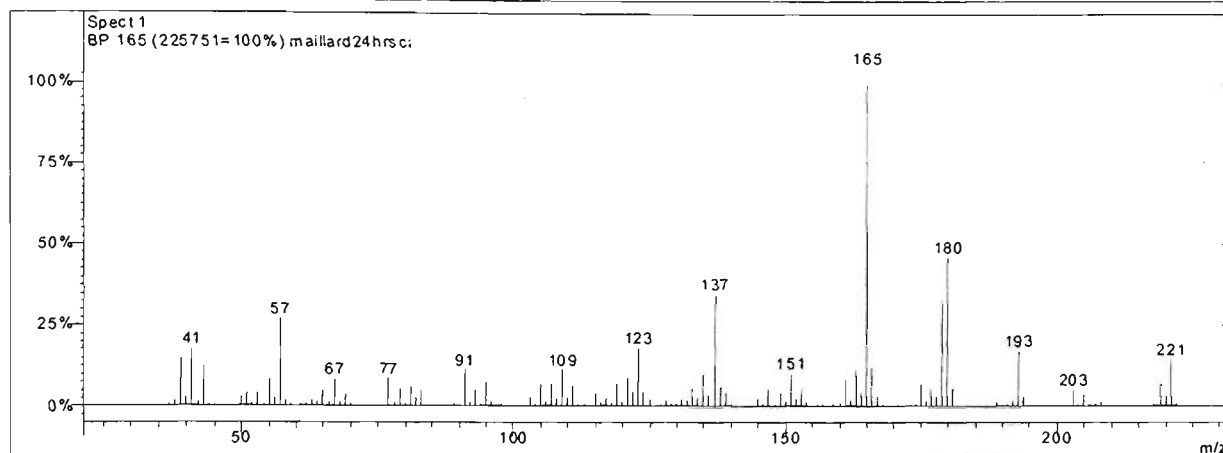
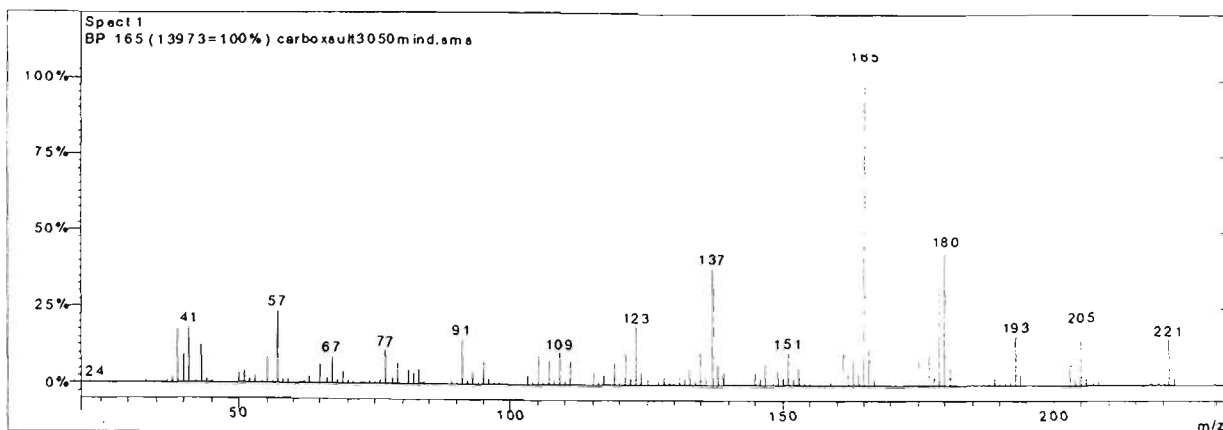
Peak 40 From Carboxen fibre sultana (top) and Carboxen fibre model (bottom)



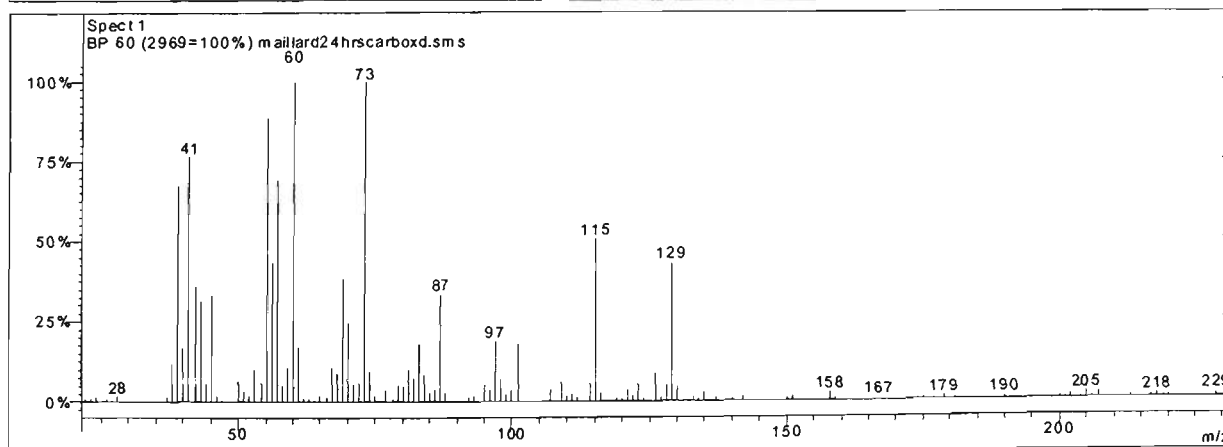
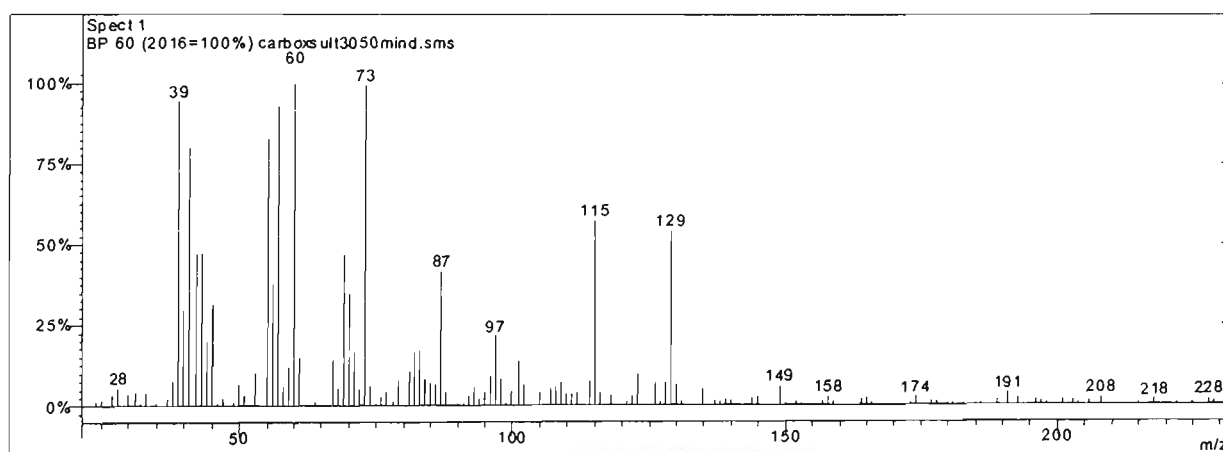
Peak 41 From Carboxen fibre sultana (top) and Carboxen fibre model (bottom)



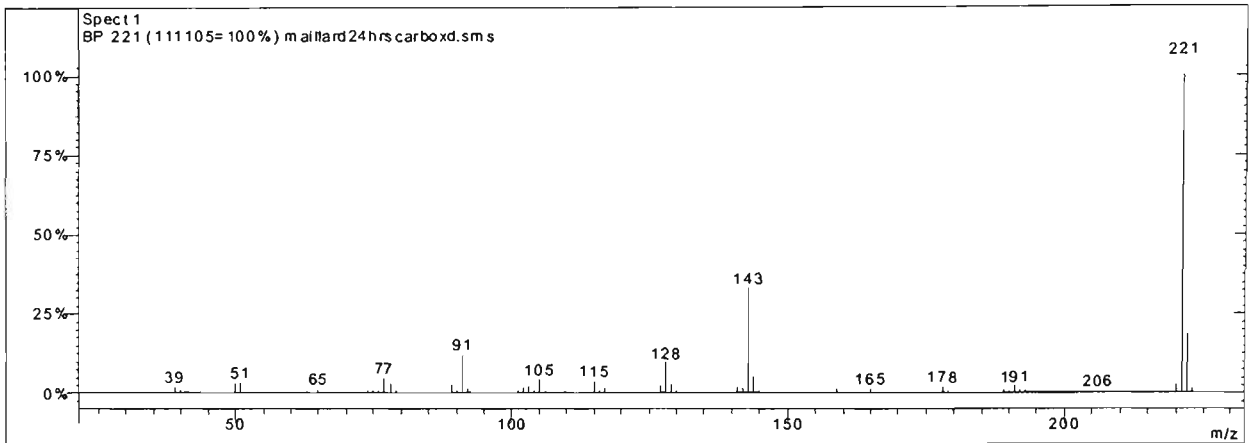
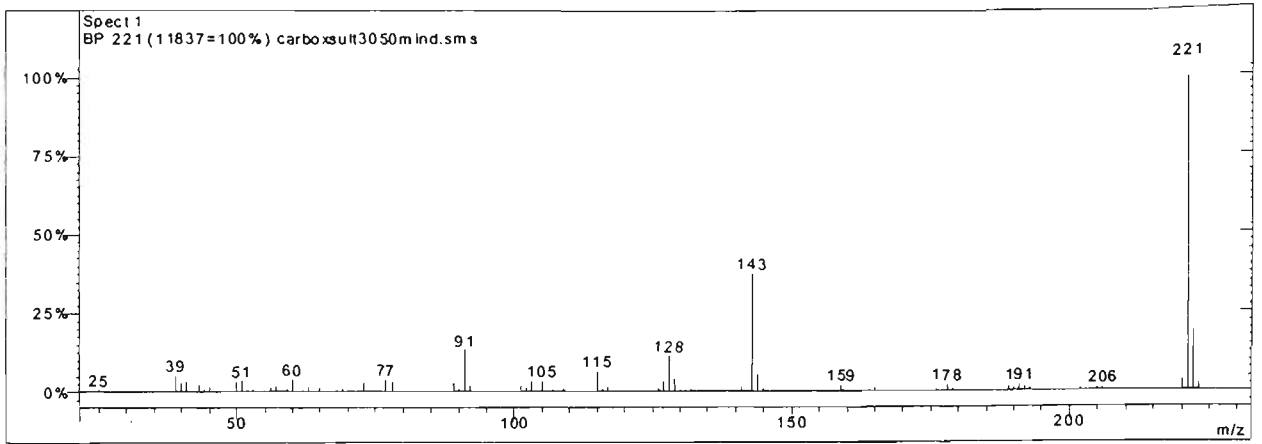
Peak 42 From Carboxen fibre sultana (top) and Carboxen fibre model (bottom)



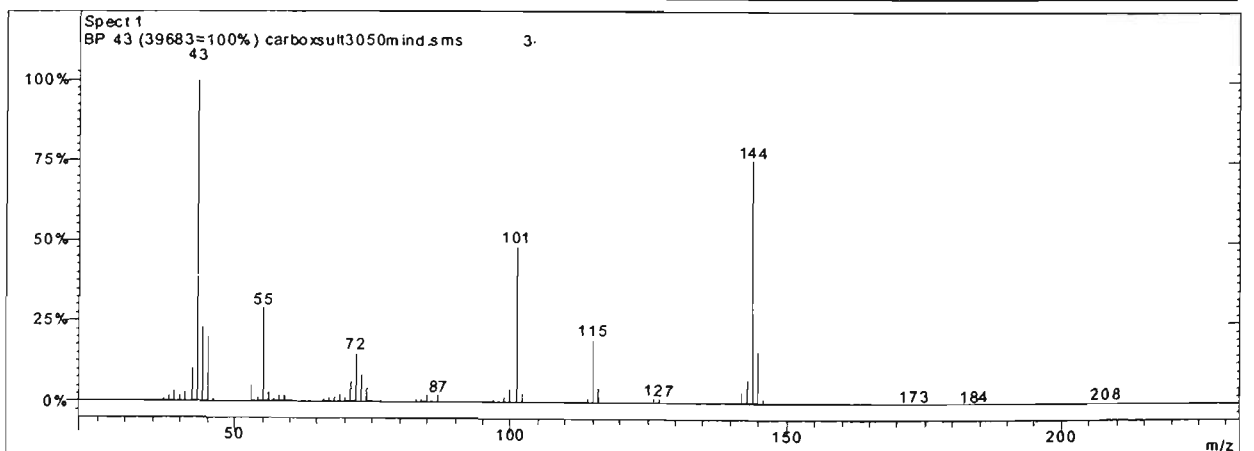
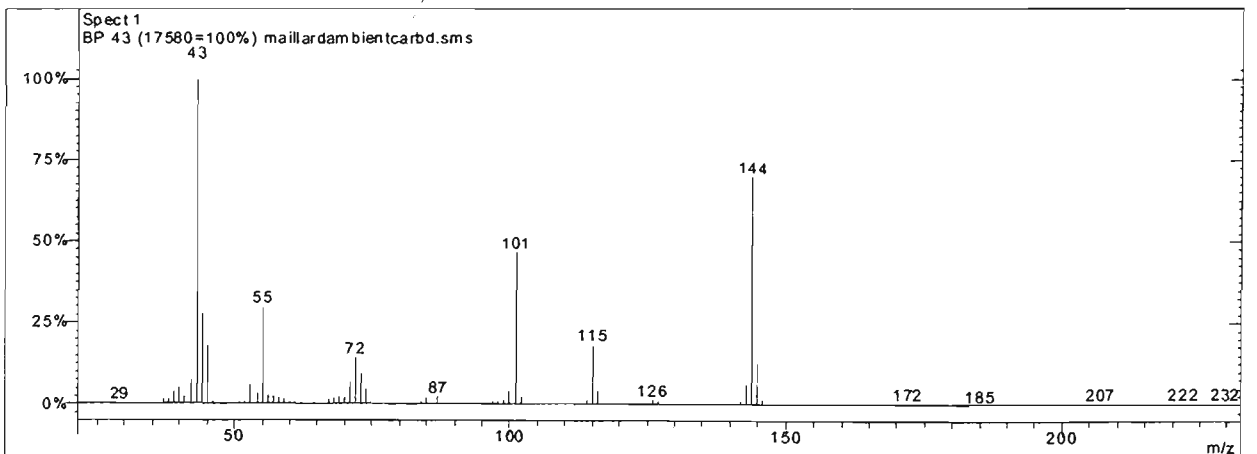
Peak 43 From Carboxen fibre sultana (top) and Carboxen fibre model (bottom)



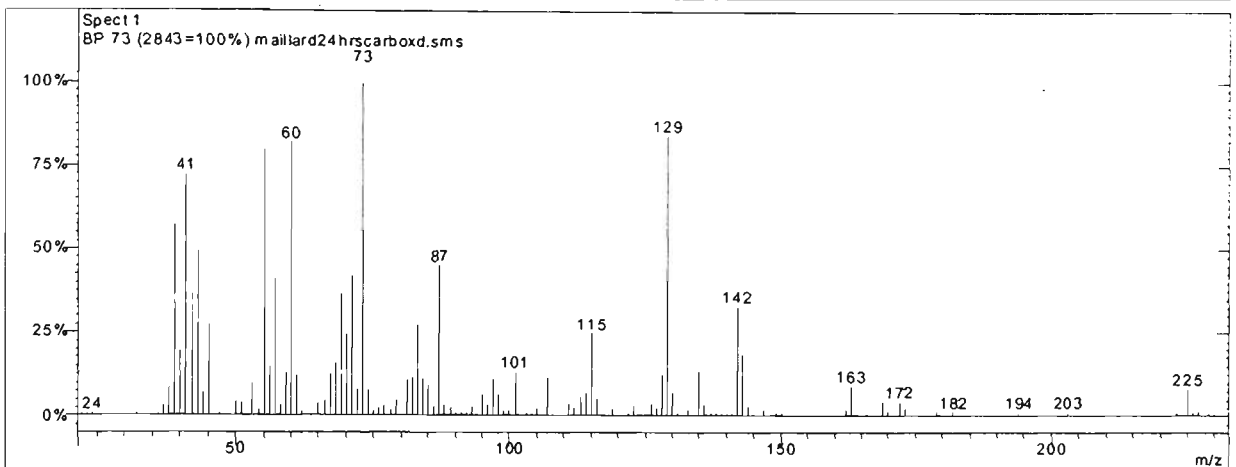
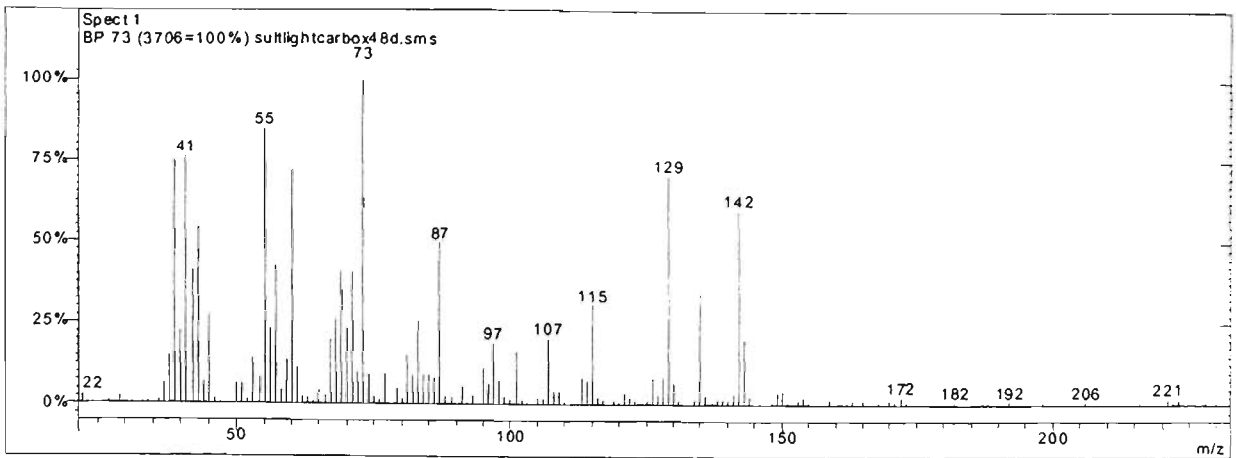
Peak 44 From Carboxen fibre sultana (top) and Carboxen fibre model (bottom)



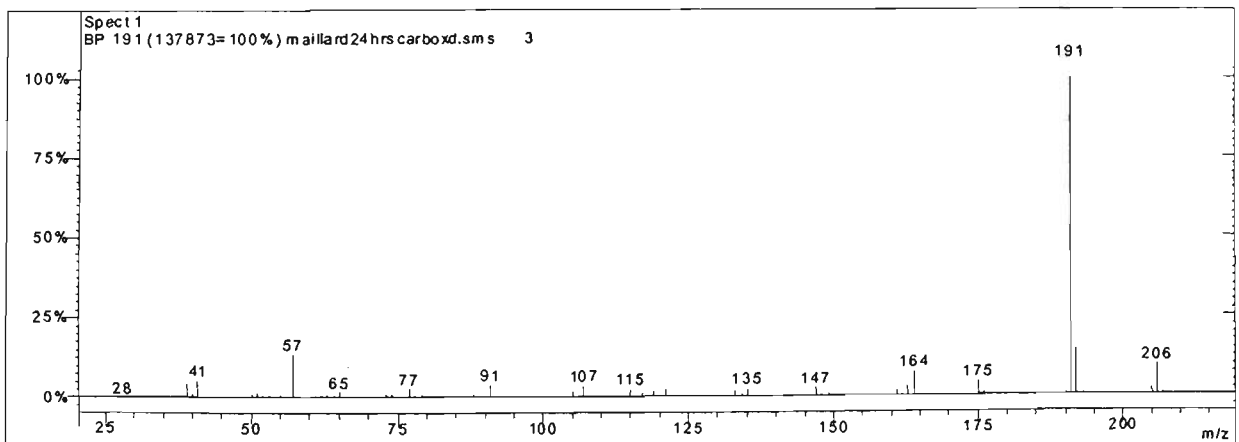
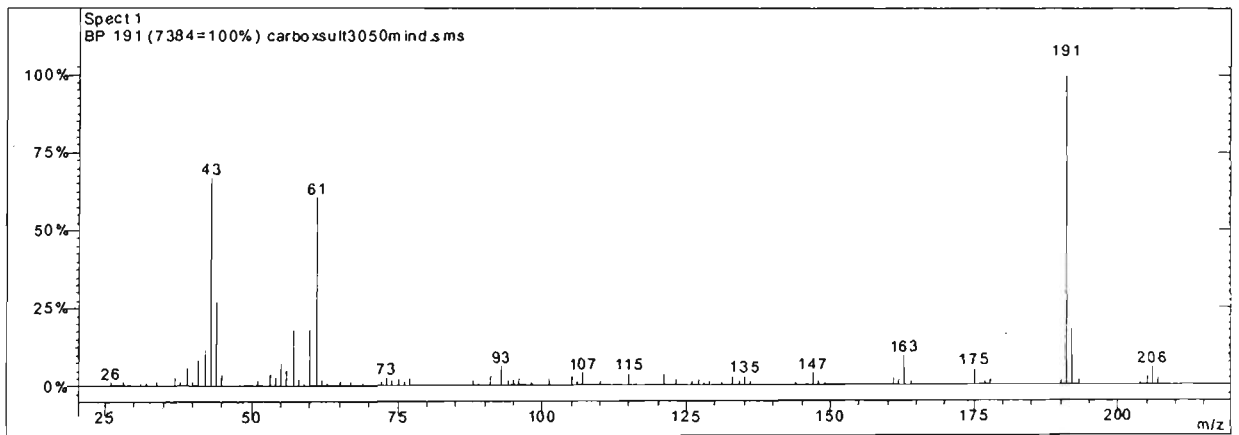
Peak 45 From Carboxen fibre sultana (top) and Carboxen fibre model (bottom)



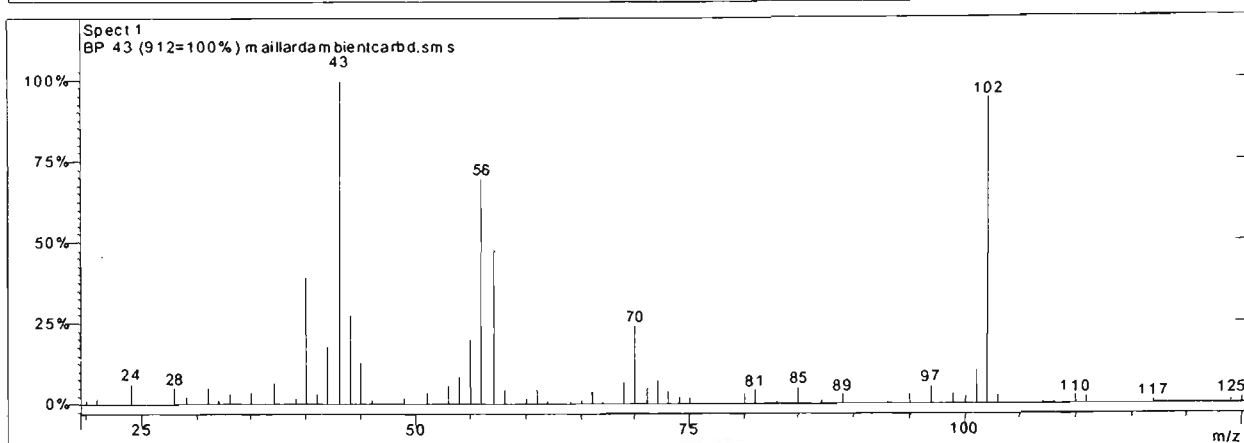
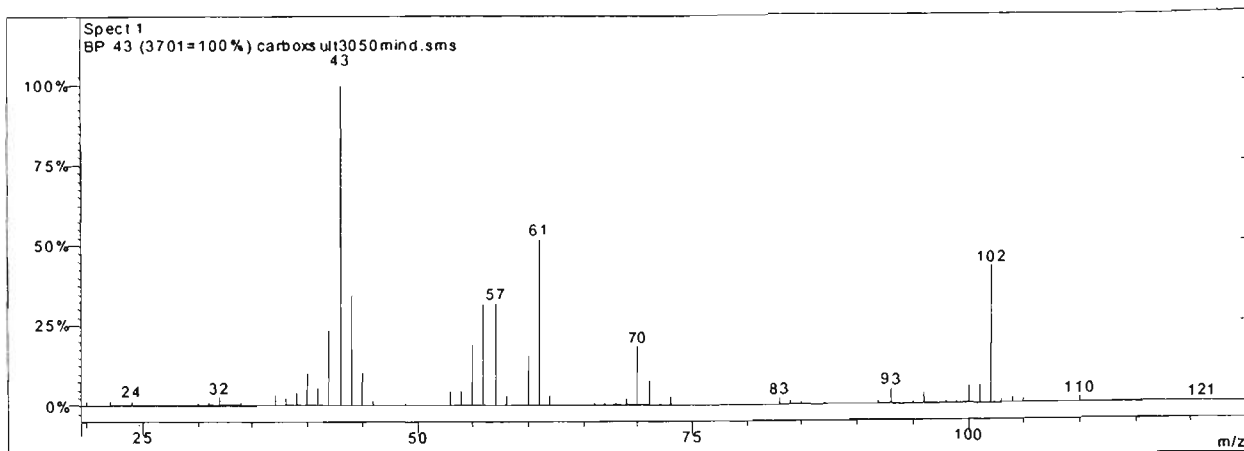
Peak 46 From Carboxen fibre sultana (top) and Carboxen fibre model (bottom)



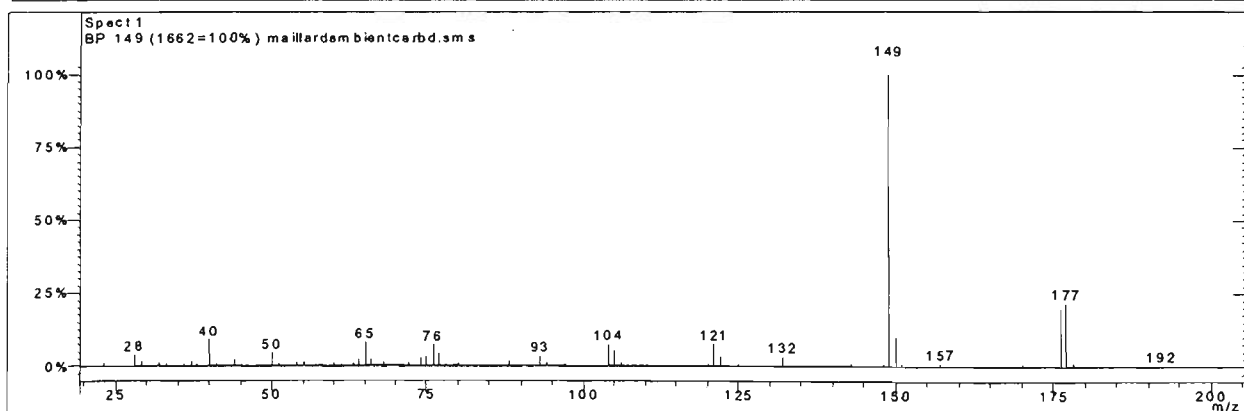
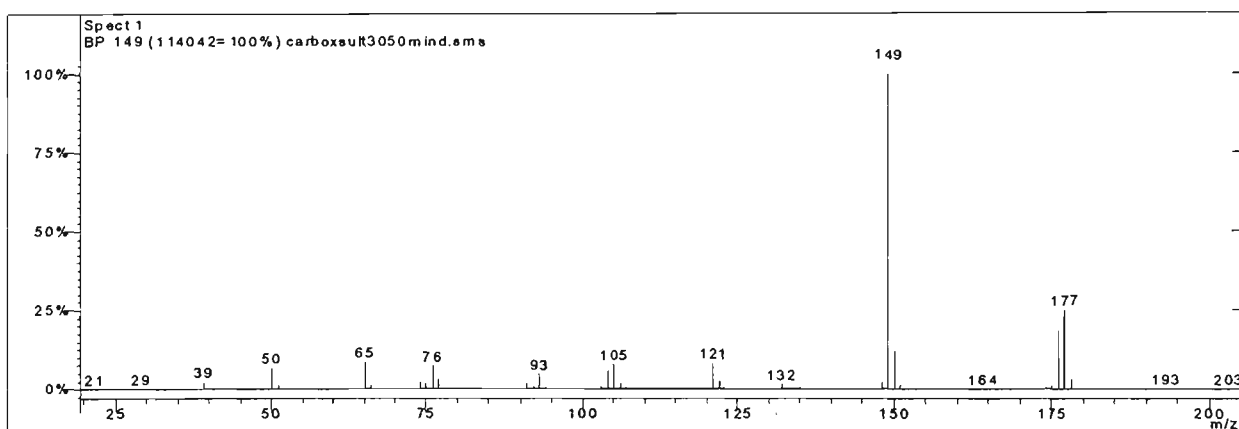
Peak 47 From Carboxen fibre sultana (top) and Carboxen fibre model (bottom)



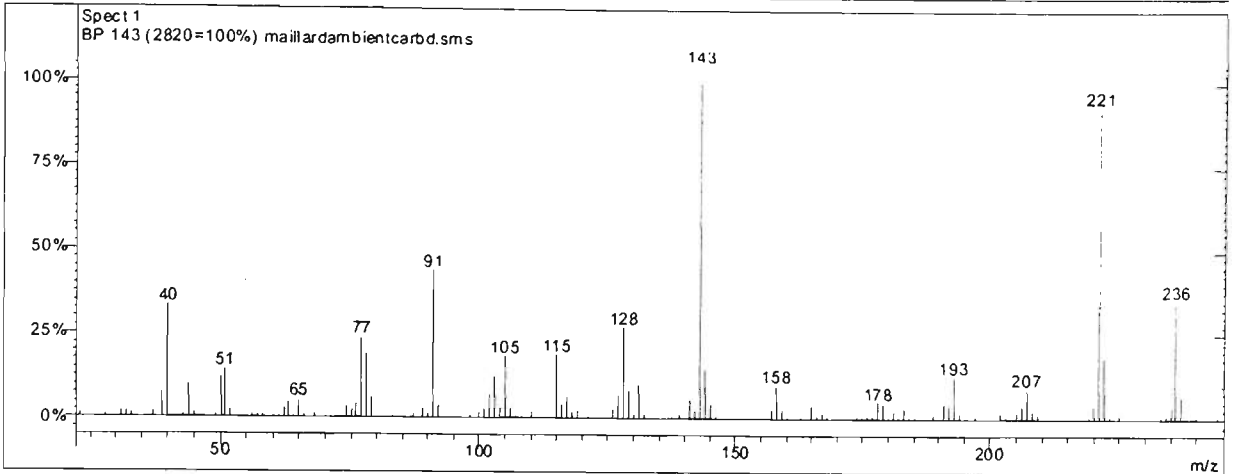
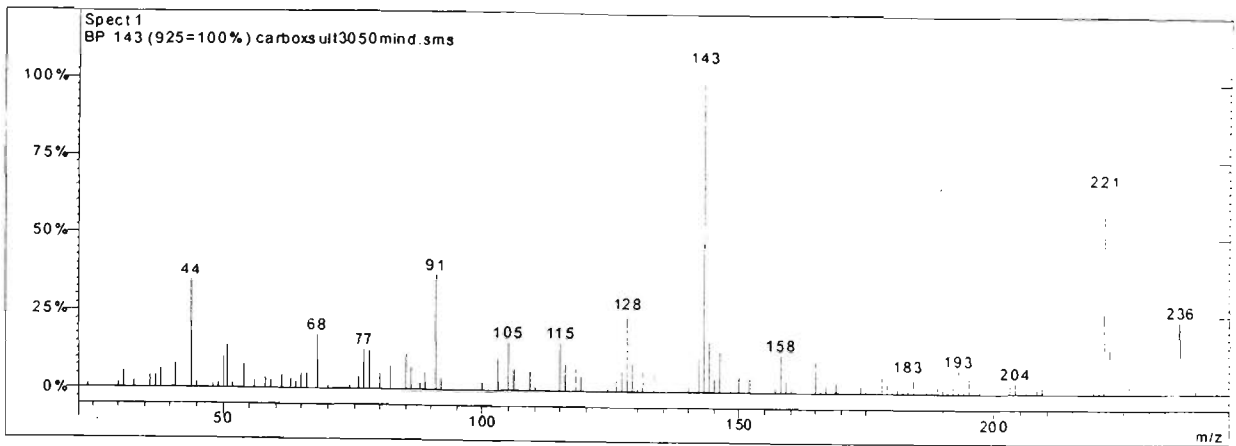
Peak 48 From Carboxen fibre sultana (top) and Carboxen fibre model (bottom)



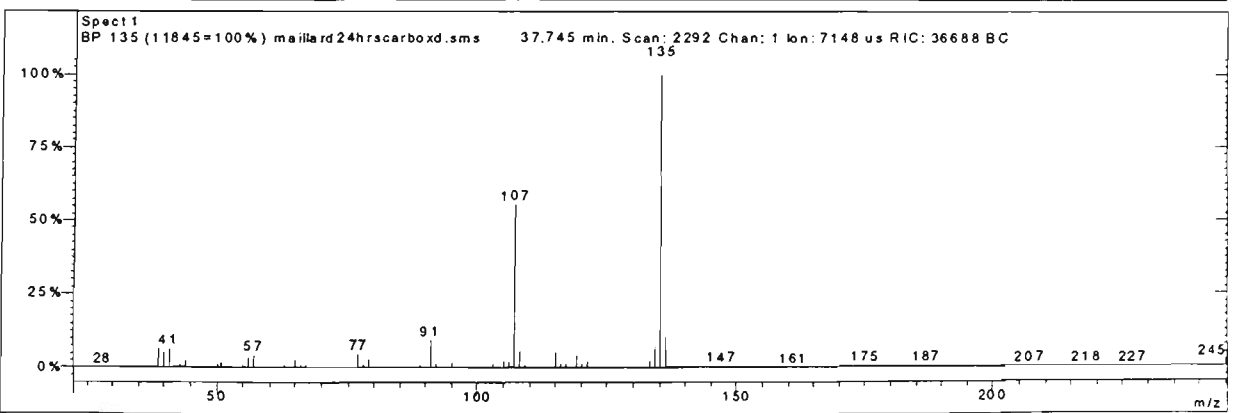
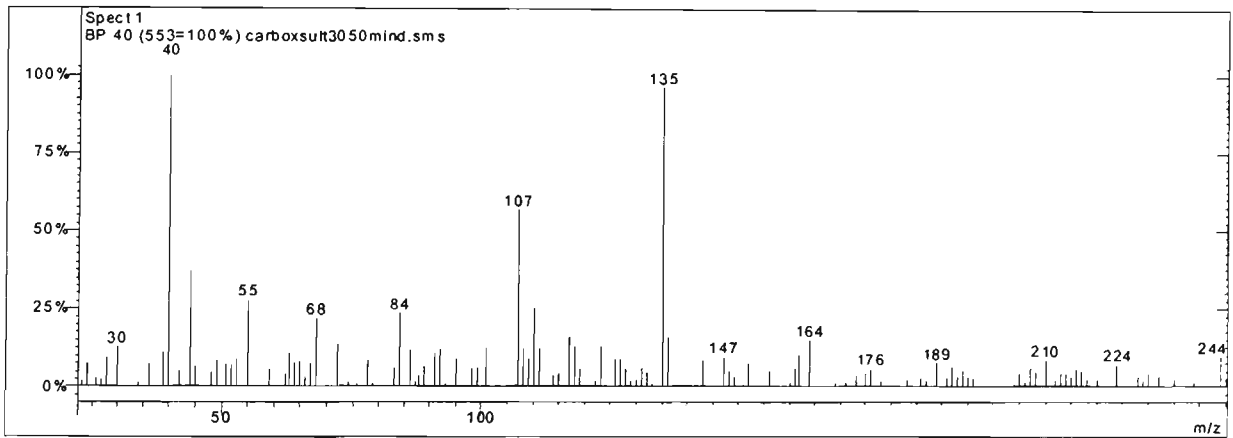
Peak 49 From Carboxen fibre sultana (top) and Carboxen fibre model (bottom)



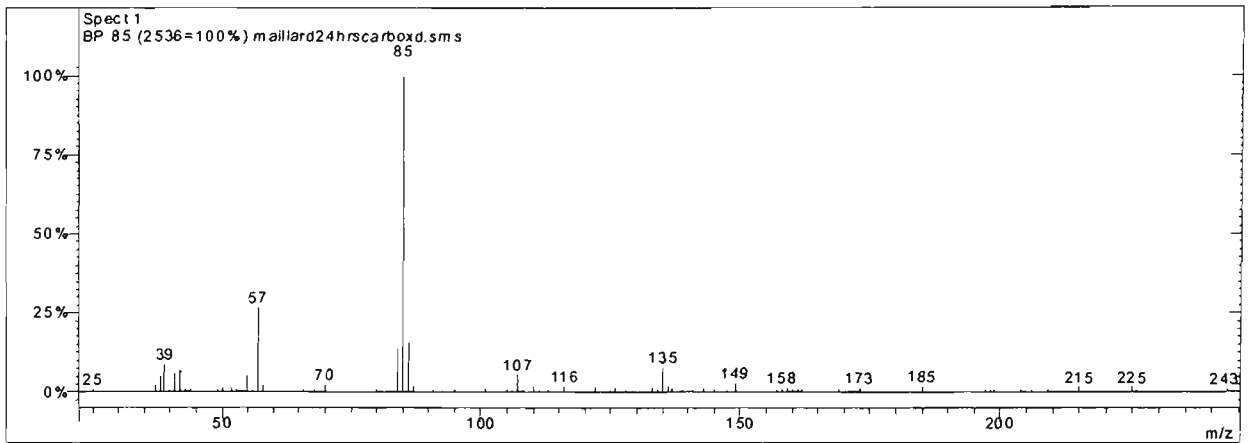
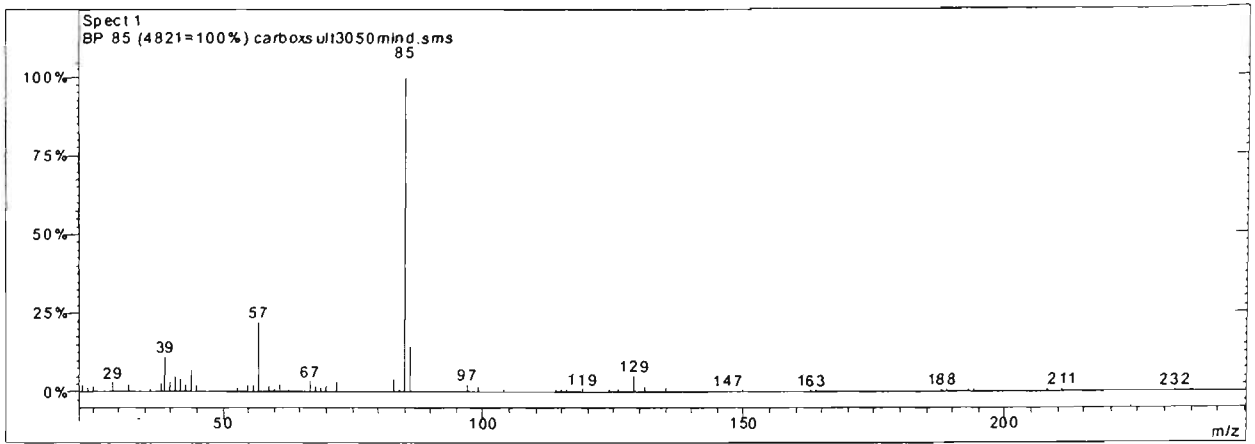
Peak 50 From Carboxen fibre sultana (top) and Carboxen fibre model (bottom)



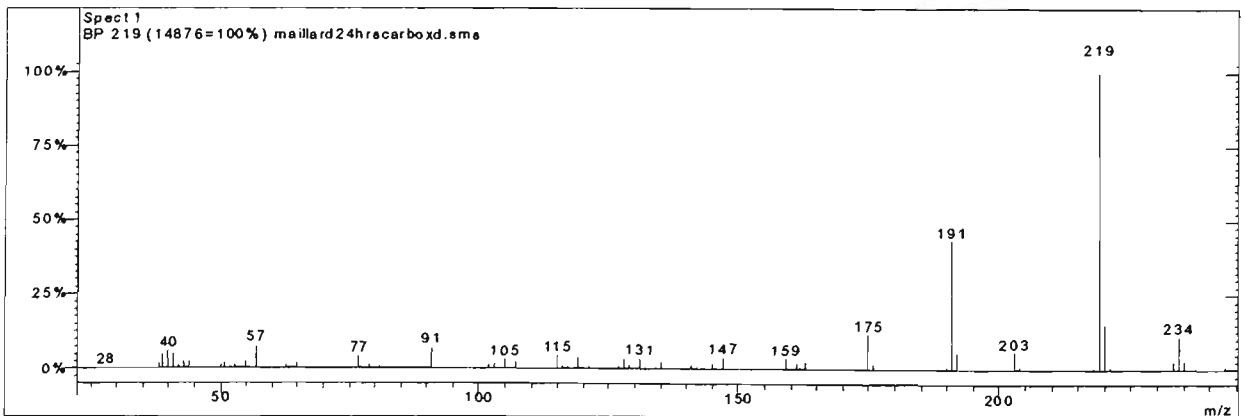
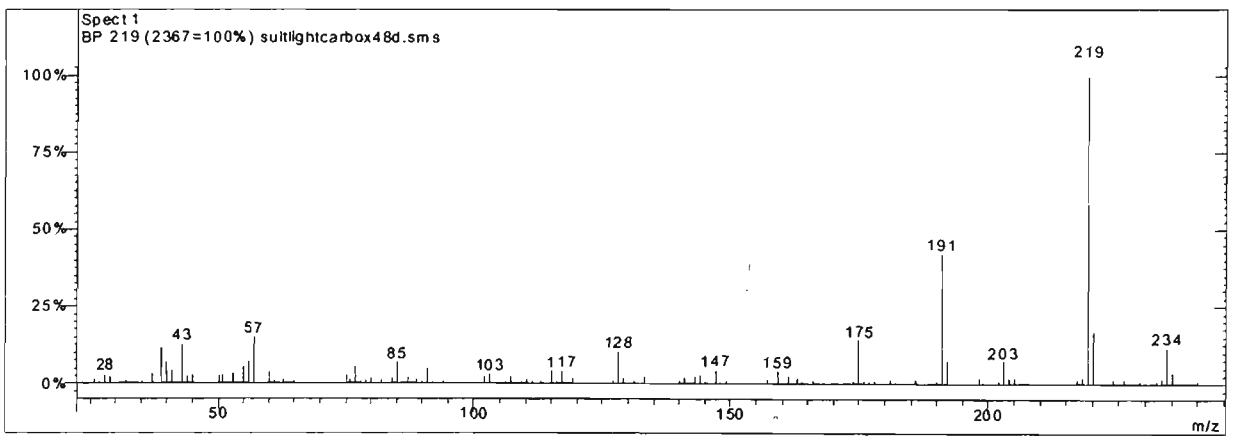
Peak 51 From Carboxen fibre sultana (top) and Carboxen fibre model (bottom)



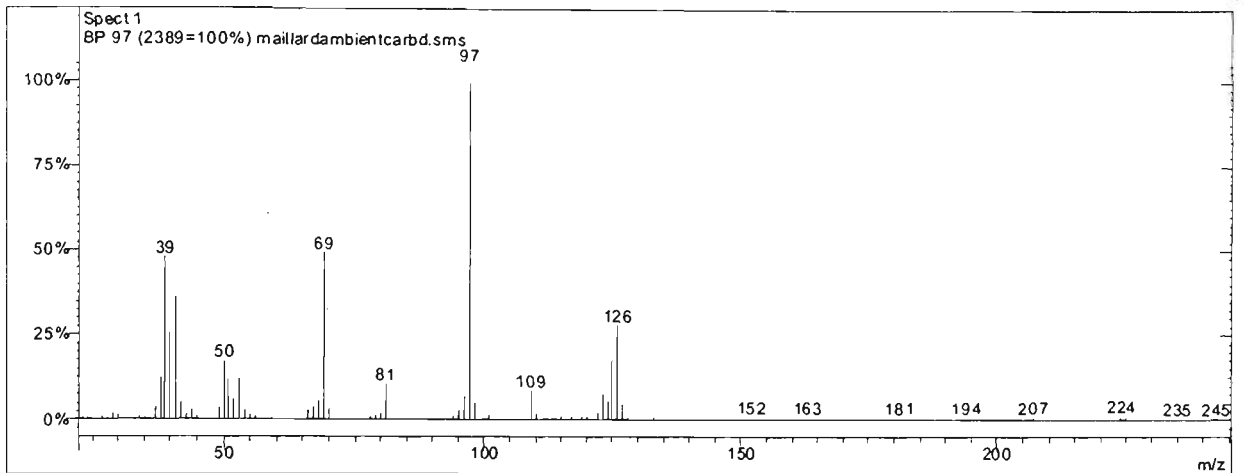
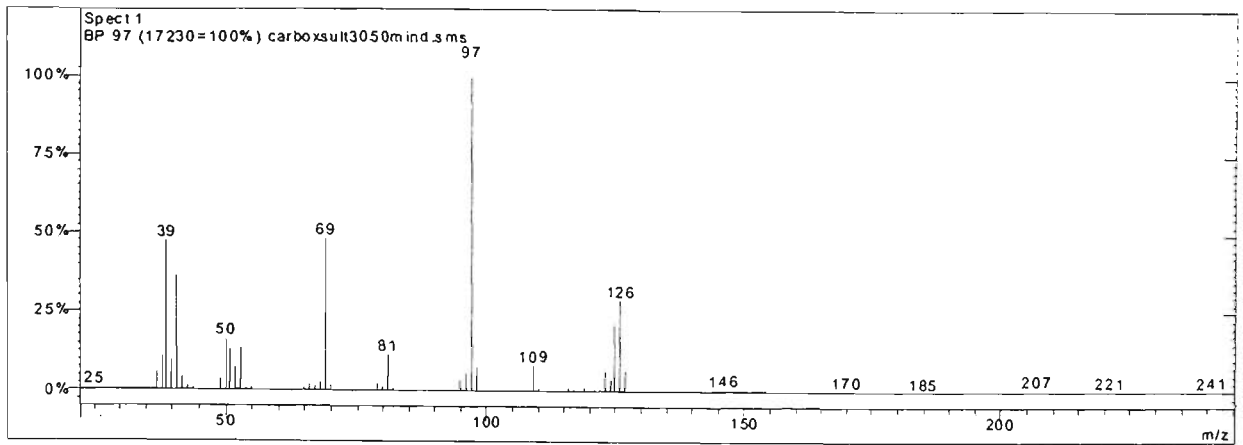
Peak 52 From Carboxen fibre sultana (top) and Carboxen fibre model (bottom)



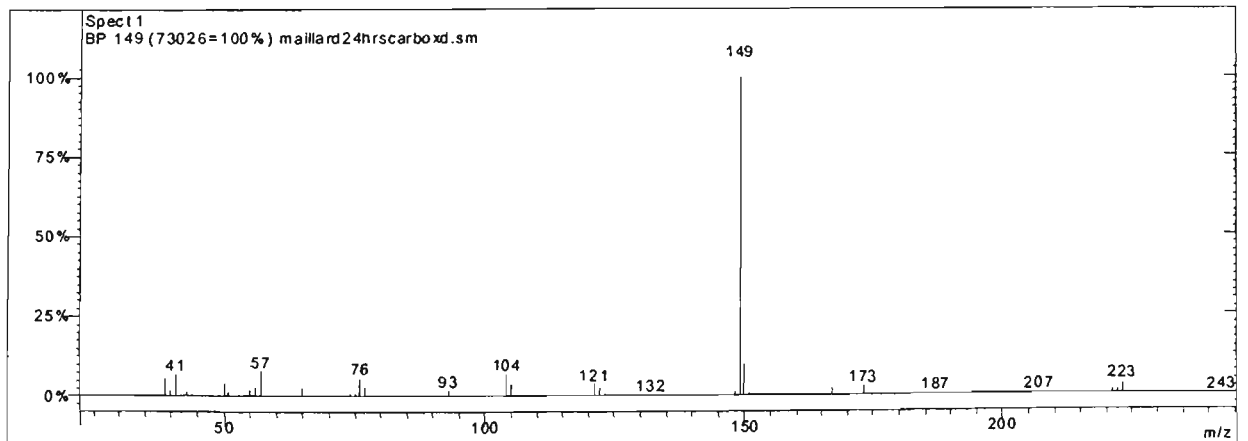
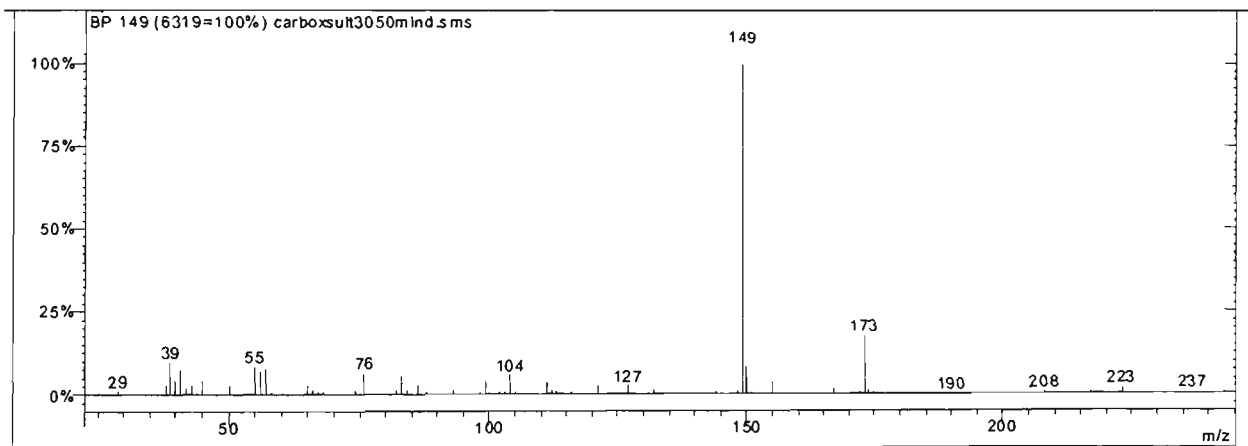
Peak 53 From Carboxen fibre sultana (top) and Carboxen fibre model (bottom)



Peak 54 From Carboxen fibre sultana (top) and Carboxen fibre model (bottom)



Peak 55 From Carboxen fibre sultana (top) and Carboxen fibre model (bottom)



Peak 56 from Carboxen fibre sultana (top) and Carboxen fibre model (bottom)















